Robert J. Howlett
Lakhmi C. Jain
Shaun H. Lee
Editors



Sustainability in Energy and Buildings

Proceedings
of the First International Conference
in Sustainability in Energy
and Buildings
(SEB'09)

Springer

Sustainability in Energy and Buildings

Proceedings of the International Conference in Sustainability in Energy and Buildings (SEB'09)

Robert J. Howlett · Lakhmi C. Jain ·
Shaun H. Lee (Eds.)

Sustainability in Energy and Buildings

Proceedings of the International Conference in Sustainability in Energy and Buildings (SEB'09)

Springer

Dr. Robert James Howlett
KES International
2nd Floor, 145-157 St. John Street
London, EC1V 4PY
UK
E-mail: rjhowlett@kesinternational.org

Dr. Shaun H. Lee
KES International
2nd Floor, 145-157 St. John Street
London, EC1V 4PY
UK
E-mail: shlee@kesinternational.org

Prof. Lakhmi C. Jain
School of Electrical and Information Engineering
University of South Australia
Adelaide, Mawson Lakes Campus
South Australia SA 5095
Australia
E-mail: Lakhmi.jain@unisa.edu.au

ISBN 978-3-642-03453-4 e-ISBN 978-3-642-03454-1

DOI 10.1007/978-3-642-03454-1

Library of Congress Control Number: 2009934312

Typeset & Cover Design: Scientific Publishing Services Pvt. Ltd., Chennai, India.

Production: Scientific Publishing Services Pvt. Ltd., Chennai, India

Printed in acid-free paper

9 8 7 6 5 4 3 2 1

springer.com

Preface

This volume represents the proceedings of the First International Conference on Sustainability in Energy and Buildings, SEB'09, held in the City of Brighton and Hove in the United Kingdom, organised by KES International with the assistance of the World Renewable Energy Congress / Network, and hosted by the University of Brighton.

KES International is a knowledge transfer organisation providing high-quality conference events and publishing opportunities for researchers. The KES association is a community consisting of several thousand research scientists and engineers who participate in KES activities. For over a decade KES has been a leader in the area of Knowledge Based and Intelligent information and Engineering Systems. Now KES is starting to make a contribution in the area of Sustainability and Renewable Energy with this first conference specifically on renewable energy and its application to domestic and other buildings. Sustainability in energy and buildings is a topic of increasing interest and importance on the world agenda. We therefore hope and intend that this first SEB event may grow and evolve into a conference series.

KES International is a member of the World Renewable Energy Congress / Network which is Chaired by Professor Ali Sayigh. We are grateful to Professor Sayigh for the collaboration and assistance of WREC/N in the organisation of SEB'09. We hope to continue to work with WREC/N in the future on projects of common interest.

In addition to featuring papers from a range of renewable energy and sustainability related topics, SEB'09 was intended to explore two innovative themes:-- The application of intelligent sensing, control, optimisation and modelling techniques to sustainability;- The technology of sustainable buildings.

This volume contains the best papers selected from a considerable number of submissions after reviews by experts in the field. The papers are grouped in the themes under which they were presented, namely Smart Sustainability, Solar and Wind Energy, Technologies for Sustainable Buildings, Clean and Renewable Energy, Engineering Intelligence and Energy Technologies, Building Energy Efficiency and Performance and Novel Techniques for Energy Efficiency.

Thanks are due to the very many people who have given their time and goodwill freely to make the SEB'09 a success. We would like to thank the Dean of the Faculty of Science and Engineering, Professor Andrew Lloyd, and the Mayor of Brighton and Hove, Councillor Garry Peltzer Dunn for opening the conference. We would like to thank the members of the International Programme Committee who were essential in providing their reviews of the papers. We are very grateful for this service, which enabled us to ensure high quality papers. We thank the high-profile keynote speakers for providing interesting talks to inform delegates and provoke discussion. Important contributors to SEB'09 were made by the authors, presenters and delegates without whom the conference could not have taken place, so we offer them our thanks. The KES Secretariat staff worked hard to bring the conference to a high level of organisation, and we thank them. Finally we thank the staff of the Holiday Inn, and the people of Brighton and Hove for welcoming the conference.

We believe these proceedings will form a record of recent research results, useful for engineers, students, professionals, managers and many others working in this leading-edge field. We intend that Sustainability in Energy and Buildings will become a regular event and we hope to see you at a future SEB conference.

Bob Howlett
SEB'09 General Chair
KES International Executive Chair

Organization

Conference General Chair

Dr Robert J. Howlett
Centre for SMART Systems, University of Brighton, UK
Executive Chair, KES International

Honorary Chair (Intelligent Systems)

Professor Lakhmi C. Jain
University of South Australia &Visiting Professor,
University of Brighton

Honorary Chair (Renewable Energy)

Professor Ali Sayigh
Chairman of World Renewable Energy Congress
Director General of WREC/N

Honorary Chair (Built Environment)

Professor Andrew Miller
Centre for Sustainability in the Built Environment, University of Brighton

Asia (excluding China) Liaison Chair

Professor Vivek Agarwal
Indian Institute of Technology Bombay, India

Australia & New Zealand Liaison Chair

Professor Bogdan Z. Dlugogorski
Director, Research Centre for Energy
The University of Newcastle, Australia

China Liaison Chair

Professor Hong Jin
Director of Green Building Research Institute
Director of Architectural Technology Department
Harbin Institute of Technology, Peoples Republic of China

Local Arrangements Chair

Mr Shaun Lee
Centre for Smart Systems, University of Brighton, UK

KES International

The organisation and operation of SEB'09 is the responsibility of the KES International organisation

Executive Chair: Dr Robert J. Howlett, University of Brighton
Founder: Professor Lakhmi Jain, University of South Australia
Operations Manager: Mr Peter Cushion
On-site Registration Executive: Ms Anna Howlett

SEB'09 International Programme Committee

Prof. Moulay-Ahmed Abdelghani-Idrissi	University of Rouen, France
Prof. Vivek Agarwal	Indian Inst. of Technology Bombay, India
Prof. Abdel Aitouche	HEI Grande Ecole, Lille, France
Prof. A.S.Bahaj	University of Southampton, UK
Prof. Frede Blaabjerg	Aalborg University Inst. of Energy Technology, Denmark
Mr Tony Book	Riomay Ltd, UK
Prof. Chris Chao	Hong Kong University of Science and Technology, China
Dr Tim Cockerill	Imperial College London, UK
Prof. Emilio Corchado	University of Burgos, Spain
Prof. Juan Manuel Corchado	University of Salamanca, Spain
Prof. Derek Clements-Croome	University of Reading, UK
Dr. Gouri Datta	University of Delhi, India
Prof. He Dexin	President, Chinese Wind Society, China
Prof Bogdan Dlugogorski	University of Newcastle, Australia
Prof. Prasad Enjeti	Texas A&M University, Qatar
Luis A. Fajardo-Ruano	Universidad Michoacana of San Nicolás of Hidalgo, Mexico
Prof Ahmed Hajjaji	University of Picardie Jules Verne, France
Prof. Jishan He	Chinese Academy of Engineering, China
Prof. Sture Holmberg	Royal Institute of Technology, Stockholm, Sweden
Dr. Robert Howlett	KES International & University of Brighton, UK
Dr. Sam C.M.Hui	University of Hong Kong, China
Dr Kenneth Ip	University of Brighton, UK
Prof. Lakhmi C. Jain	University of South Australia, Australia

Prof. Hong Jin	Harbin Institute of Technology, Heilongjiang, China
Prof. Eric Kennedy	University of Newcastle, Australia
Prof. D. P. Kothari	Vice Chancellor, Vellore Institute of Technology University, India
Dr Sumathy Krishnan	North Dakota State University, USA
Prof. Anjui Li	Xi'an University of Architecture & Technology, China
Prof. Shaohua Liu	Vice-president of Northeast Dianli University, China
Prof. Søren Linderoth	Risø National Laboratory Technical University of Denmark
Prof. Yongqian Liu	North China Electric Power University, China
Prof. Dennis L. Loveday	University of Loughborough, UK
Prof. Behdad Moghtaderi	University of Newcastle, Australia
Prof. Nordine Mouhab	University of Rouen, France
Prof. Chem V. Nayar	Curtin University of Technology, Australia
Prof. Huang Qili	Chinese Academy of Engineering, China
Prof. Ahmed Rachid	University of Picardie Jules Verne, France
Prof. V. T. Ranganathan	Indian Institute of Science, India
Prof. Saffa B. Riffat	University of Nottingham, UK
Prof. Dermot Roddy	University of Newcastle, UK
Dr Khizer Saeed	University of Brighton, UK
Dr Cesar Sanin	University of Newcastle, Australia
Prof. Abdulnaser Sayma	University of Sussex, UK
Prof. Javier Sedano	University of Burgos, Spain
Dr. Dominique Seguin	University of Rouen, France
Dr. Marina Sokolova	Kursk State Technical University, Russia
Dr. Jonathan Sprooten	HEI Grande Ecole, France
Prof. Mark Sumner	University of Nottingham, UK
Prof. Edward Szczerbicki	University of Newcastle, Australia
Prof. Alan Turner	University of Sussex, UK
Dr. Mummadi Veerachary	Indian Institute of Technology Delhi, India
Dr. T. Nejat Veziroglu	University of Miami, USA
Prof. Jianping Xiang	North China Electric Power University, China CREST, University of Loughborough, UK
Prof. Hongxing Yang	Hong Kong Polytechnic University, China
Prof. Xianhui Yang	Tsinghua University, China

Keynote Speakers

Dr. Beth Jianping Xiang

Visiting Professor at North China Electric Power University, China

The development of Wind Energy in China

Abstract. Renewable energy has been selected as one of the strategic important clean energy sources by the Chinese government to cope with the serious environmental problems incurred by the dramatic increasing energy demand as the economy has been growing in the pat 30 years. As the most commercially competitive renewable energy except large scale hydro power, wind energy has been keep developing quickly in this country in recent years.

In this presentation, we will highlight the current status and development trend of wind energy industry in China. This includes the manufacturing of wind turbine generator systems, development of wind farms, research and development of wind energy science and technologies, development of wind energy education, polices, etc.

Biography. Beth Xiang is a visiting professor at North China Electric Power University in Beijing, China. She received a BEng. in Industrial Automation from Hunan University in 1982, an MEng in Automatic Control in 1996 and a PhD in Geophysics in 2000 from Central South University, P. R. China. For several years she worked as Associated Professor in the Department of Computer Engineering, Changsha University of Science & Technology, China, until she came to the UK as a principal project investigator sponsored by a Royal Society Fellowship in 1999.

Dr Xiang has been working at universities both in China and the UK for over 27 years. Dr. Xiang started working in wave energy and wind energy in the UK since 2001. She has been involved in several research projects funded by E.U**.,** UK EPSRC, UK emda and UK Royal Society.

Dr Xiang has a long term link with Chinese organizations and universities on renewable energy, especially the Chinese Academy of Engineering and Tsinghua University. A delegation on renewable energy from the Chinese Academy of Engineering visited the UK under her efforts in 2007.

Professor Sture Holmberg

Royal Institute of Technology, Stockholm, Sweden

Sustainable Energy Solutions and Indoor Climate Conditions in Buildings

Abstract. Within the European Union (EU) there is a demand for a 20 % reduction in the total annual energy consumption before year 2020. The building sector plays a key role. Heating, ventilation and cooling of buildings is responsible for some 40 % of total energy consumption and a significant amount of CO_2 emission. The three basic elements in meeting this EU ambition are to reduce the overall energy demand of buildings, increase the energy efficiency in the building sector and increase the use of renewable energy. The demand for efficient environmental friendly heating systems has in Sweden contributed to the development of low-temperature heat emitters specially adapted to heat pump systems. Here energy (energy quality) demand of the heat emission system is low and can be satisfied by a number of different sources with great potential for reduced C02 emission to the environment. A national programme for energy efficiency and energy-smart constructions - an energy declaration of buildings - is introduced, where both energy and the important indoor environment aspects are considered.

Biography. Sture Holmberg is a professor at the Royal Institute of Technology (KTH) in Stockholm, Sweden. He received his MSc in Chemical Engineering from Åbo Akademi (Finland) in 1978, and his PhD in Mechanical Engineering from KTH in 1987. For several years he worked as Associated Professor and head of his department, Constructional Engineering and Design, until he in 2007 became regular Professor in Fluid and Climate Theory at KTH.

Fluid and Climate Technology is his new research division at the School of Architecture and Built Environment (ABE) dealing with human health and well being in the built environment, particularly indoor environment. Professor Holmberg´s research and PhD education include theory, modelling techniques and also technical solutions that can contribute to improve built environments. Computer-based flow calculations and new ways of visual presentation form the basis of better understanding of important connections between built environments and with occupants health, comfort and productivity. The ultimate goals are 'healthy and sustainable' indoor environments and energy solutions. CFD (Computational Fluid Dynamics) predictions and methodology are of particular interest in his research group. Professor Holmberg is supervising PhD students, and regularly involved in different teaching activities. His international contacts and collaborations have been of great help for the development of his research area in Sweden. In 1996 Holmberg was a visiting scientist at CSIRO Australia in Melbourne. He was invited by the Advanced Thermal Technologies Laboratory at the Division of Building, Construction and Engineering. In 1999 he was a visiting scientist at the Massachusetts Institute of Technology (MIT), invited by the Building Technology Program.

Professor Ali Sayigh

Chairman of World Renewable Energy Congress, and Director General of World Renewable Energy Network, Brighton, UK

Renewable Energy and the Changing World

Abstract. The paper will highlight the importance of Renewable Energy and the continued progress in its various forms. The annual increase in photovoltaic production, wind application and solar thermal application over the last 5 years was 30-40%. The USA used to lead in photovoltaic (PV) production, then Japan took the lead but at the end of 2008, China became the leading manufacturer of PV. In the wind industry and application, Germany is the leader followed by Spain, but it is predicted that India will be number one by 2012. Also highlighted is the large investment being made in countries such as United Arab Emirates and Portugal. Large scale marine and wave energy projects in excess of one MW is in operation and bio-fuel is being produced at a competitive price, but there is concern over the use of food crop impacting on food availability and cost. Fuel cells are coming down in price accompanied by high efficiencies. One of the advantages in using Renewable Energy is to meet the electricity demand in many of developing countries. The paper will address climate change and water shortage and demonstrate that Renewable Energy can help solve both of these issues.

Biography. Graduated from London University, & Imperial College, B.SC. DIC, Ph.D., CEng in 1966. Fellow of the Institute of Energy, and Fellow of the Institution of Electrical Engineers, Chartered Engineer. Prof Sayigh taught at Baghdad University, College of Engineering, King Saud University, College of Engineering, Saudi Arabia, and also Kuwait University as part time professor. Also Head of Energy Department at Kuwait Institute for Scientific Research (KISR) and Expert in renewable energy at AOPEC.

He started working in solar energy since September 1969. In 1984 he establish with Pergamon Press his first International Journal for Solar and Wind Technology as an Editor-in-Chief. In 1990-present Editor-in-Chief of Renewable Energy Journal incorporating Solar & Wind Technology, published by Elsevier Science Ltd, Oxford, UK. He is Founder and Chairman of the ARAB Section of ISES since 1979, was chairman of UK Solar Energy Society for 3-years and consultants to many national and international organizations, among them UNESCO, UNDP, ESCWA, & UNIDO.

Since 1977, Prof Sayigh founded and directed several Renewable Energy Conferences and Workshops in ICTP - Trieste, Italy, Canada, Colombia, Algeria, Kuwait, Bahrain, Malaysia, Zambia, Malawi, India, West Indies, Tunisia, Indonesia, Libya, Taiwan, UAE, Oman, Czech Republic, West Indies, Bahrain, Germany, Australia, Poland, USA and UK. In 1990, he established the World Renewable Energy Congress and in 1992 the Network (WREN) which have their Congresses every two years, attracting more than 100 countries each time. In 2000 he was one of the founding member of ASTF.

Prof Sayigh had supervised and graduated more than 30 Ph D students and 50 M Sc students under his supervision at Reading University and University of Hertfordshire. He edited, contributed, and written more than 20-books, and 300-papers in

various international journals and Conferences. Since 1990 cooperated with the British Council, Commonwealth Science Council, UNDP, ESCWA, UNESCO and during the last six years with ISESCO. In 2000-Present initiated and worked closely with Sovereign Publication Company to produce the most popular magazine at annual bases called Renewable Energy (2001, 2002, 2003, 2004, 2005 and 2006).

Professor Bogdan Dlugogorski

Priority Research Centre for Energy, The University of Newcastle, Australia

Assessment of Mineral Carbonation as an Option for Sequestering CO2 Emissions from Coal Power Stations in the State of New South Wales in Australia

Abstract. Geosequestration, which denotes the storage of CO_2 underground in porous rocks and saline reservoirs, remains the preferred option for storing CO_2 emissions from coal power stations in Australia. Each state in Australia, except New South Wales, has access to good geosequestration sites. In NSW, prospective sites identified in the Darling Basin require field confirmation from a drilling program. However, NSW has large deposits of ultramafic rocks, especially as part of the so-called New England Great Serpentinite Belt which crops out 100-150 km from coal power stations of the Hunter Valley. The Belt is more than 300 km in length with an outcrop width of between 10 m and 2 km. Its estimated capacity is around 400 Gt of CO_2, the equivalent of the roughly 1000 years of current Australian CO_2 emission. The belt's rocks comprise serpentinites (lizardite and antigorite minerals, with relatively small amounts of previously mined chrysotile), and partially serpentinised dunites and harzburgites. Serpentines, as sheet minerals, exhibit little reactivity to CO_2 and require energy intensive activation.

In this presentation, in addition to reviewing the Australian deposits of ultramafic rocks, we explore technical issues relating to the inclusion of mineral carbonation as an option for storing the NSW emissions of CO_2. We find that the technologies described in the literature, except for the ARC (Albany Research Council, USA) and the low-volume IET (Institute of Energy Technology, Norway) processes, are not technologically feasible for sequestering CO_2. In particular, pH swing process and the hydrochloric acid extraction processes seem to generate 4 to 7 times as much CO_2 as they consume. Likewise, the feasibility of gas/solid processes based on the carbonation of $Mg(OH)_2$ depends on the extraction of $Mg(OH)_2$ from serpentines. A recent assessment of the ARC process appears to err by excluding the CO_2 compression costs, and using electrical energy to activate serpentines. We conclude that mineral carbonation is not yet ready for pilot plant trials in Australia. Intense research is required to optimise the ARC process for serpentinites, in conjunction with serpentinite activation, followed by detailed process economic and life cycle analyses.

Biography. Bogdan Dlugogorski gained undergraduate degrees in chemical engineering and geophysics from the University of Calgary, and MEng and PhD, both in chemical engineering, from McGill University and École Polytechnique de Montrèal, respectively. Recently he was awarded a DSc degree in fire science and engineering

from the University of Newcastle. He spent 15 months at the National Fire Laboratory of the National Research Council, Canada, before joining the University of Newcastle, Australia in 1994, where he is now Professor in Chemical Engineering and Director of the Centre for Energy. He is a Fellow of the Australian Academy of Technological Sciences and Engineering, Engineers Australia, and the Royal Australian Chemical Institute. His research interests cover energy, especially CO2 sequestration, as well as fire and explosive chemistry, with special focus on fire suppression and formation of toxic products in fires. His career's output includes over 200 publications.

Professor Eric Kennedy

Priority Research Centre for Energy The University of Newcastle, Australia

Development of a non-destructive process for treatment of fluorine-containing synthetic greenhouse gases

Abstract. Fluorochemical gases are used broadly and intensively around the world, as heat transfer fluids in air conditioning, foaming agents in refrigeration and building insulation and as fire extinguishing agents. These chemicals often have high global warming potentials (generally greater than 1,000) and some compounds (such as halons and CFCs) are also ozone-depleting. There is considerable interest in minimising the emission of these chemicals into the receiving environment, and many countries have implemented measures aimed at emission reduction.

In this presentation we outline a process developed to treat these chemicals which results in the production of a valuable compound. The technology is based on the reaction of the fluorochemical with methane (which is the major component of natural gas). We hypothesise that the key elementary step involves the coupling of a CF_2 moiety (formed from the synthetic greenhouse gas) with a methyl radical (formed from methane or methane derivatives) will results in the production of $C_2H_2F_2$, (often abbreviated VDF) a highly valued monomer used in the synthesis of acid-resistant fluoropolymers.

Biography. Eric Kennedy gained undergraduate and PhD degrees from the University of New South Wales (Australia). He joined the University of Newcastle, Australia in 1994, where he is now Professor in the Department of Chemical Engineering, Deputy Director of the Centre for Energy and Assistant Dean (Research) in the Faculty of Engineering and Built Environment. His research interests include the development of technologies which reduce greenhouse gas emissions, fundamental studies on fire chemistry, formation of toxic compounds in fires and fire mitigation.

Table of Contents

Session A : Smart Sustainable Systems

Session B : Solar and Wind Energy

Session C : Technologies for Sustainable Buildings

Session D : Clean and Renewable Energy Technology

Session E : Engineering Intelligence and Energy Technologies

Session F : Building Energy Efficiency and Performance

Session G : Novel Techniques for Energy Efficiency

Smart Monitoring of Wind Turbines Using Neural Networks

Jianping Xiang[1], Simon Watson[1], and Yongqian Liu[2]

[1] Centre for Renewable Energy Systems Technology (CREST), Department of Electronic and Electrical Engineering, Loughborough University, LE11 3TU, UK
Tel.: +44 1509 635352; Fax: +44 1509 610031
J.Xiang@lboro.ac.uk
[2] North China Electric Power University, Beijing, 102206 China

Abstract. In this paper, we present a neural networks model-based method to monitor the condition of a generator bearing in a wind turbine. The temperature of the generator bearing is modelled as a function of the generator speed in the wind turbine. The difference between the temperature measurement and the model is calculated and compared to logbook records to verify the method. Other methods are also given for comparison.

Keywords: wind turbine, generator bearing temperature, system identification, neural networks.

1 Introduction

Recently, the need for proactive and predictive maintenance for wind turbines is becoming ever more necessary with the move to the offshore environment where access is severely limited. Great efforts have been made through research projects in Europe, including condition monitoring for offshore wind farms (CONMOW) [1] and Supergen Wind Energy Technologies Consortium (Supergen Wind) [2]**.** As supervisory control and data acquisition (SCADA) systems have been widely used in the wind energy industry world wide, we started to analyze the SCADA data for the purpose of the condition monitoring of wind turbines since 2005. Using the achievements from the reliability analysis [3] and experience on condition monitoring of wind turbines[4], we have developed some methodologies to tackle different aspects of the problem in wind turbines. In this paper, we present a model-based method to analyze the temperature of a generator bearing in a wind turbine by using neural networks and compare it with other methods.

In order to clarify the topics and to guide the discussion, we will give some information related to the development of the neural networks model-based method in the use of the SCADA data.

The SCADA data is usually 10-minute statistics (average, minimum, maximum and standard deviation). As a SCADA system is a huge database and is related to many wind turbine components, we have investigated the fault mode, the fault reason, the failure rate, the relationship between some parameters, etc, from the database. The

aim of this work is to find out how the failures are related to the SCADA data and what we can possibly use for the condition monitoring of the wind turbines from the SCADA data. Table 1 lists some failure modes and its related failure reasons, which shows that temperature and vibration are two important elements in many components. Table 2 indicates that around 4.9 percent of time is spent on the repair and maintenance of wind turbines in a windfarm. As failure rate is a typical measure

Table 1.

Material related fault mode	Fault description
Blade	Damaged Blade, Loose Blade Seal, etc
brake	High temp Brake Disc, etc
Gearbox	High Gear Temp, Transm Osc, Low Gear Oil Pressure, etc
Generator	High Generator Temp, High temperature Gen Bearing 1, etc
Other	Noise, Vibration, etc
Pitch Mechanism	Low Working Pressure, Oil Leak, High Hydraulic Temp, High Gear Temperature, Pitch A Positio,
Rotor	Rotor noise, Snagging in Rotor, etc
Shaft & bearing	High Temperature Generator Bearing, Transm Osc, etc
Yaw system	Yaw Gearing, etc

Table 2.

Total calendar time (day)	Total downtime /Per turbine (day)	Available time rate	Unavailable time rate for scheduled turbine service
1135	55.6	95.1%	0.4%

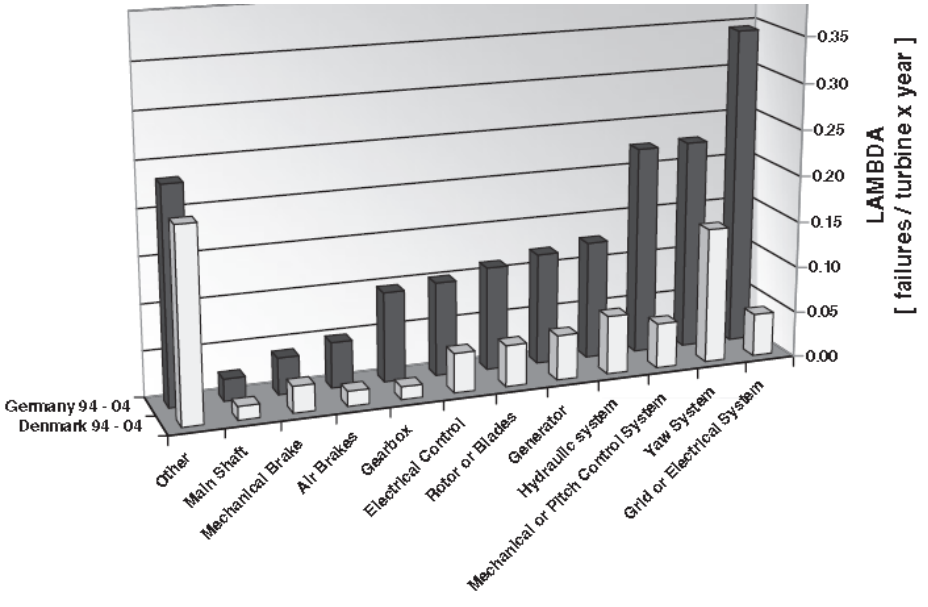

Fig. 1. Average failure rate of wind turbine components

of reliability, we investigated the failure rate under each failure mode, based on WindStats Data. Figure 1 is estimated from windfarms over Germany and Denmark. For example, nearly 10% of the gearboxes failed in Germany in one year. The above implies that wind turbines might be greatly improved, if the failure rate can be improved. In order to achieve the improvement, we have analysed a lot of data sets and found that a very clear relationship exists in many parameters, e.g. the generator bearing temperature and the generator power in wind turbines. We have also investigated the temperature lag effect that is shown in Figure 2. The clearest temperature lag effect in Figure 2 is between the generator1 temperature and the generator power in wind turbines. For example, the power is raised from 722kW to the up-limit of about 2MW in 30 minutes, but it takes 4 hours and 50 minute for the temperature to rise from 82 C^o to the up-limit of about 112 C^o. In this paper, we will focus on the condition monitoring of the generator bearing through its temperature characteristics to demonstrate the neural networks model-based method.

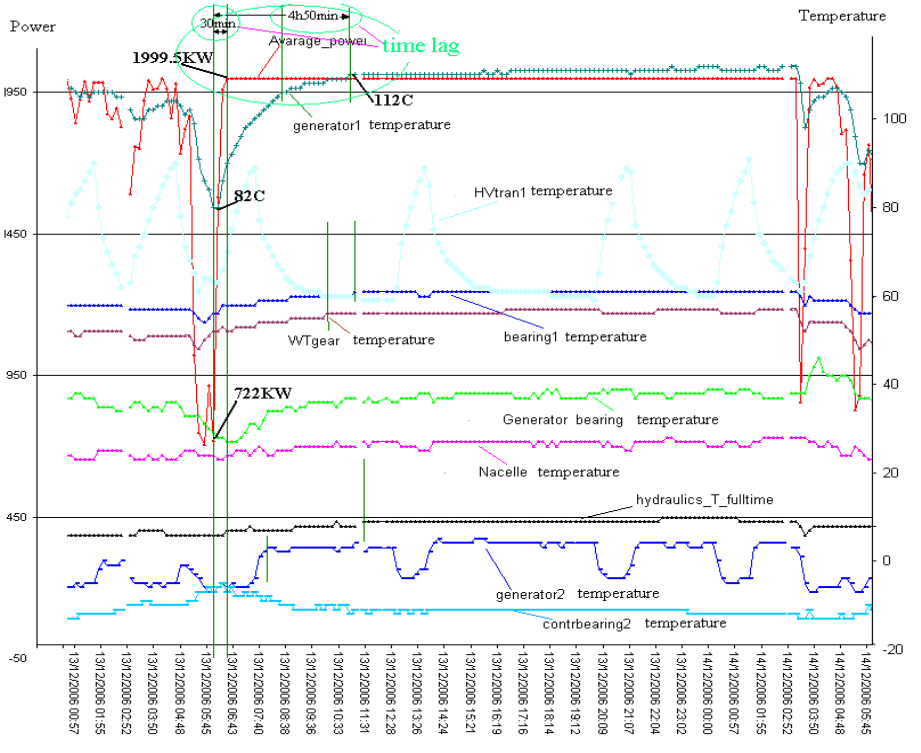

Fig. 2. The lag between temperature and power

Figure 3 gives the comparison between Generator faults and the generator bearing temperature in a daily sequence. A useful case is the time period after the LS generator is replaced with ABB generator on 20th January 2006. The bearing temperature goes down after the second generator replacement of generator on 6th

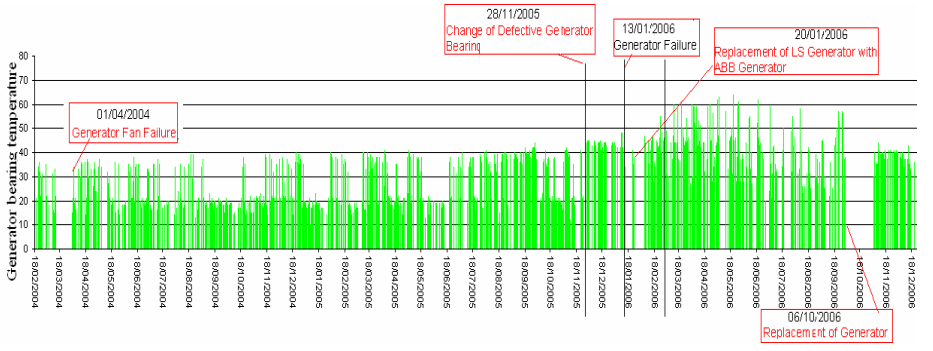

Fig. 3. Daily maximal temperature of generator bearing

October 2006. The results indicate that the generator bearing temperature is a good parameter for the condition monitoring of generator bearings.

The result in Figure 3 is the daily maximal temperature that is calculated from a screened data set, based on the linear segment of the temperature vs. power. There is a non-linear relationship between the bearing temperature and the power, but a linear characteristics can be used under some circumstances. For the case of the data that we are investigating, a linear characteristics can be chosen within the power range of 1100 ~1700KW.

As Figure 3 is based on screened data sets, only some percentage of data is used for analysis, which obviously affects the quality of the monitoring. In order to solve the problem, we have had further investigation into the temperature characteristics by using a black-box modelling approach. By using the black-box modelling approach, we have achieved some good results, but a higher order of the model is needed to obtain higher accuracy. Under such circumstance, we start to investigate the feasibility of the neural networks method.

In order to give a more clear and connected view of the subjects under consideration, in this paper, we will first present the theory related to the generator bearing. After that, we will describe the black-box modeling approach and some results. With the understanding from the black-box modeling approach, we will finally give a detailed discussion on the neural networks model-based approach and its related results.

2 Thermodynamics in a Bearing [5]

The power loss in a bearing as a result of bearing friction can be obtained using the equation (1).

$$P_R = 1.05 \times 10^{-4} Mn \tag{1}$$

where

P_R =power loss, W

M =total frictional moment of the bearing, Nmm

n =rotational speed, r/min

Under certain conditions of bearing load $P \approx 0{,}1\ C$, good lubrication and normal operating, the frictional moment can be calculated with sufficient accuracy using a constant coefficient of friction μ from the following equation

$$M = 0.5\ \mu\ L_p d \tag{2}$$

Where

M=frictional moment, Nmm

μ =constant coefficient of friction for bearing

L_p =equivalent dynamic bearing load, N

d=bearing bore diameter, mm

If the cooling factor (the heat to be removed from the bearing per degree of temperature difference between bearing and ambient) is known, a rough estimate of the temperature increase in bearing can be obtained using

$$\Delta T = P_R\ / W_S \tag{3}$$

Where

ΔT=temperature increase, °C

P_R =power loss, W

W_s =cooling factor, W/°C

Equation (3) indicates that the temperature increase is proportional to the power loss, if the cooling factor is constant.

As power loss in a bearing is not measured in our data sets, we will use the stator electrical power output, P_s, as an alternative in Equation (3). If the mechanical power captured by the wind turbine and transmitted to the rotor is P_m, the power loss in a bearing is P_R,

$$P_R = P_m - P_s - \sum_{i=1}^{n} P_i \tag{4}$$

In Equation (4), $\sum_{i=1}^{n} P_i$ is the power loss including the iron loss, copper loss, windage loss, etc.

Inserting Equation (4) into Equation (3), we have

$$\Delta T = (P_m - P_s - \sum_{i=1}^{n} P_i)\ / W_S \tag{5}$$

If P_m, $\sum_{i=1}^{n} P_i$ and W_s are fixed, the temperature increase is a linear function of P_s.

3 Black-Box Modelling of Generator Bearing Temperature vs. Power [6]

Section 2 has revealed that the generator temperature increase can be a function of the electrical power under some assumptions. Based on the theory, a MSc project was

carried out for an investigation of the temperature characteristics by using a system identification method. At the first stage, the purpose of the project is to find out if there is a suitable black-box model from the measured data. Several data sets in different months are employed for the investigating. Results show that the black-box model is reasonable as a description of the temperature behaviour. There are two key points from the results: 1) the models calculated from each month are very close; 2) The data calculated from the model is very close to the measured data. Figure 4 indicates the modelling data has a better fitting to the measured data in a higher order.

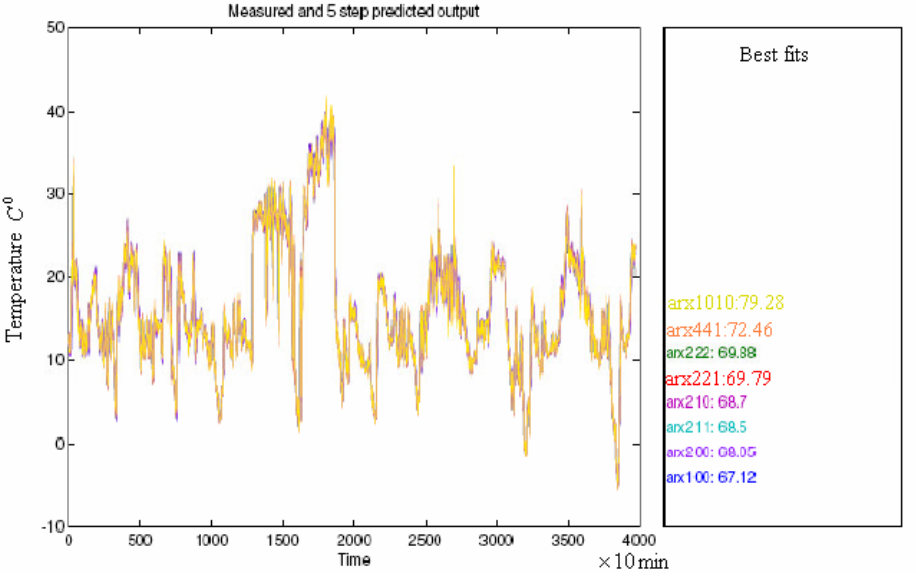

Fig. 4. Black-box modelling of bearing temperature

4 Neural Networks Modelling of Generator Bearing Temperature vs. Generator Speed [7]

As it has been mentioned that a higher order of the model is needed to obtain higher accuracy of fitting between the measured data and the modelling data for the system identification modelling method. This is because of the complexity shown in equation 5 and the noise due to many factors. In order to find a more accurate model for the complex nonlinear system, we used a neural networks model-based method to analyze the measured data of the generator temperature and compared the results with the records in a logbook. In this method, the generator speed difference is used as the input of a feed-forward backpropagation neural network and the generator temperature difference as the training target of the neural network, as the temperature increase is proportional to the rotation speed that is determined by equation 1 to 3. The measured data is then subtracted by the model dada to get a final result that will be compared to the logbook.

Results show that neural networks model-based method is a reasonable method. It can be seen that it is very difficult to find problems from the original measurements shown in Figure 5 (a), but (b) gives a much clearer picture of the problems. Figure 5 (b) shows that the temperature difference reduced each time after some maintenance is carried out. Since a key feature of neural networks is an iterative learning process, neural networks model-based method is an artificial intelligent method. The artificial neural networks model-based method can describe a highly non-linear and complex system and therefore it is a smart monitoring method of wind turbines.

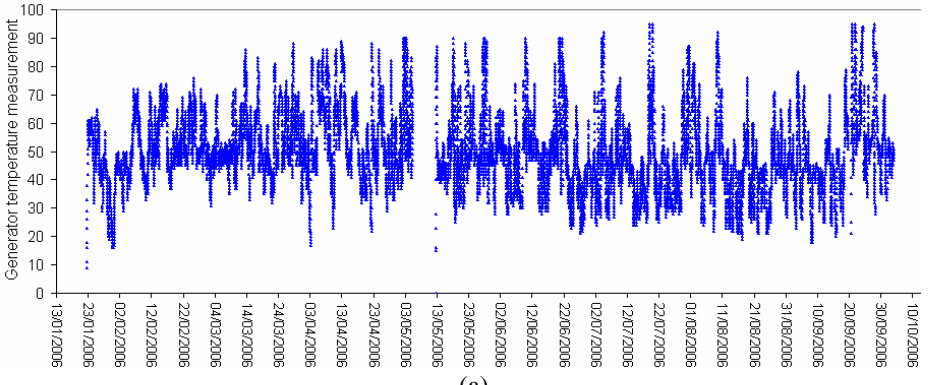

(a)

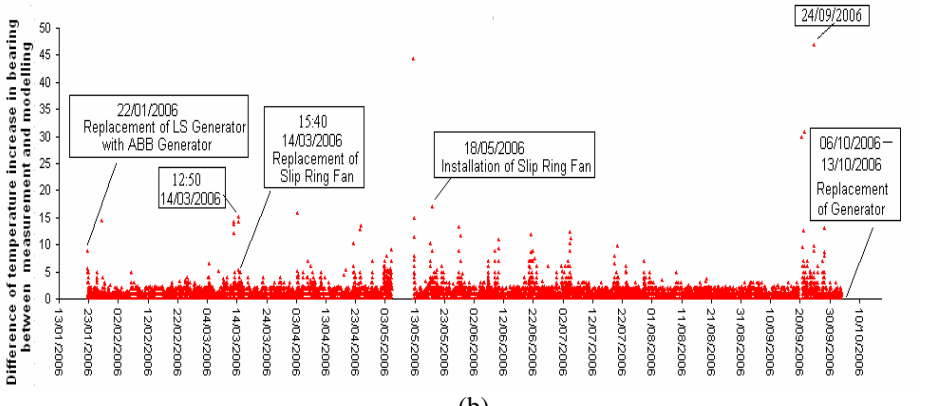

(b)

Fig. 5. Bearing temperature obtained from neural networks modelling method

5 Conclusion

This paper has presented a neural networks model-based method. It has been applied to the measured data of the generator bearing temperature in a wind turbine. The results show that the method is prospective for its ability to find informative information from complex measured data and therefore it can be used as a smart monitoring tool of some wind turbine components.

Acknowledgment

The authors would like to thank partners in EPSRC Supergen and the EU CONMOW project for their ongoing support of this work. We especially appreciate Airtricity for providing data and comments on our work.

References

1. Wiggelinkhuizen, E., Verbruggen, T., Braam, H., Rademakers, L., Xiang, J., Watson, S.: Transactions of the ASME: Journal of Solar Energy Engineering 130, 031004(1-9) (2008)
2. Xiang, J., Watson, S.J.: Practical Condition Monitoring Techniques for Offshore Wind Turbines. In: EWEC 2008 conference proceedings, Brussels Expo., Belgium, PO. 195, pp. 1–8 (2008)
3. Tavner, P., Xiang, J., Spinato, F.: Wind Energy 10, 1–18 (2007)
4. Watson, S.J., Xiang, J.: Real-time Condition Monitoring of Offshore Wind Turbines. In: European Wind Energy Conference & Exhibition, Greece, February 2006, pp. 647–654 (2006)
5. SKF, http://www.skf.com/portal/skf/home/products?paf_dm=shared&maincatalogue=1&lang=en&newlink=1_0_40
6. Chiu, W.-p.: Analysis of Wind Turbine SCADA and Maintenance Logs, M.Sc report, CREST, Loughborough University (2008)
7. Neural Network Toolbox, User's Guide

SMART Buildings: Intelligent Software Agents
Building Occupants Leading the Energy Systems

Wim Zeiler[1,2], Rinus van Houten[2], and Gert Boxem[1]

[1] TU/e, Technical University Eindhoven, Faculty of Architecture, Building and Planning.
[2] Kropman Building Services Contracting

Abstract. To further reduce the energy consumption of existing buildings, intelligent building control offers new possibilities. Intelligent Software Agents (ISA) can be implemented at different levels of building automation. Individual agents for individual climate control for each user of the building in combination with feedback on the energy consumption (costs) leads to better acceptance of the individual comfort and a reduction of the energy consumption. ISA's at room level with knowledge of the actual weather situation and orientation of the windows, improves efficiency of the used available energy resources of a building and this leads to better energy performance at lower costs. The technology was tested in field tests at different office buildings in the Netherlands.

Keywords: Software Agents, Building Automation, Thermal Comfort.

1 Introduction

In the built environment we need to reduce our environmental impact - our ecological footprint – by two thirds to a sustainable and globally equitable level to ensure future well being. This can only be reached by sustainable design.

Often decision makers assume that sustainable design is mainly about resource conservation – energy, water, and material resources. The last ten years, however, has seen a dramatic broadening of the definition of sustainability to include assurances for mobility and access as affected by land use and transportation, for health and productivity as affected by indoor environmental quality, and for the protection of regional strengths. This broader definition of sustainability is represented in the US by the LEED™ (Leadership in Energy and Environmental Design) standard of the US Green Building Council (Loftness et al. 2006).

The Center for Building Performance and Diagnostics at Carnegie Mellon University likes to expand this definition even further, to give greater emphasis to contextual and regional design goals, to natural conditioning, and to flexible infrastructures that support change and deconstruction (Loftness et al. 2006). The CBPD defines sustainable design as "a transdisciplinary, collective design process driven to ensure that the built environment achieves greater levels of ecological balance in new and retrofit

construction, towards the long term viability and humanization of architecture. Focusing on environmental context, sustainable design merges the natural, minimum resource conditioning solutions of the past (daylight, solar heat and natural ventilation) with the innovative technologies of the present, into an integrated "intelligent" system that supports individual control with negotiation for environmental quality and resource consciousness (Loftness et al. 2005). There is a strong need for more efficient and more intelligent buildings. Integration between end-user and building is the ultimate in the intelligent building concept. “Connecting” the end-user to a building is complex. User-connectivity, the combination of usability and user interface together, is studied and developed further. Information and communication technology connects people and helps them to communicate with the building (Clements-Croome 1997).

Building automation (BA) has become a crucial factor in order to adjust the requested comfort with use of the least energy. BA started with simple thermostatic controls and has become a specialized field that uses the newest available techniques in data-communication and control algorithms. Crucial data concerning the status and performance of the equipment is gathered and used to optimize the comfort in the building. Further optimisation aims at the reduction of the energy consumption, without compromise on indoor comfort. Human behaviour is an important factor to consider in the thermal exchanges between a building and its surroundings and the resulting energy consumption (Palme et al. 2006). The ability for occupants to make their own choices and control the environment is critical to the satisfaction of users are a determining factor in the comfort they feel (Isalque et al.2006). Dynamic online steering of individual comfort management and building management could save up to 20% of current energy consumption (Akkermans 2002). Further integration of user and the available systems is needed. Intelligent Software Agents (ISA) is a good concept in order to realise the further integration and optimization of building systems. Thanks to its autonomous operation, modular structure and abilities to communicate, software agents are a very flexible concept for integration of optimization at different levels.

ISA concepts are developed over the last 20 years and have been applied very different fields. The ISA used in this article can be best described as: *ISA’s are autonomous pieces of software dedicated to certain tasks; an ISA has access to resources ands is able to communicate and negotiate with other ISA’s in order to fulfil its tasks.* This definition suits the purposes for ISA within this paper, for further descriptions of the agent technology we refer to (Weiss 1999, Diane et al 2004). In this article the results are discussed of the two field experiments in office buildings. The first experiment was part of the European EBOB-project (Energy efficient Behaviour in Office Buildings). The second project was the SMART project in which the agent technology was developed for optimal setting of the comfort parameters. SMART stands for *Smart Multi Agent Technology.* The, in SMART developed, technology was tested in an extended field test in the IIGO-project, IIGO is a Dutch acronym for *Intelligent Internet mediated control in the built Environment*. The long term goal of this research program at the Technische Universiteit Eindhoven in cooperating with Kropman Building Services contracting and the Energy Research Centre Netherlands (ECN), is to develop an IAS that can be used to optimize the building performance, but also can be used as a tool during the design phase of energy infrastructures within buildings but also in the whole built environment. The structural concept of IAS is used to specify the needs and layout of the building systems.

2 Methodology

EBOB

In EBOB so called *Forgiving* Technology was developed, with this technology each user in the building was given control of his or her personal comfort in combination with feedback on the energy costs of the chosen setting.

The EBOB project is a European EU-FP5 program project with eleven partners from five countries. EBOB ran from 2002 until 2005. The field test was held at Kropman Rijswijk. A different type of technology to implement user behaviour, Forgiving Technology, was developed in EBOB. *Forgiving* Technology enables each user in the building to control his or her personal comfort in combination with feedback on the energy costs of the chosen setting. EBOB investigated new combined technical and socio-economic solutions to make energy efficient behavior natural, easy and intuitively understandable for the end-users in refurbished and new offices. By starting from the human perspective and use available and new technology, the outcome was focused on the ability to understand for the end user.

Too much heating or cooling consume a lot of energy, and at the same time these actions decrease comfort as effect of overshoot. Indoor temperature is also the most common issue in occupants' complaints. Misunderstandings and wrong conceptions about indoor environment are common. Most office users are not even aware of the fact that they can affect the energy use. Still the ability to make choices and control the environment is critical to the satisfaction of users are a determining factor in the comfort they feel (Isalgue et al.2006).

Energy consumption and the sensation of comfort are two different terms, but both are very important for evaluating the energy performance of buildings (Palme et al. 2006).

The user's behaviour is responsible for almost half the outcome of planned energy reduction. The occupant's behaviour is important to control the energetic consequences of comfort system in buildings. The end-users behaviour of building occupants needs to be taken into account. As until now the user is no part of the building comfort system control strategy, new technological development is needed to implement the behaviour of occupants of buildings.

SMART-IIGO

The, in SMART developed, technology was tested in an extended field test in the IIGO-project. From 2000 until 2002, the SMART project was carried out at the site of the Energy Research Centre of the Netherlands (ECN) near Petten. The general objective of this project was to formulate requirements for the optimization of such new climate control systems. Important was to gain experience in implementation such climate control systems in different settings. A field test in building 42-1 of ECN was held. A second, extended field-test with the SMART technology was done within the IIGO project. A period covering all seasons was used to determine the energy and cost saving potential of the SMART technology. This second field test was done at Kropman Nijmegen.

End-users were represented in the design of the SMART system by Fanger's comfort model (1970). Fanger's model predicts user's evaluations of the indoor climate in buildings. SMART determined the comfort level in a given period by measured

values of the comfort parameters of Fanger's model (Kamphuis et al.2002). By doing so it is possible to determine an individual preferable comfort profile.

The representation of situations with multi end-users was realized by developing an individual voting system for SMART, see figure 1. This approach was inspired by a pilot study with a similar system, the DUCOZT system (Oseland et al.1997, Perry & Raw 1999). The voting system implied that every user in a thermal zone could enter his vote (warmer/colder) within a voting period (e.g. one hour) while seeing the aggregated voting of other users in his zone at the moment of voting.

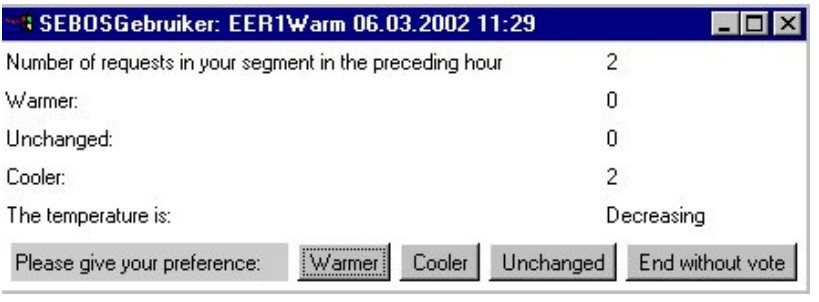

Fig. 1. Average vote and temperature as a result of individual voting system for SMART (Jelsma et al 2003)

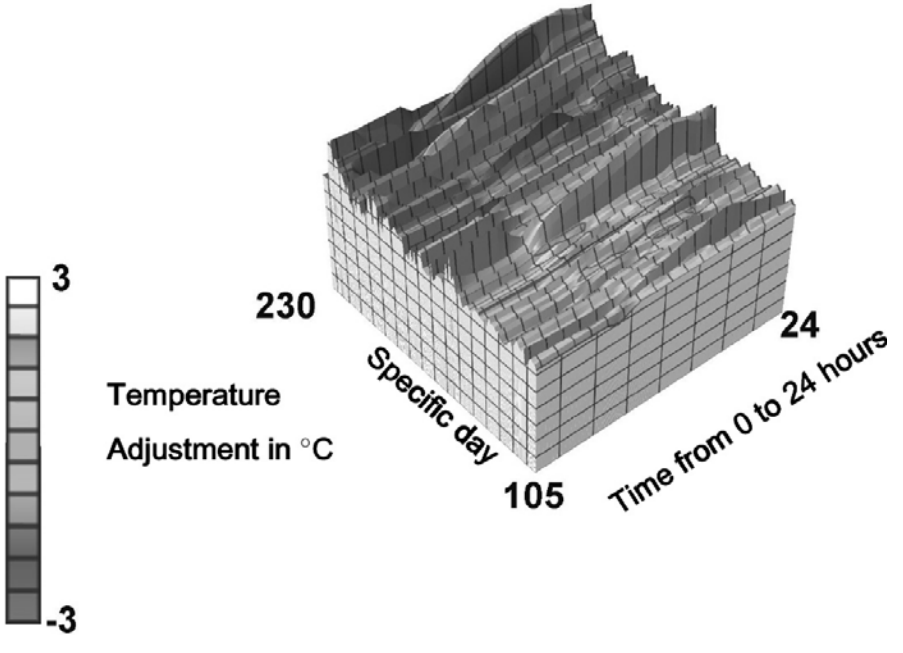

Fig. 2. Overview of the individual temperature adjustment during 125 days (Jelsma et al. 2002)

The voting system implied that every user in a thermal zone could enter his vote (warmer/colder) within a voting period (e.g. one hour) while seeing the aggregated voting of other users in his zone at the moment of voting. Figure 2 gives an overview of the temperature adjustments over a 125 days period.

The users comfort needs, based on Fanger's theory, are leading in this control strategy. The control strategy is based on a prescription of the user behaviour. The new user behaviour control strategy was implementation in a BMS (Building Management System). This BMS was extended with an external real-time information system to improve energy and comfort control.

3 Results Fieldtests

EBOB-project

In the EBOB-project the main topic was the interaction between energy use and individual comfort. This was done by giving each user a choice of 4 different modes. (1) a *Default setting*, where the system work with a default set point in the comfort band, (2) a *Comfort Zone*-setting, where the user can choose an offset of +/- 2K on the default setting, (3) an individual setting, where the user is able to choose a plus or minus offset to the standard comfort setting, and (4) an *Optimize Energy*-setting where the system operates within a wider comfort band is used to minimize energy costs. The users get feedback on the effects of their choice by information about the current outdoor weather conditions and by feedback based on the 'relative' energy consumption of the chosen mode. In figure 3 the lay-out of the user interface is given.

The field-test in the Kropman building in Rijswijk showed a reduction in energy consumption, due to a major choice for the *Optimize energy setting*. The field test learned the importance of a correct match of the offset-range to the actual ability of the

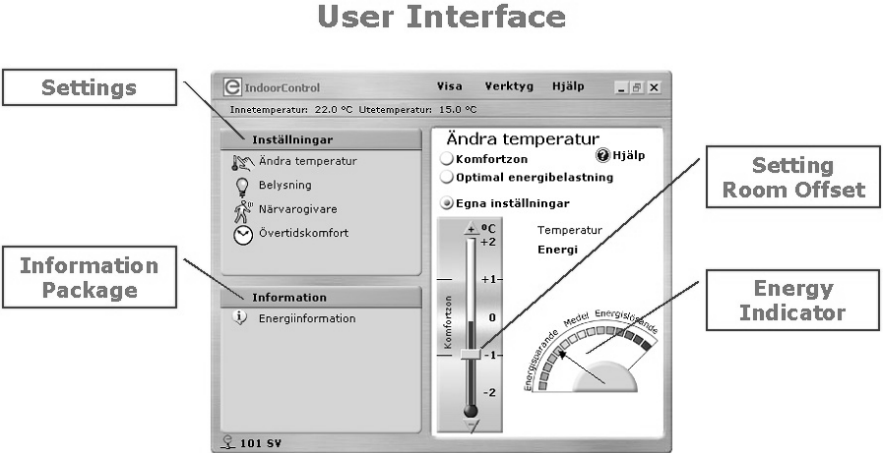

Fig. 3. PC-based user interface as developed in EBOB-project (EBOB 2004). The user can choose his preferences for temperature, and gets feedback on actual indoor and outdoor temperatures and an indication about the energy consumption of the HVAC-system.

HVAC-system. When the system is at is max. offset it should not 'promise' a cooler temperature than actual achievable. For a room with more occupants, the feedback of *the room temperature* is not representative for each individual user. For example a person near an air-outlet can perceive a cooler temperature; in fact the feedback should be made possible per workplace.

SMART-IIGO

The, in SMART developed, technology was tested in an extended field test in the IIGO-project. In the first part of the project, the agent-software for climate control was developed and tested at ECN research Centre. In the second part the technology was tested in the Kropman office of Nijmegen.The SMART-technology combined with the communication and control system developed in the IIGO was used in the field test. In the test the ISA-platform was implemented as a top layer on the existing BMS.

In figure 4 is the agent structure projected on different levels of a building. Due to the size of the building and the lay-out of the HVAC-system, *Floor-* and *Workplace Agents* had no real function. In the implemented lay-out the User Agents directly negotiated with the *Room agents* and the *Room-agents* had direct access to the *Building Agents*.

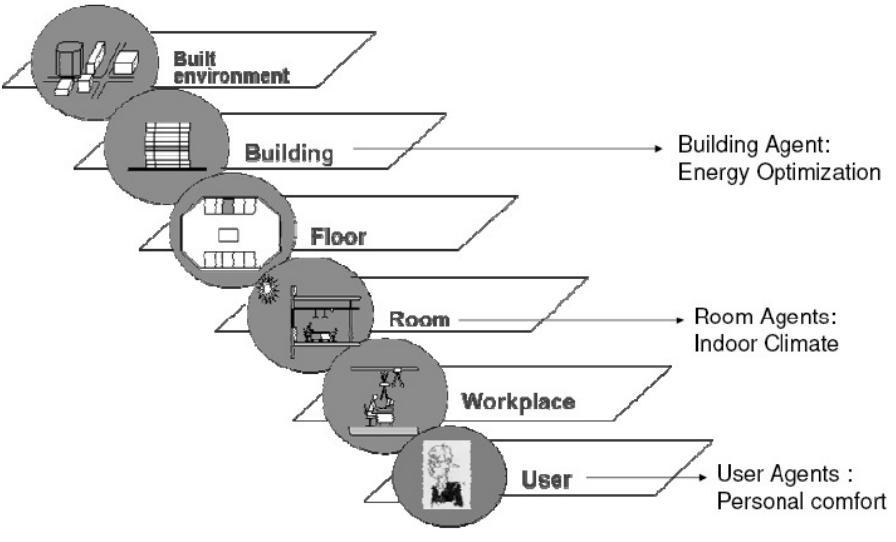

Fig. 4. At 3 levels agents are implemented: User agents for employees, Room agents for climate control of each room, and a Building agent for energy optimization.

The U*ser agents* adjust the room conditions to the needs of the user; it creates a comfort profile over time, and uses this profile to negotiate set-point adjustments with the Room-agent.

The *Room-agent* controls on basis of the SMART-set-point of figure 3, the set-point is amended by an average 'vote' of the connected User-agents, a simple 2-node room model is used to predict the actual need for heating or cooling. The 2-node

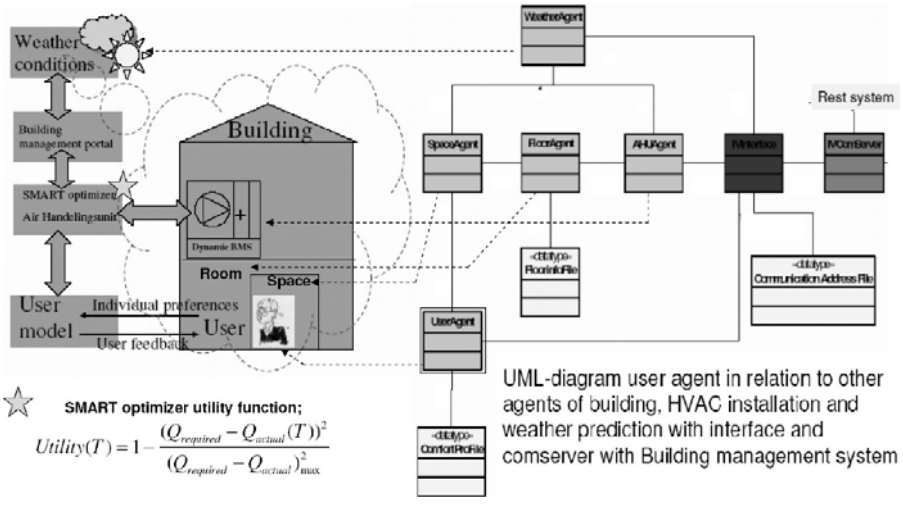

Fig. 5. Conceptual framework SMART with UML-diagram, individual adjustments/energy demands and utility function (Hommelberg 2005)

model uses weather predictions, orientation on the sun and the thermal mass of the building to predict the air- and radiant-temperatures. The prediction is used to negotiate the air-supply temperature of the building.

The optimization is based on user preferred comfort, cost, weather conditions and energy use. All the agents are communicating with other agents, representing rooms or the floors of the building. To cope with the different users and their different needs the system wide information by agents is the basis. Also there are agents representing the information about the weather forecast and the central process control of the air-handlings unit, see figure 5. The Building-agent has to weight the need for cooling/heating to a cost function which incorporates energy and production costs as function of the air-inlet temperature T. A utility function of T as given below represents the required amount of cooling in order to achieve optimal satisfaction of the users.

$$Utility(T) = 1 - \frac{(Q_{required} - Q_{actual}(T))^2}{(Q_{required} - Q_{actual})^2_{\max}}$$

The maximum difference between Cost and Utility is the most cost-effective set-point for the air inlet temperature T. The agent configuration was implemented on top of the existing BA-system and was tested for a period of 3 months, without stability problems. In figure 5 also the representation of the adjustments and the different energy needs of the different occupants are shown.

4 Discussion

The concepts developed in EBOB and SMART-IIGO have shown to be applicable in an actual building configuration. In the field test no stability problems occurred,

although in a multi-agents systems the same problems can occur as in multi-control configurations as shown by Akkermans and Ygge (Akkermans, Ygge 1999). When the agents, operating at Floor, Work-place-level are incorporated in the system, this could possibly lead to stability problems.

The intelligence of each agent can be further enhanced, for example more complex building models for use in the Room-agents gives better predictions, and extended comfort-models in the User-agents can lead to better performance. An increase in the complexity of the system balances better performance against risk of stability problems. In further research each addition to the system will be weighted to performance and robustness of the total system.

As it is yet not possible for an individual building to operate autonomous on the energy market, actual energy savings by load-shifting could not be received. Implementation of the ECN Power matcher technology should enable this. This technology was developed at ECN in the POWERMATCHER-project (CRISP 2002). The PM-technology combines local demand and supply of electricity and efficiently incorporates distributed generation into the network (Kamphuis et al. 2006, Kamphis et al. 2007).

The tuning of the cost/comfort ratio is critical; too much emphasis on costs will lead to underperformance for comfort. In the experiment the IAS was implemented as a top layer on an existing HVAC-control system. When during the design of HVAC and BA are developed with IAS in mind better performance could be achieved.

5 Conclusions

In the EBOB-project the main topic was the interaction between energy use and individual comfort. In the SMART project the agent technology was developed for optimal setting of the comfort parameters. The lessons learned in these projects are further used in the Flexergy project. In this project SMART control of the building is combined with agent technology for a flexible energy purchase on an open market.

Building automation based on Intelligent Software agents are a flexible and promising technology for efficient operation of building and offer good opportunities for energy efficient conditioning of building occupants.

In order to optimize the comfort/energy ratio of each user, further research is needed in the translation of the user needs to the optimal setting of the system. Individual controls at the workplace should be incorporated in the workplace-agent.

Acknowledgements

EBOB was partly funded by EU as projectNNE5/2001. SMART and IIGO were financially supported by SenterNovem. Partners in the following-up project Flexergy are Kropman BV, Technische Universiteit Eindhoven, ECN and Installect.

References

Akkermans, H., Ygge, F.: Journal of Artificial Intelligence Research. 11, 301–333 (1999)

Akkermans, H.: Being Smart In Information Processing. In: Technological And Social Challenges And Oppertunities, Proceedings IFIP IIP 2002 (2002)

Clements-Croome, T.D.J.: What do we mean by intelligent buildings? Automation in Construction 6, 395–400 (1997)

CRISP 2002, Distribute Intelligence in Critical Infrastructures for Sustainable Power, ENK5-LT-2002-00673, Energy Research Center Netherlands(ECN), Petten (2002)

Diane, J., et al.: Smart Environments: Technology, Protocols and Applications. John Wiley & Sons, New Jersey (2004)

EBOB 2004, Final Report, EU project: NNE5/2001/263, Helsinki University of Technology (2004)

Fanger, P.O.: Thermal Comfort. Danish Technical Press, Copenhagen (1970)

Hommelberg, M.: Careful Building, Master thesis, Technical University Eindhoven, Eindhoven (2005)

Isalgue, A., Palme, M., Coch, H., Serra, R.: The importance of users' actions for the sensation of comfort in buildings. In: Proceedings PLEA 2006, Geneva, September 6-8, P I – 393 (2006)

Jelsma, J., et al.: SMART work package, Final Report; Energy Research Center The Netherlands, Petten (2002)

Jelsma, J., Kamphuis, R., Zeiler, W.: Learning about smart systems for comfort management and energy use in office buildings. In: Proceedings ECEEE Summer study (2003) ISBN: 91-631-4001-2

Kamphuis, I.G., et al.: IIGO: Intelligent Internet mediated control in the built Environment: Description of a large-scale experiment in a utility building setting, Energy Research Center, The Netherlands, Petten (2006)

Kamphuis, I.G., Kok, J.K., Warmer, C.J., Hommelberg, M.P.F.: Massive coordination of residential embedded electricity generation and demand power response using Powermatcher approach. In: Proceedings EEDAL 2006 (2006)

Kamphuis, I.G., Warmer, C.J., Hommelberg, M.P.F., Kok, J.K.: Massive coordination of dispersed generation using powermatcher based software agents. In: Proceedings 19th International Conference on Electricity Distribution, Vienna, May 21-24 (2006)

Loftness, V., Hartkopf, V., Gurtekin, B., Hua, Y., Qu, M., Snyder, M., Gu, Y., Yang, X.: Building Investment Decision Support (BIDS^{TM}) —Cost-Benefit Tool to Promote, High Performance Components. In: Flexible Infrastructures & Systems Integration for Sustainable Commercial Buildings and Productive Organizations, AIA Pilot Report on University Research, pp. 12–31 (2005)

Loftness, V., Hartkopf, V., Poh, L.K., Snyder, M., Hua, Y., Gu, Y., Choi, J., Yang, X.: Sustainability and Health are Integral Goals for the Built Environment. In: Proceedings Healthy Buildings 2006, Lisbon, Portugal, June 4-8 (2006)

Oseland, N.A., Fargus, R.K., Brown, D.K., Charnier, A.D., Leaman, A.J.: DUCOZT, A prototype system for democratic user control of zonal temperature in air-conditioned offices. In: CIBSE 1997 Virtual Conference 'Quality for People' (1997)

Palme, M., Isalgue, A., Coch, H., Serra, R.: Robust design: a way to control energy use from human behaviour in architectural spaces. In: Proceedings PLEA 2006, Geneva, September 6-8, P I–311 (2006); Perry M., Raw G.: Power to the workers, Democratic user controls intelligent controls, Building Services Journal (December 1999)

Weiss, G. (ed.): Multi-agent Systems, a Modern Approach to Distributed Artificial Intelligence. MIT Press, Cambridge (1999)

Solar Energy Harvesting for ZigBee Electronics

Xin Lu and Shuang-Hua Yang

Department of Computer Science, Loughborough University, Leicestershire, LE11 3TU, United Kingdom
{X.Lu2,S.H.Yang}@Lboro.ac.uk

Abstract. The use of environmental energy harvesting to increase the autonomy of wireless sensor networks has recently emerged as a viable option to provide energy replacing batteries. This paper systematically analyzed the various design choices and tradeoffs which are involved in the design of solar energy harvesting modules required to design an efficient solar energy harvesting system. A prototype based on three subsystems, is presented to incorporate the results of this analysis. This prototype is then used to produce experimental results, which supports our findings.

1 Introduction

Wireless Sensor Networks (WSNs) have been growing rapidly due to the increased pace of development of Micro-Electro-Mechanical Systems (MEMS) technology together with the reduction in the cost of such components. As a result, we have witnessed the emergence of numerous WSNs platforms and applications. ZigBee technology is an exciting new area of WSNs and belongs to the class of ad-hoc networks, where the individual devices have limited computation, sensing, communication and power. Large scale applications of such networks are being considered to carry out complex tasks without human intervention. However, experience shows that it is still difficult to develop a long-lasting, large-scale, outdoor sensor network using ZigBee technology in real world situations. The largest limiting factor preventing successful development of such networks is the long term supply of power. Normally, batteries provide the dominant energy source for ZigBee systems. However, batteries are not permanent energy source and thus limit the lifetime and utility of any systems. Batteries replacement processes can become very expensive and can even turn out to be impossible for many applications. A promising technology to overcome this limitation is the emerging technology for environmental energy harvesting, which can be used as the power source in WSNs. There are several energy sources in environment that can now feasibly be harvested, such as sunlight, thermal gradient, wind, vibration, and radio frequency energy. Comparing the energy density in an average outdoor setting, the most accessible energy source is solar energy which can be harvested through Photovoltaic (PV) conversion.

In order to design a highly efficiency, simple, and permanent solar energy harvesting system to power WSNs, we initially consider, in this paper, the various characteristics

and tradeoffs of solar cells, energy storage technologies used to satisfy such power supply requirements. We then present the design and implementation of a solar energy harvesting platform for ZigBee electronic which has potential to be extremely long lasting. In order to evaluate the performance of this design, an indoor testing environment has been implemented. The results of this evaluation illustrate how this energy harvesting system can improve the efficiency by comparison with another simpler design.

The rest of the paper is organized as follows. The characteristic of solar cells are introduced in Section 2. Section 3 introduces some successful investigations in this area. Then design principles and implementations of our solar energy harvesting, which includes three subsystems, are described in Section 4. In Section 5, the prototype and another simple design are tested and the experimental results are analyzed. Finally in Section 6 we preset our conclusions.

2 Solar Cell Characteristic

Normally, the output power of a solar cell depends on the incident of light intensity, panel's temperature, and light incidence angle and load resistance. It also has a very specific voltage- current relationship that can be representing as an I-V curve, as depicted in Fig.1 (a). Obviously, the I-V characteristic of a solar cell is highly nonlinear. Likewise on Fig.1 (b) depicts the P-V curve of a solar cell from which it can be observed that the output power of the solar cell is very sensitive to its voltage. Normally, there is unique voltage point where the solar panel will provide the most power for a particular input light intensity. This special operation point is called Maximum Power Point (MPP).

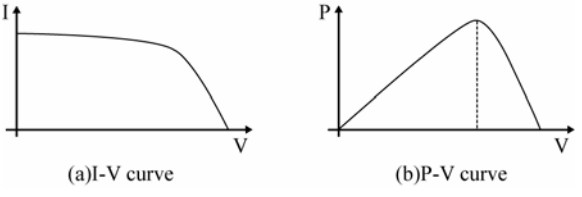

Fig. 1. I-V curve and P-V curve

Various methods of MPP tracking (MPPT) control have been discussed in existing literature [1, 2, 3] such as Perturb and Observe (P&O), maximizing load current or voltage, Fractional Open Circuit voltage (FOC), fuzzy control, neural network, and incremental conductance. Unfortunately, most of these methods were originally developed for relatively large, complex solar system and are not relevant for WSNs because of the low-power and limited computation resources available. One representative method [6] of MPPT for solar power WSNs is the running of a simple MPPT algorithm on the Micro Controller Unit (MCU). But this method will only work well, if the supply condition does not change abruptly. A further drawback of this approach is that MPPT can not work when the MCU is asleep. For these reasons, an autonomous MPPT method [7, 8], which is based on fractional open circuit voltage, is proposed. The fundamental of FOC voltage method is the near linear relationship between the open circuit voltage and the voltage at the MPP.

3 Related Works

Nowadays, more and more solar energy harvesting platforms for WSNs have been proposed. Most of them use rechargeable batteries or supercapacitors, both for energy storage. Here, we categorized the existing works by describing several harvesting system without MPPT and one with MPPT.

Prometheus [5] is autonomous solar energy harvesting system without MPPT. In order to prolong the lifetime of the system, it intelligently manages a two-stage buffer. The working principle is that the solar panel first charges the supercapacitor. When the charge level of the supercapacitor's terminal voltage is higher than a certain value, the capacitor powers the target system only. Otherwise, the system only draws current from the battery. Furthermore, when the capacitor's terminal voltage is higher than another threshold, the capacitor charges the battery and powers the system at the same time. Because Prometheus does not perform MPPT, the harvesting efficiency of this system is not very high.

The Everlast [6] system consists of a MPPT circuit but does not have a two buffers design. It only uses a 100F supercapacitor as energy reservoir. The MPPT can be achieved by measuring periodically open circuit voltage by a temporary disconnection of the solar cell from the circuit. The harvesting efficiency is much higher than that of Helimote and Prometheus. However, the drawbacks of this design are the power from the solar cell is temporarily lost because of the temporary disconnection and MPPT can not work when the MCU is sleep. A further system, based on Everlast, is called Ambimax [7]. It is considered to be the first autonomous energy harvesting system with a MPPT. Ambimax does not only harvest solar energy but also harvest wind energy. Each subsystem charges a separate supercapacitor and then use this stored energy to charge a rechargeable battery. The MPPT principle of Ambimax is based on a linear relationship between the output voltage of a light sensor and the output voltage of the MPP of the solar cell. This eliminates the drawback caused by an always running the algorithm on the MCU. Unfortunately, the power consumption required by the light sensor cannot be neglected. Bologna [8] is another autonomous solar energy harvesting system with MPPT. The MPPT principle is the same as Ambimax, but Bologna uses a miniaturized photovoltaic module instead of a photo sensor. The advantage of this is that the miniaturized photovoltaic module doses not require any additional energy supply. This enables the system to operate when the energy reservoir is empty. This approach has been adopted in our design. However, as the Bologna prototype only uses a supercapacitor as an energy reservoir, the prototype does not provide a long operational lifetime.

4 System Design and Implementation

Our system has adopted some existing works such as the MPPT circuit of Bologna, the two buffers design used in Prometheus, and control charged circuit used in Ambimax. Fig.2 depicts the functional architecture of our solar energy harvesting system which comprises three subsystems: an energy harvesting unit, a maximum power point tracking (MPPT) unit, and the power management unit.

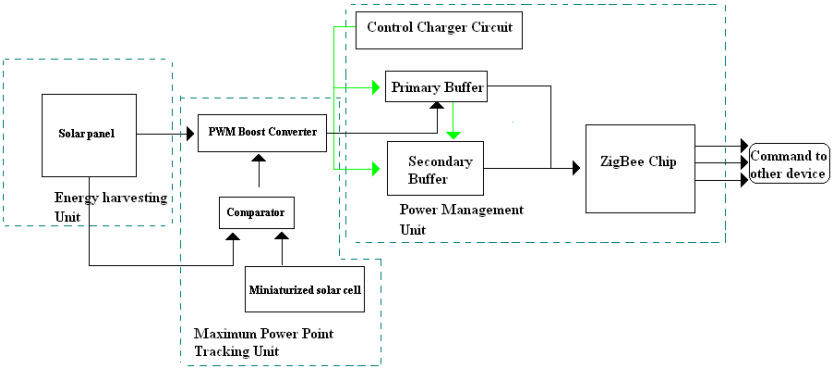

Fig. 2. Function diagram of an energy harvester system

4.1 Energy Harvesting Unit

A solar cell is used to harvest light intensities. Numerous types of solar cells are available for this task. The tradeoffs between prices, dimensions and the efficiency of solar cells were considered and the Centennial Solar CS6161 [9] was chosen as the main solar cell in our design. Because one solar cell is not sufficient to power the whole system, two solar cells, used in parallel, provided the energy harvesting unit.

4.2 Maximum Power Point Tracking Unit

The core part of a solar scavenger is the MPPT unit. The main function of this unit is to deliver the maximum power from the solar cell to the energy reservoirs. The MPPT unit consists of two parts: a Pulse Width Modulation (PWM) DC/DC converter and the MPPT circuit.

4.2.1 Pulse Width Modulation (PWM) DC/DC Converter

Because solar energy varies over time, an energy harvesting interface circuit with high power transfer efficiency needs to be developed to converter the input power conditions into a more constant value. The correct type of DC/DC converter depends on the strength of the power harvested and the operating voltage range of energy storage elements used. The test results from Ambimax showed that the conversion efficiency of LTC3401 [10] is over 85% in the 10-50mA output current range, when its output voltage is set to 4.1V. Therefore we chose this converter as the DC/DC converter in our design. There are two advantages in using this method over direct charging methods, which use a diode to connect to solar panel, in order to charge the reservoir. Firstly, this connection enables energy harvesting to continue even when the open circuit voltage of the solar cell is lower than the voltage of the energy reservoir. Secondly, using a diode to block the reverse current flow from the reservoir to the solar cell causes a 0.7V drop in the output voltage, but if the converter is used, this voltage drop can be avoided.

4.2.2 Maximum Power Point Tracking (MPPT) Circuit

The fundamental principle of our MPPT circuit is based a linear relationship between the open-circuit voltage of the miniaturized PV module and the MPP of the main solar

cell when they exposed to the same light radiation. Therefore a miniaturized PV module with a comparator can be used to perform MPPT. In our design, we have chosen a Hamamatsu S1087 [11] photodiode instead of the pilot cell, which was used in Bologna prototype as a miniaturized PV module functioning as a radiance sensor, providing feedback information to the comparator. The advantage of this design is that no additional power supply for this light sensor.

4.3 Power Management Unit

The main task for the power management unit is to manage the power supply to each part of the system. There are two reasons for the use of a multiple buffers design in our systems. As the light intensity in the environment changes, the generating voltage would vary over time, and consequently it is hard to power the target system directly. Therefore, a high density energy storage element such as rechargeable battery must be employed to accumulate the available energy delivered by the energy generator. On the other hand, the rechargeable battery has limited recharge cycles and lifetime, which limits the lifespan of the whole system. In order to prolong the system's lifespan as long as possible, the target system must be directly powered by the energy harvesting unit most of the time. Thus, two buffers design, used in Prometheus, has been adopted in our system. The primary buffer, which is directly charged by harvesting panels, powers the target system when enough power is available. Otherwise, the target system only draws current from the secondary buffer. Furthermore, if a sufficient light source is available, the primary buffer charges the secondary buffer and powers the target system simultaneously. Then the whole power management unit consists of the primary buffer, the secondary buffer and the control charger circuit.

4.3.1 Two Buffers Design

The primary buffer's purpose is to minimize access to the secondary buffer in order to prolong the energy harvesting system's lifetime. As a result of considering the design limitations, the primary buffer must have capability to handle high levels of energy throughput and frequent charge cycles but does not need to hold energy for a long time. Basically, supercapacitors have much longer lifetime higher efficiency, higher power density, fast and simpler charging circuit than rechargeable batteries. This means that supercapacitors fit all the requirements of the primary buffer.

The secondary buffer is used when the energy at primary buffer is exhausted, and needs to hold energy for a long period of time, have low current leakage, but does not need to charge or discharge frequently. Normally, rechargeable batteries have higher energy density, lower breakdown voltage, and lower leakage current than supercapacitor. For these reasons, rechargeable batteries are the preferred option in the design of the secondary buffer.

4.3.2 Control Charger Circuit

To optimize the harvested power for the whole systems, a control charge circuit is needed. We adopted the same design as Ambimax for the control charge circuit. By comparing the terminal voltage of the supercapacitors and using a configured threshold voltage, the control charge circuit determines which power source, either the primary buffer or the secondary buffer, should power the target system. In order to

enable the charging of the batteries when sufficient energy is available from the supercapacitors, another window comparator is used to compare the voltage of the capacitors and the charging threshold voltage. When the rechargeable batteries are not fully charged and the voltage of the supcapacitor is higher then this charging threshold, the rechargeable batteries are replenished by the capacitors. Furthermore, in order to enhance the lifetime of the rechargeable batteries as long as possible, an overcharge and undercharge protection is required. This is achieved by loading the overcharge and undercharge algorithm into the ZigBee chip.

5 Evaluations

In this section, we investigate the performance of our design in terms of harvesting efficiency and energy consumption caused by an analog control circuit. In order to achiever these goals, three steps were implemented. Initially, the energy harvesting circuit is tested without any power management unit. Then the power management unit is tested to verity the design principle. In addition, the power consumption of this circuit is tested. The final version is where all the units are integrated together and then tested. In order to produce a stable experimental setup, solar cells and the miniaturized PV module were illuminating by a 100W desk lamp with adjustable light intensity. In order to determine how using this artificial light compared to that using outdoor light, the solar cells were placed outside during a normal sunny day in Loughborough where the maximum 120mW could be achieved. For the desk lamp, the maximum light intensity enables the solar cells to produce about 75mW power. Therefore we consider we can use the lamp light emulate sunlight indoors correctly.

5.1 Circuit without Power Management Unit Test

Reasonable comparison, another simple direct connection implementation was also tested in this stage. For the direct connection design, solar panels were directly connected to the capacitor and a diode was used to protect the solar panel from any reverse current flow. A desk lamp placed at distances of 13cm and 20cm was used to illuminate the solar cells. In order to ensure the state of the capacitor at the beginning of each experiment was the same, the capacitor was pre-charged to 1.3V. In addition, as the MPP of a solar cell is very sensitive to its temperature, it was very important to ensure the panel's temperature was the same during the experiment. Therefore, the solar cells were illuminated by the lamp for about 20 minutes to ensure that the temperature of the solar panel has reached a stable state. The experimental results are show in table 1. For our design, the voltage of the capacitor can go as high as 4.6V, which is not limited by the voltage of the solar cell. For the direct connection, we observe that the capacitor's voltage is changed by solar cell's voltage and there is always a voltage gap between them, which is caused by the diode.

In order to compare efficiency, we measured the time for the capacitor's voltage to increase from 1.3V to 3.1V. This is because the charging time provides a simple way to interpret efficiency. Table 2 shows the charging time for each prototype form a fixed-intensity lamp light source at a distance of 20cm.

Table 1. Maximum harvesting energy for different tested circuits

Distance (cm)	Solar cell's voltage	Our design capacitor's voltage	Direct connection capacitor's voltage
13	3.33V	4.6V	2.72V
20	3.73V	4.6V	3.13V

Table 2. Charging time for the different tested circuits

Voltage range (V)	Our design charging time (second)	Direct connection charging time (second)
1.3-2.0	113	87
2.0-2.5	104	113
2.5-3.0	223	516
3.0-3.1	105	864
1.3-3.1	545	1600

For the 1.3V to 2.0V charge cycle experiments, the directly connected method shows a faster charging time than our system. This is as a result of the current limitation due to the DC/DC converter. But for other charging range, our system exhibits faster charging time than that of the direct connection. Over the total charging range, our system is able to charge the capacitor on average 3 times than the directly implementation under identical light intensity.

5.2 Power Management Unit Test

We verified our power management unit by simply connecting the primary buffer to a Direct Current (DC) power supplier. In the first scenario, the power management unit with the ZigBee chip is connected to the DC power supplier. Initially, the ZigBee chip is powered by batteries while the DC power supplier charging the supercapacitors. When the first threshold of 3.4V is met, the power management unit turns to use supercapacitors power the system. When the supercapacitors reach the charging threshold of 4.0V, the comparator switches on the adjustable current limit switch (Max890L [14]) and rapidly transfers the supercapacitors' energy to batteries. Then as we turn off the DC power supplier, the voltage of the supercapacitors drops. When the supercapacitor's voltage drops less than 4.0V, the super capacitor stop charging the batteries. When the supercapacitor's voltages drop less than 3.4V, the batteries start to power the ZigBee chip again. We can observe that all these phenomena correctly fit the design principles. For the overcharge protection and undercharge protection test, the software was loaded into the ZigBee chip. In order to simplify the testing, a supercapacitor was used to replace the batteries. The experimental results showed that the ZigBee chip monitors the supercapacitor voltage correctly and the control signal changes as required. Finally, the current consumed by the power management unit was measured. When we supply 3.0 V to the power management unit, it consumes less than 2mA.

5.3 Integrated System Test

Then we integrated all three subsystems into one and tested it in an actually environment for two days. The experiment results showed that the system works autonomously as expect without any additional power requirement. During the daytime, the system was powered by the supercapacitors most of the time and the supercapacitors charge the batteries when they have sufficient power. During the night, the system switches to use the batteries.

6 Conclusions

In this paper we presented a highly efficient solar energy harvester for ZigBee nodes. Our platform autonomously and simultaneously harvests energy from solar energy source while performing MPPT. In order to demonstrate that the MPPT unit was able to harvest more energy from ambient source, it was compared to another design, using direct connected. Furthermore, a smart power management unit was adopted in our design, to improve energy usage and prolong the lifetime of the system. The experiment results demonstrated that this system worked as predicted. Future work will be focused on designing a PCB board prototype and lowering the power consumption of the whole system.

Acknowledgments

This work was supported by Carbon Connections. Thanks to the contributions made by Fang Yao and GuiZeng Fu in the Networking Sensing and Control ResearchGroup in the department of Computer Science, Loughborough University.

References

[1] Esram, T., Chapman, P.L.: Comparison of Photovoltaic Array Maximum Power point Tracking Techniques. IEEE Transactions on Energy Conversion (2007)
[2] Koutroulis, E., Kalaitzakis, K., Voulgaris, N.C.: Development of a Microcontroller-Based, Photovoltaic Maximum Power Point Tracking Control System. IEEE Transactions on Power Electronics 16(1) (2001)
[3] Jiang, J.-A., Huang, T.-L., Hsiao, Y.-T., et al.: Maximum Power Tracking For Photovoltaic Power Systems. Tamkang Journal of Science and Engineering 8(2), 147–153 (2005)
[4] Raghunathan, V., Kansal, A., Hsu, J., et al.: Design considerations for solar energy harvesting wireless embedded systems. In: Information Processing in Sensor Networks, IPSN 2005, pp. 452–462 (2005)
[5] Jiang, X., Polastre, J., Culler, D.: Perpetual environmentally powered sensor networks. In: Information Processing in Sensor Networks, 2005. IPSN 2005, pp. 463–468 (2005)
[6] Simjee, F., Chou, P.H.: Everlast: Long-life, Supercapacitor-operated wireless sensor Node. In: Low Power Electronics and Design, ISLPED 2006 (2006), doi:10.1109/LPE.2006.4271835

[7] Park, C., Chou, P.H.: AmbiMax: Autonomous Energy Harvesting Platform for Multi-Supply Wireless Sensor Nodes. In: IEEE SECON 2006 Proceeding, pp. 168–177 (2006)
[8] Laurier, S.: Experimental analysis of photovoltaic energy scavengers for sensor nodes. In: Electonics and Information systems. University of Ghent, Belgium (2007)
[9] SC 6161 solar cell, http://www.farnell.com/datasheets/8196.pdf
[10] Linear Technology. LTC3401 1A, 3MHz micropower synchronous boost converter (2001), http://www.linear.com/pc/downloadDocument.do?navId=H0,C1,C1003,C1042,C1031,C1060,P1897,D2673
[11] Hamamatsu technology. S1087 photodiode, 56NM, Ceramic, Max voltage 10V, http://www.farnell.com/datasheets/104399.pdf

Multi-Agent Systems Technology for Composite Decision Making in Complex Systems

Marina V. Sokolova[1,2] and Antonio Fernández-Caballero[1]

[1] University of Castilla-La Mancha, Department of Computing Systems, Campus Universitario s/n, 02071-Albacete, Spain
{marina,caballer}@dsi.uclm.es
[2] Kursk State Technical University, Kursk, ul.50 Let Oktyabrya, 305040, Russia

Abstract. Information technologies have evolved into an essential tool for modeling, assessment and support in any domain requiring decision making. The paper presents an approach towards decision making in complex environmental systems. In the article, the authors review the main characteristics of complex systems and offer their general approach for decision support system creation based on the multi-agent systems paradigm. An example of the general approach applied to composite complex systems is described.

1 Introduction

Nowadays, information technologies (IT) have evolved into an essential tool for modeling, assessment and support in any domain requiring decision making. The complexity and uncertainty of the nature of environmental systems, and the heterogeneity of related information, require a complex approach for their study, based on and consisting of data management, pre-processing, modeling, simulation and, lastly, decision making support.

Sustainable development is a broad concept that spans over and across the social, economical, environmental, medical, demographical and political spheres. That is why the concept "sustainable development", as an abstract and highly complex one, includes components (in agreement with the renewed EU Strategy of Sustainable Development), which deal with climate change, sustainable transport, production and consumption, natural resources management, social issues (demography, migration, etc), and public health. The link between sustainable development and public health is obvious and even does not need to be emphasized. The "health" concept represents a complex system, which includes physical, social, mental, spiritual and biological well-being, spanning across all the spheres of their lives.

Now, the use of the multi-agent systems (MAS) paradigm for the modeling of complex systems has many successful applications, as it allows specialists to gather information quickly and process it in various ways. The final intention is to understand the real nature of the processes, their influence and interconnections, and the possible outcomes in order to make preventive actions and to make correct decisions. It also facilitate taking composite decisions, which is the only possible in case of complex systems. Intelligent methods and techniques used by intelligent entities cover the storing and retrieval of necessary records, storing and retrieval of key factors, examination of real-time data gathered from monitors, analysis of tendencies of environmental processes, retrospective time series, making short and long-term forecasting, and many others [2], [3], [4].

In order to understand the current trends and to assess the ability of current agent-based intelligent decision support research, it seems reasonable to survey the current state of the art and to conclude how it may be possible to optimize it.

2 System Approach for Complex Systems Study

The majority of real-life problems related to sustainable development and environment can be classified as complex composite ones, and, as a result, inhabit some particular characteristics, which require interdisciplinary approaches for their study. A system is an integration of interconnected parts and components (through informational, physical, mechanical, energetic exchange, etc.), which result in emerging of new properties, and interact with the environment as a whole entity. If any part is being extracted from the system, it looses its particular characteristics, and converts into an array of components or assemblies. An effective approach to complex system study has to follow the principles of the system analysis, which are:

1. Description of the system. Identification of its main properties and parameters.
2. Study of interconnections amongst parts of the system, which include informational, physical, dynamical, temporal interactions, as well as the functionality of the parts within the system.
3. Study of the system interactions with the environment, in other words, with other systems, nature, etc.
4. System decomposition and partitioning. Decomposition supposes the extraction of series of system parts, and partitioning suggests the extraction of parallel system parts. These methods can be based on cluster analysis (iterative process of integration of system elements into groups) or content analysis (system division into parts, based on physical partitioning or function analysis).
5. Study of each subsystem or system part, utilizing optimal corresponding tools (multidisciplinary approaches, problem-solving methods, expert advice, knowledge discovery tools, etc.)
6. Integration of the results received from the previous stage, and obtaining a pooled fused knowledge about the system. The synthesis of knowledge and

composition of a whole model of the system can include formal methods for design, multi-criteria methods of optimization, decision-based and hierarchical design, artificial intelligence approaches, case-based reasoning, and others such as hybrid methods [9].

3 Decision Support Systems and Their Characteristics

A decision support system (DSS) is an information system that supports decision-making and system management activities. A properly-designed DSS is an interactive software-based system intended to help decision makers in compiling useful information from raw data, documents, personal knowledge, business models, etc., to identify and solve problems and make decisions. Sprague and Carlson [16] identify three fundamental components of a DSS: (a) the database management system (DBMS), (b) the model-based management system (MBMS), and, (c) the dialog generation and management system (DGMS).

Haag et al. [5] describe these three components in more detail. The Data Management Component stores information (which can be further subdivided into that derived from an organization's traditional data repositories, from external sources, or from the personal insights and experiences of individual users); the Model Management Component handles representations of events, facts, or situations (using various kinds of models, two examples being optimization models and goal-seeking models); and the User Interface Management Component is, of course, the component that allows a user to interact with the system.

Levin [9] analyzes a number of works and names the following components as essential for a modern DSS: (1) models, which include multi-criteria techniques, problem-solving schemes, data processing and knowledge management; (2) analytical and numerical methods of data pre-processing and identification of problems for the preliminary stages of decision making; (3) human-computer interaction and its organization through graphic interface and others; (4) information support, communication with databases, web-services, etc.

According to Power [11], academics and practitioners have discussed building DSS in terms of four major components: (a) the user interface, (b) the database, (c) the modeling and analytical tools, and (d) the DSS architecture and network. The definition of a DSS, based on Levin and Power, in that a DSS is a system to support and improve decision making, represents, in our opinion, an optimal background for practical DSS creation.

4 A Novel Approach towards DSS Creation

4.1 General Requirements and Assumptions for Decision Support Systems

It is obvious that the DSS structure has to satisfy the requirements, imposed by specialists, and characteristics and restrictions of the application domain. In Fig. 1, there is a general work flow for a decision making process, which is

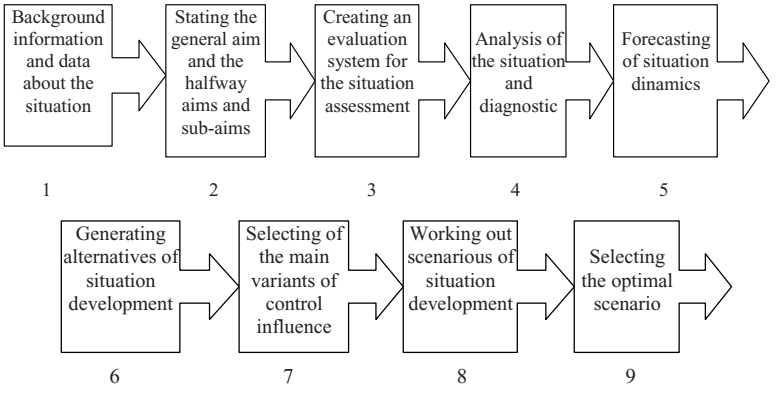

Fig. 1. The standard decision making flow

embodied in a DSS. The traditional "decision making" work flow includes the preparatory period, the development of decisions and, finally, the decision making itself and its realization.

In accordance with Fig. 2, a decision can be seen as an intersection of the spaces of possible decisions and alternatives, and the selection criteria. Complexity increases in the case when all these spaces have a composed organization. In the simplest case, possible alternatives are independent, but they can be grouped into clusters, or form hierarchies; decisions can consist of the best optimal alternative, but can also be formed as a result of a combination (linear, non-linear, parallel, etc.) of alternatives, and their subsets and stratifications; criteria can be both independent or dependent, and, commonly, hierarchically organized (see Fig. 2). Our approach towards DSS for complex system is based on the general DSS structure, discussed in the section 3. The main components of the DSS, which are (a) the user interface, (b) the database, (c) the modeling and analytical tools, and (d) the DSS architecture and network, have been determined for special features and characteristics of possible application domains. The most important difference is that the DSS is realized in form of a multi-agent system, and agents provide system functionality and realize organizational and administrative functions.

A DSS organization in form of a MAS facilitates distributed and concurrent decision making, because the idea of the MAS serves perfectly to deal with the difficulties of a complex system [17]. A MAS, which can be described as a community of intelligent entities - agents -, offers solutions because of the inherent agent properties, which are: reactivity (an agent responds in a timely fashion to changes in the environment); autonomy (an agent exercises control over its own actions); goal-orientation (an agent does not simply act in response to the environment, but intents to achieve its goals); learning (an agent changes its behavior on the basis of its previous experience); reasoning (the ability

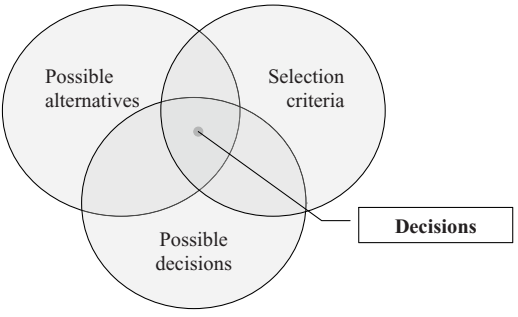

Fig. 2. The composite decision as an intersection of possible alternatives and decisions that satisfy the selection criteria

to analyze and to make decisions); communication (an agent communicates with other agents, including external entities); and, mobility (an agent is able to transport itself from one machine to another) [17], [1], [14].

4.2 Forming Composite Decisions

Composite decision making is hierarchical. It is made by agents of the lower level, then by the agents of superior levels, and is finally corrected, accepted or rejected by a specialist, who interacts with the MAS.

The decision making process needs planning, especially on the previous stages, when the MAS searches for data, retrieves, fuses and pre-processes it. As a rule, these processes can be realized automatically, when they have been planned and described before. And, the agents that execute these procedures are reactive, as the decisions they do are more rigid. Also, a supervising agent is proactive and has liberty in making decisions. The next stage is function approximation and data analysis, and the distribution of "agent rights" is similar: the data mining agents are reactive, they receive tasks from the superior agents and solve them by they means, and, the last ones have to make decisions.

In the scientific research there are several approaches to organize decision making processes (for example, decision tables, decision trees and flows). Some MAS creation tools offer analytical or graphical environments for agent diagrams creation. We have used decision trees, as this is an easily understandable visual method. The general schema of hierarchical decision making is shown on Fig. 3.

These ideas have embodied into planning and creation of an agent-based decision support system that will be discussed in the next section.

4.3 Proposal of the Generalized Agent-Based Decision Support System

We suggest implementing an agent-oriented software system dedicated to environmental situation estimation. The system receives retrospective statistical information in form of direct indicator values - water pollution, solar radiation,

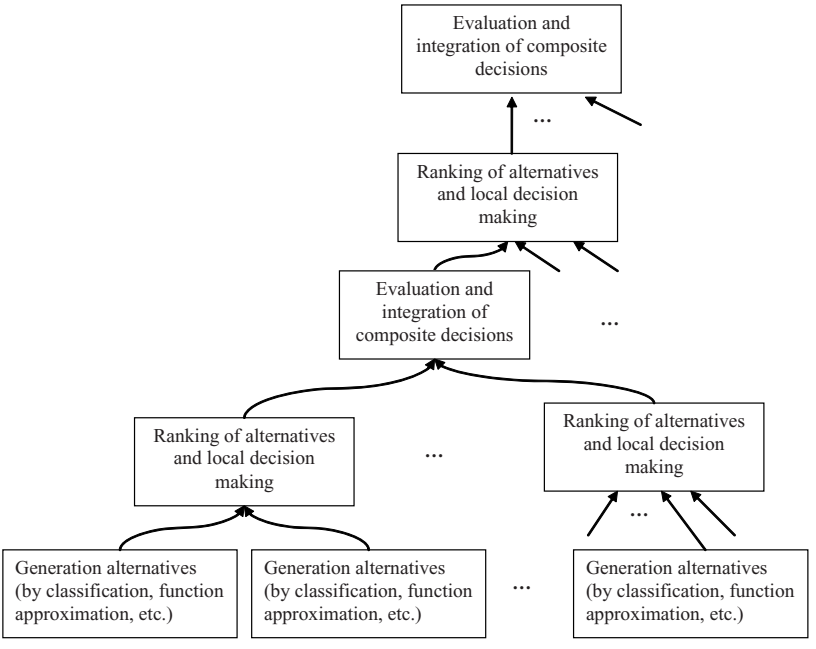

Fig. 3. Hierarchical structure of decision making (adapted from [9])

etc. - and in form of indirect indicator values - types and number of vehicles used, energy used annually and energy conserved, types and quantity of used fuel, etc. [15],[13]. The indirect indicators are utilized in accordance with ISO 14031 "Environmental Performance Evaluation" standard in order to estimate air and soil pollution [7]. The population exposure is registered as number of morbidity cases with respect to International Statistical Classification of Diseases and Related Health Problems, 10th review (ICD-10) [6].

The analysis of the system has resulted in obtaining and describing the system roles and protocols. There, the proposed system is logically and functionally divided into three layers. The first is dedicated to meta-data creation (information fusion), the second is aimed to knowledge discovery (data mining), and the third layer provides real-time generation of alternative scenarios for decision making, as shown in Fig. 4.

We use four agent teams within the system: two are within the first level, and one team on the second and third level each. Each "main" agent plays several roles. During the system work cycle, the agents play with diverse input and output information flows: data transmission protocols, messages, input and output data, etc. These information sources differ by their "life time": they can be permanent and temporary. Some can be used, modified or deleted by agents, and the decisions about others have to be taken by a system user.

The agent-based decision support system (ADSS) design has entirely been modeled following the Prometheus methodology [10], and using the Prometheus

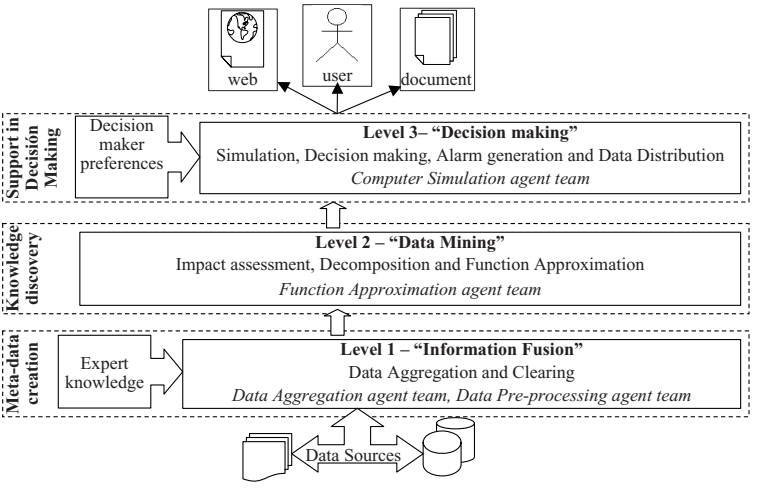

Fig. 4. The general architecture of the decision making system

Design Tool [12]. The tool provides the possibility of checking the consistency of the created system and of generating a skeleton code for JACK Intelligent Agents development tool [8], as well as design reports in HTML.

5 Design of the Environmental Impact Assessment Decision Support System

5.1 The Data Aggregation Agent Team

The Data Aggregation agent (DAA) has a number of subordinate agents under its control; these are the Domain Ontology agent (DOA) and the fusion agents: the Water Data Fusion agent (WFA), the Petroleum Data Fusion agent (PFA), the Mining Data Fusion agent (MFA), the Traffic Pollution Fusion agent (TFA), the Waste Data Fusion agent (WDFA) and the Morbidity Data Fusion agent (MFA).

First, the DAA sends the message *ReadOntology* to the DOA, which reads the OWL-file, which contains information about the ontology of domain, and make it available to the DAA. The DOA terminates its execution, sending the message *OntologyIsBeingRead* to the DAA. Next, the DAA sends the message Start Fusion to the fusion agents, which initiate to execute. When start to execute, each fusion agent searches for the files, which may contain information about the concept of its interest. Each fusion agent works with one or few concepts of the domain ontology, when it change properties (if necessary) of retrieved data and sends it to the DAA, which pools information together. Finally, DAA fills the domain ontology with data, and put data into a standard format. After that, the data files are ready to be preprocessed, and the DAA through the protocol *ReturnDF* says to the DPA, that data is fused and pre-processing can be started.

5.2 The Data Preprocessing Agent Team

The Data Preprocessing agent (DPA) provides data preprocessing and has a number of subordinate agents which specialize in different data clearing techniques: Normalization agent (NA), Correlation agent (CA), Data Smoothing agent (DSA), Gaps and Artifacts Check agent (GAA). They perform all data preprocessing procedures, including outliers and anomalies detection, dealing with missing values, smoothing, normalization, etc.

DPA starts to execute as soon as receives a triggering message from DAA. The main function of the DPA is to coordinate the subordinate agents and decide when they execute and in which order. Starting its execution, DPA sends the *StartDataConsistenceCheck* message, which triggers the GAA, which eliminates artifacts, searches for the double values and fills the gaps. Having finished execution, GAA sends to DPA a message. Then, DPA through the message *StartSmoothing* calls for DSA, which can execute exponential and weighted-average smoothing and terminates sending *SmoothingIsFinished* message to DPA. Then, NA and CA are called for in their turn. The outcomes of the DPA work are: data, ready for further processing and modeling, and additional data sources with correlation and normalization results.

5.3 The Function Approximation Agent Team

The Function Approximation agent (FAA) has a hierarchical team of subordinate agents, which serve to support the roles: "Impact Assessment", "Decomposition" and "Function Approximation". FAA has under its control a number of data mining agents: the Regression agent (RA), the ANN agent (AA), and the GMDH agent (GMDHA), which work in a concurrent mode, reading income information and creating models. Then, if any agent from this group finishes modeling, it calls for the Evaluation agent (EA), which evaluate received models, and return the list of the accepted ones, the others are banned and deleted. The FAA pools the outcome of the agents work, creates the list with the accepted models and then, once RA, AA and GMDHA finished their execution, calls for the Committee Machine agent (CMA), which creates the final models in form of committees for each of the dependent variables, and saves them.

5.4 The Computer Simulation Agent Team

The Computer Simulation agent (CSA) interacts with user and performs a set of task within Computer Simulation, Decision Making and Data Distribution roles. It has the agent team, which includes Forecasting agent (FA), Alarm agent (AmA) and View agent (VA).

The CSA execution cycle starts with asking for user preference, to be more precise, for the information of the disease and pollutants of interest, period of the forecast, and the ranges of their values change. Once the information from user is received, CSA sends a message *SimulateAlternative* to FA, which reasons

and execute one of the plans, which are *Forecasting*, *ModelSimulation*, and *CriterionApplication*. When the alternative is created, CSA sends the *StartAlarmCheck* message to AmA. The AmA compares the simulation and forecast data from the FA with the permitted and alarm levels for the correspondent indicators. If they exceed the levels, AmA generates alarm alerts.

6 Results and Conclusions

To evaluate the impact of environmental parameters upon human health in the Spanish region of Castilla-La Mancha, in general, and in the city of Albacete in particular, we have collected retrospective data since year 1989, using open information resources, offered by the Spanish Institute of Statistics and by the Institute of Statistics of Castilla-La Mancha, as indicators of human health and the influencing factors of environment, which can cause negative effect upon the noted above indicators of human health.

The MAS has a wide range of methods and tools for modeling, including regression, neural networks, GMDH, and hybrid models. The function approximation agent selected the best models, which were: simple regression - 4381 models; multiple regression - 24 models; neural networks - 1329 models; GMDH - 2435 models. The selected models were included into the committee machines. We have forecasted diseases and pollutants values for the period of four years, with a six month step, and visualized their tendencies, which, in common, and in agreement with the created models, are going to overcome the critical levels. Control under the "significant" factors, which cause impact upon health indicators, could lead to decrease of some types of diseases.

As a result, the MAS provides all the necessary steps for standard decision making procedure by using intelligent agents. The levels of the system architecture, logically and functionally connected, have been presented. Real-time interaction with the user provides a range of possibilities in choosing one course of action from among several alternatives, which are generated by the system through guided data mining and computer simulation. The system is aimed to regular usage for adequate and effective management by responsible municipal and state government authorities.

We used as well traditional data mining techniques, as other hybrid and specific methods, with respect to data nature (incomplete data, short data sets, etc.). Combination of different tools enabled us to gain in quality and precision of the reached models, and, hence, in recommendations, which are based on these models. Received dependencies of interconnections and associations between the factors and dependent variables helps to correct recommendations and avoid errors. To conclude with, it is necessary to about our future plans regarding the work. As the work appeared to be very time consuming during the modeling, we are looking forward to both revise and improve the system and deepen our research. Third, we consider making more experiments varying the overall data structure and trying to apply the system to other but similar application fields.

Acknowledgements

This work is supported in part by the Spanish CICYT TIN2007-67586-C02-02 grant and the Junta de Comunidades de Castilla-La Mancha PII2I09-0069-0994 and PEII09-0054-9581 grants.

References

1. Bergenti, F., Gleizes, M.P., Zambonelli, F.: Methodologies and Software Engineering for Agent Systems: The Agent-Oriented Software Engineering Handbook. Springer, Heidelberg (2004)
2. Bradshaw, J.M.: Software Agents. The MIT Press, Cambridge (1997)
3. Foster, D., McGregor, C., El-Masri, S.: A survey of agent-based intelligent decision support systems to support clinical management and research. In: First International Workshop on Multi-Agent Systems for Medicine, Computational Biology, and Bioinformatics, MAS-BIOMED 2005 (2006)
4. Gorodetsky, V., Karsaeyv, O., Samoilov, V.: Multi-agent and data mining technologies for situation assessment in security-related applications. In: Advances in Soft Computing, pp. 411–422. Springer, Heidelberg (2005)
5. Haag, Cummings, McCubbrey, Pinsonneault, Donovan: Management Information Systems for the Information Age. McGraw-Hill Ryerson Limited, New York (2000)
6. International Classification of Diseases (ICD), `http://www.who.int/classifications/icd/en/`
7. ISO 14031:1999. Environmental management - Environmental performance - Guidelines, `http://www.iso.org/`
8. Jack Intelligent Agents, `http://www.agent-software.com/shared/home/`
9. Levin, M.S.: Composite Systems Decisions. Decision Engineering (2006)
10. Padgham, L., Winikoff, M.: Developing Intelligent Agent Systems: A Practical Guide. John Wiley and Sons, Chichester (2004)
11. Power, D.J.: Decision Support Systems: Concepts and Resources for Managers. Westport, Conn., Quorum Books (2002)
12. Prometheus Design Tool (PDT), `http://www.cs.rmit.edu.au/agents/pdt/`
13. Sokolova, M.V., Fernández-Caballero, A.: Agent-based decision making through intelligent knowledge discovery. In: Lovrek, I., Howlett, R.J., Jain, L.C. (eds.) KES 2008, Part III. LNCS (LNAI), vol. 5179, pp. 709–715. Springer, Heidelberg (2008)
14. Sokolova, M.V., Fernández-Caballero, A.: A multi-agent architecture for environmental impact assessment: Information fusion, data mining and decision making. In: 9th International Conference on Enterprise Information Systems, ICEIS 2007, vol. 2, pp. 219–224 (2007)
15. Sokolova, M.V., Fernández-Caballero, A.: An agent-based decision support system for ecological-medical situation analysis. In: Mira, J., Álvarez, J.R. (eds.) IWINAC 2007. LNCS, vol. 4528, pp. 511–520. Springer, Heidelberg (2007)
16. Sprague, R.H., Carlson, E.D.: Building Effective Decision Support Systems. Prentice-Hall, Englewood Cliffs (1982)
17. Weiss, G.: Multiagent Systems: A Modern Approach to Distributed Artificial Intelligence. The MIT Press, Cambridge (2000)

Network-Enabled Intelligent Photovoltaic Arrays

Colin Mallett

Founder and CEO, Trusted Renewables Ltd
名誉ある 再生可能 エネルギー

Abstract. Photovoltaic (PV) solar arrays are currently fairly simple devices. In this paper we consider the architecture of a new family of intelligent PV arrays which are created by embedding a secure processor based on mobile phone technology together with a trusted platform which supports strong authentication. Installations can then become part of an integrated communications network. Being able to remotely manage the installation and 'self certify' information on how much renewable power has been created is likely to introduce new business opportunities. It would also be very difficult to falsify information. Intelligent PV arrays can also provide public communications infrastructure which in turn could allow pervasive ICT platforms to become an integrated part of an environment. Finally we describe how PV arrays could help the development of community shared wireless installations.

1 Introduction

A new generation of intelligent photovoltaic (PV) solar arrays can be created by adding a secure processor to a solar panel [1]. Fig.1 shows the control module which adds the important feature of allowing renewable energy installations to be remotely managed as well as becoming a 'thin client' in an integrated communications network connected to a remote management platform. This allows us to view individual intelligent PV arrays as a secure platform which could be dispersed over a wide area. This could support trusted commercial transactions which in turn lead to new business models associated with renewable energy. These could include sponsored carbon projects which might be compatible with Kyoto Protocol initiatives. Additional spin-offs include the provision of public radio-based communications infrastructure and centrally managed services such as solar-powered lighting.

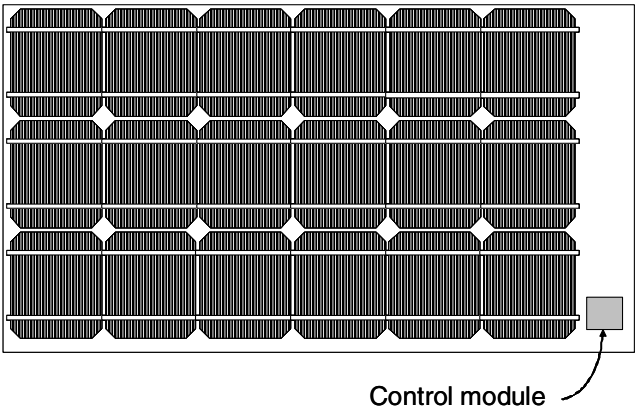

Fig. 1. Intelligent PV array

2 Architecture of Intelligent Array

2.1 Embedded Control Module

Fig. 2 shows the block diagram of the control module in more detail. It contains a digital management controller, processor and a several communications modules linked together with a data bus. This tamper-resistant module is deeply embedded in the panel so that it cannot be removed or altered without being destroyed.

We propose to re-use OEM mobile phone processors and thus benefit from volume component production and year-on-year cost reductions of proven devices. We also

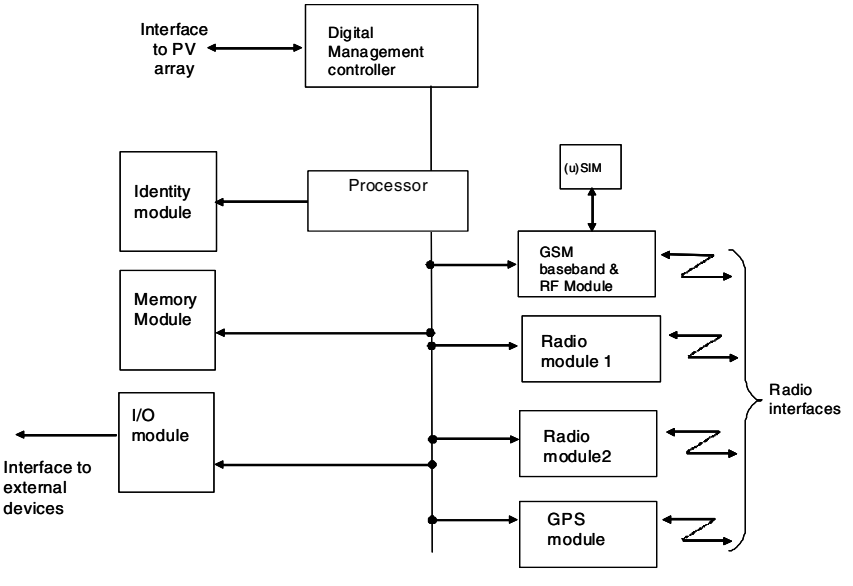

Fig. 2. Block diagram of control module

envisage the use of open source operating systems - such as Ubuntu or Linux, though Symbian and Windows CE might be equally suitable. Software would include a solar array management capability and we consider this as the ideal environment for Java applications development.

2.2 Control Module Functions

The primary function of the control module is to manage power generation from the panel. These are greatly enhanced by the addition of communications capabilities. As a bare minimum we envisage the control module communicating via the power lines themselves but equally we would expect to use radio communications where appropriate, and on the right hand side of Figure 2 are a number of module including GSM, Wi-Fi, WiMAX or other emerging wireless standards.

There is also a global positioning satellite (GPS) radio receiver. The GSM module contains a SIM[1] card which allows a mobile data subscription to be incorporated into the intelligent PV array functionality. Suitable antennae can be integrated with the PV array.

On the left hand side of Figure 2 a module provides interfaces to external, removable flash memory, such as an SD card. This can extend the hard-wired memory associated with the processor and allows the PV array to provide storage of locally gathered or downloaded data. The processor also interfaces to an I/O module which allows external devices to be connected via wired connections such as USB, Ethernet, ADSL or fibre. The intelligent panel can therefore communicate over wired or wireless links to other hardware connected to it. This can include additional PV arrays so that a complete renewable energy installation could be 'communications enabled'.

The I/O module also allows the PV array processor to interface to external transducer modules to measure various external parameters such as ionising and non-ionising radiation, vibration, sound, or in fact anything which might be transmitted and stored by the processor. We envisage being able to achieve a very high level of integration between the control module and the PV array - which results in the intelligent solar cell becoming essentially a single component. This will have significant advantages in terms of reliability and ease of use in the field.

3 Connecting an Intelligent PV Array to a Network

Fig. 3 shows the intelligent PV array connected as a 'thin client' via the Internet to a centralised management platform. Much attention has been focused on developing this kind of architecture for secure transactions and we can benefit from this application to managed renewable energy installations.

We can exploit this trend by viewing each individual intelligent PV array as a secure platform from which to conduct commercial transactions; and later in this paper we shall discuss some new interesting services and applications. This is a potentially scalable architecture so very large numbers of intelligent PV installations anywhere in the world could be managed from a single platform. This platform could be located in a different continent so that large numbers of dispersed intelligent PV arrays can

[1] The term "SIM" is used in common parlance, though it is more correct to use expression (U)SIM to indicate 2G and 3G compatible devices. For clarity we shall refer to it just as a "SIM".

become a single managed entity over a wide area. This leads to new business models associated with renewable energy.

Within a particular installation, panels can be linked together via either fixed or radio networks, in the latter case using licensed or unlicensed spectrum. This flexibility allows different technical and commercial architectures to be used according to circumstances.

One option is to use a cellular data network to connect intelligent PV arrays to the internet. In this case, a panel then becomes the equivalent of a mobile terminal activated by a 'mobile subscription' managed by the SIM card. Mobile operator airtime costs need to be carefully considered, though the data throughput required to manage these panels is low, and a degree of latency can be tolerated.

To further reduce the number of mobile subscriptions to a manageable level, it may be appropriate for just one panel in an installation to be 'mobile enabled'. This one, or perhaps two for redundancy, could then act as a secure communications node for the whole installation, with other panels could be linked together with an appropriate local communications network.

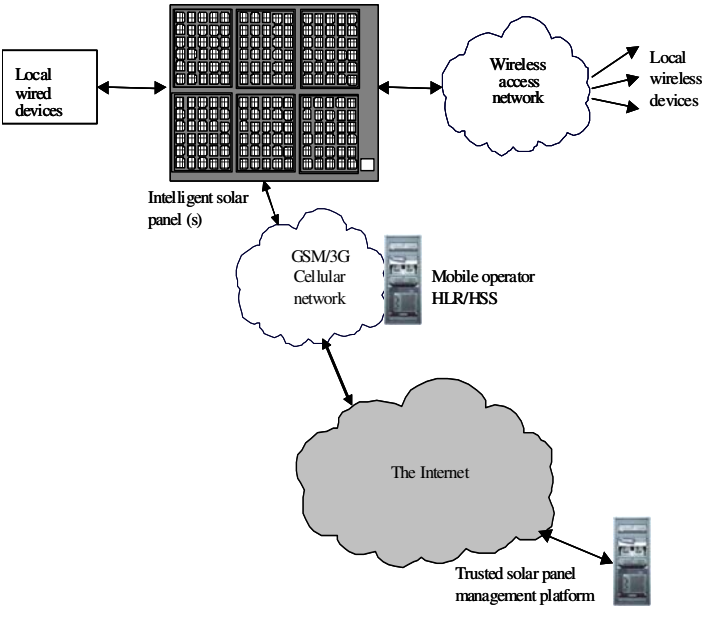

Fig. 3. Intelligent PV array communications

4 Managing Intelligent PV Array Identity and Security

4.1 The Intelligent PV Array as a Trusted Platform

We propose to use a "Trusted Platform Module" (TPM) to turn the intelligent PV array into a trusted platform with an identity module linked to the processing and communications modules as shown in Fig. 2. The TPM is a tamper-resistant silicon chip

which contains a unique identifier, encryption keys and digital certificates according to recommendations by bodies such as the Trusted Computing Group ("TCG"). Members of this group develop and promote open, vendor-neutral, industry standard specifications for trusted computing building blocks and software interfaces across multiple platforms [2].

These are often installed on the motherboard of a personal computer, and in our case the TPM allows an intelligent PV array to authenticate to a network-based host platform and allow secure access to devices, networks and services over an encrypted link. Internally, where the identity module is separate, it is linked to the processor by a dedicated, secure data bus. Intel has announced a programme to develop similar functionality which is fully integrated with the processor. This is called the "Identity-Capable Platform" (ICP) [3] and mobile chip maker ARM has a similar version called the "TrustZone" [4].

The GSM/3G SIM card is also a trusted platform, but this is inserted rather than deeply embedded in the panel and is primarily used to authenticate a mobile data subscription to the mobile operator's Home Location Register (HLR)[2]. This provides optional opportunities for a licensed cellular operator to be involved in the management of intelligent PV arrays using a standard called JSR 177 [5] which permits high speed communication between the SIM card and the digital management processor on the intelligent PV array. Having the TPM and SIM independent provides commercial flexibility in terms of whether the mobile operator is involved in managing an intelligent PV array installation. We think that keeping the two trusted platforms separate provides greatest flexibility.

4.2 Embedded Identity and Security

We envisage that the unique, embedded identity of each panel will be held in the TPM, not the SIM. This trend is happening in many other industries - such as automotive, where unique secure identifiers are often embedded into components to combat counterfeiting. The corresponding identifier used in mobile terminals is called the IMEI (International Mobile Equipment Identity) [6]. Alongside this, mobile networks use a subscriber identifier called the International Mobile Subscriber Identity (IMSI) [7] held in the SIM card. This is in effect a unique user name which is also held on the mobile operator's HLR so the two can be cross-referenced. The IMSI and IMEI can be locked together so that a stolen mobile phone or invalid SIM can be detected.

Intelligent PV arrays can use the same approach. Being relatively high value items, there is a risk, that panels may be stolen. This is particularly true in the less secure locations. However, the built-in GPS receiver can provide a regular encrypted location fix transmitted to the centralised management platform, to be cross-referenced with the value registered during installation. Unauthorised attempts to move the PV array would be detected and stolen or 'moved' intelligent PV could register itself on a 'grey' list and perhaps adopt a different operating mode. This might include disabling its power generation capability.

[2] The 3G version is called the Home Subscriber Subsystem.

5 Exploiting Intelligent PV Arrays

5.1 Sponsored Carbon Communities

There is much work to develop smart metering round the world, and an intelligent PV array could become a flexible building block for some of these solutions. Having a trusted platform deeply embedded in the structure of the intelligent PV array helps solve some of the security problems associated with smart metering. For instance the intelligent PV array can 'self meter' the power generated, and this information could be securely transmitted back to a remote management server. This platform could then aggregate data from installations throughout the world, and using a secure platform would make it very difficult to falsify the reported information.

Smart metering typically describes the metering of electricity, but could equally apply to measurement of gas and water consumption. Using interfaces from associated sensors, an intelligent PV array acting as a trusted smart meter can provide a means of matching power consumption with generation together with information about when energy was consumed. This could allow time of day and seasonal energy consumption price setting linked in with renewable energy generation.

Large scale deployment of intelligent PV arrays would help rollout of the Clean Development Mechanism (CDM) [8] which was established by the Kyoto Protocol. CDMs are projects that reduce emissions in developing countries, which must be validated to ensure that they genuinely provide "additional" carbon reductions that would not otherwise have happened. Renewable energy production clearly falls into this category, and it may be possible for the deployment of intelligent PV arrays in a developing country to be sponsored by an organisation based in Northern Europe. In return for paying for the setup costs, the organisation would receive carbon credits based on the amount of 'green energy' produced in the developing country. The electricity itself could be used locally and the value is not so much in the electricity but the fact that a clear audit trail exists from the location of a particular renewable energy installation to the carbon credits earned.

We do not currently have an opinion about how the cost of the installation would match up to that value of the offset carbon but we feel that managed intelligent PV array installations such as these could lead to new business models associated with CDMs and we feel confident that legislative changes may change the commercial viability of such a solution overnight.

5.2 Solar Powered Lighting and Provision of Secure Public Wireless Infrastructure

Intelligent PV Arrays can be distributed on buildings or landscape features, and a sunny place such as a roof is often also good for radio functions. Thus individual solar panels can also provide public communications infrastructure such as Wireless Cities [9]. This is a powerful combination.

Solar panels can be integrated into buildings as Building Integrated Photovoltaics (BIPV). With added intelligence and communications they can also contribute to the provision of secure public wireless infrastructure. This can be extended from buildings to motorway walls to provide local power for lighting and public services.

Solar-powered street lighting is particularly interesting for countries prone to natural disasters. Reliable local lighting and communications can become very important when local infrastructure is damaged. Lighting fixtures can include earthquake detectors, Tsunami warnings and similar features which can be linked to the I/O module on an intelligent PV array. They could readily send back local weather conditions which include a GPS fix.

There is considerable interest in many countries for the deployment of public wireless infrastructure (hotspots) to provide public services for citizens. In many places, public Wi-Fi services are now seen as a public utility and the first step along the pervasive ICT route. It would seem a very good idea to extend wireless cities with intelligent PV arrays, particularly as the built-in security and tamperproof nature would support secure communications. An interesting example of the software becoming available is shown by a Symbian application called JoikuSpot [10] for a Nokia Smartphone. This is free downloadable mobile software solution turns a mobile phone into a WLAN HotSpot. Clearly it is only a matter of time before this kind of application becomes widely available.

5.3 Solar Powered Pervasive Communications

Pervasive computing and communications [11] is where information and communication technology is 'everywhere,' for 'everyone', 'at all times', and is seen to be how the next generation of computing environment will emerge. By their nature, PV arrays will be placed in open positions so this kind of public infrastructure can be created at the same time as a managed solar power generation capability. Pervasive ICT platforms will become an integrated part of an environment, with buildings, walls, lampposts, and other street furniture containing integrated processors, and sensors, - all connected via distributed high-speed networks. Many of these will be in the form of ad-hoc mesh networks. An intelligent PV array as a general purpose secure radio platform shows great potential to become a key component in this evolution.

5.4 New Business Models for Community Shared Wireless

The biggest challenge is to create a business case for the additional wireless infrastructure costs, which will be more convincing if it comes from reduced operation costs rather than additional revenues which may not emerge. Fortunately there are some emerging business models and commercial architectures that might help. One of these is a system of community shared wireless networks called "FON", created by Martin Varsavsky in 2005 [12]. FON's members ("*Foneros*") agree to share their private Wi-Fi in return for free access to all other community Wi-Fi access points round the world. Routers have been designed to provide a separate channel to share with fellow *Foneros* and non-members ("*Aliens*"). There is a simple business model to receive income from the provision of a public Wi-Fi hot spot – for example in a restaurant or bar.

There may be potential to combine this business model development with the concept of intelligent PV arrays, configured to allow a user or an enterprise to benefit from becoming some form of *Fonero.* This might prove particularly attractive to enterprises that choose to deploy intelligent PV arrays as part of a BIPV installation, as

it is very likely that such a building would have an optical fibre feed to the main communications network. This could allow FON users to benefit from potentially vast data rates from PV hot spots attached to adjacent buildings in range.

We envisage that the processor used in an intelligent PV array would be able to support all the intelligence required for the router security and firewalls needed in this kind of solution.

6 Conclusions

In this paper we have outlined a new generation of intelligent PV solar arrays created by adding secure processors based on mobile phone technology. The addition of a trusted platform transforms a PV array into an intelligent communications node which can be linked to the Internet and then be centrally managed.

Because a GPS module is included, a unit can be 'locked' to a specific location recorded in a central database, and form part of an integrated communications network which is able to 'self certify' renewable power information. We consider this is a very powerful combination which can also support new business models. As an important spin-off, intelligent PV arrays can also provide public communications infrastructure, perhaps as part of a managed BIPV installation. This in turn could allow pervasive ICT platforms to become an integrated part of an environment, for example as a 'wireless city'. Furthermore, by combining intelligent PV arrays with emerging business models such as *FON* may give rise to some interesting future developments.

Acknowledgments

Thanks are due to Keith Beacham and Kevin Bosworth, colleagues in Trusted Renewables Ltd, as well as Dr Piotr Cofta, Chief Researcher in BT Innovate, and Dr Toshio Nomura of the Sharp Laboratories of Europe.

References

[1] UK Patent application number 0900082.9 filed 06 (January 2009)
[2] The Trusted Computing Group home page, `https://www.trustedcomputinggroup.org/home` (accessed February 24, 2009)
[3] A description of the ICP can be found, `http://www.intel.com/technology/techresearch/research_day/2007/demos.htm` (accessed February 24, 2009)
[4] A description of the ARM TrustZone technology can be found, `http://www.arm.com/products/security/trustzone/` (accessed February 24, 2009)
[5] The Security and Trust Services (SATSA) API for J2ME JSR 177 is described, `http://java.sun.com/products/satsa/` (accessed February 24, 2009)
[6] The IMEI is described, `http://www.gsm-security.net/faq/imei-international-mobile-equipment-identity-gsm.shtml` (accessed February 24, 2009)

[7] The IMSI is described, http://www.gsm-security.net/faq/imsi-international-mobile-subscriber-identity-number-gsm.shtml (accessed February 24, 2009)
[8] The Clean Development Mechanism (CDM) home page, http://cdm.unfccc.int/index.html (accessed February 24, 2009)
[9] An EU funded Wireless Cities project home page can be found, http://www.wirelesscities.org/index.php (accessed February 24, 2009)
[10] Description of JoikuSpot software, http://www.joikuspot.com/home.php (accessed February 24, 2009)
[11] IEEE computer society home page, http://www.computer.org/pervasive (accessed February 24, 2009)
[12] The FON home page can be found, http://www.fon.com/en (accessed February 24, 2009)

Design Ontology for Comfort Systems and Energy Infrastructures: Flexergy

Wim Zeiler[1,2], Rinus van Houten[1], Gert Boxem[1], Perica Savanovic[1], Joep van der Velden[2], Willem Wortel[2], Jan-Fokko Haan[2], Rene Kamphuis[3], and Henk Broekhuizen[4]

[1] Technische Universiteit Eindhoven, Netherlands
w.zeiler@bwk.tue.nl
[2] Kropman Building services, Nijmegen, Netherlands
[3] Energy research Centre Netherlands, Petten, Netherlands
[4] Installect, Nijkerk, Netherlands

Abstract. At present the main focus of research in Building Services is on reduction of energy consumption of buildings through high insulation and the application of high efficient equipment. In future however it will be no longer sufficient to look only at the building itself: the occupant and the energy infrastructure need also be considered too. Building, user and energy infrastructure together are linked strongly with a dominating position for the user. The strong focus on the energy reduction led to situations in which health and comfort are endangered. "Connecting" the end-user and/or the external energy sources to a climate process control system of a building is complex.

Design tools for energy installations are only available on the level of individual installations. There is a need for an Integral Design approach which describes at the conceptual level the design process as a chain of activities, which starts with an abstract problem and which results in a solution. The paper discusses an integral approach combined with that of Open Building to reach a flexible integration of end-user, building and energy infrastructure.

Keywords: design methodology, morphological overview, Flexergy.

1 Introduction

In Europe comfort in buildings needs 40% of the total energy. Global warming, caused largely by CO2 emissions as a result of energy consumption, shows an increasing effect. Climate change is becoming a major problem. As results of Global Warming (Alley 2007) become more and more prominent, it is necessary to look for new possibilities to save energy and to generate sustainable energy to be used for comfort in the built environment. Preservation of energy resources, occupant comfort and environmental impact limitation are the key issues of modern and sustainable architecture. A major portion of primary energy consumption, about 40 %, is due to create thermal comfort in buildings by heating, cooling, ventilating and lighting.

In office buildings most of the energy is needed for thermal comfort especially cooling. Present energy efficient technology is not sufficient to further reduce the energy use of buildings. New comfort control technology, such as individual control, offers new possibilities to further reduce energy consumption of office buildings. Dynamic online steering of individual comfort management and building management could save up to 20% of current energy consumption. Misunderstandings and wrong conceptions about indoor comfort and energy use are common. Most office users are not even aware of the fact that they can affect the energy use. The behavior of building occupants needs to be taken into account as it is responsible for almost half the outcome of planned energy reduction (Claeson-Jonsson 2005). When the comfort control system is not working adequately, a lot of energy is wasted by too much heating or cooling. As a result of this overshoot indoor temperature is the most common issue in occupants' complaints about thermal comfort.

As until now the user has not been part of the building comfort system control strategy in offices, the energy consequences of the user behaviour are not accounted for. New technological development is needed to incorporate the behaviour of occupants of buildings. We did some development in this field. The first experiment was part of the European EBOB-project (Energy efficient Behaviour in Office Buildings). In EBOB so called Forgiving Technology was developed, with this technology each user in the building was given control of his or her personal comfort (Claeson-Jonsson 2005). The goal of the project was, by giving the user a choice in combination with feedback on the energy consumption/cost efficient operation was enhanced. In the SMART/IIGO project the agent technology was developed for quick interaction between the user and the changes in his environment. SMART stands for Smart Multi Agent Technology (Jelsma et al. 2002) and IIGO (Kamphuis et al.2005) is a Dutch acronym for Intelligent Internet mediated control in the built Environment. The in SMART developed technology was tested in an extended field test in the IIGO-project. The lessons learned in these projects are used in the Flexergy project. In this project SMART control of the building is combined with agent technology for energy purchase on an open market. This technology was developed by ECN in the POWERMATCHER-project (PM). The PM-technology combines local demand and supply of electricity and efficiently incorporates distributed generation into the network (CRISP 2002, Kok et al. 2008). One of the most important lessons learned from these projects is the dominating influence of the occupant on the outcome of energy efficiency and comfort. The energy supply on a system level should be dominated by trends in demands by the occupants of the buildings (Fig.1).

Such novel control systems should not only improve the energy performance of the building, but should also offer benefits to users (i.e. building operators as well as workers). Comfort management should be linked with improving energy efficiency. Individual comfort management makes it possible to optimize comfort, energy efficiency and costs. This combination would be beneficial for building operators as well as occupants. Therefore in commercial buildings, the inclusion of options for individual comfort management is an important feature to make such systems attractive to end users.

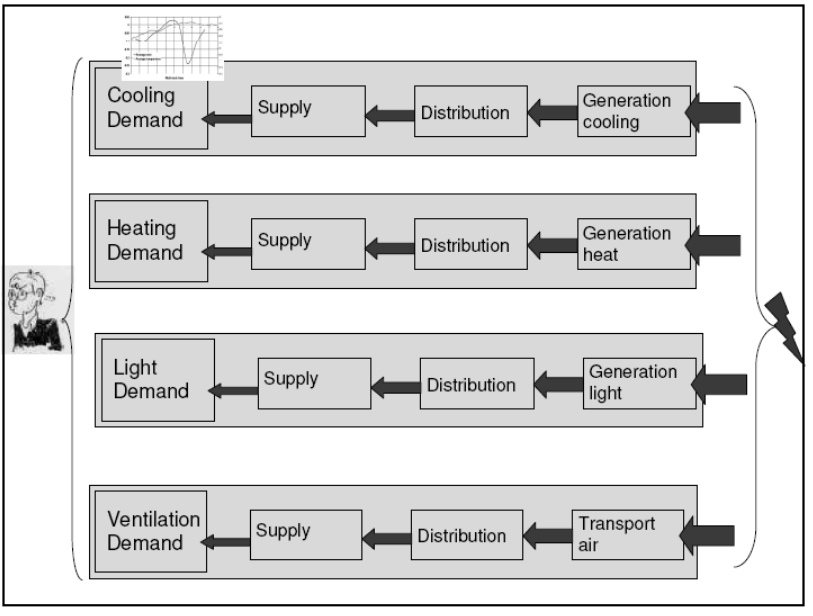

Fig. 1. Human demands and needs: temperature, light and air

2 Methodology

One of the major problems in modeling design knowledge is in finding an appropriate set of concepts to refer to the knowledge, or -in more fashionable terms- finding an ontology. In the knowledge engineering community, ontology is viewed as a shared conceptualization of a domain which is commonly agreed by all parties. It is defined as 'a specification of a conceptualization' (Gruber 1993). 'Ontology' in philosophy means theory of existence in the broadest sense. It tries to explain what is being and how the world is configured by introducing a system of critical categories to account things and their intrinsic relations (Kitamura 2006). Ontology aims to capture the conceptual structures in a domain by describing facts assumed to be always true by the community of users. Ontology is the agreed understanding of the 'being' of knowledge: consensus regarding the interpretation of the concepts and the conceptual understanding of a domain (Dillon et al. 2008). Currently the design of building environment and the necessary energy infrastructure are done by totally different and separated groups of designers. Therefore there is no shared perception (i.e. an ontology) of the design activities which designers perform in the design process of an energy infrastructure on the different levels of scale within the building environment.

Without the shared perception it would not be possible to develop adequate design methodology or approaches for design support that are systematic, consistent, reusable and interoperable.

We looked at ontology's in the built environment for integrating the users. Ontology's are formal conceptualizations not made l'art pour l'art, but to help to achieve a

goal or to perform a task by an actor. In this case, the task involves knowledge-intensive reasoning to understand the world not just static, but to serve practical purposes of action by the actor in his world (Akkermans 2008): a model to support the process at hand.

2.1 Open Building Principle

Open building developed by N.J. Habraken (Habraken 1961) attempted to integrate industrial building and user participation in housing, but Habraken's concept can also be used for office buildings. It approached the built environment as a constantly changing product caused by human activity, with the central features of the environment resulting from decisions made at various levels. During the design process participants and their decisions were structured at several levels of decision-making; the infill-level, the support-level and tissue-level. On each level, there has to be made a balance between the performances of supply and demand for buildings during the life-cycle. The levels of city structure, urban tissue, support, space and infill were usually distinguished. The "thinking in levels" approach of Open Building was introduced to improve the design and decision process by structuring them at different levels of abstraction.

To apply the principles of Open Building design to the optimization of the energy infrastructure of a building and the surrounding built environment, a methodology was developed by us to support the design process of building and its energy infrastructure.

2.2 Design Methodology

To develop our required model of design support, an existing model from the mechanical engineering domain was extended: Methodical Design. This design model by van den Kroonenberg, it was based on the combination of the German (Kesselring, Hansen, Roth, Rodenacker , Pahl and Beitz) and the Anglo-American design schools (Asimov, Matousek, Krick) (Blessing 1994). This design model was chosen as a basis because; " it is one of the few models that explicitly distinguishes between stages and activities, and the the only model that emphasis the recurrent execution of the process on every level of complexity (Blessing 1993, p.1398)".

The Integral Design process can be described at the conceptual level as a chain of activities which starts with an abstract problem and which results in a solution. A characteristic feature of Integral Design, is the occurrence of a four-step pattern of activities, see figure 2.

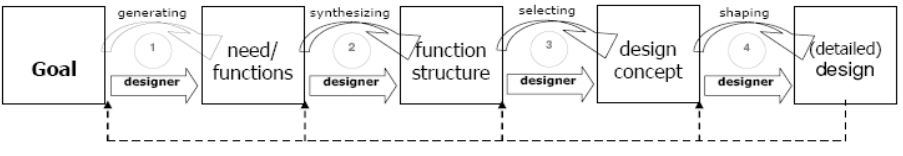

Fig. 2. The four-step pattern of Integral Design

In order to survey solutions, engineers classify them according to various features. This classification provides the means for decomposing complex design tasks into problems of manageable size. Decomposition is based on building component functions. This functional decomposition is carried out hierarchically so that the structure is partitioned into sets of functional subsystems. Decomposition is carried out until simple building components remain whose design is a relatively easy task. This like the decomposition which is described in the guidelines 2221 and 2222 of the "Association of German Engineers", VDI (Pahl et al.2006). It is possible to compare this highly abstract approach with the hierarchical abstraction of Open Building which is more commonly known in the building industry, see figure 3.

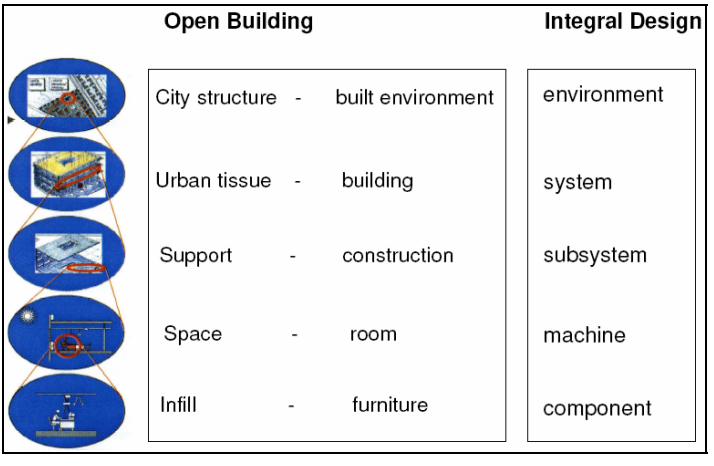

Fig. 3. Comparison Open Building and Integral Design approach

2.3 Morphological Overviews

For the synthesize activities of the Integral Design process morphological overviews can be used to generate alternatives in a very transparent and systematic way. General Morphological analysis was developed by Fritz Zwicky (Zwicky&Wilson 1967) as a method for investigating the totality of relationships contained in multi-dimensional, usually non-quantifiable problem complexes (Ritchey 2002). The Morphological overview is a key methodology that can improve the effectiveness of the concept generation phase of the design process (Weber and Condoor 1998). It is this aspect which we focus on in our research.

Based on definition of functions, morphological overviews make it possible to assess client's needs on higher abstraction levels than what a program of requirements (which is often too detailed) provides. The morphological approach has several advantages over less structured methods. We think it may help to discover new configurations, which thus far may not be so evident and could have been overlooked. The morphological chart gives a complete overview of aspect elements or sub-solutions that can be combined together to form a solution. The purpose of the vertical list is to try to establish those essential aspects and functions that must be incorporated in the

product, or that the design has to fulfil. These are often expressed in rather abstract terms of product requirements or functions. Also the morphological approach is an excellent way to record information about the solutions for the relevant functions and aspects. It aids in the cognitive process of generating the system-level design solutions (Weber and Condoor 1998). The morphological approach has several advantages over less structured methods, it may help to discover new configurations, which may not be so evident and could have been overlooked. It also has definite advantages for scientific communication and for group work (Ritchey 2002). We think like Ritchey (2002) that the morphological approach has definite advantages for communication and for group work.

2.4 Technology Layers

Design takes place in an environment that influences the process and as such it is contextually situated (Drost & Hendriks 2000, de Vries 1994). The context of a model of design is composed of a “world view”. Our model consists of 4 worlds (the real world, the symbolic world , the conceptual world and the specification world). These worlds are coupled to specific abstraction levels. The contents of the different abstraction levels are based on the technical vocabularies in use, technology-based layers (Alberts 1993):

1. Information Level: knowledge-oriented, representing the "conceptual world".

This level deals with the experts’ knowledge of the systems. One of the essential ideas behind this is that human intelligence has the capacity to search and to redirect search. This information processing capacity is based on prior design knowledge.

2. Process Level: process oriented, representing the "symbolic world".

This level deals with physical variables, parameters and processes. The set of processes collectively determines the functionality of the variables that represent the properties of a device. Modelling at the functional level involves the derivation of an abstract description of a product purely in terms of its functionality. This abstraction reduces the complexity of engineering design to the specification of the product’s desired functionality.

3. Component Level: device orientation, representing the "real world".

This level describes the hierarchical decomposition of the model in terms of functional components and is domain dependent. Generic components represent behaviors that are known to be physically realizable. They are generic in the sense that each component stands for a range of alternative realizations. This also implies that the generic components have yet to be given their actual shape.

4. Part Level; parametric orientation, representing the” specification world".

This level describes the actual shape and specific parameters of the parts in the form of which the components exist. Relevant technical or physical limitations manifest themselves in the values of a specific set of parameters belonging to the generic components. These parameters are used to get a rough impression, at the current level of abstraction, of the consequences of certain design choices for the final result.

The technology-based layers can be combined with the abstraction levels from the Integral Design methodology. The method/contents matrix, represents the recursion of the design steps of a design process from high abstraction level to lower abstraction

levels and is now combined with the principles of Open Building and the technology-based layers of building services, see fig.4, which shows the relation between the technology layers of building represented in relation to the conceptual world view model.

3 Results

Functions have a very significant role in the design process. Generally, designers think in functions before they are concerned with details. During the design process, and depending on the focus of the designer, functions exist at the different levels of abstraction. An important decomposition is based on functions. Function-oriented strategy, preferred by experienced designers (Fricke 1993), allows various design complexity levels to be separately discussed and, subsequently, generated (sub)solutions to be transparently presented. The function-oriented strategy allows various design complexity levels to be separately discussed and, subsequently, generated (sub) solutions to be transparently presented. This way the interaction with the other participants of the design process is aided, and at the same time design process information exchange is structured, see fig. 4. Combining the concept of morphological overviews with hierarchical functional abstraction levels leads to a structure of different sets of morphological overviews for cooling, heating, lighting, power supply and ventilation.

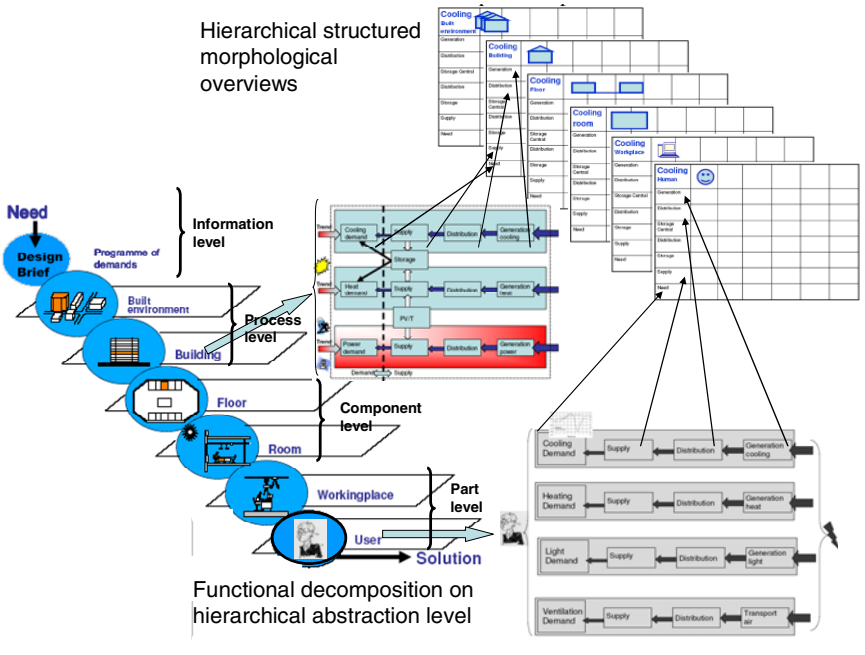

Fig. 4. Set of connected morphological overviews about cooling on the different hierarchical abstraction and the infill on the built environment level

In fig. 4 an example of the different abstraction level morphological overviews are presented. In these overviews the alternative solutions for generation, central distribution, central storage, local distribution, local storage and supply are presented to fulfill the need on the specific abstraction level of built environment, building, floor, room, workplace and person. The overviews are used to generate new possibilities for a flexible energy infrastructure in and between buildings to optimize the combination of decentralized power generation, use of sustainable energy source on building level and traditional centralized energy supply.

The overviews are used to generate new possibilities for a flexible energy infrastructure in and between buildings to optimize the combination of decentralized power generation, use of sustainable energy source on building level and traditional centralized energy supply. The energy flows of heat, cold and electricity have to be optimized together. For this a new design and control strategy based on Integral design and the use of agent technology is developed. The work on these subjects within the project will continue till 2010.

4 Conclusion

Taking the principles of Integral Design and Open Building as starting point, a new design approach is defined for the energy infrastructure within and between buildings. Central in this approach is the abstract representation the building design process which makes it possible to generate new solutions for a sustainable energy infrastructure. In order to allow a stepwise approach in which each design decision has well defined implications, four different ontological levels are distinguished for designing energetic process: Information level, Process level, Component level and Part level. These levels provide a structured framework for morphological charts to give an overview of the possibilities and to support the design process. The possibility to combine and exchange different energy flows within the building and between buildings results in a flexible energy infrastructure called Flexergy.

The participants of the Flexergy project work on new energy infrastructural concepts to use and combine energy flows on the level of building and built environment. Central in this approach is the abstract representation the building design process which makes it possible to generate new solutions for a sustainable energy infrastructure.

Acknowledgement

Kropman bv and the foundation “Stichting Promotie Installatietechniek (PIT)” support the research. Flexergy project is financial supported by SenterNovem, project partners are Technische Universiteit Eindhoven, ECN and Installect.

References

Akkermans, H.: The Business of Ontology calls for a Formal Pragmtics. Invited talk 3rd workshop on Formal Ontologies Meet Industry, FOMI 2008, Torino, Italy, June 5-6 (2008), http://e3value.few.vu.nl/docs/bibtex/pdf/HansA2008.pdf

Alberts, L.K.: YMIR: An Ontology for Engineering Design, PhD-thesis, University of Twente, Enschede (1993)

Alley, R., et al.: Climate Change 2007: The Physical Science Basis Summery for Policymakers, Intergovernmental Panel on Climate Change, Paris, France (2007)

Beitz, W.: Systematic Approach to the Design of technical systems and products, VDI 2221 0 Entwürf, VDI, Düsseldorf (1985)

Blessing, L.T.M.: A process-based approach to computer supported engineering design. In: Proceedings International Conference on Engineering design, ICED 1993, The Hague, August 17-19 (1993)

Blessing, L.T.M.: A process-based approach to computer supported engineering design. PhD thesis Universiteit Twente (1994)

Claeson-Jonsson, C.: Final publishable report, Energy Efficient Behaviour in Office Buildings (2005)

Dillon, T., Chang, E., Hadzic, M., Wongthongham, P.: Proceedings Fifth Asia-Pacific Conference on Conceptual Modelling, APCCM 2008, Wollongong, NSW, Australia (January 2008)

Drost, K., Hendriks, D.: The Role of the Design Context: In Practice and in the design Methodology. In: Proceedings 5th International Design thinking research Symposium "Designing in Contect" DTRS 2000, Delft, December 18-20 (2000)

Fricke, G.: Kostruieren als flexiber Problemlöseprozes – Empirische Untersuchung über erfolgreiche Strategien und methodische Vorgehensweisen. VDI-Verlag, Düsseldorf (1993)

Geller, J., Perl, Y., Lee, J.: Ontology Challenges: A Thumbnail Historical perspective. Editorial, Knowledge and Information Systems 6, 375–379 (2004)

Gruber, T.R.: A translation approach to portable ontologies. Knowledge Acquisition 5(2), 199–220 (1993)

Habraken, N.J.: De dragers en de mensen, Haarlem (1961) (in Dutch)

Jelsma, J., Kets, A., Kamphuis, I.G., Wortel, W.: SMART work package, final report; SMART field test: experience of users and technical aspects, research report ECN-C—02-094, ECN, Petten (2002)

Kamphuis, I.G., Warmer, C.J., Jong, M.J.M., Wortel, W.: IIGO: Intelligent Internet mediated control in the built environment: Description of a large-scale experiment in a utility building setting, ECN rapport ECN-C—05-084 (October 2005)

Kitamura, Y.: Roles of ontologies of engineering artifacts for design knowledge modeling. In: Proc. of the 5th International Seminar and Workshop Engineering design in Integrated product Development (EDIProD 2006), Gronów, Poland, September 21-23, pp. 59–69 (2006)

Kok, K., Derzi, Z., Gordijn, J., Hommelberg, M., Warmer, C., Kamphuis, R., Akkermans, H.: Agent-based Electricity Balancing with Distibuted Energy Resources, A Multiperspective case Study. In: Proceedings of the 41st Hawaii International Conference on System Sciences (2008)

Pahl, G., Beitz, W., Feldhuzen, J., Grote, K.H.: Translators. In: Wallace, K., Blessing, L. (eds.) Engineering Design, A systematic Approach, Third edn. Springer, Heidelberg (2006)

Ritchey, T.: General Morphological Analysis, A general method for non-quantified modeling. In: 16th EURO Conference on Operational Analysis, Brussels 1998 (2002)

de Vries, T.J.A.: Conceptual design of controlled electro-mechanical systems, a modeling perspective, PhD thesis Twente university, Enschede (1994) ISBN:90-9006876-7

Zwicky, F., Wilson, A.G. (eds.): New Methods of Thought and Procedure. Contributions to the Symposium on Methodologies, Pasadena, May 22-24, Springer, Heidelberg (1967)

An Innovative Building-Integrated Solar-Air Collector: Presentation and First Results

Jean Louis Canaletti, Gilles Notton, and Christian Cristofari

Laboratory "Physical Sciences for Environment" - Science Centre of Vignola
University of Corsica Pascal Paoli– UMR CNRS 6134- Route des Sanguinaires - F-20000 Ajaccio – France

Abstract. We present a new solar air collector totally integrated into a shutter. The air is moved by a fan supplied with electricity by a PV module inserted into the shutter. The produced hot air is injected in the house to heat it and to maintain a healthy air. This solar air shutter is reversible and can run in all positions. After a brief presentation of the building energy situation in France, the new concept of the solar air heater is described; then, the experiment and the collected data are shown. Finally, the first performance results are presented and discussed.

1 Introduction

There's no doubt that the fossil energy resources of our Earth have been depleting and that the strong economical development of the developing countries as China or India will increase the resources drop. On the other hand, it appears that the massive utilization of fossil fuels (and nuclear ones) threatens our Environment. The part of the used energy for building is very important and hasn't stopped increasing; to limit or to reduce this building energy consumption, it is necessary to develop some actions aiming at the rational energy management in parallel with the utilization of renewable energy sources. The reduction of the energy consumption in one's abode must not be achieved to the prejudice of the life quality nor to the health of its occupiers.

We present a new patented concept of solar air heater totally integrated in a shutter reducing the aesthetic impact and able to produce hot air from sun radiations with a total autonomy and to introduce it inside the house. It allows conserving the integrity of the architecture of the house.

2 French Building Energy Situation

The energy consumption rapid increase of the building sector is observed in many countries around the world. In France, 30 million houses use about 50% of the final energy and produce 25% of green house gases (second sector). For Europe, 500 million inhabitants in 60 million housings also consume half the energy.

The residential and tertiary sector is the first energy consumer in France (Fig. 1) with 70.6 MTOE in 2007 (French Ministry of ecology 2007) i.e. 43.59 % of the total final energy. The part of the residential and tertiary sector remains stable (around 42-43%) but in absolute value, the energy consumed in this sector increases. From 1973 to 2005, the residential-tertiary sector increased by 25% but there is a decrease of the energy consumption per square meter from 372 to 245 kWh/m².

In France, on 29.7 million housings, there are 24.5 million principal residences, 3.1 million secondary ones and 2.1 million empty houses. The first class represents about 2.1 billions of m² against 814 millions for the tertiary sector. The low turnover (1% per year) associated with the actual rate of rehabilitation induces that the total building park built before 1975 will be upgraded in one century. The part of the housings built before 1975 reached 64 % and we can consider that 50% have been thermally rehabilitated but much energy saving remain to be done in these dwellings which energy consumption is higher than the new buildings one.

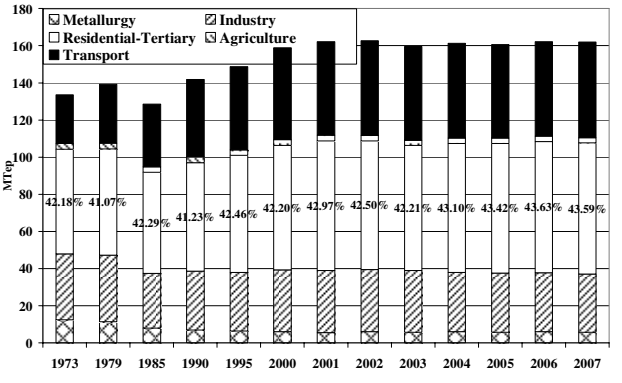

Fig. 1. Final Energy Consumption by sector in France (French Ministry of ecology 2007)

The total energy consumption of the building sector increased by about 50% over the last twenty years with a high penetration of electricity (+130%) which covers 40% of all the needs of which 50% for captive use as lighting, domestic appliances, etc ….). The repartition of the consumption by type of use for a main home in 2004 (i.e. 83% of the total of the houses) is shown in Fig.2. The heating is the most important sector in term of energy consumption and it represents 15% of household expenditure devoted to the house, or 3.7% of their total expenditure (ADEME/CEREN 2006; Besson 2008). In 2006, the household heating expenditures reached 21.3 G€. There are 3 ways making it possible to reduce energy consumption:

- by improving the thermal insulation;
- by using more efficient heating systems as classical or solar one;
- by optimizing the energy utilization of the energy in the building.

We developed an innovative concept of heating system easily building-integrated for reducing the visual impact (psychological obstacle), easy to install in both new and old houses (technical obstacle), not too expensive to install (financial obstacle) and totally environmentally friendly (environmental indoor or outdoor positive solution).

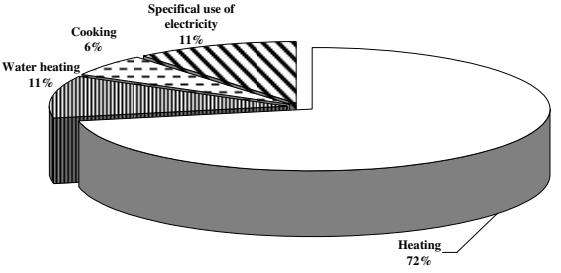

Fig. 2. Repartition of the energy consumption in housing sector (Besson 2008)

3 Presentation of the Solar Air Shutter

This new concept of solar air shutter, patented and named volet'air® allows to produce a low temperature heat directly from the sun without any other energy supply. The objective is to provide a part of the hot air needs in maintaining a healthy ambiance in the housing. This solar air shutter can be used both in principal residence occupied all the year and in secondary residence often no-occupied during a long period of the year and for which the thermal balance and ventilation are just provided by natural energy exchanges from outdoor to indoor and in isolated houses not connected to the electrical grid.

The same fluid is used both for the ventilation and the heat supply. The solar air shutter has the same aspect as a classical shutter (Fig.3.). The internal area is used as a heat converter and the frame can be built with various materials (wood, aluminium and PVC). The heat converter is composed by two glazing panels in multi-wall polycarbonate (a 10 mm depth sheets in twin wall form) specially conceived for outdoor utilization. The outdoor face is transparent and used as a cover and the indoor face is covered by a black thermal painting and is used as an absorber (Fig. 4).

Fig. 3. Window shutter with wood frame and French-window shutter with aluminium frame

a-Si photovoltaic modules are integrated into the lower part of the black face and are used to supply the air fan with electricity. The shutter runs opened, closed and even in intermediate positions thanks to its symmetrical conception. The air enters

between the two plates through two openings under the frame of the shutter and, after having been divided into two parts, runs into the channels to the top, then it continues its progression between the two black plates (one of each multi-wall polycarbonate glazing panels) when it mixes with the air coming from the other side of the shutter and at last this hot air exits by a collector located on the intern part of the frame where are situated the hinges of the shutter (Fig. 5). The air fan is located into the housing wall (Fig. 6).

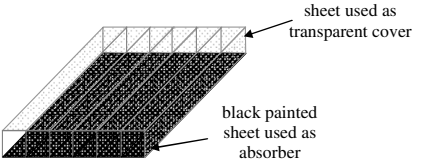

Fig. 4. Glazing panels in multi-wall polycarbonate (10 mm depth sheets in twin wall form)

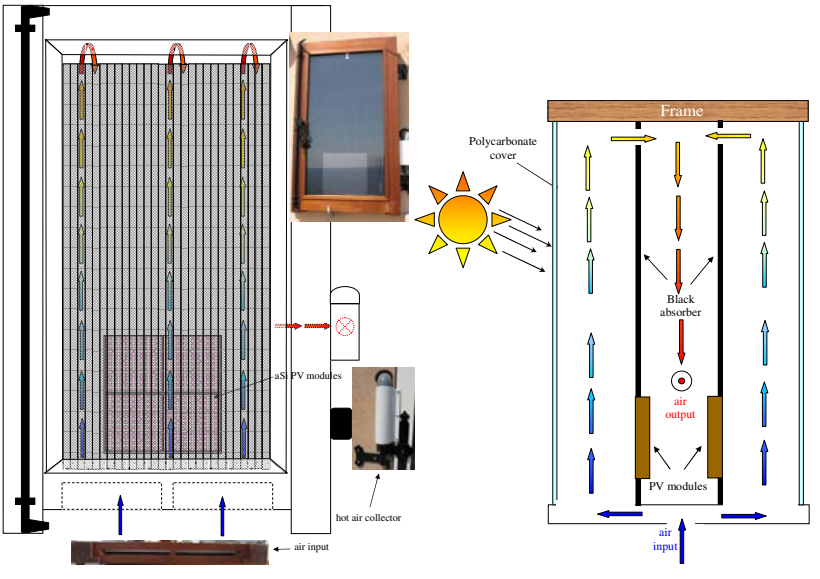

Fig. 5. The solar collector, its main components and the air circulation

This configuration does not use a thermal insulation as in a conventional solar collector and makes this solar collector thermally original; this originality will induce a special thermal modelling and will lead to a particular energy performances. In fact, the more heated the fluid is, the more it enters into the shutter which limits the conductive and convective losses with the outdoor creating thus a kind of thermal dynamic insulation.

The polycarbonate has approximately the same optical properties as glass, it lets the solar radiation in and stops the large infrared radiation emitted by the absorber creating a greenhouse effect. But it has some advantages if compared with glass, it

has a higher mechanical resistance for smaller thickness and weight (250 times more shocks resistant) with a less expensive price. The first air passage is made through channels and not between two plates (as it is with a glass cover) and consequently, the thermal exchange surface area is increased and the heat absorbed by the fluid increased during the first passage. There are conductive losses between the cover and the absorber by the sides of the channels that connect the absorber to the cover but these losses are for a great part, recuperated by the air circulating into the channels.

The frame is identical to a window frame excepted the two holes for the air passage: for the input air under the frame and for the output air on the vertical edge of the shutter near the wall. Consequently, its conception is easy to implement.

Two different air-fans are chosen according the size of the shutter and are less noisy as possible in order not to disturb the tranquillity of the inhabitants of the house. The hot air collector (Fig.6) is composed with a piece dependent on the shutter and another one dependent on the wall; the first one is cylindrical and aligned with the rotation axis of the hinges. The upper part of this cylinder is open and can easily receive the piece situated in the wall; the piece into the wall is made up of three parts: a rigid tube crossing a part of the wall, a flexible tube which is fitted onto the cylindrical part of the shutter and a O-ring providing a sealing between the two parts that run into one another and a Venturi fixed on the other end of the rigid tube that leads to the house; It incorporates a fan, a temperature sensor and supports the grid protection for the air dissemination.

Fig. 6. The hot air collector: indoor and outdoor view

To supply the air fan with electricity, a PV module is integrated in the low part of the shutter. The PV module has been chosen according to the following constraints:

- it must provide a sufficient power for the air-fan running;
- it must be perfectly integrated in the shutter and it must respect some sizes;
- it must not modify the general aestheticism of the shutter.

The second condition does not allow to use “classical” PV modules because their size is not adapted to the size of our shutter; thus, we decided to use ASI® OEM Schott PV modules in silicon thin film (Schott Solar GmbH 2008), adapted in size, shape and voltage to our needs; these small PV modules are connected in serial or parallel according to the required voltage and current.

A special electronic regulation has been designed and controls the air fan. No cable is necessary because the control signals are given to the air fan by a wi-fi connection, this regulation is composed by a central transmitter situated in the housing (measuring the indoor ambient temperature) and one electronic sensor in each solar shutter (measuring the output air temperature); thus an unique central transmitter is used for all the shutters available in the house. It regulates the air fan speed in such a way that the indoor air temperature reaches to the temperature wanted by the user.

This new concept of solar air collector has mainly the following advantages:

- a new active function is added to the shutter;
- it can produce heat in open, closed or intermediate position thanks to its symmetrical design; thus, a shutter fixed on a wall toward west or east can be opened in such a way that it is exposed towards south; the presence of shutters on the various walls of the housing allows to produce heat during all the sun trajectory;
- the vertical inclination allows to produce more in winter and less in summer;
- it can be sized for all the windows because each part of the shutter can be taken to pieces and replaced independently;
- the installation is very easy for old (existing) and new houses.
- the air is directly introduced into the house by a rotary air collector without costly and big air distribution systems
- its classical functions are preserved : sound and thermal insulation, mechanical resistance;
- it is autonomous because the fan is supplied by the integrated PV modules and it can be used in remote areas ; moreover, as the electrical grid is not necessary, it reduces the problem of cable installation and reduces the installation cost;
- it is easily removable what is useful to clean it and to preserve a clean air.

But there are some disadvantages: it is impractical to rolling shutters, the number of windows in the house implies the size of the heating system and the utilization of air as heating fluid decreases the heat production compared to a water solar collector.

4 First Experimental Results of the Solar Air Shutter

We set up an experimentation with three objectives:

- to test the thermal and electrical behaviour of the shutter, to collect experimental data in various meteorological conditions and to measure its energy performances;
- to validate a thermal model that will be developed through a future work;
- to make adjustments necessary to improve the performances and the efficiency.

We built an experimental wall with two window-openings able to receive two shutters for French windows and two shutters for classical windows (Fig. 7).

Fig. 7. The experimental wall

The meteorological data measured are solar radiations (horizontal and vertical global, horizontal diffuse), air ambient temperature and humidity, wind speed and direction. For each shutter, we measure the air output and the wall temperatures, the air output humidity, the air flow, the voltage and current for each PV generator and the air temperature in the top of the extruded polycarbonate shading and sunny cover.

The solar collectors sizes are 0.825m x 0.435m i.e. a surface area equal to 0.36m² for the small one and 1.985m x 0.46m = 0.91m² for the French-window shutter. We present here the first results of the experimentation and it is obvious that some improvements will have to be achieved to this solar shutter in the near future to increase its performances. The solar shutters were tested with the air fan powered by a stabilized electrical source (around 14 V) or by the PV modules. We show the daily thermal behaviour for the window (0.36 m²) and French window (0.91 m²) shutters with the air fan powered by a stabilized electrical sources (Fig. 8-9) and for the window-shutter with the air fan powered by PV modules (Fig.10);

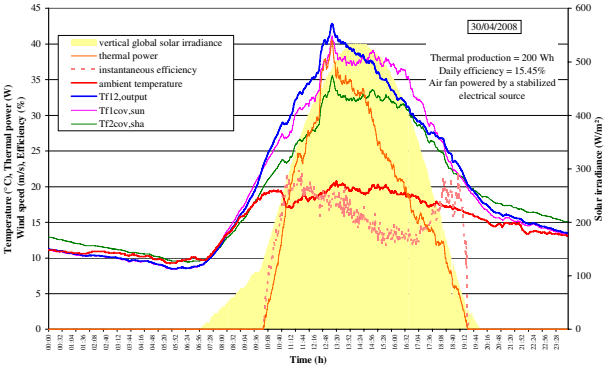

Fig. 8. Experimental results (stabilized electrical source) for the small shutter

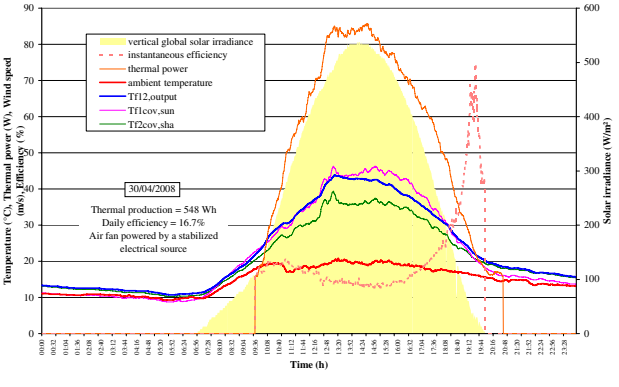

Fig. 9. Experimental results (stabilized electrical source) for the French-window shutter

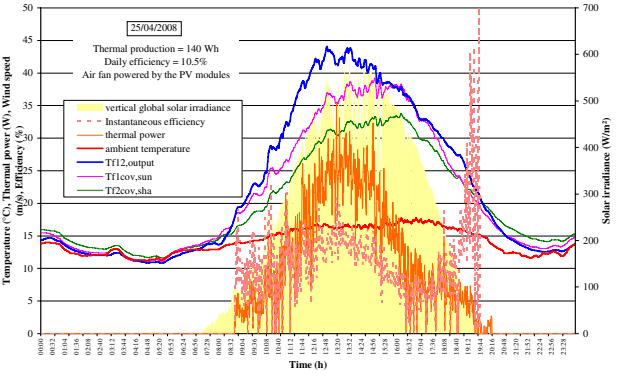

Fig. 10. Experimental results (PV electrical source) for the small shutter

We could notice that :

- the thermal production is shifted over the curve of sunshine due to the thermal inertia of the solar shutter inducing a low instantaneous efficiency at the beginning of the heat production and a high one at the end;
- comparing the output temperature $T_{f12,output}$ with the temperatures at the covers top ($T_{f1,cov,sun}$ and $T_{f2,cov,sha}$), we can see that in the first part of the day the air is heated by the second pass (between the two absorbers) and that the afternoon $T_{f12,output}$ is situated between $T_{f1,cov,sun}$ and $T_{f2,cov,sha}$ due to the combination of colder air (shading face) with hot air; under the same meteorological conditions, the maximum temperature in the air collector is approximately the same for the small and large shutter;
- the air flow rate is very low: 7 and 11.7 m^3/h for window-shutter and French-window shutter with stabilized electrical supply (30/04/2008) and up to 4.4 m^3/h (25/04/2008) for photovoltaic supply; these low air flow rates induce a low efficiency (about 15-16% in stabilized supply and 10% in PV supply) and a small daily production comparing with existing air solar collector.

This low efficiency is due to the low flow rate; in 1982, Garg and Sharma (1982) carried out an experimental study on three air plate collectors under the same operating conditions. Yidilz et al (2002) studied the performances for a air flow rate equal to 20, 43 and 65 m^3/h and showed that the collector efficiency increases with the air flow and is inversely proportional to the inlet fluid temperature; Kurtbas and Turgut (2006) and Ben-Amara et al (2005) show also this influence. The more turbulent the air flow regime is, the more the thermal exchanges are increased, but with the air flow rate in our shutter, the flow regime is laminar (Reynolds number equal to 600). In the most common air collectors, the flow rate is around 100 m^3/h for a 1.5-2 m^2 air solar collector (Sopian et al 1996; Ben-Amara et al 2005).

Moreover, the solar shutter has no conventional thermal insulation and this originality has also an influence on the performances. But, another important parameter explaining the low efficiency is the period of the test because this experiment began in April 2008 and it is not the best period to determine the performances; in fact, the vertical inclination of the solar shutter induces:

- a low solar irradiation incident on the vertical shutter whatever the season is;
- when the sun is high, the angle between the sun and the vertical surface is high and induces a small transmittance of the cover and a small absorptance of the absorber; thus a small part of the incident radiation is useful to be converted into heat;

In winter, the performances and the shutter efficiency will increase because:

- the sun incidence angle will be smaller and transmittance and absorptance higher; The useful solar energy and the heat production will be higher; at the same time, the incidence angle decreases and the PV module power increases and consequently the air flow rate will increase and will have a positive influence on the heat production;
- the efficiency will increase because, in winter, the daily heat production will increase faster than the daily solar irradiation on the vertical plane (see Fig. 11).

To confirm our hypothesis, we achieved three experiments :

- a measure of the pressure drop due to the shutter and the experimental material;
- a measure of the transmittivity of the polycarbonate;
- a measure of the influence on the IV curves of PV modules of the sun position and the connection between PV modules.

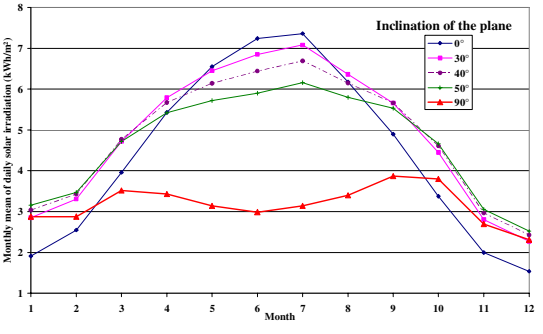

Fig. 11. Monthly mean values of the daily solar irradiation on tilted planes for Ajaccio calculated by Calsol Software (INES 2008)

We measured the pressure drop into the two shutters: for the French-window shutter 7.5 Pa and for the small one 6 Pa; The French-window shutter has a length twice as large as the small one, consequently the pressure drop in the shutter is mainly due to the presence of numerous singularities, more than to a pressure loss through the channel. In the experiment, the shutter is connected to a measuring system introducing additional losses which are much higher than shutter pressure drops. The pressure drop due to the measuring system varies between 10 Pa (big shutter) and 5.5 Pa (small shutter). It is necessary to modify the flow rate measurement system in such a way that the pressure drop is greatly decreased and the measured flow rate is near

the flow rate in real running conditions (without instrumentation). With only the pressure drop of the shutter, the air fan characteristics predict an air flow rate equal to 20 $m^3.h^{-1}$ (7 $m^3.h^{-1}$ now) for the small shutter and 50 $m^3.h^{-1}$ for the French-window one (12 $m^3.h^{-1}$ now); with these "real" flow rates, the performances should be greatly improved.

We measured the transmittivity of the 10 mm multi-wall polycarbonate glazing panels for sun radiation in normal incidence equal to 80%; this transmittivity is due to the two polycarbonate plates but also to the perpendicular sides of the channel which diffuse the solar radiation entering the cover; with a high incidence angle between the sun and the normal of the surface, this transmittivity was measured at 30%; this result confirms the high influence of the season on the solar collector performance;

The previous measures of the transmittivity influence also the PV modules power moreover, the PV modules connection (4 in serial - 2 series in parallel) reduces the power by 15% and 35% in normal and high incidence angle compared with the power of the 8 individual modules. The two effects (transmittivity and PV modules association) increase the seasonal influence on the PV module productivity and on the flow rate. In a future version, an unique PV module will replace the 8 small ones.

These three experiments confirm that the performances of the solar collector should be improved during the winter i.e. the heating season. We must wait for the winter results to give more complete and realistic performances But we can already give a few ways to improve the performances of the shutter:

- by increasing the flow rate through changing for a more efficient fan, or increasing the PV power (but if more solar energy is converted into electricity, less will be into heat);
- by reducing the pressure drop by using larger channel without changing the thickness because the thickness of the shutter must stay the same.
- by elaborating an automatic system which cuts the air passage in the shading face with three possible influences ; increasing the flow rate in the sunny side, avoiding mixing the air coming from the sunny side with cooler air from the shading one and increasing the thermal insulation for the shading face.

5 Conclusion

A new concept of solar air collector with a high integration level in the building was presented. The «solar shutter» called «Volet'air®» can be applied not only in new houses but also in existing buildings. The technical particularities of this solar shutter are that it works in all positions and does not use thermal insulation. An experiment has been implemented and the first results for the performances show a small efficiency due, mainly, to the period of measures that is not the period the solar collector was designed for; in winter, for the same daily solar irradiation incident on the vertical plane the cover transmittivity and absorber absorptivity will increase and the useful solar energy too. These hypotheses were confirmed by three experiments on pressure drop, transmittivity and PV modules performances. It is necessary to increase the air flow because it influences directly the performances. The low flow rate is due to the pressure drop in the shutter but mainly by the measuring system; we must modify the measuring system in such a way it can't modify the real flow rate into the shutter.

References

ADEME/CEREN: Statistical data on energy consumption (2006), http://www.ifen.fr/uploads/media/menages2a.pdf

Besson, D.: Consommation d'énergie: autant de dépenses en carburants qu'en énergie domestique. ISEE Première 1176 (February 2008)

French Ministry of Ecology, French Ministry of Economy: L'énergie en France - Chiffres clés (2007)

SCHOTT Solar GmbH: ASI® OEM Outdoor Solar Modules (2008), http://www.schott.com

Garg, H.P., Sharma, V.K.: Evaluation of the performance of air heaters of conventional designs. Solar Energy 29, 523–533 (1982)

Yildiz, C., Togrul, I.T., Sarsilmaz, C., Pehlivan, D.: Thermal efficiency of a air thermal collector with extended absorption surface and increased convection. Int. Comm. Heat Mass Transfer 29(6), 831–840 (2002)

Kurtbas, I., Turgut, E.: Experimental Investigation of Solar Air Heater with Free and Fixed Fins: Efficiency and Exergy Loss. International Journal of Science & Technology 1(1), 75–82 (2006)

Ben-Amara, M., Houcine, I., Guizani, A.A., Maalej, M.: Efficiency investigation of a new-design air solar plate collector used in a humidification–dehumidification desalination process. Renewable Energy 30, 1309–1327 (2005)

Sopian, K., Yigit, K.S., Liu, H.T., Kakac, S., Veziroglu, T.N.: Performance analysis of photovoltaic thermal air heaters. Energy Convers. Mgmt. 37(11), 1657–1670 (1996)

National Institute of Solar Energy (INES): Calsol software (2008), http://ines.solaire.free.fr/gisesol_1.php#

Development and Strategies of Building Integrated Wind Turbines in China

Bin Cai and Hong Jin

School of Architecture, Harbin Institute of Technology, Harbin 150001, China
jinhong_777@yahoo.com.cn

Abstract. In China, almost 1/3 energy consumption are caused by buildings today. Most of these energy are from fossil fuel which will lead to serious environmental problems and large amount of CO_2 emissions. The Chinese government is seeking for a safe, clean and sustainable energy to help with reducing the environmental pollutions. Wind energy which is clean and renewable is a very good choice. Now scientists and architects begin to integrate wind turbines into buildings to provide electricity energy as well as an aesthetic appearance. Although there are only a few cases of building integrated wind turbine projects at present, more and more people have shown a great interest in this new developed technique. This paper will review the development of the wind energy in China followed by a summary of the current status of building integrated wind turbine projects. It will also give out some strategies to overcome the problems which building integrated wind turbines are facing today as well as a prospect of the wind energy inverting into buildings in the future.

Keywords: wind turbines, renewable energy, green building design, sustainable building technology.

1 Introduction

China, the biggest developing country with a huge number of populations, has seen a great amount of energy consumption during the last decade. Most of these energy are from coal which can not be regenerated in the short future. And with the development of architectural industry, more than 1/3 of the total energy consumption is caused by buildings. Now, the total areas of existing buildings are over $3.6x10^{11}$ m^2, and this number will keep increasing in a rapid speed. It is predicated that by the year 2020, the total energy consumption by buildings will be three times as it is now, and China will become the country with the largest CO_2 emission at that time.

To solve this problem the Chinese government are seeking for solutions to reduce the energy consumption by buildings as well as employing safe, clean and sustainable energy into buildings. They wish that, in the year 2010, renewable energy would take 10% in the total energy consumptions, and 16% in 2020.

So far, in China the electricity energy generated from PV system is 1.1GW in 2007. And China has the largest number of solar thermal collections to provide hot water. Now the government begins to focus more on the wind energy which is safe, clean and renewable with lower prices.

2 Development of the Wind Energy in China

During the early years, wind turbines have not been developed very fast as most of them were large, noisy with lower efficiency. Ever since the 20s and 30s in the last century, energy crisis made the scientists began to seek for energy which is more sustainable and stable. Wind energy with low emissions and costs was definitely a good choice. And thanks to the development of wind turbine mechanism, modern wind turbines, which are being used on a significant scale with much higher efficiency, are available in various sizes and power output and can operate over a range of wind speeds.

China, which has the largest potential resources of wind energy, has seen progressively growth in wind power development in the last decade. In the early 1970s, China began to develop wind energy to provide electricity energy to people living in the remote areas without national electricity grid connection. For more than 20 years development, the renewable energy technologies has achieved a great progress and the large-scale wind turbines have entered into a stage of commercialization. By the end of 1997, the total capacity installed of wind power is 160 MW in China. Over 170,000 sets of small-sized wind turbine generators with a capacity of 100W have been installed in the whole country, around 80% of which, 140,000 sets, were installed in the Inner Mongolia Autonomous Region [1]. By 2000, the total installed capacity of wind turbines in China reached 344.8MW with the total installed units of 727. At present, there are 40 wind farms in 14 provinces around China. At the same moment, the development of small wind turbine technique makes it possible to install wind turbines into buildings.

3 Current Status of Building Integrated Wind Turbines

3.1 Examples of Building Integrated Wind Turbine Projects

Now in China, there are a lot of examples of building integrated PV systems and solar thermal collections, but building integrated wind turbines is still at its beginning stage.

Wind turbines being mounted on, integrated into or even close to the buildings are called Building mounted/integrated wind turbines (BUWT). The first building integrated wind turbine project in China is the Youth apartment in Tianshan Road, Shanghai (Fig. 1). It is a 3kw small wind turbine mounted on the roof of the apartment. It has been working since Sep 2007. The cut-in wind speed is 2.2 m/s, and it is working with a PV system, which could help each other to increase the stability of the whole system.

A plan for Zhujiang building in Guangzhou also planned to adopt wind energy into buildings (Fig. 2). It is called the first zero energy-costing commercial building in China. This high-rise building is 309m high with 71 floors and is going to be built in 2009. In spite of the PV system, two air holes were designed in the facade of the building to integrate the wind turbines.

Fig. 1. Youth apartment in Tianshang Road, Shanghai

(http://blog.tom.com/lujianzhou78/article/1713.html)

Fig. 2. Zhujiang building

(http://www.ycwb.com/gdjsb/200708/21/content_1591362_2.htm)

Fig. 3. Shanghai centre

(http://news.163.com/08/0815/03/4JC141710001124J.html)

Another plan of a high-rise building in Shanghai which is called the centre of Shanghai also employed wind power into buildings (Fig. 3). The total areas of the building are 558,806m^2 with 127 floors, and it is in the centre of Lujiazui CBD in Shanghai. The height of the building is 632m and it is going to be the highest building in Shanghai in the future. Designers of this tallest building wanted to install 72 wind turbines into the roof of the building. And each of the turbines is a 10Kw small wind turbine.

3.2 Hurdles Facing Development of Building Integrated Wind Turbines

Meanwhile, using wind turbines in an urban area involves many different difficulties. From a planning perspective, there are several challenges presented by building integration of micro wind turbines that are not important for other micro

generation technologies [2]. These challenges can be summarized as: noise, vibration, shadows, access for installation and maintenance, and electricity interference, etc. Also, when designing wind turbine systems, wind speed is a crucial point to the performance of wind turbines, because the energy output of a wind turbine is cubic to the wind velocity. Since the built environment around a building has relatively lower average wind speed and higher turbulence levels. This has a great influence on the performance of a building integrated wind turbine. So far, there are some existing building integrated projects and upcoming projects in the near future, but few researches have been conducted to investigate the wind flows over the buildings for wind power utilization purpose, and no research was performed to compare the advantages of building integrated wind systems with remote stand-alone wind systems [3]. And in China, considering her own situation, there are some important hurdles which need to be overcome.

3.2.1 The Electricity Grids

The quality of a power grid will not be affected by wind power if the portion of wind installations is less than 10% of total generation. However, due to the random nature of wind speeds, wind power can not be dispatched, and it is impossible to replace the conventional installed capacity which can guarantee meeting load demand [4]. And once the quality of wind power is under 10%, storage systems will be considered to be designed to store the extra electricity energy generated from wind power. In China, the quality of the electricity grid is around 12%. However, there are still some accidents which caused the breaking down of the electricity grids. So that, the power grid of the new buildings need to be designed strong enough to hold the energy generated from wind.

3.2.2 Social Impacts

Generally speaking, building integrated wind turbines are not totally understood and accepted by the society in China at the moment. For one thing, when wind turbines are working, the noise, vibration and shadows caused by the turbines will definitely influent the users of the building. For another, as there are still few cases of building integrated wind turbine projects, the appearance of building integrated wind turbines are not very popular in China. However, if there could be more examples of real projects and buildings cloud be designed properly to reduce the influence of the turbines, all these problems will be solved respectively.

3.2.3 Economic Impacts

As the technology develops the cost of wind power may continue to drop, but at the moment in China, the tariff for wind electricity is 0.3-0.4 Yuan/kWh higher than coal fired power. For a wind farm with installed capacity of 100MW and an annual energy production of 250GWh, the consumers of the provincial power grid would have to pay 75-100 million Yuan more a year for purchasing wind power [4].

In buildings, the installation of wind turbines during the initial periods will increase the payment of the investors in a certain level. And in order to get more energy from wind, building integrated wind turbines must be used in areas with higher wind power density. As a result, whether or not employing the wind energy into buildings depends on the local wind power resources. There is another way to reduce the cost of

wind energy. Since the price of initial installation of wind turbines is high, if more components can be made locally, it will bring the cost down.

3.2.4 Policies

At present there are some existing policies to encourage the using of renewable energy in architectural industry such as the "Green House Identification Project". However, as it is still an under development area of inserting wind power into buildings, more incentive policies are need to encourage the development of building integrated wind turbines. And it is recommended that the administrative agencies should promote policies to remove the financial and technical barriers, to provoke the market demand and to promote the development of renewable energy industry.

4 Strategies of Inverting Wind Turbines into Buildings

4.1 Wind Power Utilizations According to Different Wind Energy Distributions

Because the power in the winds is proportional to the cube of wind speed, when designing building integrated wind turbine systems, the local wind resource is crucial to the electricity energy output. The ideal local annual average wind velocity should be >3m/s, the total hours of the wind speed which is 3-20m/s should be >3000h, and the density of wind energy power at wind speed between 3 to 20 m/s should be >100W/m^2.

Fig. 4 shows the density of wind energy distributions in China. There are two areas with high wind resource density in China. One is in the "three northern" part of China which includes most of the areas of northeastern, northern and northwestern parts in China. In these areas, the wind power density is over 200-300W/m^2, and sometimes can reach to 500 W/m^2, the total hours of high wind velocity is over 5000hrs. Another area is along the coastline in the southeastern part of China. The wind power density is around 200W/m^2, and in some islands it can reach to 500 W/m^2, the total hours of high wind velocity is around 7000-8000hrs [5]. It is very effective to install wind turbines in these areas with high wind density. The only problem is to avoid turbulent flows and extreme climates such as the storm, thunder and snow.

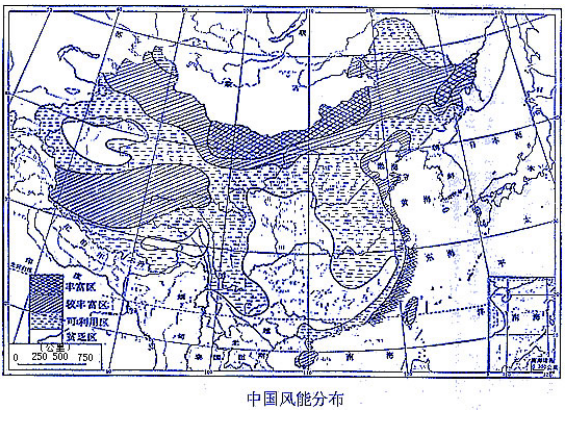

Fig. 4. Wind Energy Distribution in China

(http://www.lrn.cn/science/energyCollection/200705/t20070529_62674.htm)

In the areas with medium wind resource density which is around 100W/m^2, with total hours 3000hrs, wind turbines can be also installed into buildings. However,

when designing the buildings, some strategies must be used to enhance the air flow over the wind turbines. And in areas with low wind resource such as the middle parts of China where wind power density is under 100W/m^2, it is not suitable to install wind turbines.

4.2 Designing Electricity Grids in Buildings

Generally speaking, electricity generated from a stand alone building integrated wind turbine system can not meet all the energy demands of the building. And the national electricity grid is needed to supply most of the energy needs of the building at present. In China, the existing electricity grids are not strong enough to afford the portion of electricity generated from wind energy. And it is not allowed to supply extra electricity to the national grids either. So it is better to separate the two grids system from each other. The grids of wind turbines can provide electricity to some specific areas (such as the bathrooms, kitchens and offices etc) or equipments (such as lighting) in the buildings.

As the electricity energy is supplied to the building through a battery in the wind turbine system, keeping the balance of input and output power will last the life of the battery. So the best way to achieve effective utilization of the wind turbine system is to design the electricity demand according to the changes of wind velocity and frequency.

4.3 Controlling Noise and Vibration of Building Integrated Wind Turbines

The noise of the wind turbines are usually correlated to the vibration, the size of the turbines and the turbulence levels over the turbines. There are some solutions to reduce the influence of noise and vibration on the users of the buildings. The first one is to separate the supporting structure of the turbines from the buildings. And if it is impossible, some soft mount systems can be designed between buildings and turbines to give a damping to reduce the noise and vibration. The second solution is to choose the size of wind turbines and to avoid turbulent locations when integrating them into the buildings. The last one is to integrate wind turbines in the positions with high surrounding noise-levels or place them into the least sensitive locations where the noise of turbines is not significant.

4.4 Enhancing Wind Power Flow over Wind Turbines

4.4.1 Rising the Height of Wind Turbines

Because with the height of the buildings wind velocity increases. In small buildings, increasing the height of wind turbines will raise the amount of electricity energy output. However, raising the height of turbines means longer wire is needed and the longer the wire the more the electricity lost. It is a challenge for designers to decide a property height of the turbines. In high-rise buildings, as higher wind speed happens on more places, there are more optimize positions to install wind turbines such as the roof, facade and places between two towers. Once designing the positions of wind turbines, designers should consider both the wind speed and turbulent flows around the building. In order to make an accurate decision, sometimes, using CFD (Computational Fluid

Dynamic) simulation can provide a much more accurate result during the design process.

4.4.2 Taking Use of Special Places on Buildings

Sometimes, turbines can be installed in some special positions in the buildings such as the air outlets, solar chimney in the buildings and even places between two towers. These areas are usually specifically designed to augment the flow through the turbines in the new buildings. And for the existing buildings, a CFD simulation should be used to exploit any potential positions where the highest wind speed happens. And as well the turbulent flow should also be avoided during the design process.

4.5 Complementing to Other Renewable Energy Systems

In some areas with both plenty of solar insulation and wind energy distributions, wind turbines can work parallel with PV systems or solar thermal collections. PV system is quiet and can be easily installed into buildings, but expensive and lower in efficiency. It can be only working during the day time, and the highest power output happens in the mid day. Compared with PV systems, wind turbines are noisy and heavy, but cheap and higher in efficiency. The advantage of building integrated wind turbines is that they can work during the sun set time and also in the cloudy days when PV system can not work effectively. When these two systems work together, the combined system is called wind-solar hybrid system. It can cover the shortcomings of each other and take advantages of these two kinds of renewable energy.

5 Conclusions

The contribution of renewable energy is quite small compared with the huge amount of fossil fuel consumption at the moment in China. However as the renewable energy resources in China are extensive, the actual development of renewable energy has the potentiality to be as many times as now in the short future. And the most urgent task now is to reduce the cost of renewable energy and remove constrains which stop the development of renewable energy techniques.

Acknowledgments. Project Supported by “National Key Project of Scientific and Technical Supporting Programs Funded by Ministry of Science & Technology of China（2006BAJ04B05-4）”.

References

[1] Liu, W.-Q., Gan, L., Zhang, X.-L.: Cost-competitive incentives for wind energy development in China: institutional dynamics and policy changes. Energy Policy 30, 753–765 (2002)

[2] Domestic installation of micro generation equipment—Final report from a review of the permitted development regulations, ENTEC DCLG (April 2007)

[3] Refocus, D.E.: Wind energy in buildings: Power generation from wind in the urban environment — where it is needed most 7(2), 33–38 (2006)

[4] Shi, P.: Planning of Wind Farm Development in China. Renewable Energy Congress VI (WREC), 1176–1178 (2000)
[5] Wind distribution in China, Resource Document China Renewable Energy (2007), http://www.lrn.cn/science/energyCollection/200705/t20070529_62674.htm
[6] Vertical axis wind turbines — make it possible of building integrated wind turbines, http://blog.tom.com/lujianzhou78/article/1713.html
[7] Zhujiang building –To create the world's most environmentally friendly skyscraper (2007), http://www.ycwb.com/gdjsb/2007-08/21/content_1591362_2.htm
[8] Shanghai Center will be up to 632 meters, Resource Document Eastern World (2008), http://news.163.com/08/0815/03/4JC141710001124J.html

Missing Data Interpolation of Power Generation for Photovoltaic System

Kun-Jung Hsu

Department of Construction Technology, Leader University
No. 188 An-Chung Rd. Sec. 5, Tainan 709, Taiwan (ROC)

Abstract. The data acquisitions of Photovoltaic system (PVs) and Building Integrated Photovoltaic system (BiPVs) include the quantities of electric power generated, temperature, current and voltage, solar radiation from field installations. In the practice of PVs and BiPVs field data collection, we often encounter some missing and outlier data because of computer shut down, the electric pulse to sensitive sensor, thus affect the reliability of the whole data. Without complete data, we cannot catch the whole picture of the annual electric power generated respect to the PV system. Using the moderator regression model and the field data collected from a PV system installed on the roof of a high technology facility, this paper showed how the missing and outlier data can be interpolated properly. The null hypotheses of the explanatory variables have no effect on PV electric power output is rejected at 1% significance level. Using the estimates coefficient of the estimators the missing and outlier data were interpolated. Finally, the daily yields of the PV system across the whole year were plotted.

Keywords: Photovoltaic system, Regression model, Missing and outlier data, Interpolation method.

1 Introduction

In order to monitor the effective or efficiency of the installed Photovoltaic systems (PVs), we always set up monitor systems, and use computer program to collect data from field installations. These PVs data acquisition include the quantities of electric power generated, temperature, current and voltage, solar radiation. But sometime we also encounter the missing data and outlier data occurring in the observed data set. These phenomenon may source from computer shut down, the electric pulse to sensitive sensor, thus affect the reliability of the whole data.

In these cases, the analysis processes become trouble because of the data set incompletion. Without complete data, we cannot catch the whole picture of the annual electric power generated respect to the PV system. The analyzer cannot catch the essence of the empirical insight. One of the results is giving up the data already collected. But if these are most often situation we met in PVs/BiPVs field site, give up the whole data set should not be the best way one hope to choice.

Using daily yield record of the PV/BiPV system and the weather data collected by the field monitor system, if we can construct a best estimation model and interpolate these missing data. The whole data set should be still has its representative respect to

the PV/BiPV system. According the theoretical framework of PVs electric power yield, with the stochastic property of field attribute, the statistic model should be constructed. Using the estimated parameters respect to data collect from field, the missing and outlier point then can be interpolated.

This paper uses the statistic estimation tools to explore the ways of interpolating missing/outlier data of the PV system. In the following paragraphs, we construct a moderator regression model first. Then using the effective records of a high technology facility located at mid-Taiwan, the parameters of the model were estimated first. Including the field-nearby irradiation and temperature records of Center Weather bureau of Taiwan, the missing and outlier data then was estimated. The missing and outlier of the data set then were interpolated. Finally, the conclusions were drawn.

2 The Model

According laboratory researches, we know that the major effects of electric power generation from PV system include solar irradiance, cell temperature, wind, and solar incidence angle (The German Solar Energy Society 2005). Solar incidence angle of PVs was decided by the latitude of its installation location during planning and design stage. Supposing the solar incidence angle already was optimized at the PVs design stage, the major factors which affect daily output of the system should be solar irradiance and cell temperature. Solar irradiance is the major source of solar cell. Also, a PV module's expected power output under Standard Test Conditions (STC) always character as temperature sensitivity.

Following the basic concepts of the previous researches, the sources of electric power generation from photovoltaic system are majorly from solar irradiation, cell temperature, wind, and solar incidence angle (Whitaker et al. 1991, Emery et al. 1995, Emery et al. 1996, Katz et al. 2001, Green 2003, The German Solar Energy Society 2005). Normally, the monitor system of PVs field site doesn't record the wind data in Taiwan. And the solar incidence angle of the PV panel respect to the location of the field site always is optimized at the design phase. So the solar irradiation and the cell temperature should be the major factors which affect the daily yield of the PV system.

Excluding the effect of wind and solar incidence angle, the output of electric power generated from PV system P_i, can be summarized as $P_{REF}\left(\frac{R_i}{R_{REF}}\right)\left[1+\beta\left(T_i-T_{REF}\right)\right]$. Where P presents as the output of electric power (KW); R presents as plane-of array irradiance (W/m^2); T presents as module temperature (°C); β is the temperature coefficient of maximum power (1/°C); and subscript i indicate the desired conditions of the PVs, and REF represent as reference conditions. The final cause-effect of a PV system now can be interpreted as follow: first part of the effects majorly from solar irradiation, and the second part of the effects from the interaction of irradiation and cell temperature. With the random residual, ε_i, which represent the unaccounted system level effect from the field

environment, the estimation model of the field electric power output of a PV system can be written as follows.

$$E_i = a + bR_i + c(R_i T_i) + \varepsilon_i. \tag{1}$$

Where R_i repsents the direct solar irradiation of the observation *i*; and T_i repsents the interaction of solar irradiation and modular temperature; and E_i repsents the electric power output of a fixed interval.

Whenever there are missing and outlier data in annual data set, the respect records of power output, solar irradiation and temperature records of the field site miss. In this situation, we don't have solar irradiation and modular temperature records respect to those missing/outlier data. We need some information outside the field of PVs; for example, the general daily solar irradiation and temperature records of the nearby local weather bureau may be useful now. Generally, the local weather bureaus will provide the long term weather monitor records. If we can access the records of the field-nearby weather monitor station, and give some reasonable assumption or/and estimation, the quality of wanted interpolation can be improved in advanced. The local weather records of the nearby Local Weather Bureau can be treated as an instrument variable and substitute the solar irradiation and temperature information of the field site, which affect electric output of the PVs.

With general information of the local irradiation and temperature respect to the installation-nearby area, we have different approaches to interpolate the missing and outlier data. As we know, module temperature are affected by solar irradiation and ambient temperature (T_i^*) together. The ambient temperature of the installation can be seen as a moderator variable which interacts with irradiation and the result is the total electric output of the PVs in a fixed interval. With the environmental random effect, its random residual term μ_i, the relationship can be represented as follows,

$$T_i = \alpha + \beta R_i + \gamma T_i^* + \mu_i. \tag{2}$$

Substituting Eq.2 into Eq. 1, and replaced variable $R_i T_i^*$ as R_i^*, replaced residual term $cR_i \mu_i + \varepsilon_i$ as ε_i^*, we attain,

$$E_i = a + (b + c\alpha) R_i + (c\beta) R_i^2 + (c\gamma) R_i^* + \varepsilon_i^*. \tag{3}$$

Simplified the notation in Eq. 3, we let $c_0 = a$, $c_1 = b + c\alpha$, $c_2 = c\beta$, $c_3 = c\gamma$; Eq. 3 thus can be rewritten as follows,

$$E_i = c_0 + c_1 R_i + c_2 R_i^2 + c_3 R_i^* + \varepsilon_i^*. \tag{4}$$

We can use the field observations of the PVs to estimate the parameters: c_0, c_1, c_2, c_3 in Eq. 4. Then the general solar irradiation and temperature information adopted from the nearby weather monitor station can be treated as the approximation value of

the missing and outlier data of the field-site. Thus we can use these local solar irradiance and temperature records, and apply Eq. 4 to estimate the missing and outlier output of the PVs. Without other information, these results should be one of the best estimations, thus it can be interpolated into the missing/outliers of the whole year.

3 Data and Analysis

Concerning the renewable energy issue, the Bureau of Energy Ministry of Economic Affairs in Taiwan has proposed a subsidized program for those PV system users from 2000. Grid-connected PVs were subsidized from 2002. Until now, only a few grid-connected cases have annual data of electric power generated from PV system. Most of PVs were installed on roof of the buildings; some of them were integrated into curtain wall system of the buildings. Considering the electric power output of the stand-alone system cannot feed into the battery properly whenever full-charge, thus loss some efficiency of the power generated, this study uses the grid-connected PVs case as an illustrative example.

This paper uses the annual computer records of a grid-connected PV system installed at roof of a high technology facility located in Science Park of mid-Taiwan as an illustrative of the model estimation and missing/outlier data interpolation. The record period of the illustrative case start from October 01, 2005 to September 30, 2006. Each of the observations includes hour accumulation solar irradiance, temperature

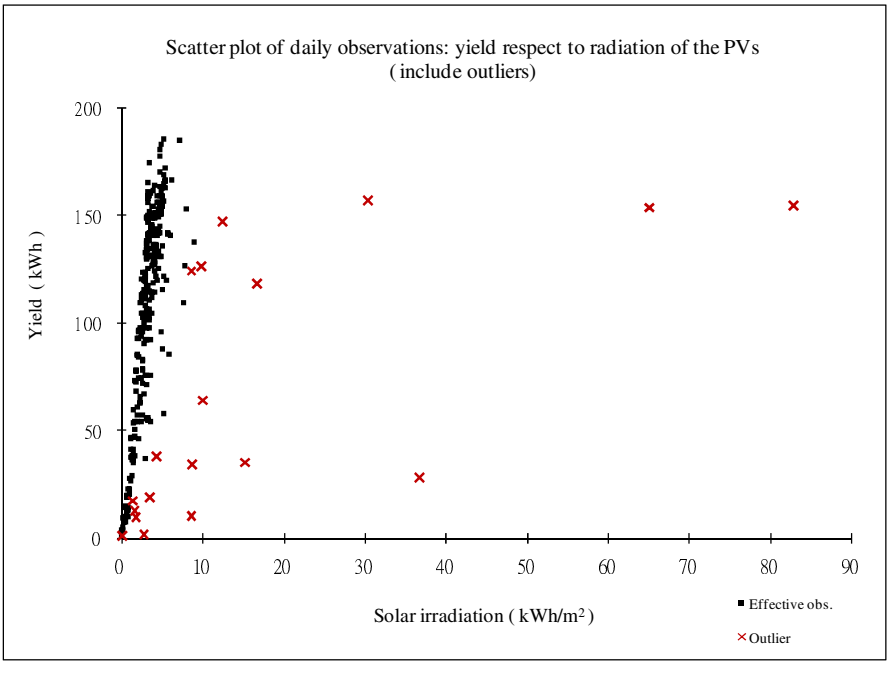

Fig. 1. The daily yield of the illustrative PV system: include yield outlier

record underneath the modular panel, and hour accumulation electric power generated. These data were recorded using computer programming by the installed PV Company, Hengs Technology Co., LTD. After examining the daily records set, we find there are 80 missing observations (Fig. 1).

The unreasonable electric minute power generated data and irregular modular temperature records totally were omitted 19 records, which were showed in Fig. 1. With these missing and outlier data, Fig. 2 showed the daily yield respect to temperature underneath the modular. Excluding the missing data and outliers, Table 1 summarized that total missing and outliers are 99 records, and the total numbers of the effective observations are 266 records.

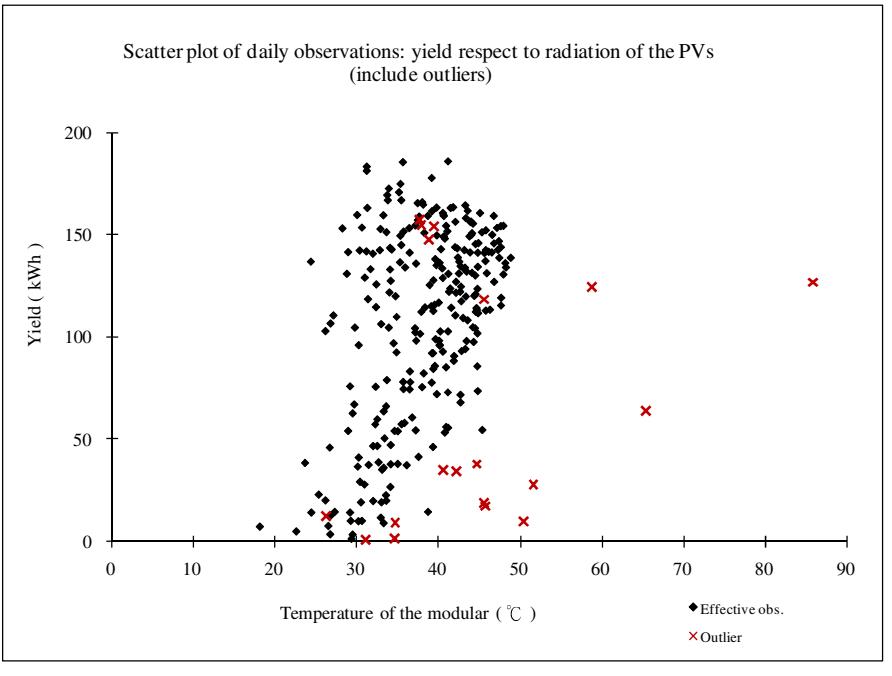

Fig. 2. The daily yield of the illustrative PV system: include outliers

Table 1. The missing/outlier records of daily observation of the illustrative case

Missing data	Unreasonable solar irradiance and temperature outliers	Total missing & outliers	Total effective observations
80	19	99	266
22%	6%	27%	73%

Fig. 3 showed the 266 effective observations by date sequence, which was drawn by daily electric power generated across the whole year. The missing and outlier data are majorly located among two periods: the first one is middle November 2005, the second one with largest period from middle January 2006 to February 2006.

By using the regression analysis, the test statistics F of the model of Eq. 4 is 345.47, which shows the model estimated is at level of significance of 0.00000. The goodness fits of the model; the coefficient of determination R^2 is 0.798, which showed 79.8% variation of the data information can be explained by the model. The t-statistics of coefficient for Solar irradiance (R) and Square-irradiance (R^2) are 10.87 and -12.30 respectively, which all show the estimates are significant at the 1% level; and the t-statistics of coefficient for interaction of Solar irradiance and temperature (RT^*) is 4.94, which shows the estimate is also significant at the 1% level. Therefore the null hypotheses of these variables have no effect on PV electric power output is rejected at acceptable significance level.

The above statistical results were tabulated in Table 2. Table 2 shows that the null hypothesis of each variable has no effect on the electric power output of the PVs can reject at 1% level (Null hypotheses, H_0: the coefficient = 0). These showed that the estimates of coefficients for all variables respect to Eq. 4 are at an accepted significant level.

Table 2. Results of parameter estimation of the regression model

		Coefficients	Std. Errors	t-statistics	p-value
Interception	c_0	-21.06***	4.81	-4.38	0.00002
Solar Irradiance (R)	c_1	44.01***	4.05	10.87	0.00000
Square-irradiance (R^2)	c_2	-4.51***	0.37	-12.30	0.00000
Interaction of Solar irradiance and temperature (RT^*)	c_3	0.34***	0.07	4.94	0.00000

N=266; R^2= 0.798; F-value= 345.47; Significance=0.00000

*** Significant at the 0.01 level (2-tailed)

** Significant at the 0.05 level (2-tailed)

* Significant at the 0.10 level (2-tailed)

Using the local solar irradiance and temperature records of the nearby weather monitor station, we can apply the estimated coefficient of Eq. 4 to predict the missing and outlier data of the whole year. After the predicted value of the missing and outlier were estimated, the incomplete data set can be interpolated. The daily yield of the PV system respect to the whole year profile finally was plotted. Figure 4 showed the final profile of the daily electric power generated of the PV system respect to the study period from October 01, 2005 to September 30, 2006.

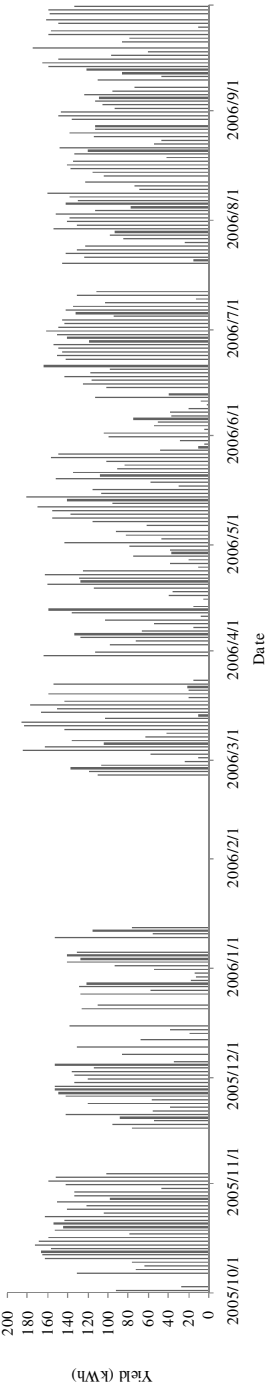

Fig. 3. Daily yield of the PVs with missing/outlier data

Fig. 4. Daily yield of the PVs after interpolating the missing/outlier

4 Conclusions and Discussions

This paper constructed a regression model as a tool of interpolating the missing and outliers. The effective records of a high technology facility located at mid-Taiwan then were used to estimate the parameters of the model. By using the regression analysis, the test statistics F of the model is 345.47, which shows the model estimated is at level of significance of 0.00000. The goodness fits of the model showed that 79.8% variation of the data information can be explained by the model. The null hypothesis of each explanatory variable has no effect on PV electric power output all can be rejected at 1% significance level. Including the field-nearby irradiation and temperature records of local weather bureau, the missing and outlier data of was estimated. Using the estimates coefficient of the estimators, the missing and outlier data of the whole data set thus were interpolated. The daily yields of the PV system of the whole year finally were plotted.

In general, the practices of interpolating the missing and outlier data for PVs/BIPVs highly depend on the availability of the data and its attributes. First, the accumulated electric power generated from PV system is measured by a desired interval, e.g. by minute, by hour, or in this paper the accumulated electric power is by day and for whole year. Different kinds of interval for accumulating the electric power generated will result different parameters interpretation of the model. Secondly, how solar irradiation and temperature affect the electric power generated from PVs will periodic-specific, parameters respect to different period may highly sensitive. For example, with different weather and temperature characteristic, different season (or month) will have present different estimates of the model, and should accompany with different meaning and interpretations. Thus different periodic model can be estimated and compared, e.g. by year, by season, or by month. But if there are too many missing and outlier data embedded in a short-period, say in monthly, the small sampling size problem may lead the month model obsolete.

On the other hand, even year model and season model are with larger samples size, in order to verify which one is the better; the statistic testing processes of the interpolation need be developed. Moreover, if the field solar irradiation and/or field temperature data not available in computer records, how the model should be adjusted? How the weather records of local weather bureau can be an auxiliary of the field observation respect to such model fitting? These different kinds of problem respect to field data set have its specific characteristics, but the respect interpolation methods/tools still need be redeveloped in advance.

Acknowledgments

The authors would like to thank the National Science Council of the Republic of China for financially supporting this research under Contract No. NSC 96-2221-E-426-008, No. NSC 97-2221-E-426-012-MY2; and Fulbright Senior Research Grants 2008-09. The field data was provided by Hengs Technology Co., LTD; my student Chai-Hao Hu helped with field data collection; and the Department of Construction Management, University of Nebraska-Lincoln provided a good research environment for the completion of this paper. Comments and helpful suggestions were provided by

Professor Chi-ming Lai. Many thanks to all those who assisted me in this research! The contents of this paper are the sole responsibility of the author.

References

The German Solar Energy Society. Planning and installing Photovoltaic Systems: A guide for installers, architects and engineers. James & James, London (2005)

Katz, E.A., Faiman, D., Tuladhar, S.M., Kroon, J.M., Wienk, M.M., Fromherz, T., Padinger, F., Brabec, C.J., Sariciftci, N.S.: Temperature dependence for the photovoltaic device parameters of polymer-fullerene solar cells under operating conditions. J. Appl. Phys. 90, 5343–5551 (2001)

Whitaker, C.M., Townsend, T.U., Wenger, H.J., Iliceto, A., Chimento, G., Paletta, F.: Effect of irradiance and other factors on PV temperature. In: Proceeding of the 22nd IEEE Photovoltaic Specialists Conference, pp. 608–613 (1991)

Emery, K., Caiyem, J., Dunlavy, D., Field, H., Rummel, S., Ottoson, L.: Temperature and irradiance behavior of photovoltaics devices. In: Photovoltaics Performance and Reliability Workshop, NREL Tech. Rep. TP-411-20379 (September 1995)

Emery, K., Burdick, J., Caiyem, Y.: Temperature dependence of photovoltaic cells, modules and systems. In: 25th IEEE PVSC, pp. 1275–1278 (1996)

Green, M.A.: General temperature dependence of solar cell performance and implications for device modeling. Prog. Photovoltaics: Res. and Appl. 11, 333–340 (2003)

Development of Short-Term Prediction System for Wind Power Generation Based on Multiple Observation Points

Muhammad Khalid[1] and Andrey V. Savkin[2]

[1] School of Electrical Engineering and Telecommunications,
The University of New South Wales, UNSW Sydney, NSW 2052, Australia
m.khalid@student.unsw.edu.au
[2] School of Electrical Engineering and Telecommunications,
The University of New South Wales, UNSW Sydney, NSW 2052, Australia
a.savkin@unsw.edu.au

1 Introduction

Wind energy is becoming the fastest growing energy technology in the world. As wind power provides a clean and cheap opportunity for future power generation, many countries have started harnessing it [1], [2], [3], [4]. Wind is a highly fluctuating resource. A reliable prediction system is required in order to absorb a large fraction of wind power in the electrical systems. As electricity markets are moving towards wind energy, a reliable and accurate wind power prediction system will be beneficial for all wind plant operators, utility operators and for utility customers as well. Only accurate predictions can make it possible for grid operators to schedule the efficient and economic power generation in order to meet the demand of utility customers.

Our system for the prediction of power generation is based on measurements from multiple observation points. These measurements are transmitted over communication channels to our designed predictor. In fact, our system is an example of a networked state estimation system. Such systems have attracted a lot of attention in recent years [5], [6], [7].

Due to intermittent nature and built-in uncertainty of the wind, the efficient and cost effective integration of wind power into electricity grid has become the greatest challenge. Therefore, only an accurate and reliable wind power prediction system can improve the efficiency of power system operation. The better we can predict the wind power, the more valuable the wind power. Prediction can contribute to the economic and secure large-scale wind integration in a power system, and make it possible for efficient management of wind production even in the challenging conditions.

Depending on the intended application, the prediction of the wind power generation may be considered at different time scales. Very short-term predictions ranging from milliseconds up to a few minutes ahead are used for turbine active control. For the power system management and energy trading, the short-term predictions ranging from 48-72 hours ahead are useful. These short term predictions may also be used for optimizing the scheduling of the conventional power plants. Long term predictions are used with longer time scales up to 5-7 days ahead for planning the maintenance of wind farms, conventional power plants and transmission lines [8].

Although wind power prediction has gained significant interest in recent years but none of the system for very short- term has gained the industry acceptance as yet [9]. Normally the persistence technique is used for short term wind power predictions. We focus on two important time scales; 5-min-ahead and 10-min-ahead predictions. The effective use of this type of wind predictions would vary depending on the market structure of the electric power industry [10]. For example, predictions at this time scale help in making the decision to accept or reject the bids from generators.

As a case study, a wind power prediction system for 10-min ahead predictions has been developed utilizing the data from Woolnorth wind farm site in Tasmania, Australia. As Tasmania and southern regions of Australia are rich in wind resources, the number of planned wind farm installations in this region is the highest [11].

Fig. 1. Location of Woolnorth wind farm site in Australia

2 Overview of Existing Prediction Techniques

Although three main classes of techniques have been identified for wind forecasting, which are numerical weather prediction (NWP) methods, statistical methods, and methods based on artificial neural networks, however, time series models like Kalman filter [12], Autoregressive models [13], the autoregressive moving average (ARMA) models [14], neural networks [15], and some advanced hybrid approaches are usually preferred for short-term wind power prediction. For detailed history of wind power prediction, refer to [16] and references therein.

3 The Persistence Model

This is the simplest model also known as naive predictor. This model is presently an industry benchmark for very short-term wind power prediction. It assumes that the power at time step $t-1$ is the same as the power at time step t.

$$P_t = P_{t-1} \tag{1}$$

In other words, the persistence is based on the assumption of a high correlation between the present and future wind values. The accuracy of this model degrades with increasing prediction horizon.

4 The Grey Predictor Model

These systems refer to any system with partially known information about its parameters. The Grey predictor models have been involved in many prediction applications, for example, predicting non-periodic time series such as wind data series, stock price indices, etc. There are several Grey predictor models currently in use. We are focusing on traditional *GM (1, 1)* model [17]. The procedure of the *GM (1, 1)* model is as follows. In the first stage of *GM (1, 1)*, the first order accumulated generating operation (AGO) series is generated i.e.

$$X^{(1)}(k) = \sum_{t=1}^{k} X^{(0)}(t) \quad \forall k = 1, ..., \mathrm{n} \tag{2}$$

where $X^{(1)}$ is the accumulated data series and $X^{(0)}$ is the original data series. In the second stage, the model's differential equation that relates its dependent variables with the independent ones is formulated. This differential equation is known as the Grey dynamic model. For the traditional *GM (1, 1)* model, this differential equation is represented by one independent variable and no dependent variables and can be expressed as follows

$$\frac{dX^{(1)}}{dt} + aX^{(1)} = b \tag{3}$$

where X represents the independent variable for the traditional *GM (1, 1)* and (a, b) are the model parameters. The parameters a and b of the *GM (1, 1)* can be determined by the method of least squares as follows

$$A = \begin{bmatrix} a \\ b \end{bmatrix} = \left[\beta^T \beta\right]^{-1} \beta^T Y \tag{4}$$

where

$$\beta = \begin{bmatrix} -Z^{(1)}(2) & 1 \\ -Z^{(1)}(3) & 1 \\ \vdots & \vdots \\ -Z^{(1)}(n) & 1 \end{bmatrix} \tag{5}$$

$$Y = [X^{(0)}(2)\ X^{(0)}(3)\ \cdots\ X^{(0)}(n)]^T \tag{6}$$

and

$$Z^{(1)}(t) = \frac{X^{(1)}(t-1) + X^{(1)}(t)}{2} \tag{7}$$

The following equation calculates the predicted values of the AGO series $\hat{X}^{(1)}$.

$$\hat{X}^{(1)}(t+1) = \left(X^{(0)}(1) - \frac{b}{a})\right) e^{-at} + \frac{b}{a} \tag{8}$$

where $X^{(0)}(1)$ represents the first data in the original time series. Finally the forecasted AGO series of data is transformed back to its original form using the inverse accumulated generating operation (IAGO) mathematically represented as

$$\begin{aligned} &\hat{X}^{(0)}(1) = \hat{X}^{(1)}(1) \\ &\hat{X}^{(0)}(t+1) = \hat{X}^{(1)}(t+1) - \hat{X}^{(1)}(t)\ \ \forall t = 1, 2, 3, ... \end{aligned} \tag{9}$$

5 The Proposed Model

The two stages of proposed wind power prediction system are explained in the following sub-sections.

5.1 Wind Speed and Direction Predictions

In the first stage, the proposed model demonstrates that wind speed predictions at a given turbine can be improved by using the wind speed observations from nearby turbines. As there is strong coupling between wind speed and direction, accurate prediction of wind speed as well as the direction can make the operation of wind turbines intelligent and efficient. Therefore, the wind speed and the direction are predicted simultaneously using the proposed model. Hence to achieve the goal, wind data is converted to wind vectors as shown in Fig. 2.

Generally this model can be represented as

$$Y = MX \tag{10}$$

where

$$Y = [Y(t+1),\ \cdots, Y(t-N+1)\,]^T \tag{11}$$

$$X = [c_1,\ \cdots,\ c_K]^T \tag{12}$$

$$M = [V_1,\ \cdots,\ V_K] \tag{13}$$

where

$$Y(t+1) = \sum_{i=1}^{K} c_i^T\, \upsilon_i(t) \tag{14}$$

with

$$c_i = [\alpha_{i,1}, \cdots,\ \alpha_{i,n_i}]^T \in \Re^{n_i} \tag{15}$$

and

$$\upsilon_i(t) = [v_i(t), v_i(t-1), \cdots, v_i(t-n_i)]^T \tag{16}$$

$$V_i = \begin{bmatrix} v_i(t) & v_i(t-1) & \cdots & v_i(t-n_i) \\ v_i(t-1) & v_i(t-2) & \cdots & v_i(t-1-n_i) \\ \vdots & \vdots & \ddots & \vdots \\ v_i(t-N) & v_i(t-N-1) & \cdots & v_i(t-N-n_i) \end{bmatrix} \tag{17}$$

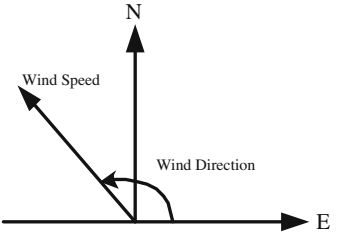

Fig. 2. Wind vector representation

where K is the number of the turbines and N is the number of the historical data points taken. n_i is the order of the autoregressive (AR) models of the i-th turbine, $v_i(\xi)$ is the wind speed recorded at the i-th turbine at time ξ. The vector c_i contains the coefficients of the AR model of the i-th turbine. The vector X containing the coefficients of the model for K turbines is estimated using the method of adaptive least squares at each time step. The coefficients are computed using the following relation,

$$X = (M^T M)^{-1} M^T Y \tag{18}$$

The novel idea is to convert wind data into wind vectors i.e. V_x and V_y.

$$\begin{aligned} V_x &= V \cos\theta \\ V_y &= V \sin\theta \end{aligned} \tag{19}$$

where θ is the direction of the wind in degrees. The proposed model in (10) is utilized to predict the individual wind vectors i.e. $\hat{V}_x^2$ and $\hat{V}_y^2$. Finally, the wind speed and the direction predictions at each time step are obtained using the following relations.

$$\hat{V} = \sqrt{\hat{V}_x^2 + \hat{V}_y^2} \tag{20}$$

$$\hat{\theta} = \tan^{-1}\left(\frac{\hat{V}_y}{\hat{V}_x}\right) \tag{21}$$

In this way both wind speed and direction are predicted simultaneously. Depending upon the predicted direction, the appropriate power curve is selected to determine the predicted power output. This is achieved by feeding the predicted wind speed to the input of power curve. In our case, the power curve models are sub sector direction dependent empirical power curves based on the historical wind speed and power measurements for a given turbine. As a case study, we consider 4 power curve models for 4 direction sectors as explained in Sec. 5.2. It has been observed that sub-sector power curves can lead to slight improvement in wind power predictions at the single turbine. In fact, the small improvement in the power prediction at turbine level can lead to the significant improvement in the prediction accuracy of the wind farm power output by extending the idea efficiently over the entire wind farm.

5.2 Power Curve Modeling

The power curve of a wind turbine is a graph that indicates how large the electrical power output will be for the turbine at different wind speeds. The wind power of a wind turbine depends on the wind speed; which depends on regional weather patterns, seasonal variations, and terrain types. It is well known that the theoretical relation between the energy (per unit time) of wind that flows at speed v (m/s) through an intercepting area A (m^2) is

$$p = \frac{1}{2}\rho A v^3 \tag{22}$$

where ρ is the air density (kg/m^3), which depends on the air temperature and pressure. However, the true relation between the power generated at an actual wind farm and the speed of the wind is more complex than (22).

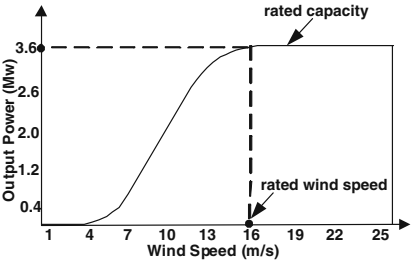

Fig. 3. A typical machine power curve

Fig. 3 illustrates the machine power curve of a particular wind turbine. From this machine power curve, we can see that below some minimum wind speed, called connection speed, the wind turbine does not produce power. After this connection speed, the power increases as the wind speed increases. When the speed increases and reaches the nominal speed, the power reaches the rated capacity of the wind turbine. After the nominal speed, the output power is kept constant for some range of the wind speed. Finally, when the wind speed surpasses the disconnection speed, the wind turbine is disconnected to prevent damages from excessive wind.

The deterministic machine power curve shown in Fig. 3 is different from the empirical power curve obtained in the real operation at a wind farm [18]. That's why the power curve is derived from measured wind speed and power. Different studies have shown that using a power curve derived from measured wind speed and power can improve the forecast root mean square error (RMSE) significantly in comparison to use the manufacturer's power curve only. In addition, due to the non-linearity of the power curve, wind speed forecasting errors are amplified in the high-slope region between the cut-in wind speed of the turbine and the plateau at rated wind speed, where errors are dampened. That is, the nonlinearity of the wind turbine power curves lead to further amplification of the error, and the small deviations in the wind speed may result in large deviations in the power.

The wind power generation is also influenced by the wind direction due to strong coupling between them. However, the influence of the wind direction on power output is less significant as compared with wind speed due to the fact that turbines are directed to face the wind during its operation [19]. Again it varies from site to site. In our study we are focusing on improvement in the power generation at turbine level, hence the small improvement can result in the significant improvement at the wind farm power output. Therefore, our power curves are based on direction distribution at the particular turbine at the given wind farm site. Fig. 4 shows the 4 direction sectors based on direction distribution of one of the turbines at Woolnorth for the year 2006. The idea is to model independent power curves for each direction sector using historical data provided that data for each small sector should be rich enough to represent the complete speed and power relation. The number of direction sectors can also vary from site to site. Although any appropriate method of power curve modeling can be used for modeling those curves, we are using method of bins [20].

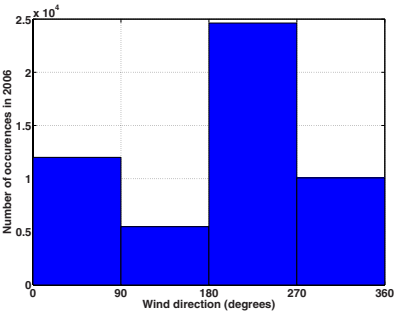

Fig. 4. Wind direction representation at Woolnorth for individual turbine with 4 direction sectors for the year 2006

6 Data Bases

The wind farm observation data used in this paper consists of 37 turbines, Roaring 40s Woolnorth wind farm in Tasmania, Australia as shown in Fig. 1. The data is of 10 min resolution of wind speed, wind direction and wind power for the year 2006 and January 2007 measured at the hub height.

7 Results and Discussion

Complete 2006 year data is used for power curve modeling, which is found sufficient to capture the complete speed and power relation for each direction sector. Data for January 2007 is selected for model testing and evaluation. The optimal number of turbines involved in the prediction, the order of autoregressive terms for each turbine involved in the prediction, and the number of historical data points is determined by experiments. Model is tested and validated for different groups of turbines. As an example results from one of the experiments are presented where 50 historical wind speed and direction observations have been used to determine the model coefficients at each time step. Wind speed predictions at a given turbine for future 500 points have been computed.

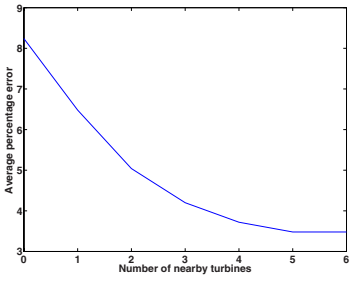

Fig. 5. The effect of increasing the number of turbines in one step ahead predictions of wind speed over average percentage error

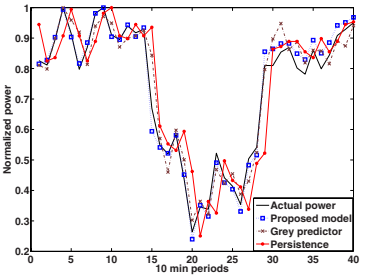

Fig. 6. Normalized wind power predictions for different models

Table 1. Average percentage error in wind power predictions

Model	1 Step ahead	2 Step ahead	3 Step ahead
Persistence	17.38	24.42	38.5
Grey predictor	14.85	18.37	28.82
Proposed model[a]	11.0	15.1	26.3

[a] using information from 5 turbines

The results are presented for the optimal number of the turbines involved in the prediction with the best auto regression order. In order to get the predicted output power, the wind speed predictions at each time step are used at the input of appropriate power curve model which is selected based on predicted wind direction. For clarity and good visibility of the graphs, performance of the methods as in Fig. 6 is shown only for 40 data points. For confidentiality, normalized power is shown in Fig. 6 instead of actual power at the given wind farm.

8 Conclusion

A complete prediction system for wind power generation has been developed in this paper. This system is capable of predicting the wind power at short-term prediction scale, however, we presented the results for 10 minute ahead prediciton. The proposed methodology is based on the use of multiple observation points which led to the significant improvement in wind speed predictions. A reasonable accuracy improvement in wind power predictions at the turbine level has been achieved due to these improved wind speed predictions. The experimental results reveal the effectiveness of proposed approach over the reference models.

Acknowledgements. This work was supported by the Australian Research Council. We would like to thank Hugh Outhred, Iain MacGill, Merlinde Kay, and Nicholas

Cutler at the Centre of Energy and Environmental Markets (CEEM), UNSW for their assistance in getting the required data. We are also grateful to Roaring 40s for their co operation in terms of providing the required time series data to carry out this research.

References

1. Schwartz, M., Milligan, M.: Statistical wind forecasting at the US National Renewable Energy Laboratory. In: Proceedings of the First Joint Action Symposium on Wind Forecasting Techniques. International Energy Agency (IEA), Norrköping (2002)
2. Benoit, R., Yu, W.: Developing and testing of wind power forecasting techniques for Canada. In: Proceedings of the First Joint Action Symposium on Wind Forecasting Techniques. International Energy Agency (IEA), Norrköping (2002)
3. Ernst, B., Rohrig, K.: Online-monitoring and prediction of wind power in German transmission system operation centres. In: Proceedings of the First Joint Action Symposium on Wind Forecasting Techniques. International Energy Agency (IEA), Norrköping (2002)
4. Cutler, N., et al.: The first Australian installation of the wind power prediction tool. In: Proceedings of the Global Wind Energy Conference. Australian Wind Energy Association, Adelaide (2006)
5. Matveev, A.S., Savkin, A.V.: The problem of state estimation via asynchronous communication channels with irregular transmission times. IEEE Transactions on Automatic Control 48(4), 670–676 (2003)
6. Savkin, A.V.: Analysis and synthesis of networked control systems: topological entropy, observability, robustness, and optimal control. Automatica 42(1), 51–62 (2006)
7. Matveev, A.S., Savkin, A.V.: Estimation and Control over Communication Networks. Birkhauser, Boston (2009)
8. Giebel, G., Brownsword, R., Kariniotakis, G.: The state-of-the-art in short-term prediction of wind power; a literature overview, Deliverable report of the EU project ANEMOS (2003)
9. Potter, C.W., Negnevitsky, M.: Very short-term wind forecasting for Tasmanian power generation. IEEE Transactions on Power Systems 21(2), 965–972 (2006)
10. Bathurst, G.N., Weatherill, J., Strbac, G.: Trading wind generation in short-term energy markets. IEEE Transactions on Power Systems 17(3), 782–789 (2002)
11. Negnevitsky, M., Potter, C.: Innovative short-term wind generation prediction techniques. In: Proceedings of the IEEE/PES General Meeting, Montreal, Canada, June 18-22 (2006); CD-ROM, IEEE Catalog Number 06CH37818C, ISBN 1-4244-0493-2
12. Bossanyi, E.A.: Short-term wind prediction using Kalman filters. Wind Engineering 9(1), 1–8 (1985)
13. Fukuda, H., et al.: The development of a wind velocity prediction method based on a data-mining type auto-regressive model. In: Proceedings of the European Wind Energy Conference, Copenhagen, Denmark, June 2-6, pp. 741–744 (2001) ISBN 3-936338-09-4
14. Torres, J., García, A., Blas, M.D., Francisco, A.D.: Forecast of hourly average wind speed with ARMA models in Navarre (Spain). Solar Energy 79(1), 65–77 (2005)
15. Kariniotakis, G.N., Stavrakakis, G.S., Nogaret, E.F.: Wind power forecasting using advanced neural networks models. IEEE Transactions on Energy Conversion 11(4), 762–767 (1996)
16. Costa, A., et al.: A review on the young history of the wind power short-term prediction. Renewable and Sustainable Energy Reviews 12(6), 1725–1744 (2008)
17. El-Fouly, T.H.M.: Grey predictor for wind energy conversion systems output power production. IEEE Transactions on Power Systems 21(3) (2006)

18. Sanchez, I.: Short-term prediction of wind energy production. International Journal of Forecasting 22, 43–56 (2006)
19. Li, S., Wunsch, D.C., O'Hair, E.A., Giesselmann, M.G.: Using neural networks to estimate wind turbine power generation. IEEE Transactions on Energy Conversion 16(3), 276–282 (2001)
20. Cabezon, D., et al.: Comparison of methods for power curve modeling, Global Windpower, Chicago, Illinois USA, a report (2004)

Electricity Supply to a Remote Village Using Grid-Connected Wind Generators

Eric Paalman[1] and Roger Morgan[2]

[1] SP PowerSystems Ltd
[2] Liverpool John Moores University, UK

Abstract. The optimum site for a wind turbine, accessing the best available wind, can be too remote for optimum connection to the grid. Unless there is a high-voltage transmission line nearby, the cost of connection to the 33 kV or 66 kV system can render a small wind farm uneconomic. As a result, small scale wind generation is often connected into the 11 kV rural distribution system. This can cause unacceptable voltage excursions. In this paper, a method is discussed for connecting generation capacity, whether wind-powered or otherwise, into a rural distribution system, and for solving the resulting voltage control problems. The method uses standard voltage control hardware. It has been implemented for wind generators in a remote location in North Wales. Records of voltage measurements are presented, and it is shown that the voltage stability is much improved. Some problems have been experienced, and solutions are proposed.

1 Introduction

Distributed generation capacity using grid-connected natural energy sources such as wind turbines offers an attractive option for electricity supply to remote villages. Local generation can supply the bulk of the local load when the wind is blowing, and the grid is available to supply any shortfalls and usefully absorb any surplus power. However, the existence of reverse power flows, and the need for reactive power supply to the generators, can create voltage stability problems. This arises partly from the original design of the public utility power supply network, which was intended for stabilising the voltage when supplied from a central supply, rather than from a mixture of central and distributed generation. It is made more difficult by long overhead lines with relatively high impedance.

The problem can be outlined [1] in the following diagrams. In the traditional arrangement (figure 1) the voltage on the line to the consumers is controlled at the sub-station so as to ensure that all customers remain within the tolerance band of (typically) + and – 2%. The current into the line is sensed, and the voltage at the sub-station is raised when the current is high, so as to compensate for the drop in voltage along the line. When a source of distributed generation is added on to the line, there is

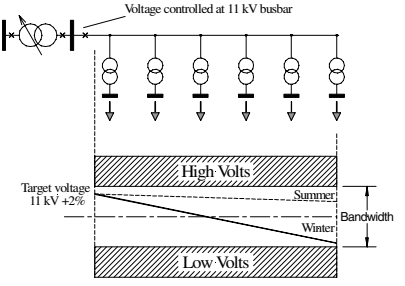

Fig. 1.

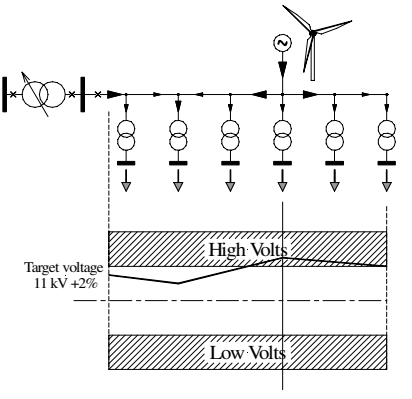

Fig. 2.

a local rise in voltage which can take some consumers outside the permitted tolerance band (figure 2).

In the past, this problem led supply companies to set very severe restrictions on connection of generating capacity on to the distribution network. Nowadays however, there is increasing pressure on utility companies to accommodate small-scale distributed generation, often using very variable sources of energy such as wind power. In particular, the Snowdonia National Park Management Plan [2] has emphasised the importance of community generation schemes. This makes a solution to this type of problem immediately desirable.

2 The Present Project

In this study, a remote rural village community with a typical peak load of about 2MW had an existing supply from a three-phase 11kV overhead line, some 20km long, with a maximum capacity of not much more than 2MW. A group of three wind generators, with a maximum output of about 2MW, was installed by an independent company. This was connected to the public utility's 11kV rural distribution network, as there were no 33kV or higher voltage lines in the vicinity, and the cost of bringing one in would have been prohibitive.

Even in the early stage of the project, with only one turbine generating, there was some degradation of the voltage stability for customers in the village, approaching the permitted band limit when the wind was blowing strongly at times of low demand (see figure 3).

To allow another 1.7MW of wind farm generation and provide greater voltage stability an innovative idea was trialled. The system has been retro-fitted with an active voltage control system (figure 4) consisting of two pole-mounted automatic tap changing voltage stabilisers, located at the point where the feed from the wind generators was connected into the 11kV distribution network. These stabilisers

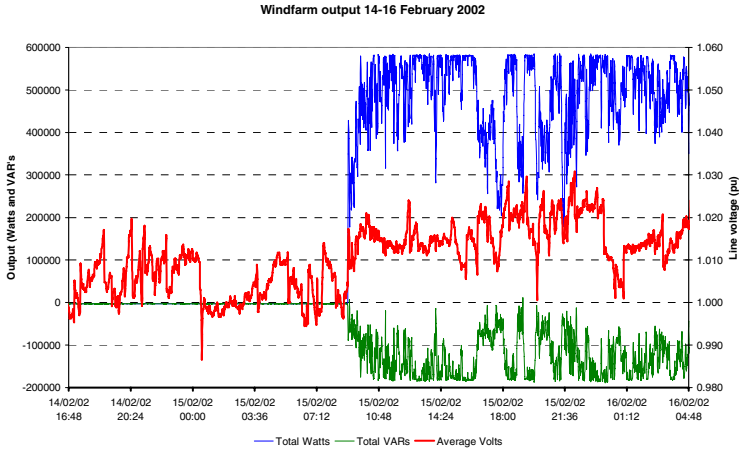

Fig. 3.

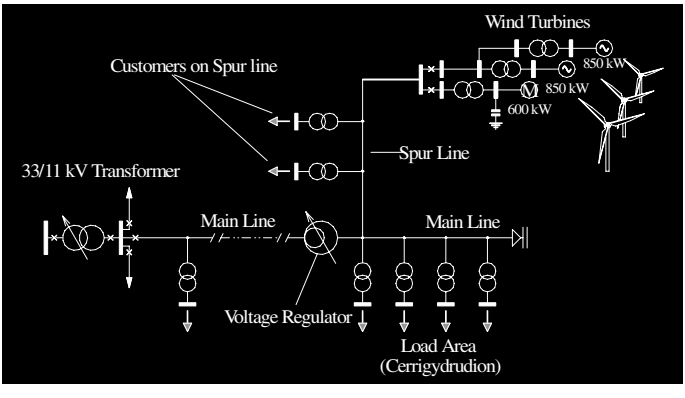

Fig. 4.

operated in conjunction with the voltage control of the wind generators, located at the generators themselves, and with the voltage control located at the 33kV/11kV grid sub-station.

Although traditionally designed for conventional single-direction power flows, the arrangement has proved very effective in the bi-directional power flows encountered in this installation. Even in windy conditions and with all three turbines generating, the voltage remained within the permitted band (figure 5).

In setting up the operating conditions, the characteristics of three separate (and essentially unconnected) control systems have to be optimised. It has been found empirically that the sub-station voltage control looks after voltage fluctuations for durations in excess of 80 seconds, the control at the generators themselves looks after fluctuations up to 30 seconds duration, and the pole-mounted voltage stabilisers look after durations between 30 and 80 seconds.

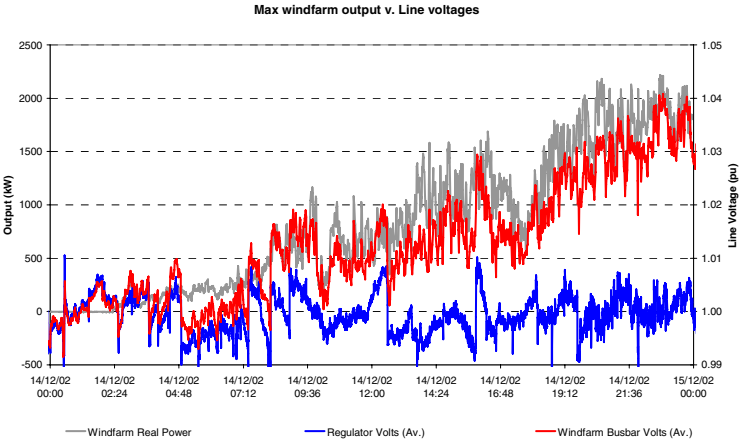

Fig. 5.

3 Discussion

Despite the overall success of the project, some operating conditions could prove difficult. To understand the problem, we can look at four extreme situations.

1. No wind, no generation, some load. In this situation, all the power supplied flows out of the sub-station into the load in the traditional way. Here the regulator works in the 'forward' direction.
2. Windy conditions, light load. In this situation, some of the power from the wind generators flows to the load, but there is a large flow of power back into the sub-station. Here the regulator works in the 'reverse' direction.
3. Windy conditions, medium load. In this situation most of the power from the wind generators flows to the load, but a small amount flows back into the sub-station. Here the regulator works in the 'reverse' direction.
4. Windy conditions, heavy load. In this situation all of the power from the wind generators flows into the load, and is supplemented by power flowing from the sub-station. Here the regulator works in the 'forward' direction.

Situation number 4, with windy conditions and heavy load, can lead to excessive voltage rise for the small number of customers located on the spur line to the generators. Up to now this scenario has not caused problems, and no action is foreseen at present. Situation number 2, with windy conditions and light load, can cause a voltage rise for the significant number of customers on the main line on the sub-station side of the point of connection of the generators. This is because of the heavy power flow towards the sub station. Here the solutions contemplated include restricting the power factor of the generators, tapping down the transformers, upgrading the conductors of the main line, and lowering the bus-bar voltage at the sub-station.

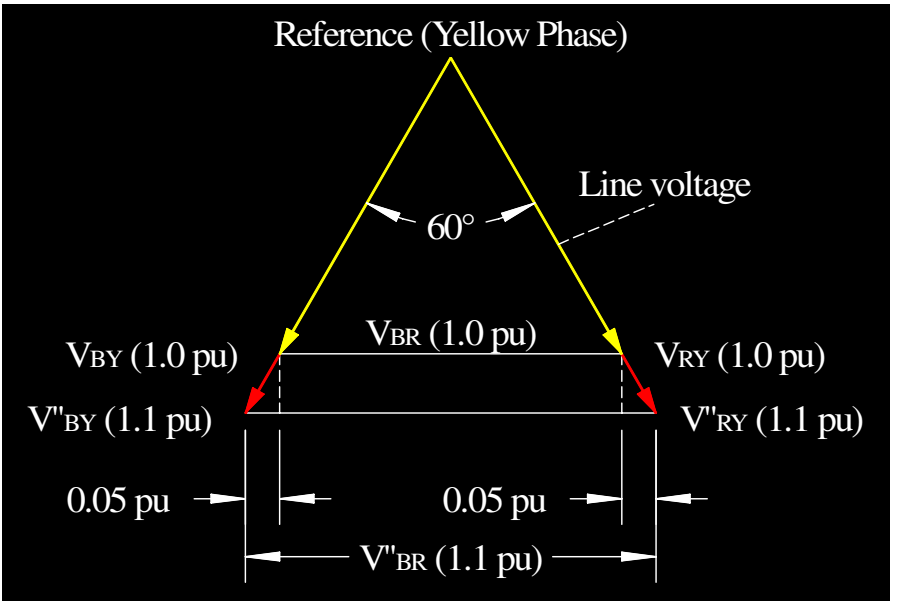

Fig. 6.

In addition, the present set-up (figure 6) with only two voltage regulators serving the three phases can cause the virtual neutral point to vary enough to cause a fault trip during short term parallel operation. To this the obvious solution is to use three voltage regulators instead of two, restoring the virtual neutral point to where it should be, but there are interesting geometrical problems in locating the third transformer within the confines of conventional wiring practice at 11 kV.

One unexpected success of the project arose when the 33kV /11kV transformer at the substation failed, leaving customers to be supplied by the wind generators along with an 11 kV supply from another sub-station some kilometres away. In this situation the customers in the area had a satisfactory voltage, at least partly because of the supply of real power from the wind generators, but the customers on the main line on the sub-station side of the point of connection suffered fluctuating voltages. The situation was made worse by the transfer of the reactive power required by the generators, from the still-functioning 33/11kV transformer along the 11kV line between the two sub-stations.

4 Future Plans

A new problem now seems likely to emerge. The company which owns the existing three wind generators requested to install a fourth, which is probably the limit of local authority planning restrictions. This fourth turbine brings to the total generation to 3.15MW from the site. This increase of generation is likely to cause problems because of additional ‘reverse’ power flow, that is, flow back into the sub-station, as shown in figure 7. The utility company allowed the connection utilising another innovative

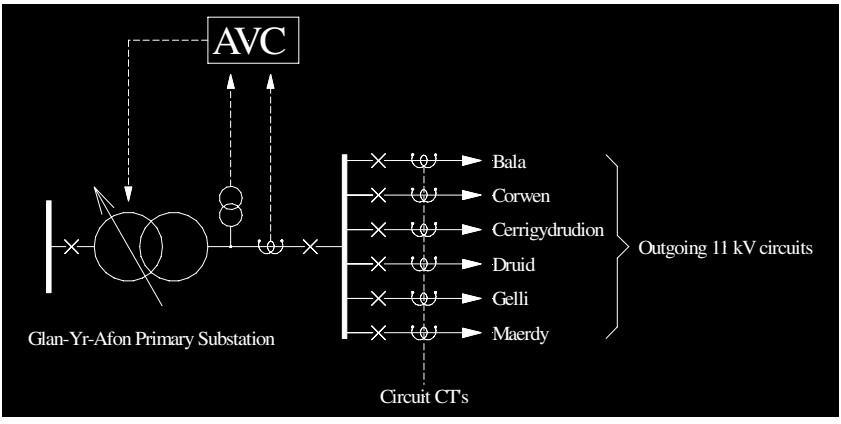

Fig. 7.

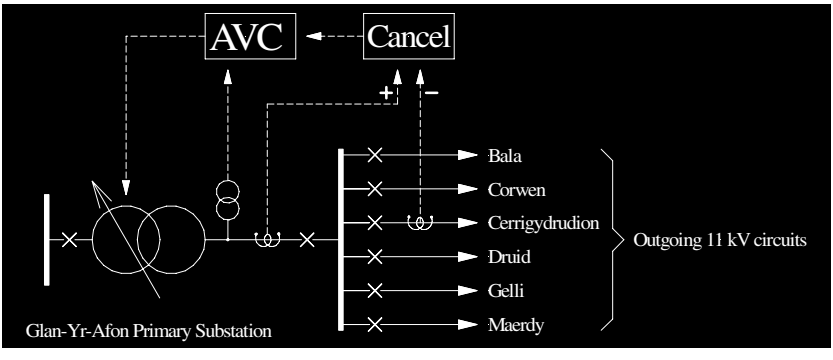

Fig. 8.

idea. Besides the upgrade of the spur line connection to the wind farm a set of cancellation current transformers (CT) was installed at the Primary substation. These CTs measure the line with the wind generators on it (figure 8) so that the current on the feeder is subtracted from the current drawn by the Primary transformer before directing it to the Automatic Voltage Control relay (AVC). The local Voltage at the 11kV bars at the substation is not affected by the large power flows on the 11kV feeder to the wind farm since that input to the relay has been cancelled out.

The voltage control at the primary substation is now governed by the remaining circuits feeding the local network. In that way a proper account can be taken of power flows, and the sub-station voltage control can adjust the voltage on the outgoing line appropriately.

5 Conclusions

This project has proved successful. It has shown how distributed generation can be incorporated into weak rural distribution networks without major voltage excursions.

Problems have emerged, but solutions are available which are more economical than major upgrades of the network. The method has applications far beyond this particular site.

Acknowledgements

The authors thank PowerSystems Ltd for funding the project and for permission to publish. Some of the work was supported by a grant from the United Kingdom Government's Department of Energy. The earlier part of the paper has been presented by the authors at the 2003 Power Plant and Power Systems Symposium of the International Federation of Automatic Control.

References

[1] Paalman, E., Morgan, R.: Voltage regulation for distributed wind generators. In: IFAC PPS Symposium 2003, Seoul, Korea (September 2003) paper 227
[2] Snowdonia Local Development Plan, Topic paper on Energy (March 2007)

The Role of Photovoltaics in Reducing Carbon Emissions in Domestic Properties

F.J. O'Flaherty[1], J.A. Pinder[2], and C. Jackson[3]

[1] Centre for Infrastructure Management, Sheffield Hallam University, UK
[2] Positive Sum Ltd., Sheffield, UK
[3] South Yorkshire Housing Association, Sheffield, UK

Abstract. The paper reports on the performance of photovoltaic (PV) systems which were installed on 23 new build properties at Henley Rise in Rotherham, South Yorkshire, UK. A total of 17 properties were fitted with 3.02 kiloWatt peak (kWp) photovoltaic systems designed to supply up to 2400 kiloWatt hours (kWh) of solar energy per annum whereas the remaining six systems were 3.75 kWp systems providing up to 3000 kWh per annum. The photovoltaic panels were integrated into the roofs of all properties. Datum readings were taken at the time of commissioning in the Summer of 2007 with subsequent readings taken during Winter 2008/09.

The results show that there is a significant difference in performance across the 23 PV systems. Variables which may have had an influence on the performance included system capacity, roof pitch and effect of shading on the panels. The paper also investigates the impact of air temperature, solar irradiance, cracked cells and shunt resistance that has been shown to influence the performance of PV systems. Comparisons are made with the performance of PV systems elsewhere in the World. An estimate in annual reduction of carbon emissions from a typical installation is also made and related to the Government's 2050 carbon reduction targets.

1 Introduction

Since the housing sector currently accounts for almost 30 percent of energy used in the UK [1]; renewable energy technologies, such as solar photovoltaics, offer an opportunity to reduce carbon dioxide (CO_2) emissions from homes and contribute to the Government's target of generating 10 percent of the UK's electricity supplies from renewable sources by 2010 [2].

A project is underway which will investigate the impact of renewable energy technologies in reducing CO_2 emissions in domestic housing. The study focuses on the South Yorkshire Housing Association's (SYHA) Henley Rise Eco-Homes Development in Rotherham, South Yorkshire. The development was completed in September 2007 and consisted of 23 three bedroom affordable homes with state of the art renewable energy technologies. All homes were fitted with solar photovoltaic and solar hot water systems, this paper concentrates on the performance of the photovoltaic systems only. Surplus electricity generated from the homes is exported back to the grid and the money savings generated will be offset against residents' electricity bills. Residents of the development

(a mix of low-income and key-worker households) were also provided with carbon coaching to help them derive maximum benefit from the technology.

2 Research Significance

A review of the sustainability of existing buildings was conducted in 2006 [3] and found that 152 million tonnes of carbon (MtC) were produced by the UK in 2004. The domestic building stock was responsible for 41.7 MtC of this total, or 27% of the total carbon emissions [3]. The report goes on to say that domestic emissions will have to fall by 24.7 MtC to 17 MtC by 2050 if the domestic sector is to reduce in line with overall carbon emissions targets [3]. In addition, The Stern Review has also predicted that, due to climate change, there will be less cold related deaths in the winter but more heat related deaths in the summer. As a result, gas consumption will decrease in the winter but due to an increased use of air conditioning in the summer months to cool homes, electricity consumption will increase [3]. Regardless, the onus remains on the use of eco technology to reduce building stock emissions and the project results will help determine if 2050 emission targets are feasible.

3 Henley Rise Eco Development

A plan of the Henley Rise Eco Development is given in Fig. 1. The development consists of detached (5 No.) and semi-detached (18 No.) properties. Referring to Fig. 1, properties labelled 'A' were fitted with a 3.02 kWp photovoltaic system (58 PV tiles) on a roof pitch of 40°. Properties labelled 'B' had a similar photovoltaic design except the roof pitch was 27°. Property type 'C' (Fig. 1) were supplied with a 3.75 kWp photovoltaic system (72 photovoltaic tiles) on a 27° pitch. All properties were also fitted with solar thermal tiles (12 No., 4.67m^2 but their performance is not considered in this paper.

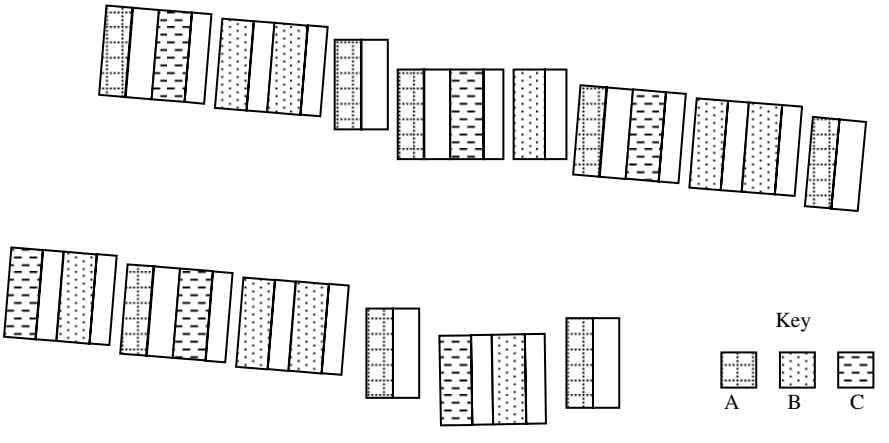

Fig. 1. Plan of Henley Rise Eco Scheme, Rotherham, UK

The plan view of the solar roofs is shown in Fig. 2. Referring to Fig. 2, the majority of the south facing roof is composed of 58 photovoltaic tiles, each covering 0.39m^2. Some shading is evident from the roof of the adjacent property meaning this area was not utilized for solar panels. However, on roofs where shading was not a problem, an extra 12 tiles were installed resulting in a 3.75 kWp PV system.

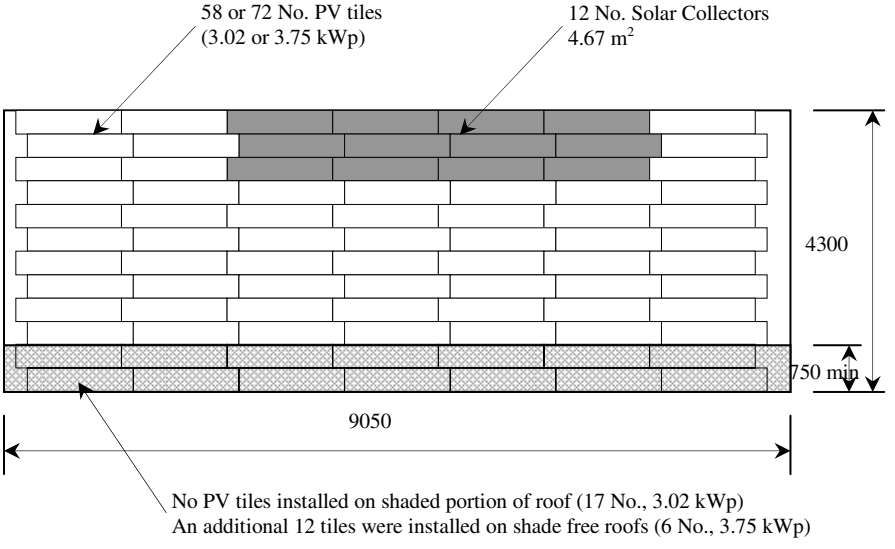

Fig. 2. Roof plan showing PV layout

4 Monitoring Solar Energy

The solar tiles (Fig. 2) are linked together to form a circuit back to an inverter. The inverter converts solar DC electricity to AC and was mounted in the loft space. An AC cable connects the inverter to the main distribution board via an isolator and kWh meter. Each property was also supplied with a display unit which had a wireless connection to the inverter meaning that each resident could monitor, for example, daily or yearly energy generation or usage. The energy generated from the photovoltaic panels were manually monitored using both the display unit and the electricity unit. Electricity meter datum readings were taken upon commissioning the systems in August or September 2007. Subsequent readings were taken in during Winter 2008/09 (November to February) as it was not possible to obtain all readings on the same day due to unavailability of residents and access to unoccupied properties. Meters readings also tied in with interviews which were conducted with the residents to gauge their response to living in an eco house [4].

5 Efficiency of Solar Photovoltaic Systems

5.1 Cumulative Performance

Table 1 gives details of the solar systems and energy generated over the monitoring period (Summer 2007 - Winter 2008/09). The house identification is given in col. 1.

Two readings are given for the majority of the twenty-three properties - one from the electricity meter (col. 2, Table 1) and one from the display unit (col. 3), except houses I, B, U and V where the display units were either not working or missing from the property. The ratio of the two readings (col. 2/col. 3) is given in col. 4. Two roof pitches were used in the design of the properties (27° and 40°) and these are shown in col. 5. Col. 6 shows if some of the roofs were subjected to shading. The monitoring period for each property is given in col. 7.

Referring to Table 1, col. 2, the best performing photovoltaic system generated 3485 kWh during the monitoring period whereas the worst system generated 633 kWh. It is clear that there is quite a considerable variation between the various properties and possible reasons will be investigated in the following sections. In addition, the meter readings are on average 8% lower than the reading from the display unit. Is likely that heat losses have occurred in the AC cable connecting the inverter to the electricity meter whereas the display unit remotely monitors energy generation direct from the inverter.

Table 1. PV monitoring data from Henley Rise

1	2	3	4	5	6	7
House ID	Energy (kWh) Elec. Meter	Energy (kWh) Display Unit	Ratio	Roof Pitch (degrees)	Shading	Monitoring Period
I	3485	-	-	27	no	Aug 07 - Dec 08
Q	3194	3434	0.93	27	no	Aug 07 - Dec 08
F	2879	3064	0.94	40	no	Aug 07 - Dec 08
K	2861	3052	0.94	27	no	Aug 07 - Nov 08
A	2621	2912	0.90	40	no	Aug 07 - Nov 08
T	2512	2745	0.92	27	some	Aug 07 - Dec 08
R	2480	2649	0.94	27	no	Aug 07 - Dec 08
H	2236	2497	0.90	40	no	Sep 07 - Feb 09
P	1876	2103	0.89	27	some	Aug 07 - Dec 08
O	1828	2065	0.89	27	some	Aug 07 - Nov 08
L	1601	1725	0.93	27	no	Aug 07 - Feb 09
C	1574	1681	0.94	40	no	Aug 07 - Feb 09
B	1515	-	-	40	no	Aug 07 - Jan 09
D	1411	1496	0.94	40	no	Aug 07 - Feb 09
G	1383	1532	0.90	40	no	Sep 07 - Nov 08
S	1299	1394	0.93	27	some	Aug 07 - Dec 08
N	1114	1256	0.89	27	some	Aug 07 - Feb 09
U	1061	-	-	27	no	Sep 07 - Feb 09
W	998	1078	0.94	27	some	Sep 07 - Jan 09
M	963	1082	0.89	27	some	Aug 07 - Feb 09
J	906	992	0.91	27	some	Aug 07 - Feb 09
V	727	-	-	27	some	Sep 07 - Dec 08
E	633	685	0.92	40	no	Aug 07 - Dec 08

The key data tabulated in Table 1 (cols. 1, 2, 5, 6) is illustrated in Fig.3. The plotted data is from the electricity meters, col. 2, Table 1 as the energy generated is available for all properties. Referring to Fig. 3, four of the higher design capacity systems (3.75 kWp) perform well in relation to the other properties. However, properties L and U both have 3.75 kWp systems installed and perform less well, property U being the sixth worst performer. However, six of the nine properties which were categorized

by the designer as being affected by shading exhibit a performance at the lower end of the graph, occupying six of the lowest eight positions in Fig. 3. Shade affected properties T, P and O perform better. The 40° roof pitches are all fitted with 3.02 kWp systems and are shade free. However, their performance varies considerably, property F having the third best performing system but property E having the worst. Further investigations are required to determine the reasons for the considerable variation in performance and this is considered in Section 6.

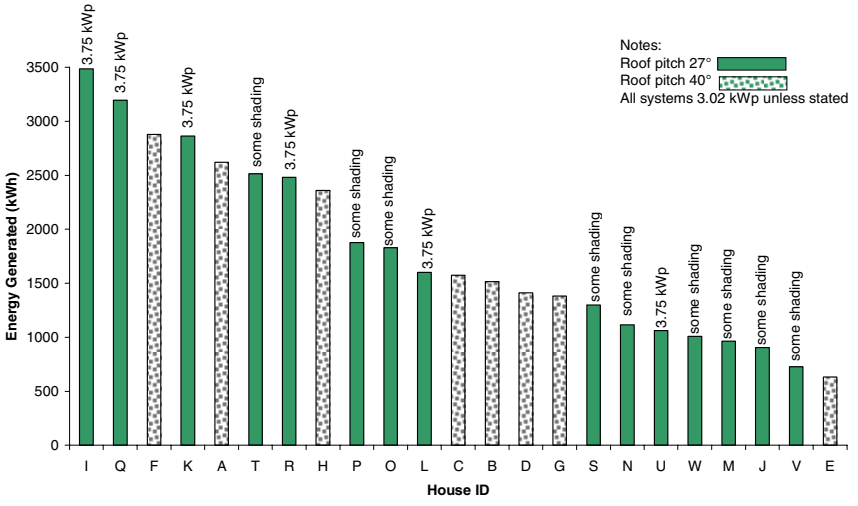

Fig. 3. Performance of PV systems at Henley Rise

5.2 12 Month Performance

Referring to Fig. 3, two of the twenty-three properties (H & W) had manual meter readings taken periodically over the monitoring period. This enabled an evaluation of their performance over a twelve month period to be undertaken. Referring to Fig. 4, readings between September 2007 and January 2009 are given although some meter readings between November 2007 and April 2008 were unavailable. It is estimated that after one year of operation, the photovoltaic system on property H generated approximately 1835 kWh of solar electricity. The same analysis is done for property W but only approximately 900 kWh of solar electricity was generated (Fig. 4). Both systems are 3.02 kWp, designed to provide up to 2400 kWh of solar electricity, or 795 kWh/kWp per annum. The output was 608 and 298 kWh/kWp for properties H and W respectively. However, further analysis is required to determine the under performance but possible reasons are given in Section 6.

The following provides performance data for other PV systems elsewhere in the UK and the world. It must be noted, however, that variations in annual irradiation, system design, location etc. will influence the performance so these figures are given only as a guide. A 34 kWp PV system in East Anglia, on a south facing façade on the top floor of a building in the UK, produced 647 kWh/kWp in 2005 [5], slightly higher

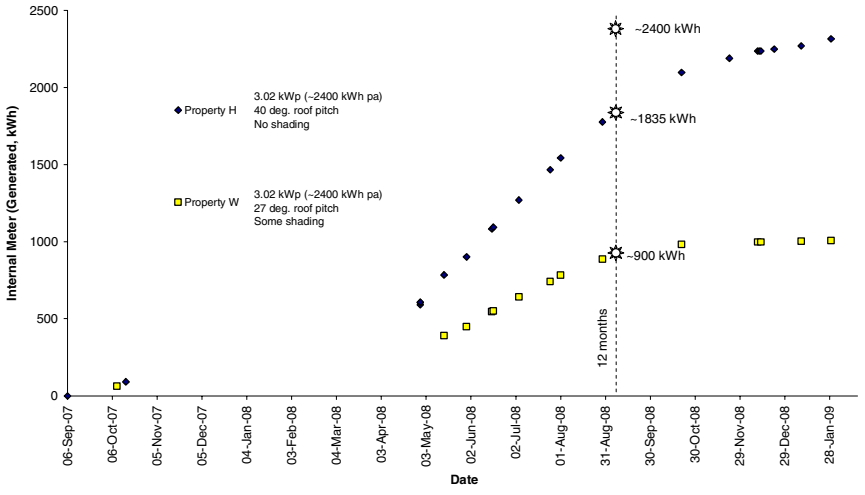

Fig. 4. PV performance over 12 month period for two properties

than property H at Henley Rise. The average of nine PV systems, commissioned in the South of England in 2004, was 807 kWh/kWp. Elsewhere in Europe, a 1 kWp PV system in Poland generated 740 and 680 kWh in two consecutive years (740 and 680 kWh/kWp) [6]. Annual yields varied between 430 and 875 kWh/kWp in Northern Germany on PV systems monitored in the 1990s [7]. A PV park on the island of Crete in Greece yielded 1337 kWh/kWp in 2007 [8] whereas a PV system in the south of Spain yielded a very similar 1339 kWh/kWp, again in 2007 [9]. In Canada, a 3.2 kWp PV system continuously produced approximately 662 kWh/kWp over a five year period from 1995 [10].

6 Degradation Mechanisms

Further research is required to pinpoint the reasons for the varied performance of the photovoltaic systems shown in Fig. 3. However, a literature review has determined the following to be reasons for poor performance in photovoltaic tiles which may or may not have influenced performance at Henley Rise.

6.1 Air Temperature and Wind Speed

Up to 14% of potential energy production can be lost when photovoltaic tiles are operating above ambient temperature. The nominal operating cell temperature of a single crystalline silicon module will be in excess of 40°C. However, wind speed has the effect of lowering the ambient temperature and, hence, the tile temperature which is beneficial for power production [11].

6.2 Solar Irradiance

Current and voltage do not vary at the same rates with increased irradiance. Current exhibits a linear increase due to increased irradiance whereas voltage varies

logarithmically [11]. This would not explain the variations in performance at Henley Rise, but if the photovoltaic tiles contained different cell materials, then a variation is possible. Solar cell performance is strongly dependent on spectral distribution and PV tiles comprising different cell materials will have different spectral outputs, which will vary as the spectral distribution varies [11].

6.3 Cracked Cells

A panel with a cracked cell can potentially produce less power. Previous research elsewhere has shown that even with a cracked cell, a module may lose as little as 2% of power [11], but the losses are dependant on the severity of the crack. A cracked cell will heat up during dissipation of the power and irreversible cell damage may occur. These mismatched cells, if not protected by bypass diodes, may enable hot spots to occur, resulting in damage to the cell. A bypass diode is a form of short-circuiting to prevent power generation and in practice, covering one cell leads to the entire substring being short-circuited if properly designed [12].

6.4 Shading

When shading occurs, the affected cell will produce less current. If the cell is connected in series to other string cells, it becomes reversed biased by the voltage generating capabilities of the other string cells. The shaded cell will operate in the negative voltage range where it becomes a dissipater of power in the form of heat. High cell temperatures will result with higher reverse bias and higher power dissipation. If the reverse bias exceeds the breakdown voltage of the cell, irreversible damage will be caused by hot spot formation, cell cracking and melting solder [13]. It was reported elsewhere that 10% shading of the cell area resulted in a power loss of 2.6% and 50% shading resulted in a power loss of 38% [13].

6.5 Shunt Paths

Low resistance precision resistors are used to measure electrical currents in the solar tiles by measuring the voltage drop across the resistance [11]. It is possible that an alternate current path for the light-generated current is developed in these high conductivity paths (shunts) [13]. This reduces current flowing through the solar cell junction and consequently reduces the voltage from the solar cell. They are typically due to manufacturing defects rather than poor solar cell design. Low light levels aggravates this problem since there will be less light-generated current. The loss of this current to the shunt, therefore, has a larger impact [14]. It was reported that a low shunt resistance in a previous experiment resulted in a power loss of up to 63% [13].

7 Carbon Reductions due to Photovoltaics

In order to estimate the impact of photovoltaics in reducing carbon emissions, the solar energy generated by Property H will be used as an example. The PV installed on this property performed above average as shown in Fig. 3. The following calculation

is used to estimate the impact of photovoltaic on one property and this figure is extrapolated to cover all domestic properties in the UK.

- Property H: 1835 kWh solar electricity generated pa (Fig. 4)
- 1 kWh of solar energy generated in place of electricity eliminates 0.568 kg CO_2
- Carbon emissions saved by Property H: 1835 x 0.568 kg = 1042 kg, say 1.042 tonnes
- There are approximately 24.8m domestic properties in the UK [15]. If every domestic property in the UK is fitted with a 3.02 kWp photovoltaic system performing as per property H, CO_2 savings would be 24.8m x 1.042 tonnes = 25.8 MtC
- Savings (25.8 MtC) > Target (24.7 MtC, Section 2), therefore, target exceeded!

However, it is perhaps too much to expect that every domestic property in the UK will be fitted with photovoltaics to a design similar to that at Henley Rise. The fact remains, however, that on average, each domestic property will have to save approximately 1 tonne of CO_2 if the Government reduction target is to be met. Application of renewable energy technologies will help in meeting this target but low cost, non-technological changes, for example, changing peoples behaviour by using more energy efficient white goods, installing more insulation for energy conservation, switching off or using standby mode on TV or audio appliances etc. will contribute significantly to this target.

8 Conclusions

The following are the main conclusions from the information presented in the paper:

- Photovoltaics are an effective way of reducing carbon emissions. However, to ensure the technologies are working at full capability, post application monitoring and maintenance is required to ensure optimum performance.
- An above average performance of one of the 3.02 kWp photovoltaic systems over a 12 month period (Property H) produced 1835 kWh of solar energy (608 kWh/kWp), less than the design value of approximately 2400 kWh (795 kWh/kWp). Property W produced only approximately 900 kWh (298 kWh/kWp).
- Property H has contributed to a reduction in carbon emissions of approximately 1 tonne as a result of installing the photovoltaic system.
- A saving of approximately 1 tonne of carbon dioxide is required by every domestic property in the UK if Government targets in CO_2 reductions are to be met by 2050.
- Reductions in carbon emission are possible not only through on-site micro generation (high cost) but also through changing peoples behaviour on how they use energy (low cost).

Acknowledgments

The authors' wish to acknowledge the financial support received for the Economic and Social Research Council's Business Engagement Scheme and South Yorkshire Housing Association. The contribution of Rotherham Metropolitan Borough Council is also acknowledged.

References

1. DTI: UK Energy in Brief, Department of Trade and Industry, London. DTI/Pub 8340/4.5k/07/06/NP. URN 06/220 (July 2006)
2. DTI: Meeting the Energy Challenge: A White Paper on Energy, Department of Trade and Industry, London (May 2007)
3. DCLG: Review of Sustainability of Existing Buildings, The Energy Efficiency of Dwellings – Initial Analysis, Department for Communities and Local Government, Product code 06 BD 04239 (November 2006)
4. Jackson, C., O'Flaherty, F.J., Pinder, J.A.: Managing change in domestic renewable energy schemes. In: SEB 2009 International Conference on Sustainability in Energy and Buildings, April 29-May 01. University of Brighton, UK (2009)
5. Tovey, K., Turner, C.H.: Carbon reduction strategies at the University of East Anglia. In: Proc. Ins. Civ. Eng. Mun. Eng., UK, December 2006, vol. 159(ME4), pp. 193–201 (2006)
6. Pietruszko, S.M., Gradzki, M.: 1 kW grid-connected PV system after two years of monitoring. Opto-Electronics Review 12(1), 91–93 (2004)
7. Decker, B., Jahn, U.: Performance of 170 grid connected PV plants in Northern Germany - Analysis of yields and optimization potentials. Solar Energy 59(4-6), 127–133 (1997)
8. Kymakis, E., Kalykakis, S., Papazoglou, T.M.: Performance analysis of a grid connected photovoltaic park on the island of Crete. Energy Conversion and Management 50, 433–438 (2009)
9. Sidrach-de-Cardona, M., Mora Lopez, L.: Performance analysis of a grid-connected photovoltaic system. Energy 24(2), 93–102 (1999)
10. Thevenard, D.: Performance monitoring of a northern 3.2 kWp grid-connected photovoltaic system. In: Photovoltaic Specialists Conference, Conference Record of the Twenty-Eighth IEEE, Anchorage, AK, USA, pp. 1711–1714 (2000), ISBN: 0-7803-5772-8, DoI: 10.1109/PVSC.2000.916233
11. van Dyk, E.E., Meyer, E.L., Vorster, F.J., Leitch, A.W.R.: Long-term monitoring of photovoltaic devices. Renewable Energy 25, 183–197 (2002)
12. Woyte, A., Islam, S., Belmans, R., Nijs, J.: Two years analytical monitoring results of an experimental photovoltaic system set-up under determined shadowing conditions. PV in Europe, Rome, Italy, October 7-11 (2002)
13. Meyer, E.L., van Dyk, E.E.: The effect of reduced shunt resistance and shading on photovoltaic module performance IEEE 0-7803-8707-4 1331-1334 (2005)
14. Honsberg, C., Bowden, S.: Photovoltaics CDROM `http://pvcdrom.pveducation.org/celloper/shunt.htm` (accessed March 20, 2009)
15. Technology Strategy Board: Materials for Energy (2007), `http://www.matuk.co.uk/docs/TSB_Materials07.pdf` (accessed March 20, 2009)

Armature and Field Controlled DC Motor Based Wind Turbine Emulation for Wind Energy Conversion Systems Operating over a Wide Range of Wind Velocity

Rahul Patel, Chetan V. Patki*, and Vivek Agarwal

Dept. of Electrical Engineering, Indian Institute of Technology-Bombay, Powai, Mumbai – 400 076, India
chetanp@ee.iitb.ac.in

Abstract. A Wind Turbine Emulator (WTE), which can mimic the steady-state wind turbine characteristics, is reported. It can be used for research and development work in the area of wind energy conversion systems, without depending on natural wind energy resources and is especially suited for testing and experimentation work in the laboratory environment. It offers a controllable test environment that allows the evaluation and improvement of control schemes for electric generators which is hard to achieve with an actual wind turbine since the wind speed varies randomly. The proposed WTE uses a Digital Signal Processor (DSP) TMS320F2812 system and a 1.1kW separately excited DC motor. A PC interface is also developed to provide friendly user interface and real time control of experiments.

1 Introduction

The ever increasing demand for **R**enewable **E**nergy (RE) has given a big boost to research on RE sources and systems. One such source is wind. Wind offers several advantages such as emission less operation, low maintenance cost and abundance. At the same time, it offers many challenges such as uncertainty about its presence and speed, relatively high initial investment and so on. Experiments on **W**ind **E**nergy **G**eneration **S**ystems (WEGS) are usually quite involved – especially in the laboratory environment because it is seldom possible to have an actual wind source in the laboratory environment. Therefore, for research on WEGS involving electric generators, power electronic converters and **M**aximum **P**ower **P**oint **T**racking (MPPT) algorithms, the usual trend is to use a wind turbine emulator in place of an actual wind energy source.

Several authors have reported **W**ind **T**urbine **E**mulators (WTE) in the past. These emulators are built either using an induction motor [1] or a DC motor [2-5]. Control of DC motors being easy, these emulators are more popular for the WTE applications-especially the armature controlled separately excited DC motors. Chinchilla et al. [3] have used a separately excited DC motor with torque control to emulate a wind turbine with user interface. Farret *et al.*, [4] have proposed a WTE, used a DC motor

* Corresponding author.

with dual closed-loop control. The scheme involves the measurement of power delivered by the generator and is, therefore, more complex. However, they have used only armature voltage control. Rabelo *et al*., [5] have emulated static as well as dynamic wind turbine characteristics.

In this paper, a WTE, based on a separately excited DC motor is described. Only the static torque-speed characteristics are emulated. The salient feature of the proposed scheme is that it uses both armature and field control for emulating the turbine. This facilitates emulation of characteristics over a wider wind speed range. This is in contrast to the earlier emulation methods which only relied on armature control of the DC motor. A PC interface has also been developed to make it user friendly and to enable real time control during the experiments.

2 Wind Turbine Characteristics and Model

A mathematical model is required to emulate the steady-state characteristics of a wind turbine. According to the aerodynamic characteristics of a wind turbine, its output mechanical power is given by [2, 6]:

$$P_m = \frac{1}{2} C_p(\lambda, \beta) \rho A V_{wind}^3 \tag{1}$$

where P_m is the mechanical output power of the turbine; C_P is the power coefficient of the turbine; ρ is the air density(g/m^3); A is the area swept by the turbine in m^2 (A = π R^2, where R is the rotor blade radius), V_{wind} is the wind speed (*m/s*). The power coefficient of a turbine is related to its tip speed ratio (λ) and rotor pitch angle (β) according to the following equation[6]:

$$C_p(\lambda, \beta) = C_1 (C_2 / \lambda_i - C_3 \beta - C_4)^{-c_5 / \lambda_i} + C_6 \lambda \tag{2}$$

where, the coefficients C_1 = 0.5176; C_2 = 116; C_3 = 0.4; C_4= 5; C_5 = 21 and C_6 = 0.0068. λ_i is given by the following equation[6]:

$$\lambda_i = \frac{1}{\dfrac{1}{\lambda - 0.02\beta} - \dfrac{0.003}{\beta^3 + 1}} \tag{3}$$

$$\Rightarrow \quad \lambda = \frac{\omega_r R_r}{V_{wind}} \tag{4}$$

There are two methods by which wind turbine characteristics can be obtained – (i) The **L**ook **U**p **T**able (LUT) method and (ii) Using steady-state model equations of the wind turbine. Implementation of the LUT method is easy but not that accurate. Another issue with this approach is that if the turbine parameters are changed, the table should be totally replaced (changed). In the second method, by merely changing some of the parameters, WTE can be made to emulate different turbines. In this method,

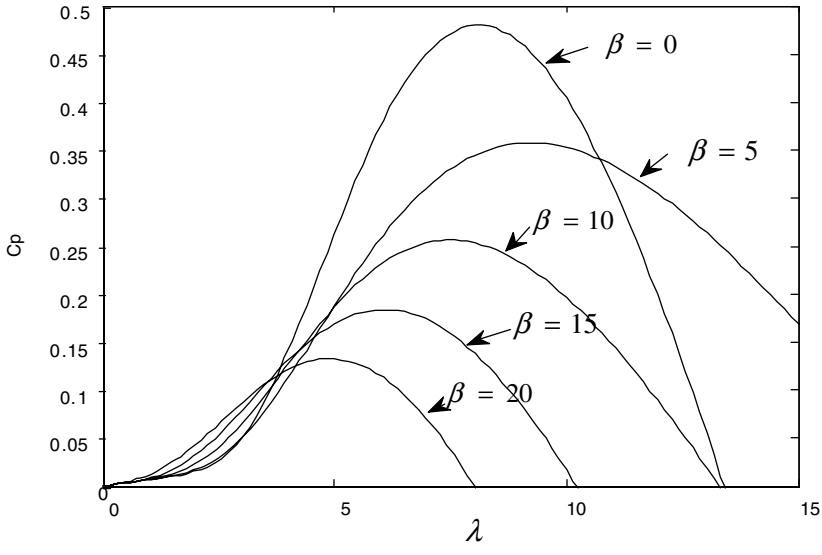

Fig. 1. Cp-λ curve for various pitch angles

first the *Cp-λ* curves are obtained according to which the DC motor reproduces the expected torque versus speed characteristic. Maximum power produced by a WTE should not exceed the rated power of the induction generator used. When the wind speed crosses a certain threshold value, pitch angle control is introduced so that the rated power of the induction generator is not exceeded in spite of a higher wind speed.

3 Steady State Model of the Wind Turbine Emulator and Simulations

For testing the MPPT, the WTE should satisfy various requirements of a Wind Energy Conversion System. It should accurately produce expected shaft torque and speed. In this situation, the output torque can be calculated by:

$$T = \frac{1}{2}\pi C_T(\lambda,\beta)\rho R_r^3 V_{wind}^2 \tag{5}$$

$$C_T = \frac{C_p}{\lambda} \tag{6}$$

The steady state mathematical model of a DC motor is given by [2]:

$$E = K_e \phi \omega \tag{7}$$

$$V = E + R_a I_a \tag{8}$$

$$T_e = K_t \phi I_a \tag{9}$$

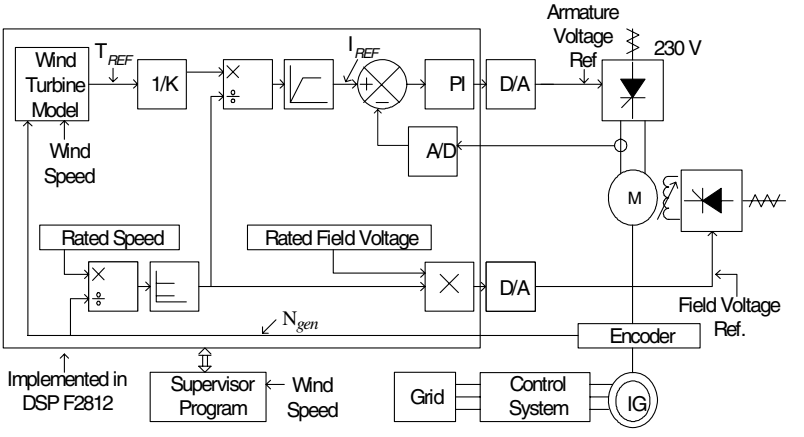

Fig. 2. Control diagram of the torque control scheme

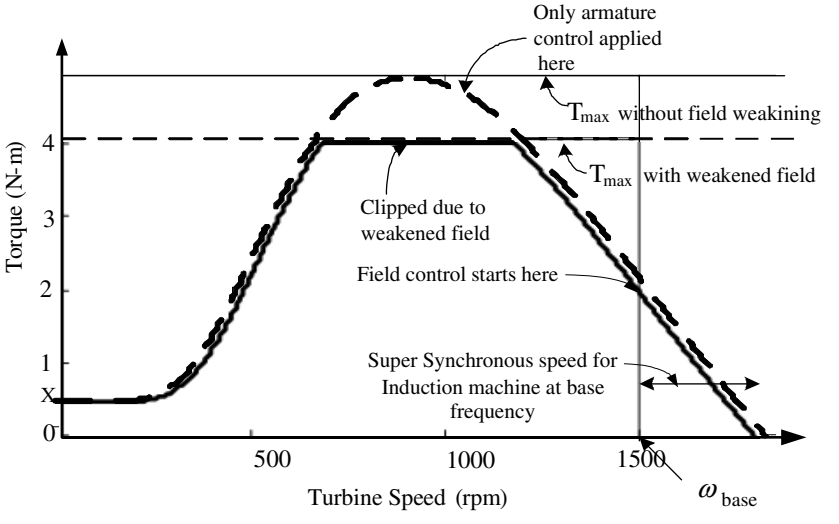

Fig. 3. Torque-Speed characteristics of Wind Turbine Emulator

where, K_e, K_t are the electromagnetic and torque constants respectively of the machine, ω is the angular speed of the DC motor, ϕ and T_e are the air gap flux and electromagnetic torque respectively. In contrast with the direct current control method used earlier [2,4], in this work, the DC motor current is directly controlled (with rated field voltage) up to the rated speed. Beyond the rated speed, field voltage is reduced and the reference current is changed according to the reference torque and field voltage. Fig. 2 shows the block diagram and the scheme of the entire control system. The simulated speed versus torque characteristics from the proposed WTE are shown in Fig. 3. It must be noted that for higher wind speeds, it is imperative for the dc motor based emulator to operate beyond its base speed (ω_{base}). But this is not realizable with armature voltage control alone without exceeding the motor voltage rating.

Hence, field control is the only option. A weakened field right from the beginning (point 'x' in Fig. 3) extends the speed range of the emulator, but brings down the maximum realizable torque. Fig. 3 shows the clipping of 'T_{max}' due to field weakening. A better option is to use field weakening beyond the based speed of dc motor by when the torque requirement reduces anyway.

This also conforms to a typical laboratory set-up, which usually consists of a dc machine-induction machine pair, with both machines of comparable ratings. In order to emulate a wind turbine with such set-ups, a typical scenario will involve the induction motor operating at super-synchronous speed, i.e. a speed greater than its base speed and that of the dc motor. This, again, supports the proposition that the field weakening is applied only beyond the base speed.

4 Wind Turbine Emulator

The emulation of the wind turbine is implemented by means of a 1.1 kW, 1500 RPM DC motor using armature/field control. A current reference is generated from the

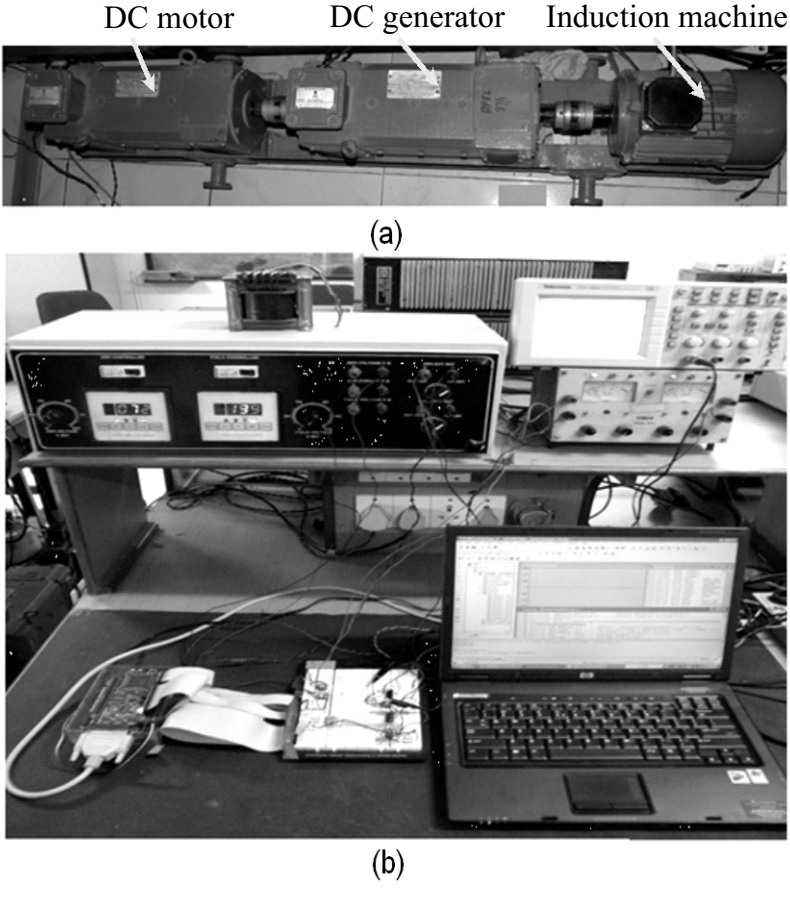

Fig. 4. (a) DC motor-generator set; (b) Control circuitry and DC motor drive

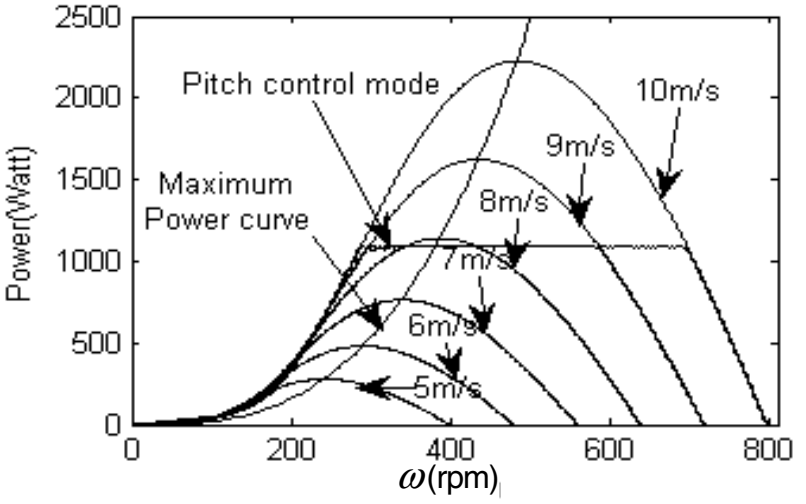

Fig. 5. Power-Speed curve for different wind speed

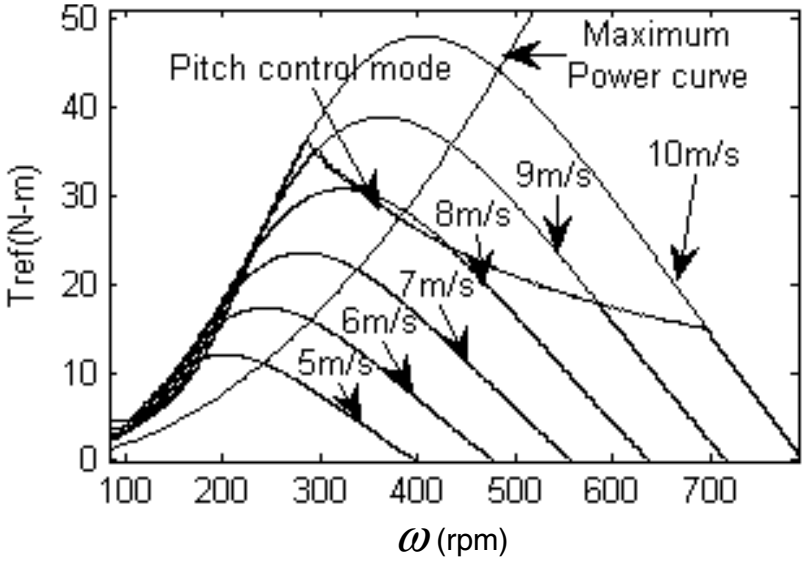

Fig. 6. Torque-Speed curve for different wind speed

torque reference obtained though a **W**ind **T**urbine **M**odel (WTM) implemented on a Digital Signal Processor (DSP) TMS320F2812 using (2) through (6) and passed on to an intelligent power supply module through a D/A converter on the control board, which, in turn, controls the DC drive's voltage. In order to calculate the reference torque, the control program communicates with a supervisory program running on a PC to acquire information about the wind velocity. The motor's speed (N_{gen}) is measured online. The supervisory program provides a user-friendly interface and wind turbine parameters and wind velocity values can be easily changed. Fig. 4 shows the hardware set-up for the proposed WTE.

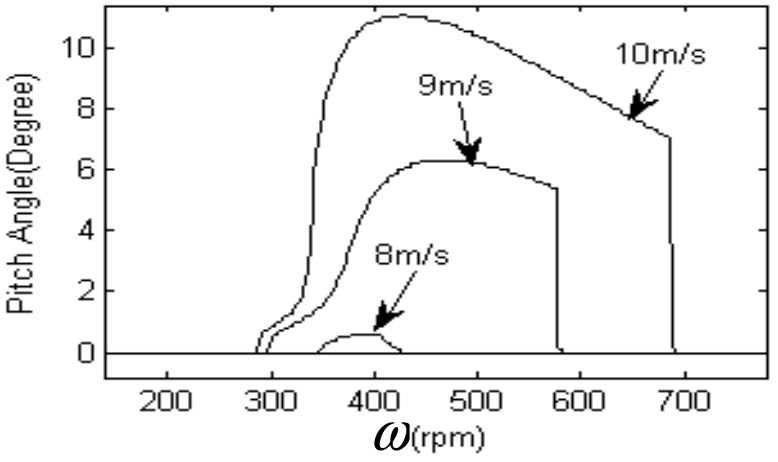

Fig. 7. Pitch angle-Speed curve in Pitch angle control mode for different wind speed

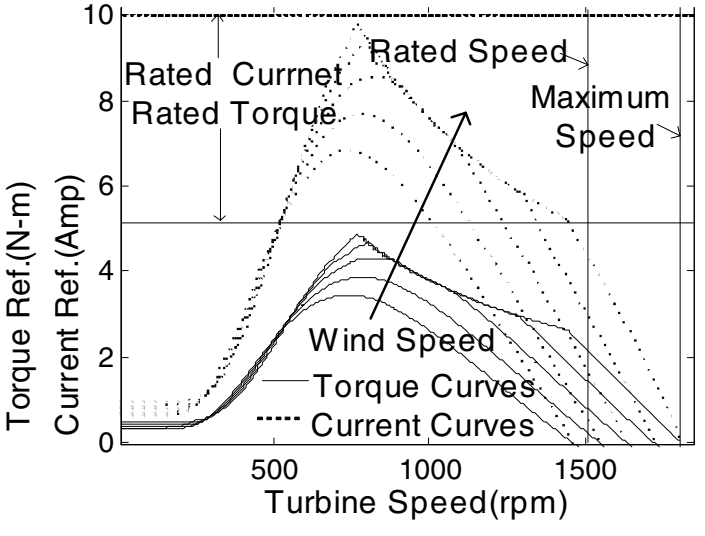

Fig. 8. Reference Current-Speed and Reference Torque-Speed curve for WTE

Figs. 5 and 6 show the power versus speed and torque versus speed curves respectively, obtained from the WTM for different wind speeds (turbine rotor radius, R=1.6m). Output of WTM becomes the torque reference for DC motor. Fig. 7 shows the pitch angle versus speed curves for a turbine with rotor radius R=1.6m. DC motor being used in emulation has rated current of 10Amp. Fig. 8 shows reference current and reference torque verses speed graph generated by DSP for different wind speeds.

5 Experimental Results

In this section some of the key experimental results of the developed WTE are given and compared with the actual Wind Turbine characteristics. As mentioned earlier, in order to calculate the reference torque, the control program communicates with a

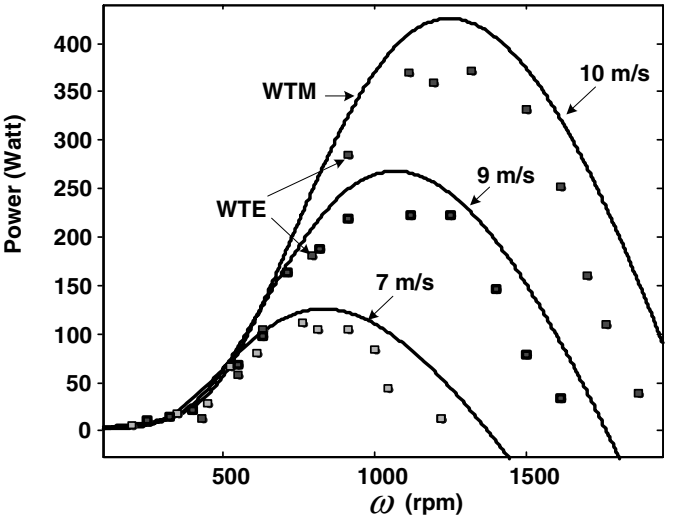

Fig. 9. Experimental Results: Comparison of Power-Speed characteristics obtained using WTM and WTE

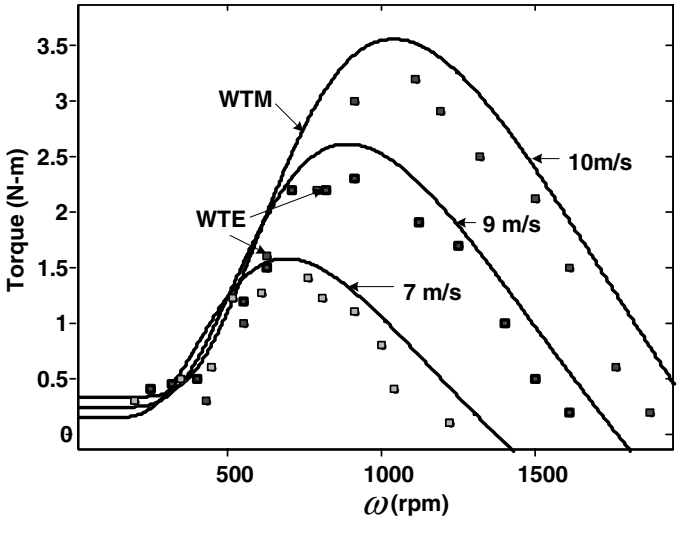

Fig. 10. Experimental Results: Comparison of Torque-Speed characteristics obtained using WTM and WTE

supervisory program running on a PC to acquire the wind velocity and the expected operating mode (armature control or field weakening mode control) is determined. Turbine radius in our experiments is 0.7m and the experiment has been conducted for wind speeds of 7m/s, 9m/s and 10m/s..Fig. 9 shows comparison between simulated Power-Speed characteristics with the experimental results obtained for the same during constant pitch angle(β =0) Fig. 10 shows comparison between simulated Torque-Speed characteristics with the experimental results obtained for the same during constant pitch angle(β =0). As the load increases, both the motor speed and tip speed ratio decreases and C_p is increased, as clearly as indicated by wind turbine Cp-λ characteristic of Fig.1. But in pitch angle control mode, the pitch angle is increased to limit the value of C_p such that the output is limited to 1.1 kW.

6 Conclusion

A WTE is a convenient option which facilitates research on WECS. It provides a controlled and flexible test environment for wind turbine related experiments. Simulation and experimental results obtained with the proposed WTE have demonstrated its effectiveness as the characteristics obtained using emulation are found to match well with those of the actual wind turbine. The combination of armature and field control has rendered a WTE that can work over a wide wind velocity range without violating the power rating of the induction generator.

The limitation of the proposed system, however, is that it can emulate only steady-state characteristics. Work is underway on an emulator which can provide both steady-state and dynamic characteristics. This will be presented in a future paper.

References

[1] Kojabadi, H.M., Changand, L., Boutot, T.: Development of a Novel Wind Turbine Simulator for Wind Energy Conversion Systems Using an Inverter-Controlled Induction Motor. IEEE Trans. Energy Conversion 19(3), 547–552 (2004)

[2] Li, W., Xu, D., Zhang, W., Ma, H.: Research on Wind Turbine Emulation based on DC Motor. In: 2nd IEEE Conference on Industrial Electronics and Applications, Harbin, China, May 2007, pp. 434–436 (2007)

[3] Chinchilla, M., Arnaltes, S., Rodriguez Amenedo, J.L.: Laboratory set-up for Wind Turbine Emulation. In: IEEE International Conference on Industrial Technology Hammamet, Tunisia, pp. 553–557 (2004)

[4] Farret, F.A., Gules, R., Marian, J.: Micro-turbine Simulator based on Speed and Torque of a DC Motor to Drive Actually Loaded Generators. In: First IEEE international Caracas Conference on Devices, Circuits and Systems, Caracas, Venezuela, December 1995, pp. 89–93 (1995)

[5] Rabelo, B., Hofmann, W., Gluck, M.: Emulation of the Static and Dynamic Behaviour of a Wind-turbine with a DC-Machine. In: 35th Annual IEEE Power Electronics Specialists Conference (APEC), Aacken, Germany, pp. 2107–2112 (2004)

[6] Heier, S.: Grid Integration of Wind Energy Conversion Systems. John Wiley and Sons Ltd, Chichester (1998), ISBN 0-471-97143-X

[7] Petru, T., Thiringer, T.: Modeling of wind turbines for power system studies. IEEE Trans. Power Systems 17(4), 1132–1139 (2002)

Utilization of Fly-Ash Products from Biomass Co-combustion and Zeolite 13X for Building Energy Conservations

C.W. Kwong[1] and C.Y.H. Chao[2,*]

[1] Environmental Engineering Program, School of Engineering, The Hong Kong University of Science and Technology, Clear Water Bay, Hong Kong
[2] Department of Mechanical Engineering, The Hong Kong University of Science and Technology, Clear Water Bay, Hong Kong
Tel.: (852) 2358 7210; Fax (852) 2358 1543
meyhchao@ust.hk

Abstract. Catalytic ozonation of volatile organic compounds (VOCs) using biomass combustion derived fly-ash products and zeolite 13X was investigated for applications in an integrated air purification and desiccant cooling system. Fly-ash products from rice husk- coal co-combustion at different biomass blending ratios were used. The material characteristics such as metal content and surface area were compared and correlated with the catalytic activities. It was found that the surface area and the metal constitutes have made the catalytic activities over the fly-ash products from biomass combustion superior to that from coal-only combustion. The elevated reaction temperatures from 25°C to 75°C also have significant effects to the catalytic activities. On the other hand, the potential synergy to Zeolite 13X was explored. The combined catalytic ozonation and adsorption not only enhance VOCs removal, but also minimize intermediate species emission. Furthermore, the hydrophilic properties of Zeolite 13X can be utilized to handle the latent load of the conventional air conditioning system for energy conservations.

1 Introduction

The use of biomass for power generation has been regarded as one of the attractive green house gas reduction strategies. Co-combustion of biomass with coal is a practical and attractive approach for renewable energy generations [1, 2] and thus, it is anticipated that significant amount of fly-ash products (FAP) will be produced with the use of biomass energy. Currently, the FAP produced from most of the power plants is land-filled or stored in ash lagoons [3]. These disposal methodologies do not only increase the burden of the landfills, but also create significant impacts to the surrounding environments. The disposals of FAP are problematic, yet it can be a useful resource for various applications if handled appropriately.

Numerous researchers have pioneered the conversion of FAP from coal and biomass combustion into various adsorbents [4-6] or catalysts [7] for environmental

* Corresponding author.

applications. The attractiveness of using biomass FAP as catalyst originates from its low cost and abundance from biomass power plants. Recent research [7] has shown that the metal compounds present in the biomass FAP may serve as the effective active sites for various molecular decompositions, such as ozone decomposition. These metal compounds include manganese, iron and magnesium [8] and they decompose ozone into oxygen and some active species, like atomic oxygen and free radicals for the elimination of volatile organic compounds (VOCs). Although ozone itself can be an indoor air pollutant, the use of ozone for the catalytic oxidation (ozonation) of low concentration VOCs with FAP has several advantages over the use of the traditional adsorption and catalytic combustion methods. It converts VOCs into the innocuous final products such as CO_2 and H_2O at room temperature so that intensive heat source and frequent regeneration are not required. VOCs ozonation over the FAP combines the advantage of those traditional methods while minimizing energy consumption. In addition, FAP can combine with an appropriate hydrophilic adsorbent, such as zeolite 13X, to further improve the removal of VOCs and simultaneously control the relative humidity (RH) of the process air. From the perspective of energy conservations, the removal of VOCs enhances the indoor air quality (IAQ) so that the fresh air supply to the building environment can be reduced. Also, the hydrophilic property of the adsorbent shares the latent cooling load of the ventilation system. These characteristics are attractive when incorporating the FAP into the building environment to improve the indoor environmental quality (IEQ) and energy performance. In this paper, the ozonation of VOCs using various FAP from biomass co-combustion and the combination of FAP and zeolite 13X were evaluated. The conceptual design of a hybrid ventilation system was also discussed.

2 Experimental

The FAP used in this study was produced from the bench scale pulverized fuel combustion facility [2]. Coal and rice husk were the fuels for co-combustion and the fuel characterization were described in our previous study [2]. The combustion parameters including the excess air ratio and the relative moisture content were set at 30% and 8%, respectively. The BET surface area and the bulk chemical compositions of FAP were determined by the N_2 physisorption analysis (Coulter, model: SA 3100) and the X-ray Fluorescence (XRF) analysis (JEOL, model: JSX-3201Z), respectively. The FAP from 100% (Ash_{100}), 30% (Ash_{30}) and 0% (Ash_0) biomass blending ratios (BBR) were used to represent the FAP produced from biomass only combustion, co-combustion at optimum ratio [2] and coal only combustion, respectively. They were collected by cascade impactors in the size range of 3.3- 9 μm and around 1 g of FAP was extracted and distributed over the ceramic wool in the first round of experiments. The high porosity (~0.9) of the ceramic wool enables a large surface area for FAP loading for enhanced mass transport. In the second round of experiments, around 1g of Zeolite 13X was loaded after the FAP to study the combined performance. Zeolite 13X was obtained commercially (Sigma- Aldrich) and its properties were reported previously [9, 10].

Catalytic ozonation experiments were carried out in a fixed bed flow reactor as shown in Fig. 1. The FAP and zeolite 13X were loaded in quartz tubes with 7mm

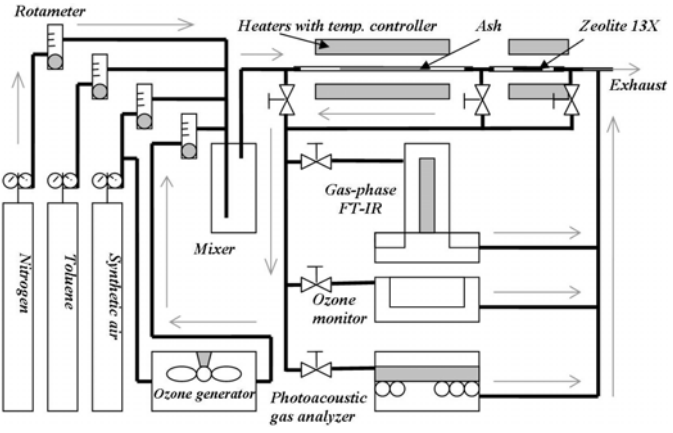

Fig. 1. Schematic diagram of the fixed bed flow reactor

inner diameter. Toluene was used as the VOCs source and the reaction gas was prepared from a standard toluene gas cylinder with 5 ppmv balanced in nitrogen. This was mixed with synthetic air so that the toluene concentration at the reactor inlet was maintained at 1.5 ppmv. Ozone was synthesized from the molecular oxygen in the synthetic air by a corona discharge ozone generator and it was maintained at 36 ppmv at the reactor inlet. This inlet concentration ensured the ozonation process was not limited by the ozone supply [10]. Besides, the RH level was maintained at 0% to eliminate the effect of moisture to the ozonation process. The gas flow rate was fixed at 0.21 m^3/h and the gas outlet was coupled with a photoacoustic multigas monitor (Innova, model: 1312) for real time RH, toluene and carbon dioxide (CO_2) monitoring. Also, the ozone concentration was monitored by an ozone monitor (API ozone monitor, model: 450) and the intermediate species was analyzed by a gas phase Fourier Transform Infrared (FT-IR) spectrometer (Bruker, model: Tenser 27) equipped with a gas cell of 35 m path length (Infrared Analysis, model: 35-V-H). The temperature of the reactor was maintained at around 25 ^oC, 50^oC and 75 ^oC to study the effect of temperature to the ozonation activities and it was regulated by a temperature controller (Cole Parmer Digi Sense, model: 89000-05) with a K-type thermocouple. Before each round of experiments, the FAP and zeolite 13X were heated at 350 ^oC for 4 h to remove the containing moisture and organic contaminants. In addition, control experiments were conducted to evaluate the effect of the ceramic wool on ozone and toluene decompositions.

3 Results and Discussions

FAP as Catalyst

The ozonation of toluene over ceramic wool was evaluated and it was found that the toluene and ozone adsorption/ conversion were less than 3% and 5%, respectively, and hence its effect was neglected in our discussions. Fig. 2 shows the time courses of toluene ozonation over three kinds of FAP. It is seen that the adsorption-desorption

equilibrium [11] was attained in around 50- 100 min. Coal fly-ash (Ash_0) attained the equilibrium in around 50 min, followed by Ash_{30} and Ash_{100} in 65 min and 100 min respectively. This time scale probably depended on the surface area of the FAP. As showed in table 1, the BET area of Ash_{100} is much larger than Ash_{30} and Ash_0. The released volatile from the biomass structure during the combustion process led to significant pore-development [12] and thus Ash_{100} was demonstrated to adsorb more pollutant in the initial adsorption stage.

After the adsorption– desorption equilibrium, various FAP demonstrated the net ozonation activities towards the elimination of toluene. The ozonation process was initiated by a range of metals in the form of manganese oxides (MnO_x), iron oxides (Fe_2O_3) and magnesium oxides (MgO) present in the FAP as shown in Table 1. These metal oxides were found to have the highest ozone decomposition activity among the other metal oxides [8]. It is seen that around 15- 54% of toluene were converted with various FAP. In particular, Ash_{100}, Ash_{30} and Ash_0 reduced the 1.5 ppmv inlet toluene to around 0.7 ppmv, 1.0 ppmv and 1.3 ppmv at steady state, respectively. Ash_{100} recorded the highest performance among the other FAP. This was probably because of the largest surface area for enhanced mass transfer and the metal oxide constitutes to generate active species such as atomic oxygen for toluene decomposition. In contrast, the reduced surface areas of Ash_0 and Ash_{30} might offset the effect of high oxide constitutes so that the toluene conversions were weaker than Ash_{100}.

Table 1. BET surface analysis and the bulk elemental analysis by XRF

BET surface area (m^2/g)		Elemental composition analysis by XRF (wt%)										
Fly-Ash products	S_{BET}	SiO_2	Al_2O_3	Fe_2O_3	CaO	MgO	SO_3	Na_2O	K_2O	P_2O_5	MnO_x	Rest
Ash_0	3.8	15.9	15.1	20.4	17.5	3.8	20.6	3.4	1.8	0.1	0.2	1.2
Ash_{30}	22.6	47.1	7.4	11.3	11.8	3.6	8.2	2.2	3.8	1.3	0.4	2.9
Ash_{100}	58.5	82.2	1.7	2.3	1.5	2.1	-	1.4	6.3	0.6	0.8	1.1

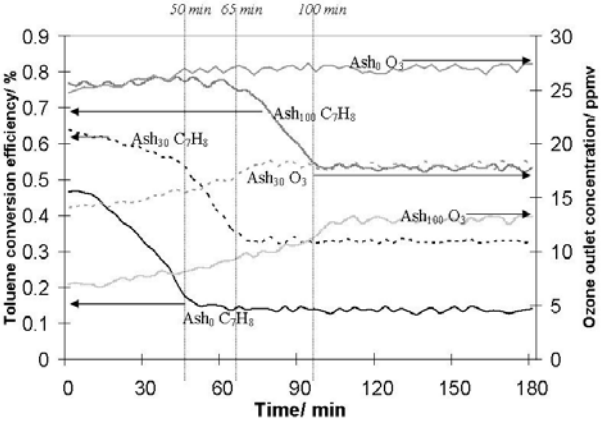

Fig. 2. Toluene conversion efficiencies and outlet ozone concentrations over various FAP. Experimental conditions: Toluene, 1.5 ppmv; Ozone, 36 ppmv; Mass of FAP, 1 g; Residence time, 0.15 s; Temperature, 24-26 ^oC.

Fig. 2 also shows the time courses of ozone outlet concentrations over various FAP. It is seen that the transient states of ozone outlet concentration took around 50-100 min. This time range was consistent with the adsorption- desorption equilibrium time for toluene as described earlier. During these transient states, the combined effects of adsorption and reaction over the fly-ash surface might contribute to the high removal for both toluene and ozone. When steady states were attained i.e.: adsorption-desorption equilibrium, the removal efficiencies were maintained at the levels lower than the transient states, depending on the fly-ash composition. The net removal of toluene at steady state was solely by the ozonation effects as the adsorption-desorption equilibrium was attained in the earlier stage. The ozonation behaviors of FAP were different with the adsorbents such as zeolites and MCM-41 materials [9, 10]. The ozonation reactions from the FAP would continue after the initial adsorption stage, while the ozonation reactions over the pure adsorbent system could only occur during the initial adsorption stage. In the ozonation system with pure adsorbent, all the reaction products remained in the adsorbed phase, therefore the active sites would be deactivated after the initial adsorption stage when the Lewis acid sites were fully occupied and blocked by the reaction products. On the contrary, the reaction products from the FAP desorbed to gas phase after the reactions. As a result, they would not accumulate at the metal sites and the reactions could continue after the initial adsorption stage.

Effect of Temperature on Ozonation Activity

Fig. 3 showed the effect of temperatures to the ozonation activity on various FAP. Results showed that the toluene conversions increased with the temperature for all cases and the performance of Ash_0 was the most sensitive to the change of temperature. In particular, the toluene conversation efficiencies of Ash_0, Ash_{30} and Ash_{100} were enhanced to 42%, 57% and 67% at a reaction temperature of 75°C, respectively. On the other hand, the outlet ozone concentrations diminished with temperature as showed in the same figure. The elevated reaction temperatures might further reduce the energy barriers of the reaction and hence the conversion efficiencies of for both toluene and ozone increased.

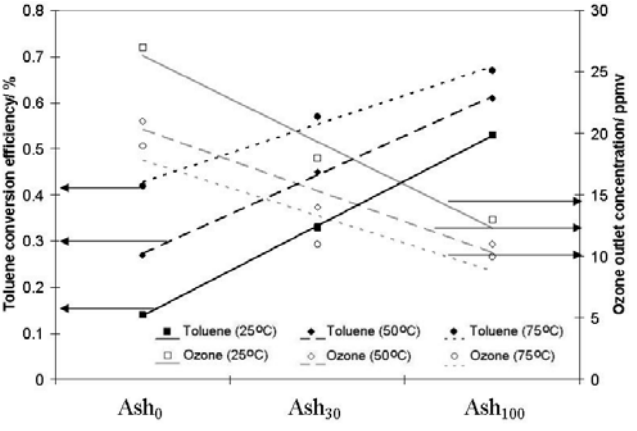

Fig. 3. Effect of temperature on steady state toluene conversion efficiency and ozone outlet concentration over various FAP. Experimental conditions: Toluene, 1.5 ppmv; Ozone, 36 ppmv; Mass of FAP, 1 g; Residence time, 0.15 s; Temperature, 25-75 °C.

Reaction Products

The gas phase FT-IR analysis indicated that CO_2 and H_2O were the major reaction products from the ozonation process and this was consistent with our previous findings [9, 10]. However, trace amounts of intermediate species were also found in the gas spectra. They included aldehydes, formic acids and carbon monoxide (CO). These were the incomplete reaction products from the catalytic ozonation and their concentrations were small compared with the major reaction products such as CO_2 and H_2O. Most of them were also found in the ozonation process over Zeolite and MCM-41, except CO. This was probably because of the different reaction mechanisms involved. The active sites of ozonation were Lewis acid sites for adsorbents and metal sites for FAP. The incomplete ozonation of VOCs over metal sites such as MnO_x might lead to the formation of CO [8]. The formation mechanism of CO and the corresponding concentrations of the intermediate species will be further investigated.

Combined FAP and Zeolite 13X

The release of intermediate species from the FAP was undesirable as discussed in the last section and this might limit the use of FAP in the building environments. However, if the FAP is combined with Zeolite 13X, the intermediate emissions can be minimized. Since the intermediates released from the FAP can either be oxidized in the zeolite or kept in the adsorbed phase.

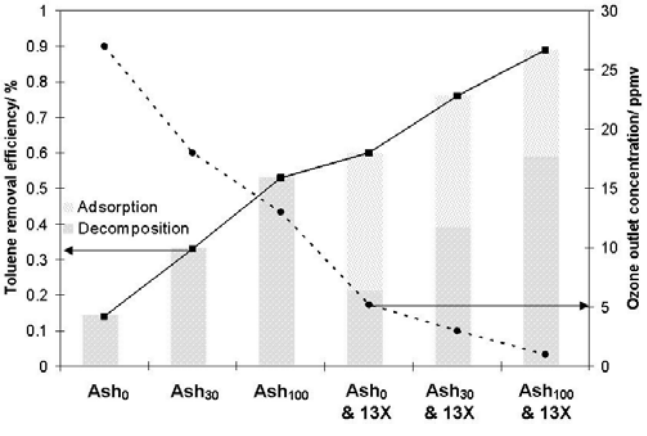

Fig. 4. Effect of the combined use of FAP and zeolite 13X on steady state toluene conversion efficiency and ozone outlet concentration. Experimental conditions: Toluene, 1.5 ppmv; Ozone, 36 ppmv; Mass of FAP, 1 g; Mass of Zeolite, 1 g; Residence time, 0.15 s (FAP only), 0.22 s (FAP+ 13X); Temperature, 24-26 ^oC.

Fig. 4 showed the results of the toluene removal over various FAP and Zeolite 13X at room temperature. The breakdown of the total removal efficiency contributed by adsorption and decomposition were also indicated. It was seen that the overall removal efficiency climbed to around 90% and the residual ozone was reduced to 1 ppmv in the case of the combined Ash_{100} and zeolite 13X. The enhanced effect was the combination of adsorption and catalytic ozonation (decomposition) over the FAP

and Zeolite. The decomposition fraction were estimated to account for around 60-70% of the total removal of toluene. This estimation was the summation of the fly-ash activity showed in Fig. 3 and the zeolite activity based on the adsorption- desorption results presented in our previous ozonation study [10]. The combined removal efficiency was higher than that of wither the pure FAP or the Zeolite 13X system [10]. On the other hand, most of the intermediate species including aldehydes and formic acids were retained in the adsorbed phase of the zeolite because they were not found in the downstream FT-IR gas spectra. On the contrary, the CO generated from the ozonation of toluene over the fly-ash surface was not adsorbed by the zeolite and existed in the downstream gas spectra. Its concentration was nevertheless well below the safety exposure limit as the major reaction products were CO_2 and H_2O.

Design of the Integrated Air Purification and Desiccant Cooling System

The second advantage in combining FAP and zeolite 13X is that they might be utilized as integrated air purification and cooling system. The zeolites 13X not only adsorbs pollutants, but also adsorb moisture from the air stream. The latent cooling load of the building can then be handled separately for energy conservations. Fig. 5 shows the design of the integrated air purification and cooling system. In the process air side, the air will be mixed with the optimum amount of ozone through the ozone generator (I). This optimum amount can be calculated from the VOCs sensor based on the inlet VOCs concentration. The air containing ozone, moisture, VOCs etc will first pass through the FAP filter (II) for the first stage ozonation process. In this process, most of the VOCs will be degraded into CO_2 and H_2O, together with some intermediate species as described in the last section. This air mixture will then go through the second stage ozonation process across the zeolite 13X filter (III). Most of the remaining VOCs, intermediates and moisture will be removed in this stage. After this stage, the temperature of the process air will be elevated to around 40- 70^oC (depending on the amount of moisture adsorbed) due to the heat of moisture adsorption on the zeolite 13X. This heat will be recovered to the regeneration side through a heat wheel (IV) and the pre-cooled and dry air will pass through the evaporator (V) of a conventional vapor compression (VC) system for temperature control.

On the other hand, most of the heated and humidified air from the conditioned space (VI) will be returned to process (1) and part of them will be ducted to the regeneration side. In this side, the air will be humidified to the saturation point by an evaporative cooler (VII) in order to reduce the air temperature for effective heat transfer over the heat wheel (IV). The pre-heated air will be mixed with the exhaust air stream from the condenser of VC system (VIII). The air mixture will further heat up to the regeneration temperature by the solar assisted electric heater (IV). The regeneration temperature depends on mass flow rate, the loading and the types of pollutants adsorbed on the zeolite, temperature as low as 65^oC [13] and 100^oC [14] can be used for the regeneration of moisture/ CO_2 and VOCs, respectively. The residual heat after the regeneration of the zeolite wheel (III) will be extracted by a heat exchanger (X) to heat up the FAP for enhanced ozonation. In addition, the exhaust heat can be recovered to preheat the regeneration air.

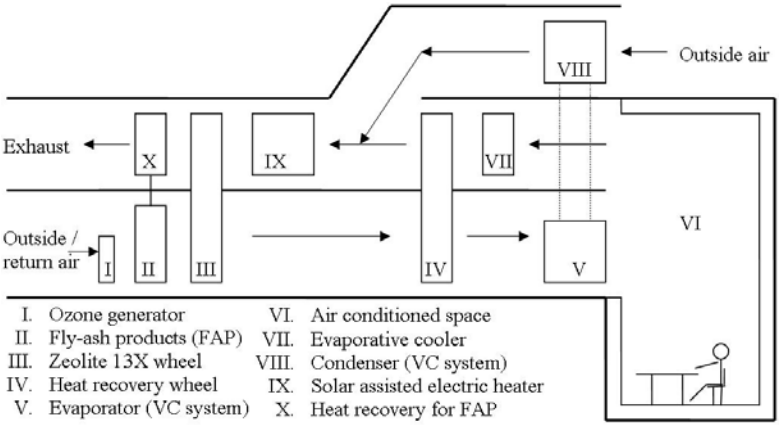

Fig. 5. Schematic diagram of the air purification and desiccant cooling system

With the use of the integrated system described above, individual IEQ parameters can be adjusted independently. For instance, the IAQ and the RH levels can be controlled by adjusting the amount of air passing through the FAP and Zeolite filter. Moreover, the sharing of the latent cooling loads helps to reduce the energy consumption of the VC system, particularly in the seasons with high humidity ratio [15]. Also, the indoor air temperature can be maintained close to the upper limit of the thermal comfort range with a relatively low RH level for further energy conservations.

4 Conclusions

In this paper, we have shown that the FAP from pure biomass combustion (Ash_{100}) demonstrated the highest degree of ozonation activity on the elimination of toluene, followed by Ash_{30} and Ash_0. Results also suggested that the combined use of FAP and zeolite 13X have not only enhanced the removal of VOCs, but also suppressed the release of the intermediates by holding them in the adsorbed phase over zeolite. The moisture and pollutant removal characteristics of the combined FAP and zeolite 13X system may be applicable for the use in an integrated air purification and desiccant cooling system for building energy conservations. Further research is required to understand the effect of moisture to the ozonation activity and determine the ozonation kinetics, the regeneration characteristics and the quantification of the intermediate species from various FAP.

Acknowledgements

Funding for this study was provided by the Hong Kong SAR Government through RGC Grant 611507.

References

[1] Demirbas, A.: Sustainable cofiring of biomass with coal. Energy Convers Manage 44, 1465–1479 (2003)

[2] Kwong, C.W., Chao, C.Y.H., Wang, J.H., Cheung, C.W., Kendall, G.: Co-combustion performance of coal with rice husks and bamboo. Atmos Environ. 41, 7462–7472 (2007)

[3] Haynes, R.J.: Reclamation and revegetation of fly ash disposal sites – Challenges and research needs. J. Environ. Manage. 90, 43–53 (2009)

[4] Fan, Y., Zhang, F.S., Zhu, J., Liu, Z.: Effective utilization of waste ash from MSW and coal co-combustion power plant—Zeolite synthesis. J. Hazard Mater. 153, 382–388 (2008)

[5] Hui, K.S., Chao, C.Y.H.: Synthesis of MCM-41 from coal fly ash by a green approach: Influence of synthesis pH. J. Hazard Mater. 137(2), 1135–1148 (2006)

[6] Hui, K.S., Chao, C.Y.H.: Methane emissions abatement by multiion-exchanged zeolite A prepared from both commercial-grade zeolite and coal fly ash. Environ. Sci. Technol. 42, 7392–7397 (2008)

[7] Kastner, J.R., Ganagavaram, R., Kolar, P., Teja, A., Xu, C.: Catalytic ozonation of propanal using wood fly ash and metal oxide nanoparticle impregnated carbon. Environ. Sci. Technol. 42(2), 556–562 (2008)

[8] Dhandapani, B., Oyama, S.T.: Gas phase ozone decomposition catalysts. Appl. Catal. B.-Environ. 11, 129–166 (1997)

[9] Kwong, C.W., Chao, C.Y.H., Hui, K.S., Wan, M.P.: Removal of VOCs from indoor environment by ozonation over different porous materials. Atmos. Environ. 42, 2300–2311 (2008)

[10] Kwong, C.W., Chao, C.Y.H., Hui, K.S., Wan, M.P.: Catalytic ozonation of toluene using zeo-lite and MCM-41 materials. Environ. Sci. Technol. 42, 8504–8509 (2008)

[11] Einaga, H., Futamura, S.: Effect of water vapor on catalytic oxidation of benzene with ozone on alumina-supported manganese oxides. J. Catal. 243, 446–450 (2006)

[12] Raveendran, K., Ganesh, A.: Adsorption characteristics and pore-development of biomass-pyrolysis char. Fuel 77(7), 769–781 (1998)

[13] Shen, C.M., Worek, W.M.: The second-law analysis of a recirculation cycle desiccant cooling system: cosorption of water vapour and carbon dioxide. Atmos. Environ. 30(9), 1429–1435 (1996)

[14] Baek, S.W., Kim, J.R., Ihm, S.K.: Design of dual functional adsorbent/catalyst system for the control of VOC's by using metal-loaded hydrophobic Y-zeolites. Catal. Today 93–95, 575–581 (2004)

[15] Yadav, Y.K.: Vapour- compression and liquid desiccant hybrid solar space-conditioning system for energy conservation. Renew. Energ. 7, 719–723 (1995)

The Effect of Metal Ions on Calcium Carbonate Precipitation and Scale Formation

Jitka MacAdam and Simon A. Parsons

Centre for Water Science, Cranfield University, Cranfield, Bedfordshire, MK43 OAL, UK
j.macadam@cranfield.ac.uk

Abstract. Scale formation in domestic heating appliances is a widespread problem in the UK. Scale affects the life of energy intensive domestic devices such boilers with a potentially significant impact on their energy efficiency. A number of metallic cations, such as copper and zinc have been reported to affect $CaCO_3$ precipitation and scale formation. This study aimed to investigate closely the effect of zinc and copper on calcium carbonate ($CaCO_3$) formation and two sets of laboratory tests were performed. The effect of both metals on $CaCO_3$ precipitation was investigated using a standard jar tester. The longest delay in precipitation was obtained by zinc. To study $CaCO_3$ formation on a heated surface, a rapid scaling test was developed. This test was conducted at 42°C and 70°C to examine the effect of zinc dosing on $CaCO_3$ scale formation. The results show that zinc is effective in inhibiting scale formation on a heated surface particularly at 42°C.

1 Introduction

Scale affects the life of energy intensive domestic devices such as boilers, dishwashers, washing machines, coffee machines, kettles and irons and will also impact on new devices such as solar water heating. Space heating and hot water systems are the largest users of energy in domestic homes (85%) but there is little information on what impact the water has on performance. For example installing 5 million A rated condensing boilers is proposed to save 0.6 million tonnes of CO_2 per annum per year but scale formation could reduce its energy rating within just a few weeks of use. The deposits are usually poor thermal conductors causing a decline in the thermal transmission efficiency of the heat transfer equipment (Ming *et* al., 2006). Fouling of heat transfer equipment by inverse solubility salts, such as calcium carbonate ($CaCO_3$), known as crystallisation fouling represents a serious problem in all processes where water is used. Crystallisation fouling is probably the most serious single fouling mechanism in heat exchangers (Bansal and Müller-Steinhagen, 1993). $CaCO_3$ crystals can be found in different forms and the most common are calcite, aragonite and vaterite. Mineral or organic impurities can have a major influence on the crystal growth in terms of both the rate and the form. Calcite is a thermodynamically stable crystal form under normal conditions, but aragonite appears to be a stable form when certain impurities are present, including Mg^{2+}, Ni^{2+}, Co^{2+}, Fe^{3+}, Zn^{2+} and Cu^{2+}. The presence of these impurities can result in a prolonged induction period leading to slower precipitation (Műller-Steinhagen and Branch, 1988).

A number of metallic cations, such as iron, copper and zinc have been reported to affect $CaCO_3$ precipitation and scale formation (Takasaki *et al.*, 1994; Katz and Parsiegla, 1995; Pernot *et al.*, 1998; MacAdam and Parsons, 2004). Compared with other metals, zinc has received the greatest interest and has shown the most potential (Lisitsin *et al.*, 2005; Ghizellaoui *et al.*, 2007; Ghizellaoui and Euvrard, 2008). Zn(II) is an ion which is very common in raw waters where its concentration can reach several milligrams per litre. Several effects of metal ions on $CaCO_3$ precipitation have been observed. As mentioned above, metal ions can delay nucleation of $CaCO_3$ (Coetzee *et al.*, 1998) and promote the formation of aragonite crystals (Wada *et al.*, 1998). Other reported effects include retardation of crystal growth (Meyer, 1984) and encouragement of bulk precipitation (Pernot *et al.*, 1999). The mechanism behind these effects has received some attention although it is not yet fully understood.

This paper aims to enhance the understanding of the effect of zinc and copper on the formation of $CaCO_3$. Here, we report the findings of a practical evaluation of the effect of these metals on the nucleation and precipitation of $CaCO_3$. Further, the effect of zinc on the formation of $CaCO_3$ was observed.

2 Methods and Materials

2.1 Materials

The majority of chemicals were supplied by Fisher Scientific UK and were all AnalaR grade. Deionised water with an electronic resistance of 15 MΩ was used to prepare stock and test solutions. The water was prepared by reverse osmosis using Purelab water purifier (ELGA Labwater UK). Synthetic $CaCO_3$ test solutions were prepared by mixing the appropriate amount of $NaHCO_3$ and $CaCl_2.2H_2O$ stock solutions, made by dissolving the chemicals in deionised water. The solutions were prepared fresh prior to each experiment. Stock solution of each metal (250 $mg.l^{-1}$) was prepared and the chemicals used to make up these solutions were $Zn(NO_3)_2$ and $CuSO_4$.

2.2 Analytical Techniques

The pH and temperature were measured using a Jenway pH Meter equipped with a Merck Gelplas General Purpose pH Probe and Merck Temperature Probe. Calibration of the probe was achieved through the use of pH 7.00 and pH 10.01 buffer solutions (Merck). Conductivity was measured with a Jenway 3410 Electrochemistry Analyser. Calibration was carried out according to the supplier's specifications using KCl AnalaR standard solution (Merck). Hardness levels were determined by the EDTA titrimetric method 2340 C and alkalinity levels were determined by the HCl titrimetric method 2320 B (APHA , 1992).

Calcium, zinc and copper concentrations were determined using Inductively Coupled Plasma Atomic Emission Spectrophotometry (ICP-AES). The equipment used for ICP-AES analysis was a Thermo Jarrell Ash Atomscan 16 unit (Sci-Tek Instruments). Prior to analysis, all samples were filtered to remove any suspended solids. 100 ml of each sample was prepared and 0.5% of nitric acid was added to the samples. Calibration of the instrument was carried out using ICP standard solutions (typically 1000 $mg.l^{-1}$) purchased from Fisher Scientific and diluted accordingly. The

prepared standards were tested separately to ensure the accuracy and reliability of the unit.

All scale samples were dissolved in 0.1% HCl. The calcium content in dissolved scale samples was then analysed as above using ICP-AES and the amount of scale formed then calculated. The crystal morphology and scale structure were determined using a Scanning Field Emission Gun (SFEG), manufactured by FEI Company™, where prior to analysis, $CaCO_3$ scale samples were fixed onto a stud and coated with a mixture of gold and platinum to make them conductive.

2.3 Laboratory Batch Experiments

2.3.1 Precipitation Trials

This batch method was used to investigate the precipitation of $CaCO_3$ under specified conditions. A Sedimentation Jar Tester, designed and manufactured by Aztec Environmental Control Ltd. with six plastic stirrers (80 rpm) was used for the experiments. Experiments were conducted in duplicates. Two solutions ($CaCl_2$ and $NaHCO_3$) were freshly prepared before each experiment to ensure that the final concentration of $CaCO_3$ in the test solution was 300 $mg.l^{-1}$. The pH of the bicarbonate solution was lowered to 7.3 – 7.4 by the addition of concentrated hydrochloric acid. After 30 minutes the bicarbonate solution was mixed with calcium chloride solution by magnetic stirring. All the tested solutions (final volume 500 ml) were then left to stand for 10 minutes at room temperature before being placed into the water bath (40ºC). pH was then measured continuously throughout the experiment using a Jenway pH meter and precipitation curves were obtained by plotting the pH against time. Three of the tested solutions were used as controls. The remaining three were spiked with a potential inhibitor, zinc (Zn^{2+}) or copper (Cu^{2+}), prior to placing the test solutions into the water bath. The delay was obtained from the comparison of the precipitation curves for the spiked solutions, with the controls' precipitation curves.

2.3.2 Rapid Scaling Test

The experimental rig manufactured by Model Products Ltd. (Bedford, UK) consisted of a plastic tank, a submerged heating element, covered by a removable sleeve and was temperature controlled. During the experiments synthetic $CaCO_3$ test solution was used. The test solution was heated to either 42ºC or 70ºC for 45 minutes (1 repeat). It was then discharged and replaced by a new $CaCO_3$ solution in which the heater was allowed to cool for 15 minutes and then reheated. The test solution was magnetically stirred throughout the entire experiment. After either ten or five repeats (dependant on the temperature used), the sleeve was removed from the heater, with $CaCO_3$ scale dissolved and analysed. The stock solution of zinc was dosed prior to the $CaCO_3$ test solution being heated.

3 Results and Discussion

3.1 Effect of Metal Ion Dosing on Calcium Carbonate Precipitation

Two metal ions ($Zn^{2+}$and Cu^{2+}) were dosed here and their effects on $CaCO_3$ precipitation, specifically the induction period are reported. A number of methods can be

employed to determine the induction period (t_{ind}) of $CaCO_3$ precipitation. The pH method was used here and the experimental data are presented as precipitation curves (pH vs. time).

The effects of the metals on $CaCO_3$ precipitation were investigated at 40°C. Each experiment consisted of three controls and three tests and each experiment was repeated at least twice to minimise error. All results are summarised in Table 1. In some cases the standard deviation of the repeats within one experiment exceeded the average delay between the dosed solutions and the controls. In these cases, the delay was not considered noteworthy.

Table 1. Summary of the induction period delays recorded in the precipitation experiments

Exp.	Inhibitor ($mg.l^{-1}$)	Induction period of single samples (min)				**Delay (min)**
	zinc	Control*	(stdev)	inhibitor	(stdev)*	
1	0.05	98	9.2	96	0	**0**
2		132	42.0	132	10.4	**0**
3	0.1	135	15.6	165	13.9	**30**
4		109	20.1	132	3.5	**23**
5		107	12.5	129	3.5	**22**
6		114	23.1	132	6.9	**18**
7		107	10.4	135	3.5	**28**
8	0.5	131	24.7	266	0	**135**
9		111	33.5	210	0	**99**
10		117	20.0	235	15.0	**118**
11		133	25.2	244	18.5	**111**
12		102	2.8	203	20.8	**101**
13		146	28.9	293	5.8	**147**
	copper					
14	0.05	116	3.5	120	3.5	**4**
15		104	9.2	108	6.9	**4**
16	0.1	98	9.2	98	3.5	**0**
17		100	0	117	19.6	**17**
18		70	0	76	18.0	**6**
19	0.5	94	6.0	106	6.0	**12**
20		82	6.0	94	17.0	**12**

*average from 3 jars

Better results were obtained when zinc was dosed. The effects of three different zinc concentrations were investigated here. It can be seen that as the concentration of zinc increased as did the induction time. At a zinc dose of 0.1 $mg.l^{-1}$, the induction period increased on average by 24 minutes, whilst with a dose of 0.5 $mg.l^{-1}$ in experiment 8, no precipitation was recorded over the length of the run, which lasted 266 minutes. The average delay recorded at a 0.5 $mg.l^{-1}$ dose of zinc was 119 minutes. There was no delay recorded at the lowest dose used (0.05 $mg.l^{-1}$). These results are significant and strongly support the inhibitory effect of this metal ion described in the literature. It was suggested previously, that trace amounts of zinc can slow down the

nucleation rate of $CaCO_3$ and also encourage its crystallisation in aragonite form, even under conditions favouring calcite (Coetzee *et al*., 1998). Meyer (1984) found out that zinc ions can significantly reduce the crystal growth of calcite, 2 x 10^{-7} mol.l^{-1} was enough to inhibit calcite crystal growth by 80%. Although a number of researchers investigated the effect of zinc on crystallisation of $CaCO_3$, the mechanism has not yet been agreed. Several suggestions have been made, including the involvement of the free metal ion during the nucleation process (Coetzee *et al*., 1998) or during the crystal growth phase (Meyer, 1984).

The same concentration levels were investigated in the case of copper (0.05, 0.1 and 0.5 mg.l^{-1}). In comparison with the zinc experiments, copper was much less effective. A delay of just 12 minutes was observed using 0.5 mg.l^{-1} copper dose (experiment 19) while no obvious delay was recorded at the lower doses. This is supported by data in the literature, where it is reported that a higher concentration of Cu^{2+} ions in comparison to Zn^{2+} ions is necessary to achieve a similar effectiveness (Ghizellaoui *et al.*,2007; Wen-jun *et al.*, 2008). Coetzee *et al.* (1998) have shown that copper was only half as effective as zinc. As reported previously, if the water is metastable, certain substances, including Cu^{2+} or Zn^{2+} ions decrease the probability of nucleation (Lédion *et al*., 2002). Their findings suggest that copper has a strong inhibitory effect on $CaCO_3$ scale formation.

3.2 Effect of Zinc Dosing on Calcium Carbonate Scaling Rate

In the previous section, zinc has shown great potential to inhibit the nucleation of $CaCO_3$. Here, the effect of zinc dosing on $CaCO_3$ scale formation was studied. The scaling experiments were conducted at 42°C and 70°C and the influence of chemically dosed zinc was examined over a range of concentrations.

The scaling results show that zinc not only prolonged the induction time of $CaCO_3$ precipitation, but also effectively reduced the scale formation (Figure 1), particularly

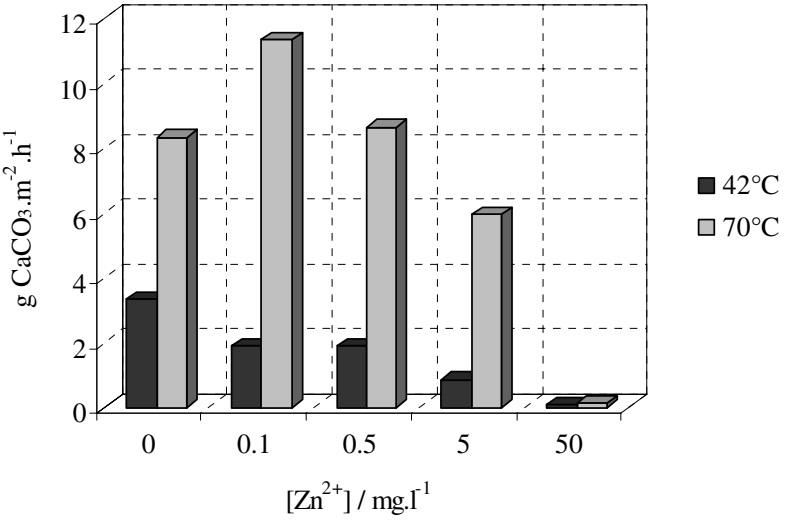

Fig. 1. Effect of zinc dosing on $CaCO_3$ scaling rate (300 mg.l^{-1} as $CaCO_3$, stainless steel surface at 42°C (10 repeats) and 70°C (5 repeats).

at the lower temperature. At 42°C, a zinc dose of 0.1 $mg.l^{-1}$ reduced scaling by 43%, whilst at 5 $mg.l^{-1}$concentration the reduction increased to 74%. At a dose level of 50 $mg.l^{-1}$, the scale formation was almost completely inhibited (98%). The effect of zinc was diminished at higher temperatures, with the two lowest concentrations (0.1 and 0.5 $mg.l^{-1}$) having no positive inhibitory effect on $CaCO_3$ scale formation at 70°C. A 5 $mg.l^{-1}$ zinc dose was needed to obtain a significant reduction (35%) at this temperature, whilst again a 50 $mg.l^{-1}$ dose completely inhibited scale formation.

The effect of zinc on $CaCO_3$ precipitation and crystal growth was previously discussed. The resulting reductions in scaling were not as significant as expected at the lower doses used, particularly at 70°C. Although it was mentioned that Meyer (1984) reduced the growth of calcite by as much as 80% by adding 2 x 10^{-7} $mol.l^{-1}$ (~ 0.0131 $mg.l^{-1}$), his experiments were conducted at 20°C. The negative effect of increased temperature was cancelled at high zinc concentrations. As previously mentioned, the excessive dose of 50 $mg.l^{-1}$ almost completely inhibited the scale formation at both temperatures.

Zinc addition led to changes in the structure of the crystals formed. In comparison to the crystal structure of $CaCO_3$ from the control experiment, where 0.5 $mg.l^{-1}$ of zinc was dosed (both experiments conducted at 42°C), it is clearly visible in Figure 2 below that zinc has not only affected the size of the aragonite crystals but also their organisation. The effect of zinc on the size of $CaCO_3$ crystals was also reported by Ghizellaoui *et al.* (2007) where crystals precipitated from zinc doped solution were smaller than those precipitated from an untreated solution.

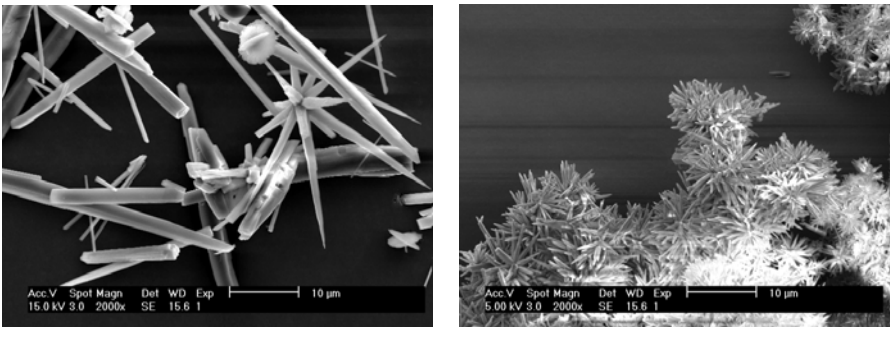

(a) (b)

Fig. 2. The SEM analysis of crystals collected from the heater cover (stainless steel surface) after the scaling test (a) control (300 $mg.l^{-1}$ as $CaCO_3$, 42°C) and (b) zinc dosed experiment (300 $mg.l^{-1}$ as $CaCO_3$, 42°C, 5 $mg.l^{-1}$ Zn^{2+})

These crystals were collected from the heated surface, where the temperature significantly exceeded the bulk temperature of 42°C. Aragonite was the preferred crystal phase formed in the control experiment as well as in the presence of zinc and thus any conclusion regarding the ability of zinc to promote the formation of aragonite as opposed to calcite could not be made.

Zinc has been reported to possess potential as a low dose scale inhibitor and this is supported by the results shown above. Zinc increased the induction period of $CaCO_3$ precipitation by almost 2 hours at 0.5 $mg.l^{-1}$ concentration and proved to be an effective scale formation retardant. The tests have further shown that zinc can affect the growth of $CaCO_3$ crystals causing them to grow at a slower rate and into a different organisation. The main advantage of zinc dosing is that together with copper it can be released into the solution electrolytically. The principle is that two metals such as copper and zinc combined in the device, generate a current and are subsequently released into the water as free ions (López-Sandoval *et al.*, 2007). This method is already in use in a number of domestic physical conditioners but their effectiveness varies considerably.

To understand why and subsequently improve the range of products available, it is necessary to address the inhibitory mechanism issue. Whilst a number of different inhibitory effects of zinc on $CaCO_3$ scale formation have been described previously, the mechanism of the inhibitory action of zinc is still not known (Chen and Chan, 2000). The aim here is to form a better understanding of the zinc inhibitory action.

A number of researchers have studied the inhibitory effects of zinc on $CaCO_3$ in the past and several mechanisms of zinc inhibitory action have been proposed (Table 2). The precipitation of zinc in the most likely form of $ZnCO_3$, which is isomorphous to calcite, was mentioned by Pernot *et al*. (1999). However, what must also be considered are the quantities of zinc involved. The zinc level required to have a measurable effect on $CaCO_3$ formation is very low (< 1 $mg.l^{-1}$) compared to the

Table 2. Summary of the observed inhibitory effects of zinc on $CaCO_3$ formation

	OBSERVED EFFECT	PROPOSED MECHANISM	REFERENCE
(a)	Delayed nucleation of $CaCO_3$	Possible involvement of free metal ions during the nucleation stage	Coetzee *et al.* (1998)
(b)	Retardation of calcite crystal growth	Adsorption of the impurities at the growth sites	Meyer (1984)
(c)	Encouragement of bulk precipitation	The formation of $Zn(OH)_2$ and/or $ZnCO_3$ which act as a heteronuclei in the bulk of the solution	Pernot *et al.* (1999)
(d)	Preferential formation of aragonite crystals	1.Inhibition of growth of the metastable phase (aragonite) by adsorption of the impurity cations 2.Formation of the unstable solid solution of calcite through transformation of aragonite	Wada *et al.* (1995)

concentrations of calcium and carbonate ions (Lédion *et al*., 2002). The literature on zinc and scale formation shows that zinc not only affects the growth of $CaCO_3$ crystals but also claims the formation of aragonite rather than calcite crystals (Coetzee *et al.*, 1998). Pernot *et al*. (1999) also suggested that zinc may act as an accelerator of heterogenous nucleation in the bulk of the solution instead of on the surface, therefore reducing the formation of $CaCO_3$ on the heated surface. The promotion of bulk precipitation was also reported by López-Sandoval *et al.*, 2007.

No change in crystal habit was observed in the scaling trials conducted here though at surface temperatures above 42°C a preferential formation of aragonite would be expected (Gabrielli *et al*.,1999; Andritsos *et al*., 1997). However, these findings also suggest that zinc had an effect on the aragonite formation. It is possible only to speculate at this point, if the reduction in scaling on the heating element observed during the rapid scaling tests was entirely the result of the prolonged induction period. As the bulk precipitation was not measured during the experiment due to unsatisfactory data reproducibility, the possibility that zinc enhanced the bulk precipitation and thus reduced the deposition on the heated surface cannot be ruled out. As previously described in the case of copper the competition mechanism is unlikely as the concentrations of zinc are very low compared to both carbonate and calcium ions (Ledion *et al*., 2002).

The crystal morphology of $CaCO_3$, including the structural isomers of calcite, aragonite, and vaterite, is determined by the crystallization conditions, such as the supersaturation, temperature, concentration of reagents, pH, and residence time in the reactor. According to Gabrielli *et al*. (1999), $CaCO_3$ scale precipitates as calcite at room temperature, or as aragonite at temperatures higher than 50°C. Some reports suggest predominant formation of aragonite at 45°C (Andritsos *et al*., 1997). Vaterite is more rarely observed. Impurities can also have a major influence on the crystal growth process, some even at very low concentrations. It is known from the experiments reported by Söhnel and Mullin (1982), that impurities have a great effect on shape and size of $CaCO_3$ crystals. In particular calcite was the thermodynamically stable form under normal conditions, but aragonite appeared to be the stable form when certain impurities are present. The actual phase formed and the rate of phase transition was affected by the temperature and the type of impurity. It was found that impurities with a small ionic radius and higher hydration energy than that of Ca^{2+} resulted in aragonite formation. As reported by Ming *et al.* (2006), the growth of aragonite crystal nucleus was retarded by the replacement of some of the Ca^{2+} ions on the crystal surface by Zn^{2+}, and the transition of $CaCO_3$ from aragonite to calcite was blocked.

The current study funded by Carbon Connections and also Sentinel Performance Solutions Ltd. is based on the above data and focuses on quantifying and controlling the impact of scale formation derived from the secondary (domestic hot water) circuit on domestic boiler efficiency. This project is the first to quantify the link between scale formation and domestic boiler efficiency. Further, a novel treatment solution based on $CaCO_3$ inhibition by zinc is being developed and its impact on energy efficiency will be quantified.

4 Conclusions

The observed inhibitory effect of zinc on $CaCO_3$ precipitation was significant: As the concentration of zinc increased as did the induction time of $CaCO_3$ precipitation. The average delay recorded at a 0.5 $mg.l^{-1}$ dose of zinc was 119 minutes.

In comparison with the zinc experiments, copper was much less effective. A delay of just 12 minutes was observed using 0.5 $mg.l^{-1}$ copper dose while no obvious delay was recorded at the lower doses.

Zinc has further shown great potential as a scale inhibitor. When dosed chemically, at 42°C a zinc dose of 0.1 $mg.l^{-1}$ reduced scaling by 43%, whilst at 5 $mg.l^{-1}$ concentration the reduction increased to 74%. The effect of zinc was diminished at higher temperatures whilst a 5 $mg.l^{-1}$ zinc dose was needed to obtain a significant reduction (35%). A 50 $mg.l^{-1}$ dose completely inhibited scale formation at both temperatures.

References

Andritsos, N., Karabelas, A.J., Kontopoulous, M.: Morphology and structure of CaCO3 scale layers formed under isothermal conditions. Langmuir 13, 2873–2879 (1997)

APHA, Standard Methods, 18th edn. American Public Health Association, Washington (1992)

Bansal, B., Müller-Steinhagen, H.: Crystallisation fouling in plate heat exchangers. J. Heat. Trans. 115, 584–591 (1993)

Chen, T.Y., Chan, S.-H.: Novel biological inhibitors of fouling and scale formation on heat transfer surfaces through genetic engineering. Microscale Therm. Eng. 4, 103–108 (2000)

Coetzee, P.P., Yacoby, M., Howall, S., Mubenga, S.: Scale reduction and scale modification effect induced by Zn and other metal species in physical water treatment. Water. SA. 24, 77–84 (1998)

Gabrielli, C., Maurin, G., Poindessous, G., Rosset, R.: Nucleation and growth of calcium carbonate by an electrochemical scaling process. J. Cryst. Growth. 200, 236–250 (1999)

Ghizellaoui, S., Euvrard, M.: Assessing the effect of zinc on the crytallisation of calcium carbonate. Desalination 220, 394–402 (2008)

Ghizellaoui, S., Euvrard, M., Ledion, J., Chibani, A.: Inhibition of scaling in the presence of copper and zinc by various chemical processes. Desalination 206, 185–197 (2007)

Katz, J.L., Parsiegla, K.I.: Calcite growth inhibition by ferrous and ferric ions. In: Amjan, Z. (ed.) Mineral Scale Formation and Inhibition. Plenum Press, New York (1995)

Lédion, J., Braham, C., Hui, F.: Anti-scaling properties of copper. J. Water SRT-AQUA 51, 389–398 (2002)

Lisitsin, D., Yang, Q., Hasson, D., Semiat, R.: Inhibition of CaCO3 scaling on RO mem-branes by trace amounts of zinc ions. Desalination 183, 289–300 (2005)

López-Sandoval, E., Vazquez-López, C., Zendejas-Leal, B.E., Ramos, G., San Martín-Martínez, E., Muñoz Aquirre, N., Reguera, E.: Calcium carbonate scale inhibition using the "allotropic cell" device. Desalination 217, 85–92 (2007)

MacAdam, J., Parsons, S.A.: Calcium carbonate scale formation and control. Rev. Environ. Sci. Biotechnol. 3, 159–169 (2004)

Meyer, H.J.: The influence of impurities on the growth rate of calcite. J. Cryst. Growth. 66, 639–646 (1984)

Ming, X., Liang, J., Ou, X., Tang, Q., Ding, Y.: Interaction of ions in water system containing copper-zinc alloy for boiler energy saving. Rare. Metals 25, 405–410 (2006)

Műller-Steinhagen, H., Branch, C.A.: Calcium carbonate fouling of heat transfer surfaces. In: Proceedings of CHEMECA 1988, Sydney (1988)

Pernot, B., Euvrard, H., Simon, P.: Effect of iron and manganese on the scaling potentiality of water. J. Water SRT-Aqua. 47, 21–29 (1998)

Pernot, B., Euvrard, H., Remy, F., Simon, P.: Influence of Zn(II) on the crystallisation of calcium carbonate application to scaling mechanisms. J. Water SRT-Aqua. 48, 16–23 (1999)

Söhnel, O., Mullin, J.W.: Precipitation of calcium carbonate. J. Cryst. Growth. 60, 239–250 (1982)

Takasaki, S., Parsiegla, K.I., Katz, J.L.: Calcite growth and the inhibitory effect of iron(III). J. Cryst. Growth. 143, 261–268 (1994)

Wada, N., Yamashita, K., Umegaki, T.: Effects of divalent cations upon nucleation, growth and transformation of calcium carbonate polymorphs under conditions of double diffusion. J. Cryst. Growth. 148, 297–304 (1995)

Wada, N., Yamashite, K., Umegaki, T.: Effects of silver, aluminum, and chrome ions on the polymorphic formation of calcium carbonate under conditions of double diffusion. J. Colloid. Interf. Sci. 201, 1–6 (1998)

Wen-jun, L., Hui, F., Lédion, J., Xing-wu, W.: The influence of metal ion on the scaling in the mineral water tests. Ionics 14, 449–454 (2008)

Lateral Stability of Prefabricated Straw Bale Housing

Christopher Gross[1], Jonathan Fovargue[2], Peter Homer[3], Tim Mander[4], Peter Walker[1], and Craig White[5]

[1] BRE Centre for Innovative Construction Materials, University of Bath, UK
[2] Eurban Construction, London, UK
[3] Agrifibre Technologies Ltd, Biggleswade, UK
[4] Integral Structural Design, Bath, UK
[5] White Design Associates Architects, Bristol, UK

Abstract. Straw bales have been use for building for about 140 years. Until recently bales were only used for load bearing Nebraskan style building or for infill on timber framed buildings. ModCell panels are a prefabricated straw bale panel consisting of a timber frame, straw bale infill and lime rendered faces. ModCell panels have been used for cladding on several framed buildings and are now being developed to be load bearing. In order to allow this sufficient racking shear resistance needs to be developed. This paper reports on a series of joint tests and full scale panel racking shear tests at the University of Bath. Refinements to the joint and bracing details have improved the racking shear resistance of the panels.

1 Introduction

Straw has been used for thousands of years as a building material. Traditionally straw was mixed with clays in earth construction techniques such as wattle and daub, cob and adobe in order to reinforce the earth (King 2006). During the late 1800s, baling machines were invented in the USA and farmers in Nebraska started to use the bales produced from their crops to build houses. These buildings had load bearing straw bale walls which were then rendered both inside and out. This type of building has become known as Nebraskan style and some of these buildings survive to this day (Jones 2002). Bales have also been used in a non-load bearing applications as infill for timber framed buildings (Chiras 2000).

The first straw building in the UK was built in 1994. Generally speaking all the straw bale buildings built in the UK have been one off projects built by individuals who have an interest in building with straw. This trend is reflected in the fact that between 1994 and 2002 only about 70 straw bale buildings were constructed in the UK (Jones 2002). ModCell (from Modular Cellulose) panels were developed by White Design and Integral Structural Design in order to try and combat this trend and move straw bale building into the mainstream construction sector. The idea behind ModCell panels is that they are prefabricated off site in a local factory and then transported to site, removing the presence of straw bales onsite and the associated problems (storage, weather protection, fire risk).

Fig. 1. ModCell Panels used at Knowle West Media Centre, Bristol

The ModCell panel (Figure 1) consists of a laminated timber frame, infilled with straw bales and rendered with a formulated lime render. Generally the timber frames they are formed to accommodate the modular size of a standard bale (approximately 1.0 x 0.45 x 0.35 metres). The bales are stacked in running bond and held together using timber stakes. Additional timber stakes are inserted through holes in the frame to secure the bales. Stainless steel threaded bar is used to brace the frame. The height of the panels is designed to allow some pre-compression of the bales in order to alleviate any potential settlement. The panels are covered with two coats of lime render which is allowed to harden for at least seven days before the panels are delivered to site and installed.

To date ModCell panels have been used in six buildings. Five of these applications have been as cladding to framed buildings. The other was as the load bearing ground floor of the Grand Designs Live house at Excel in London in 2008 (ModCell 2009). By using the ModCell panels in a load bearing application the need for a structural frame is removed, reducing the amount of material used and so reducing the embodied carbon content of the construction.

2 Previous Work

There has been very little previous research on prefabricated straw bale panels. Ash et al. noted that render is key to improving shear resistance in their investigation on in plane cyclic loading of straw bale walls. This work tested straw bale walls measuring 2.44 metres square with different renders and mesh reinforcement. An in plane horizontal load was applied to the top of the walls. This work found that by changing the

render type and the reinforcement in the render the racking shear resistance of the walls could be increased by almost six times. A wall with cement render reinforced with chicken wire gave a load of 28.4 kN (11.64 kN/m) at a displacement of 35mm. Carrick and Glassford (1997) also tested straw bale walls subject to in plane loading. They tested walls 3.6 metres wide by 2.7 metres tall with a 30mm thick sand and cement render reinforced with chicken wire. They found that a 10 kN (3.7 kN/m) load produced a 2.4mm deflection.

At the University of Bath Lawrence et al. (2009) carried out tests on corner joints to investigate the resistance offered to racking shear, but still limited to a cladding application. This work found that even with corner bracing the joints were not sufficient alone to resist the required racking forces. Lawrence et al. (2009) then confirmed this by testing a two metre by two metre ModCell timber frame, timber frame with the straw bales and finally a fully rendered panel. The rendered panel was 3.5 times stronger than the straw filled panel. Racking shear load resistance tests were then performed on full size ModCell panels measuring 3.08 metres wide, by 3.34 metres high, by 0.48 metres thick. Panels reinforced with steel bracing as well as unreinforced panels were tested. Cracks developed in the render of the reinforced panel at 1.25 times the load in the unreinforced panels and that failure occurred at nearly three times the load. It was observed that load capacity and lateral stiffness of the frame is significantly influenced by the joint details. In addition Lawrence et al. (2009) also observed that the render is a key contributor to the shear resistance of the panels. This observation is in keeping with other straw bale building techniques.

3 Aims

This investigation aims to establish the racking shear resistance of ModCell panels in order to ascertain if they can be used in two or three storey load bearing construction. In load bearing ModCell construction vertical loads are transferred through the timber frame. In plane racking shear loads need to be resisted by the panels in order to meet wind load criteria. The total racking shear load on a 6.8 metre by 6.8 metre two storey ModCell house caused by the effects of wind is in the order of 35 kN. This needs to be resisted by the ModCell panels with a maximum horizontal displacement of 5.2 mm (h/500) per storey.

4 Testing and Results

In order to establish the racking shear resistance the following testing was carried out: joint tests; and, four full size ModCell panel tests. The previous testing by Lawrence et al. (2009) showed that ModCell panels could resist the racking shear loads applied to them in a two storey load bearing application, but not within the serviceability deflection requirements (h/500). Therefore these tests will determine if the ModCell panels can resist the racking shear loads at the serviceability deflection limit.

4.1 Joint Testing

Joint tests were carried out in order to establish the most appropriate joint type. Previous work showed that the joints were a limiting factor. Although these failures

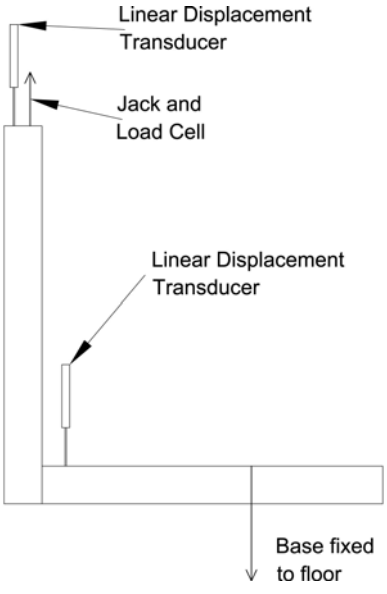

Fig. 2. Joint Testing Set up

occurred at maximum load the strength of the joints will have an effect on the serviceability performance of the panels. When the panels are loaded during laboratory testing and also in service in buildings the racking shear load is applied to the top horizontal member of the frame. This load has to be transferred into the sides of the frame though the corner joints. During testing of complete panels this tends to pull the joint apart with the panel side moving vertically up from the base.

Vertical pull out tests were carried out on three different types of joint; dove tailed joints, dowelled finger joints and screwed finger joints. The set up for the test is shown in Figure 2. The joints were set up at 90^{o} and the horizontal piece was fixed to the laboratory floor. The vertical piece was then loaded using a hydraulic jack and hand pump and the vertical displacement measured. All the joints were made from 1 metre lengths of laminated timber as used in the ModCell frames. The dove tailed joints were simply push fitted together. The dowelled joints were made with a three piece finger joint through which a stainless steel dowel was inserted. The screwed joints used the same three piece finger joint but were screwed together with twelve screws.

The average results for each type of joint are shown in Figure 3. From the results it is clear that the screwed joints displayed the highest load capacity (64.21 kN average) and stiffness (8.29 kN/mm). The joints remained intact until a load of 50 kN when the timber being loaded by screws in shear split. The dove tail joints showed a large amount of initial deflection as there was some play within the joints due to them only being a push fit. The joints tightened as they were loaded and once this had occurred the stiffness was similar to that of the screwed joints. Sudden failure occurred by splitting of the vertical timber along its major axis at an average load of 26.53 kN. The dowelled joints developed some ductility as the dowel deformed, however the timber split in a brittle manner at the dowel location.

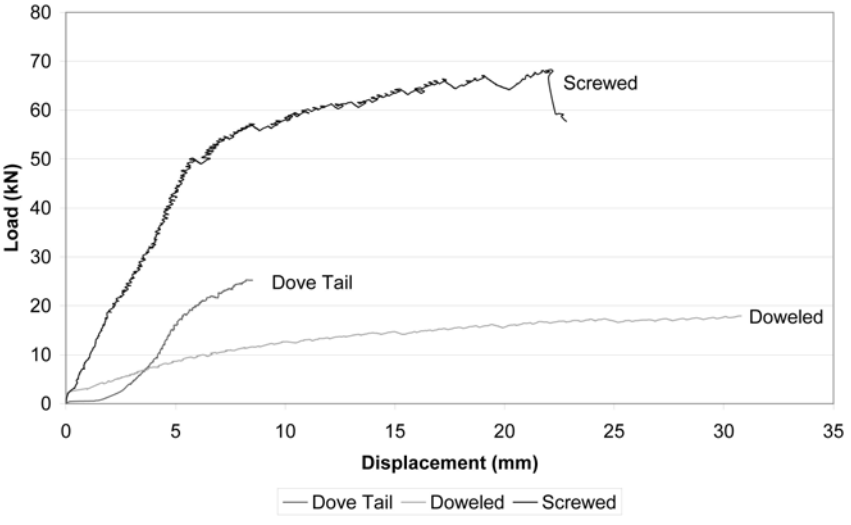

Fig. 3. Joint Testing Results

4.2 Full Size Racking Shear Tests

The racking shear test set up used for this investigation is shown in Figure 4. The ModCell panel is fixed to the floor to prevent it from sliding and rotating freely. A horizontal load was applied to the top of the timber frame at the corner by means of a hydraulic jack and hand pump. The displacement of the panels was measured using Linear Voltage Displacement Transducers (LVDT) at set locations around the timber frame and the load was measured using a load cell at the jack. In all of the tests the panels were loaded until a deflection at the top corner opposite the jack reached a set displacement. The load was then removed and the residual settlement recorded. This was done at displacements of h/500, h/300 and h/100. After this the panels were loaded to failure. It should be noted that no vertical load was applied to the panels during these racking tests.

Four panels were tested, two three bale panels and two two bale panels. The panels used were 3.2 metres long by 2.6 metres high by 0.49 metres thick. All of the panels used the screwed joints. Two types of bracing were used. One three bale panel and one two bale panel were constructed with stainless steel bar corner bracing; the two other panels had stainless steel bar diagonal cross bracing.

Figure 5 shows the results of the racking shear tests on the panels. It can be seen that the three bale panels carry about three times the load of the two bale panels at deflections of h/500 and h/300. At the h/500 deflection limit the loads being carried by the panels were 12.4 kN/m (39.7 kN) for the three bale corner braced panel; 10.7 kN/m (34.2 kN) for the three bale cross braced panel; 4.3 kN/m (13.7 kN) for the two bale corner braced panel; 3.1 kN/m (10.0 kN) for the two bale cross braced panel. In all of the racking shear tests the render cracked at displacements above h/300. When the load was removed after loading the three bale corner braced panel to a displacement of h/500 a residual displacement of 1.8 mm was recorded.

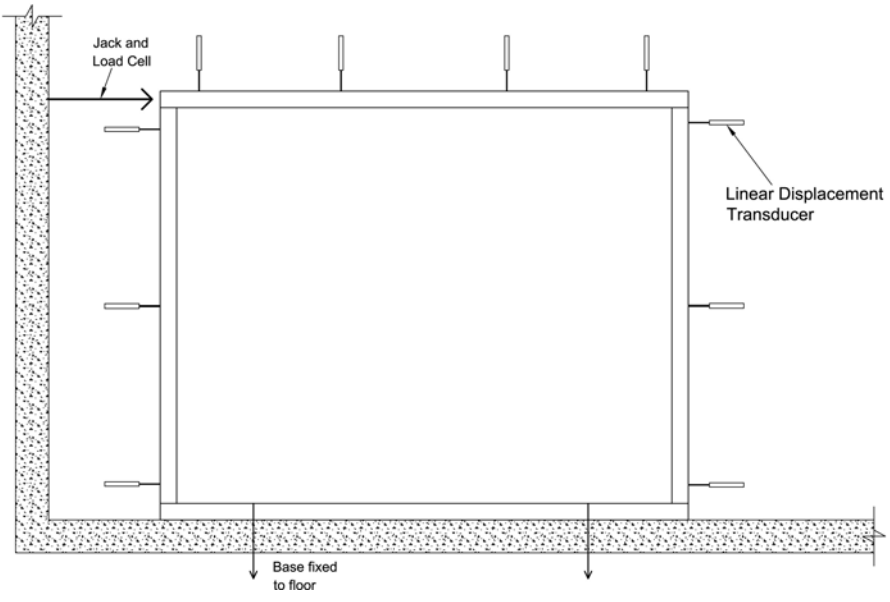

Fig. 4. Racking Shear Test Set up

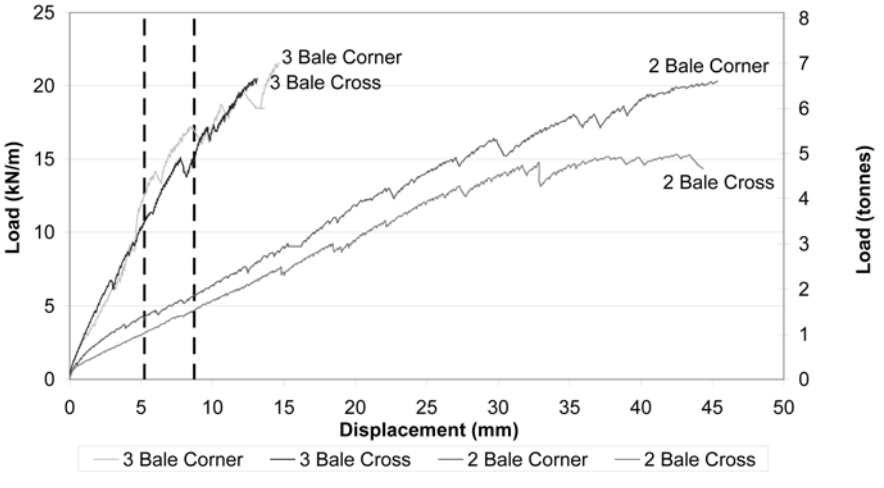

Fig. 5. ModCell Panel Racking Shear Testing Results

The cross braced and corner braced panels both performed similarly, with the two bale corner braced panel outperforming the two bale cross braced panel. One reason for this is that the two bale cross braced panel did not have any vertical steel reinforcement due to the overlapping of the bracing bars at the centre. If the vertical reinforcement had been present then there would have been three bars on top of each other, which would have resulted in unsatisfactorily thick render. As the panel racks

the top and bottom frame elements move closer together putting the render into compression. The vertical reinforcement prevents uplift of the top element of the frame and vertical pull out of the joints and as a result the render remains in compression and the panel strength is increased.

4.3 Other Testing

During construction of the full size test panels render specimens were taken and tested in flexure and compression at the same time as the racking test (14 days after manufacture) in accordance with BS EN 1015-11. The average flexural strength was 1.22 N/mm^2 and the average compressive strength was 2.85 N/mm^2. The density and moisture content of the bales was also recorded to ensure that they were within the specified limits for ModCell panels. The bales used had an average density of 113.4 kg/m^3. At the time of panel construction the bale moisture content varied between 12% and 14%. A computer model of load bearing ModCell panels is currently being developed with the aim of comparing modelled results and test results. If the results are comparable it is hoped that this model may then be used for assessing future developments to the ModCell panels.

5 Conclusions

The racking shear strength of ModCell panels has been improved. This has been achieved through refinement of the bracing design and investigation into the joint detailing. Four racking shear tests have demonstrated that the joints are adequate. The tests have also shown that corner bracing is adequate and that cross bracing the panels offers little structural advantage. During these racking shear tests two bale ModCell panels were tested for the first time. It has been shown that they are weaker than the three bales panels and this needs to be taken into consideration when designing with ModCell panels.

This investigation set out with the aim of improving the ModCell panels so that they could be used in two or three storey load bearing construction. This has been achieved for two storeys at least and potentially three dependant upon where two and three bale panels are used. The results in this investigation do however need to be confirmed by further racking shear tests, but the future of load bearing ModCell panels looks promising.

Acknowledgements

The authors firstly would like to acknowledge the support of Carbon Connections funding for the work outlined in this paper. The Carbon Connections project consortium is comprised of White Design Associates Architects, Integral Structural Design, Agrifibre Technologies, and Eurban Construction. The input from our University of Bath colleagues is also gratefully acknowledged.

References

Ash, C., Aschheim, M., Mar, D.: Inplane cyclic tests of plastered straw bale wall assemblies. University of Illinois report, http://www.ecobuildnetwork.org/pdfs/InPlane_Wall_Tests_Large.pdf (21/01/2009)

BS EN 1015-11: Methods of test for mortar for masonry – Part 11: Determination of flexural and compressive strength of hardened mortar. BSI (1999)

Carrick, J., Glassford, J.: Preliminary Test Results Straw Bale Walls. University of New South Wales, Building Research Centre (1997), http://www.strawbalebuilding.ca/pdf/Carrick%20Test%20results.pdf (21/01/2009)

Chiras, D.D.: The natural house: a complete guide to healthy, energy-efficient, environmental homes. White River Junction, Chelsea Green, Vt. (2000)

Jones, B.: Building with straw bales: a practical guide for the UK and Ireland. Green, Totnes (2002)

King, B.: Design of straw bale buildings: the state of the art. Green Building Press, San Rafael (2006)

Lawrence, M., Drinkwater, L., Heath, A., Walker, P.: Racking Shear Load Resistance of Prefabricated Straw Bale Panels. ICE Journal of Construction Materials (accepted, 2009)

ModCell (2009), http://www.modcell.co.uk/page/projects (22/01/2009)

Monitoring of the Moisture Content of Straw Bale Walls

Mike Lawrence, Andrew Heath, and Pete Walker

BRE Centre for Innovative Materials, Dept of Architecture & Civil Engineering,
Bath University, UK

Abstract. This paper describes an investigation into moisture levels in straw bale walls used to clad a newly constructed building. The moisture content was monitored up to 10 months after the building was handed over. The sensors used for this purpose were readily available, low cost and easily installed. The moisture levels fluctuate during the first 4 months following installation of the instrumentation, followed by a period of greater stability where it is believed that the straw acts as a moisture buffer, managing the humidity levels within the building and contributing to a healthier internal environment. This ongoing study makes a contribution towards raising confidence levels in the use of straw bales as low carbon building material in mainstream construction.

1 Introduction

Straw has been used as a building material for thousands of years either as an additive to clay in the form of adobe or cob, or as a water resistant layer in the form of thatch. With the invention of mechanical baling in the 19th century, it became possible to use compressed straw bales as oversized building blocks. This technique was used to good effect in Nebraska in the USA where other building materials were in short supply [1]. By the end of the 19th century the technique lost popularity as railway transportation allowed ready availability of more flexible materials such as stone, brick, timber and steel. During the second half of the 20th century interest in the technique was revived, particularly in the state of California. By the end of the century interest in straw bale construction had developed in Europe because of the perceived need for low environmental impact building materials. Straw was seen as a useful contributor to low environmental impact construction for a number of reasons:

- Straw has excellent thermal insulation properties
- Straw has excellent sound insulation properties
- The production of straw is a low energy process compared with other building materials
- Straw sequesters carbon dioxide (CO_2) thereby reducing atmospheric CO_2

Straw is an organic material that carries particular risks with it in the context of living accommodation. These risks include:

- Fire – straw is inherently flammable
- Rodent and insect infestation – straw can contain protein and carbohydrates which can sustain life

- Decay – under the right environmental conditions straw is subject to both aerobic and anaerobic decay
- Structural instability – straw bales have low compressive and flexural strength and stiffness

Detailing has been developed to address many of these problems. Such detailing includes rendering with fire resistant material, which also inhibits access by rodents; protection of the junction between render and timber from wind driven rain; use of a drip detail at the base of the panel which protects from ingress by water flowing down the face of the panel; steel reinforcement to improve stiffness of the panels. The use of lime based or cementitious renders results in walls which meet statutory fire resistance criteria in the USA, in the UK and in Europe. Rendered walls have been shown to be resistant to rodent and insect attack [2]. Render also provides an outer layer which is resistant to moisture ingress from rainfall. Many structural tests have been conducted on straw bale walls both with and without render, and with and without additional reinforcement within the render [3,4,5,6]. These studies have shown that straw bale walls can be designed to be sufficiently robust to act as single storey structural walls, and in some cases two storey structural walls.

The issue of long term durability is the area of straw bale construction which attracts the most concern from all interested parties, including architects, builders, specifiers, regulators, financiers, insurers and end users. The most likely risk to long term durability is the potential of decay within the straw, initiated by excess moisture content. This paper addresses this issue, and discusses the use of sensors embedded within the walls of buildings to monitor the condition of the straw. The use of appropriate sensors provides long term data which adds to our understanding of the performance of straw bale construction. It also provides early warning of any incipient decay within the structure and improves the level of certainty about the condition of the walls.

2 Causes for the Decay of Straw

Straw can decay in one of two modes: anaerobic and aerobic. Anaerobic decay occurs in the absence of oxygen and requires elevated moisture levels [7]. In the context of straw as a building material, such conditions almost never occur. This is because the straw is generally above ground protected from moisture ingress by damp proof courses, and moisture resistant membranes or barriers such as renders or a rainscreen. The risk of decay in straw bale buildings is, therefore, confined to aerobic decay. The four main conditions that affect the rate of microbial decay in straw are:

1. nutrients contained in the straw
2. availability of oxygen in the straw
3. temperature of the straw
4. free moisture on the straw

The nutrients in straw are relatively low compared with materials such as hay, and are not possible in any event to be controlled. Temperature is similarly difficult to control in a built environment where internal wall temperatures are determined by the

requirement to maintain a suitable environment for accommodation and external temperatures are subject to the vagaries of the weather.

The moisture content of the straw in a built wall can be limited by good detailing, but accidental inundation can still occur from time to time. Excessive water content will limit access of oxygen since saturated straw will only have access to the little oxygen dissolved in the water. Straw that has been rendered will also have reduced access to atmospheric oxygen.

Fungal and bacterial growth is not very active below 10ºC and few species will survive above 70ºC. Decay is very limited below 25% moisture content on a dry basis with the rate of decay decreasing above 120%[8]. There is therefore a limited range of moisture content in straw that will support decay, from a minimum of 25% to a maximum of around 120%, when free water starts to limit the availability of atmospheric oxygen, with saturation occurring at 400%.

The moisture content is the controlling factor in the decay of straw, as without a suitable moisture content any nutrients and oxygen in the straw cannot be consumed by fungi and bacteria. Since this is the case, knowledge of the moisture content within a constructed straw bale wall will provide reassurance as to their integrity.

3 Measurement of Moisture Content of Straw

Measurement of the moisture content of straw can be conducted either directly or indirectly.

Direct measurement involves the gravimetric method. This requires the weighing of the specimen followed by drying and re-weighing. The moisture content on a dry basis is calculated by expressing the weight loss as a percentage of the dry weight of the straw. This technique does present a number of difficulties:

1. The technique is highly invasive.
2. Relatively large amounts of material (render/rainscreen and straw) are removed from the structure which then require replacement.
3. Obtaining moisture profiles through the thickness of the wall is problematic, and requires an even more invasive approach.

It is possible to place a known weight of straw in a ventilated container inside a hollow ventilated tube within the wall which can then be periodically removed and weighed [9]. This technique is cumbersome and would only be usable in limited numbers within a building without becoming visually invasive and compromising the integrity of the wall.

Moisture content can be measured indirectly by measuring the relative humidity (RH) of the air in the immediate vicinity of the straw sample and converting this measurement into an equivalent moisture content using isotherm data. The moisture content of timber samples embedded within the straw wall can be measured using timber moisture meters and this measurement equated to straw moisture content using suitable isotherm data [10]. Straw bale moisture probes designed for use by farmers use similar science to timber moisture meters by measuring electrical resistivity. These probes have a diameter of around 10mm and are inserted into the straw bale to a measured distance. The electrical resistivity is converted into a moisture content

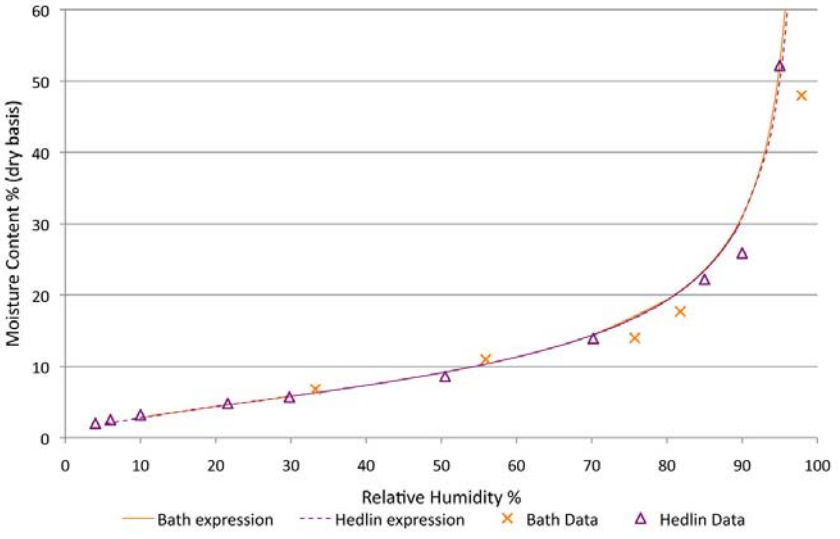

Fig. 1. Wheat straw isotherms and associated expressions

using calibration data for different straw types. This technique is also invasive and destructive in that it leaves a hole in the superficial render / rainscreen and a void in the straw.

The authors have developed an empirical expression [11] which relates RH measurements into MC data over the range 5% to 100% MC. This can be used in conjunction with RH sensors embedded in the straw walls to produce continuous readings of moisture content through the depth of the wall. This allows moisture profiles to be measured as well as measuring the response of the wall to wetting and drying from rainfall and sunshine. The data gathered from these sensors can be used to demonstrate the way in which straw bale walls can be considered to 'breathe', thereby buffering the effect of variations in moisture. In addition to these useful data, most importantly the technique can monitor the condition of the walls providing reassurance as to the absence of decay.

The expression used by this technique is a development of prior work by Malmquist [12,13] and Hedlin [14]. This expression takes the form:

$$C = \frac{C_s}{1 + n\left(\frac{K_m}{\varphi} - 1\right)^{i/3}} \tag{1}$$

C_s is defined as the fibre saturation moisture content,C is the equilibrium moisture content at relative humidity φ. n, K_m and i are constants where n= $C_s/C_{50\%\ RH}$.

The moisture content of saturated wheat straw (C_s) has been taken as 400%. This value corresponds to fibre saturation assumed by Hedlin using the suction technique for high relative humidities as used by Penner [15] at a suction of 1 cm. It should be noted that the value of C_s can be varied substantially without changing the form of the calculated isotherm below 95% relative humidity if corresponding adjustments are made to the

values of n and K. [14]. The constants used in these expressions, empirically determined by Hedlin, are:

$$n = 44;\ K_m = 0.9773;\ K = 0.0227;\ i = 1.6$$

The data gathered by Hedlin and those gathered by the authors are shown in Figure 1 together with the line described by the above expression and that described by the more complex expression developed by Hedlin.

It is clear that both expressions give very similar results, and that both have a slight tendency to overstate the moisture content as measured by experimentation for a given RH%. Further refinement is required to the expression, but is its considered that the current expression offers a factor of safety at higher RH levels where moisture content is most critical.

4 Instrumentation

Rendered straw bale walls have been monitored in a newly constructed media centre in Bristol, UK (Figure 2) since August 2008. The sensor used was a Humirel HTM1735LF capacitive humidity sensor with an accuracy of ± 2% @ 55%RH. The sensor requires a 5v supply which was supplied from a Grant Instruments Squirrel 2020 data logger.

The sensors were inserted into ventilated 20mm ø polypropylene tubes and installed into the straw bale panel during construction (Figure 3). Sensors were positioned at the centre of the base of the panel just behind the render at both the exterior and the interior of the panel. Instrumentation was inserted into one panel on each

Fig. 2. Media Centre in Bristol constructed from straw bales

Fig. 3. Sensor inserted just below the external render (prior to final rendering)

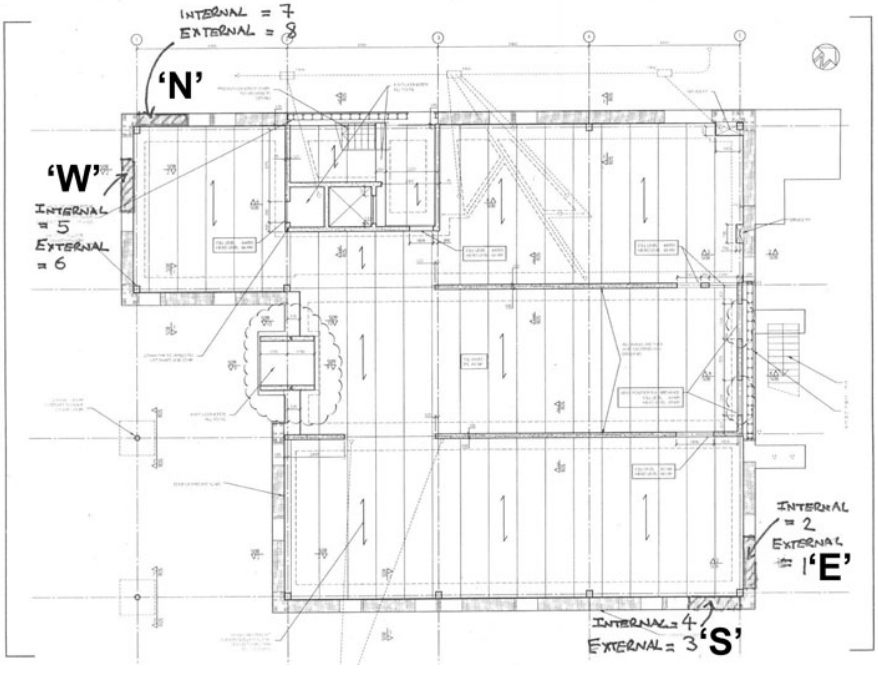

Fig. 4. Location plan of sensors on the building

elevation of the building (Figure 4), although subsequently it was found that the wiring to the sensors in the 'West' elevation was damaged during construction, and data from these were not accessible.

Wiring from the sensors was taken to a central point in the building and connected to the data logger, where data were logged at 60 minute intervals. Daily temperature and rainfall information were recorded from a publicly available weather station 500m from the building.

5 Data Acquisition

The raw RH% data are presented in Figure 5.

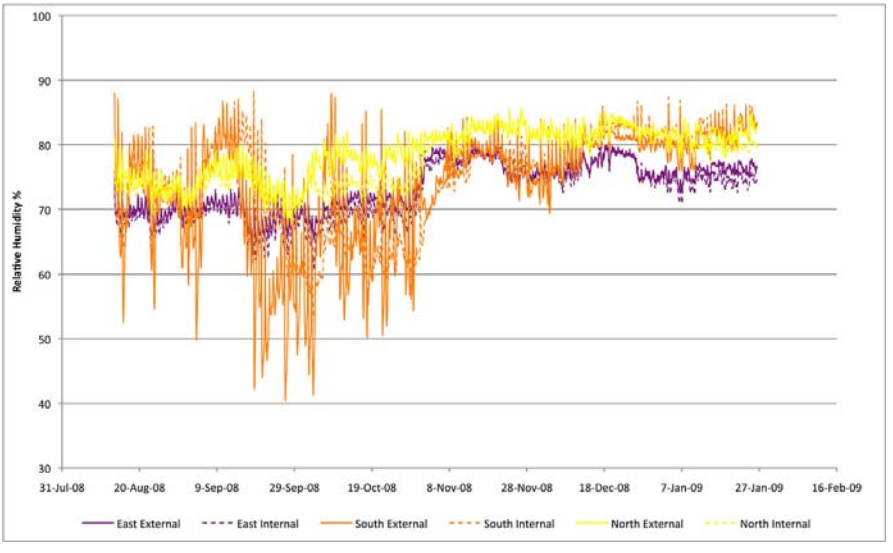

Fig. 5. Raw RH% data from sensors

The expression described above was then applied to these raw data to produce moisture content (MC) data. In order to smooth out the hourly variations and obtain a curve which is more readily able to be interpreted, the resultant MC data were averaged using a rolling 24 hour average. For a given point the previous 24 hourly measurements were averaged. This produces a curve which takes out significant individual variations to produce a smoother curve which is more readily interpreted. It was decided to use a rolling average based on a 24 hour cycle because this was felt to best represent the diurnal pattern of external humidity. The rolling average of the previous 24 hours resulted in a figure which was 12 hours out of phase (earlier) than the time point on the x axis. Resultant data were therefore moved backwards by 12 hours in order to be in phase, and therefore directly comparable, with any weather events. These data are presented in Figure 5 together with daily rainfall from a nearby weather station.

It can be seen that the curve does not show the large individual variations seen in the RH data from Figure 4.

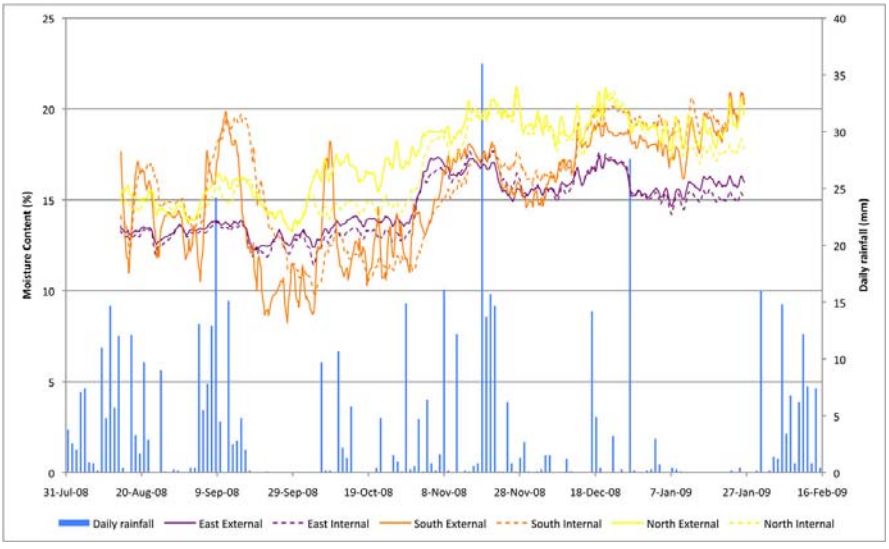

Fig. 6. Smoothed moisture content data and daily rainfall data

6 Data Analysis and Interpretation

There appear to be two distinct phases to the moisture content data. The first phase runs to about 8th November. In this phase the moisture content of the straw oscillates over a wide range of values from 8% to 20%. The moisture content increases relatively rapidly about 8 days after a rainfall incident and then reduces about 6 days after the rainfall ceases. The prevailing wind is from the South West and the most exposed face of the building is the Southern elevation. It can be seen that the data from the South elevation varies by the greatest amount with the internal MC slightly out of phase and behind the external MC. This is likely to be due to the wind driven rain increasing moisture content more rapidly than on the other two elevations. When the rainfall ceases, drying will occur more rapidly on the exposed southern elevation. The East elevation is the most protected of the three elevations, and it can be seen that there is much less variation in moisture content, both internally and externally.

Between 1st November and 15th November there was a general rise in moisture content, but subsequently the MC varies over a lower range than in the first phase, varying between about 14% and 21%, a range of 7% compared with 12% in the first phase. The moisture content during the second phase appears to be less associated with external rainfall, and appears to be buffering the moisture in the building. Individual elevations vary by between 3% and 5%, compared with over 12% in the first phase.

It is noteworthy that the differential in moisture content between the interior and the exterior is quite small, of the order of 1% or 2% only, where straw bale moisture probing has shown a differential of up to 5%. An increased scope for air flow around the frame edge is expected to have contributed to this effect. From these limited data it would appear that the straw bale moisture level takes around 8 months to establish an accommodation between the internal and the external humidity conditions, after

which time they act as a buffer, maintaining relatively steady moisture content. Further readings are required, in this building and in a number of future projects, to establish wider trends. However, other studies using periodic measurements of timber discs [10] have shown differences in MC between interior and exterior of 1%-2% with variations of between 2% and 5% between dry and wet periods depending on the orientation of the wall to the prevailing weather. This compares well with the data gathered in this study.

The data gathered to date accord with the reported environmental benefits of inhabiting straw bale buildings, where not only does the straw act as an effective thermal insulation, but also maintains a much more comfortable environment within the building.

7 Conclusions

The study is still at an early stage, and environmental data for the interior of the building are now becoming available, which will in future be correlated with the moisture content of the straw bale walls in order to establish the contribution that straw bale walls make to the internal environment of the building. Over the first 8 months of occupation of the building there had been 582mm of rainfall, with a total of 828mm to the date at which this analysis terminates (26th January 2009). During this period there has been very little opportunity for the building to dry out. During the drier months of the year it is expected that the walls will lose some of their moisture content through radiant drying.

This study suggests that straw bale walls might respond to the external environment during the early stages of the building's life, and that after about 6 months they may begin to act as a moisture buffer, maintaining a relatively constant moisture level, which should make a considerable contribution to the internal environment of the building. These tentative conclusions need to be underpinned by further planned studies. The sensors used are relatively low cost, and future buildings will be able to be instrumented to a greater extent in the knowledge that such instrumentation will provide valuable data on the performance of straw bale walls in modern construction.

Acknowledgements

The authors firstly would like to acknowledge the support of the Technology Strategy Support (TSB) Technology Programme funding for the work outlined in this paper. The TSB project consortium is comprised of White Design Associates Architects, Integral Structural Design, Agrifibre Technologies, Eurban Construction, Lime Technology and The Centre for Window and Cladding Technology. The kind co-operation of the Knowle West Media Centre, Leinster Avenue, Bristol and support and input from our University of Bath colleagues is also acknowledged.

References

[1] King, B.: Design of Straw Bale Buildings. Green Building Press, San Rafael (2006)
[2] Wooley, T.: Natural Building. Crowood Press, Marlborough (2006)

[3] Grandsaert, M.: A Compression Test of Plastered Straw-Bale Walls. In: Proceedings of the First International Conference on Ecological Building Structure, San Rafael, 43 p. (2001)
[4] Nichols, J., Raap, S.: Straw Bale Shear Wall Lateral Load Test. In: Proceedings of the First International Conference on Ecological Building Structure, San Rafael, 24 p. (2001)
[5] Faine, M., Zhang, J.: A Pilot Study Examining the Strength, Compressibility and Serviceability of Rendered Straw Bale Walls for Two Storey Load Bearing Construction. In: Proceedings of the First International Conference on Ecological Building Structure, San Rafael, 14 p. (2001)
[6] Walker, P.: Compression Load Testing of Straw Bale Walls, Technical Report. University of Bath (2004), http://people.bath.ac.uk/abspw/straw%20bale%20test%20report.pdf (Accessed September 9, 2008)
[7] Acharya, C.N.: Studies on the anaerobic decomposition of plant materials. Biochem. J. 29, 528–541 (1935)
[8] Summers, M.D.: Moisture and Decomposition in Straw: Implications for straw bale construction. In: King, B. (ed.) Design of Straw Bale Buildings. Green Building Press, San Rafael (2006)
[9] Canada Mortgage and Housing Association, Straw Bale Moisture Sensor Study (2000), http://www.cmhc-schl.gc.ca/publications/en/rh-pr/tech/96-206.pdf (Accessed January 27, 2009)
[10] Lawrence, M., Heath, A., Walker, P.: Determining moisture levels in straw bale construction. Construction and Building Materials (in press)
[11] Goodhew, S., Griffiths, R., Wooley, T.: An investigation of the moisture content in the walls of a straw bale building. Building and Environment 39, 1443–1451 (2004)
[12] Malmquist, L.: Sorption as deformation of space. Kylteknisk Tydskrift 4, 49–57 (1958)
[13] Malmquist, L.: Sorption of water vapour by wood from the standpoint of a new sorption theory. Holz als Roh und Werkstoff 5, 171–178 (1959)
[14] Hedlin, C.P.: Sorption Isotherms of five types of grain straw at 70ºF. Canadian Agricultural Engineering 9(1) (1967)
[15] Penner, E.: Suction and its use as a measure of moisture contents and potentials in porous materials. In: Proceedings of the International Symposium on Humidity and Moisture, Washington DC, IV, pp. 245–252 (1963)

An Evaluation of Environmental and Economic Performance of Sustainable Building Technologies for Apartment Houses in Korea

Hae Jin Kang[1], Jin-Chul Park[2], and Eon Ku Rhee[2]

[1] Doctoral Candidate, Dept. of Architecture, Chung- Ang University, Seoul, Korea
[2] Professor, Dept. of Architecture, Chung- Ang University, Seoul, Korea

Abstract. This study aims to evaluate economic and environmental performances of sustainable building technologies applicable to multi-family residential buildings in Korea. The technologies investigated for the study include; 'exterior insulation', 'double envelope system', 'floor radiant heating/cooling system', 'solar hot-water system' and 'photovoltaic system'. Energy performance of each technology was evaluated using "EnergyPlus" as the simulation program. A sensitivity analysis was conducted in order to determine the relative influence of each technology in terms of energy consumption reduction in a sample building. A life-cycle cost analysis of a sample building designed with conventional technologies was also conducted to compare the result with the sustainable building technologies. The result of the study indicates that the sustainable building technologies, although the initial investment costs are higher than conventional technologies, are more economical in terms of life-cycle cost due to the reduction of energy and environmental costs.

Keywords: Sustainable Technologies, Apartment Houses, Energy Analysis, CO_2 Emission Reduction, Life Cycle Cost Analysis, CO_2 Emission Right Price.

1 Introduction

Unprecedented global warming in recent days has led to a great concern worldwide for the reduction of CO_2 emissions. In Korea, the housing sector constitutes about 10% of total CO_2 emissions energy consumption in Korea. Since apartment houses account for 85% [1] of housing market in Korea, in order to effectively reduce CO_2 emission in the building sector, apartment houses should be the first place to be considered. However, since there are few research data related to CO_2 emission performance and economic feasibility of applicable building strategies, it is difficult for architects and engineers to determine viable solutions in building design and construction. The objectives of the study are to analyze the performance of sustainable building technologies and to provide designers and engineers with reliable technical data in terms of CO_2 emissions reduction economic feasibility.

2 Research Scope and Methodology

A sample building, a typical 18-story apartment building with 72 households in Asan City, was selected for the study. The actual energy consumption data of the building with relevant weather data and user pattern was collected for one year from October 2006 to September 2007. At the same time, the energy performance of the sample building was simulated with "EnergyPlus" program, and the result was compared with the actual consumption data. Afterwards, sustainable building technologies were applied to the building and the energy performances were analyzed. The energy consumption data were then converted to CO_2 emissions data by using carbon emission factor(CEF) of various fuel resources. Finally, life cycle analyses were conducted considering energy cost and environmental cost.

3 Identification of Sustainable Technologies Applicable to Apartment Houses

In order to identify major sustainable building technologies applicable to apartment houses in Korea, relevant research was reviewed. Technologies were classified in terms of design components and their energy consumption characteristics were examined. (Table 1)

Table 1. Classification of Sustainable Technologies

Component	System	Technology		Energy Resources					Index
				Natural Gas		Electricity		Water (elec)	
				Heating	Hot Water	Cooling	Lighting Etc.		
Water Resources Utilization	Grey Water System	Biological Water Treatment						●	[3],[4]
		Grey Water Reuse System						●	[3],[4]
	Rainwater Harvest	Rainwater Collection and Reuse						●	[3],[4]
Building Design	Shape	Aspect Ratio, SVR		●		●			[2],[5]
	Envelope	Exterior Insulation (Air-Tightness, High Insulation)		●		●			[3],[5]
	Aperture	Triple Glazing, Shading Device	Double Envelope	●		●			[3],[5]
		Natural Ventilation		●		●			
	Plan	Space Allocation		●		●			
Mechanical System	Heating System	Radiant Ceiling Heating		●					[3],[4]
		Radiant Floor Heating	Radiant Floor Heating/Cooling System	●					[3],[4]
	Cooling System	Radiant Floor Cooling				●			
	Water/Sanitary System	Water Efficient Appliances						●	[3],[4]
Primary Energy/ Electricity	Ventilation System	Heat Recovery System		●					[5]
	High Efficiency Equipment	District Heating System		●					[2],[4]
		Co-generation System		●		●	●		[5]

Table 1. (*continued*)

Component	System	Technology	Energy Resources					Index
			Natural Gas		Electricity		Water (elec)	
			Heating	Hot Water	Cooling	Lighting Etc.		
	Renewable Energy	Photovoltaic System			●	●		[3],[5]
		Solar Thermal System	●	●		●		[3],[5]
		Geothermal System	●		●	●	●	[5]
		Wind Power System			●	●		[5]
		Biomass System	●			●		[5]

Table 1 indicates that building technologies which affect more than two energy resource, thus have greater energy potentials, are; *Aspect Ratio and SVR, Exterior Insulation, Double Envelope System, Space Allocation, Radiant Floor Heating/Cooling System, Co-generation System, Photovoltaic System, Solar Thermal System, Geothermal System, and Biomass System*. These strategies can be used in apartment houses to reduce energy consumption, and consequently to reduce CO_2 emissions. Among these, co-generation system, biomass systems were excluded from analysis due to insufficient technologies development and/or economical feasibility. Building shape and plan were also not considered, as they are more related to subjective aspects of building design. Therefore, it was finally determined to include *Exterior insulation, Double Envelope System, Radiant Floor Heating/Cooling System, Photovoltaic system, Solar Thermal System, Geothermal System* as sustainable technologies applicable in apartment houses in Korea.

4 Validation of Simulation Tool

4.1 Simulation Tool

In order to estimate energy performance, 'EnergyPlus' program was selected as a simulation tool. The program is based on DOE-2.1E and BLAST, and is useful in modeling building heating, cooling, lighting, ventilating, and other energy flows. The program includes many innovative simulation capabilities such as time steps of less than an hour, modular systems and plant integrated with heat balance-based zone simulation, multi-zone air flow, thermal comfort, and renewable energy systems such as photovoltaics.(Drury, B. C., Jon, W. H. Michael K. Brent T. 2008)[6]

4.2 Comparison of Actual Energy Consumption and Simulated Energy Consumption

In order to secure the validity of energy simulation, actual energy consumption data of a sample apartment house was compared with the result of 'EnergyPlus' simulation. Since the actual gas consumption data read from the meter did not separate

heating, hot water and cooking, a representative household energy consumption data[7],[8] obtained from Korea Energy Economics Institute were used to distinguish the use pattern. Actual electricity consumption data were classified into cooling and electric appliances based on the appliance use pattern obtained from questionnaire survey[9]. The weather data of the area gathered from Korea Meteorological Administration was used for the simulation. The result shown in figure 1 indicates that the deviation of gas consumption is less than 10%, while the difference in electricity consumption data. Moreover, the annual patterns of consumption are found to be very similar with one another. Therefore, the simulation data can be considered quite reliable, and 'EnergyPlus' can be used as a simulation tool with a high confidence.

4.3 Energy Saving Effects of Sustainable Technologies

Table 2 shows the energy saving effects of sustainable technologies when they were applied to the sample building. Negative(-) values indicate the reduction of energy consumption when a technology was applied to the building. It was found that the magnitude of reduction is greater as the following order; ***geothermal system> double envelop system > exterior insulation> solar thermal system > photovoltaic system> radiant floor heating/cooling system.*** The increase of electricity consumption in geothermal, solar thermal and double envelope is due to the increased fan and pump operation for the technologies.

Table 2. Actual Energy Consumption of Sample Apartment House

	Jan	Feb	Mar	Apr	May	Jun	Jul	Aug	Sep	Oct	Nov	Dec
Natural Gas (㎥)	18286	14303	10302	4458	3149	2210	1952	1916	2443	3750	10063	16449
Electricity (KWh)	26928	23328	25272	23688	25056	25560	28368	28800	24624	24192	23544	27864
Water (ton)	1080	936	1296	1296	1512	1584	1584	1656	1440	1296	1152	1080

5 Energy Performance of Sustainable Technologies

5.1 Energy Simulation of a Prototype Apartment House

The energy consumption of prototype apartment house was simulated using 'Energy-Plus'. A typical apartment house, an 18- story apartment with 72 household with 120m^2 floor area each, was selected as the prototype house. The liquefied natural gas(LNG) was used for heating and electricity for cooling. The major input data for the simulation are show in Table 3.

The heating energy consumption of the building was simulated to be 1022.18MWh/yr, while cooling energy was 272.51MWh/yr. Overall, the building's energy requirement was 1294.79MWh/yr., and monthly energy consumption was shown in Figure 1.

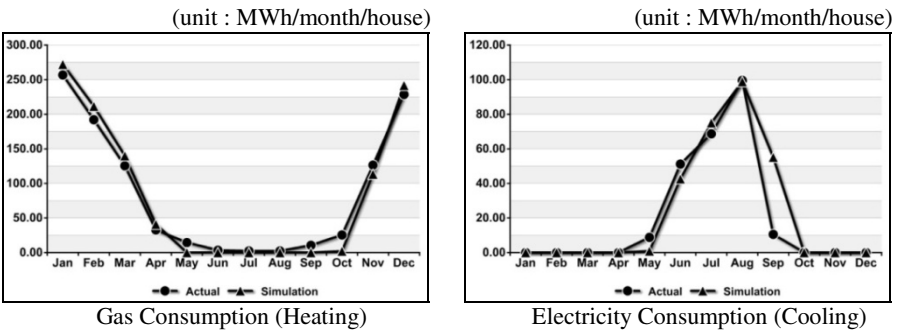

Fig. 1. Comparison of Actual Energy Consumption and Simulation Result

Table 3. Input Data for Simulation

variables		specification	Input
temp setting		-	22℃ ~ 26℃
ventilation rate		-	0.5ACH
activity	Weekday	1~7h 100%, 8h 50%, 9~12h 25%, 13~15h 0%, 16~17h 25%, 18~19h 50%, 20h 75%, 21~24h 100%	sensible heat: 70W latent heat: 45W
	Weekend	1~7h 100%, 8~9h 75%, 10~13h 50%, 14~15h 25%, 16~17h 50%, 18~20h 75%, 21~24h 100%	
internal gain		1~7h 0%, 8~9h 100%, 10~18h 18%, 19~20h 100%, 21~24h 18%	total: 9.46W/㎡
wall	exterior	concrete 180mm, insulation 90mm, board 9.5mm	U-value: 0.49(W/m²℃)
	interior	mortar 24mm, concrete 108mm, Mortar 24mm	U-value: 3.1(W/m²℃)
window		clear glazing 5mm, air gap 6mm, clear glazing 5mm	U-value: 2.7(W/m²℃)
slab		Mortar 40mm, light concrete 50mm, insulation 30mm, concrete 150mm, board 9.5mm	U-value: 0.65(W/m²℃)
heating period		-	Nov, Dec, Jan, Feb, Mar
cooling period		-	Jun, Jul, Aug

5.2 Energy Saving Effects of Sustainable Technologies

Energy simulations were conducted for the technologies previously identified Table 4 shows the conditions of sustainable technologies applied to the prototype apartment house. Each technology was applied to the house, and the result was compared with the one without the application. Double Envelope system was a box-shape with a 300mm cavity space. Radiant floor heating/cooling system utilized existing radiant heating coils for cooling. Photovoltaic panels were mounted on the building roof, while solar evacuated tubes installed in the balcony guard rails. Geothermal heat-pump system was a vertical closed circuit type using bore holes.[10]

Table 4. Characteristics of Sustainable Technologies

Technology	Applied Location	Energy Serve	Type/Size
Exterior Insulation	Exterior Wall	Heating/Cooling	200mmTHK dry construction type
Double Envelope	South Window	Heating/Cooling Ventilation	box-shape double envelope, glazing U-value: 2W/㎡K
Radiant Floor Heating/Cooling	Existing Floor Heating Coil	Heating/Cooling	refrigerator capacity: 3.6RT/house, COP 3.0
Photovoltaic	Roof	Electricity	144 panels(1,584mm*787mm, 170w each) total area of array: 180㎡
Solar Thermal	Balcony Guard Rail (Evacuated Tube)	Heating Hot water	40 houses in upper 10 floors (9~18F), 12㎡ @each house, avg radiation: 3,500kcal/㎡day
Geothermal	Underground	Heating/Cooling	vertical closed circuit type heat pump, 100RT each building

Table 5. Energy Saving Effects of Sustainable Technologies

	Natural Gas Saving (MWh)			Electricity Saving (MWh)				Total MWh	Order
	Heating	Hot Water	Total	Cooling	Individual elec. use	Collective elec. use	Total		
Exterior Insulation	-174.1	-	-174.1	-4.6	-	-	-4.6	-178.7	3
Double Envelope	-260.6	-	-260.6	-48.7	+5.3	-	-43.4	-304.0	2
Radiant Heating/Cooling	-	-	-	-7.1	-	-	-7.1	-7.16	6
Solar Thermal	-	-175.6	-175.6	-	+11.7	-	+11.7	-163.9	4
Photovoltaic	-	-	-	-	-	-28.9	-28.9	-28.95	5
Geothermal	-659.7	-	-659.7	-	+207.9	-	+207.9	-451.8	1

Table 5 shows the energy saving effects of sustainable technologies. Negative(-) values indicate the reduction of energy consumption when a technology was applied to the building. It was found that the magnitude of reduction is greater as the following order. ; *Geothermal System> Double Envelope System > Exterior insulation> Solar thermal System > Photovoltaic System> Radiant Floor Heating/Cooling System.* The increase electricity consumption in geothermal, solar thermal and double envelope is due to the increased fan and pump operation for the technologies.

6 Analysis of CO_2 Emission Reduction Performance of Sustainable Technologies

6.1 Carbon Dioxide Emission Factor (CEF)

Carbon emission factor(CEF) is the carbon content per unit of energy released for a particular fuel. CO_2 emission factor is the product of CEF multiplied by CO_2 conversion

factor. In order to estimate the amount of CO_2 emissions released from building energy use, CEF each fuel type should be established. Since there are no standard CEF values developed in Korea, CEF values issued by IPCC(inter-governmental Panel on Climate Change)[11] was used for liquefied natural gas(LNG) and CO_2 emission factor developed by KEE(Korea Energy Economics Institute) [12] was used for electricity in the study.(see Table 6)

Table 6. Carbon Dioxide(CO_2) Emission Factor

fuel	unit	TOE	Carbon Emission Factor (CEF)	CO_2 Coversion Factor	CO_2 Emission Factor
electricity	MWh	-	-	0.424	0.424
natural gas (LNG)	Nm^3	0.000955	0.6370	44/12	0.002231

6.2 CO_2 Emission Reduction

Among the sustainable technologies, *Double Envelope* was found to have the best performance in CO_2 emission reduction, followed by *Exterior insulation, Geothermal, Solar thermal*, *Photovoltaic, and Radiant heating/cooling* in descending order. The order of CO_2 emission reduction performance was different from that of energy performance, because the majority of electricity in Korea is produced by nuclear plants which emit less CO_2. Table 7 show the result of CO_2 emission reduction of each technology. Negative(-) values indicate the reduction of CO_2 emission when technology was applied to the building.

Table 7. CO_2 emission reduction of Sustainable Technologies

	CO_2emissionreduction from Natural Gas(LNG), ton			CO_2emissionreduction from Electricity, ton				Total	Order
	heating	hot water	Sub Total	cooling	Individual elec. Use	Collective elec. use	Sub total		
Exterior Insulation	-31.7	-	-31.7	-1.9	-	-	-1.9	-33.6	2
Double Envelope	-47.3	-	-47.3	-20.6	+2.2	-	-18.4	-65.7	1
Radiant Heating/Cooling	-	-	-	-4.9	-	-	-4.9	-4.9	6
Solar Thermal	-	-31.9	-31.9	-	+5.0	-	+5.0	-26.9	4
Photovoltaic	-	-	-	-	-	-12.3	-12.3	-12.3	5
Geothermal	-120.0	-	-120.0	-	+88.1	-	+88.1	-31.9	3

Table 7 shows the amount of CO_2 emission reduction of sustainable technologies when they were applied to the sample building. Among the sustainable technologies, ***double envelope*** was found to have the best performance in CO_2 emission reduction, followed by ***exterior insulation, geothermal, solar thermal, photovoltaic and radiant heating/cooling*** in descending order. For geothermal system, although energy reduction potential is the greatest, the effect of CO_2 emission reduction has decreased because of the increased electricity consumption for the increased pump operation power.

7 Analysis of Economic Performance

7.1 Life Cycle Cost Analysis Method

Since sustainable building technology shares life cycle with buildings and realizes environment performance during the life cycle of buildings, life cycle cost analysis was performed to identify economic feasibility of sustainable technologies. In the analysis, energy cost and CO_2 emission trading cost during the life cycle of the building were put emphasis on.

The values of economic variables such as discount rate, inflation rate, energy price escalation, etc. were set as the average values during the last ten years in Korean market. The life span of the analysis was set to be 40 years. The initial costs of installing systems were supplied from corresponding manufacturers, while the government incentive for renewable technologies were set to be 50% of installation cost. The CO_2 emission trading cost was estimated based on IPCC practice, which at the time of the study was about 25 euros per ton.(Yeom,Y.S. 2008)[10] The life cycle cost analysis based on these variables well represents the current trend and situation in Korea. However, the kaleidoscopic nature of global economic market and energy situation may not secure any definite analysis for future perspectives.

7.2 Economic Assessment of Sustainable Technologies

Table 8 presents the result of the life cycle cost analysis of sustainable technologies. The negative(-) sign indicates additional cost which occurs when the technology is applied to the building, compared to the case without such application. The positive(+) sign, on the other hand, represents financial gain which can be achieved, compared to the case without technology application. The result indicates that ***geothermal system*** has the best performance in life cycle cost saving, followed by ***double envelope, solar thermal, exterior insulation and radiant heating/cooling*** in descending order. However, ***photovoltaic system*** shows negative value, meaning that total life cycle cost of the system is greater than conventional system due to excessive initial cost, thus economically unfeasible even considering energy saving and CO_2 emission reduction.

Table 8. CO_2 emission reduction of Sustainable Technologies

	Exterior insulation	Double Envelope system	Radiant heating cooling	Solar thermal system	Photo-voltaic System	Geo-thermal system
Initial Cost	-231,597	-269,942	-18,523	-307,200	-225,938	-1,023,796
Financial Incentive	-	-	-	154,920	113,716	649,850
Sub-total	-231,597	-269,942	-18,523	-152,280	-112,222	-373,946
O&M	-7,074	-176,218	138,415	-218,062	-23,021	43,097
Energy Cost	652,239	1,487,276	79,250	796,804	28,820	3,067,837
CO_2Right Price	86,408	183,867	3,135	113,474	7,387	391,949
Sub-total	731,573	1,494,925	220,800	695,197	13,186	3,502,884
Total	499,975	1,224,983	202,277	542,917	-99,035	3,128,938

8 Conclusion

Since apartment houses account for 85% of housing market in Korea, in order to effectively reduce CO_2 emission in the building sector, apartment houses should be the first place to be considered. However, since there are few research data related to CO_2 emission performance and economic feasibility of applicable building strategies, it is difficult for architects and engineers to determine viable solutions in building design and construction. The objectives of the study are to analyze the performance of sustainable building technologies and to provide designers and engineers with reliable technical data in terms of CO_2 emissions reduction economic feasibility.

The technologies examined in the study are those being developed for apartment buildings as a part of the Korean government's "Low Energy Sustainable Apartment Program". A typical apartment building was selected as a sample building for the study. The actual energy consumption data of the building with relevant weather data and user pattern was collected and compared with the simulated energy performance using "EnergyPlus" program. Afterwards, sustainable building technologies were applied to the building and the energy performances were analyzed. The energy consumption data were then converted to CO_2 emissions data by using carbon emission factor(CEF) of various fuel resources. Finally, life cycle analyses were conducted considering energy cost and environmental cost. The result of the study can be summarized as follows.

1) Among the sustainable technologies, it was found that the magnitude of energy saving is greater as the following order; ***geothermal system> double envelop system > exterior insulation> solar thermal system > photovoltaic system> radiant floor heating/cooling system***.
2) On the other hand, ***double envelope system*** was found to have the best performance in CO_2 emission reduction, followed by ***double envelope, exterior insulation, geothermal, solar thermal, photovoltaic and radiant heating/cooling*** in descending order. For geothermal system, although energy reduction potential is the greatest, the effect of CO_2 emission reduction has decreased because of the increased electricity consumption for the increased pump operation power.
3) The result indicates that ***geothermal system*** has the best performance in life cycle cost saving, followed by ***double envelope, solar thermal, exterior insulation and radiant heating/cooling*** in descending order. However, ***photovoltaic*** shows negative value, meaning that total life cycle cost of the system is greater than conventional system due to excessive initial cost, thus economically unfeasible even considering energy saving and CO_2 emission reduction.
4) The result of the life cycle cost analysis presented in this study well represents the current trend and situation in Korea. However, considering the kaleidoscopic nature of global economic market and energy situation, the result should be used only as a reference in design decision-making. It is recommended that future analysis should consider a variety of scenarios and provide a number of alternative suggestions.

As global warming and energy scarcity are threatening human sustainability, all sectors of the society should make energy efforts to reduce energy consumption and CO_2 emission. The application of the findings may be limited to apartment houses design and engineering in Korea,. Although more detailed technical and energy data are needed for future refinement, the result of the study can be used as a guideline for selecting sustainable building technologies to effectively reduce CO_2 emission in apartment houses in Korea.

References

[1] Korea Energy Management Corporation, Consumption Record of Housing [Data file], http://www.kemco.or.kr/data/e_static/energy_chart
[2] Korea Institute of Energy Research. Zero Energy Town(ZET) – Construction and Technologies. Korea Research Council of Public Science & Technology. Korea (2006)
[3] Housing Research Institute. A Model Development of Environmentally Friendly Housing Estates. Korea National Housing Corporation. Korea (1996)
[4] Hyeon, S.K., Tae, K.A., Jae, S.K., Hey, S.P.: The Korean Federation of Science and Technology. In: A Study on the Development of Green Town. Korea Institute of Construction Technology, Korea (2000)
[5] Architectural Institute of Korea. A Study for Improvement of Green Building Rating System of Korea. The Korean Federation of Science and Technology Societies. Korea (2007)
[6] Drury, B.C., Jon, W.H., Michael, K., Brent, T.: Contrasting the capabilities of building energy performance simulation program. Building and Environment 43(4), 661–673 (2008)
[7] Korea Energy Economics Institute (eds.): 2006 Energy Consumption Survey. Ministry of Commerce Industry and Energy. Korea (2006)
[8] Korea Institute of Construction Technology. The Study of the Development of Energy Performance Assessment Method and Policy in Buildings. Ministry of Commerce Industry and Energy. Korea (2007)
[9] Korea Power Exchange Power Planning Dept., Survey on Electricity Consumption Characters of Home Appliance. Korea Power Exchange. Korea (2006)
[10] Yoem, Y.S.: A Study on Evaluation of Sustainable Technology for Multi-family Residential Buildings based on Life Cycle Analysis. M. Arch. Thesis: Chung-Ang University. Korea (2008)
[11] Eggleston, H.S., Buendia, L., Miwa, K., Ngara, T., Tanabe, K. (eds.): 2006 IPCC Guideline for National Greenhouse Gas Inventories. Inter-governmental Panel on Climate Change (2006)
[12] Jae, W.I.: A Study on the Basic Research for Preparation of the 3rd National Communication of the Republic Korea under the United Nations Framework Convention on Climate Change. Korea Energy Economic Institute. Korea (2005)

Managing Change in Domestic Renewable Energy Schemes

Craig Jackson[1], Fin O'Flaherty[2], and James Pinder[3]

[1] Senior Architectural Technician, South Yorkshire Housing Association
[2] Senior Lecturer, Centre for Infrastructure Management, Sheffield Hallam University
[3] Director, Positive Sum Ltd.

Abstract. The UK Government proposal to reduce carbon dioxide emissions from the residential sector to as close to zero as possible by 2050 is highly ambitious. Many proposals, strategies and technologies exist to meet this target, however there is currently a lack of empirical research and peer-reviewed data to measure their comparative effectiveness in meeting that target. The paper reviews current literature and applies lessons learned from two case studies where renewable technologies (solar thermal and photovoltaics) were installed. User attitudes towards the renewable technologies are evaluated in both case studies. The study finds that the 2050 target is unlikely to be met using the "fit and forget" approach to renewable technologies traditionally taken by house builders and housing providers. The paper posits that an understanding of the interaction between individuals and renewables is critical to their long term success and that future renewable installations will need to be accompanied by a programme of behavioural change management to ensure the maximum benefits, both in financial and environmental terms, are obtained.

1 Introduction

The housing sector currently accounts for 30 percent of energy consumed in the UK and 27 percent of carbon dioxide emissions (Boardman, 2007). Micro renewable energy technologies, such as solar photovoltaics, solar thermal hot water systems and ground source heat pumps, have the potential to help reduce CO_2 emissions from homes and contribute to the Government's target of reducing the UK's CO_2 emissions to as close to zero as possible by 2050 (DECC, 2009). Micro renewable energy technologies also have the potential to help reduce levels of fuel poverty in the UK[1]. This is particularly pertinent, given that recent increases in domestic energy prices have posed a serious impediment to the Government's aim of eradicating fuel poverty in vulnerable households by the year 2010 and all households by 2016.

This paper looks at the importance of managing change in domestic renewable energy technology schemes. In doing so, this paper will draw on the findings from the recent evaluation of two domestic renewable energy technology schemes in Rotherham and Birmingham. This paper will begin with a critical review of the literature on

[1] "The generally accepted definition of fuel poverty is when a household has to spend 10% or more of its income on energy to maintain a warm home" (DTI, p.76; 2007).

the performance of domestic renewable energy technologies and household attitudes and behaviour towards energy consumption in the home. The case study schemes will then be described and the findings from the evaluations discussed. This paper will conclude with a discussion of the common themes from both evaluations and recommendations for improving the implementation of domestic renewable energy schemes through the use of structure change management initiatives.

2 Literature Review

Despite the increasing use of renewable technologies at a domestic scale in the UK, relatively few robust empirical studies measuring performance in everyday use currently exist. This is worrying at a time when significant political pressure is being exerted to ensure that carbon reductions become the dominant factor in future development in general and within the domestic sector in particular. Measuring the effectiveness and performance of renewable technologies in use is therefore very important as a tool to enable future strategic decisions to be made.

One recent study in the UK (O'Flaherty *et al.* 2009) has shown that significant carbon dioxide reductions can be achieved using domestic scale renewables. The study also found that not all installed technologies operated at their optimum design level. This raises doubts as to whether design level outputs can be used as accurate indicators of future installed performance.

In addition to these performance issues, domestic renewable technologies are also dependant upon customer usage. For a system to operate to its optimum performance there will therefore need to be an element of user interaction with the installed technology. This can range from a periodic inspection of components to more involved user interaction. The latter will by necessity involve an element of behavioural change from the currently accepted norm (O'Flaherty *et al*. 2009).

Published studies related to behavioural change in its broadest sense are widely available, although again there are few papers which directly discuss renewable energy technologies in the domestic sector. Attitudinal research exists across many other fields and the lessons of affecting behavioural change in other sectors may be beneficial in this context (Barr, 2007).

A number of studies have found that there are significant disconnections between individuals' stated preferences and their subsequent actions or inactions (Faiers *et al.* 2006; Poortinga *et al.* 2002). These manifest themselves in findings which suggest that householders are unsure of how much they pay for their energy, how much energy they actually use or where their energy comes from. Generally it would appear that environmental factors only influence behaviour in the absence of other issues. There appears to be a tendency for individuals to demand high rates of return for their investment (short payback periods) before they consider the implementation of energy efficiency technologies (Brook Lyndhurst, 2007; Ansar and Sparks 2008).

The UK Government has recognised the importance of education and awareness regarding environmental issues and energy efficiency. Typical UK householders have become accustomed to receiving what appears to be an endless and cheap supply of energy to support their lifestyles (Brook Lyndhurst, 2007). Energy labelling has so far been used as the mechanism for enabling individuals to make informed choices,

however in practice this approach appears to be flawed as increased public awareness does not necessarily lead to improved energy efficiency (Gram-Hanssen *et al.* 2006; Benders *et al.* 2005; Pichert and Katsikopoulos 2007; Whitmarsh, 2009). Studies of UK households have shown that behaviours such as leaving appliances on standby remain prevalent despite the knowledge that doing so is costly in both financial and environmental terms. (Brook Lyndhurst, 2007)

In part, this can be ascribed to Jevons' Paradox (Jevons, 1865; Sorrell, 2008) which states that economically justified efficiency improvements can increase energy consumption, rather than decrease it. It is noted that this is more likely to be the case in the early stages of newer technologies or efficiency improvements as is currently the case with renewable solar technologies. At its logical extreme Jevons' Paradox supports a scenario whereby money saved by an individual via energy saving efficiencies is recycled into the market by, say, buying tickets for long haul flights which emit more carbon dioxide than was originally saved. Clearly this scenario is counterproductive, however reliance on free market markets and the assumption that individuals are capable of making rational, informed choices carries a risk that carbon reductions will not occur at the expected rate.

Human behaviours in such situations are highly complex but are becoming more clearly understood (Whitmarsh, 2009; Hansla *et al.* 2008; Ohtomo and Hirose, 2007). There has been a great deal of research into the psychological and theoretical aspects of the subject, however the application of established processes and techniques to domestic energy efficiency has yet to be clearly defined. A series of studies across EU Member States into the provision of energy efficiency advice found that issues are being tackled in diverse ways with each project adopting its own approach (IEE, 2008). An element of allowing markets, technologies and policy to develop in parallel is accepted as being necessary across the EU, however mechanisms are clearly required to ensure best practice and measurably effective methods are disseminated and adopted (SErENADE, 2007).

The UK Government accepts the need to respond to these shortcomings. The consultation document for the proposed Heat & Energy Savings Strategy (DECC 2009) attempts to place energy efficiency at the top of government policy agenda. It makes specific reference to improvements not just in raising awareness, but in the application of new methods for initiating and sustaining wider behavioural change. The aim is for individuals to ultimately associate waste and wastefulness with the same negative social connotations currently bestowed upon drink driving and smoking in public places.

It is important to note that behavioural change is not confined to individuals after technologies are installed. It will also be required as part of the wider project planning process within the built environment to ensure those technologies are installed in the first place (van der Waals, 2002). Despite political and regulatory reform designed to increase the implementation of carbon saving products, processes and technologies, there remains a underlying decision making structure based on simplified assessments of economic or technical issues. The ability of individuals to act as "change agents" who can assess carbon savings in a broader, more holistic sense to facilitate their introduction into a project will clearly be a key factor in the implementation of carbon reductions in the future.

3 Case Studies

The paper is based on the findings of two case studies undertaken between September 2007 and March 2009 and cover both new build and refurbishment of properties. Details of the case studies follow below.

3.1 Henley Rise Eco-Homes Scheme

South Yorkshire Housing Association's Henley Rise Eco-Homes scheme is located in the Masborough area of Rotherham, South Yorkshire, and was completed in September 2007. The scheme consists of 23 new super-insulated three bedroom homes fitted with an integrated 3.02 kWp or 3.75kWp solar photovoltaic system and a solar thermal hot water system. The development comprises a mix of rented and owner-occupied housing, the latter of which were sold on a fixed-equity basis. An evaluation of the scheme was funded by the Economic and Social Research Council and undertaken by Sheffield Hallam University between October 2007 and March 2009. The evaluation involved:

- Monitoring the renewable energy technologies in two of the homes over an 18 month period, commencing October 2007, together with prevailing weather conditions, such as solar radiation, air temperature and wind speed. Local influences such as pitch of the roof and shading were also investigated.
- The collection of energy generation and consumption data from the meters fitted to all 23 homes and utility bills provided by households. Meter readings were taken on a monthly basis.
- Semi-structured face-to-face interviews with residents in order to examine the useability of the technologies, establish whether residents felt "better off" living in the homes and to investigate whether living in homes fitted with renewable energy technologies had affected residents' attitudes and behaviour towards energy consumption in the home.

This paper will focus primarily on the findings from the interviews with residents; the findings from the analysis of the monitoring and meter reading data can found in O'Flaherty *et al.* (2009).

3.2 Summerfield Eco Neighbourhood Scheme

The Summerfield Eco Neighbourhood scheme represents the latest stage in the regeneration process of the Summerfield area of Birmingham, an area containing a diverse range of housing types, demographics and households. All of the 329 homes covered by the Eco Neighbourhood scheme were fitted with solar thermal hot water systems. Solar panels were mounted predominantly on south facing roof pitches, although homes without south facing roof pitches had panels fitted on east and west facing roof pitches. Approximately 40-50 percent of homes were found to have heating systems that were either obsolete or incompatible with the solar thermal system. These systems were replaced with grade 'A' efficiency combi-boilers or system boilers.

The primary objectives of the Eco Neighbourhood project was to address the problem of fuel poverty in the area, by mitigating against future energy price rises, and to

reduce carbon dioxide (CO_2) emissions. Households with an income of less than £22,000 were eligible for free installations, on the basis that they were more likely to be suffering from fuel poverty. The scheme was managed on behalf of Birmingham City Council by Family Housing Association, the largest registered social landlord in the area. Family Housing Association commissioned Sheffield Hallam University to conduct an independent evaluation of the scheme between March and June 2008. The evaluation involved:

- Semi-structured interviews with 17 stakeholders in the Eco Neighbourhood scheme, including representatives from Family Housing Association, Birmingham City Council, Urban Living (one of the scheme's funders) and New World Solar (the contractor). Interviews were undertaken face-to-face or over the telephone and sought to identify lessons and good practice from the project.
- A questionnaire survey of 250 residents that had changes made to their homes as part of the scheme. Recipients of the questionnaire were asked, amongst other things, to indicate their satisfaction with the installation process and the renewable energy technologies, and whether they had noticed any difference in their energy bills since the installation. Forty-seven questionnaires were returned, constituting an 18% response rate.
- Semi-structured face-to-face interviews with 30 residents that had participated in the scheme. Interviewees were asked a series of questions about the changes made to their home and their attitudes towards environmental issues. The interviews encompassed a broad diversity of ages of residents, including elderly residents living alone, young families, multi-generational households, and a cross-section of ethnic backgrounds.

4 Findings

Data were obtained via a number of different methods and some themes emerged consistently across both case studies. Verbatim comments from individuals are used to supplement other data throughout the paper. It is acknowledged that these do not necessarily represent the majority view in all cases, so quotes have only been used where they are either repeated or supported by other respondents.

Generally, residents across both case studies were happy with the renewable technologies installed in their homes. At Henley Rise, interviews elicited a number of positive responses.

> "Brilliant. Couldn't get me out of here, I love it. Absolutely love it."
> (Henley Rise resident)

In Summerfield, questionnaire results suggested that a large majority of residents were satisfied with their solar panels (See Fig 1), however the majority of residents hadn't seen any financial benefits from the installations (See Fig 2). This could be attributed to a number of factors, including that:

- The solar thermal system had only been recently installed, which means that residents had not had sufficient time to notice any year-on-year difference in their energy bills ("We've got big hopes for the summer months that the bills will be less")

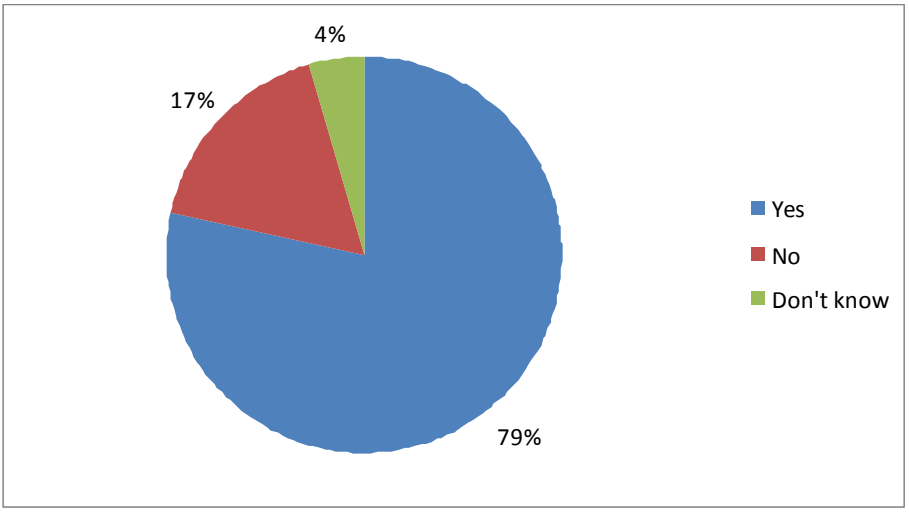

Fig. 1. Are residents satisfied with their solar heating systems?

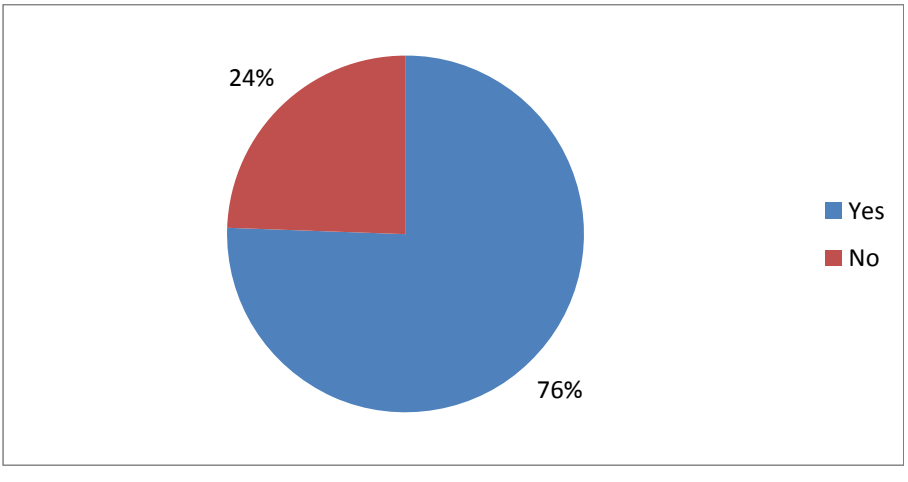

Fig. 2. Has the installation of a solar hot water heating system in your home made you think differently about how you use energy?

- Residents were focusing on the cost rather than the number of units of energy consumed, which means that any savings may have been obscured by recent increases in energy prices ("It has made a difference, but increasing fuel prices, that's the killer because it's hard to see a difference").
- Residents had not received a gas or electricity bill since the solar thermal system had been installed.
- Residents are making payments on a fixed monthly Direct Debit basis.

Some of the residents that had noticed a reduction in their energy bills had made small changes to their daily routines in order to derive maximum benefit from the solar thermal system:

> "I changed my lifestyle in as much as I realised that in the evening we'd have heated water from the sun, whereas in the morning it might well have cooled down. So rather than having an early morning shower, I'll leave the washing until the evening, and I'll have a shower in the evening, so I don't have to use the back up. At the moment I'm not using it at all."
> (Summerfield resident)

> "I think you tend to work out when is the best time, so now if I want to do the washing … I know if it's really hot that it'll keep going and I'll have that free hot water."
> (Summerfield resident)

Despite this, the question of how to get the best from the systems across both case studies remains an issue. A lack of coaching, instruction or advice was cited as a key factor. One resident suggested a visit once the system has been in place for a while would be useful:

> "It took a while for me for it to plot how the actual boiler works, but then to use the controls, to understand what kicks in when and what to expect. Looking back, if it was me running the thing, I would have another visit a few months in, because at the time you don't know what questions to ask. … But the reality is, from a customer service perspective, I would have preferred a visit about a month or two afterwards."
> (Summerfield resident)

Because:

> "You don't know the questions to ask until you're in what I call the 'solar season'"
> (Summerfield resident)

Many residents found the systems very complicated to operate:

> "I think most people had problems with the controls because they're so complicated…. It's too detailed I think for most people."
> (Summerfield resident)

> "They showed us the boiler, and I was like, that is amazing, I've never seen a boiler like that in my life, it were like something out of Star Wars."
> (Henley Rise resident)

Other indications about the problems that remain with regard to public perception of renewable technologies were found with residents being particularly unsure of future maintenance implications. A number expressed concern about what would happen if something went wrong with their systems.

> "I know we're guaranteed for a year, but it's like, after that what happens? And it's having sufficient people that are willing to do it at a reasonable price is a risk. That's an issue I think. It's the potential for being ripped off I think. They're not common yet. …"
> (Summerfield resident)

> "At some point something's going to go wrong with it, and we want to know what we've got to do."
> (Summerfield resident)

The inherent problems associated with long term maintenance of these technologies, especially for individuals on low incomes was also evident.

> "If it costs a lot to repair we might not bother, as we don't have a lot of money."
> (Summerfield resident)

The effect of a lack of effective ongoing maintenance could be significant in the drive to reduce carbon emissions. Projections for the total carbon dioxide savings anticipated will not be met where systems are inadequately maintained or are allowed to operate below their optimum performance. The need to adequately and accurately monitor and respond to changes in these systems is therefore critical to the long-term success of renewable technologies.

Householders therefore need to be given the tools to assess and monitor their own systems. This was an aspect that was lacking in both case studies.

> "I realise I got something for free but this could have been done better - particularly explaining how it works. My neighbour who doesn't speak English didn't know how to use the system"
> (Summerfield resident)

Despite this, some residents were aware of the potential of their renewable technologies and were able to notice a difference in how their system operated and the benefits that were accruing.

> "Although in the winter there was no sunshine, I noticed how quickly the water heated using the back-up heating, because the water was not hot, but it certainly wasn't cold as it would have been without the solar panel. It was just topping it up."
> (Summerfield resident)

> "If things stay how they are, then I think it should do (make a difference). I reckon it will be massive. I know everyone's complaining about fuel bills going up, but mine seems to have gone down, so I've kept quiet at work. … I can't complain!"
> (Henley Rise resident)

This was supported by responses to questionnaires at Summerfield which suggested that over 75% of respondents thought differently about how they used energy (See Fig 3). It also acted as an indicator to one of the wider outcomes from both projects which was to ascertain whether living in an "eco" house had a positive effect on attitudes and behaviours towards "green" issues generally. The study found interesting and encouraging correlations across both case studies with many residents reporting changes in their attitudes and/or behaviours.

> "Went to Currys and said I'm moving into an eco-house … they told me ways to save money, save water. … They were very good explaining which were the best appliances to buy."
> (Henley Rise resident)

> "You want to leave a good place for your children, so you should do what you can do, it doesn't affect your life, it won't kill you. So you should recycle, you should turn things off, you should use less heat, you should use solar installations and so on. It saves you money as well at the end of the day."
> (Summerfield resident)

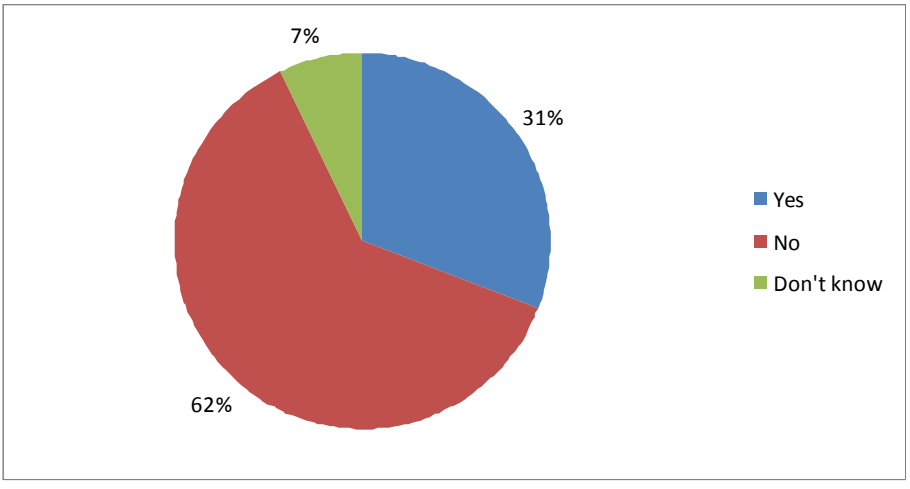

Fig. 3. Have you noticed any difference in your energy bills since the installation of your new hot water heating system?

"With the recycling, before I were just like, sling it in the bin, but now we're more like, at it."
(Henley Rise resident)

"I think we should all do as much as we can to make changes to the way we use energy and think more about the long term consequences to the environment"
(Summerfield resident)

"I've just signed up for that paperless billing. I never thought I'd do that, but I heard about it, and I said to them 'well will I save any money?' and they said 'well you're saving trees', so I said 'go on then'
(Henley Rise resident)

5 Conclusions

This paper set out to discuss whether change management initiatives can improve the efficiency and effectiveness of micro renewable energy technologies in low-income housing. Analysis of the interview and questionnaire survey data from the Henley Rise and Summerfield case studies highlighted a number of change management issues that were common to both schemes. Foremost amongst these were:

- The importance of providing residents with appropriate information and guidance about the use of the renewable energy technologies installed in their homes.
- The positive impact that the installation of renewable energy technologies can have on residents' attitudes and behaviour towards energy consumption and the environment.
- The importance of managing residents' expectations about the impact of the renewable technologies installed in their homes.

- The need to develop appropriate strategies for servicing and maintaining the renewable energy technologies.

6 Recommendations

Future eco-home projects should include a structured programme of "carbon coaching", whereby residents are educated on a range of energy efficiency issues, such as how to make best use their renewable energy technologies, how to understand and read their utility bills, and how to save energy in the home. Such programmes could be delivered on a one-to-one basis or in groups, depending on the nature and scale of the project. The carbon coaching programme could also provide carbon footprint profiling for residents, so that they can see their environmental impact before and after the installation of the low carbon technologies.

The installation of "smart meters" should be considered in all eco-home projects in order to help residents to understand where and how much energy they are consuming. Evidence from other eco-home developments[2] suggests that such metering devices can have a positive influence on helping residents to reduce their carbon footprint. Smart metering was considered at the outset of the Summerfield Eco Neighbourhood project and a bid was submitted in partnership with Birmingham City Council but unfortunately was unsuccessful.

Any future projects of this type should, from the outset, include a programme of independent monitoring so that the impact of the projects can be evaluated using robust quantitative data. Such data are critical in helping to understand the benefits of low-carbon technologies and encourage their adoption by home owners. This is particularly the case with the Summerfield Eco Neighbourhood project, given the number and diversity of homes and the wide range of household types. Residents could also be engaged in the data collection process, for instance by asking them to log meter readings at regular intervals. Post-project evaluations should take place at least six months after the installation of the low-carbon technology in order to allow sufficient time for residents to notice the benefits gained.

Funding should be made available to enable a suitably qualified contractor to provide free planned and reactive maintenance services to residents in order ensure that the solar thermal systems continue to operate at optimum efficiency over their 20-25 year life-cycle. Many residents, most of whom are on low incomes, may not have the funds to maintain or repair the technology, despite the benefits they will derive in terms of lower fuel bills. The homes may also change ownership over time and the new owners may not have the awareness, funds or inclination to repair the panels. The cost of such a maintenance service should therefore be factored into the budgets of future eco-home projects, for instance through the use of a credit union to establish a sinking fund, which could also be used to pay for the replacement of any solar thermal panels, when required, and the glycol (heat exchange fluid) in the panels, which needs replacing every 5-7 years. Such a fund could be developed as a social enterprise to include training of solar panel and gas servicing maintenance engineers.

[2] For example, see Darby, S. (2006) *The effectiveness of feedback on energy consumption,* Department for Environment, Food and Rural Affairs.

Future eco-home projects, particularly those on the scale of the Summerfield Eco Neighbourhood, should be delivered in discrete phases with opportunities for reflection at the end of each phase. Funding streams should be structured to ensure phasing can be incorporated into the project timetable. Such an approach will allow lessons to be learnt and applied during the course of the project. A longer lead time should also be built into future project to enable adequate planning and resourcing, and to enable homes to be surveyed in advance. This will also enable the managing contractor to develop the trust of residents and strategic relationships with installers and suppliers in order to gain larger discounts on equipment and installation costs, thereby enabling more homes to be upgraded.

Incentives are required to encourage equity rich home owners and those on higher incomes to participate in future eco-home projects. The Summerfield Eco Neighbourhood project was successful at engaging a small number of "afford to pay" residents by part-funding the cost of the technology, however, other incentives, such as interest free loans, should also be considered in future projects. Clear information on eligibility criteria and part funding should be provided to residents at the start of the project in order to manage expectations, aid transparency of decision-making and maximise participation amongst residents. For larger projects it might be worth providing an online "self-assessment" tool or application form in order to speed up the application process and reduce the administrative burden on the managing contractor.

Other forms of low-carbon and renewable energy technologies should be considered for use in future eco-home projects, including new build housing developments. Examples include photovoltaic arrays, combined heat and power (CHP), bio mass (wood pellet burners), large wind turbines and ground source heat pumps. Such technologies might be used to provide energy to groups of homes and feed electricity back into the national grid, making the project more financially viable. Experience from other projects suggests that it is possible negotiate with energy suppliers and obtain a higher rate for units of electricity returned to the national grid. A proposal for a guaranteed income via a Feed-in Tariff and the Renewable Heat Initiative is currently being considered by the UK Government.

7 Further Research

The paper recommends that further research is necessary in understanding the complex relationships between individuals and the renewable technologies which will form a significant part of the UK commitment to carbon reductions by 2050.

Methods to accurately measure baseline data, energy in use and carbon dioxide savings in a practical, comparative sense will need to be developed, measured, analysed and the findings disseminated.

Acknowledgements

The authors would like to thank the Economic and Social Research Council, South Yorkshire Housing Association and Family Housing Association for funding the evaluations, and Peggy Haughton for her assistance with the interviews and data analysis.

References

Ansar, J., Sparks, R.: The experience curve, option value, and the energy paradox. Energy Policy 37, 1012–1020 (2008)

Barr, S.: Factors influencing environmental attitudes and behaviours: A UK case study of household waste management. Environment & Behavior 39(4), 435–473 (2007)

Benders, M.J., et al.: New approaches for household energy conservation – in search of personal household energy budgets and energy reduction options. Energy Policy 34, 3612–3622 (2005)

Lyndhurst, B.: Public understanding of sustainable energy consumption in the home. Department for Environment Food & Rural Affairs (2007)

Boardman, B.: Home Truths: A low carbon strategy to reduce UK housing emissions by 80%. Research Report for Co-operative Bank and Friends of the Earth, November 27 (2007)

Darby, S.: The effectiveness of feedback on energy consumption. Department for Environment, Food and Rural Affairs (2006)

DECC, Heat & Energy Saving Strategy Consultation Department of Energy & Climate Change, London (2009)

DTI, Meeting the Energy Challenge: A White Paper on energy, The Department of Trade and Industry, London (2007)

EEA, Household consumption and the environment, European Environment Agency, Office for Official Publications of the European Communities (2005)

Faiers, A., et al.: The adoption of domestic solar power systems: Do consumers assess product attributes in a stepwise process? Energy Policy 35, 3418–3423 (2006)

Gram-Hanssen, K.: Do home owners use energy labels? A comparison between Denmark & Belgium. Energy Policy 35, 2879–2888 (2006)

Hansla, A., et al.: Psychological determinants of attitude towards and willingness to pay for green electricity. Energy Policy 36, 768–774 (2007)

Jevons, W.S.: The Coal Question, Can Britain Survive? In: Flux, A.W. (ed.) The Coal Question: An Inquiry Concerning the Progress of the Nation and the Probable Exhaustion of Our Coal Mines. Augustus M. Kelley, New York (1865)

IEE, Energy efficient homes and buildings. The beauty of efficiency Intelligent Energy-Europe Project Report No. 2. Executive Agency for Competitiveness and Innovation of the European Commission (2008)

O'Flaherty, F., et al.: The role of photovoltaics in reducing carbon emissions in domestic properties (2009)

Ohtomo, S., Hirose, Y.: The dual-process of reactive & intentional decision-making involved in eco-friendly behavior. Journal of Environmental Psychology 27, 117–125 (2007)

Pichert, D., Katsikopoulos, K.V.: Green defaults: Information presentation and pro-environmental bahviour. Journal of Environmental Psychology 28, 63–73 (2007)

Poortinga, W., et al.: Household preferences for energy-saving measures: A conjoint analysis. Journal of Environmental Psychology 24(2003), 49–64 (2002)

SErENADE, Energy Advice in Europe 2007: A review of current practice in advice on sustanable energy in the countries of the European Union Intelligent Energy-Europe. Executive Agency for Competitiveness and Innovation of the European Commission (2007)

Sorrell, S.: Jevons' Paradox revisited: The evidence for backfire from improved energy efficiency. Energy Policy 37, 1456–1469 (2008)

Whitmarsh, L.: Behavioural responses to cliamte change: Assymetry of intentions and impacts. Journal of Environmental Psychology 29, 19–23 (2008)

Optimum Energy Management of a Photovoltaic Water Pumping System

Souhir Sallem, Maher Chaabene, and M.B.A. Kamoun

Unité de Commande de Machines et Réseaux de Puissance CMERP-ENIS, Tunisia
Mba.kamoun@enis.rnu.tn, maherchaabene@gmail.com,
souhirsallem@gmail.com

Abstract. This paper presents a new management of the energy of a photovoltaic water pumping installation composed of a battery, a water pump and a photovoltaic panel. The approach makes decision on the optimum connection times of the installation elements using fuzzy rules considering the battery safety on the first hand and the forecasted Photovoltaic Panel Generation (PVPG) on the second hand. The approach extends the operation time of the water pump with respects to multi objective management criteria. The system assessment confirms an improvement of about 90% of the pumped water volume referring to the stand alone management method.

Keywords: photovoltaic, water pumping, modeling, optimization, energy management.

1 Introduction

Researches published in photovoltaic water pumping were interested essentially either in water pump modeling and control [1-2] or in overall system modeling and simulation [3] so as to bring a contribution to the study of the behaviors of the photovoltaic generators and converters used to feed an asynchronous machine actuating a centrifugal pump [4].

Other researchers developed strategies in order to offer optimum energy management of PVP systems [5-6]. Thus, many algorithms are developed to forecast climatic parameters behavior during daylight [7]. Forecasted data are placed in a PVP model in order to predict the Photovoltaic Panel Generation (PVPG) during a considered day [8-9]. The estimated PVPG constitutes a determinant factor in photovoltaic installation sizing and energy management.

Some recent works combined the previous thematic in order to build optimum control tools based on the energy management of the photovoltaic plants produced energy [5-7-8]. This paper presents a continuation of previous published works which stated algorithms that forecast the instantaneous PVPG since the sunrise of a considered day on the basis of the climatic parameters behavior during the day before. In view of the estimation results of the PVPG during a considered day, an intelligent fuzzy rules based algorithm makes decision on the connection ways and times of the components of a PVP/battery/water pump plant. Decisions must maximize the pumping period on the one hand and guarantee a sufficient depth of discharge in

the battery (dod less than 0.5) during the day, a total use of PVPG and a power supply stability for the pump motor on the other hand.

Following section 2 presents the energy management strategy. The fuzzy algorithm is given in section 3. Section 4 presents the system assessment. Finally, section 5 gives a conclusion.

2 The Management Strategy

The interconnection mode and instants of PVP installation components: a lead acid battery, a pumping motor and a PVP is decided on the basis of the following criteria:

- To reserve a PVPG power margin of +10%: the connection of the water pump to PVP output cannot be decided unless PVP estimated available power is more than 110% of the load operating power, which guarantees continuous electric supply for water pump face to possible climatic perturbations.
- To store in the battery the generated energy which is either supplementary to the load need or insufficient to operate the water pump.
- To guarantee a depth of discharge in the battery (dod) less than 0.5 in order to protect the battery against excessive discharge.

Figure 1 traces the synoptic schema of the proposed approach. The estimated PVPG is managed to supply either the pumping motor or a lead acid battery or both. In addition, the connection time of the pumping motor to the battery is computed so as to keep the $dod < 0.5$ and to ensure a continuous power supply to the load. The PVPG and the *dod* calculations are based on published and validated models [7-8-10].

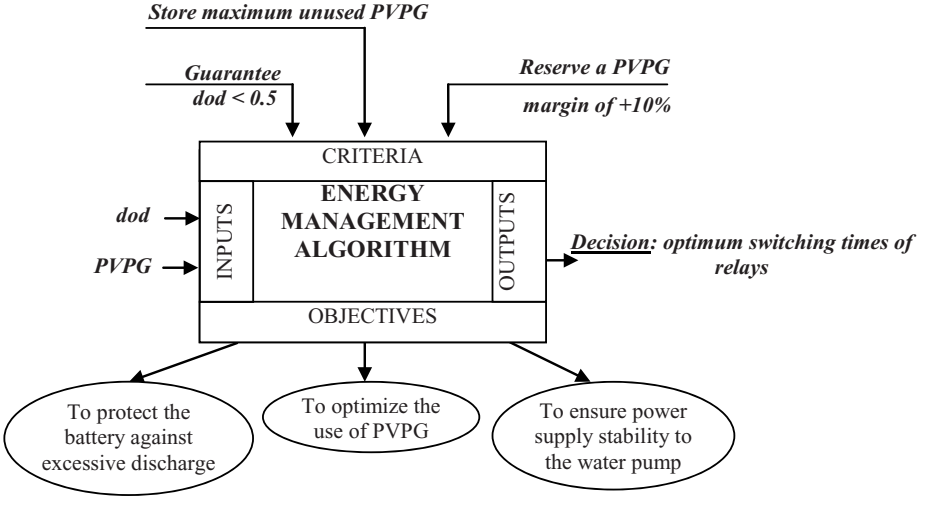

Fig. 1. The synoptic schema of the proposed approach

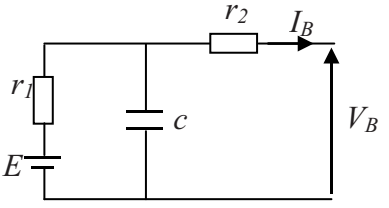

Fig. 2. The equivalent circuit of a cell lead acid battery

2.1 The Battery Model

A non linear dynamic model of a lead acid battery is used. Figure 2 gives the equivalent circuit of a lead acid battery. I_B is the algebraic value of the battery current (positive when charging and negative when discharging), V_B is the output voltage and R (function of r_1 and r_2) is the internal equivalent resistance of a battery. The open circuit voltage E (Eq.1) is proportional to the battery depth of discharge ($dod = 0$ when the battery is fully charged and $dod = 1$ when the battery is empty) [10].

$$E = n(2.15 - dod(2.15 - 2)) \tag{1}$$

$$dod = \frac{C_R}{C_P} \tag{2}$$

where n is the number of cells in the battery, C_R is the value of the battery capacity and C_P is the Peukert Capacity (Eq. 3):

$$C_P = I_B^k T \tag{3}$$

where k is the Peukert coefficient $(k = 1.12)$ and T is the constant-current discharge time. Referring to figure 2, the output voltage is:

$$V_B = E - RI_B \tag{4}$$

The output power is then expressed as a quadratic equation:

$$P_B = V_B I_B = (E - RI_B) I_B \tag{5}$$

This yield to the calculation of algebraic value of the battery current:

$$I_B = \frac{E - \sqrt{E^2 - 4RP_B}}{2R} \tag{6}$$

Hence, the instantaneous charge removed from the battery at a considered current I_B is:

$$\frac{\delta C_R}{\delta t} = \frac{I_B^k}{3600} Ah \tag{7}$$

2.2 The PVP Generation Model

In a previous published work [8], authors give a dynamic prediction model of solar radiation and ambient temperature. Prediction is based on climatic parameters behaviours during the day before and on time distribution models. The algorithm forecasts solar radiation ($\hat{G}_{d|d-1}$) and ambient temperature ($\hat{T}_{d|d-1}$) for a considered day, on the basis of their evolutions during the previous days. Forecasted climatic parameters are used as inputs to a PVP generation model in order to predict the PVPG ($\hat{P}_{pv_{d|d-1}}$) during a considered day (d). Consequently, a 1kWp PVPG generation of a PVP is given:

$$\hat{P}_{pv_{d|d-1}} = 20(3.33 + 1.2\,10^{-3}(\frac{\hat{G}_{d|d-1}}{1000}(\hat{T}_{d|d-1} + \frac{1}{40} - 25) + 3.35(\frac{\hat{G}_{d|d-1}}{1000} - 1)u_{pv} \tag{8}$$

Yet, the predicted current generated by PVP is:

$$\hat{I}_{pv_{d|d-1}} = \frac{\hat{P}_{pv_{d|d-1}}}{u_{pv}} \tag{9}$$

3 The Fuzzy Management Algorithm (FMA)

The switching strategy consists of Four possible operating modes are fixed (figure 3). In the first mode (M_1: only R_1 is switched ON), the battery supplies the pump motor while $dod < 0.5$. This mode is suitable in the morning before sunrise. In the second mode (M_2: R_1 and R_2 are switched ON), the battery and the PVP provide the pump motor required power if the predicted PVPG power is less than 110% of the motor pump power and if $dod < 0.5$. This mode is suitable in the morning just after sunrise. The third mode (M_3: R_2 and R_3 are switched ON) is decided if the predicted PVPG is more than 110% of the pump motor power. Thus, the PVP supplies at the same time the battery and the pump motor. In the fourth mode (M_4: only R_3 is switched ON), the predicted PVPG power is less than 110% of the pump motor power. This mode is suitable in the afternoon in order to store unused energy in the battery for the next day. During a considered day, the instantaneous power balance of the system is:

$$\hat{P}_{pv_{d|d-1}} + \overline{P_B} = P_i \tag{10}$$

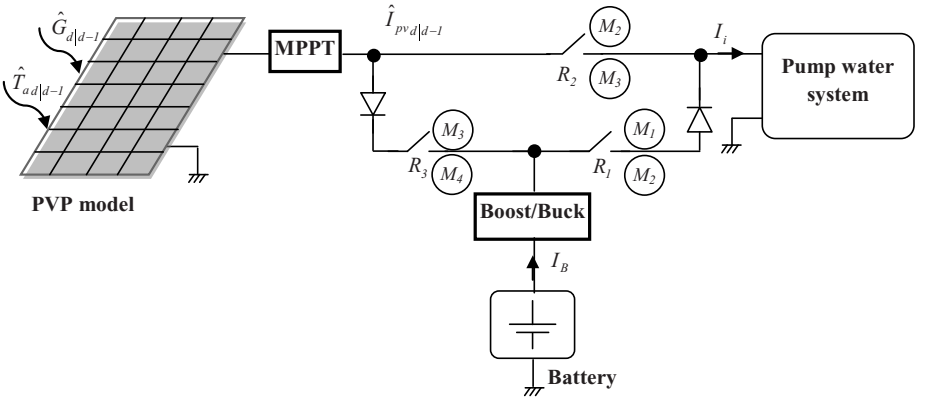

Fig. 3. The switching strategy for the PVP/ Battery/Load system

Since the voltage supply is fixed to $12V$, then:

$$\hat{I}_{pv_{d|d-1}} + \overline{I_B} = I_i \tag{11}$$

where I_i is the input current of the pump water system.

Figure 4 gathers the different operating modes. The switching strategy aims to determine the instant t_c for which the pump motor should start in order to offer continuous and longer time of water pumping. Considering t_{10} and t_{11} as the intersection times of $\hat{P}_{pv_{d|d-1}}$ and P_i curves, the connection time t_c of the load to the battery is computed to guarantee at the instant t_{10} a battery $dod_{\max}$ equal to 0.5. The first connection time of the battery to the load is calculated knowing dod_i and dod_f .

Hence, the proposed approach extends the overall operation time of the water pump to the period ΔT (Eq. 12) instead of the duration ΔT_3 observed in the conventional pumping mode.

$$\Delta T = \Delta T_1 + \Delta T_2 + \Delta T_3 \tag{12}$$

Where $\Delta T_1 = t_{sr} - t_c$, $\Delta T_2 = t_{10} - t_{sr}$ and $\Delta T_3 = t_{11} - t_{10}$.

Since the energy management is based on cases study, it is obvious to choose the fuzzy logic tool to decide the optimal connection mode of the system. Known as an intelligent tool, fuzzy logic offers fast decision using multi-rules resolution for multi-variable consideration [11-12].

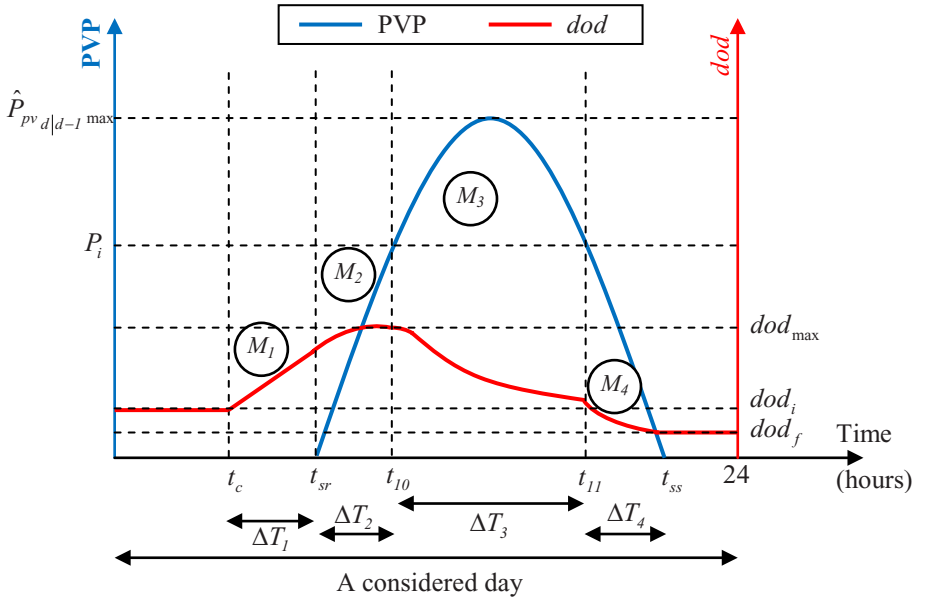

Fig. 4. The different operating modes

According to the management criteria given in section 2, the management algorithm is based on the following fuzzy rules:

- If $dod \in [0,0.5]$ and $P_{pv} \in [0,50]$ and *time is am* then R_1 is ON
- If $dod \in [0,0.5]$ and $P_{pv} \in [50,450]$ and *time is am* then R_1 and R_2 are ON
- If $dod \in [0.5,1]$ and $P_{pv} \in [0,450]$ and *time is am* then R_3 is ON
- If $dod \in [0,1]$ and $P_{pv} \in [450,1000]$ and *time is am* then R_2 and R_3 are ON
- If $dod \in [0,0.2]$ and $P_{pv} \in [0,50]$ and *time is pm* then R_3 is ON
- If $dod \in [0,0.2]$ and $P_{pv} \in [50,450]$ and *time is pm* then R_1 and R_2 are ON
- If $dod \in [0.2,1]$ and $P_{pv} \in [0,450]$ and *time is pm* then R_3 is ON
- If $dod \in [0,1]$ and $P_{pv} \in [450,1000]$ and *time is pm* then R_2 and R_3 are ON

4 The System Assessment

The approach is validated on an installation composed of a $1KWp$ PVP equipped with a maximum Power Point Tracker, a $420Ah$ lead acid battery and a $400W$ pump motor supplied through a three phase voltage inverter. The installation is controlled by a PC computer equipped with Matlab7 software and an Input/output interface card. At the end of each day $(d-1)$, the management algorithm is executed so as to compute the switching times of the relays (Figure 1) for the next day (d). The procedure consists of:

step 1: Predict the PVP generation for the day (d) on the basis of the climatic parameters forecast [8] for the day (d) and equation 8.

step 2: Acquire the battery current I_B and calculate the battery dod relative to the end of the day $(d-1)$.

step 3: Compute the switching times (ON and OFF) of the different relays for the day (d) by executing the fuzzy rules of the management algorithm which are based on the predicted PVP generation (given by step 1) and the battery dod (given by step 2).

During the day (d), the computer controls instantaneously the whole installation by switching ON and OFF the relays at the times planned by step 3 and controls the pumping motor.

The system has been tested during 2007. For clarity reason, the results are given for arbitrary days relative to the moderate season [7-8]. Since the visualization behavior during the day before is necessary to achieve calculation, results are shown for three consecutive days. Each set of results (figure 5) is composed of:

- The predicted and measured PVP generation,
- The switching traffic of the relays,
- The instantaneous state of the battery *dod*,
- The installation currents: generated by PVP $(\hat{I}_{pv_{d|d-1}})$, absorbed by the pumping motor I_i and delivered or received by the battery I_B.
- A comparative histogram giving the cumulated volume of pumped water using both a stand alone classical mode and our approach.

By analyzing the different seasons' results, it can be seen that the predicted and measured PVPG converge which proves the efficiency of the prediction approach, thing already confirmed by previous works [8-9].

The relays' timings, trough the different seasons, given by Figure 5.a confirms that the relay R_1 connects the load to the battery at the computed time t_c. At sunrise time, the load becomes provided through R_1 and R_2 by both the PVP and the battery.

Table 1. Experimental results across seasons

		dod_i	dod_f	t_c	ΔT	ΔT_3
Moderate Season	*October22nd*	*0*	*0.247*	*2h 28 mn*	*12h 44mn*	*5h 45 mn*
	October23rd	*0.247*	*0.219*	*5h 16 mn*	*10h 07mn*	*6h 04 mn*
	October24th	*0.219*	*0.245*	*5h 06 mn*	*10h 07mn*	*5h 35 mn*

This mode continuous until the PVP output reaches $440W$. At this moment, R_1 is switched OFF and R_3 is switched ON in order to charge the battery by the unused PVP power. As for R_2, it remains ON so as to guarantee a continuous load supply. In the classical control mode, the load is supplied only when PVP generation is more than $400W$ (this mode is represented by ΔT_3 in figure 4). Compared to this mode, the developed strategy offers a time function (ΔT : figure 4) starting at the time t_c until the switching OFF time of the relay R_2. Thus, the approach extends the operation time to ΔT instead of ΔT_3 (figure 4).

Table 1 summarizes for the chosen days of October 2007, the computed time t_c and the operation times in both the classical (ΔT_3) and the proposed approach (ΔT). In addition, the average of the time operation of water pumping relative to the classical ($\Delta T_{3\,AV}$) and the new approach (ΔT_{AV}) over the three considered days is $\Delta T_{AV} = 10h59mn$ instead of $\Delta T_{3\,AV} = 5h48mn$.

Considering the chosen days as typical, the daily mean improvement of the water pumping time is $5h11mn$.

Figure 5.b gives the state of discharge of the battery, the currents assessment and the volume of pumped water for the above considered days.

During experiment, the battery dod of the first day is assumed equal to zero which means that the battery starts at a full state. At the end of each day, the battery dod is less than *0.247*. Moreover, during the day, the battery dod is maintained less than 0.5. This should protect the battery against deep discharge thanks to the third management criteria (section 2).

Referring to current curves, the current assessment (Eq.11) is respected along the day. These curves reflect the dod variation. In fact, starting t_c time the battery is discharged at constant current until sunrise after which it is discharged in a manner that respects Eq.11 so as to provide at constant current the load. Since instant t_{10}, the

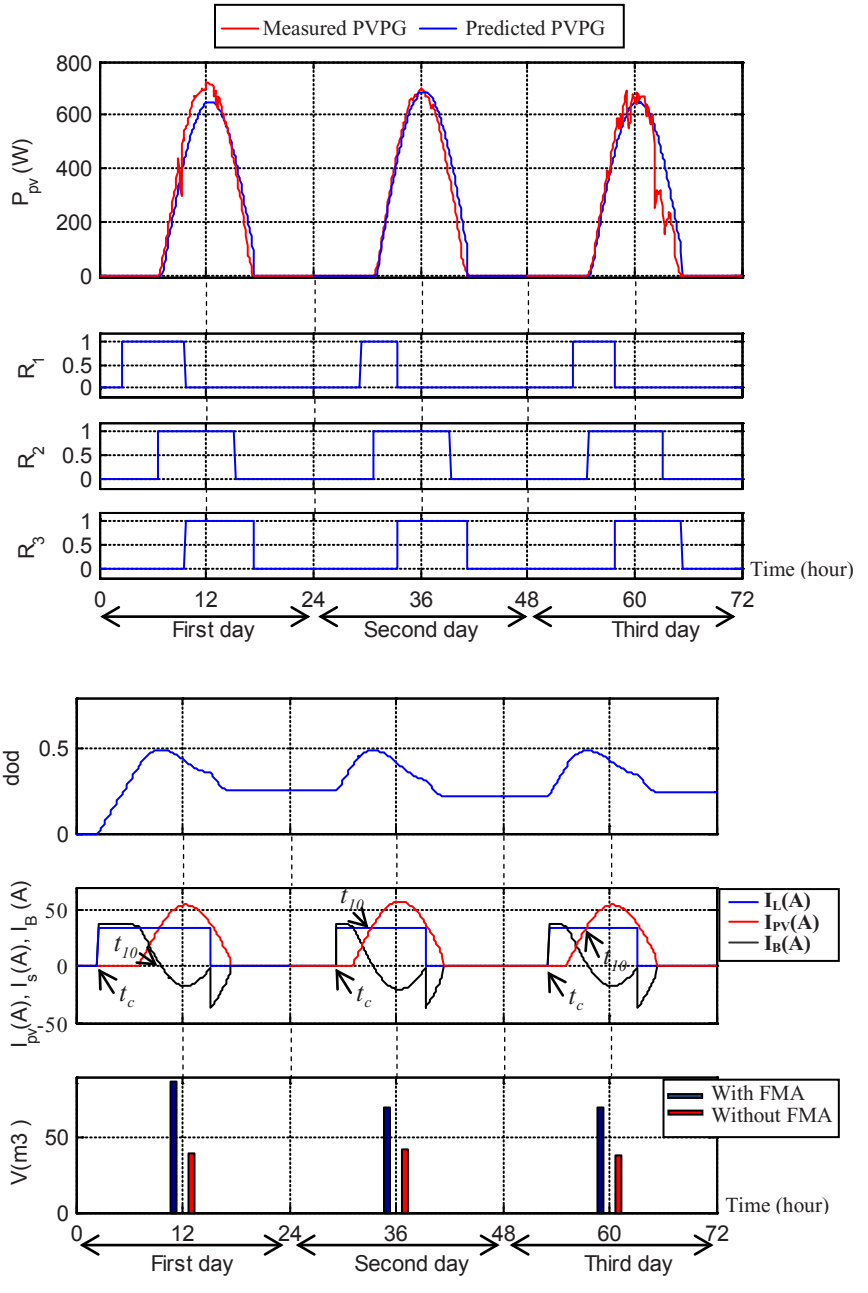

Fig. 5. The experimental results for the typical day: a) The PVP Generation and the relays switching, b) The battery *dod* , the current assessment, the pumped water

battery current becomes negative which charges the battery and involves a battery dod decrease. This phenomenon is maintained until sunset so as to guarantee a dod less than *0.247* at the end of the day.

The mean pumped water during the considered days which is produced by the classical method is $V_{AV} = 39.66m^3$ while that produced with the new approach is $V_{FMA_{AV}} = 75.08m^3$, it is observed that the new approach offers an improvement of 89.1% for moderate season. Consequently, the overall daily mean pumped water is $35.42\,m^3$.

5 Conclusion

A daily predicted energy produced by a PVP is managed to decide the adequate interconnection mode for the components of a water pumping system. This later is composed of a $1kWp$ PVP, a $420Ah$ battery and a $400W$ water pump. The decision is taken through fuzzy rules that respect optimal management criteria. The algorithm aims to optimize the utilization of the PVP generation by extending the water pump operation period on the first hand and to carry out security to the battery against deep discharge on the second hand. After implementation, the algorithm effectiveness is shown over experimental results taken during three consecutive days of the moderate season. The system assessment confirms an improvement of 89% of the water pump operation time by keeping the battery dod less than 0.5 during the day and less than *0.247* at the end of the day. Actually, the approach is investigated to carry out an optimization of an electric vehicle using photovoltaic energy by controlling its speed depending on the available energy.

References

[1] Hadj Arab, A., Benghanem, M., Chenlo, F.: Motor-pump system modelization. Renewable Energy 31, 905–913 (2006)

[2] Amer, E.H., Younes, M.A.: Estimating the monthly discharge of a photovoltaic water pumping system: Model verification. Energy Conversion and Management 47, 2092–2102 (2006)

[3] Manolakos, D., Papadakis, G., Papantonis, D., Kyritsis, S.: A stand-alone photovoltaic power system for remote villages using pumped water energy storage. Energy 29, 57–69 (2004)

[4] Arrouf, M., Ghabrour, S.: Modelling and simulation of a pumping system fed by photovoltaic generator within the Matlab/Simulink programming environment. Desalination 209, 23–30 (2007)

[5] Ben Salah, C., Chaabene, M., Ben Ammar, M.: Multi-criteria fuzzy algorithm for energy management of a domestic photovoltaic panel. Renewable Energy 33, 993–1001 (2008)

[6] Jeong, K.-S., Lee, W.-K., Kimm, C.-S.: Energy management strategies of a fuel cell/battery hybrid system using fuzzy logics. J. Power Sources 145(2), 319–326 (2005); Electrical Power and Energy Systems 29, 783–795 (2007)

[7] Chaabene, M., Ben Ammar, M.: Neuro-fuzzy dynamic model with Kalman filter to forecast irradiance and temperature for solar energy systems. Renewable Energy 33, 1435–1443 (2008)
[8] Chaabene, M.: Measurements based dynamic climate observer. Sol. Energy (2008), doi:10.1016/j.solener.2008.03.003
[9] Cao, J., Lin, X.: Study of hourly and daily solar irradiation forecast using diagonal recurrent wavelet neural networks. Energy Conversion and Management 49, 1396–1406 (2008)
[10] Larminie, J., Lowry, J.: Electric Vehicle Technology Explained, ISBN 0-470-85163-5
[11] Beccali, M., Cellura, M., Ardente, D.: Decision making in energy planning: the ELECTRE multicriteria analysis approach compared to a FUZZY-SETS methodology. Energy Convers. Manage. 39(16-18), 349–355 (1998)
[12] Sallem, S., Ammar, M.B., Chaabene, M., Kamoun, M.B.A.: Fuzzy rules based energy management of a PVP/battery/load system. In: World Renewable Energy Congress X and Exhibition, Glasgow – Scotland, July 19-25 (2008)

Diagnosis by Fault Signature Analysis Applied to Wind Energy

Ouadie Bennouna and Houcine Chafouk

IRSEEM (Institut de Recherche en Systèmes Electroniques Embraqués), Technopôle du Madrillet, avenue Galilée, BP 10024, 76801 Saint Etienne du Rouvray, France
Tel.: 0033232915821
{benouna,chafouk}@esigelec.fr

Abstract. Historically, man has needed energy to feed, to move… It comes in several forms. Today, technology allows its production in large quantities, using all possible resources (fossil, water, wind, sun ...). In the twenty-first century, energy remains a major challenge in several fields: political, economic, scientific and environmental. In this context, the present paper introduces a method to develop renewable energy and especially wind power by detecting, localizing and identifying gross errors in the Doubly Fed Induction Generator (D.F.I.G) of a wind turbine. An experimental benchmark emulating the working of this last is used to validate the technique. This approach is dedicated, in general, to linear dynamic systems. It is based on fault signature analysis. A technique presented in a previous article which uses dynamic reconciliation by polynomial approximation will be compared to the current method.

1 Introduction

There is an increasing demand for industrial processes to become more safe and reliable. Indeed, imprecision on instruments can lead to poor decisions that will affect many parts of the process. It is therefore necessary to have a rigorous monitoring able to detect, localize and identify errors. In the case of energy, and in particular renewable one, its development becomes a global priority. It has to be safe, reliable and available.

This paper introduces a method to develop wind power using diagnosis and error detection techniques. It is based on fault signature analysis using the system model. Chafouk (Chafouk et al. 2007a, b) used parity space approach for data validation which remains a powerful method. In the context of renewable energies, several studies have emerged. Hameed (Hameed et al. 2009) developed algorithms to monitor the performance of wind turbines as well as for an early fault detection to keep them away from catastrophic conditions due to sudden breakdowns. Other authors studied especially the Doubly Fed Induction Generator (D.F.I.G.); Hansen (Hansen et al. 2007) worked on the fault ride-through capability of D.F.I.G. wind turbines, Sang (Sang et al. 2008) presented a modeling and a control of the same generator at a variable speed.

In previous articles (Bennouna et al. 2005, 2007), a method was developed using polynomial approximations for data validation and gross error detection. It was

applied to the Doubly Fed Induction Generator (D.F.I.G) of a wind turbine using an experimental benchmark. Promising results were obtained. Indeed, errors can be detected and estimated. In this paper, we propose to use another technique which is based on fault signature analysis. The aim is always to detect errors, then to compare if both methods lead to the same result. Another paper (Bennouna et al. 2009) dealt with the same problem, but in the case of a wind turbine operating at variable speed.

The layout of this article is as follows. Section 2 presents the fault signature analysis technique. Section 3 describes the application and gives the results corresponding to our tests. Concluding remarks are presented at the end.

2 Fault Signature Analysis

Relying on the polynomial representation of different variables of the system, a technique was developed for data validation in the absence of errors. Otherwise, they are identified and estimated. Let's consider the classic model of linear dynamic systems represented by the following equation:

$$\frac{dx}{dt} = Ax + Bu \tag{1}$$

Where,

x is the state variable.

u is the input variable.

A, B are two matrices.

Suppose that the presence of errors in the system is modeled by the following equations:

$$x = \sum_{k=0}^{s} \alpha_k t^k + \delta\,,\; u = \sum_{k=0}^{s} \beta_k t^k + \delta' \tag{2, 3}$$

δ and δ' are errors.

The procedure already presented in a previous article can detect these errors and estimate their values using a polynomial representation of all variables.

In this paper, fault signature analysis is proposed to compare the results of both techniques. Thus, using a simple linear combination, some variables can be eliminated, and the equation (1) can be rewritten as follows:

$$C_i \frac{dx_i}{dt} = A_i x_i + B_i u \tag{4}$$

i is an indice varying from 1 to n which is the number of subsystems.

Fault signature analysis based on equation (4) will validate the results of the polynomial representation technique.

Please note that this approach is developed only through an example (the DFIG model). A numerical algorithm of state elimination in the general case is being studied (with the choice of the eliminated states, and the matrix C_i).

3 Application

The technique used concerns all linear dynamic systems represented by equation (1). In this study, we chose to treat the case of the Doubly Fed Induction Generator (D.F.I.G) of a wind turbine. The mathematical model of this generator is as follows:

$$\frac{d}{dt}\begin{pmatrix} i_{\alpha s} \\ i_{\beta s} \\ i_{\alpha r} \\ i_{\beta r} \end{pmatrix} = \frac{1}{(L_s L_r - L_h^2)} \begin{pmatrix} -R_s L_r & \omega_m L_h^2 & L_h R_r & \omega_m L_r L_h \\ -\omega_m L_h^2 & -R_s L_r & -\omega_m L_r L_h & L_h R_r \\ L_h R_s & -\omega_m L_s L_h & -R_s L_r & -\omega_m L_s L_r \\ \omega_m L_s L_h & L_h R_s & \omega_m L_s L_r & -R_s L_r \end{pmatrix} \begin{pmatrix} i_{\alpha s} \\ i_{\beta s} \\ i_{\alpha r} \\ i_{\beta r} \end{pmatrix} + \frac{1}{(L_s L_r - L_h^2)} \begin{pmatrix} L_r & 0 & -L_h & 0 \\ 0 & L_r & 0 & -L_h \\ -L_h & 0 & L_s & 0 \\ 0 & -L_h & 0 & L_s \end{pmatrix} \begin{pmatrix} u_{\alpha s} \\ u_{\beta s} \\ u_{\alpha r} \\ u_{\beta r} \end{pmatrix} \tag{5}$$

Where:

$i_{\alpha s,\beta s}$, $i_{\alpha r,\beta r}$ are respectively the currents of the stator and the rotor on the phase's alpha and beta.

$u_{\alpha s,\beta s}$, $u_{\alpha r,\beta r}$ are respectively the voltages of the stator and the rotor on the phase's alpha and beta

ω_m is the rotational speed of the generator.

L_s, L_r, L_h are respectively the inductance of the stator, the rotor and the mutual inductance.

R_s, R_r are respectively the resistance of the stator and the rotor.

The D.F.I.G model can be rewritten as equation (1), with:

$$x = \begin{pmatrix} i_{\alpha s} \\ i_{\beta s} \\ i_{\alpha r} \\ i_{\beta r} \end{pmatrix}, \; u = \begin{pmatrix} u_{\alpha s} \\ u_{\beta s} \\ u_{\alpha r} \\ u_{\beta r} \end{pmatrix}, \; B = \frac{1}{(L_s L_r - L_h^2)} \begin{pmatrix} L_r & 0 & -L_h & 0 \\ 0 & L_r & 0 & -L_h \\ -L_h & 0 & L_s & 0 \\ 0 & -L_h & 0 & L_s \end{pmatrix}$$

$$A = \frac{1}{(L_s L_r - L_h^2)} \begin{pmatrix} -R_s L_r & \omega_m L_h^2 & L_h R_r & \omega_m L_r L_h \\ -\omega_m L_h^2 & -R_s L_r & -\omega_m L_r L_h & L_h R_r \\ L_h R_s & -\omega_m L_s L_h & -R_s L_r & -\omega_m L_s L_r \\ \omega_m L_s L_h & L_h R_s & \omega_m L_s L_r & -R_s L_r \end{pmatrix}$$

Please note that some hypotheses are necessary for this approach: all variables are measured. The model is supposed perfect, and there are no uncertainties about model's parameters.

Using a linear combination, equation (5) can be rewritten in the form of equation (4). According to the eliminated variable (one of the four currents), four subsystems can be obtained.

- 1st subsystem

$$x_1 = \begin{pmatrix} i_{\beta s} \\ i_{\alpha r} \\ i_{\beta r} \end{pmatrix},\ u = \begin{pmatrix} u_{\alpha s} \\ u_{\beta s} \\ u_{\alpha r} \\ u_{\beta r} \end{pmatrix},\ C_1 = \begin{pmatrix} R_s & \omega_m L_h & 0 \\ 0 & \omega_m L_s & -R_s \end{pmatrix}$$

$$A_1 = \frac{1}{(L_s L_r - L_h^2)} \times \begin{pmatrix} -(R_s^2 L_r + \omega_m^2 L_s L_h^2) & -\omega_m L_h (L_r R_s + R_r L_s) & L_h (R_r R_s - \omega_m^2 L_s L_r) \\ -L_h (\omega_m^2 L_s^2 + R_s^2) & -\omega_m L_h (L_s R_r + R_r L_s) & L_s (-\omega_m^2 L_r L_s + R_s R_r) \end{pmatrix}$$

$$B_1 = \frac{1}{(L_s L_r - L_h^2)} \begin{pmatrix} -\omega_m L_h^2 & R_s L_r & \omega_m L_h L_s & -R_s L_h \\ -\omega_m L_h L_s & R_s L_h & \omega_m L_s^2 & -R_s L_s \end{pmatrix}$$

- 2nd subsystem

$$x_2 = \begin{pmatrix} i_{\alpha s} \\ i_{\alpha r} \\ i_{\beta r} \end{pmatrix},\ u = \begin{pmatrix} u_{\alpha s} \\ u_{\beta s} \\ u_{\alpha r} \\ u_{\beta r} \end{pmatrix},\ C_2 = \begin{pmatrix} R_s & 0 & -\omega_m L_h \\ 0 & R_s & \omega_m L_s \end{pmatrix}$$

$$A_2 = \frac{1}{(L_s L_r - L_h^2)} \times \begin{pmatrix} -(R_s^2 L_r + \omega_m^2 L_s L_h^2) & L_h (R_r R_s - \omega_m^2 L_r L_s) & \omega_m L_h (L_r R_s + L_s R_r) \\ L_h (\omega_m^2 L_s^2 + R_s^2) & -L_s (R_s R_r - \omega_m^2 L_r L_s) & -\omega_m L_s (L_r R_s + L_s R_r) \end{pmatrix}$$

$$B_2 = \frac{1}{(L_s L_r - L_h^2)} \begin{pmatrix} R_s L_r & \omega_m L_h^2 & -L_h R_s & -\omega_m L_s L_h \\ -L_h R_s & -\omega_m L_s L_h & L_s R_s & \omega_m L_s^2 \end{pmatrix}$$

- 3rd subsystem

$$x_3 = \begin{pmatrix} i_{\alpha s} \\ i_{\beta s} \\ i_{\beta r} \end{pmatrix},\ u = \begin{pmatrix} u_{\alpha s} \\ u_{\beta s} \\ u_{\alpha r} \\ u_{\beta r} \end{pmatrix},\ C_3 = \begin{pmatrix} \omega_m L_r & R_r & 0 \\ \omega_m L_s L_r & 0 & -L_h R_r \end{pmatrix}$$

$$A_3 = \frac{1}{(L_s L_r - L_h^2)} \times \begin{pmatrix} -(\omega_m R_s L_r^2 + \omega_m R_r L_h^2) & (\omega_m^2 L_h^2 L_r - R_s R_r L_r) & (\omega_m^2 L_h L_r^2 + L_h R_r^2) \\ -\omega_m L_s (R_s L_r^2 + L_h^2 R_r) & L_h^2 (\omega_m^2 L_s L_r - R_r R_s) & L_s L_h (\omega_m^2 L_r^2 + R_r^2) \end{pmatrix}$$

$$B_3 = \frac{1}{(L_s L_r - L_h^2)} \begin{pmatrix} \omega_m L_r^2 & R_r L_r & -\omega_m L_h L_r & -R_r L_h \\ \omega_m L_r^2 L_s & R_r L_h^2 & -\omega_m L_s L_r L_h & -R_r L_s L_h \end{pmatrix}$$

- 4th subsystem

$$x_4 = \begin{pmatrix} i_{\alpha s} \\ i_{\beta s} \\ i_{\alpha r} \end{pmatrix},\ u = \begin{pmatrix} u_{\alpha s} \\ u_{\beta s} \\ u_{\alpha r} \\ u_{\beta r} \end{pmatrix},\ C_4 = \begin{pmatrix} R_r & -\omega_m L_r & 0 \\ 0 & \omega_m L_s L_r & L_h R_r \end{pmatrix}$$

$$A_4 = \frac{1}{(L_s L_r - L_h^2)} \times \begin{pmatrix} -(R_s R_r L_r - \omega_m^2 L_r L_h^2) & \omega_m (L_h^2 R_r + R_s L_r^2) & L_h (R_r^2 + \omega_m^2 L_r^2) \\ -L_h^2 (\omega_m^2 L_s L_r - R_r R_s) & -\omega_m L_s (R_s L_r^2 + R_r L_h^2) & -L_h L_s (\omega_m^2 L_r^2 + R_r^2) \end{pmatrix}$$

$$B_4 = \frac{1}{(L_s L_r - L_h^2)} \begin{pmatrix} R_r L_r & -\omega_m L_r^2 & -R_r L_h & \omega_m L_r L_h \\ -L_h^2 R_r & \omega_m L_s L_r^2 & L_s L_h R_r & -\omega_m L_r L_s L_h \end{pmatrix}$$

3.1 Tests and Results

Tests were performed using the experimental benchmark of the University of Mondragon. It consists of a DC machine of 25 kW emulating the aerodynamic and mechanical behaviour of a wind turbine, and a D.F.I.G of 15 kW emulating the electrical generator (figure 1).

This benchmark presents physical characteristics that are close to wind turbines the most used. The control of electric machinery is through a Digital Signal Processor (DSP); communication between these DSP and electronic components of the bench is done via Digital to Analog and Analog to Digital Converters (DAC / ADC).

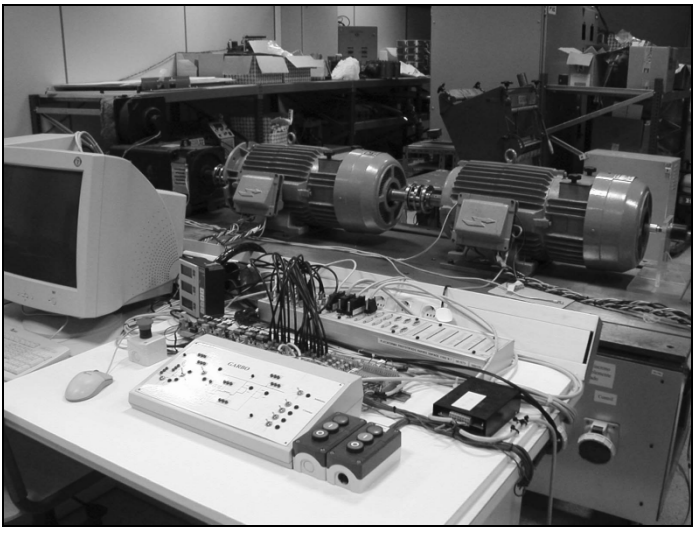

Fig. 1. Experimental benchmark

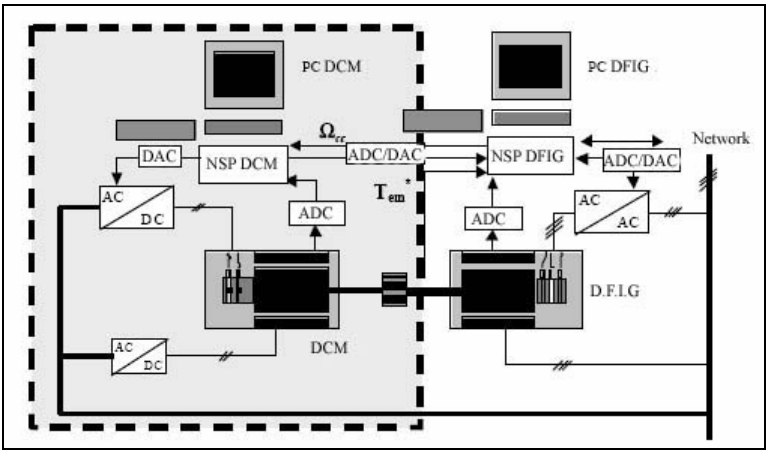

Fig. 2. Composition of the benchmark

During these tests, the rotational speed of the generator is 1250*rpm*, the sampling period is 0.0002*s*, and samples are equal to 500. From sample 100, a bias was added to the variable $i_{\alpha s}$. Residuals corresponding to each of these subsystems are calculated. They are represented in the following figures:

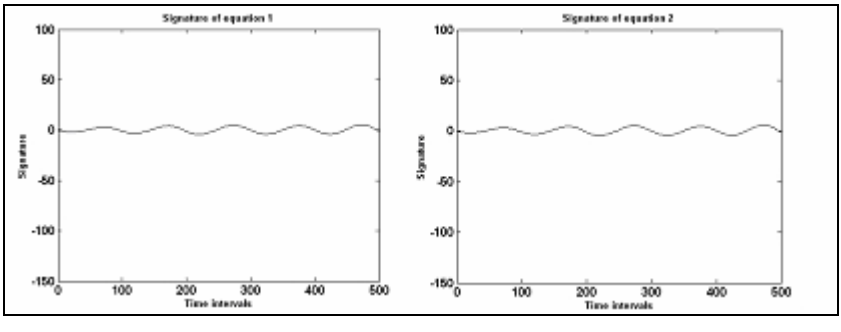

Fig. 3. Residuals of subsystem 1

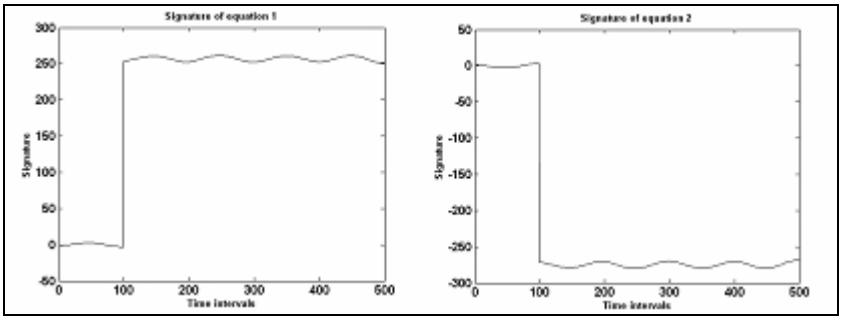

Fig. 4. Residuals of subsystem 2

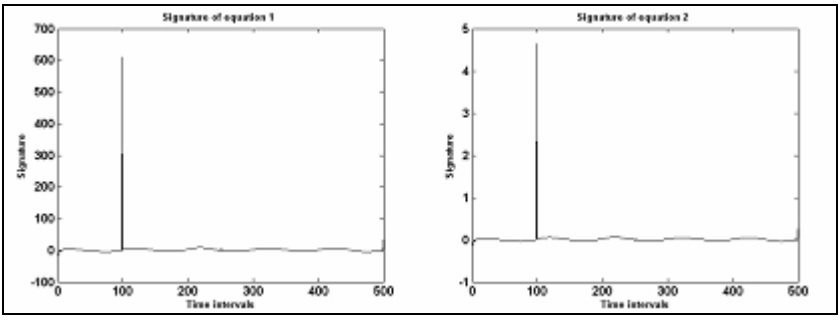

Fig. 5. Residuals of subsystem 3

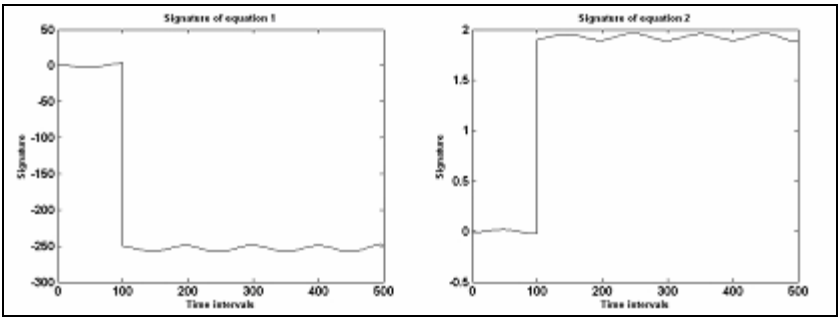

Fig. 6. Residuals of subsystem 4

Please note that time intervals are given by the number of sampling.

3.2 Fault Signature Analysis

All generated relationship can be grouped as shown in the following table:

Table 1. Generated relations

	$i_{\alpha s}$	$i_{\beta s}$	$i_{\alpha r}$	$i_{\beta r}$
EQ1		**1**	**1**	**1**
EQ 2		**1**	**1**	**1**
EQ 3	**1**		**1**	**1**
EQ 4	**1**		**1**	**1**
EQ 5	**1**	**1**		**1**
EQ 6	**1**	**1**		**1**
EQ 7	**1**	**1**	**1**	
EQ 8	**1**	**1**	**1**	

From the previous table, fault signature vectors corresponding to the four currents can be calculated:

$$s_1 = (00111111)^T \tag{6}$$

$$s_2 = (11001111)^T \tag{7}$$

$$s_3 = (11110011)^T \tag{8}$$

$$s_4 = (11111100)^T \tag{9}$$

Taking into account the statistical aspect of each residue, a change in its average value can be detected. Thus, a binary vector of consistency (bvc) can be formed, which, in our case, is:

$$vbc = (00111111)^T \tag{10}$$

A comparison of this vector with fault signature vectors provides information on the status of the system: normal operation or failure. In this work, the distance of Hamming is used to make this comparison. It is defined by:

$$D_i = \|vbc - s_i\| \qquad i=1,...,4 \tag{11}$$

The previous binary vector of consistency gives the following results:

Table 2. Table of Hamming distances

Variables	$i_{\alpha s}$	$i_{\beta s}$	$i_{\alpha r}$	$i_{\beta r}$
D	0	4	4	4

The closest fault signature to vbc is $i_{\alpha s}$ (since the corresponding Hamming distance is equal to zero). We can infer that failure is present at this variable. This method has allowed thus confirming the results of polynomial representation technique.

4 Conclusion

We have presented a method for identifying errors for linear dynamic systems. It is used in tandem with another procedure based on polynomial representation. This method is applied to the Doubly Fed Induction Generator (D.F.I.G) of a wind turbine using an experimental benchamrk. Results are honorable, and the two techniques lead to the same decision.

Our next work will focus on systems partially measurable with the ability to estimate no measured variables.

References

Bennouna, O., Héraud, N., Camblong, H., Rodriguez, M.: Diagnosis of the doubly fed induction generator of a wind turbine. Wind Engineering 29(5), 431–448 (2005)

Bennouna, O., Héraud, N., Rodriguez, M., Camblong, H.: Data reconciliation & gross error detection applied to wind power. Journal of Systems and Control Engineering 221(3), 497–506 (2007)

Bennouna, O., Héraud, N., Camblong, H., Rodriguez, M., Kahyeh, M.A.: Diagnosis and fault signature analysis of a wind turbine at a variable speed. Journal of Risk and Reliability 223(1), 41–50 (2009)

Chafouk, H., Hoblos, G., Langlois, N., Le Gonidec, S., Ragot, J.: Soft computing algorithm to data validation in aerospace systems using parity space approach. Journal of Aerospace Engineering 20(3), 165–171 (2007)

Chafouk, H., Hoblos, G., Langlois, N., Le Gonidec, S., Ragot, J.: Soft computing approach for data validation. Journal of Aerospace Computing, Information, and Communication 4(1), 628–635 (2007)

Hameed, Z., Hong, Y.S., Cho, Y.M., Ahn, S.H., Song, C.K.: Condition monitoring and fault detection of wind turbines and related algorithms: A review. Renewable & Sustainable Energy Reviews 13, 1–39 (2009)

Hansen, A.D., Michalke, G.: Fault ride-through capability of DFIG wind turbines. Renewable Energy 32, 1594–1610 (2007)

Sang, H., Gab, G., Ho, N., Pyo, W.: Modeling and control of DFIG-based variable-speed wind-turbine. Electric Power Systems Research 78, 1841–1849 (2008)

A Novel Self-organizing Neural Technique for Wind Speed Mapping

Giansalvo Cirrincione[1] and Antonino Marvuglia[2]

[1] Laboratoire Modélisation, Information et Systèmes (MIS), Université de Picardie Jules Verne, 33, rue Saint Leu - 80039 Amiens Cedex 1
[2] Dipartimento di Ricerche Energetiche ed Ambientali (DREAM), Università degli Studi di Palermo, viale delle scienze, edificio 9 -90128 Palermo, Italy

Abstract. Systems with high nonlinearities are, in general, very difficult to model. This is particularly true in geostatistics, where the problem of the estimation of a regionalized variable (RV) given only a small amount of measurement stations and a complex terrain surface is very challenging. This paper introduces a novel strategy, which couples the Curvilinear Component Analysis (CCA) and the Generalized Mapping Regressor (GMR). CCA, which is a nonlinear projector of a data manifold, is here used in order to find the intrinsic dimension of the data manifold, just giving an insight on the nonlinearities of the problem. This analysis drives the pre-processing of the data set used for the training phase of GMR. GMR is an incremental, self-organizing neural network which is able to model nonlinear functions by transforming the approximation into a pattern recognition problem. The presented approach is tested on the spatial estimation of the wind speed over the complex terrain of the isle of Sicily, in Italy. Wind speed maps resulting from this technique are presented and compared with a deterministic interpolator, the Inverse Distance Weighting (IDW) method.

Keywords: Discontinuity, Curvilinear Component Analysis, Generalized Mapping Regressor, spatial estimation, wind.

1 Introduction

Nonlinear problems very often arise in science and engineering: in general they are inverse, have discontinuities and depend on several variables. They are not only difficult to analyse and model, but also difficult to be visualized. There are few techniques able to yield good results, and most of them require strong assumptions for simplifying the problem. It should be desirable to solve it without additional assumptions by using the raw data. In general, neural networks can model nonlinear systems, but are not able to give an insight of the problem. They also have problems with discontinuities and multiple solutions. The Generalized Mapping Regressor (GMR) [1], [2], applied in this work to achieve the task of wind speed spatial mapping, is able to model nonlinear functions with any kind of discontinuities and any number of solutions. It is a self-organizing neural network which tries to model the manifold to which all data belong. The use of GMR has been here coupled with the application of another basic neural tool: the Curvilinear Component Analysis (CCA) [3]. It is, in general, used for

visualization properties because it projects the input manifold in a nonlinear way by respecting the small interpoint distances. CCA and GMR share the same self-organization philosophy and so they can be coupled (indeed, CCA has been used as a pre-processor for GMR). However, in this paper, a different use of CCA is made. It is used to assess the degree of nonlinearity of the problem and as a support tool to estimate the intrinsic dimension of the manifold. The coupling of CCA and GMR is interesting not only because it works well for this kind of problems, but it can also be used for a geometrical analysis of the data manifold (in this case, the accuracy of the GMR modelling can serve as a validation tool for CCA).

The problem tackled in the paper deals with the spatial interpolation of observations drawn from a limited number of stations over the complex terrain of the isle of Sicily, in Italy.

2 Curvilinear Component Analysis

CCA is a very powerful data analysis method, conceived to extract relevant information from data. This method makes it possible to determine the so-called intrinsic dimension of a data set, i.e. the minimum number of free variables needed to generate the data. CCA is a self-organizing neural network which gives a revealing low-dimensional mapping of the manifold of a high-dimensional and nonlinearly related data set. The goal is to find the dimension of the average manifold of the data and to map it onto a space of lower dimension (*representation space*). In summary, the algorithm proceeds to a global unfolding followed by a local projection onto the average manifold (Fig. 1).

The main idea is the following: for every couple of distinct points (x_i, x_j) every interpoint distance $X_{ij}= \left| x_i - x_j \right|$ in the input space is computed and the corresponding interpoint distance $Y_{ij}= \left| y_i - y_j \right|$ in a lower-dimensional output representation space is taken. This can be done by minimizing the following quadratic form:

$$E = \sum_{i,j} E_{ij} = \sum_{i,j} \left(X_{ij} - Y_{ij} \right)^2 \tag{1}$$

For each couple of points x_i and x_j in the input space, the correspondent points y_i and y_j in the output space are moved so that the terms E_{ij} are minimized, for example by means of a gradient descent algorithm.

In order to map the average manifold of the data, two cases are to be considered: first, it is needed a global unfolding of the average manifold of the data and second it is necessary to carry out a local projection of these data onto their average manifold. In the case of global unfolding alone, only some of the E_{ij} terms in Eq. (1) need to be minimized: those for which the distance Y_{ij} is smaller than some pre-defined distance λ. Thus, allowing the matching for only short distances is a way to respect the local topology. The choice of λ strongly depends on the data. The case of local projection is the opposite of the preceding one. Let us suppose that data have already projected onto their average manifold; the interpoint distances Y of the projected data will locally minimize the following quadratic error:

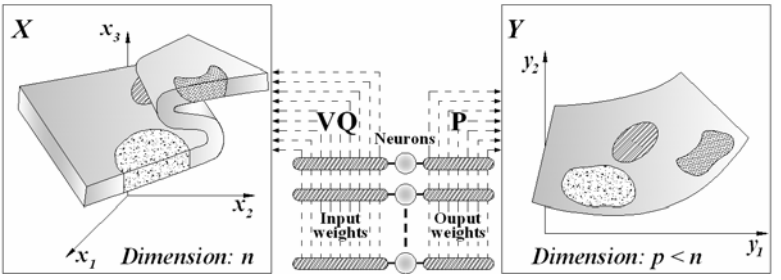

Fig. 1. Principle of the CCA algorithm. The input weights first proceed to a vector quantization (VQ) of the input data space (X) in *n* dimensions. Then, the output weights map the local topology of the input average manifold by projecting it (P) onto an output representation space (Y) of dimension $p < n$. This way, tasks like classification and recognition are highly facilitated in an unfolded and lower-dimensional output space.

$$\left(X_{ij}^{2} - Y_{ij}^{2}\right) \tag{2}$$

Because of the projection, this should apply only when $Y_{ij} \leq X_{ij}$. Conversely, when $Y_{ij} \geq X_{ij}$, there is unfolding. Hence, the two situations (unfolding or projection) do not overlap, and the global cost function should merge the functions related to the two cases, provided that the continuity between them is assured at $Y_{ij}=X_{ij}$. The global function to be minimized is then:

$$E = \sum_{ij} \left[E_{ij}\Big|_{Y_{ij} > X_{ij}} + \frac{1}{4X_{ij}^{2}} E_{ij}\Big|_{Y_{ij} < X_{ij}} \right] F_{\lambda}\left(Y_{ij}\right) \tag{3}$$

where F_{λ} is the function defined as follows:

$$F_{\lambda}(\cdot) = \begin{cases} 1 & \text{if } Y_{ij} < \lambda \\ 0 & \text{if } Y_{ij} > \lambda \end{cases} \tag{4}$$

This cost function is invariant under transformations like translation, rotations, or inversion of axes. This property can be exploited by adding constraints suitable for various goals in data mining.

If the output space has the same dimension as the input one, all the input interpoint distances are equal to the corresponding output interpoint distances and, as a consequence, the joint distribution of input distances (*dx*) versus output ones (*dy*), called *dy-dx* diagram, lies on the first quadrant bisector *dx=dy*.

If the dimension of the output space is lower than the one of the input space, the joint distribution *dx/dy* presents two aspects: in the case of unfolding, the points lie on the *dy>dx* side of the first diagonal and, in the case of projection, they lie on the *dy<dx* side. A "good" mapping is obtained when there is an unfolding for large *dy* values and a projection for small values. Then, the aspect of the joint distribution on the graph which plots *dx* versus *dy* is very useful [4]. In fact, if the distribution lies on the first diagonal, it is possible to lower the output dimension, and if the distribution

becomes thicker, the output dimension is too small to correctly represent the data manifold. Once the good dimension has been chosen, the quality of the mapping can be improved varying the minimum value of λ to reduce the scattering around dx=dy for medium values of dy. Looking at the maximum of dx near dy=0 gives an idea of the spreading of the data near the average manifold.

CCA is therefore a useful method for redundant and non linear data structure representation. It provides revealing curvilinear views of even strongly folded structures whereas Principal Component Analysis (PCA) or other linear methods fail to give such a suitable information.

3 Generalized Mapping Regressor

GMR is mainly an incremental self-organizing neural network. Its algorithm transforms the mapping problem f:$x \rightarrow y$ into a pattern recognition problem in the augmented space Z represented by vectors $z = [x^T \; y^T]^T$, where T is the transpose operator, which are the inputs of GMR. In this space, the branches of the mapping become clusters which have to be identified. The weights of the first layer are continuous and represent the Z space, while the other ones are discrete (chains between neurons) and represent the mapping branches mapping. The first layer weights are computed (training phase) by a multiresolution quantization phase, the second layer weights are computed (linking phase) by a PCA technique [5].

The training phase concerns the vector quantization of the Z space. This can be obtained by using different neural approaches, which must be incremental, i.e. the number of neurons is not predefined but changes according to the complexity of the mapping to be approximated. At the presentation of each input of the training set (TS), there are two possibilities: either creation of a new neuron (whose weight vector is equal to the input vector) or adaptation of the weight vector of the closest neuron (in input/weight space). Given a threshold ρ (*vigilance threshold*), a new neuron is created if the hyperspheres of radius ρ, centered in the already created weight vectors, do not contain the input (and so is unable to represent the input). The parameter ρ is very important: it determines the resolution of training.

Learning can be divided into two sub-phases: *coarse quantization* and *fine quantization*. The coarse quantization is obtained by using EXIN SNN [1], [2], [6] with a high value for ρ, say ρ_1. Here more than one epoch are accepted. In general, the first epoch defines the number of neurons needed for mapping and the others adapt their weights for a better approximation. The neurons thus obtained identify the *objects*, which are compact sets of data in Z. The resulting neurons are called *object neurons*. In the second sub-phase, at first, a preprocessing is required for labeling each neuron with the list of the input data which had the neuron as winner; it can be accomplished by presenting all data (*production phase*) to GMR and recording the corresponding winning neurons. At the end, for each neuron a list of the inputs for which it won is stored. This list represents the *domain* of the object neuron. Every list is considered as the TS for a subsequent secondary *EXIN SNN*. Hence, as many EXIN SNN's as the object neurons are used in parallel in order to quantize each object domain. These intra-domain learning phases need a threshold lower than ρ_1, say ρ_2, whose value is determined by the required resolution. At the end, the neural network is composed of the

neurons generated by the secondary learning phases (*pool of neurons*), labeled as belonging to an object by the corresponding object neuron, which however is not included in the pool.

Resuming, the augmented Z space is quantized by means of a coarse sub-phase, a labeling processing requiring a production phase (presentation of the TS to the network) and a fine sub-phase requiring a parallel implementation. This multiresolution quantization can also be obtained by using other neural networks: what is important is to obtain a pool of neurons and compute its weights with respect to the input (first layer weights).

In the recall phase, the input (from now on called x) can be any collection of the components of z (the input space is defined as X). Hence the output y is the vector composed of the other elements of z (the output space is defined as Y). All weight vectors are also projected onto X. This projection is easily accomplished by using only the elements of the weight vector whose position indices correspond to the position indices of the input elements in the augmented vector Z. For example, if the first three elements of the vector z are taken as input, the projected weight vectors are composed of only the first three elements of the weight vectors. In X space, each neuron is replaced with a Gaussian which represents the neuron domain. Its parameters (mean, covariance) are given by the Maximum Likelihood (ML) estimates (the sample mean and sample unbiased covariance). When there are at most two points in the domain (e.g. under-represented portions of branches of the mapping to be approximated), the Gaussian, as defined before, makes no sense and is replaced by a spherical Gaussian centered in the neuron weight, whose variance is given by the final vigilance threshold in order to respect the resolution of the training. When an input vector x is fed to GMR, the Gaussians are sorted in decreasing order according to their value in x (the value of the Gaussian in x is here considered as a metric). Following this order, each Gaussian is labeled as *level one* if the hypersphere, centered in the mean and whose radius is the domain radius, contains the input (level one test) and *level two* if it is not level one, but is directly linked to a level one Gaussian. This labeling is controlled by the following stop criterion: if the Gaussian is neither classified as level one nor as level two, then the labeling is stopped. All level one Gaussians and level two neurons which are connected each other (even not directly) are considered as belonging to the same mapping branch. Then, for each Gaussian k the complement of the weight of the corresponding domain is defined as t_k. The outputs are associated to the level one Gaussians. For each of these Gaussians, say the i-th, the interpolation phase considers the two Gaussians (either level one or level two) directly linked to it. Call them p_{i-1} and p_{i+1}. The associated output y_i is given by the following kernel interpolation formula:

$$y_i = \frac{t_{i-1} p_{i-1}(x) + t_i p_i(x) + t_{i+1} p_{i+1}(x)}{p_{i-1}(x) + p_i(x) + p_{i+1}(x)} \tag{5}$$

If one of the two Gaussians does not exist or is neither level one nor level two, its value is set to zero. If the i-th Gaussian has no links, the interpolation is given by:

$$y_i = t_i p_i(x) \tag{6}$$

No interpolation is required if the value of the i-th Gaussian in x is nearly one (with respect to the training resolution). In the end, as a consequence of the interpolation,

each level one Gaussian yields an output *y*. Two different outputs belong to the same branch if they correspond to Gaussians belonging to the same branch. All level one Gaussians and the branches or portions of branches containing only level one Gaussians constitute a discretization of the equilevel hypersurfaces.

4 Application to Wind Speed Spatial Estimation in Sicily

The application proposed in this paper deals with the creation of a wind speed map for the Sicily isle in Italy. The wind data used to train the final model are the hourly mean values of wind speed at 10 meters above the ground level (a.g.l.), recorded in 29 different anemometric stations spread on the Sicilian territory. The temporal information contained in the available wind time series has been resumed in the corresponding Weibull distributions fitted to the data in [7] and only their means (i.e. the first order statistical moment) have been retained for the neural network training.

Two very important factors affecting regional wind fields are represented by terrain orography and land cover (that influences wind velocity through a term called *surface roughness length,* generally referred to as z_0). In order to take into account these two important variables, the GMR network used for the spatial estimation of the wind speed is trained with a set of *5*-dimensional vectors obtained as explained in the following. A regular grid of points is created and for each point the corresponding value of the elevation a.g.l. is obtained from the Digital Elevation Model (DEM) of the island, while the value of the parameter z_0 is obtained from the map of the roughness lengths created as described in [8]. In this way it is possible to create a set of *4*-dimensional vectors, in which the first two components are represented by the geographical coordinates of the point (*Easting* and *Northing*) and the third and fourth components are the corresponding values of the elevation and roughness length, respectively. The fifth component is the value of the mean wind speed previously estimated in the point represented by its first two coordinates by the application of the inverse distance weighting (IDW) method [9]. The GMR trained with this *5*-dimensional data set has to estimate the mean wind speed at 10 m a.g.l. in every point of Sicily. However, it is to be noticed that in such an irregular terrain like the Sicilian one, a factor which can strongly affect the results of the accomplished analysis is the lack of data. In fact only 29 stations are not sufficient to completely describe the features of the wind manifold because some areas of Sicily are not represented.

4.1 CCA Analysis

Here the CCA approach is used in an original way. Indeed, it is not used simply as a nonlinear projector, but its diagrams (mainly the *dy-dx* diagram) are used as tools for the detection and analysis of the nonlinearities.

The fact that the intrinsic dimension be less than five stems from the empirical observation that the physical variables *x, y, z*, the roughness and the wind influence themselves. For CCA, initial TS is built by using the information derived from a grid covering the whole Sicily, as previously explained. For the purpose of visualization, CCA is used by projecting the TS in 2D. Fig. 2 shows the projection and Fig. 3 the corresponding *dy-dx* diagram. In this plot it can be noticed that dimension 2 is not

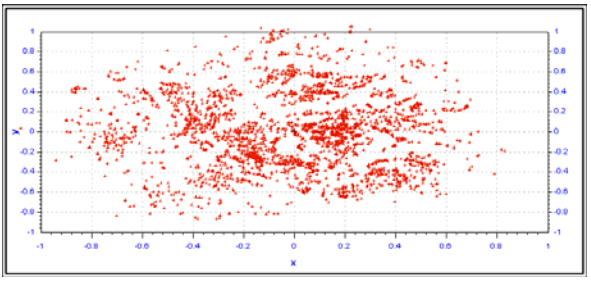

Fig. 2. 2D projection of the five-dimensional training set

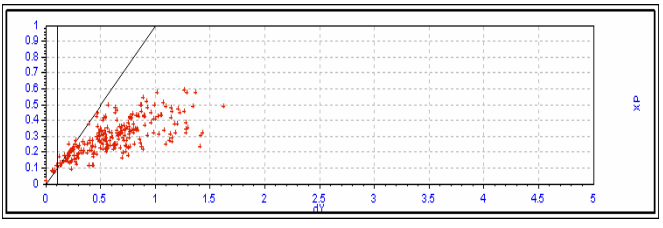

Fig. 3. *dy-dx* diagram of the 2D pojection of the five-dimensional training set

suitable to correctly represent the data (observe the bending of the data cluster from the bisector).

By the observation of the analogous diagrams for CCA projections of the data in 3D and 4D, it was inferred that the intrinsic dimension of the data manifold is between 3 and 4.

4.2 GMR with Data Projected in a 4- and 3-Dimensional Space

At first GMR works with a TS obtained by projecting the original TS in a 4-dimensional space by using PCA. Then data were statistically normalized. Only 2 objects are recovered by using the PCA method with $k = 4$, which is the final choice here. The grid containing Sicily was divided in two sub-grids of the same size by picking out one point out of two for the TS and leaving the other one for the data set to be used to validate model results (*validation set*). In Fig. 4 it is showed the map obtained by feeding GMR with the data of the validation set.

A projection of the TS in a 3-dimensional space by PCA has also been accomplished. According to the previous analysis, this choice constraints all the variables forcing the wind speed to be linked to the other features.

In other words, by projecting in a dimension which is slightly lower than the intrinsic dimension, the components of the original vectors are linked to each other in such a way that the variables known with a higher level of precision (in this case the spatial coordinates and the *roughness length*) polarize the learning process of the features of those variables that are known with a lower degree of precision (in this case the wind mean speed). In a very large sense, the described approach can be seen as a non-linear co-kriging technique [10]. However, unlike co-kriging, it does not require the estimation of

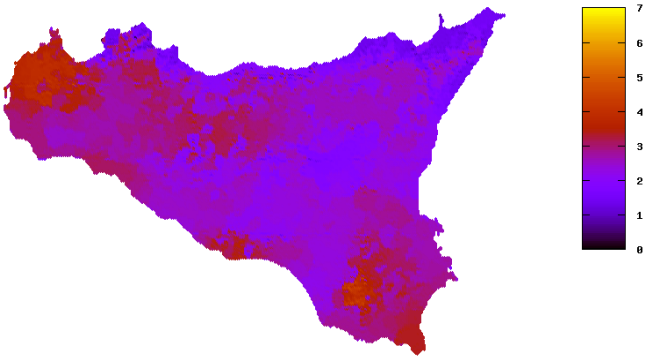

Fig. 4. Map of the average wind speed (m/s) at 10 m a.g.l. obtained with the validation set by the GMR neural network trained with data projected in a 4-dimensional space

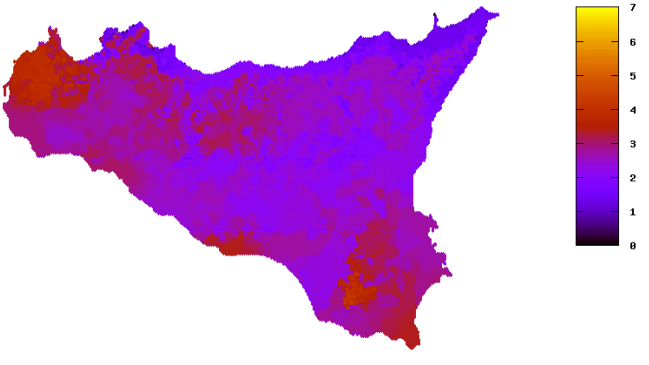

Fig. 5. Map of the average wind speed (m/s) at 10 m a.g.l. obtained with the validation set by the GMR network trained with data projected in a 3-dimensional space

all the cross-covariance functions, which can be a computationally intensive task. The map obtained by feeding GMR with the data of the validation set is showed in Fig. 5.

5 Conclusions

A novel neural approach has been used in this paper in order to tackle the problem of wind speed spatial estimation over the territory of the isle of Sicily (Italy), starting from the measurements recorded in a set of anemometric stations.

It represents the first application of GMR neural network to this kind of problem and is the result of the synergy between a careful exploratory data analysis and the exploitation of the NNs capability to extract the knowledge directly from the data. The core of the pre-processing phase is represented by the application of the CCA technique for the estimation of the intrinsic dimension of the “wind manifold”. The final result of the work is a map of the estimated average wind speed at 10 m a.g.l. Starting from this first estimate, by using the power low that is well known in wind

studies, it is possible to obtain the wind speeds at the wind turbines' hub height, which could represent the starting point for the evaluation of the wind potential of the region and the selection of the best areas in terms of yearly theoretical wind power producibility.

The presented approach is applicable in any geographical context, provided that enough information about the features of the territory (orography, land coverage and any other additional item) is known. However, it has to be underlined that, in general, the results of any mathematical model are to be taken only as a guide criterion for the selection of the most suitable sites for wind energy exploitation and an even short monitoring of the selected areas is always desirable before starting economic investments.

References

[1] Cirrincione, G.: Neural structure from motion. Ph.D. Thesis, LIS INPG, Grenoble, France (1998)

[2] Cirrincione, G., Cirrincione, M., Van Huffel, S.: Mapping approximation by the GMR neural network. In: Proc. of the Wolrd Multiconference on Circuits, Systems, Communications & Computers, Athens, Greece, July 2000, pp. 1811–1818 (2000)

[3] Demartines, P., Herault, J.: Curvilinear component analysis: A self-organizing neural network for nonlinear mapping of data sets. IEEE Trans. on Neural Netw. 8(1), 148–154 (1997)

[4] Demartines, P.: Mesures d'organisation du réseau de Kohonen. In: Cottrell, M. (ed.) Congrès Satellite du Congrès Européen de Mathématiques: Aspects Théoriques des Réseaux de Neurones (1992)

[5] Berthold, M., Hand, D.J. (eds.): Intelligent data analysis: an introduction. Springer, New York (1999)

[6] Cirrincione, G., Cirrincione, M.: A Novel Self-Organizing Neural Network for Motion Segmentation. Appl. Intell. 18(1), 27–35 (2003)

[7] Cellura, M., Cirrincione, G., Marvuglia, A., Miraoui, A.: Wind speed spatial estimation for energy planning in Sicily: Introduction and statistical analysis. Renew. Energy 33, 1237–1250 (2008)

[8] Cellura, M., Cirrincione, G., Marvuglia, A., Miraoui, A.: Wind speed spatial estimation for energy planning in Sicily: A neural kriging application. Renew. Energy 33, 1251–1266 (2008)

[9] De Smith, M.L., Goodchild, M.F., Longley, P.A.: Geospatial Analysis: A Comprehensive Guide to Principles, Techniques, and Software Tools, 2nd edn. (2008), http://www.spatialanalysisonline.com

[10] Kanevsky, M., Maignan, M.: Analysis and modelling of spatial environmental data. EPFL Press, Lausanne (2004)

Integral Fuzzy Control for Photovoltaic Power Systems

A. El Hajjaji, M. BenAmmar, J. Bosche, M. Chaabene, and A. Rabhi

Laboratoire de Modélisation, Information et Systèmes
Université de Picardie Jules Verne
7, rue Moulin Neuf, 80000, Amiens, France
ahmed.hajjaji@u-picardie.fr

Abstract. This paper addresses the control problem for a photovoltaic generator coupled to a boost DC-DC converter taking into consideration the nonlinearities and the parametric uncertainties of the model. After the analysis and modeling of the photovoltaic power system by a Takagi-Sugeno (TS) fuzzy model, the design strategy of the control law is proposed and the stabilization conditions are formulated in terms of Linear Matrix Inequalities (LMIs) which can be solved very efficiently using convex optimisation techniques. Simulation and experimental results will be given to demonstrate the performance of the proposed methods.

Keywords: Photovoltaic energy, Fuzzy control, LMI, Stabilisation.

1 Introduction

Photovoltaic energy is considered as an alternative energy to meet the ever increasing demand for energy in the world because it comes from solar energy which is abundant, renewable, clean and free. This energy is not only widely used in space applications but also in terrestrial applications. To obtain this energy we have essentially need of a photovoltaic generator and a Buck DC-DC converter, a Boost DC-DC converter or a combination of the two. Despite the research developed on photovoltaic systems in the least years, the problem of the maximum power continues to be studied because photovoltaic conversion systems are nonlinear and uncertain. To extract the maximum power from PV generators, control algorithms are usually used [1, 2 , 3, 4, 5, 6 ,7]. Many methods have been developed to track the maximum power point. Thus, in [5], a perturbed and observe (PO) method is proposed and an incremental conductance algorithm is used in [6]. Recently, the robust control like sliding mode, Youla parametrization [2], and Neural Networks [3,4,5] have also been proposed. In this work, we propose a design method to ensure the maximum power point, using integral TS fuzzy controllers, largely developed in literature in control and diagnosis fields of nonlinear systems [8,9,10,11]. It is well know that the I-V photovoltaic characteristic changes depending on the insulation and temperature as illustrated in figures 1 and 2. The purpose of this study is to develop an MPPT to extract the maximum power panel by developing a integral TS fuzzy controller for a photovoltaic system taking into account the weather conditions.

This paper is organized as follows; in section 2, we present the main characteristics of a photovoltaic panel and the influence of different weather and material factors on these features. Section 3 is devoted to fuzzy control design based on TS fuzzy representation of PV systems. Simulation and experiment results to illustrate the feasibility of the proposed algorithm and to demonstrate its high performances are presented in section 4. Finally, we conclude this work in section 5.

2 Modelling and Characterization of PV Systems

The PV generator consists in combination of many PV cells connected in series and parallel modes to provide the desired value of output voltage and current. I-V characteristics of the photovoltaic generator can be obtained using its equivalent circuit. Atmospheric variables dramatically affect the available insulation for photovoltaic generators. Consequently, the current–voltage (*I–V*) curves and maximum power points (MPPs) of photovoltaic modules change with the solar radiation, as illustrated in Figure 1. Besides insulation, another important factor that influences the characteristics of a photovoltaic module is the cell temperature, as shown in Figure 2. The variation of cell temperature greatly changes the MPP along the *x*-axis. Fig. 3 illustrates the insulation effect based on the relationship of photovoltaic power and current.

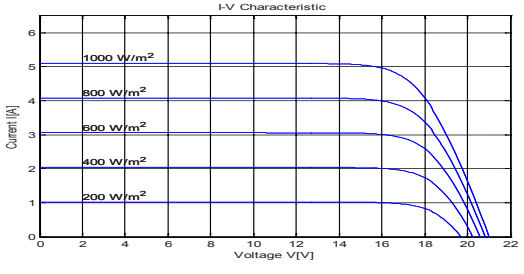

Fig. 1. I-V characteristics with insulation variations and constant cell temperature

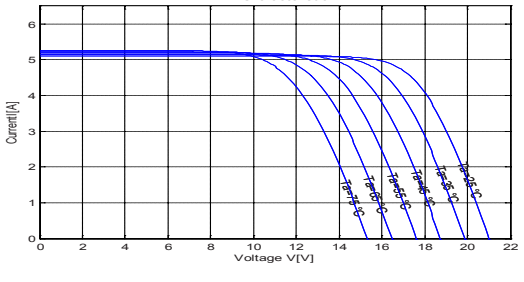

Fig. 2. I-V characteristic with cell temperature variation and constant insulation

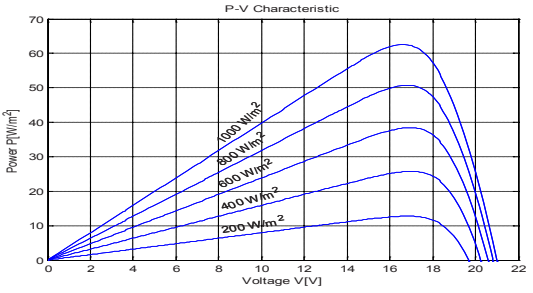

Fig. 3. P-V characteristics with insulation variations and constant cell temperature

Now, we develop a dynamic model of our laboratory benchmark shown in figure 4.

Fig. 4. Laboratory benchmark

This PV system is composed of a photovoltaic generator (100 Watts), a DC-DC boost converter and a battery (24 Volts). The equivalent circuit is presented in figure 5.

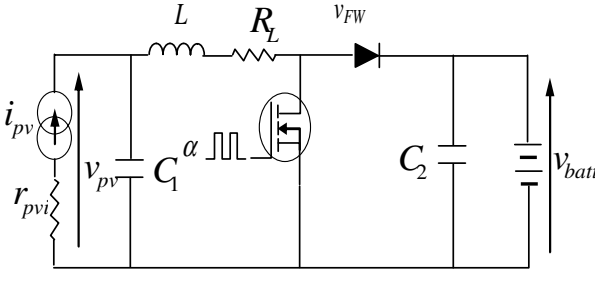

Fig. 5. PV equivalent circuit

The differential equations of the circuit can be described as follows [2]:

$$\frac{d}{dt}\begin{bmatrix} i_L \\ v_{pv} \end{bmatrix} = \begin{bmatrix} -\frac{R_L}{L} & \frac{1}{L} \\ -\frac{1}{C_1} & \frac{1}{r_{pvi}C_1} \end{bmatrix}\begin{bmatrix} i_L \\ v_{pv} \end{bmatrix} + \begin{bmatrix} -\frac{V_{bat}+V_{FW}}{L} \\ 0 \end{bmatrix}\alpha$$

$$y=\begin{bmatrix} 0 & 1 \end{bmatrix}\begin{bmatrix} i_L \\ v_{pv} \end{bmatrix}$$

Where r_{pvi} denotes the dynamic resistance of PV panel defined by $r_{pv} = \frac{dv_{pv}}{di_{pv}}$. For fixed cells temperature and insulation, the I-V characteristics of the PV (T=25°C, G=1000W) system is represented in figure 7.

To obtain the fuzzy model, we have approximated this curve by a fuzzy model with 4 Takagi Sugeno (TS) rules using the Levenberg-Marquardt optimisation algorithm:

The obtained fuzzy rules are:

$$\text{If } V_{PV} \text{ is } F_1 \text{ Then } I_{pv} = 0.43V_{pv} + 8.54$$

$$\text{If } V_{PV} \text{ is } F_2 \text{ Then } I_{pv} = 0.61V_{pv}$$

$$\text{If } V_{PV} \text{ is } F_3 \text{ Then } I_{pv} = 0.29V_{pv}$$

$$\text{If } V_{PV} \text{ is } F_4 \text{ Then } I_{pv} = -0.35V_{pv}$$

Where membership functions *Fi (i=1,2,3,4)* are represented in figure 6.

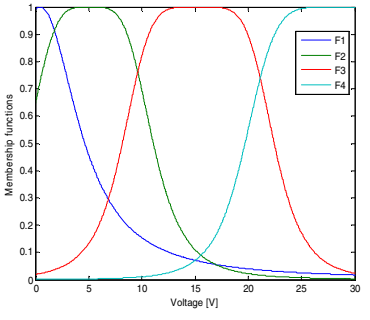

Fig. 6. Membership functions

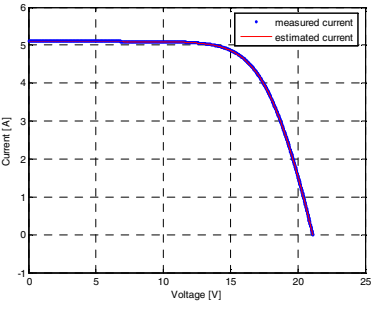

Fig. 7. I-V photovoltaic charactistic

Using this idea, state model (1) can be described by the following TS Fuzzy model :

If V_{PV} is F_i then $\dot{x} = A_i x + B_i u + w$ (i=1,2,3,4)

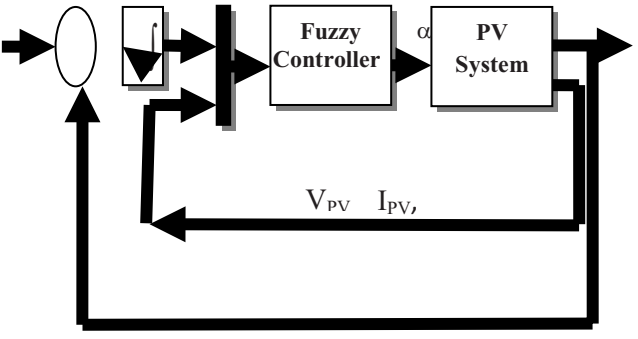

Fig. 8. Block diagram

where

$$A_i = \begin{bmatrix} -\frac{R_L}{L} & \frac{1}{L} \\ -\frac{1}{C_1} & \frac{a_i}{C_1} \end{bmatrix}, \quad B_i = \begin{bmatrix} -\frac{V_{bat}+V_{FW}}{L} \\ 0 \end{bmatrix}, x = \begin{bmatrix} i_L \\ V_{PV} \end{bmatrix}, u = \alpha$$

$$a_1 = 0.43,\ a_2 = 0.61,\ a_3 = 0.29,\ a_4 = -0.35,\ w = \begin{bmatrix} 0 & 8.54 \end{bmatrix}^T$$

The final output of the fuzzy system is inferred as follows

$$\dot{x}(t) = \sum_{i=1}^{4} h_i(vpv(t))\{A_i(x(t)) + B_i u(t) + w\} \qquad (1)$$

with

$$h_i = \frac{F_i(V_{PV})}{\sum_{i=1}^{4} F_i(V_{PV})}$$

It is easy to check that $h_i(V_{PV}) \geq 0, \quad \sum_{i=1}^{4} h_i(V_{PV}) = 1.$

In order to guarantee zero steady state regulation error, we develop an integral T-S fuzzy control. Let r be a constant reference, the objective is to achieve that $V_{pv} \rightarrow r$ when $t \rightarrow \infty$. To this end, we introduce an added state variable to account for the integral of output regulation error. Let us define the new state variable as:

$$\dot{e} = r - V_{PV} \qquad (2)$$

The TS fuzzy model given in (1) augmented by the error dynamics given in (2) becomes:

$$\dot{\overline{x}} = \sum_{i=1}^{4} h_i(V_{pv})\left\{\overline{A}_i(x(t)) + \overline{B}_i u(t) + W\right\} \qquad (3)$$

Where $\overline{A}_i = \begin{bmatrix} A_i & 0 \\ -C & 0 \end{bmatrix} \overline{B}_i = \begin{bmatrix} B_i \\ 0 \end{bmatrix} W = \begin{bmatrix} w \\ r \end{bmatrix}, C = \begin{bmatrix} 0 & 1 \end{bmatrix}.$

3 Control Strategies

In this work two control strategies are studied:

1) Incremental Conductance Method
This method consists in looking for the MPP. During the accurate tracking cycle, the output voltage of the photovoltaic array (PV) is adjusted by comparing the values of the incremental conductance and its instantaneous value.

$$P = V \cdot I$$
$$\frac{1}{V}\frac{dP}{dV} = \frac{I}{V} + \frac{dI}{dV}, V > 0$$
$$dP/dV > 0 \quad \text{if } G > \Delta G$$
$$dP/dV = 0 \quad \text{if } G = \Delta G$$
$$dP/dV < 0 \quad \text{if } G < \Delta G$$
$$G = I/V$$
$$\Delta G = -dI/dV$$

where I/V is the conductance of the PV array, and dI/dV is defined as the incremental conductance.

The test procedure is shown by the following algorithm. This algorithm tracks the operating voltage point at which the instantaneous conductance is equal to the incremental conductance.

2) Integral TS Fuzzy Controller Method
We consider the well known PDC structure defined as:

If V_{PV} is F_i then $u = -K_i \overline{x}$ (i=1,2,3,4).

The designed fuzzy controller uses the same fuzzy sets as in the premise parts with the plant and has local linear controllers in the consequence parts. The global output of the fuzzy state feedback controller is given by :

$$u(t) = -\sum_{i=1}^{4} h_i(V_{pv}) K_i \overline{x}(t) \tag{4}$$

By substituting (4) into (3), the closed loop fuzzy system can be represented as

$$\dot{\overline{x}}(t) = \sum_{i=1}^{4}\sum_{j=1}^{4} h_i h_j G_{ij} \overline{x}(t) = \sum_{j=1}^{4} h_i^2 G_{ii} \overline{x}(t) + \sum_{\substack{j=1 \\ i<j}}^{4} h_i h_j \left(G_{ij} + G_{ji}\right) \overline{x}(t) + W \quad \text{With}$$

$$G_{ij} = \overline{A}_i - \overline{B}_i \overline{K}_j = \begin{bmatrix} A_i & 0 \\ -C & 0 \end{bmatrix} - \begin{bmatrix} B_i \\ 0 \end{bmatrix} \begin{bmatrix} K_i & K_{Ii} \end{bmatrix}$$

The objective is to find $\overline{K}_i$ so that the closed loop system described by (3) is quadratically stable.

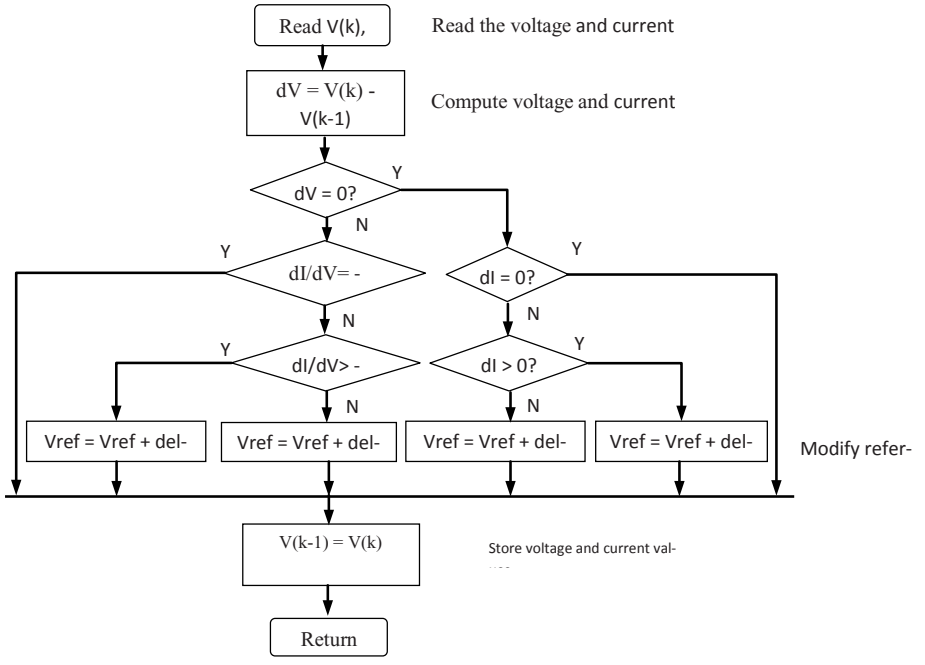

Fig. 8. Flow chart of the MPPT Incremental Conductance Method

The diagram block of integral TS fuzzy control is shown in figure 8.

Using the relaxed stabilisation conditions proposed in [9], we can say that the equilibrium point of the PV system described by TS fuzzy model (2) is quadratically stabilisable via fuzzy controller 4) if there exist matrices $Q>0$, Y_i,(i=1,2,3,4), Y_{iii},(i=1,2,3,4),$Y_{jii}=Y_{iij}^T$ and Y_{iji} ,(i=1,2,3,4, j≠i,j=1,2,3,4) and $Y_{ijl}=Y_{lji}^T$, $Y_{ilj}=Y_{jji}^T$, $Y_{jil}=Y_{lij}^T$,(i=1,2,j=i+1 …3,l=j+1,…,4) satisfying the following LMI:

$$QA_i^T + A_iQ - Y_i^T B_i^T - B_iY_i < Y_{iii}$$

$$2QA_i^T + QA_j^T + 2A_iQ + A_jQ - \left(Y_i + Y_j\right)^T B_i^T$$
$$- Y_i^T B_j^T - B_i\left(Y_i + Y_j\right) - B_jY_i \le Y_{iij} + Y_{iji} + Y_{iij}^T$$

$$
\begin{aligned}
&2Q(A_i + A_j + A_l)^T - \left(Y_j + Y_l\right)^T B_i^T - \left(Y_i + Y_j\right)^T B_l^T \\
&\quad - \left(Y_i + Y_l\right)^T B_j^T + 2(A_i + A_j + A_l)Q - B_i\left(Y_j + Y_l\right) \\
&\quad - B_l\left(Y_i + Y_j\right) - B_j\left(Y_i + Y_l\right) \le Y_{ijl} + Y_{ilj} + Y_{jil} \\
&Y_{ijl}^T + Y_{ilj}^T + Y_{jil}^T \\
&\quad \begin{bmatrix} Y_{1i1} & Y_{1i2} & Y_{3i1} & Y_{1i4} \\ Y_{2i1} & Y_{2i2} & Y_{2i3} & Y_{2i4} \\ Y_{3i1} & Y_{3i2} & Y_{3i3} & Y_{3i4} \\ Y_{4i1} & Y_{4i2} & Y_{4i3} & Y_{4i4} \end{bmatrix} \le 0
\end{aligned}
$$

Moreover, in this case, the fuzzy local state feedback gains are $K_i = Y_i Q^{-1}$

Proof : See [9].

4 Simulation and Experiments Results

To validate the proposed algorithm, simulation and experiment results are carried out. The simulations are developed in the matlab/simulink software and the experiment tests are achieved on a laboratory benchmark composed of the UNI-SOLAR PV generator (Pmax= 65 W, Voc =21.1 V, Isc=5.1 A, 124 Wp), a Boost DC-DC converter, Two Batteries (12 Volts, 40 Ah), two flash lights, a fan and a PIC18F-4520 microcontroller to receive the control laws as shown in figures 10, 11 and 12.

Based on the Incremental conductance method, we have charged a 24V battery, powered a fan and flash light with a power efficiency of 94.89% as shown in figure 12.

In simulation, we consider that the MPP is obtained with considering a reference voltage equal to 15,5 volts. The simulation results using the integral TS fuzzy control given in figure 13 show the regulation performance of the algorithm proposed.

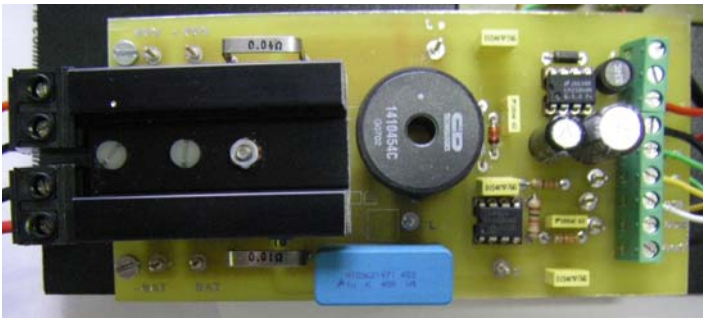

Fig. 10. Power block of PV system

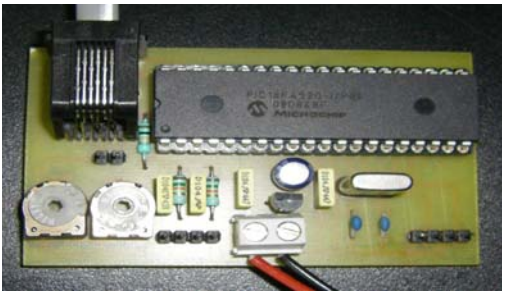

Fig. 11. PIC 18F-4520 Microcntroller

Fig. 12. Generated Power

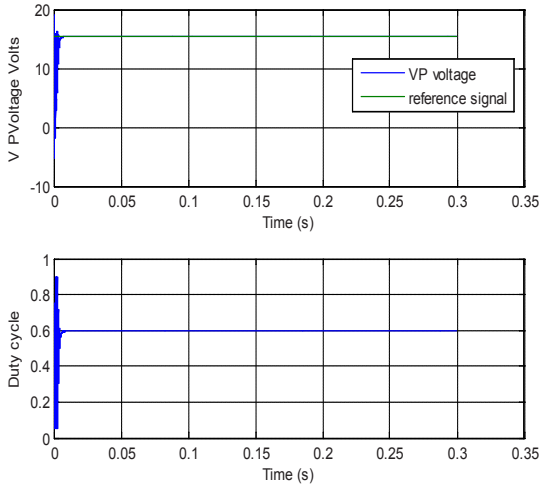

Fig. 13. The response of output voltage and the control input

5 Conclusion

In this paper, a method based on the TS fuzzy system has been used to modelize, analyse and control the PV systems. The controller design conditions are formulated in LMI terms and an MPPT was developed to implement the proposed MPPT Methods.

References

[1] Petrone, G., Spagnulo, G., Vitteli, M.: Analytical model of mismatched photovoltaic fields by means of Lambert W-function. Solar Energy Materials & Solar Cells, 1652–1657 (2007)
[2] Xiao, W., Dunford, W.G., Palmer, P.R., Capel, A.: Regulation of Photovoltaic Voltage. IEEE Transactions on Industrial Electronics 54(3) (June 2007)
[3] Bahgat, A.B.G., Helwa, N.H., Ahmad, G.E., El Shenawy, E.T.: Maximum power point tracking controller for PV systems using neural networks. Renewable Energy 30, 1257–1268 (2005)
[4] Leyva, R., Alonso, C., Queinnec, I., Cid-Pastor, A., Lagrange, D., Martinez, L.: MPPT of photovoltaic systems using Extremum- Seeking Control. IEEE Transaction on Aerospace and Electronic Systems 42(1), 249–258 (2006)
[5] Femia, N., Petrone, G., Spagnuolo, G., Vitelli, M.: Optimization of perturb and observe maximum power point tracking method. IEEE Trans. Power Electron. 20(4), 963–973 (2005)
[6] Tafticht, T., Agbossou, K., Doumbia, M.L., Chériti, A.: An improved maximum power point tracking method for photovoltaic systems. Renew. Energy, 1–9 (2007)
[7] Hussein, K., Muta, I., Hoshino, T., Osakada, M.: Maximum photovoltaic power tracking: an algorithm for rapidly changing atmosphere conditions. IEEE Proc. Inst. Electr. Eng. 142(1), 59–64
[8] Tanaka, K., Ikeda, T., Wang, H.O.: Fuzzy Regulators and Fuzzy Observers: Relaxed Stability Conditions and LMI-Based Designs. IEEE Trans. on Fuzzy Systems Journal 6(2), 250–265 (1998)
[9] Fang, C., Liu, Y., Kau, S., Hong, L., Lee, C.: A New LMI-Based Approach to Relaxed Quadratic Stabilization of T–S Fuzzy Control Systems. IEEE Transactions on Fuzzy Systems 14(3) (June 2006)
[10] Oudghiri, M., Chadli, M., El Hajjaji, A.: One-Step Procedure For Robust Output H∞ Fuzzy Control. In: CD-ROM of the 15th Mediterranean Conference on Control and Automation, IEEE-Med 2007, Athens, Greece, June 27-29 (2007)
[11] El Messoussi, W., Bosche, J., Pages, O., El Hajjaji, A.: Non-Fragile Observer-Based Control of Vehicle Dynamics Using T-S Fuzzy Approach. In: Proceeding of the 17th IFAC World Congress, Seoul Korea, July 6-11 (2008)

MACSyME: Modelling, Analysis and Control for Systems with Multiple Energy Sources

A. Naamane and N.K. M'Sirdi

LSIS, CNRS UMR 6168, Domaine Univ. St Jerome, Av. Escadrille
Normandie-Niemen. 13397, Marseille Cedex 20, France
Aziz.naamane@lsis.org, nacer.msirdi@lsis.org

Abstract. MACSyME[1] project aims to design and develop new systems combining different Energy sources: The process to control is made of three parts (production sources, the energy consumption and storage parts). The production sources (depend on wind or sunlight intensity) have stochastic behavior and are not fully controllable. Energy consumption has to be estimated and predicted. The instantaneous equilibrium of production, consumption and storage has to be maintained in an optimal level which depends on the system state, production state of charge and the demands. We have to design coupled prediction, estimation and control systems to optimize energy costs and satisfy demand. This paper describes the first work done for this project with. a specific urban wind turbine.

1 Introduction

According to IEA World Energy Oulook 2008'' The world is facing an energy and climate crisis. Globally, the energy sector emits 26 billion tonnes of CO2 each year and electricity production alone accounts for 41% of emissions. The International Energy Agency expects CO2 emissions in 2030 to have increased by 55% to reach more than 40 billion tonnes of CO2. The share of emissions coming from electricity production will increase to 44% in 2030, reaching 18 billion tonnes of CO2 ''The EWEA is fairly confident about the projections of wind power in the EU to 2030.

In these scenarios Urban wind turbines is an industry and technology that is still at development stage. It supposes that one can install and exploit wind in urban environment. Turbines have to be designed as part of the building itself (architecturally integrated). These turbines need compact wind devices able to supply a decentralized production, free from transport and generated losses,and is likely to make a tangible contribution to energy savings.

The offshore environment may allow the relaxation of a number of constraints on turbine design, such as aesthetics and noise level. However, addressing urban conditions, noise and reliability issues create new challenges in the urban sector. This will lead to a significant modification for the development of specific urban designs in

[1] MACSyME: Modeling, Analysis and Control for Systems with Multiple Energy sources. Definition of this project has been started in the LSIS in 2007 and involve several collaborating research laboratories.

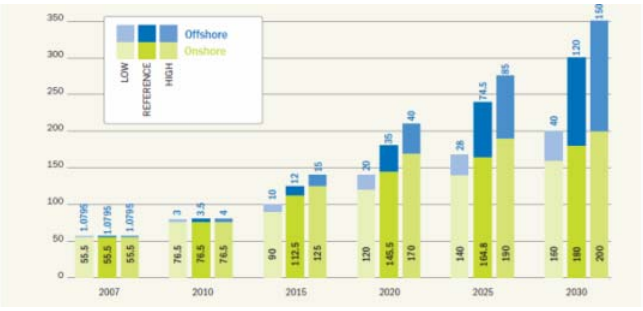

Fig. 1. EWEA's three wind power scenarios (in GW)

the medium and long term. So the aim of the research prioritized by our Laboratory is to develop technology that enables to deliver highly cost efficient wind turbines for individual wind turbine, by:

- applying recent and advanced control methods to optimize the dynamic behavior of variable-speed wind energy conversion systems (WECS).
- equipping WECS with sensors and control systems implementing supervision and data acquisition concept. The challenging open problem in WECS control is to ensure good quality electrical delivered energy while using a profoundly irregular primary source (the wind) and in most time very irregular demand.
- trying to develop new systems for control and management of power energies in the system with some following features:

  - Modelling subsystems to be able to optimize costs and consumption.
  - Analysis tools for design and supervision of multidisciplinary systems (system of systems).
  - Control and supervision taking into account subsystems features using prediction, forecasting and control.
  - Systems design using mechatronic approaches: A wind power system is a sophisticated combination of components and sub-systems that have to be designed in an interdisciplinary and integrated manner.
  - Management of the switching control between the different power sources in order to optimize energy consumption.
  - Energy sources and Energy storage have to be controlled via observers, estimators and diagnosis tools for the optimization of the whole studied system depending on weather and environment.

2 The MacSyME Project

The process to be controlled is composed by three parts as depicted by the scheme of figure 2. It has the following features:

- The energy production sources are not controllable. They have stochastic behavior as they depend on wind or sunlight intensity.

- The energy consumption has also to be estimated and predicted.
- The instantaneous equilibrium of production consumption and storage optimal depend on state of the previous system parts.

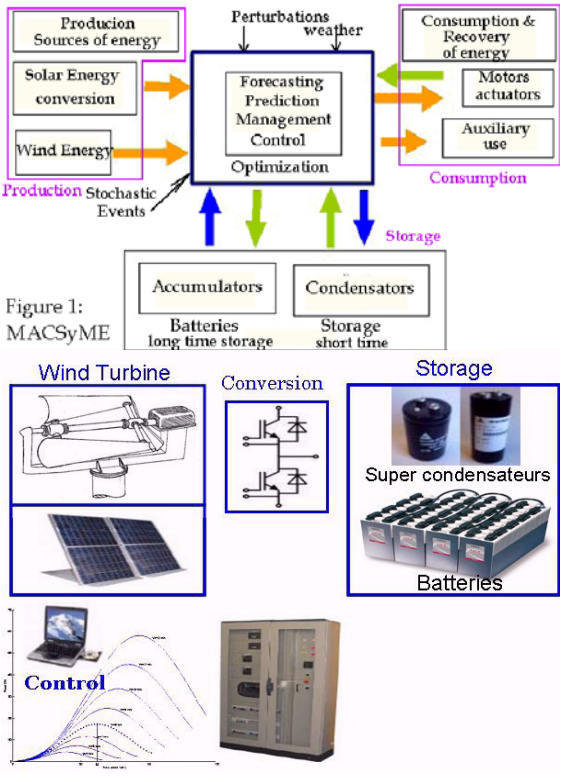

Figure 1: MACSyME

Our approach consists in a first stage to develop appropriate models (for control and management) for each part of the system, and to use these models for forecasting, estimating the system state and prediction of demand targets. The next step will consist to manage the production sources, use of power and storage (for long and short time) to optimize the costs and to lead to stable behaviors.[4]

Once the power target is defined (depending on energy demand) contribution of each source (solar, wind and storage) has to be defined in correlation with forecasting (stochastic events, perturbations and weather fluctuations) and prediction of demand during a selected period (to avoid redundant switching).

Several variables have to be measured: the system state variables and all parameters describing interactions between the system parts describing energy exchanges. Thus sensors can be used for most of them but measurements have to be observed or estimated.

The last part to develop is the control of sources and power managements. Optimization has to consider different cost functions, the system stability and safety in the same time as the protection of the subsystems from failures and faults which may be due to bad operating points or excessively demanding operating modes components.

3 The Studied Wind Turbine

3.1 Wind Turbine Characterization

The wind Turbine prototype used in this study has a particular shape as it is shown in figure 2.

Fig. 2. Wind turbine prototype

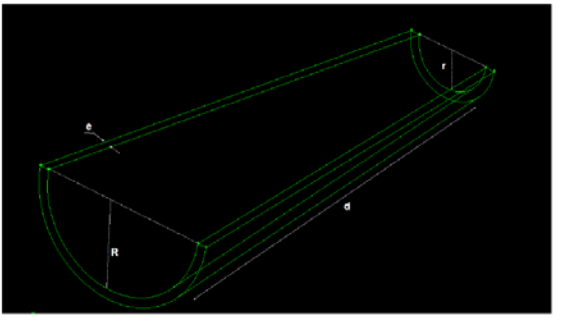

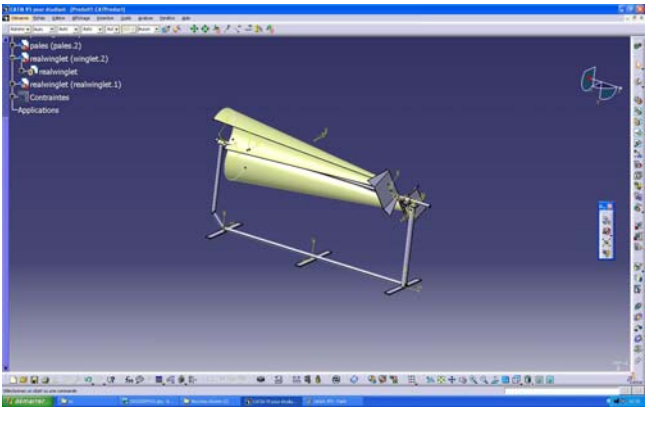

Fig. 3. Catia models

The first work carried out for this project dealt with the geometrical characterisation of the wind turbine and its behaviour under different wind speeds .

We have used for this purpose CATIA (Computer Aided Three Dimensional Interactive Application) software to assist us in prototyping the wind turbine. We have also used FLUENT for CATIA which gives fluid flow analysis and provides a full generative relationship between our manufacturing-ready geometry models and the flow analysis model.

In the following figures are presented the simulations results from Catia Software. These simulations allowed us to .optimize the geometrical parameters of the turbine.

In this part, the Catia software and Fluent were used in order to determine the difference in pressure inside and outside the blades. Different simulations with different configurations were accomplished. As a main conclusion, we have demonstrated that the axis of the two blades must have an angle of 15°with the central axis.

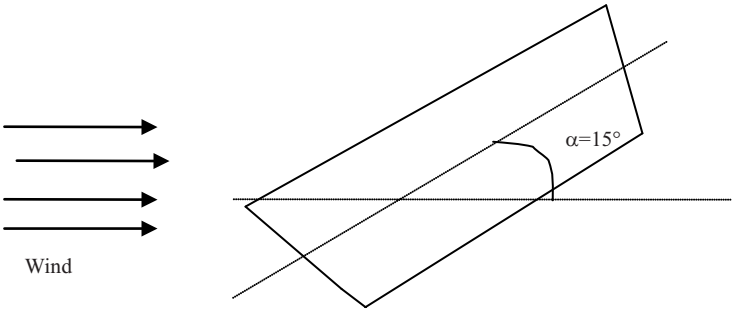

In the following figures are represented the results obtained with fluent software.

For this model, the geometry and the angle α are taken into account, we can obtain the velocity contours profiles and air flow pathlines. These simulations were carried out to appreciate the forces exerted by the air on the blades.

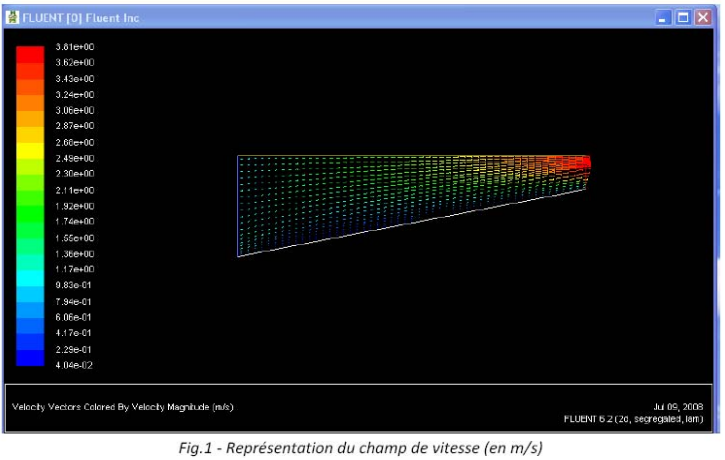

Fig.1 - Représentation du champ de vitesse (en m/s)

Fig. 4. Velocity field representation

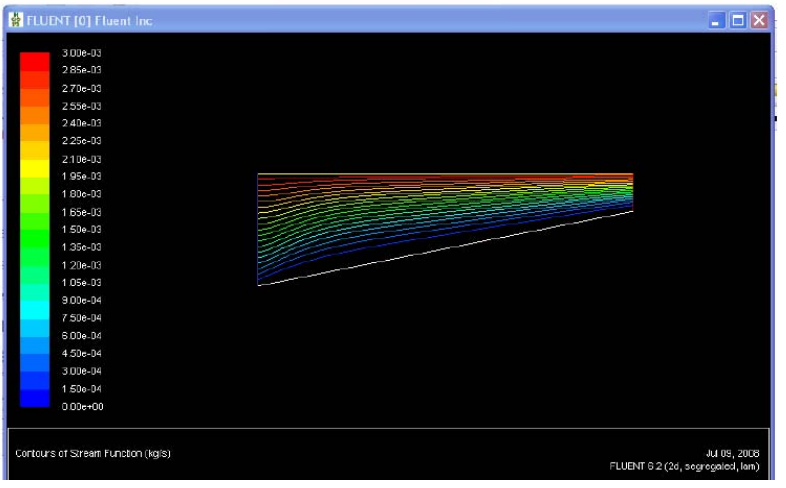

Fig. 5. Contours of stream function (Kg/s)

It is to be noticed that the half-cone shape, makes it possible to have an acceleration in end of the blade (like the Venturi effect).

These simulations indicated us that the value of the force is tripled when the value of α passes from 0 to 15°.

4 System Modeling and Simulation

4.1 Preliminaries

A Wind Energy conversion System WECS is characterized by the involved power speed characteristics. The Tip Speed Ratio (TSR), λ is defined by:

$$\lambda = R\omega_t / v_w \tag{1}$$

Where ω_t denotes the rotation velocity of turbine, v_w is the wind speed.

The mechanical power P_{turb} (power produced by turbine in W) that can be captured from the wind, in steady state, with a wind energy converter with effective area A_r is given by:

$$P_{turb} = 1/2\ \rho\pi R^2 v_w^3\ Cp(\lambda,\theta) \tag{2}$$

Where $Cp(\lambda,\theta)$ called power coefficient of turbine, the aerodynamic efficiency which depends on the power captured by the blades, P_{turb} can be calculated using (2)=$T_{turb}\ \omega_t$. the aeorodynamic torque acting on the blades, T_{turb} is obtained by:

$$T_{turb=} 1/2\ \rho\pi R^3 v_w^2\ C_T(\lambda,\theta) \tag{3}$$

If Cp is known, the aerodynamic torque can also be calculated from:

$$T_{turb=} 1/2\ \rho\pi R^3 v_w^2\ C_p(\lambda,\theta)/\ \omega_t \tag{4}$$

$$P_{turb=}1/2\ \rho\pi R^5\ \omega_t^3\ C_p(\lambda,\theta)/\ \lambda^3 \quad (5)$$

It can be seen from the above two equations that C_T and Cp are a function of λ and θ.

For our studied turbine q namely pitch angle is constant, Therefore C_T and C_p depend on λ only.

4.2 Wind Simulation

Modeling wind speed effect is difficult. The modeling of wind speed is important because it dictates how to evaluate the performances of wind generators and determines the features of the system dynamics for prediction of energy output. The turbulence of the wind speed is random in time and space and often described by a stationary Gaussian process [1,2,3]. The nature of wind speed may generally be assumed as made of two components, a steady state average flow and a time varying turbulence. The turbulent part is characterized by random fluctuations of the wind speed with some quasi periodic components and drifts. The mean average of wind speed increases with the elevation.

The wind speed v(t) [5]is simulated as a function of time by the following equation:

$$v_w(t)= A_0 +\Sigma A_i \cos(\omega_i t+\varphi_i) \quad (6)$$

In our case for the sake of simplicity, a single value of wind speed is applied to the whole wind turbines.

In the following figures,it is represented the block diagram of the whole system: the wind turbine part and the electrotechnical part.

The first experimental results achieved concern the curves of mechanical power versus Rotation velocity of the wind turbine and the torque versus Rotaional velocity. for different wind speeds.

The second part, achieved was the choice and the principle of functioning of the Generator to use for a maximum efficiency.

A Doubly Fed Induction Generator (DFIG) is chosen among several asynchronous generators. It is composed of a wound rotor induction generator connected to the electric grid within rotor and stator. The stator is directly connected to the grid and the rotor is connected to the grid by the unified power flow controller (UPFC). Such system has the capacity to track the maximum of power for different wind speeds and deliver the electric power by minimizing the Distorsion Harmonics Rate(DHR).[10,11].

Four phases of operation of the wind turbine at variable speed are considered:

- The launching phase of the machine. The electric production starts when the mechanical speed reached approximately 70% the speed of synchronism of the generator. The electric output remains rather low.
- The phase of extraction of the maximum power or phase MPPT (Maximum Power Point tracking). In this zone, mechanical speed varies and can reach a value close to nominal speed. The electric output increases quickly. In this zone, The maximum power is thus obtained for each value of mechanical speed and average speeds of wind.

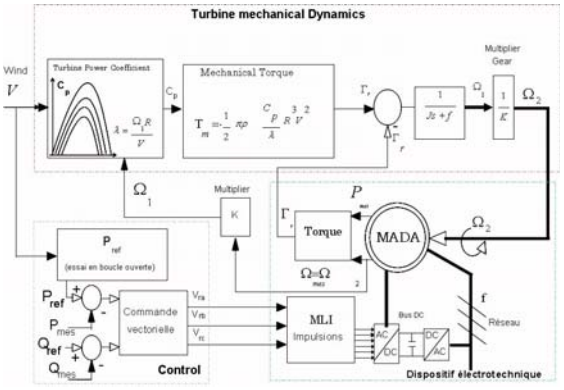

Fig. 6. Block diagram of the studied system

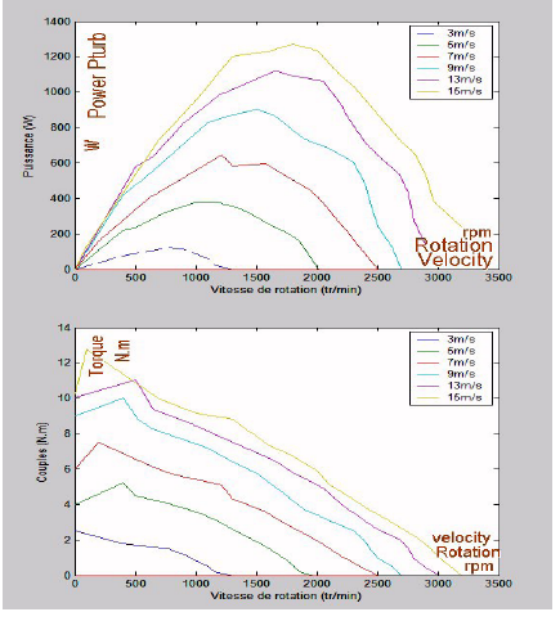

Fig. 7. Simulation results :Power and Torques Vs velocity rotation

- The phase at quasi constant mechanical speed. the electric output increases very quickly.
- The phase at constant power.

It is to be noticed that transfers of power in the MADA is achieved thanks to the bidirectional converters of power; [8,9]. In the circuit of the rotor, the MADA is able to work as a generator or engine in hypersynchronous way or in hyposynchronous way.

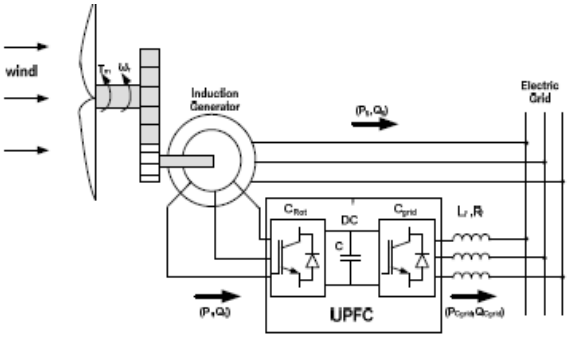

Fig. 8. DFIG configuration

The electrical part described above is currently simulated with PSIM software and will be tested in order to validate the approach.

5 Conclusions

In this paper, we have presented the first results obtained in ongoing project dealing with the optimization of Energy production. An urban wind turbine prototype was presented and characterized. The first experimental results in a laboratory environment are very promising. Experimentations under real conditions are envisaged on the roof of the Laboratory to confirm these first results. Another wind turbine of four larger time's dimensions will be used... This site would enable us to highlight the power ratio which exists between various wind turbines of different sizes. Theoretically, while multiplying by four the scale of the basic model, the power supplied by the wind turbine is 64 (4^3) times more important compared to the same wind speed of wind. We are in the presence of a concept exploiting volume of the blades covered by the wind instead of considering a surface.

References

[1] Watson, S.: Predicting the performance of small wind turbines in the roof-top urban environment. In: The proceedings of the Europe's premier wind event 7-40, Milan, Italie (May 2007)

[2] Paquette, J.: Increased strength in wind turbine blades through innovative structural design. In: The proceeding s of the Europe's premier wind event 7-40, Milan, Italie (May 2007)

[3] Holttinen, H.: State of the art of design and operation of power systems with large amount of wind power. In: The proceedings of the Europe's premier wind event 7-40, Milan, Italie (May 2007)

[4] Panel 1a: Les expériences d'utilisation des sources d'énergies renouvelables dans les villes. Est-il possible de développer le potentiel des énergies renouvelables dans un environnement urbain? In: BERLIN 2004: La conférence sur les énergies renouvelables. 19 au 24 Janvier (2004)

[5] Van der Hoven, I.: Power spectrum of horizontal wind speed in the frequency range from.0007 to900 cycles per hour. Journal of Meteorology 14, 160–164 (1957)
[6] Neammanee, B., Sirisumrannukul, S., Chatratana, S.: Development of a Wind Turbine Simulator for Wind Generator Testing. International Energy Journal 8, 21–28 (2007)
[7] Munteanu, I., Cutululis, N.A., Bratcu, A.I., Ceanga, E.: Optimization of variable speed wind power systems based on a LQG approach. Elsevier Tran. on Control Engineering Practice (2004)
[8] Hansen, L.H., Helle, L., Blaabjerg, F., Ritchie, E., Munk-Nielsen, S., Bindner, H., et al.: Conceptual survey of generators and power electronics for wind turbines. RIS_ National Laboratory, Roskilde, Denmark, Tech. Rep. RIS_-R-1205(EN) (2001)
[9] De La Salle, S.A., Reardon, D., Leithead, W.E., Grimble, M.J.: Review of wind turbine control. International Journal of Control 52(6), 1295–1310 (1990)
[10] Carlin, P.W., Laxson, S., Muljadi, E.B.: The history and state of the art of variable-speed wind turbine technology. National Renewable Energy Laboratory, U.S.A., Tech. Rep. NREL/TP-500-28607 (2001)
[11] Boukhezzar, B., Lupu, L., Siguerdidjane, H., Hand, M.: Multivariable Control Strategy for Variable Speed, Variable Pitch Wind Turbines. Renewable Energy International Journal (2006)

Structural Analysis for Fault Detection and Isolation in Fuel Cell Stack System

Quan Yang[1], Abdel Aitouche[1], and Belkacem Ould Bouamama[2]

[1] LAGIS UMR CNRS 8146
Hautes Etudes d'Ingénieur, 13, rue de Toul, 59046, Lille, France
Tel.: +333 2838 4822
quan.yan@hei.fr, abdel.aitouche@hei.fr
[2] LAGIS UMR CNRS 8146
Polytech-Lille, Rue Paul Langevin, 59655, Villeneuve d'Ascq, France

Abstract. This article deals with structural analysis for fault detection and isolation in fuel cell stack system. Analytical redundancy relations (ARRs) are computed by means on structural analysis with residuals generation. Then, structural monitorability (detectability and isolability) of fuel cell stack system is given. Through the fault signature's table, it has been shown that drying, flooding, contamination by gas pipe, compressor faults (mechanical, hydraulic, controller), compressor's current and velocity sensor faults and air mass flow sensor fault are detectable and isolable.

Keywords: fuel cell system, fault tree, structural analysis, analytical redundancy relations, oriented graph, detectability, isolability, monitorability, fault signatures, Fault Detection and Isolation, PEMFC.

1 Introduction

In the past few years, the fuel cell is the interest focus as the most promising power generation technology. Fuel cell development has generated much interest in technological and research community. Fuel cells, the devices that convert chemical energy, such as hydrogen, are an ideal electrical power source: lower/zero emission, silent, high efficiency. A fuel cell produces only electricity, water, and heat, thereby eliminating pollution at the energy conversion. This is one of the reasons why fuel cell is attractive.

Research and development of fuel cell systems for various applications has dramatically been increased in the last decade. Proton exchange membrane fuel cell (PEMFC) system is one of the most promising candidates to substitute traditional systems such as internal combustion engines. The PEMFC is an attractive candidate not only for transportation systems but also for other applications such as stationary systems, portable systems due to its higher power density and lower operating temperature compared to other types of fuel cells.

Recently, the research community of fuel cell has shown a considerable interest for diagnosis in view to ensure safety, security, fault detection and isolation when faults occur. These faults must be detected early and some time estimated and accommodated.

The main faults as shown in Figure 2 are: hydrogen circuit faults, air compressor faults and fuel cell stack faults. Most works focus on the detection of faults in the fuel cell heart. Main faults are flooding (accumulation of water on the canals), drying and contamination by gas (carbon monoxide or carbon dioxide or nitrogen).

All these faults are susceptible to affect the stack and thus generate a voltage drop. Generally, this drop will be detected but not located. Other parameters are necessary in this case to differentiate the various faults including temperature, loss of load and humidity reactive gas flow.

In the literature, to detect those faults, most methods are based on experiences. Liu, *et al.* (2005) have used phenomena between current density and formation of water in fuel cell to detect drying and flooding. These two phenomena are based on an analytical model of fuel cell. Methods based on images to detect flooding developed by Pekula, *et al.* (2005) have been ameliorated to detect drying and flooding in the fuel cell.

Most authors as Kramer *et al.* (2005) and Brunet *et al.* (2004) use spectrometric impedance technique. All these methods provide good results for the detection of flooding or drying in fuel cell, their implementation is still complex and costly related to the instrumentation required. All those methods based on experiment analysis can not detect and isolate faults on the global fuel cell stack system (FCSS) from which the idea of this paper is to use an alternative approach such as dynamic model based fault detection and isolation (FDI).

Few papers deal with FDI dynamic model based approaches applied to FCSS. Performances of such methods depend essentially on the model accuracy. Furthermore the FDI performances in term of isolability and detectability don't need any additional experiments since faulty analytical models can be obtained.

The problematic for model based FDI of fuel cell consists in that the model is complex and the numerical values are not always known. This is why structural model (based on existence or not of the links between variables and the relations) is well suited. The basic tool for structural analysis is based on the concept of matching on a bipartite graph (Staroswiecki, 2000).

Once the dynamic model obtained, methods on Analytical Redundancy Relations (ARRs) could be used (Patton *et al*., 1989 and Aitouche *et al*., 1999). Analytical redundancy approach consists to eliminate unknown variables and therefore generate formal ARRs. Those relations could be determined by using the technique of elimination theory and represented by an oriented graph.

Numerical evaluation of ARRs gives fault indicators named residuals. The set of residuals generates a binary sequence where a 0 represents a null residual and a 1 a non-null residual. Those binary sequences are called signatures. A table of fault signatures is provided. It will be shown (before industrial design) which faults can be detected and or isolated and how to make them monitorable with given instrumentation architecture.

This paper is organized as follows. The second section presents the fuel cell stack system: description and its faults tree. The third section presents the structural analysis of FCSS and the oriented graph of its each subsystem. In the fourth section, monitorability of FCSS is provided and the effectiveness of this method is proved.

2 Fuel Cell Stack System

2.1 Description

Figure 1 shows the scheme of fuel cell system. This system consists in four circuits of matter and energy: air, hydrogen, humidification and electrical circuit.

- Hydrogen valve: it is used to control the flow of fuel gas H_2.
- Air filter and compressor: The purpose of the air filter is to remove solid particles such as dust, pollen, molds and bacteria. The motor-compressor's role is to increase the air pressure by reducing its volume.
- Humidifier: it is a device that increases the moisture in the air compressed and filtered through the circuit of humidification.
- Fluid manifold: with one input and multiple outputs, it can distribute the gas under uniform guaranteeing the supply of fuel gas of each cell of stack.
- PEMFC: it is the heart of the system which consists of several cells depending on the power that was almost required.
- Cooling group: an electric fan is placed next to the compressor and the humidifier to cool. A second fan ensures the low temperature of the stack in normal operation.
- Batteries and converter DC / AC: batteries allow storage of electrical energy generated by the battery and inverter allows conversion DC / AC.

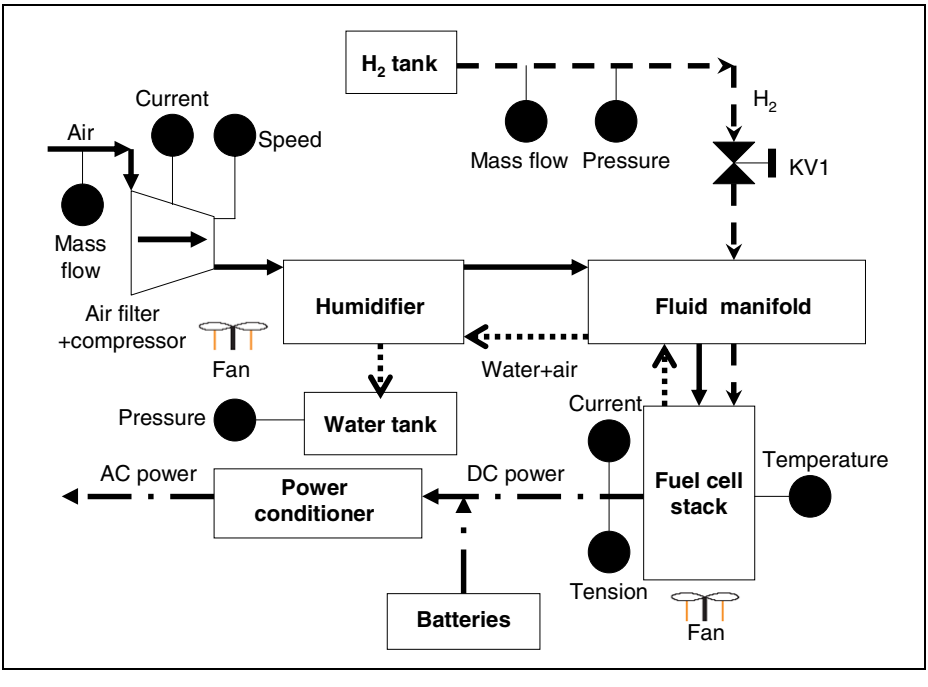

Fig. 1. Scheme of fuel cell stack system

To measure the physical variables of fuel cell system (FCS), several sensors were installed: flow and pressure of hydrogen, air flow, current and velocity of compressor, water pressure coming out of stack current, voltage and temperature of stack.

2.2 Faults Tree of Fuel Cell Stack System

Figure 2 shows the scheme of faults tree of fuel cell stack system. In our case, there are three classes of failure at high level for the global system: failure of hydrogen circuit, compressor failure and failure of fuel cell stack. In each class, it was shown several types of faults at second level and causes of failures at third level (Fig. 2.). From this fault tree, we can see that the hydrogen circuit is sensitive to leak faults of hydrogen and capping. Two possible failures can affect the compressor on the mechanical and electrical part. In addition, there is also a failure of the regulator which controls the engine and a hydraulic failure due to the reduction of the effect of compressibility. Inside the fuel cell (the heart of the system) it is shown that the distribution of water in the channel of the membrane may cause drying or flooding. In addition to water generated by the electrochemical reaction, the temperature of the fuel cell can affect drying faults and flooding.

Because of the existence of parasitic reaction, it is possible to detect contamination of the feed gas by N_2, CO or CO_2 especially in stack systems that use hydrogen produced from a fuel reformer or for systems operating in an environment polluted.

Table 1 shows the details of faults tree of fuel cell stack system. First column contains all kinds of failures corresponding to the first level in Fig. 2. Second column is

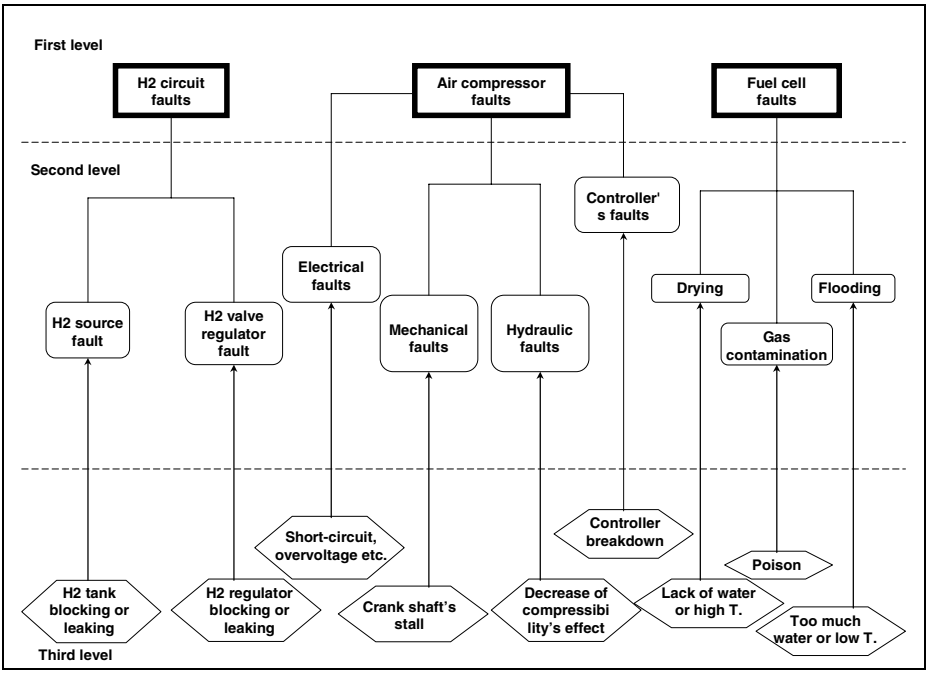

Fig. 2. Faults tree of fuel cell stack system

composed by all fault details under each kind of failures. Third column hierarchically presents causes of faults. Based on this table, the distribution of water is the most important effect to faults of fuel cell.

Table 1. Structural details of faults tree of fuel cell stack system

Failures of FCSS	Fault details	Causes		
H_2 circuit failures	H_2 source fault	H_2 tank blocking or leaking		
	H_2 valve regulator fault	H_2 valve regulator blocking or leaking		
Air compressor failures	Electrical faults	Short-circuit, over-voltage etc.		
	Mechanical faults	Crank shaft's stall		
	Hydraulic faults	Decrease of compressibility's effect		
	Controller's faults	Controller breakdown		
Fuel cell failures	Catalyst support oxidation	Parasite reaction caused by lack of reagents	Water accumulation in channels	Too much water or low temperature or under stoichiometry
			Water accumulation in the distribution areas	
	Membrane piercing	Parasite reaction caused by lack of reagents		
		Deterioration in physical and chemical properties	Water accumulation in the distribution areas	Too much water or low temperature or under stoichiometry
			Drying	Lack of water or high temperature or over stoichiometry
		Pressure difference		
	Catalyst agglomeration and migration	Water accumulation in the distribution areas		
		Irregular distribution of the current density	Water accumulation in channels	
			Water accumulation in the distribution areas	Too much water or low temperature or under stoichiometry
			Poisons	

3 ARRs Generation by Structural Analysis

A controlled system is a set of interconnected components interacting with each other to achieve the systems goal. Each components behavior can be described by a set of algebraic and/or dynamic equations defining the trajectory of a set of variables. Structural analysis only deals with the structural information contained in the model, i.e. which variables appear in which equation. Generally, this kind of relationship between variables and equations can be presented by bipartite graph (Steinder *et al*., 2004) since its causality. In this paper, oriented graph is used for the presentation of this relationship (mathematical model) and furthermore for the generation of ARRs by structural analysis.

This is a completely qualitative model, which does not consider the numerical form of the equations. The purpose of this section is to present an algorithm for ARRs generation by means of structural analysis. An analytical redundancy is a relation where all variables are known and can be written under following form:

$$f(K) = 0 \tag{1}$$

where K is the set of known variables.

$$K = [De, Df, Se, Sf, MSe, MSf, \theta, u] \tag{2}$$

Where:

De: sensor of effort, Df: sensor of flux, Se: supply of effort Sf: supply of flux
Mse: modulated supply of effort MSf: modulated supply of flux
ɵ: parameters set of system u: inputs set

Therefore, the expression of the ARR equation can be written as:

$$f(De, Df, Se, Sf, MSe, MSf, \theta, u) = 0 \tag{3}$$

The residual which represents the indicator of faults is then:

$$r = f(De, Df, Se, Sf, MSe, MSf, \theta, u) \tag{4}$$

It will be remembered that the system is no faulty if the residual is zero or below a certain threshold. In this work, it is assumed in ideal case, so the residual will be zero if fault is missing. In this paper, all variables in the form of De_X , Df_X , Se_X , Sf_X , u_X are known variables in which X is unknown variable that can be deduced from these known variables. All other variables are referenced in Table 4. To explain the ARRs generation through oriented graph, we suppose that the constraints Φ as path from known variables to unknown variables so that unknowns can be deduced from all known variables (observations, controls etc.). Since that all unknowns are got resolved, analytical redundancy relations can be obtained in the structural constraint as form of equation (3).

The details of all variables are given in the nomenclature.

3.1 ARRs Generation for H_2 Valve

According to structural properties of H_2 valve, the set of unknown variables is $X = [P_{in}, P_h, P_{out}, \dot{m}_h, x]$ With several sensors installed at the valve, the set of known

variables is $K=(Se\_P_{in}, De\_P_{out}, Df\_\dot{m}_{H2}, u\_V_x, c_v, c_p, \rho_{H2})$. In order to generate ARRs, four kinds of constraints can be written as follows:

- Structural constraints:

$$\Phi_s : P_{in} = P_h + P_{out} \tag{5}$$

- Component constraints:

$$\Phi_{c1} : P_h = \left(\frac{\dot{m}_h}{c_v \times f(x)} \right)^2 \times \rho_{H_2} \tag{6}$$

- Measurement constraints:

$$\Phi_{m1} : P_{out} = De\_P_{out} \tag{7}$$

$$\Phi_{m2_2} : \dot{m}_h = Df\_\dot{m}_{H_2} \tag{8}$$

- Controller constraints:

$$\Phi_{ctr1} : x = u\_V_x \tag{9}$$

$$\Phi_{ctr2} : P_{in} = Se\_P_{in} \tag{10}$$

From these constraints, one analytical redundancy relation can be deduced by eliminating all unknown variables through the oriented graph in Fig. 3.

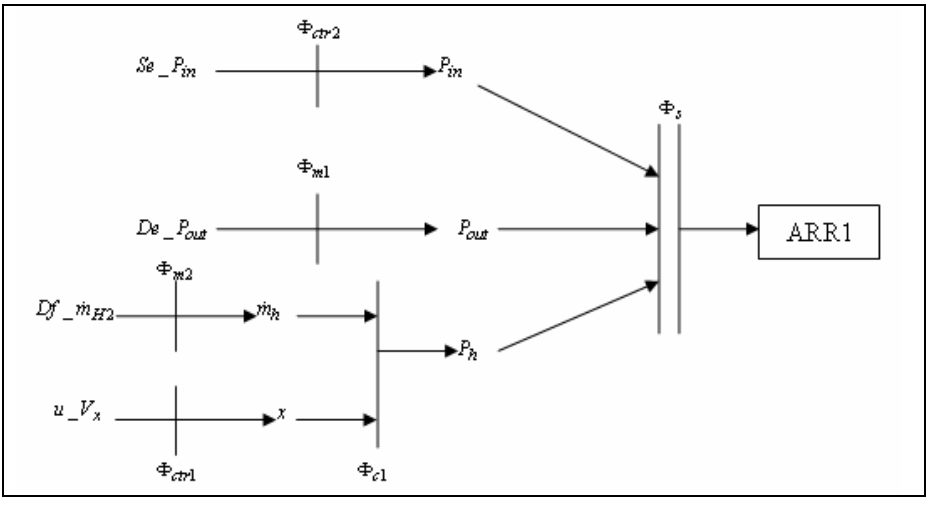

Fig. 3. Oriented graph for H_2 valve

The ARR1, which is sensible to the valve regulator and three sensors, is:

$$Se\_P_{in} - \left[\frac{Df\_\dot{m}_{H2}}{c_v \times f(u\_V_x)} \right]^2 \times \rho_{H_2} - De\_P_{out} = 0 \tag{11}$$

and its residual is R1.

3.2 ARRs Generation for Centrifugal Air Compressor

According to structural properties of centrifugal air compressor, the set of unknown variables is:

$$x = (U_c, i_c, U_R, U_e, \omega, \Gamma_{in}, \Gamma_I, \Gamma_{th}, \Gamma_{out}, P_{in}, \dot{m}_{in}, P_{out}, \dot{m}_0, \dot{m}_C, \dot{m}_{slip}, \dot{m}_{out})$$

With several sensors installed around the compressor, the set of known variables is $K = \left(Df\_\omega, Df\_i_c, De\_P_{in}, Df\_\dot{m}_{in}, Se\_U_e, r, \eta_p, b, C, I, R_e, \rho_{O_2}\right)$. The constraint equations are as follows:

- Structural constraints:

$$\Phi_{s1} : \Gamma_{in} = \Gamma_I + \Gamma_{th} + \Gamma_{out} \tag{12}$$

$$\Phi_{s2} : \dot{m}_0 = \dot{m}_C + \dot{m}_{slip} + \dot{m}_{out} \tag{13}$$

$$\Phi_{s3} : U_e = U_c + U_R \tag{14}$$

- Component constraints:

$$\Phi_{c1} : U_c = r \times \omega \tag{15}$$

$$\Phi_{c2} : \Gamma_{in} = r \times i_c \tag{16}$$

$$\Phi_{c3} : \Gamma_I = I \times \frac{d\omega}{dt} \tag{17}$$

$$\Phi_{c4} : \Gamma_{th} = \omega \times f\left(1 - \frac{\Gamma_{out}}{\Gamma_{in}}\right) \tag{18}$$

$$\Phi_{c5} : \dot{m}_0 = b \times f(P_{in}, P_{out}, \omega) \tag{19}$$

$$\Phi_{c6} : \Gamma_{out} = b \times f(P_{in}, P_{out}) \tag{20}$$

$$\Phi_{c7} : \dot{m}_C = \frac{d}{dt}(C \times P_{out}) \tag{21}$$

$$\Phi_{c8} : \dot{m}_{slip} = \frac{P_{out}}{f\left(1 - \frac{\dot{m}_{slip}}{\dot{m}_{out}}\right)} \tag{22}$$

$$\Phi_{c9} : U_R = R_e \times i_c \tag{23}$$

$$\Phi_{c10} : \dot{m}_{in} = \dot{m}_{out} \tag{24}$$

$$\Phi_{c11} : P_{out} = \eta_p \times P_{in} \tag{25}$$

- Measurement constraints:

$$\Phi_{m1} : \omega = Df\_\omega \tag{26}$$

$$\Phi_{m2} : i_c = Df\_i_c \tag{27}$$

$$\Phi_{m3} : P_{in} = De\_P_{in} \tag{28}$$

$$\Phi_{m4} : \dot{m}_{in} = Df\_\dot{m}_{in} \tag{29}$$

- Controller constraints:

$$\Phi_{ctr} : U_e = Se\_U_e \tag{30}$$

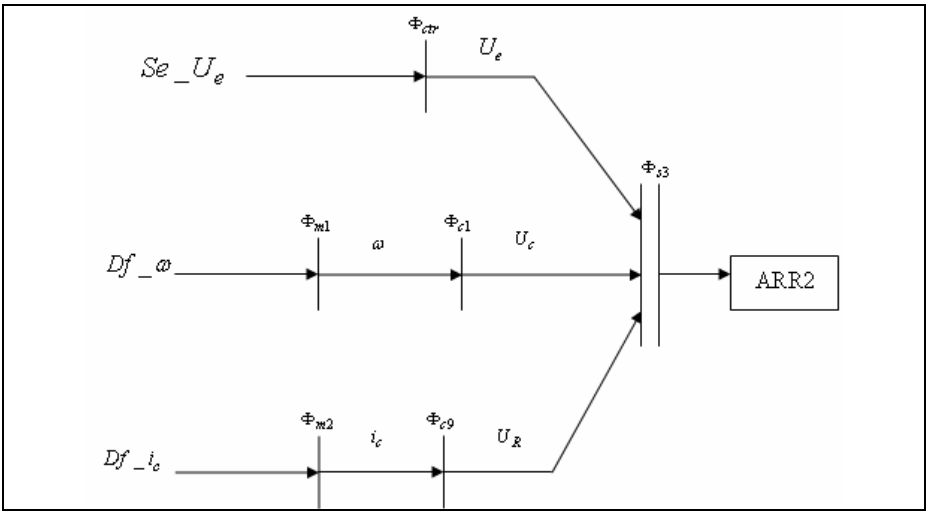

Fig. 4. Oriented graph for electric part of the compressor

From these constraints, three ARRs can be deduced respectively by oriented graph in Fig. 4., Fig. 5. and Fig. 6. The ARR2 sensible to the electric part of the compressor is:

$$Se\_U_e - r \times Df\_\omega - R_e \times i_c = 0 \tag{31}$$

and its residual is R2.

The ARR3 sensible to the mechanic part of the compressor is:

$$r \times Df\_i_c - I \times \frac{d(Df\_\omega)}{dt} - Df\_\omega \times f\left[1 - \frac{b \times f\left(De\_P_{in}, \eta_p\right)}{r \times Df\_i_c}\right] - b \times f\left(De\_P_{in}, \eta_p\right) = 0 \tag{32}$$

and its residual is R3.

The ARR4 sensible to the hydraulic part of the compressor is:

$$b \times f(De\_P_{in}, \eta_p, Df\_\omega) - \frac{d}{dt}\left(C \times \eta_p \times De\_P_{in}\right) - f\left(\eta_p, De\_P_{in}, Df\_\dot{m}_{in}\right) - Df\_\dot{m}_{in} = 0 \tag{33}$$

and its residual is R4.

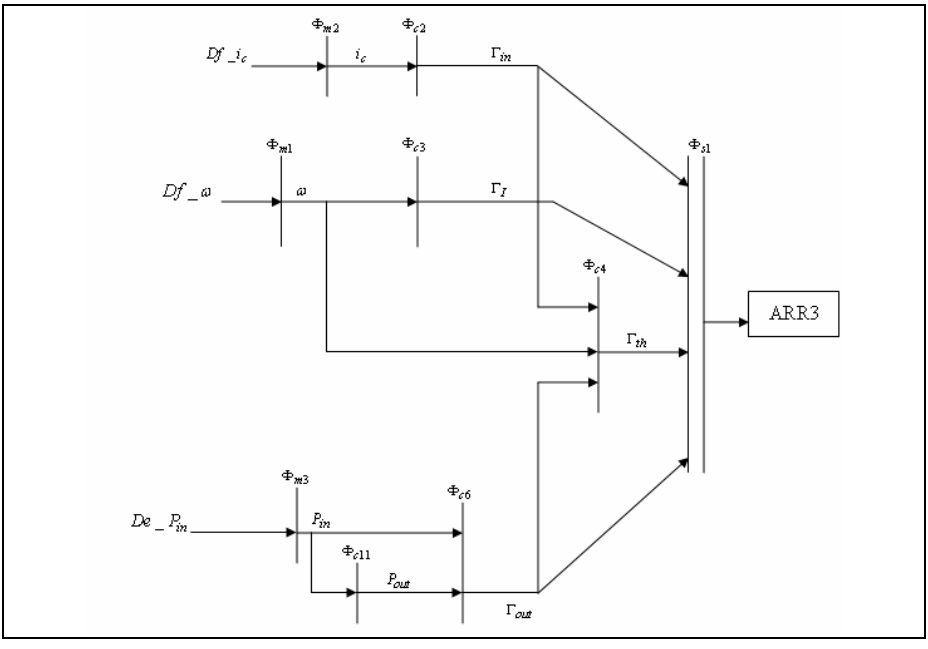

Fig. 5. Oriented graph for mechanic part of the compressor

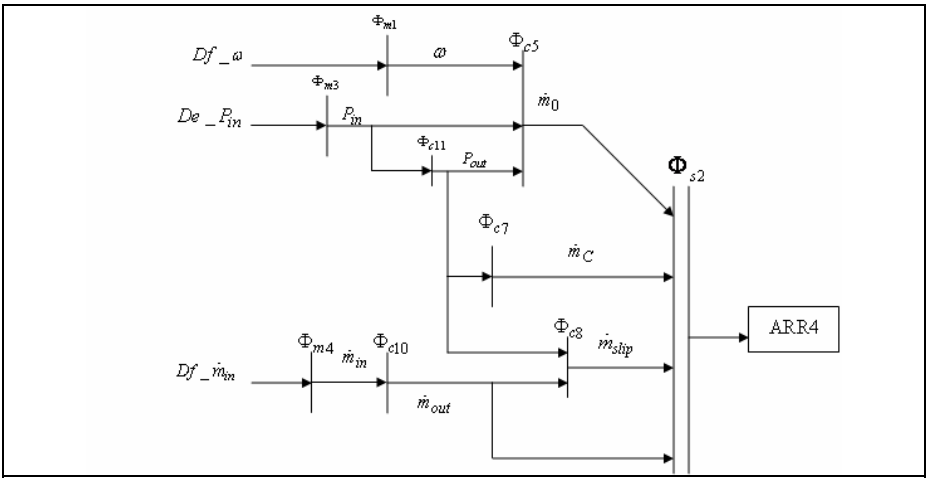

Fig. 6. Oriented graph for hydraulic part of the compressor

3.3 ARRs Generation for Fuel Cell

According to structural properties of fuel cell, the set of unknown variables is

$$x = \begin{pmatrix} \mu_{H_2}, P_{H_2}, \mu_{O_2}, P_{O_2}, \mu_{H_2O}, P_{H_2O}, \dot{m}_{H_2}, \dot{m}_{O_2}, T_{H_2}, T_{O_2}, \\ T_e, A_{H_2}, A_{O_2}, A_{H_2O}, \Delta G, E, i, \eta_a, \eta_c, \eta_e, \eta_{act}, \eta_{diff}, U \end{pmatrix}.$$

With several sensors installed, the set of known variables is

$$K = \left(\begin{array}{l} Df\_i, De\_U, De\_P_{H_2}, De\_P_{O_2}, De\_P_{H_2O}, Df\_\dot{m}_{O_2}, Df\_\dot{m}_{H_2}, \\ De\_T_{H_2}, De\_T_{O_2}, De\_T_e, \mu_0, R, P^*_{H_2}, P^*_{O_2}, P^*_{H_2O}, n, F, R_a, R_c, R_e, i_0, i_l \end{array} \right).$$

The constraint equations are as follows:

- Structural constraints:

$$\Phi_{s1} : A_{H_2} + A_{O_2} = A_{H_2O} - \Delta G \tag{34}$$

$$\Phi_{s2} : E = U + \eta_a + \eta_e + \eta_c + \eta_{act} + \eta_{diff} \tag{35}$$

- Component constraints:

$$\Phi_{c1} : \mu_{H_2} = \mu_0 + RT_{H2} \ln\left(\frac{P_{H_2}{}^*}{P_{H_2}} \right) \tag{36}$$

$$\Phi_{c2} : \mu_{O_2} = \mu_0 + RT_{O_2} \ln\left(\frac{P_{O_2}{}^*}{P_{O_2}} \right) \tag{37}$$

$$\Phi_{c3} : \mu_{H_2O} = \mu_0 + RT_e \ln\left(\frac{P_{H_2O}{}^*}{P_{H_2O}} \right) \tag{38}$$

$$\Phi_{c4} : A_{H_2} = \mu_{H_2} \tag{39}$$

$$\Phi_{c5} : A_{O_2} = \frac{1}{2}\mu_{O_2} \tag{40}$$

$$\Phi_{c6} : A_{H_2O} = \mu_{H_2O} \tag{41}$$

$$\Phi_{c7} : E = -\frac{\Delta G}{nF} \tag{42}$$

$$\Phi_{c8} : \eta_a = R_a i \tag{43}$$

$$\Phi_{c9} : \eta_c = R_c i \tag{44}$$

$$\Phi_{c10} : \eta_e = R_e i \tag{45}$$

$$\Phi_{c11} : \eta_{act} = \frac{2RT_e}{nF} \sinh^{-1}\left(\frac{i}{2i_0} \right) \tag{46}$$

$$\Phi_{c12} : \eta_{diff} = \frac{RT_e}{nF} \ln\left(1 - \frac{i}{i_l} \right) \tag{47}$$

- Measurement constraints:

$$\Phi_{m1} : T_e = De\_T_e \tag{48}$$

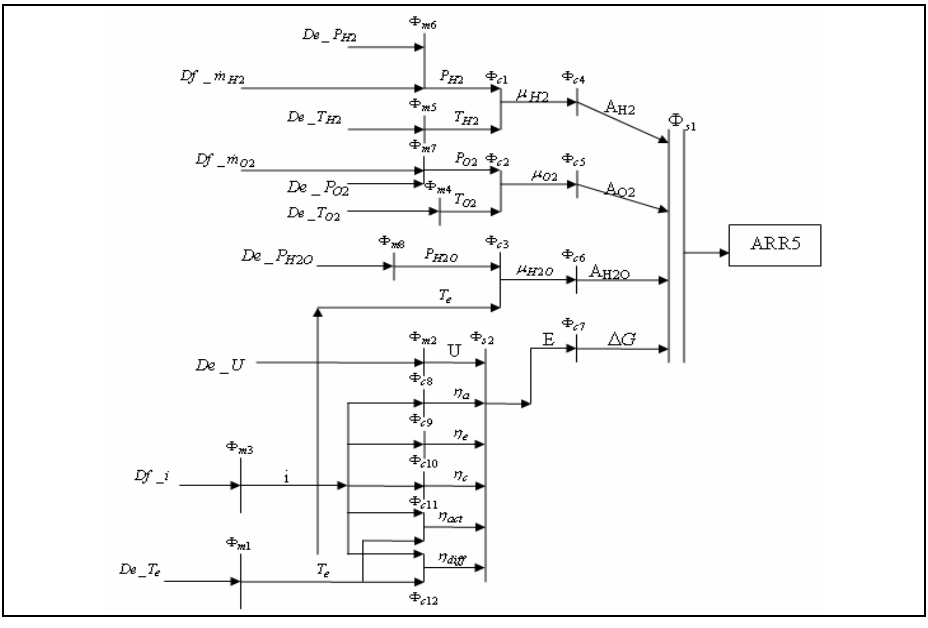

Fig. 7. Oriented graph for chemical part of fuel cell

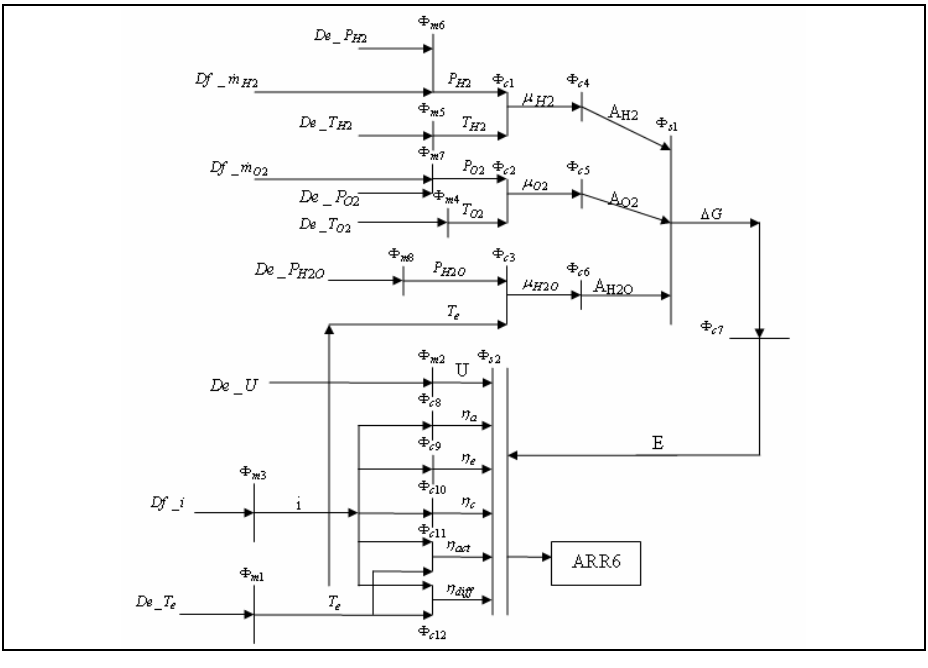

Fig. 8. Oriented graph for electric part of fuel cell

$$\Phi_{m2} : U = De\_U \tag{49}$$

$$\Phi_{m3} : i = Df\_i \tag{50}$$

$$\Phi_{m4} : T_{O_2} = De\_T_{O_2} \tag{51}$$

$$\Phi_{m5} : T_{H_2} = De\_T_{H_2} \tag{52}$$

$$\Phi_{m6} : P_{H_2} = f(De\_P_{H_2}, Df\_\dot{m}_{H_2}) \tag{53}$$

$$\Phi_{m7} : P_{O_2} = f(De\_P_{O_2}, Df\_\dot{m}_{O_2}) \tag{54}$$

$$\Phi_{m8} : P_{H_2O} = De\_P_{H_2O} \tag{55}$$

From these constraints, two ARRs can be deduced respectively by oriented graph in Fig. 7. and Fig. 8. The ARR2 sensible to the electric part of the compressor is:

From these constraints, two ARRs can be deduced respectively by oriented graph in Fig. 7. and Fig. 8. The ARR5 sensible to the chemical part of the fuel cell is:

$$\begin{aligned} &R\times De\_T_{H_2}\times\ln\left[\frac{P_{H_2}{}^*}{f\left(De\_P_{H_2}, Df\_\dot{m}_{H_2}\right)}\right]+\frac{1}{2}\mu_0+\\ &\frac{1}{2}R\times De\_T_{H_2}\times\ln\left[\frac{P_{O_2}{}^*}{f\left(De\_P_{O_2}, Df\_\dot{m}_{O_2}\right)}\right]-R\times De\_T_e\times\ln\left(\frac{P_{H_2O}{}^*}{De\_P_{H_2O}}\right)-\\ &nF\times\left[De\_U+\left(R_a+R_e+R_c\right)\times Df\_i+\frac{2R\times De\_T_e}{nF}\sinh^{-1}\left(\frac{Df\_i}{2i_0}\right)+\frac{R\times De\_T_e}{nF}\ln\left(1-\frac{Df\_i}{i_l}\right)\right]=0 \end{aligned} \tag{56}$$

and its residual is R5.

The ARR6 sensible to the electric part of the fuel cell is:

$$\begin{aligned} &\frac{1}{nF}\left\{\begin{aligned}&R\times De\_T_{H_2}\times\ln\left[\frac{P_{H_2}^*}{f\left(De\_P_{H_2}, Df\_\dot{m}_{H_2}\right)}\right]+\frac{1}{2}\mu_0+\\&\frac{1}{2}R\times De\_T_{O_2}\times\ln\left[\frac{P_{O_2}^*}{f\left(De\_P_{O_2}, Df\_\dot{m}_{O_2}\right)}\right]-R\times De\_T_e\times\ln\left(\frac{P_{H_2O}^*}{De\_P_{H_2O}}\right)\end{aligned}\right\}-\\ &De\_U-\left(R_a+R_e+R_c\right)\times Df\_i-\frac{2R\times De\_T_e}{nF}\sinh^{-1}\left(\frac{Df\_i}{2i_0}\right)-\frac{R\times De\_T_e}{nF}\ln\left(1-\frac{Df\_i}{i_l}\right)=0 \end{aligned} \tag{57}$$

and its residual is R6.

4 Detectability and Isolability Analysis

Table 2 shows the failures designation for all fault symbols used in nomenclature.

Table 3 shows the fault signature in which the monitorability (possibility of detection and isolation of failures) of the whole plant will be analyzed. The set of residuals generates a binary sequence where "0" represents a null residual and "1" a non-null residual. Those binary sequences are called signatures.

The columns of Db and Ib respectively represent the detectability and isolability of faults. A value of 1 appears in the table, if it is detected or isolated. We can see that all faults are detected but not isolated. The faults of drying and flooding can be

Table 2. Failures designation

Symbol	Failures designation
Se:H_2	H_2 source fault
Se:U_c	Compressor electrical source fault
Se:x	H_2 valve regulator fault
CF1	Compressor electrical fault : short circuit, overvoltage, etc.
CF2	Compressor mechanical fault : crank shaft stall
CF3	Compressor hydraulic fault : compressibility decrease
CF4	Compressor's controller fault
FF1	Drying
FF2	Flooding
FF3	H_2 contamination by gas (N_2, CO, CO_2)
Df:F_{H2}	H_2 mass flow sensor fault
Df:F_{O2}	Air mass flow sensor fault
De:P_{H2}	H_2 pressure sensor fault
De:P_{H2O}	H_2O pressure sensor fault
Df:I_c	Compressor current sensor fault
Df:V_c	Compressor velocity sensor fault
Df:I_{fc}	Fuel cell current sensor fault
De:U_{fc}	Fuel cell voltage sensor fault
De:T_{fc}	Fuel cell temperature sensor fault
De:T_{H2}	H_2 temperature sensor fault

Table 3. Faults signature

Fault	Db	Ib	R1	R2	R3	R4	R5	R6
Se:H_2	1	0	1	0	0	0	0	0
Se:U_c	1	0	0	1	0	0	0	0
Se:x	1	0	1	0	0	0	0	0
CF1	1	0	0	1	0	0	0	0
CF2	**1**	**1**	0	0	1	0	0	0
CF3	**1**	**1**	0	0	0	1	0	0
CF4	**1**	**1**	0	0	1	1	0	0
FF1	**1**	**1**	0	0	0	0	1	0
FF2	**1**	**1**	0	0	0	0	1	0
FF3	**1**	**1**	0	0	0	0	0	1
Df:F_{H2}	1	0	1	0	0	0	1	1
Df:F_{O2}	**1**	**1**	0	0	0	1	1	1
De:P_{H2}	1	0	1	0	0	0	1	1
De:P_{H2O}	1	0	0	0	0	0	1	1

Table 3. (*continued*)

Df:I_c	**1**	**1**	0	1	1	0	0	0
Df:V_c	**1**	**1**	0	1	1	1	0	0
Df:I_{fc}	1	0	0	0	0	0	1	1
De:U_{fc}	1	0	0	0	0	0	1	1
De:T_{fc}	1	0	0	0	0	0	1	1
De:T_{H2}	1	0	0	0	0	0	1	1

5 Nomenclature

Table 4. Nomenclature

Variable	Description
P	Total pressure(bar)
$\dot{m}$	Mass flow(kg s-1)
x or V_x	Valve position
c_v	Specific volume(J kg-1 m-3)
c_p	Specific thermal(J kg-1 K-1)
ρ	Mass density(kg m-3)
U	Voltage(V)
i	Current(A)
U_e	Source voltage(V)
ω	Angle velocity(rad s-1)
Γ	Torque(N m)
r	Compressor electric-mechanic ratio
η_p	Compressibility
b	Valve state(0 or1)
C	Compatibility(in compressor)
I	Inertia(in compressor)
R_e	Compressor equivalent resistance(Ω)
μ	Chemical potential
T	Temperature
A	Chemical affinity
ΔG	Gibbs energy variation
E	Electrical potential from ΔG in fuel cell
η_j (j=a, c, e, act, diff)	Electrical potential in fuel cell
R	Idea gas constant
P^*	Partial pressure
n	Exchanged electron number
F	Faraday constant
R_j (j=a, c, e)	Resistance inside of fuel cell
i_l	Current density for activation or diffusion Subscription
in	Input
out	Output
h	Hydraulic
a	Anode
c	Cathode

Table 4. (*continued*)

e	Electrolyte
diff	Diffusion
act	Activation
C	Compatibility(in compressor)
0	Initial condition
R	Compressor equivalent resistance

isolated based on the sign of the residual R6. That means if R6<0 or less than a certain threshold, there exists drying caused by the augmentation of resistances in fuel cell. On the contrary, if R6>0 more than a certain threshold, there exists flooding caused by the diminution of its resistances.

6 Conclusions

Our work presents a structural analysis for fault detection and isolation of fuel cell stack system. The results of structural monitorability of fuel cell stack system show that drying, flooding, contamination by gas pipe, compressor faults (mechanical, hydraulic, controller), and compressor's current and velocity sensor faults and air mass flow sensor fault are detectable and isolable. To isolate other failures, we just need to add sensors, i.e., for hydrogen leakage.

As perspective, we will take account into humidifier and fluid manifold in view to monitor the global fuel cell stack system. Further work consists to compute some residuals by means of numerical models of fuel cell stack system.

Aknowledgments. This research was supported by the research department of the Region Nord Pas de Calais, Hautes Eudes d'Ingénieur of Lille and the Centre National de Recherche Scientifique (CNRS) in France which are gratefully acknowledged.

References

Aitouche, A., Busson, F., Ould Bouamama, B., Staroswiecki, M.: Multiple Sensor Fault Detection of Steam Condensers. Computers Chemical Engineering Science Supplement 23, S585–S588 (1999)

Brunetto, C., Tina, C., Squadrito, G., Moschetto, A.: PEMFC Diagnostics and modelling by Electrochemical Impedance Spectroscopy. In: IEEE MELECOM, pp. 1045–1050 (2004)

Kramer, D., Zhang, J., Shimoi, R., Lehmann, E., Wokaun, A., Shinohara, K., Scherer, G.G.: In situ diagnostic of two-phase flow phenomena in polymer electrolyte fuel cells by neutron imaging: Part A. Experimental, data treatment, and quantification. Electrochimica Acta 50-13, 2603–2614 (2005)

Liu, Z., Mao, Z., Wu, B., Wang, L., Schmidt, V.M.: Current density distribution in PEMFC. Journal of Power Sources 141(2), 205–210 (2005)

Patton, R.J., Frank, P.M., Clark, R.N.: Fault Diagnosis in Dynamics Systems, Theory and Applications. Prentice-Hall, London (1989)

Pekula, N., Heller, K., Chuang, P.A., Turhan, A., Mench, M.M., Brenizer, J.S., Unlu, K.: Study of water distribution and transport in a polymer electrolyte fuel cell using neutron imaging. Nuclear Instruments and Methods in Physics Research A 542, 131–141 (2005)

Steinder, M., Sethi, A.S.: A survey of fault localization techniques in computer networks. Science of Computer Programming 53, 165–194 (2004)

Efficiency Analysis of Cross-Flow Plate Heat Exchanger for Indirect Evaporative Cooling

Xuelai Liu[1,2,*], Yong'an Li[2], Jizhi Li[1], Hongxing Yang[3], and Hengliang Chen[4]

[1] Department of machinery and electricity engineering, China Petroleum University, Dongying, China

[2] Department of thermal engineering, Shandong Jianzhu University, Jinan, China

liuxuelai147@163.com

[3] Department of Building Service Engineering, The Hong Kong Polytechnic University, Hong Kong, China

[4] Shandong Institute of Supervision & Inspection on Product Quality, Jinan, China

Abstract. This paper established the mathematic model of the cross-flow plate heat exchanger for indirect evaporative heat exchanger. The mathematic model is solved according to the finite volume method. Through the numerical solution of the mathematic model, the temperature distribution of the primary air and the secondary air in the flow directions are obtained. The efficiency of cross-flow plate heat exchanger for indirect evaporative cooling is analyzed by the ε—*NTU* (the number of heat transfer unite) method. The suitable number of heat transfer unite for the design of the cross-flow plate heat exchanger for indirect evaporative cooling is put forward under the sensible heat exchange condition of the primary air. The suitable number of heat transfer unite of the primary air passage and the secondary air passage is 0.8-2.5 and 0.5-1.7 respectively in actual design of the cross-flow plate heat exchanger for indirect evaporative cooling.

Keywords: Evaporative cooling, Mathematic model, effectiveness, NTU, Temperature distribution.

1 Introduction

The cross-flow plate heat exchanger for indirect evaporative cooling has the potential for widespread applications in air-conditioning systems for energy recovery. Outdoor air that called primary air in this paper is cooled without adding moisture to it, and the energy of indoor air that called secondary air in this paper is recovered. As the result the energy consumption of air-conditioning system can be reduced. Water is sprayed in the secondary passage of the cross-flow plate heat exchanger of indirect evaporative cooling; The primary air and the secondary air are flowing crossly; The heat of the primary air is transferred to the secondary air passage through the plate, and then the water is evaporated. As the result the humidity ratio and enthalpy of the secondary air

* Xuelai Liu, Man, be born 1965, The Dr. student, Department of thermal engineering Shandong Jianzhu University, The fengming road, Lingang development area, Jinan city, Shandong Province, China Postcode 250101.

are added[1]. The structure of the cross flow plate heat exchanger for indirect evaporative cooling is shown schematically in Fig. 1.

The heat and mass transfer are transferred at the same time in the cross flow plate heat exchanger for indirect evaporative cooling. The heat transfer characteristics of the primary and secondary air are changed that caused by the latent heat of the vaporization of water, so the process of transfer is very complex. In order to do some study of the heat exchanger of evaporative cooling, assumptions should be made respectively. Maclaine-cross and Banks [2] assumed the evaporating water film of the secondary air passage is stationary and continuously replenished at its surface with water at the same time, and assumed the moisture content of the air in equilibrium with the water surface is a linear function of the water surface temperature. These authors have proposed a linear approximate model for wet surface heat exchangers, with which they have proved that the same equation or graphical representations can be used determine the wet surface heat exchanger effectiveness. Stoitchkov and Dimitrov [3] developed a short-cut method for calculating the effectiveness of the wet surface cross-flow plate heat exchangers. It introduces a correction for the effectiveness estimated according to the method of Maclaine-cross and Banks. The correction developed by Stoitchkov and Dimitrov [3], together with the estimation of the mean surface water temperature and consideration of the barometric pressure, gives a reliable and fast procedure for real performance of wet surface heat exchangers by analogy to that of dry surface heat exchangers. This paper will establish the mathematical model of the cross-flow plate heat exchanger for indirect evaporative cooling based on the mathematical model of Stoithkov and Dimitrov [3]. In order obtain the temperature distribution of the primary and secondary air in the flow directions, the mathematical model is resolved according to the finite volume method [4]. The effectiveness of the cross-flow plate heat exchanger for indirect evaporative cooling is analyzed by the ε—*NTU* method.

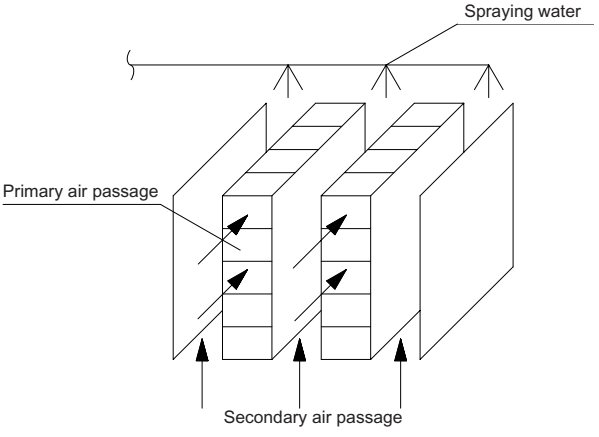

Fig. 1. Structure of the cross-flow plate heat exchanger for evaporative cooling

2 Mathematic Model

At first, make the following assumptions. The model is satisfies the following assumptions:

1) c_p, c_w, c_v, r_0, B and p_w are constant;
2) There is only the sensible heat transfer in the primary air passage, d_1 is constant;
3) The Lewis relation is satisfied.

2.1 The Energy Balance Equation of the Primary Air Passage

When the plate surface temperature inside the primary air is higher than the dew point temperature, there is only the sensible heat flow in the primary air passage. The sensible heat flow:

$$dQ_{s,1} = -k_1(t_1 - t_w)dxdy \tag{1}$$

The total heat balance equation:

$$m_1 \frac{\partial h_1}{\partial x} dxdy = dQ_{s,1} \tag{2}$$

Substituting Equation (1) into (2), we obtain:

$$m_1 \frac{\partial h_1}{\partial x} = k_1(t_w - t_1) \tag{3}$$

Where $h_1 = c_a t_1 + d_1(c_v t_1 + r)$, substituting this equation into (3), we obtain:

$$m_1 \frac{\partial t_1}{\partial x} = \frac{k_1}{c_a + c_v d_1}(t_w - t_1) \tag{4}$$

2.2 The Heat Balance Equation of the Secondary Air Passage

The total heat flow consists of the sensible and latent heat flow:

$$dQ_{s,2} = -\alpha_2(t_2 - t_w)dxdy \tag{5}$$

$$dQ_{L,2} = h_v m_2 \frac{\partial d_2}{\partial y} dxdy \tag{6}$$

The total heat balance equation:

$$m_2 \frac{\partial h_2}{\partial y} dxdy_1 = dQ_{s,2} + dQ_{L,2} \tag{7}$$

Substituting equations (5) and (6) into (7) , we obtain:

$$m_2 \frac{\partial h_2}{\partial y} = \alpha_2(t_w - t_2) + h_v m_2 \frac{\partial d_2}{\partial y} \tag{8}$$

Where $h_2 = c_a t_2 + d_2(c_v t_2 + r)$, $h_v = c_v t_2 + r$. Substituting those equations into (8), we obtain:

$$m_2 \frac{\partial t_2}{\partial y} = \frac{\alpha_2}{c_a + c_v d_2}(t_w - t_2) \tag{9}$$

2.3 The Heat Balance Equation of the Water Film

The sensible heat flow:

$$dQ_{s,w} = k_1(t_1 - t_w)dxdy + \alpha_2(t_2 - t_w)dxdy \tag{10}$$

The latent heat flow:

$$dQ_{L,w} = -h_v m_2 \frac{\partial d_2}{\partial y} dxdy \tag{11}$$

The total heat balance equation:

$$(m_w dx + \frac{\partial m_w}{\partial L_2} y)(h_w + \frac{\partial h_w}{\partial y} dy) - m_w dy h_w = dQ_{s,w} + dQ_{L,w} \tag{12}$$

Substituting equations (10) and (11) into (12), we obtain:

$$m_w \frac{\partial h_w}{\partial y} + h_w \frac{\partial m_w}{\partial y} + \frac{\partial m_w}{\partial y}\frac{\partial h_w}{\partial y} dy = k_1(t_1 - t_w) + \alpha_2(t_2 - t_w) - h_v m_2 \frac{\partial d_2}{\partial y} \tag{13}$$

The decrement of the water film is equal to the increment of the water vapor in the secondary air:

$$\frac{\partial m_w}{\partial y} = -m_2 \frac{\partial d_2}{\partial y} \tag{14}$$

Where $h_w = c_w t_w$, $h_v = c_v t_2 + r$, substituting those equations into (13), we obtain:

$$m_w c_w \frac{\partial t_w}{\partial y} = k_1(t_1 - t_w) + \alpha_2(t_2 - t_w) - m_2(c_v t_2 - c_w t_w + r)\frac{\partial d_2}{\partial y} \tag{15}$$

The total mass flow balance equation:

$$\frac{\partial m_w}{\partial y} dxdy = \sigma_w(C_w - C_2)dxdy \tag{16}$$

According to the Lewis relation: $\sigma_w = \dfrac{\alpha_2}{\rho c_p}$ (17)

C_w is water mass fraction of the saturation wet air near the water film. C_2 is the water mass fraction of the secondary air. According the reference [6]:

$$C_w = \frac{p_w}{RT_w} \tag{18}$$

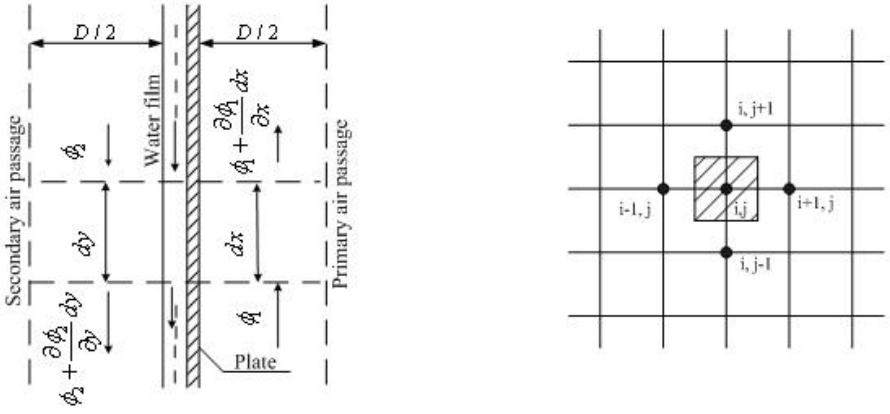

Fig. 2. Structure of mathematical model and the discrete format

$$C_2 = \frac{p_v}{RT_2} \tag{19}$$

p_v and d_2 have the following relation:

$$p_v = \frac{d_2 B}{0.622 + d_2} \approx \frac{d_2 B}{0.622} \tag{20}$$

Substituting equation (17), (18), (19), (20), into (16), we obtain:

$$\frac{\partial m_w}{\partial y} = \frac{\alpha_2}{\rho c_a R}\left(\frac{p_w}{T_w} - \frac{d_2 B}{0.622 T_2}\right) \tag{21}$$

The differential equations (4), (9), (14), (15) and (21) are the mathematic description of the cross-flow plate heat exchanger for indirect evaporative cooling. The structure of the mathematical model and the discrete format are shown in Fig.2. With known geometrical characteristics and the inlet boundary conditions of the cross-flow plate heat exchanger for evaporative cooling, those differential equations can be solved according to the finite volume method[4], the outlet parameters of water film, primary air and secondary air will be obtained.

3 Introduce the Effectiveness ε and the Number of Heat Transfer Unite (*NTU*)

According to the Maclaine-cross and Banks [2], the effectiveness of the cross-flow plate heat exchanger for evaporative cooling is:

$$\varepsilon = \frac{t_{1,i} - t_{1,o}}{t_{1,i} - t'_{2,i}} \tag{22}$$

According to the references [2] and [3], introduce the dimensionless parameter NTU (the number of heat transfer unite). The number of heat transfer unites of the primary air passage is defined as:

$$NTU_1 = \frac{kA}{M_1 c_a} \tag{23}$$

The number of heat transfer unites of the secondary air passage is defined as:

$$NTU_2 = \frac{kA}{M_2 \overline{c_2}} \tag{24}$$

Where $\overline{c_2}$ is the mean wet temperature specific heat capacity of the secondary air[7]:

$$\overline{c_2} = \frac{c_a \overline{t_2} + \overline{d_2}(c_v \overline{t_2} + r_0)}{t'_{2,i}} \tag{25}$$

The overall heat transfer coefficient k is calculated by the following equation:

$$k = \frac{1}{\frac{1}{\alpha_1} + \frac{\delta_w}{\lambda_w} + \frac{\delta_p}{\lambda_p} + \frac{1}{\alpha_2}} \tag{26}$$

The thickness of the water δ_w film is so thinly that the heat resistance of the water film can be neglected, therefore:

$$k = \frac{1}{\frac{1}{\alpha_1} + \frac{\delta_p}{\lambda_p} + \frac{1}{\alpha_2}} \tag{27}$$

The heat transfer coefficient of the primary air passage k_1 is:

$$k_1 = \frac{1}{\frac{1}{\alpha_w} + \frac{\delta_w}{\lambda_w} + \frac{1}{\alpha_1}} \tag{28}$$

As the same, neglected the heat resistance of the water film, therefore:

$$k_1 = \frac{1}{\frac{1}{\alpha_w} + \frac{1}{\alpha_1}} \tag{29}$$

The heat transfer coefficient $\alpha_1=\alpha_2$ for dry heat transfer are calculated with the following equation given by Stoithkov [3]:

$$\alpha = 36.31(\rho V)^{0.68}(\frac{L}{D_e})^{-0.08} \tag{30}$$

The heat transfer coefficient α_w is calculated with the following equation [6]:

$$\alpha = 0.644\frac{\lambda}{(L\nu)^{1/2}}V^{1/2}\,\mathrm{Pr}^{1/3} \tag{31}$$

4 Efficiency Analyses

Adopted different inlet parameters of the primary and secondary air and different number of heat transfer unite, then solved the mathematical model above according to finite volume method. The effectiveness distribution following the NTU_1 and NTU_2 is obtained as shown in the Fig.3. We can see from the Fig.3 that the effectiveness of the cross-flow plate heat exchanger of indirect evaporative cooling is increased as the numbers of heat transfer unite of the primary and secondary air, but the range of increasing is decreased gradually. When the NTU_1 is higher than 4 and the NTU_2 is higher than 2.5, the curve of effectiveness is nearly a straight line. Therefore adopt the number of heat transfer unite very greatly (that is adopt the heat plate size greatly) is unmeaning for advance the effectiveness of the cross-flow heat exchanger for evaporative cooling in physically design. Therefore the suitable number of heat transfer unite of the primary air passage and the secondary air passage is 0.8-2.5 and 0.5-1.7 respectively in physically design of the cross-flow plate heat exchanger for indirect evaporative cooling.

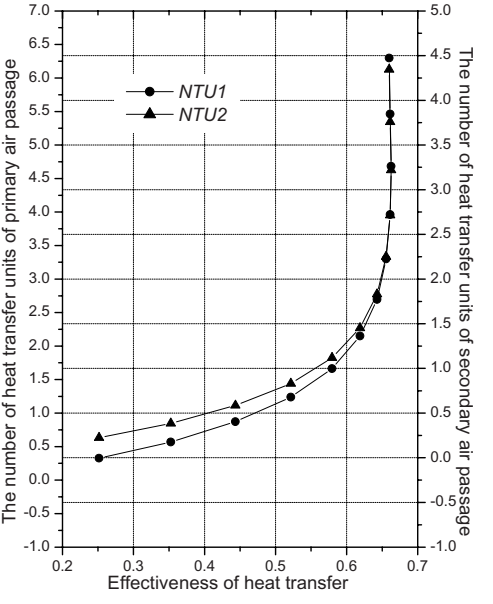

Fig. 3. Effectiveness distribution

5 The Temperature Distribution of the Primary and Secondary Air

The temperature distribution of the primary air in the flow direction is shown in Fig. 4. The inlet state of the curve 1 in the Fig.4 is: $t_{1.i}$=32℃, $d_{1.i}$=24.3g/(Kg·dry-air),$t_{1.d}$=25.8℃;

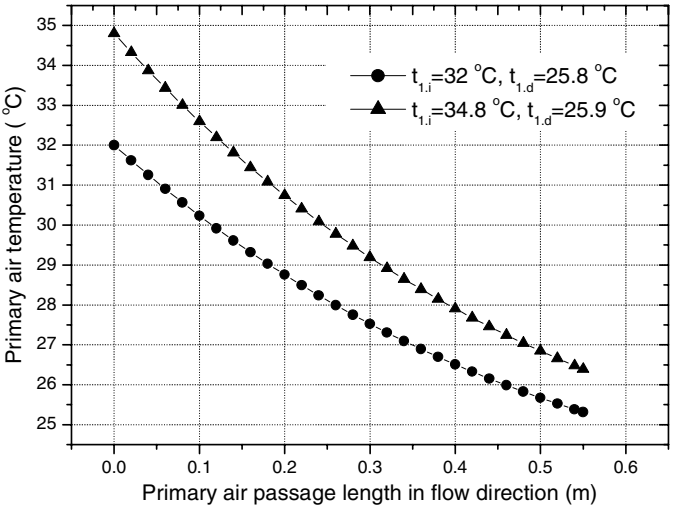

Fig. 4. Temperature distribution of primary air

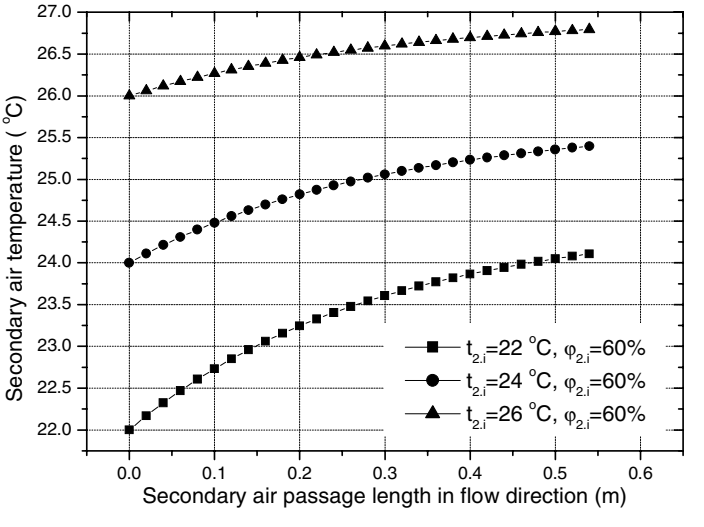

Fig. 5. Temperature distribution of secondary air

the inlet state of the curve 2 is: $t_{1.i}$=34.8℃, $d_{1.i}$=21.1g/(Kg·dry-air),$t_{1.d}$=25.9℃. Under the first inlet state, the outlet temperature of the primary air is lower than dew point temperature of inlet. That is meant that water is condensed from the primary air stream. The mathematical model in this paper isn't suitable for the condensation condition.

The condensation condition needs a further research. Fig.5 shows the temperature distribution of the secondary air in the flow direction. The inlet state of the curve 1 in the Fig.5 is: $t_{2.i}$=22℃, $\varphi_{2.i}$=60%; the inlet state of the curve 2 is: $t_{2.i}$=24℃, $\varphi_{2.i}$=60%; the inlet state of the curve 3 is: $t_{2.i}$=26℃, $\varphi_{2.i}$=60%. The temperature distribution curve of the secondary air is nearly a horizontal line. The temperature difference of inlet and outlet is no more than 2.2℃, through the calculation to various difference inlet and outlet states. Therefore the processing process of the secondary air can be seemed as isothermal humidification in the physical design of the cross-flow plate heat exchanger for indirect evaporative cooling.

6 Conclusions

This paper established the mathematical model of the cross-flow plate heat exchanger for indirect evaporative cooling. The mathematic model is solved according to the finite volume method. Through the numerical solution of the mathematic model, the temperature distribution of the primary air and the secondary air in the flow directions are obtained. The efficiency of cross-flow plate heat exchanger for indirect evaporative cooling is analyzed by the ε—*NTU* (the number of heat transfer unite) method. The number of heat transfer unite very greatly (that is adopt the heat plate size greatly) is unmeaning for advance the effectiveness of the cross-flow heat exchanger for evaporative cooling in physically design. The suitable number of heat transfer unite of the primary air passage and the secondary air passage is 0.8-2.5 and 0.5-1.7 respectively in physically design of the cross-flow plate heat exchanger for indirect evaporative cooling under the dry cooling condition of the primary air.

At last, when the humidity ratio of the primary air is higher too much, water may be condensed from the primary air stream. The mathematical model in this paper is established under the dry cooling condition. When water is condensed from the primary air stream, the efficiency of cross-flow plate heat exchanger for indirect evaporative cooling should be analyzed further more.

Acknowledgement

This research is supported by Ministry of Construction science and technology developing project(No.2008-K1-29) and cooperation-project of Hong Kong and Mainland of China(No.2005HK-CN-01).

Nomenclature

A	heat transfer surface area (m^2)	d	dew point
B	atmospheric pressure (Pa)	i	inlet of passage
C	water mass fraction	o	outlet of passage
c	specific heat capacity (kJ Kg^{-1} K^{-1})	w	water
D	distance between two plates(m)	s	sensible
D_e	equivalent diameter (m)		
d	humidity ratio (Kg Kg^{-1} dry-air)	Greeks	
h	specific enthalpy of primary air (kJ Kg^{-1})	α	heat transfer coefficient (W m^{-2} K^{-1})
L	passage length in flow direction (m)	λ	effectiveness of heat transfer
k	heat transfer coefficient (W m^2 K^{-1})	σ	thermal conductivity(W m^{-1} K^{-1})
M	mass flow rate (Kg s^{-1})	φ	mass transfer coefficient(Kg m^{-2} s^{-1})
m	mass flow rate in flow direction (m=M/L Kg s^{-1} m^{-1})	ρ	relative humidity
		δ	density(Kg m^{-3})
p	pressure (Pa)	ν	thickness(m)
r	correlation coefficient; latent heat of vaporization of water (kJ Kg^{-1})	ϕ	kinematic viscosity(m^2 s^{-1})
T	temperature (K)		current variable
t	temperature (℃)		
t′	wet bulb temperature(℃)		
Subscripts			
1	primary air	a	dry air
2	secondary air		

References

[1] Rey, M.F.J., Velasco Gómez, E.: Comparative study of two different evaporative systems: an indirect evaporative cooler and a semi-indirect ceramic evaporative cooler. Energy and Buildings 36, 696–708 (2004)

[2] Maclaine-cross, I.L., Banks, P.J.: A general theory of heat exchanger and its application to regenerative evaporative cooling. Journal of Heat Transfer 103(8), 579–585 (1981)

[3] Stoithkov, N.J., Dimitrov, G.I.: Effectiveness of cross-flow plate heat exchanger for indirect evaporative cooling. Int. J. Refrig. 21(6), 463–471 (1998)

[4] Xiaoqing, Z., Peilin, C.: Thermal analyse is of the in direct evaporative cooler. HV&AC 30(1), 39–42 (2000)

[5] Pescod, D.: A heat exchanger for energy saving in an air-conditioning plant. ASHRAE Transactions 85(2), 238–251 (1998)

[6] Rohusenow, W.M.: Handbook of heat transfer applications. Science Technique Publisher, Qi xin (1992)

[7] Wenxuan, T.: Numerical of heat transfer. Xi'an Jiaotong University Press, Xi'an (2001)

Thermal Work Condition Analysis of Teaching Building Heating Network in Winter Vacation with User Regulation

Shuang Li*, Hua Zhao, and Jianing Zhao

School of Municipal and Environmental Engineering, Harbin Institute of Technology, Harbin, China
lishuang1006@126.com

Abstract. Indoor temperature of teaching building should be reduced properly in winter vacation in order to save heating energy consumption as much as possible, and acceptable indoor temperature should keep pipe network of teaching building from frozen and wall surface of teaching building isn't damaged because of dew. This paper concentrates on heating network of teaching building in extremely cold areas of China with user regulation, and analyzes thermal work condition of teaching building heating network with lower indoor temperature. The two schemes, supply water mixed with return water by mixing pump to reduce supply water temperature and flow reduction of teaching building, are applied to reduce indoor temperature. The supply water of heating network changes with outdoor temperature based on constant flow control and centralized control with flow varied by steps. Supply and return water temperature and flow of teaching building in four work condition with lower indoor temperature was calculated respectively. The calculated result shows that relative flow of building in scheme 1 keeps constant and is less than 0.35 in scheme 2. The conclusion is that scheme 1 of mixed with return water is better than scheme 2 of building's flow reduction, and centralized control with flow varied by steps on supply water of heating network is better than constant flow control in winter vacation.

Keywords: Teaching building heating network, thermal work condition, user regulation.

1 Introduction

According to fundamental realities of Chinese heating, greater heating scale, dense urban building, so much indirect-connected heating network, one substation(heating scale 5×10^4~$40\times10^4 m^2$) [1] usually supply heat quantity for several buildings which was regulated uniformly in substation, so several buildings have the same supply water temperature. In the countries of northern Europe, heating system is advanced variable flow system, and auto-control equipments were installed in system, such as

* Corresponding author.

dynamic balanced valves(flow control valve and self-operated pressure control valve), frequency pumps[2], and so on, so hydraulic and thermal balance can be realized easily in heating network with user regulation. In China, Central heating is widely used in cold area and heating system has more branches. It's usually install mixing pump which is used to draw off return water mixed with supply water to reduce supply water temperature or flow reduction in building inlet when single building's load is reduced because of special demand [3]. Single building was seen as one user, and supply water of heating network was regulated in building inlet, and then entered user. To research thermal work condition of teaching building which has lower indoor temperature in winter vacation with building inlet regulation, this paper analyze regularity of supply and return water temperature and flow of teaching building in winter vacation.

In China, according to design standard, heating design indoor temperature of classroom is 18℃[4], and there is nobody in classroom during winter vacation(5-6 weeks), at this time, indoor temperature of classroom should be reduced as much as possible, and acceptable indoor temperature should keep pipe network of teaching building from frozen and wall surface of teaching building avoid dew. Firstly, Indoor temperature should be above 5℃ for avoiding frozen network pipe, secondly, indoor temperature must be above dew temperature to avoid dew in inside of external wall which reduced building life. It is rather dry in winter in north China with dew-point temperature below 2℃, so inside temperature of external wall is more than 2℃, thirdly, the permissible temperature difference between indoor air and room inner surface is 6℃ [5], finally, it can be obtained that indoor temperature is 8℃ without persons in the classroom based on above views.

2 Method

For research goal of this paper, theoretical calculation is the most suitable method. Calculation results can be obtained easily and it costs short time.

2.1 Physical Model

In winter vacation, supply water from outdoor heating network is regulated at building inlet. The two schemes are as follows:

Scheme 1: Mixing pump is installed in building inlet, which is used to draw off return water, and mixed with supply water, so the supply water temperature of user can be reduced, and user's flow keep constant.

Scheme 2: The user's supply water temperature keeps constant and the user's flow is reduced, so the return water temperature decreases, and indoor temperature is decreased.

2.2 Mathematic Model

Here is the mathematic model used to calculate supply and return water temperature and flow of user. Neglecting heat loss of pipe network, heating load of pipe network

is equal to heat dissipating capacity of user's radiator, and also equal to heating load of user's when heating network run steadily, so the ratio of actual value and design value in three is also equal, shown in equation (1). For scheme 1, flow of teaching building keeps constant all the time. Heat medium average temperature can be calculated by formula (3) at indoor temperature t_n=8℃. Supply and return water temperature difference at indoor temperature t_n=8℃ can be obtained from formula (4), and finally, supply and return water temperature at indoor temperature t_n=8℃ can be got from formula (5) and (6). The mixed water ratio can be calculated based on heat balance of mixed water point. For scheme 2, supply water temperature keeps constant, and user's flow was reduced, so system flow is variable. The larger calculated error is produced with formula (2), and heat dissipating capacity of radiator should be calculated with log mean temperature difference [6]. The supply and return water temperature and relative flow can be got with formula (7) at indoor temperature t_n=8℃. The regularity of supply /return water temperature and relative flow can be got with the different outdoor temperature, and it can be found in the following Figures.

$$Q_r = \frac{q_1}{Q_1} = \frac{q_2}{Q_2} = \frac{q_3}{Q_3} \tag{1}$$

$$\mathrm{Q_r} = \frac{\mathrm{t}_n - t_w}{T_n - T_w} = \left(\frac{t_{pj} - t_n}{T_{pj} - T_n} \right)^{1+b} = G_r \cdot \frac{t_g - t_h}{T_g - T_h} \tag{2}$$

$$t_{pj} = t_n + 0.5 \times (T_g + T_h - 2 \times T_n) \times Q_r^{\frac{1}{1+b}} = 0.5 \times (t_g + t_h) \tag{3}$$

$$\Delta t = Q_r \cdot (t_g^{'} - t_h^{'}) \tag{4}$$

$$t_g = t_{pj} + 0.5 \cdot \Delta t \tag{5}$$

$$t_h = t_{pj} - 0.5 \cdot \Delta t \tag{6}$$

$$Q_r = \frac{t_n - t_w}{T_n - T_w} = \left(\frac{\dfrac{t_g - t_h}{\lg \dfrac{t_g - t_n}{t_h - t_n}}}{\dfrac{T_g - T_h}{\lg \dfrac{T_g - T_n}{T_h - T_n}}} \right)^{1+b} = G_r \cdot \frac{t_g - t_h}{T_g - T_h} \tag{7}$$

Where

T_w, T_n design outdoor and indoor temperature,℃;

T_g, T_h design supply and return water temperature,℃;

Q_r, G_r relative heating load and relative flow; constant flow control G_r=1; centralized control with flow varied by steps t_w=-26~-17℃, G_r=1; t_w=-17~-8℃, G_r=0.8; t_w=-8~5℃, G_r=0.6;

b index of radiator heat transmission coefficient;
t_{pj} heat medium average temperature of radiator, ℃;
△t supply and return water temperature difference at indoor temperature tn=8℃;
Q_1, q_1 building design heating load and actual heating load on a certain outdoor temperature, W;
Q_2, q_2 heat dissipating capacity of radiator on outdoor calculated temperature and actual heat dissipating capacity of radiator on a certain outdoor temperature, W;
Q_3, q_3 heat quantity delivered by heating network to users on outdoor calculated temperature and actual heat quantity delivered by heating network to users on a certain outdoor temperature, W;

2.3 Operation Schemes

Supply water of heating network changes with outdoor temperature can be shown in Table 1.

Table 1. Regulation method of heating network

Scheme 1	Scheme 2
Constant flow control Centralized control with flow varied by steps	Constant flow control Centralized control with flow varied by steps

2.4 Selection of Heating Parameters

This paper takes Harbin in extremely cold areas of China for instance, and Harbin is located on east longitude 126°38' and northern latitude 45°. Outdoor calculated temperature is lower in Harbin, so it can widely represent urban areas in cold area of China. Heating outdoor calculated temperature of Harbin is T_w=-26℃; Design indoor temperature of teaching building is T_n=18℃; Heating outdoor temperature range is -26~5℃; Design supply and return water temperature of indoor heating system is T_g=95℃, T_h=70℃; Radiator M132 is selected, and index of radiator heat transmission coefficient is b=0.3[4]. The supply and return water temperature can be got with the known relative flow G_r and indoor temperature t_n. From the formula (1.2), stage points of outdoor temperature t_w are -17℃ and -8℃ when relative heating load Q_r is 0.8 and 0.6 respectively.

3 Results Analysis

Supply and return water temperature and relative flow of teaching building is analyzed during normal use and in winter vacation with different schemes and different regulation methods of heating network.

3.1 Thermal Work Condition Analysis of Teaching Building in during Normal Use

As shown in Fig. 1 and Fig. 2, supply and return water temperature and relative flow of teaching building during normal use can be obtained which change with outdoor temperature based on constant flow control and centralized control with flow varied by steps.

During normal use, supply water temperature of heating network regulated by centralized control with flow varied by steps is better than constant flow control, and centralized control with flow varied by steps make supply and return water temperature difference increased, so radiator of indoor can be controlled very well.

3.2 Thermal Work Condition Analysis of Teaching Building in Winter Vacation

Indoor temperature of teaching building is reduced in winter vacation without persons in, so heating load is also lower. The two schemes, mixed with return water and flow reduction, are applied to reduced indoor temperature, at the same time, the thermal work condition of two schemes are analyzed.

3.2.1 Thermal Work Condition Analysis of Scheme 1

When winter vacation come, indoor temperature is reduced to t_n=8℃ in order to save heating energy consumption. The supply water temperature of teaching building is reduced by mixed with return water with mixing pump, and the flow of teaching building keeps constant. The supply water temperature is reduced and heat medium average temperature of radiator is also lower, therefore, indoor temperature is reduced.

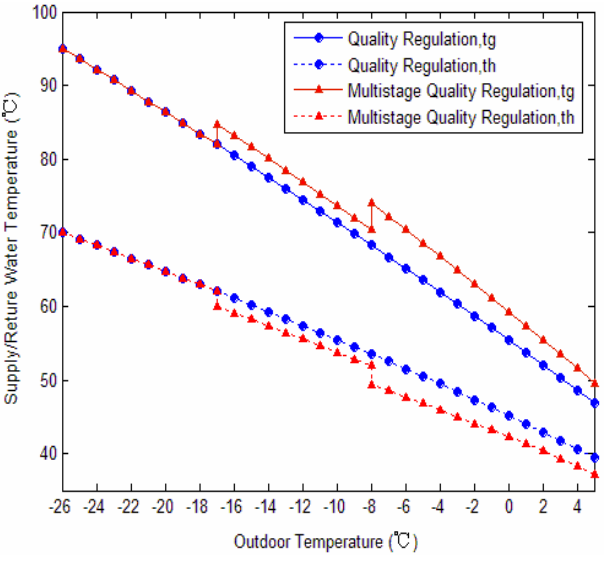

Fig. 1. Regulated curve of teaching building during normal use

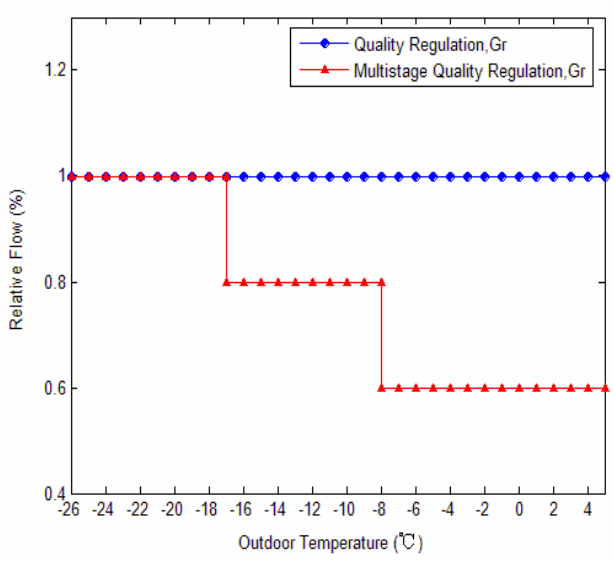

Fig. 2. Relative flow of teaching building during normal use

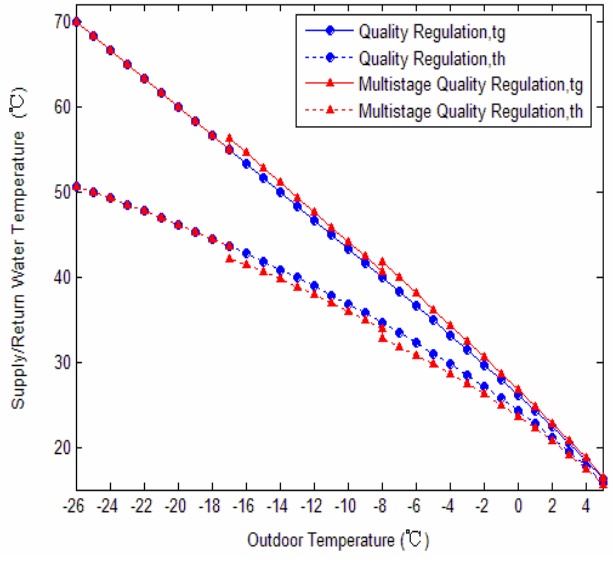

Fig. 3. Regulated curve of teaching building in winter vacation with scheme 1

From Fig. 3 and Fig. 4, supply water of heating network is regulated with constant flow control and centralized control with flow varied by steps. Maximal supply and return water temperature difference is 20℃, and flow of teaching building keeps unchanged, but mixed water ratio is increased when outdoor temperature rises. Centralized control with flow varied by steps has larger supply and return water temperature difference and a smaller mixed water ratio compared with constant flow control,

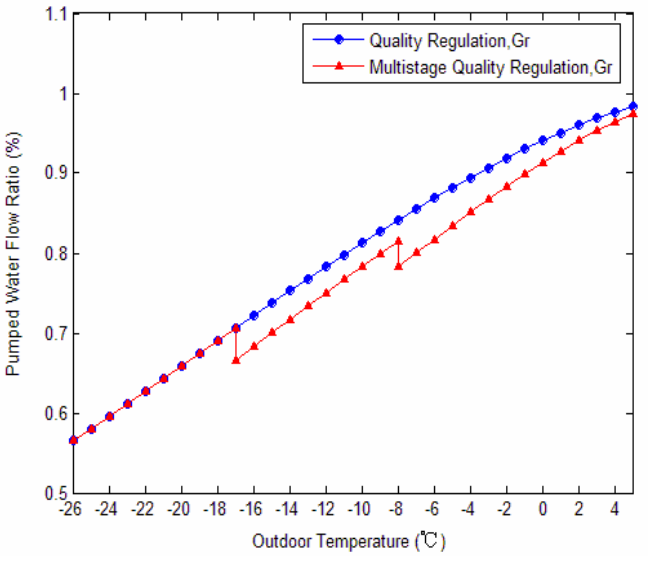

Fig. 4. Return water ratio of teaching building in winter vacation with scheme 1

so centralized control with flow varied by steps can save more mixing pump consumption in winter vacation. The trend of supply and return water temperature in winter vacation is the same to the one during normal use, but supply and return water temperature change with outdoor temperature quickly in winter vacation.

3.2.2 Thermal Work Condition Analysis of Scheme 2

Supply water temperature of heating network keeps unchanged, and the flow of teaching building is reduced to get lower indoor temperature when winter vacation come. As shown in Fig. 5 and Fig. 6, compared with constant flow control, centralized control with flow varied by steps has larger supply and return water temperature difference and smaller relative flow, and it produced the same return water temperature with the two regulation methods. In winter vacation, supply water temperature keeps constant, and return water temperature is reduced greatly. The maximal supply and return water temperature difference is 56℃ and relative flow is Gr<0.35. For vertical single pipe indoor heating system widely used in China, the larger supply and return water temperature difference is, the more easily vertical hydraulic misadjustment is produced, so the indoor temperature of user in low story will reduce, and requirement of user can not be satisfied.

Thus, to sum up the points, user's flow is constant in Scheme 1, and is variable in Scheme 2. For scheme 1, additional mixing pump which is used to draw off return water and mixed with supply water is installed in teaching building inlet. The mixed ratio is more than 0.7, and so the main circulating pump energy can be reduced largely.

For scheme 2, flow of teaching building is reduced on building inlet easily by turning down regulated valve. Relative flow is less than 0.35 when indoor temperature

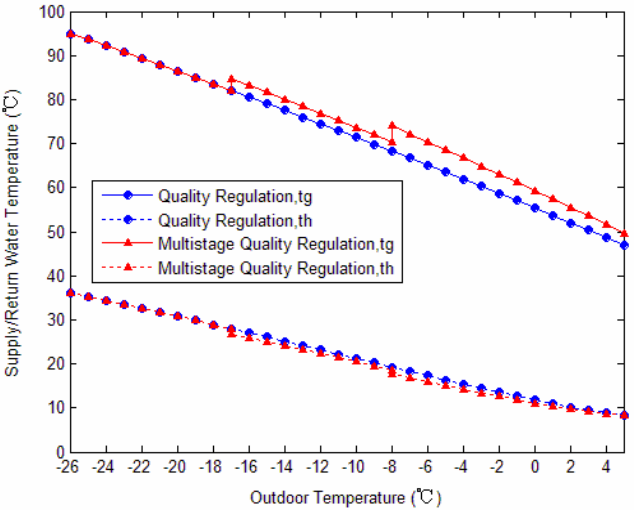

Fig. 5. Regulated curve of teaching building in winter vacation with scheme 2

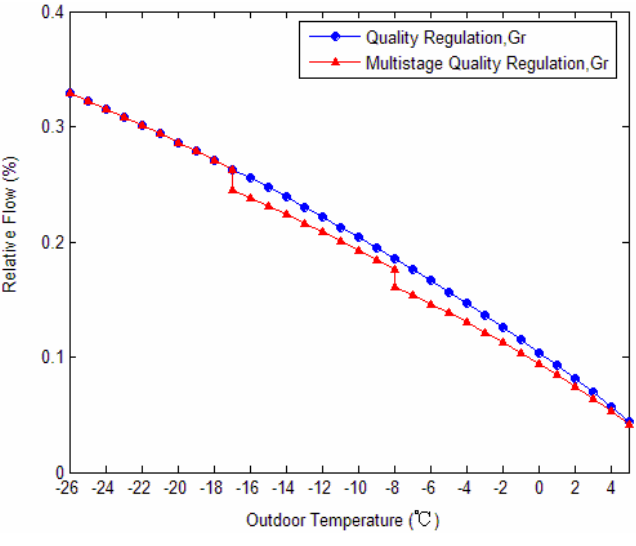

Fig. 6. Relative flow of teaching building in winter vacation with scheme 2

is 8℃. Though technology feasibility and operational guidance in scheme 2 is better than ones in scheme 1, scheme 1 is better than scheme 2 on the point of "larger flux and smaller temperature difference" in interior of the building. For scheme 2, it will produced larger hydraulic misadjustment in indoor heating system, therefore, scheme 1 of mixed with return water can keep better hydraulic balance by installing an additional mixing pump used to draw off return water mixed with supply water.

4 Conclusion

Indoor temperature of teaching building is set 8℃ without persons in when winter vacation came, which can keep pipe network of teaching building from damage and avoid dewing. The two schemes are proposed, mixed with return water and reduced flow. The conclusion can be obtained by theoretical analysis, and centralized control with flow varied by steps on supply water of heating network is better than constant flow control during normal use or in winter vacation, and mixed with return water by mixing pump in scheme 1 is better than reduced flow in scheme 2 in winter vacation.

Acknowledgments. This work was supported by the Ministry of Construction of China for the 11th Five-Year Projects on "Key Technologies Research and Demonstration of Building Energy Conservation". (Serial Number: 2006BAJ01A04).

References

1. Sheng, X.: Optimal Heating Scale Determination in Cold Area. Low Temperature Architecture Technology 4, 77–78 (2003)
2. Petitjean, R.: Balancing of Control Loops. Tour & Andersson Hydronics AB, Sweden (1999)
3. He, P., Sun, G.: Heating Engineering. China Building Industry Press (1993)
4. Code for Design of Heating Ventilation and Air Conditioning China. GB50019-2003. 10-13
5. Lu, Y.: Design Handbook Heating and Air Conditioning China, pp. 48–49 (2005)
6. Tu, G.: Technology of heat metering. China Building Industry Press (1993)

Integrated Building Management Systems for Sustainable Technologies: Design Aspiration and Operational Shortcoming

Abbas Elmualim

ICRC, The School of Construction Management and Engineering,
The University of Reading, UK
a.a.elmualim@rdg.ac.uk

Abstract. There is an increasing adoption of innovative sustainable design measures such as the application of hybrid natural and air-conditioning ventilation technologies. Such innovative systems are controlled via Integrated Building Management Systems (IBMS) whether stand alone or integrated with Computer-aided Facilities Management (CAFM). Post-occupancy evaluation study was conducted to evaluate the utility of such IBMS in realising the design benefits of hybrid natural ventilation and air-conditioning system. Indoor air quality parameters (temperature, humidity and CO_2) and external wind conditions, temperature, humidity and solar radiation were monitored for the investigated building. The monitored results of the summer and winter months operations the building employing hybrid natural ventilation and air-conditioning systems showed that the indoor air quality parameters were kept within the design target range. It was found that system and software engineers for the building services control systems were consulted to devise the systems after the completion of the building which contributed to the failure of the control strategy of the IBMS devised at the design stage. The investigation of this building provided indispensable knowledge and information to be incorporated into the maintenance and operation of building as well as the early design stage of new projects. The study calls for the involvement of FM professionals in the early design stage of projects in order to maximise the opportunities offered by innovative sustainable technologies in mitigating and adapting to the pressures of climate change.

Keywors: IBMS, hybrid ventilations, controls, facilities management, system engineers.

1 Introduction

Designing for comfortable internal conditions in buildings is a necessary goal for occupants' good health, well-being and high productivity. The application of passive design principles can help to achieve this goal with less energy consumption and at no extra cost to the building. Such passive design principles include the employment of

wind catchers for natural ventilation in buildings. Predictive design tools are commonly used during the early design stage for sizing of systems. These prediction tools, such as thermal models and CFD, are based on steady state conditions and cannot accurately establish the performance of ventilation components in building, particularly when the external and internal conditions are transient and occupants' pattern and activities are changing [1]. It is critically important to gauge building occupants' feed back through post occupancy evaluation studies. Such studies are, rarely taken in the building industry in the UK for cost reason. Government's initiative such as the Building Regulations future performance certification of buildings, air pressurisation and thermo-graphic testing promote such studies to develop energy performance indicators for new and existing buildings [2].

The wind catcher/tower system is a passive ventilation system which not only extracts air using passive stack principles but also utilises the concept of a wind tower to supply air to the spaces as well. Traditionally, wind catchers were employed in buildings in the Middle East for many centuries and they are known by different names in different parts of the region. They were constructed, traditionally, from wood-reinforced masonry with openings at height above the building roof ranging from 2 m to 20 m. With taller towers capturing winds at higher speeds and with less dust [3]. Their application in the hot arid region of the Middle East is to provide for natural ventilation/passive cooling and hence thermal comfort. Wind catchers are traditionally used in places of high urban densities where surrounding buildings obstruct free stream air flow. Traditional wind catchers can be beautiful objects, feasible architectural feature additions to buildings and are inherently durable [4, 5].

In modern design of wind catchers, the two ventilation principles of wind tower and passive stack are combined in one design around a stack that is divided into two halves or four quadrants with the division running the full length of the stack. As the wind direction changes so do the functions of each of the halves or the quadrants in the wind catcher. This renders the wind catcher as being operational whichever way the wind is blowing. As there are no free parts to the wind catchers, their maintenance is very small. It has the benefit of taking supply air at roof level, which is often cleaner than air supplied at ground level, particularly where the building is adjacent to a road in urban areas [5].

Post-occupancy performance evaluation of indoor environment in buildings where innovative technologies such as wind catchers are installed will assist in validating the systems and test their applicability in buildings for natural ventilation. The subjective assessment of occupants' satisfaction with indoor air quality and their ability to control the operation of wind catcher, hence controlling their environment, is an important criteria in validating the application of the hybrid air-conditioning and wind catchers. Furthermore, such studies will enable the understanding of the success/failures in the design and operation for such systems. This further will provide vital information and knowledge for designer and facilities managers. In this paper, sample quantative results of post-occupancy evaluation studies was carried at the Bluewater Shopping Malls, Kent to ascertain the functionality of the IBMS for the control of an integrative air-conditioning and natural ventilation system.

2 Description of the Building

Bluewater Shopping Malls in Kent are newly constructed, out off town, shopping malls. The buildings incorporate wind catchers to ventilate the malls. The wind catcher cowl is inspired by the old form of a Kent oats houses as seen in Figure 1. These forms of oats houses were widely used in the area and became an architectural feature in modern buildings around Kent. The building is an innovative application for wind catchers in the UK and provides the opportunity for validating the application of wind catchers in a temperate climate, such as the UK. The building is managed via an Integrated Building Management System. The wind catchers are automatically controlled in conjunction with mechanical ventilation system.

The Bluewater building consists of three rectilinear form shopping malls with other reception halls and ancinary services (Figure 2). The three malls are forming a

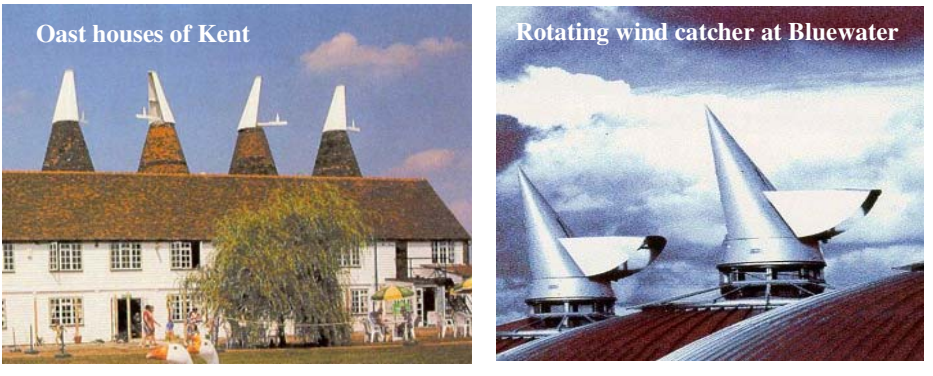

Fig. 1. Traditional and modern rotating wind catcher at Bluewater shopping malls, Kent

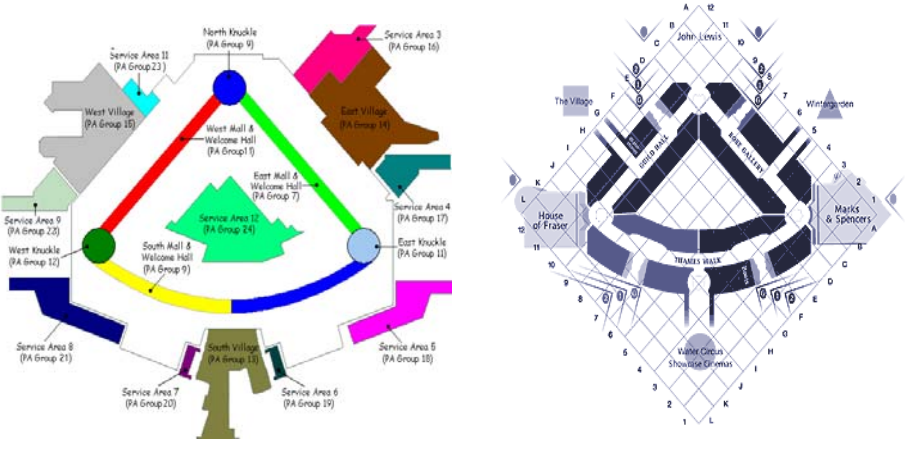

Fig. 2. Plans of the shopping malls at Bluewater, Kent

triangular shape with south, west and east facing malls and service courtyard in between. Shops were distributed around the three mall streets over two floors. The malls were ventilated using a mixed mode of natural ventilation applying wind catchers and air-conditioning system using the air handling units located on the roof of the buildings. There are 39 rotating wind catcher units distributed along the malls (13 units in each mall street). The performance investigation is carried out by taking the centre of each mall as a monitoring point. Indoor air quality parameters such as temperature, humidity and CO_2 level were controlled by the AHU units.

3 Results and Discussions

The Integrated Building Management System (IBMS) provided the interface for operating all building equipment and their operations. The system is mainly used to check on the operation of the equipment. Alarms were sent to the IBMS console about any failure and malfunctioning of the equipment such as the air handling units and wind catchers. The IBMS log external weather conditions parameters, AHU status and operation data and internal air quality parameters at an interval of 15 minutes. The IBMS system has been operational for more than three years.

The recorded data is saved into MS Access software. The database is then interrogated via a program in MS Excel developed using MS Visual Basic programming tool. The Excel program provide the data required for any week in the year. The saved database for the year 2001 was interrogated and analysed to investigate the operation of the ventilation system and establish the performance of wind catchers at one central point in each malls street (south, west and east malls). Particularly, their contribution to the indoor air environment and energy savings achieved if any. For investigating the summer operation the database was interrogated for different weeks in the summer period. Figure 3 gives the results for one week in August in the south mall street. The indoor air quality monitors were kept within the design target providing acceptable indoor air environments for the shoppers. The CO_2 never exceeded 1000 ppm, which is an acceptable level according to ASHRAE recommendations [6].

To investigate the co-ordinated operation of the wind catchers with the AHU, fan pressures were plotted across the external wind speed, external temperature and humidity. The results show that the fan pressure was at its highest, approximately 130 Pa, while the recorded external wind speed at its peak with a recorded maximum measurement of 3.7 m/s (Figure 4). It was well established by observation that all the wind catchers units were facing the prevailing wind direction. The results show that in all the malls the fans were at their highest operations at the same time the external wind speed was in the range of 1-3 m/s for the full wind catchers' operation, hence not reducing fan pressure by operation of the wind catchers. This was due to the lack of co-ordination between wind catchers and the AU which is not considered in the IBMS system. This control system failure greatly emphasises the need for the inclusion of facilities managers, software and system engineers at the early stage of the design of the project, i.e. at day one in the inception of the project.

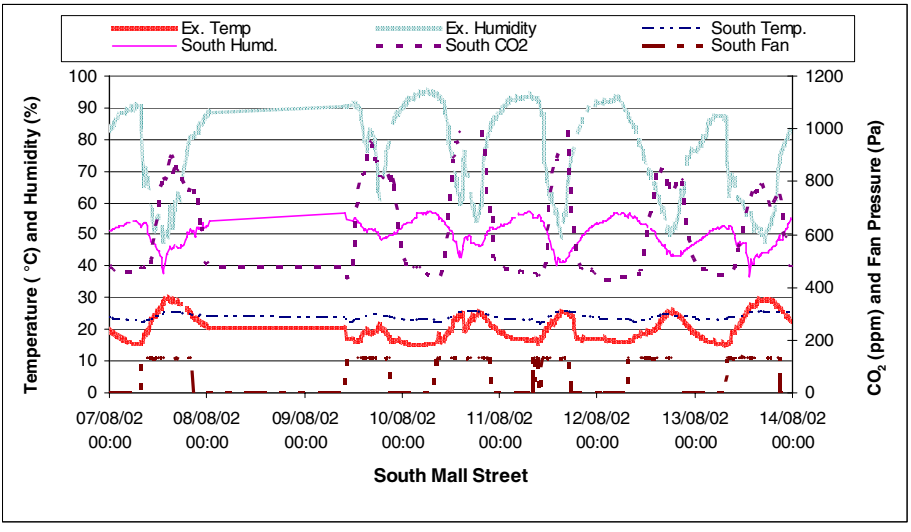

Fig. 3. Measured indoor air quality parameters and fan pressure in the centre of the south mall street

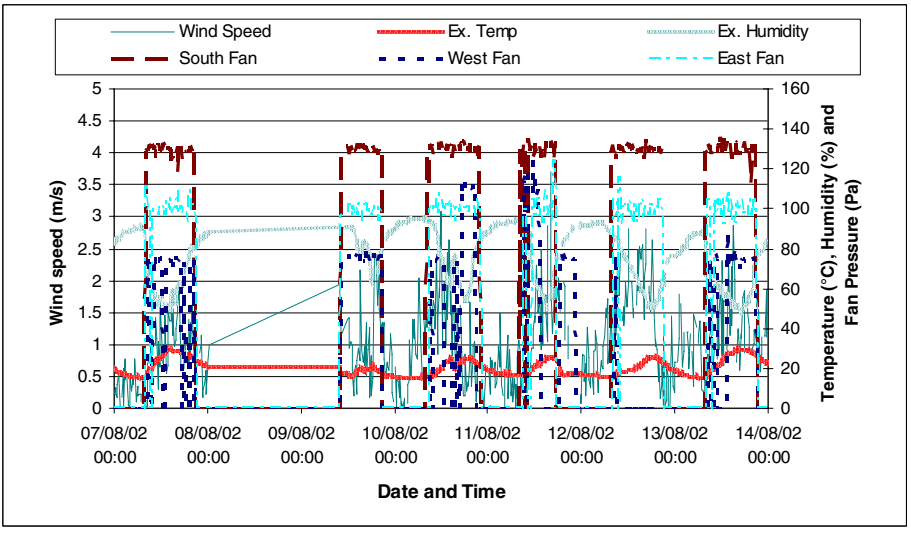

Fig. 4. Plotted external wind speed against fan pressure and external temperature and humidity

4 Conclusions

There is increasing application innovative sustainable design technologies. These technologies are manged via an integrated building management system (IBMS) or via computer aided facilities management (CAFM). A case study was carried out to

investigate the application of IBMS to control a hybrid air-conditioning and natural ventilation systems. The case study was at Bluewater Shopping Malls in Kent. Monitoring of indoor environment in real weather conditions was conducted to evaluate the indoor air quality within the buildings to ascertain the functionality of the IBMS.

The Bluewater Shopping Malls in Kent provided an innovative application of a wind catchers integrated with the mechanical ventilation system (hybrid). The integrated system is controlled via the Integrated Building Management System (IBMS) which recorded all external and internal parameters into a computer database. The summer month operation showed that the indoor air quality parameters were kept within the design target range. It showed that the fans came into operation whenever the CO_2 level was reaching a set-point of 1000 ppm. The operation of the fan increased the ventilation rate and hence reduced the CO_2 concentration to the recommended value. While the wind catchers were operational, no data was recorded regarding their operation, opening time and position. Though the control strategy implemented was working effectively in monitoring the operation of mechanical ventilation systems, i.e. AHU, it did not cover the integration of the natural ventilation system, i.e. wind catchers, with the mechanical ventilation. Controlling the operation of the wind catchers via the AHU led to isolation of these systems in the event of malfunctioning of the AHU, hence the wind catchers will remain shut. Due to the shortcoming of the control strategy implemented in this project, it was found difficult to quantify and verify the contribution of the natural ventilation systems (wind catchers) to the internal conditions and, hence, energy savings. uch studies will enable emerging concept of learning from use, which facilitate much needed integrative approach for building design and operation. Particularly, integration of FM and software and system engineers at early stage of the design processes.

Looking beyond the figures, post-occupancy evaluation studies provide an ideal tool for processes improvements and understanding of behavioural changes through the various stages of the construction cycle of a project. The studies will provide indispensable knowledge and information to be incorporated into new project and thus achieving the goal of client/user centred integrative design and service delivery.

References

[1] Croome, D.J., et al.: Evaluation of Thermal Comfort and Indoor Air Quality in Offices. Building Research and Information 20(4), 211–225 (1992)
[2] Bordass, B., et al.: Forum Walking the Tightrope: the Probe team's response to BRI commentaries. Building Research and Information 30(1), 62–72 (2002)
[3] Bahadori, M.N.: Viability of Wind Towers in Achieving Summer Comfort in the Hot Arid Regions of the Middle-East. Renewable Energy 5(5-8), 879–892 (1994)
[4] Gage, S.A., Graham, J.M.R.: Static Split Duct Roof Ventilation. Building Research and Information 28(4), 234–244 (2000)
[5] Elmualim, A.A.: Modelling of a Windcatcher for Natural Ventilation. In: Sayigh, A.A.M. (ed.) World Renewable Energy Congress VIII (WREC 2004), Denver, Colorado, USA, National Renewable Energy Laboratory, 29 August–3 September (2004)
[6] ASHRAE. ASHRAE STANDARD: Ventilation for Acceptable Indoor Air Quality. ASHRAE 62-1999. The American Society of Heating, Refrigerating, and Air-Conditioning Engineers, Inc., Atlanta, Georgia, USA (1999)
[7] Lead Technology, SPSS for Windows, 11. Lead Technology(2000), http://www.spss.com

Smart Use of Knowledge: A Case Study of Constructing Decisional DNA on Renewable Energy

Cesar Sanin[1], Edward Szczerbicki[1], and Paul Cayfordhowell[2]

[1] School of Mechanical Engineering
The University of Newcastle, Faculty of Engineering and Built Environment
{Cesar.Sanin,Edward.Szczerbicki}@newscastle.edu.au
[2] School of Software Engineering
University Drive, Callaghan, NSW 2308

Abstract. Knowledge engineering techniques are becoming useful and popular components of hybrid integrated systems used to solve complicated practical problems in different fields. Knowledge engineering techniques offer the following features: learning from experience; handling noisy and incomplete data; dealing with non-linear problems; and predicting. This paper presents a knowledge engineering case study by constructing a chromosome of Energy Decisional DNA. Decisional DNA, as a knowledge representation structure, offers great possibilities on gathering explicit knowledge of formal decision events as well as a tool for decision making processes. In this case study, several Sets of Experience of geothermal energy were collected for the construction of a geothermal chromosome within the Energy Decisional DNA. This chromosome is then implemented in an ontology model aiming to be used for predicting purposes. Thus, it enhances different systems with predicting capabilities and facilitates knowledge engineering processes inside decision making.

Keywords: Knowledge Engineering, Decisional DNA, Knowledge Representation, Renewable Energy, Set of Experience Knowledge Structure, Decision Making.

1 Introduction

The term knowledge engineering has been defined as a discipline that aims to offering solutions for complex problems by the means of integrating knowledge into computer systems [7]. It involves the use and application of several computer science domains such as artificial intelligence, knowledge representation, databases, and decision support systems, among others. Knowledge engineering technologies make use of the synergism of hybrid systems to produce better, powerful, more efficient and effective computer systems.

Among the features associated with knowledge engineering systems are human intelligence capabilities such as learning, interpolation and forecasting from current knowledge or experience. In our case, experience is the main and most appropriate source of knowledge and its use leads to useful systems with improved performance.

Knowledge engineering techniques have been used in several domains and applications and the energy field is not an exception [4], [5], [10], [11], [12].

Renewable energy (RE) resources have great potential and can supply the present world energy demand. RE can reduce atmospheric emissions, offer diversity in energy supply markets, and guarantee long-term sustainable energy supply [2]. In addition, the use of RE resources has been outlined as a research focus in many developed countries.

One promising RE technology is geothermal energy. A geothermal system's performance, i.e. it can work properly, efficiently and economically to meet the desired load requirements under local ground conditions, depends upon several factors, including ambient and ground temperatures, pressures, and ground matter, etc. In any geothermal system, sizing represents an important part of the system design, e.g., the optimal pressure or the temperatures associated with those pressures which determine the size of certain components. Thus, in order to size a geothermal system, the characteristic performance of each component in the system is required.

The present paper explains the process of implementing a knowledge engineering technology that can collect, use and offer trustable knowledge in the geothermal energy domain. We make use of the Set of Experience (SOE) as a knowledge structure that allows the acquisition and storage of formal decision events in a knowledge-explicit form. It comprises variables, functions, constraints and rules associated in a DNA shape allowing the construction of the Decisional DNA of an organization. Having a powerful knowledge structure such as the SOEKS in the Decisional DNA and apply it to the construction of a geothermal energy chromosome can enrich and develop RE research.

2 Background

2.1 Set of Experience Knowledge Structure (SOEKS) and Decisional DNA

Arnold and Bowie [1] argue that "the mind's mechanism for storing and retrieving knowledge is transparent to us. When we 'memorize' an orange, we simply examine it, think about it for a while, and perhaps eat it. Somehow, during this process, all the essential qualities of the orange are stored [experience]. Later, when someone mentions the word 'orange', our senses are activated from within [query], and we see, smell, touch, and taste the orange all over again". The SOEKS has been developed to keep formal decision events in an explicit way [14]. It is a model based upon existing and available knowledge, which must adjust to the decision event it is built from (i.e. it is a dynamic structure that relies on the information offered by a formal decision event); besides, it can be expressed in OWL as an ontology in order to make it shareable and transportable [15], [16]. Four basic components surround decision-making events, and are stored in a combined dynamic structure that comprises the SOE; they are: *variables V*, *functions F*, *constraints C*, and *rules R*.

Additionally, the SOEKS is organized taking into account some important features of DNA. Firstly, the combination of the four nucleotides of DNA gives uniqueness to itself, just as the combination of the four components of the SOE offer distinctiveness. Moreover, the elements of the structure are connected among themselves imitating

part of a long strand of DNA, that is, a gene. Thus, a gene can be assimilated to a SOE, and in the same way as a gene produces a phenotype, a SOE produces a value of decision in terms of the elements it contains. Such value of decision can be called the efficiency or the phenotype value of the SOE [14]; in other words, the SOEKS, itself, stores an answer to a query presented.

A unique SOE cannot rule a whole system, even in a specific area or category. Therefore, more Sets of Experience should be acquired and constructed. The day-to-day operation provides many decisions, and the result of this is a collection of many different SOE. A group of SOE of the same category comprises a decisional chromosome, as DNA does with genes. This decisional chromosome stores decisional "strategies" for a category. In this case, each module of chromosomes forms an entire inference tool, and provides a schematic view for knowledge inside an organization. Subsequently, having a diverse group of SOE chromosomes is like having the Decisional DNA of an organization, because what has been collected is a series of inference strategies related to such enterprise (Fig. 1).

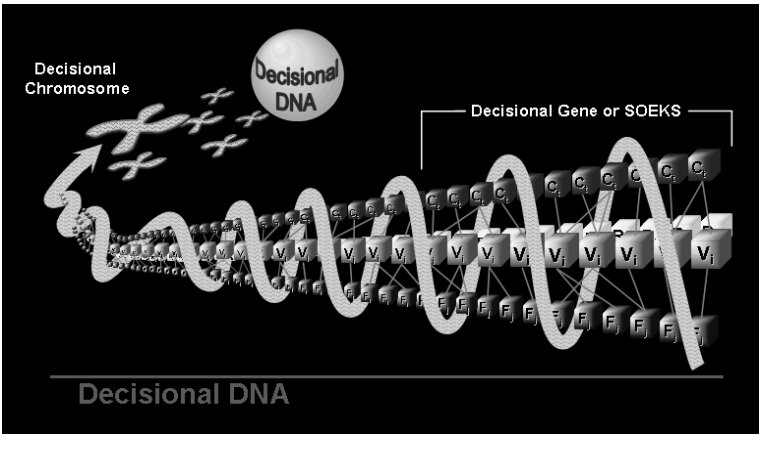

Fig. 1. SOEKS and Decisional DNA

In conclusion, the SOEKS is a compound of variables, functions, constraints and rules, which are uniquely combined to represent a formal decision event. Multiple SOE can be collected, classified, and organized according to their efficiency, grouping them into decisional chromosomes. Chromosomes are groups of SOE that can accumulate decisional strategies for a specific area of an organization. Finally, sets of chromosomes comprise what is called the Decisional DNA of the organization [13].

2.2 The Geothermal Laboratory

The University of Newcastle counts with a geothermal laboratory controlled by the Geothermal Research Group (GRG) on a project sponsored by Granite Power and AusIndustry through the Renewable Energy Development Initiative (REDI) grant.

The GRG develops several experiments aiming for efficient and optimal production of power cycles for generation of electricity from geothermal reservoirs [13].

The geothermal laboratory simulates traditional geothermal power cycles in which a working fluid is used to convert heat energy into mechanical energy (fig. 2). The pressure of the working fluid is increased in the Compression Unit and passed on to the Heat Generator (1) where the fluid temperature is raised by the waste heat from a latter part of the cycle. This partially heated fluid (1') is then passed through the High Temperature Heat Exchanger where heat exchange with the geothermal fluid will raise the working fluid temperature to its maximum. The hot working fluid (2) then passes through the Turbine, where its expansion forces the rotation of the turbine that drives an electrical generator. This expansion step reduces the temperature and pressure of the fluid. The exiting stream from the turbine (3) passes through the Heat Generator where energy is recovered and injected into the cooler compressed fluid (1). Following the Heat Generator, a separate Cold Fluid in the Low Temperature Heat Exchanger cools the working fluid (3') to its lowest temperature. The cold, working fluid (4) now re-enters the Compression Unit to be cycled once again [13].

In order to collect the research knowledge and experience created for this geothermal power cycle laboratory, several instruments and sensors are positioned in the system.. Due to the experimental nature of the work, the geothermal system incorporates a state of the art digital control system to continuously monitor, control, and record all process parameters. The primary roles of the digital control system are monitoring the process and collect online data from all the process sensors. Additionally, the digital control systems acts as a safe-fail device that controls the process and safely shut down the system in the event of a safety breach. The electronic system was supplied by Emerson Process Management Pty. Ltd. and consists of: a PC based control centre, a Foundation Field bus digital control system (DeltaV), 16 pressure transmitters, 24 temperature transmitters and 3 flow meters (a section of the laboratory is shown in fig. 3). The PC is connected to the field instruments via the DeltaV, digital control system.

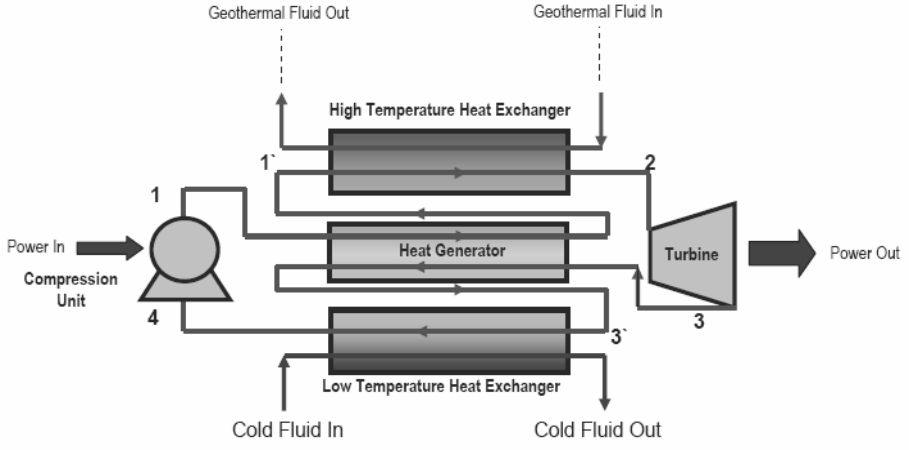

Fig. 2. Geothermal power cycle flow diagram [13]

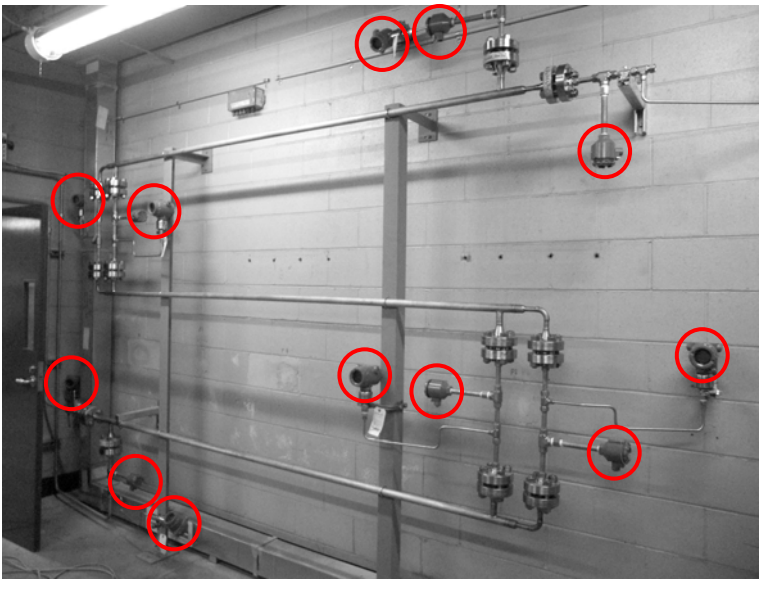

Fig. 3. Section of the geothermal laboratory with process sensors

The PC based remote operator control panel operates the Emerson PlantWeb software, which provides a visual user interface. The PC is connected to the field instruments via the DeltaV and collects all the real time online information of the process sensors. This is the repository of information.

3 Chromosome on Geothermal Energy

Experimental Research produces myriads of information and data which is collected and, sometimes, analyzed and stored; however, after a while, this information is commonly disregarded, not shared, and put behind. Little of this collected information survives, and in some cases, over time, it becomes inaccessible due to poor knowledge management practices or technology changes such as different software, hardware or storage media [3], [6], [8], [9]. These events indicate that there is a clear deficiency on information storage of experimental research, resulting in lost knowledge of the experimental processes. We suggest that some of the reasons could be a lack of technologies, not encouragement of the academic environment, and additional work involved on storing such experience. Through our project we proposed three important elements: *(i)* a knowledge structure able to store and maintain experiential knowledge, *(ii)* a solution for collecting experience that can be applied to experimental research, and *(iii)* a way to automate decision making by using such experience. In this case study we apply the three elements on RE.

Our plan aimed for the construction of a chromosome on geothermal energy which involved the implementation of the Decisional DNA, and within it, the use of

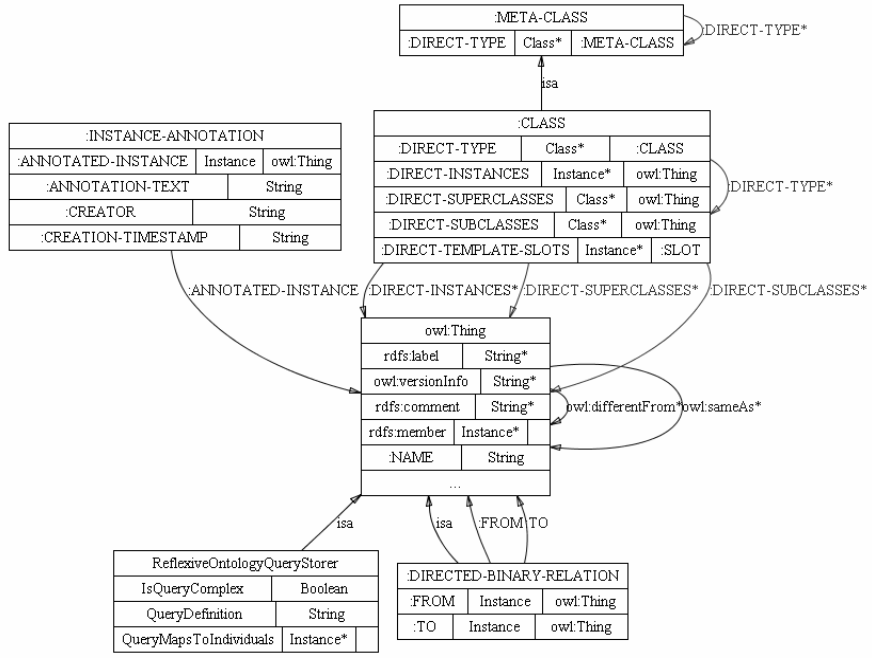

Fig. 4. Reflexive Ontology class schema

the SOEKS, to store and maintain experimental experience. Such plan requires different steps, they are as follows:

a) Run experiments at the geothermal laboratory,
b) Gather online information from the 43 sensors into the DeltaV,
c) Convert information to SOEKS compliant XML (eXtensible Markup language) by parsing the information onto metadata,
d) Feed an ontology chromosome with Sets of Experience, and
e) Check Energy Decisional DNA by querying the system with samples.

At the geothermal laboratory, experiments can run continuously for about 20 hours and information from each sensor can be collected at defined intervals between 1 second and 1 hour. For testing purposes, samples from two different experiments involving 2 fluids at intervals of 1 minute are sufficient. Such experiments produced 2400 events, each one involving variables of 43 sensors at a time. This information collected by fieldbus technology arrives to the DeltaV and it is stored in comma separated values (CSV) files.

Having these files, a parser written in Java, built up the XML trees which are then uploaded by using a Java API into protégé (an ontology software used for the construction of the Decisional DNA). Once the geothermal chromosome is constructed and ready in protégé, an additional extension for ontologies was applied:

Reflexive Ontologies

Reflexivity addresses the property of an abstract structure of a knowledge base (in this case, an ontology and its instances) to "know about itself". When an abstract knowledge structure such as the SOEKS is able to maintain, in a persistent manner, every query performed on it, and store those queries as individuals of a class that extends the original ontology, it is said that such ontology is reflexive, i.e. a reflexive ontology (RO). Therefore, any RO is an abstract knowledge structure with a set of structured contents and relationships, and all the mathematical concepts of a set can be applied to it as a way of formalization and handling. A RO must fulfill the properties of: Query retrieval (storing every query performed), integrity update (updating structural changes in the query retrieval system), autopoietic behaviour (capacity of self creation), support for logical operators (mechanisms of set handling), and self reasoning over the query set (capacity of performing logical operations over the query system) [17]. The advantage of implementing RO relies: Speed on the query process, incremental nature, and self containment of the knowledge structure in a single file.

The RO consists of an extension which adds a new class to the base ontology with the needed schema for the reflexivity; in our implementation, we call this the "ReflexiveOntologyQueryStorer class" (fig. 4).

The extension hangs from the OWL:Thing super class and it has the following OWL properties (Table 1).

Table 1. Reflexive class properties

Property	Type	Comment
isQueryComplex	Data	Boolean
QueryDefinition	Data	String
QueryMapsToIndividuals	Object	Collection of individuals

The last part of the implementation is the reflexiveness itself and it provides the ontology (programmatically) with a mechanism to perform queries and some logic on the queries that allows the handling of the reflexiveness. For our implementation we used protégé, its API's and the OWL-DL subspecies of the OWL specification [18].

A query is used to exemplify this case study. The query is defined in the code as:

```
public static String SIMPLE_RFLEXIVE_QUERY="CLASS
variable with the PROPERTY var_name EQUALS to X1";
```

Notice that this is a value type query. Such query is written in a human-like readable form which means "retrieve all the variables of the ontology that have the variable name X1".

The execution of the code offers information about the type of query executed and the successful saving of the query executed with results within the Reflexive Ontology Structure. Following in figure 5, the results can be seen as a query successfully executed with the new instance in the SOEKS-OWL transformed into a Reflexive Ontology:

```
----------------------------START-------------------------
Testing Simple query : CLASS variable with the PROPERTY
var_name EQUALS to X1
------------------------------------------------------------
... saving successful.
File modification saved with 0 errors.
-----------------------------------END-----------------
```

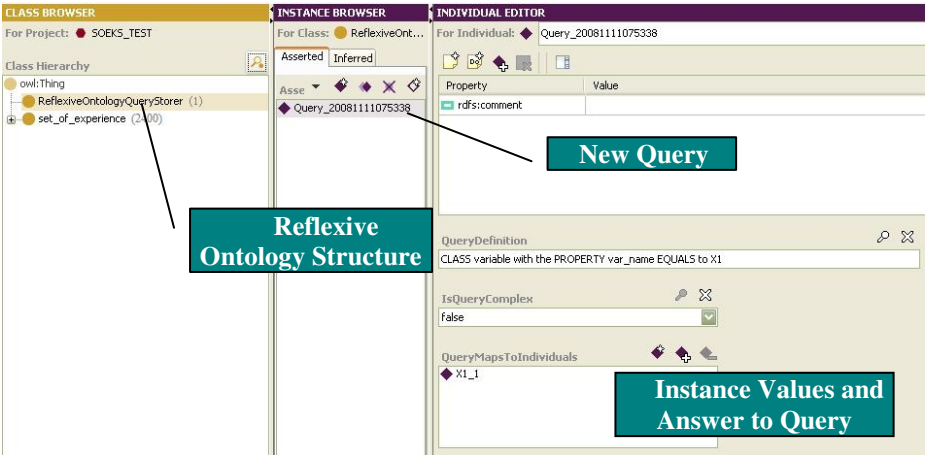

Fig. 5. Query performed on the RO geothermal chromosome

Such query performed over 2400 instances takes about 25 seconds; however, after the first time, a new similar query could take about 0.05 seconds.

4 Conclusions

This paper presents a case study for the implementation of knowledge engineering in the renewable energy field. It explains a practical case of collecting research experience from a geothermal laboratory, and then, use this information for the construction of a geothermal chromosome of an Energy Decisional DNA.

Decisional DNA and the Set of Experience were applied as a knowledge representation structure for gathering the geothermal experience. Afterwards, they were implemented in an ontology structure with reflexivity characteristics in order to use it as a tool for decision making processes that can enhance different systems with predicting capabilities and facilitates knowledge engineering processes inside decision making.

References

1. Arnold, W., Bowie, J.: Artificial Intelligence: A Personal Commonsense Journey. Prentice Hall, New Jersey (1985)
2. Asif, M., Muneer, T.: Energy supply, its demand and security issues for developed and emerging economies. Renewable Sustain Energy Rev. 111, 388–413 (2007)
3. Blakeslee, S.: Lost on Earth: Wealth of Data Found in Space. New York Times, C1 (March 20, 1990)
4. Chau, K.W.: A review on the integration of artificial intelligence into coastal modelling. J. Environ. Manage. 80, 47–57 (2006)
5. Chau, K.W.: A review on integration of artificial intelligence into water quality modelling. Mar. Pollut. Bull. 52, 726–733 (2006)
6. Corti, L., Backhouse, G.: Acquiring qualitative data for secondary analysis. Forum: Qualitative Social Research 6, 2 (2005)
7. Feigenbaum, E., McCorduck, P.: The Fifth Generation. Addison-Wesley, Reading (1983)
8. Humphrey, C.: Preserving research data: A time for action. In: Preservation of electronic records: new knowledge and decision-making: postprints of a conference - symposium 2003, pp. 83–89. Canadian Conservation Institute, Ottawa (2004)
9. Johnson, P.: Who you gonna call? Technicalities 10(4), 6–8 (1990)
10. Kalogirou, S.: Artificial intelligence for the modeling and control of combustion processes: a review. Prog. Energy Combust. Sci. 29, 515–566 (2003)
11. Kalogirou, S.: Artificial Intelligence in energy and renewable energy systems. Nova Publisher, New York (2007)
12. Kyung, S.P., Soung, H.K.: Artificial intelligence approaches to determination of CNC machining parameters in manufacturing: a review. Artif. Intelligence Eng. 12, 121–134 (1998)
13. Moghtaderi, B., Doroodchi, E.: Development of a novel power cycle for geothermal energy. REDI Grant (unplublished, 2007)
14. Sanin, C., Szczerbicki, E.: Set of Experience: A Knowledge Structure for Formal Decision Events. Foundations of Control and Management Sciences 3, 95–113 (2005)
15. Sanin, C., Szczerbicki, E.: Extending set of experience knowledge structure into a transportable language extensible markup language. International Journal of Cybernetics and Systems 37(2-3), 97–117 (2006)
16. Sanin, C., Toro, C., Szczerbicki, E.: An OWL ontology of set of experience knowledge structure. Journal of Universal Computer Science 13(2), 209–223 (2007)
17. Toro, C., Sanín, C., Szczerbicki, E., Posada, J.: Reflexive Ontologies: Enhancing Ontologies with Self- Contained Queries. International Journal of Cybernetics and Systems 39(2), 171–189 (2007)
18. Zhang, Z.: Ontology query languages for the semantic Web. Master's thesis. University of Georgia, Athens (2005)

A Study of Photo physical Properties of End Polymeric Material

Jahangir Payamara

Shahed University Physics Department, Science Faculty
P.O. Box: 18151-159
Tehran, Iran
jahangirpayamara@yahoo.com

Abstract. There have been investigated luminescence features of organic matter of GACH deparafinization GD and on its base PEHP have been developed. It is established that at excitation of organic matter of GD and developed on its base polymeric modification by light of 363 nm of mercury they transform effectively IR radiation into visible light. From temperature dependence of photoluminescence intensity it is determined activation energy of traps taken place in the quenching process of photoluminescence. This paper presents the experimental result of establishment new organic photo luminophore, development of its introduction technology into polymeric matrix and study of photo physical properties of end polymeric material.

Keywords: Photo physical properties, Luminophore, Transform, IR radiation, PEHP, GD.

1 Introduction

Luminophores implanted in the polymeric matrices are used extensively in creation of systems for optical recording information display, radiation converters and for extension of polymeric lifetimes. Decision of this problem requires detailed study of physico-chemical properties of polymer- luminophore systems introduction, methods of functional groups of luminophore in polymer and photo physical processes being at its absorption of light. Into feedstock photoluminescence modification of polyethylene of high pressure (PEHP) by method of mechanical mixing there has been dropped proposed impurity in amount of 0.5-6.0% (in mass).

2 Measurements

For attainment of homogeneous distribution of luminophore of GD in PEHP composition it is made then repeat regranulation. Film formations of PEHP granules and modifications on its base are carried out by extrusion method with inflation of industrial equipment of LRP 45-700M model. Film thickness is of 40 micrometer.

Samples from the set of developed films and of luminophore of GD as disk of $2\times10^{-2}\times2\times10^{-3}$ square meter in size at temperature T 453°k, 313°k and pressures 10,

30 MPa are obtained respectively. In stationary regime in the temperature range 100-300°k samples are excited by light of 365 nm of mercury and automatic recording of radiation spectra are carried out installation mounted on the base of spectrometer SDL-1 (N. Georgobiani 1995 & G.C.Righin,2005). Subjects of research are PEHP of various model (10803-020, 15302-003, 15803-020, 17504-006) and photo luminophore of organic matter of GD. Results of photo luminophore (PL) of organic matter of GD at temperature 293°k are listed in fig.1, curve 1.

3 Mathematical Method

Taking into consideration that probability of radioactive transition does not depend on temperature and probability without irradiative transition is defined by charge release with luminescence centre and consequently it grows with T rise proportionally with the factor Boltzmann [M. Gurvich, 1982 & G. Esposito, 2005].

$$I/I_0 = \frac{1}{1+q\exp\left(-\frac{E_A}{KT}\right)}$$

Where q-pre-exponential factor including the relation of concentration of quenching centre to concentration of luminescence centre, K-Boltzmann constant, T-absolute temperature, E_A-activation energy of luminescence centre, I_0-luminescence intensity at quenching absence, I-at quenching presence of luminophore of GD(curve1). This equation expresses the regularity of increasing of role of quenching processes with temperature rise.

4 Results and Discussion

Investigation results of photo luminophore (PL) of organic matter of GD at T 293K are listed in fig.1, curve1. For comparison in fig.1, it is listed luminescence spectrum of PEHP of 15803-020 model with GD impurity in 40% (in mass) (curve 2). The similar results are obtained for other models of PEHP. It should be noted that PEHP of various models without luminophore impurity at their excitation by IR-radiation they do not have PL.

It is seen from fig.1 that PL of spectrum of organic luminophore and obtained on its base modification of PEHP curves the range 400-590 nm with maximum at 495nm. At the same time at identical equal conditions the intensity of PL of given organic luminophore of GD composition of PEHP is distinctly reduced. It is mainly can be connected with the character of polymeric medium in matrix of which it is implanted photo luminophore and also with the feature of polymetric modification structures on over-molecular level [Abbasov T.F., 1991, & G.C.Righini,2005]. In fig.2 there have been listed dependence of intensity of PL, I/I_0 on temperature, where I- at quenching presence of luminophore of GD (curve 1) and developed of its base modification of PEHP (curve 2).

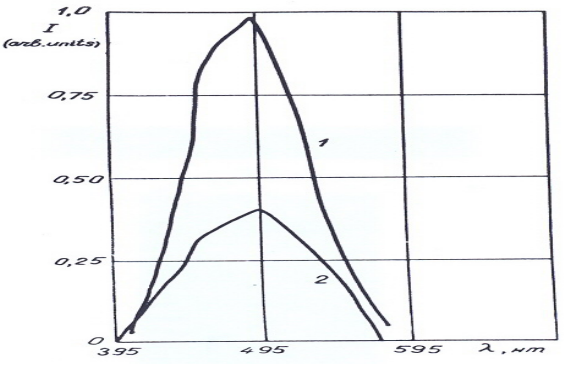

Fig. 1. PL spectra wavelength VS intensity

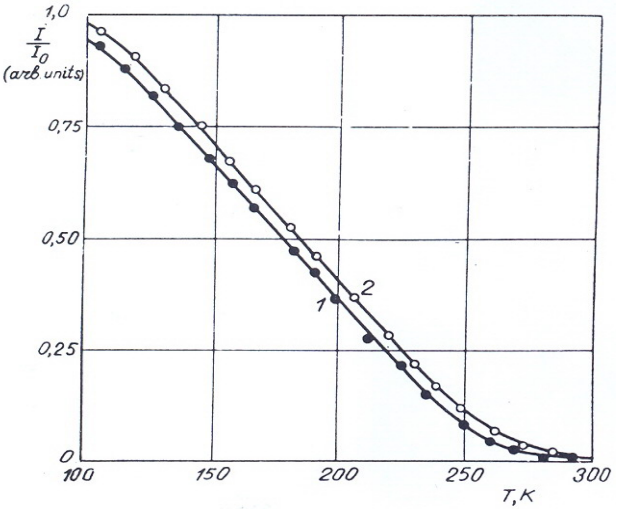

Fig. 2. Temperature dependence versus I/Io

It is seen that with the rise of temperature the intensity of PL of luminophore of GD & PEHP modifications is reduced. It can be connected with the quenching in deep electron lraps at the expense of recombination interaction of impurity centre having usually effective charges of opposite sings. Thus at recombination interaction part of non -irradiative transitions will be grown with the rise of temperature and decrease of excitation intensity.

It is also seen that quenching plays a significant role as earlier as less E_A, i.e. than nearer level of luminescence centre to valence band. To estimate activation energy E_A of luminescence centre on the base of obtained data it has been constructed dependence $\lg\left(\frac{I}{I_0}-1\right)$ on $\frac{1}{T}$. These results are shown in fig.3. It is seen that in

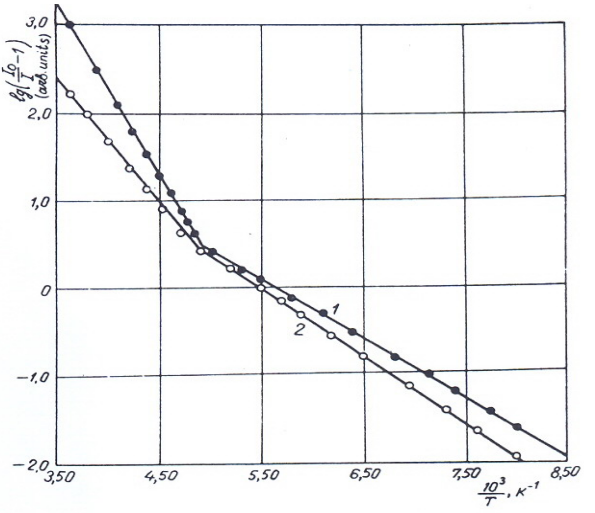

Fig. 3. Temperature dependence versus 1/T

mentioned coordinate for both samples there have been formed straight lines with band, for each sections to slope of which one can determine E_A. Thus, observed band of straight lines in coordinate $\lg\left(\frac{I}{I_0}-1\right)\approx\frac{1}{T}$ denotes that in suggested luminophore and developed on its base modifications of PEHP there are two different energy levels of luminescence centre. It is evidenced by calculation results of E_A to slope of first and second section of straight lines which are 0.163, 0.028 for luminophore of GD and for PEHP with impurities are 0.126, 0.066 ev respectively. Obtained evidence of activation energy of luminescence centre allows to pre determine of decisive role of local levels in this process.

5 Conclusions

New organic luminophore is revealed and on its base photo luminescent polymer material is developed. It is shown that at excitation of organic matter GD & on its base developed modifications of PEHP by light of 365 nm of mercury transforms IR radiation into visible light with intensity maximum of luminescence of wave length 498nm. On the base of obtained results there have been calculated activation energies of luminescence centre responsible to photo luminescent processes.

Acknowledgments

This work carried out with the financial support of the research centre of Shahed University. We would like to thank the staff at the Plasma Phys. Research Centre of I.A. University for their help.

References

1. Georgobiani, A.N., Tagiev, B.G., Tagiev, O.B., Tzzatov, B.M.: Photoluminescence of rare-earth elements in $CaGa_2S_4$ compounds. Neorganicheskiye Materiali 31(1), 19–22 (1955)
2. Righini, G.C., Ferrari, M.: Photoluminescence of rare-earth-doped glasses. Jr. Photoluminescence of Rare-earth Elements 28(12), 1–35 (2005)
3. Gurvich, A.M.: Introduction to physical chemistry of crystallophosphors. Moskva, Vischaya shkola, p. 29 (1982)
4. Esposito, G., Marmo, G.: From Classical to Quantum Mechanics, Cambridge, p. 485 (2005)
5. Abbasov, T.F.: Pecularities of electrophysical mechanical properties and structures of polymers modified by small impurities, p. 185 (1991)
6. Wunderlich, B.: Thermal Analysis of Polymeric Materials, p. 796. Springer, Heidelberg (2005)

Renewable Energy Source Emulator

Chu Chin Choon, Colin Coates, and Aparna Viswanath

School of Electrical Engineering and Computer Science
University of Newcastle, Callaghan, NSW 2308, Australia
eloh1230@hotmail.com, Colin.Coates@newcastle.edu.au,
Aparna.Viswanath@newcastle.edu.au

Abstract. Small scale solar and wind turbines are finding increased application in stand-alone, grid-connected and micro grid scenarios. New controllers for these devices are continually being developed. This paper documents the design and development of a low cost circuit to emulate the electrical characteristics of both photovoltaic arrays and wind turbines. The emulator circuit is intended as a tool to aid in the development of new wind turbine and photovoltaic controllers. The emulator consists of a DC / DC converter controlled by a microprocessor. A separate Maximum Power Point Tracking (MPPT) module is also described.

1 Introduction

The scarcity of the Earth's natural resources has driven research and investment into various forms of renewable energy. The two most widely recognized renewable energy systems are wind and solar. However, other systems such as bio-power/ biomass, geothermal and fuel cells are also receiving increased attention [1].

With the focus on renewable energy there is ongoing effort to develop improved controllers for these sources. Other research is considering how a number of these sources might interact with each other in a micro grid scenario. In progressing both these research areas, it is advantageous to be able to emulate the electrical characteristics of a renewable source in a controlled and repeatable manner rather than relying on the vagaries of the weather.

This paper presents the design and development of a low cost emulator of the electrical behavior for both solar and wind energy systems. Solar and wind are chosen as the use of both has grown considerably over the past two decades. The methods used can be readily extended to other sources.

The emulator is based around a controlled DC / DC boost converter. The prototype was developed at extra low voltage as an undergraduate student project for cost and safety reasons. The power circuit can be scaled to the voltage and power levels normally associated with small solar and wind energy systems.

2 Modeling of PV Array

A photovoltaic (PV) system will normally consist of an array of PV cells producing a variable DC voltage and current in response to lighting and load conditions. A

controller would be connected to the PV array to convert the variable DC voltage into a form appropriate to the intended load. Our purpose here is to model the voltage - current characteristic of the PV [2] array so that it can then be emulated.

Solar cells are normally used in modules or arrays, where multiple cells are connected in parallel and series to achieve desired current and voltage ratings. The current - voltage equation when adapted for module use is given by [3],

$$I = n_p \left[I_{sc} - I_s \left[e^{\frac{q\left(\frac{V}{n_s} + \frac{IR_s}{n_p}\right)}{A_f KT}} - 1 \right] - \frac{\left(\frac{V}{n_s} + \frac{IR_s}{n_p}\right)}{R_p} \right] \quad (1)$$

Where,

n_p is the number of cells in parallel

n_s is the number of cells in series

R_p is the intrinsic parallel resistance of the PV cell (Ω)

R_s is the intrinsic series resistance of the PV cell (Ω)

K is Boltzman's constant at 1.38×10^{-23} JK^{-1}

q is the charge on an electron at 1.6×10^{-19} C

T is temperature (K)

A_f ideality factor, it determines the deviation of p-n junction characteristics.

I_s is the reverse saturation current (A)

I_{sc} is the short circuit photo current generated under a given solar insolation.

3 Modeling of Wind Turbine

Small wind turbines normally operate at variable speed and use power electronic converters to interface to either the grid or battery storage. Typically, the turbine is coupled to a generator (induction or permanent magnet machine). The output of the generator is then rectified in preparation for the power electronic converter. The aim here is to emulate the DC voltage / current relationship in this system at the output terminals of the rectifier [2].

The emulation of the wind turbine rectifier voltage-current characteristic is uncommon. Most frequently wind turbine characterization is limited to either the turbine power vs. rotor speed, electrical output power vs. wind speed, rotor efficiency vs. tip speed ratio or torque vs. wind speed relationships. The turbine, generator and rectifier characteristics are combined in the following discussion.

The power extracted from the wind by turbine rotor blades is given by [4],

$$P_{turbine} = \frac{1}{2} \rho a v^3 C_p(\lambda) \text{ watts} \quad (2)$$

Where,

ρ is the density of air (kg/m^3)
a is the area of the turbine (m^2)
v is the wind velocity (m/s)
C_p is the performance coefficient or rotor efficiency of the turbine

$\lambda = \frac{\omega_m r}{v}$ is the tip speed ratio of the turbine

The relationship between C_p and λ is turbine dependent. For the present discussion the following relationship is used [5],

$$C_p(\lambda) = 0.00044\lambda^4 - 0.012\lambda^3 + 0.097\lambda^2 - 0.2\lambda + 0.11 \tag{3}$$

Equation (3) represents the wind turbine mechanical power at its shaft. A generator is coupled to the wind turbine shaft. For the present discussion it is assumed the generator is directly coupled to the turbine shaft although it is recognized that a gearbox may be employed. To convert the mechanical power to electrical, the following equation is applied,

$$P_{turbine} = 3V_{ph}I_s + 3R_s I_s^2 + P_{iron} \tag{4}$$

Where,

V_{Ph} is the per phase AC voltage at terminal output
R_S is the stator resistance of the wind turbine generator
I_S is the current flows through the stator
P_{iron} is the iron losses of the wind generator

Equation (4) can be further simplified under the assumption of an ideal lossless generator. Armature resistance and iron losses are ignored. The generator output is then rectified in which case [6-8],

$$P_{turbine} = 3V_{ph}I_S = V_{DC}I_{DC} \tag{5}$$

$$\begin{aligned} V_{DC} &= \frac{P_{turbine}}{I_{DC}} \\ &= \frac{1}{2}\frac{\rho\pi r^2 v^3(0.00044\lambda^4 - 0.012\lambda^3 + 0.097\lambda^2 - 0.2\lambda + 0.11)}{I_{DC}} \end{aligned} \tag{6}$$

4 Hardware Design of Emulator

Figure 1 shows a functional overview of the emulator system. A boost converter is used to provide a controllable dc source. A discussion of the circuit implementation and operation follows.

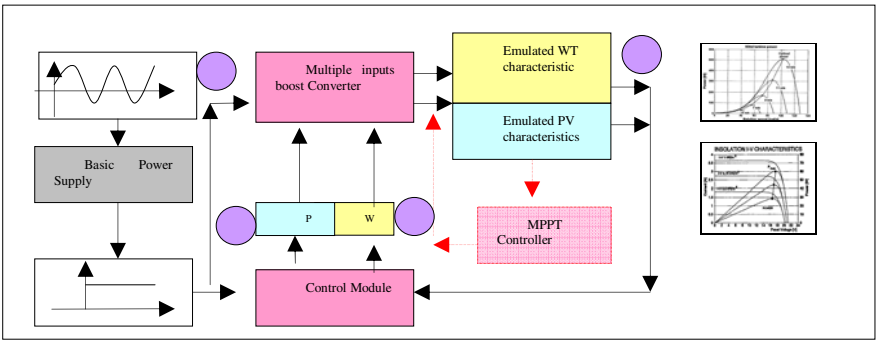

Fig. 1. Overview of Emulator System Hardware

At point 1, a fixed DC voltage is supplied to the input of the DC-DC boost converter. The prototype emulator was implemented as an undergraduate project so an extra low voltage input was chosen. However, the voltage and powers can be readily scaled to more practical values if desired.

At point 2, the boost converter output is controlled to emulate the electrical characteristic of the renewable energy source. The voltage and currents closely follow those of a renewable energy source under similar load conditions.

At point 3, a microcontroller implements the closed loop control. The boost converter output voltage and current are monitored and adjustments in the duty cycle made to ensure the desired characteristic is tracked.

At point 4, a MPPT controller is added between the converter and the loads. The MPPT controller is an independent DC-DC converter that can vary the effective load on the emulator system driving it to its optimal operating point.

Figure 2 shows the hardware assemblies. The emulator comprises of three assemblies being the power board, dc-dc converter and control module.

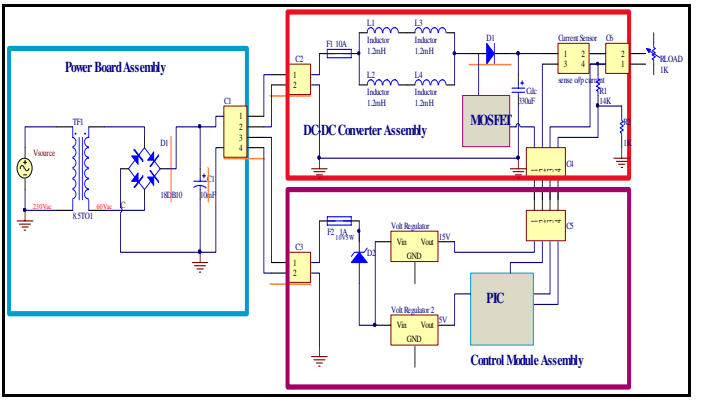

Fig. 2. Emulator interface schematic

4.1 Emulating Solar Energy Characteristics

To evaluate the emulator a resistive load is connected to the output of the emulator's boost converter. The output voltage and current are measured and fed back to the microcontroller in the control module. The microcontroller generates a lookup table that defines the solar array characteristic. The microcontroller adjusts the duty cycle of the boost converter to allow the output voltage to track the defined characteristic.

The emulator can be driven to its optimal operating point with the insertion of a MPPT controller between the converter and the load. The microcontroller in the MPPT independently monitors output voltage and current values and computes output power. Using a perturbation and observation type method the MPPT is able to adjust its duty cycle forcing the emulator to its optimal operating point.

4.2 Emulating Wind Turbine Characteristics

A wind turbine system has complex dynamic behavior. It will only reach equilibrium when the turbines mechanical torque is equal to the generators electrical torque. While this condition is not met the generator will either accelerate or decelerate impacting on its output voltage and current. To model this faithfully, a closed loop feedback path is needed to automate the adjustment of rotor speed at each new measurement of voltage or current. In its initial conception, the automated adjustment of rotor speed was deemed too complex given the available project hardware. Simplifying assumptions and approximations are made to account for this.

To achieve principle with fixed voltage and varying current (due to varying power over different wind speeds), the emulator will require the MPPT controller in the emulation process.

5 Experimental Results

To ascertain the performance of the emulator, various tests were carried out to collect data and plotted against the theoretical curves.

Figure 3 compares the emulated PV module output with the theoretical output under different temperature conditions. Good alignment is demonstrated between the emulated and actual curves.

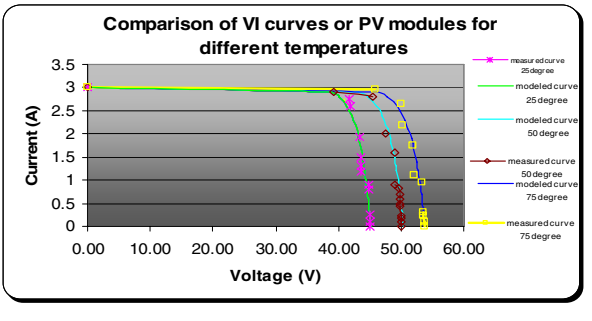

Fig. 3. Comparison of emulated and theoretical PV module curves (I_{sc} = 3A)

Figure 4 shows the theoretical wind turbine power and current curves along with the emulator current output when the DC bus is held at 60V. Once again there is good alignment between the theoretical and emulated outputs.

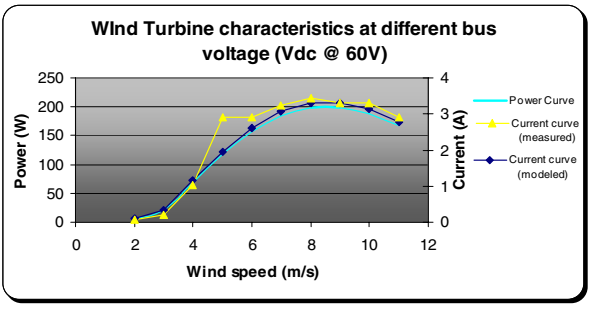

Fig. 4. Comparison of modeled wind turbine characteristics against measured data (V_{DC} =60V)

Figure 5 shows the emulated and theoretical currents and powers when the turbine is operating in constant speed winds at various generator speeds.

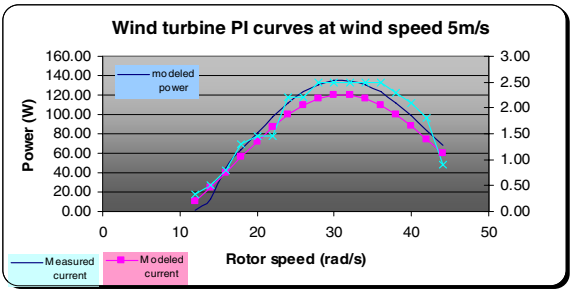

Fig. 5. Wind turbine power current curves at wind speed 5m/s

The MPPT was connected to the emulator to drive the system to its optimal operating point. Tests were repeated to locate the average MPP for different current settings. Figure 6 shows one set of test results. The maximum power point is successfully tracked.

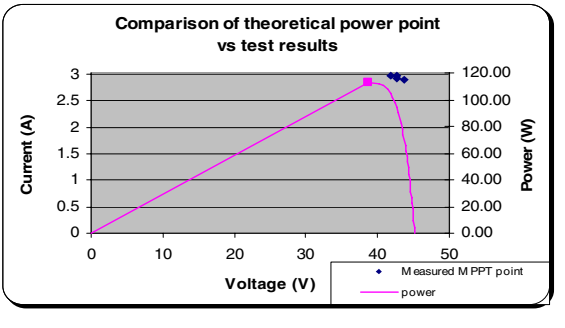

Fig. 6. MPPT test for $I_{SC} = 3A$

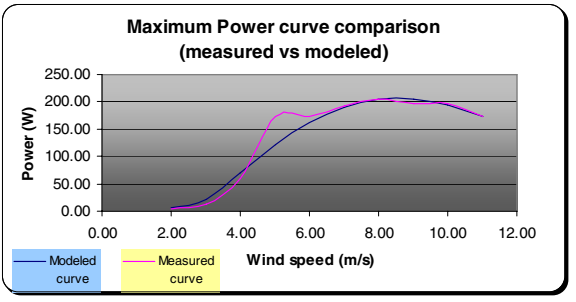

Fig. 7. Comparison of modeled and measured MPPT for wind turbine

Similarly, the MPPT test is carried for the wind turbine emulator and the results are plotted in Figure 7. It is noted that the measured curve generally follows the behavior of the modeled power curve.

6 Conclusions

The primary objective of this project was to design, build, and test a low cost emulator for selected renewable energy sources. The emulator system constructed has met this objective and other design goals stipulated in the earlier sections of this report.

The control module is designed to take in 2 renewable sources thus forming a hybrid system emulator. For the solar energy emulation, the hardware design allowed variable input parameters such as I_{SC} varying from $0\,A$ to $4\,A$ rated current. Typical temperatures settings such as 25^0C, 50^0C *and* 75^0C are also considered in the design. For wind turbine emulation, input parameters allowed for are temperature settings which affect the air density. Typical temperatures setting such as 15^0C, 25^0C *and* 35^0C are considered in this paper. Wind and rotor speeds are also included as variables in the design, this allows good variation of tip speed ratio. Due the hardware design limit, wind speeds variations are restricted. To achieve modeling of the wind turbine at different voltages, 3 different V_{DC} settings have been considered.

In order to optimize the energy utilization of the renewable energy source, it is important to operate the equipment at the maximum power point. A MPPT controller is included as an added feature to support the operation of the emulator. The MPPT controller is attached to the emulator to allow maximum power transfer. Converters that operate at maximum power point will no doubt help in maintaining the cost effectiveness of renewable energy source generation.

Acknowledgments. The authors sincerely thank the University of Newcastle for extending the Faculty of Engineering Research grant that helped submission of this paper.

References

[1] Stanley, R.: Bull, Invited paper, Renewable Energy Today and Tomorrow. Proceeding of the IEEE 89(8) (August 2001)
[2] Choon, C.C.: Renewable Energy Source Emulator. University of Newcastle, Final year project report (2008)
[3] Enrique, J.M., Duran, E., Sidrach-de-Cardona, M., Andujar, J.M., Bohorquez, M.A., Carretero, J.: A New Approach to obtain I-V and P-V curves of Photovoltaic Modules by Using DC-DC converters. IEEE Transactions on Industrials on Industrial Electronics (2005)
[4] Gilbert, M.: Masters. Renewable and Efficient Electric Power Systems (2003)
[5] Arifujjaman, M., Iqbal, M.T., Quaicoe, J.E.: Maximum Power Extraction From A Small Wind Turbine Emulator Using A DC-DC Converter Control led By Microcontroller. In: 4th International Conference on Electrical and Computer Engineering, ICECE 2006, Dhaka, Bangladesh, December 19-21 (2006)
[6] Tafticht, T., Agbossou, K., Cheriti, A.: DC Bus Control of Variable Speed Wind Turbine Using a Buck-Boost Converter. IEEE Transactions on Industrial Electronics (2006)
[7] Muljadi, E., Drouilhet, S., Holz, R., Georgian, V.: Analysis of Wind Power For Battery
[8] Bialasiewicz, J.T.: Furling control for Small Wind Turbine Power Regulation. IEEE Transactions on Industrial Electronics (2003)

Geothermal Active Building Concept

Wim Zeiler and Gert Boxem

Technische Universiteit Eindhoven, Netherlands
w.zeiler@bwk.tue.nl

Summary. Building integrated geothermal energy systems promise to reduce the energy consumption of the built environment. The passive building concept is the present trend in energy efficient sustainable dwellings. Within the passive building concept every effort is made to minimize the energy use. The ventilation capacity of many of these passive houses is critical. Energy saving and sustainability is very important but not at the risk of endangering health of the occupants. This was the starting point for a new approach, which led to an alternative concept: the active house concept. By using ground air collectors, labyrinth foundation, muro-causter and hypo-causter, the whole building envelope and construction is thermally activated by natural pre-cooled air in the summer and natural pre-heated air in winter. A first design is presented to illustrate the concept.

Keywords: active house, passive house, sustainable building envelope.

1 Introduction

The built environment uses around 40% of our total energy demands. This results in environmental problems and exhaustion of fossil fuels. This has to change and new approaches have to be developed. One such approach is the latest trend on low energy housing: the Passive House. In Germany and Austria more than 5.000 Passive houses have been built and a lot experience was gained. Also in other European countries the passive house concept is promoted, still only a few houses in the other countries have been built. Designing and building of passive houses in a country is not a matter of straight forward following the experience of the already built examples from Germany or Austria. Each country has its own building tradition, architecture, building technologies, climate and culture (Kaan en de Boer 2005). In Germany, the Passiv Haus Institut took the traditional concept of passive solar building as a starting point and developed concepts for very low energy buildings by combining the principles with a very well insulated and air tight building envelope (Kaan & de Boer 2005). In France as an example only a few passive houses have been built (Thiers and Peuportier 2008), mainly for experimental purposes and the first attempt to reach the Passive House standard in France has failed (CEPHEUS project in Rennes (Feist et al., 2005)).

The general definition of a Passive House is that the energy consumption is limited to around maximum 15 kWh/m² for space heating and around maximum total of 120 kWh primary energy/m² for heating, domestic hot water and electrical consumption

by electrical equipment and lighting. To meet these criteria, the Passive House concept focuses first and foremost on reducing the energy demand of the building. Analysis of Passive House solutions shows high priority with regard to the performance of the thermal envelope: high insulation of walls, roofs, floors and windows/doors, thermal bridge-free construction and air tightness (Storm et.al 2006). For good insulated low energy houses the needed heating energy for the ventilation air is around 50 to 65% of the total heat demand (Pottler et.al. 1999). This is the reason that often the ventilation are strongly reduced, some mention values as low as a ventilation rate of 0,4 (de Boer et.al 2005). There is a competition between energy saving on the one hand and a good indoor air quality on the other hand. Storm et.al (2006) state; "However, since Passive Houses have air tightness, sufficient ventilation must be paid to the actual realization in practice of the required ventilation rate."

In the Netherlands architect Erik Franke has built the first Passive Houses in the Netherlands according to the 'Passivhaus Projectierungs Paket'(PhPP) (Franke 2005). The PhPP is a package of tools for architects to help them with the design of passive houses and was developed by the German 'Passivehaus Instituut' in Darmstad. Though in the Netherlands a number of houses have been built according to PhPP, the actual performance of these houses was not yet thoroughly investigated. The aim of a study at the Technische Universiteit Eindhoven was to investigate if the ventilation levels reached by the installed mechanical ventilation systems in these Dutch passiv houses are sufficient (Balvers et.al. 2008). The use and application of mechanical ventilation systems in such low-energy house is the critical aspect for creating an acceptable level of IAQ. As the present passive house concept has some critical aspect related to adequate ventilation, we started to look at other ways for building to utilize the available on-site energy resources in a way that minimizes the need for purchased energy and still maintaining a satisfactory indoor environment.

2 Methodology: Active Versus Passive

There are many possibilities for direct inter-action between the building fabric and the environment in order to reduce the need for additional energy for conditioning to achieve the desired comfort and cover the residual demand. It is difficult to categorize the various passive systems because they often combine strategies for power generation, passive cooling, passive heating as well as heat storage, heat recovery or avoidance of the various external and internal heat gains.

Besides passive solutions, there are also active systems designed to utilize the environment to either produce power, or to operate in conjunction with some mechanical devices to utilize renewable energy to provide heating and cooling (Wachenfeldt and Bell 2003).

Sometimes it is good to go back all the way to the beginning, the basis. The basis of conditioning buildings are from the Greek and Romans. The Greek historian Xenophon mentioned the teaching of the Greek philosopher Socrates (470-399 BC) about the correct orientation of dwellings to have them cool in summer and warm in winter. The Romans pioneered with heating using double hollow floors through whose core the hot fumes of a fire were passed (Florides et al. 2002). They used with their

'hypocaust' and 'murocaust' the materials of the build construction to condition the building with hot air, see figure 1.

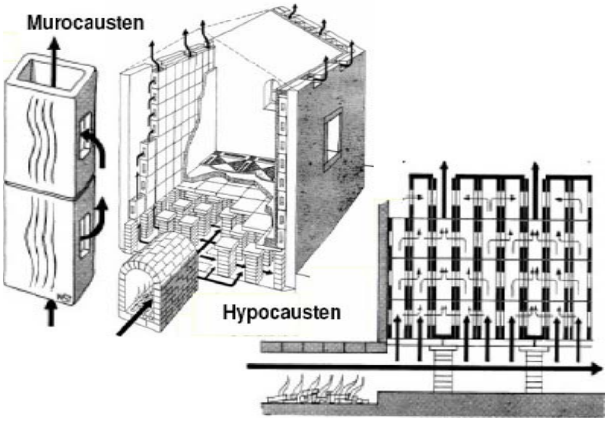

Fig. 1. The Roman thermo- and muro-causten system (Florides et al. 2002)

People ruled by Romans assimilated their building techniques and technologies that became one thing with the local ones (Sansone 1999). This was not the only Roman/ Italian influence: Kenda (2006) focused on the beneficial integration of architecture and medicine in Renaissance Italy: Sixteenth century pneumatic architecture, especially the examples of hygienico-pneumatic villas, figure 2.

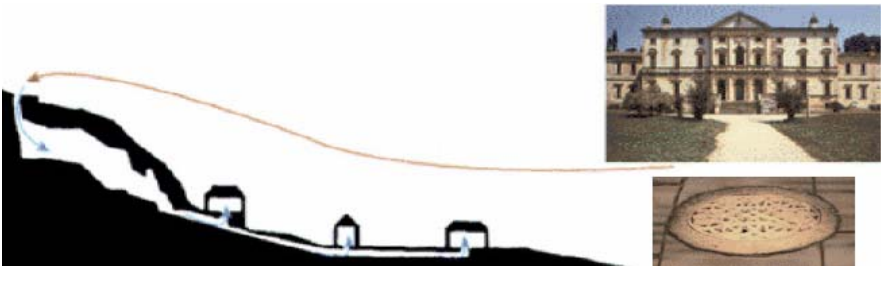

Fig. 2. Natural ventilation Villa Costozza, Italy (Bellow 2004)

The villas are connected underground by labyrinth caves and wind channels to provide a unique natural ventilation system. Renaissance architects considered pneuma (air, wind, breath, spirit, soul) from Aeolus, the god of winds to be the fundamental condition in the harmonic relationship of the human body, a building and the cosmos (Kenda 1998). Therefore, the integral aim in the making of Renaissance pneumatic architecture was to augment the powers of pneuma so as to foster the art of well-being. The direct inter-action between the building fabric and the environment in offers many possibilities to reduce the need for additional energy for conditioning in order to achieve the desired comfort and cover the residual demand. It is difficult to

categorize the various active systems from true passive systems because they often combine strategies for power generation, passive cooling, passive heating as well as heat storage, heat recovery or avoidance of the various external and internal heat gains (Wachenfeldt and Bell 2003).

A modern variant is the use of the accumulative capacity of concrete constructions to flatten and damp the effect of fast changing outdoor temperatures. One of the first applications of a 'thermolabyrinth' was the 1977 Royal Academy of Music complex in London existing of theatres and music studios by Bill Holdsworth (Holdsworth 2005). Also in Germany there are several project with so called 'Thermo labyrinth' systems built, par example Stadttheater Heilbron and Terminal 1 Hamburg Airport. Recently Atelier Ten has enjoyed considerable success with thermal labyrinths on some prestigious projects such as the Federation Square in Melborne project were the outside air is led in a labyrinth under the square and blown into the atrium of the main building (Bellew 2004, AIRAH 2003). Patrick Bellow principal of Atelier Ten has long believe in thermal labyrinhs (Bunn 2004).Other projects a business school designed by Cesar Pelli Architects for the University of Illinois, the Grand Rapids Art Museum in Michigan and the Earth Centre in Doncaster by FeildenClegg Bradley Architects. By doing this a significant cooling effect was realized, see figure 3.

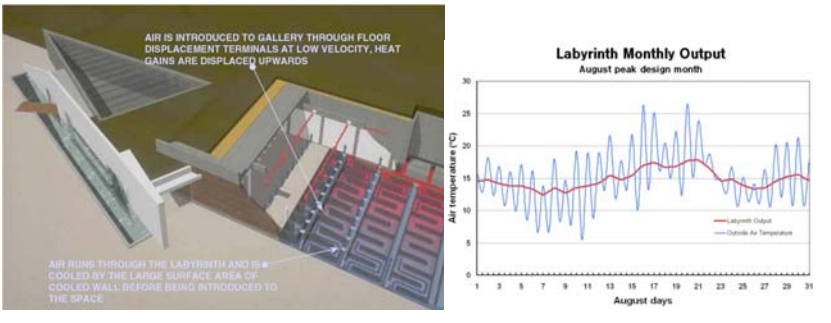

Fig. 3. Principle schematic of labyrinth ventilation and its effect on reducing the temperature of the ventilation air the earth centre- Fielden Clegg Bradley Architects (Bellow 2005)

An interesting modern technology related to the principles of 'thermo labyrinth' systems are earth-air heat exchangers, or ground tubes, or ground-coupled air heat exchangers (De Paepe and Janssens 2003). In the Netherlands only a few of these systems were applied, e.g. the firebrigade stations of Deventer and Soest by the architect Jòn Kristinsson (Kristinsson 2002). In Germany this principle is far more popular and applied in many buildings and passive houses (Pfafferot 1998), mostly with concrete or HDPE tubes as ground collectors. Atelier Ten has now developed the system further in the Butterfield Business Village. Concrete sewer pipes are used to line long underground ducts. These are 900 mm in diameter , 80 m long and are buried 1,2 m below the surface (Lane 2006).

A concept to use the accumulation capacity of a building in combination with its envelope is the Lega beam Building System (Toft 1993). Hereby between the outer and inner building walls a concrete core is placed, see figure 4 A and B. In the space

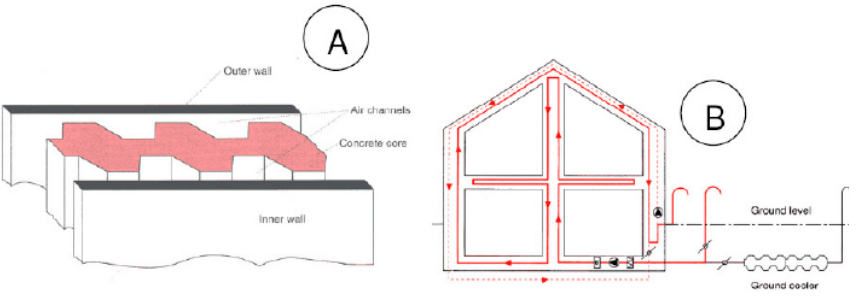

Fig. 4. A & B. Legabeam Building Systeem (Toft 1993)

between the walls and the concrete core air flows which can also be cooled of heated with a ground-air collector.

The goal of Task 19 was to facilitate the use of solar air systems for residential, institutional and industrial buildings. In 1988 they published a manuscript for an engineering handbook to provide the planner with detailed how-to information six different system types, depending on the needs of the building, climate and budget. One example system types they mentioned was the solar air system with sun collector connected to murocaust and hypocaust, see figure 5.

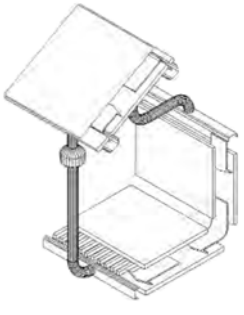

Fig. 5. Type 4:collector to murocaust and hypocaust (Hastings 1998)

Some of these systems already have been applied in projects: Lutzstrassen Apartments in Berlin (Hastings and Mørk 1999) and Gardstens Bostäder aparmentscomplex in Gothenburg (SHINE 2006). These are systems which supply the heat of a thermal suncollector to the floors or walls (BINE 2006). Heat from air collectors can be transferred to mass using the room air, or, as in the Lutzstrassed Apartments in Berlin, warmed air can be blown, using fans, through hollow cores in a massive floor, called a hypocaust (Hastings, 1999, pp. 92-95). The building has a closed loop from collectors in the south facade through tubes embedded in the concrete floor, and back to the collector. Discharge is by radiant transfer through the slab. This has the advantage of keeping the indoor air temperature from rising rapidly when the collector is heated by the sun. In the apartment Block in Gothenburg, Sweden, by Christer Nordstrom ((Hastings and Mørk 1999)) air warmed from rooftop collectors is ducted by

mechanical ventilation to a murocaust cavity in the external walls, formed by adding an insulated layer outside the existing not insulated masonry wall. Termodeck, developed by two Swedish engineers Andersson and Isfalt in the 1970s, uses the slab as a means of ducting ventilation through the building through oval or round shaped ducts (hollow-cores) within the concrete structure (Wachenfeldt and Bell 2003). In Summer the supply air fans at night bring in the cool air into the hollow slabs to cool the building and the warm outside air is cooled in the daytime. It utilizes the hollow cores within pre-cast concrete floor slabs as ventilation ducts to produce an environment which is thermally stable (Barton et al., 2002). The TermoDeck system relies on heat being exchanged between the air in the core to the concrete of the slab, through the interface which is the surface of the core. Heat is conducted radially through the concrete from this interface until it reaches the surface (top and bottom of the slab) or to where the temperature gradient becomes small—in the horizontal direction between cores. As the temperature difference between the cores is relatively low, the high heat capacity of the concrete means that it is possible to neglect the influence of adjacent cores (Barton et al. 2002). The TermoDeck system employs low air velocities (i.e. approximately 1 m/s) with the result that buildings using this system tend to consume little energy (Barton et al. 2002). For example, the Elizabeth Fry Building consumes very little energy; its average electrical energy consumption for 1997 was only 61 kWh/m² and its gas consumption was 37 kWh/m² (Standeven et.al1998), figures which are less than half of the targets values for good practice air conditioned office buildings in the UK (DETR 1998). Typical energy consumption for heating and ventilation for the UK is around 200 kWh/m²/y (Wachenfeldt and Bell 2003). The Elizabeth Fry Building uses mechanical ventilation with heating and no mechanical cooling at all. Mixed flow ventilation is used throughout the building except the Lecture Theatre where displacement ventilation is used (Wachenfeldt and Bell 2003). The building was monitored for occupant satisfaction by the Professional Organization of Building Examiners (PROBE) team: it was perceived by its occupants to be a particularly comfortable building (Bordass et al. 1999) and also recorded the highest comfort scores recorded by the independent survey specialists Building Use Studies (Wachenfeldt and Bell 2003). In Norway, the TermoDeck system was installed in some buildings in the early 80's. The thermal performance was reported to be good. However, various problems were identified (Wachenfeldt and Bell 2003):

- Smell and dust from the un-treated concrete ducts.
- The connections between the ducts were not tight, resulting airflow at unwanted places and reduced performance.
- The ventilation systems were often under-sized, resulting in insufficient ventilation airflow to maintain comfort.

Due to these above mentioned problems, since the 1990s , there have been installed few, if any, ThermoDeck systems in Norway (Wachenfeldt and Bell 2003). Most of the TermoDeck systems delivered before this period have been rebuilt in order to increase the airflow rates and avoid especially the problem with concrete dust. The ducts within the concrete structure have therefore been abandoned, and were replaced by regular HVAC duct systems.

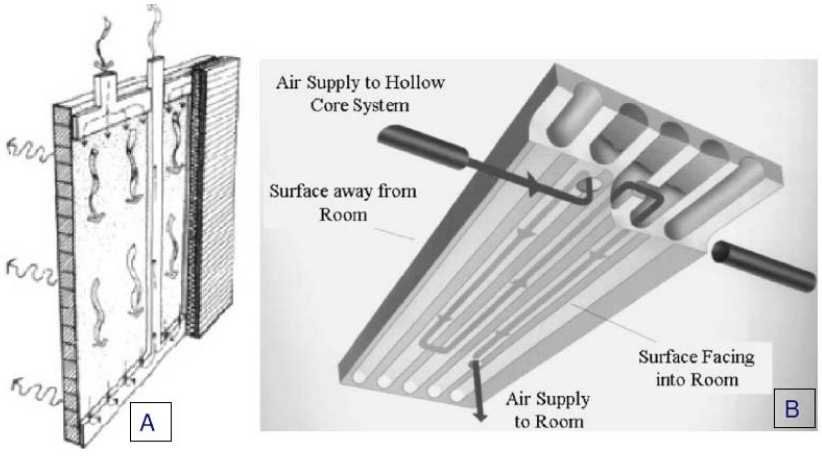

Fig. 6. A Murocaust apartment Block in Gothenburg (Hastings and Mørk 1999) B Hypocaust Thermo deck system (Barton et al. 2002)

3 Proposed Active Envelope Solution; Geothermal Active House

In the air ducts in the ground of the ground-air collectors and also in the labyrinth foundation by cooling of supply air, high relative humidity can occur. Often because of this effect air out these air-ground collectors is some what steel and not that suited to supply directly to the rooms. Especially at humid days there is condensation (Koene & Lightart 2001) When there is a long period of high relative humidity of condensation there is no way to avoid bacteria growth. By these systems there is contact between the fresh outside air and the concrete, something which we think is not optimal, as dust and participles from the concrete can easily absorbed by the air. A system which does not have that drawback is the ConcreteCool system: concrete core cooling with supply air utilizes the high storage capacity of the concrete ceiling with aluminum ducts within the concrete. The supply air flows through the cooling tubes consisting of aluminum with high thermal conductivity.. To improve the heat transfer from the tube to the air, the inner surface was tripled. This system is already used in several German projects (Schröder 2002, Kiefer 2003), see figure 7.

To avoid the negative effects of this possible bacteria growth the choice is been made for a separate system with strict moisture barriers by aluminum ducts in the buildings constructions, which carries the air through floors and walls. With a heat exchanger energy is exchanged between supply air and exhaust air, so there is no direct contact between the air directly blown into the rooms and air which went through the air-ground collector and the labyrint foundation. In our proposed system the outside air is let through a ground-air collector and through a labyrinth foundation into the building. There is a separation of the air into one part used for ventilation and one part for conditioning. The air for ventilation is supplied into the rooms through a separate floor cooling system. The air for the conditioning is used to cool or heat the total building envelope. The ground with its nearly constant temperature is used as source for cooling or heating for the floors, walls and ceilings. Activating of the buildings'

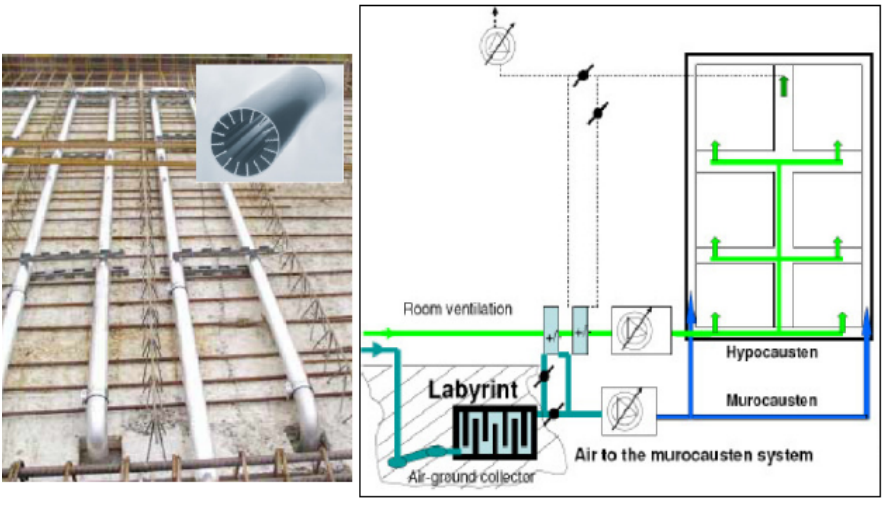

Fig. 7. The concrete core activating system ConcreteCool and Principe schematic of the hypocausten /murocausten system in combination with air-ground collector and labyrinth foundation collector

envelope by air supplied concrete core can be done with the ConcreteCool systems of e.g. Kiefer in combination of hypocausten and murocausten, see the schematic in figure 7.

4 Conclusion

Passive houses are a real hype, but good indoor ventilation is critital. Energy saving and sustainability is very important but not at the risk of endangering health of the occupants. This was the starting point for a new approach, which led to an active house concept. By using ground air collectors, labyrinth foundation, muro-causter and hypocauster, the whole building envelope and construction is thermally activated by natural pre-cooled air in the summer and natural pre-heated air in winter. This principle could play a significant role in the design of healthy buildings and change the present hype of passive building concepts.

References

AIRAH, The Labyrinth cooling federation square. The official Journal of AIRAH (February 2003)

Alley, R., et al.: Climate Change 2007: The Physical Science Basis Summery for Policymakers. In: Intergovernmental Panel on Climate Change, Paris, France (2007)

Balvers, J.R., Boxem, G., de Wit, M.H.: Indoor air quality in low-energy houses in the Netherlands, Does mechanical ventilation provide a healthy indoor environment? In: Proceeding Indoor Air 2008, Copenhagen (2008)

Barton, P., Beggs, C.B., Sleigh, P.A.: A theoretical study of the thermal performance of the TermoDeck hollow core slab system. Applied Thermal Engineering 22, 1485–1499 (2002)

Becker, R.: Computational model for analysis of dynamic thermal performance of a hybrid slab-collector system with passive discharge. Solar Energy 55(6), 419–433 (1995)

Becker, R.: Performance evaluation of an intelligent hybrid floor-collector system. Automation in Construction 6, 427–436 (1997)

Bellew, P.: Energy, Sustainability and influencing Architectural Design. In: CIBSE conference 2004 (2004)

Bellow, P.: Resource)%, New approaches to sustainable cooling for non domestic buildings, Patrick%20Bellew2.pdf (2005)

BINE informationsdienst, themeninfo II/02 Solare Lufsystemen (2002), http://www.kommen.nrw.de/.../object/downloadfile.cgi/Solare_Luftsysteme.pdf?lang=1&oid=1320&ticket=guest

Bordass, W., Leaman, A., Ruyssevelt, P.: PROBE strategic review: Report 4 Strategic Conclusions. Department of the Environment, Transport and the Regions (August 1999)

Bunn, R.: Termite tutors, Building Design (October 29, 2004), http://www.bdonline.co.uk/story.asp?storyCode=3042882

Coldhamarchitects (2006), http://www.coldhamarchitects.com/greenbuilding/greengrandtour/UK_ElizFry/uk_elizfry_desc.htm

De Paepe, M., Janssens, A.: Thermo-hydraulic design of earth-air heat exchangers. Energy and Buildings 35, 389–397 (2003)

DETR, Energy use in offices, Energy Consumption Guide 19, Department of the Environment, Transport and the Regions (1998)

EU (2007), http://europa.eu.int/comm/energy/demand/legislation/domestic_en.htm

Feist, W., Schnieders, J., Dorer, V., Haas, A.: Re-inventing air heating: convenient and comfortable wihin the frame of the Passive House concept. Energy and Buildings 37, 1186–1203 (2005)

Florides, G.A., Tassou, S.A., Kalogirou, S.A., Wrobel, L.C.: Review of solar and low energy cooling technologies for buildings. Renewable & Sustainable Energy Reviews 6, 557–572 (2002)

Hastings, S.R.: Solararchitektur, TASK 19: Solar Air Systems in IEA Solar Heating & Cooling Programme 1998 Annual Report, Morse Associates, Inc. Washington, IEA/SHC/AR 1998 (1998)

Hastings, S.R., Mørk, O.: Solar Air Systems. A design Handbook (1999)

Holdsworth, B.: Energised concrete. Concrete engineering international (2005)

IEA, Rivierdijk, Sliedrecht the Netherlands, Waaldijk, Dalem, the Netherlands, IEA-SCH Task 28/ ECBCS Annex 38: Sustainable Solar Housing (2003)

Kaan, H.F., de Boer, B.J.: Passive Houses: Achievable concepts for low CO2 housing. In: Proceedings ISES conference 2005, Orlando, USA, September 2005, ECN-RX—06-019 (2005)

Kenda, B.: Pneumatology in Architecture: The Ideal Villa. In: Proceedings of Healthy Buildings, Lissabon, June 5-8 (2006)

Kenda, B.: Medical aspects of Renaissance pneumatic architecture, PhD thesis, University of Pennsylvania (1998)

Kiefer, C.: Erfahrungen aus einem Rekord-Sommer. Betonkernkühlung mit Zuluft, Technik am Bau, 12/2003 (2003)

Lane, T.: An answer in the cold, cold earth. Building, 51–53 (March 17, 2006)

Piggins, J.: International CIB W67 Symposium Energy Moisture and Climate in Buildings, September 3-6, Rotterdam. Air Infiltration Review, vol. 12(1) (December 1990)

Pottler, K., Haug, I., Beck, A., Fricke, J., Würzburg: Erdreichwärmetauscher für Wohngebäude, Vermessung, Modellierung und Anwendung, HLH Bd.50. Nr.10 Oktober (1999)

Standeven, M., Cohen, R., Bordass, B., Leaman, A.: PROBE 14: Elizabeth fry building. Building Services Journal 20, 37–42 (1998)

Sansone, C.: Traditional Bio-Climatic Building Techniques. In: Proceedings Sharing Knowledge on Sustainable Buildings, Mediterranaen Conference, Bari, December 16-17 (1999)

Schröder, D.: Betonkernkühlung mit Zuluft, Besser konditionieren mit weniger Energieverbrau, Heizung Lüftung/Klima Haustechnik, Heft 3, seite 47-54 (2002)

SHINE, Solar housing through innovation for the natural environment, EHEN, European housing ecology network, brochure Social housing leads the way in low energy solar design (2005)

Strom, I., Joosten, L., Boonstra, C.: Passive House Solutions, 2006, final version Working paper 1.2 PEP Promotion of European Passive Houses, rapport nr. DHV_WP1.2, 23-05-2005 (May 2006)

Sustainable buildings (2006), http://www.sustainable-buildings.org/viewCaseStudy.php?id=CS6

Thiers, S., Peuportier, B.: Thermal and environmental assessment of a passive building equipped with an earth-toair heat exchanger in France. Sol. Energy (2008), doi:10.1016/j/solener.2008.02.014

Toft, H.: Building structure as heat exchanger – The Legabeam System. CADDET Newsletter (4) (1993)

Wachenfeldt, B.J., Bell, D.: Building Integrated Energy Systems in Smart Energy Efficient Buildings – A state-of-the-art. SINTEF Project report, STF22 A04503 (2003)

Heating Supply in Kazakhstan: Concept - Simulation - Comparison

G. Tleukenova[1], L. Kühl[2], M. Heuer[2], N. Fisch[2], and R. Leithner[1]

[1] Institut für Wärme- und Brennstofftechnik, TU Braunschweig, Germany
g.tleukenova@tu-bs.de, r.leithner@tu-bs.de
[2] Institut für Gebäude- und Solartechnik, TU Braunschweig, Germany
kuehl@igs.bau.tu-bs.de, heuer@igs.bau.tu-bs.de, igs@tu-bs.de

Abstract. Heating and cooling consume a high amount of energy, which is today mainly provided by fossil fuels. To save fossil resources and simultaneously reduce pollutants and CO2 heating and cooling energy consumption should be reduced by improved insulation and renewable energy should be increasingly used. Biomass and solar energy are examples of these renewable energies. The selection of usable technology is dependant on the energy requirements, climate of the area, existing and exploitable renewable resources and economic efficiency. In the paper presented, the simulation of a residential building in the city of Ust-Kamenogorsk, Kazakhstan has been carried out by using two simulation programs (PREBID and IISIBAT from TRNSYS). This work corresponds with the construction standards and the energy-saving regulations. The layout of the zones (heating, cooling, internal gains) was defined in such a way that the operating times and conditions are simulated as accurately as possible. The result of this simulation is the annual heating demand of the high- rise building in Kazakhstan. The building model is designed in the program IISIBAT taking into account the climatic conditions and the effects of human presence. Then different simulations were carried out in order to determine the annual energy demand of the building and whether improvements were needed or not. The obtained results were compared with the simulation results of the same building insulated according to the German EnEV standards. Based on this comparison, various proposals for heating systems are given.

Keywords: simulation, heating requirements, energy systems, TRNSYS, continental climate conditions.

1 Introduction

To provide the energy - and heat supplies of industrial and residential buildings by an increasing share of renewable energy is a very important issue as far as the limited fossil fuel resources, pollutants and CO2 emission are concerned. Kazakhstan has a great potential of renewable energy sources, which includes water and wind power, solar radiation as well as biomass. The resulting energy could become a significant

part of the existing energy supplies of the country, but the potential of renewable energy sources in Kazakhstan is little exploited so far. In the primary energy balance of the country, the share of renewable energy sources is not more than 2%. However, according to various forecasts, in the next fifteen to twenty years, renewable energy sources will have a significant portion in energy requirements. This will save the limited reserves of fossil fuels and reduce the resulting pollutants and CO2 emissions [11].

An important tool for assessing and analyzing the buildings and energy systems are dynamic simulations in computers. With the program "TRNSYS", different building designs with parameter variations can be simulated quite accurately. In carrying out the simulation studies for various locations, the climate conditions have to be accounted for. The following investigation is presented for the location of Ust-Kamenogorsk in Kazakhstan.

2 Research Objective

Research objective is the development of an energy supply concept, which not only guarantees for the buildings under consideration an uninterrupted supply of renewable energy, but is at the same time, economically efficient or at least reasonable. With the help of the simulation program TRNSYS, a one-zone model is created, which determines the heating requirement of the location chosen.

As the first step, the following characteristics of a building are identified:

- Wall-construction and/or U-values (heat transfer coefficients) ;
- Areas of the all zones ;
- Ventilation ;
- Number of occupants.

In the second step, these data are used as input data for TRNSYS [14]. This program is developed by TRANSSOLAR Energietechnik GmbH. For the verification purpose, the building is simulated using the weather data from Germany, so that the simulation results can be compared from statistical verification procedures (e.g., energy saving regulation – EnEV) or with existing performance data of the buildings of similar construction and usage. Later, the heat requirement of the building is determined using Kazakh weather data. The resulting simulation results can be viewed as realistic. The required energy supply systems can be designed by using these simulation results (heating requirement, heating load). A cost analysis and an ecological assessment is included in this investigation.

3 Climate Data

Kazakhstan is the ninth largest country in the world with an area of 2,717,300 km². With its geographical location in the center of Eurasia, there exists an extremely continental climate. Due to the continental climate summer and winter temperatures are extremely different. The average January temperature is -19 ° C in North,

-19.3 ° C in South. In July, the corresponding figures are 20 ° C in the North and 28 ° C in the South. In summer the temperatures can reach 45 ° C and in winter - 45 ° C is possible [2]. For dynamic building simulations, therefore, the climate data from the weather stations near to the building place concerned has been used in the standard weather data format "TM2". The weather data are resolved on an hourly basis. It includes the data on the solar radiation, air temperature, humidity, wind speed and the wind direction.

4 Buildings Description

The investigated settlement in Kazakhstan (Ust-Kamenogorsk) consists of five multi-family homes (134 residents per house) of the same type. Site plan is shown in Figure 1. These buildings are reinforced with concrete skeleton in prefabrication.

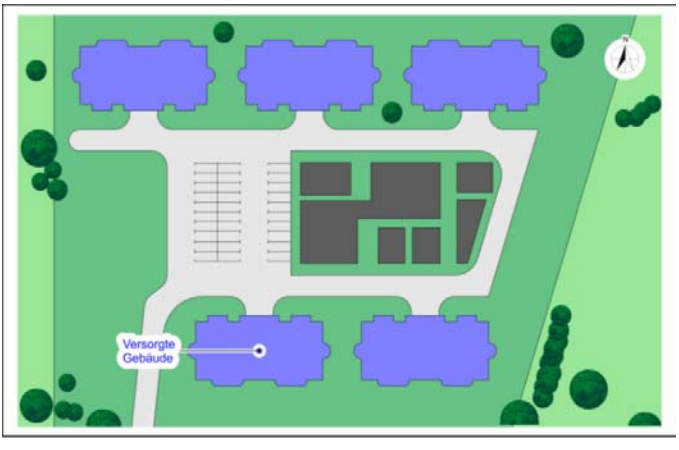

Fig. 1. Site plan of residential building in Ust- Kamenogorsk

Fig. 2. North façade of the building (main entrance)

Fig. 3. Northeastern view of the building

Figures 2 and 3 show north and north-eastern facade. All buildings have basements and flat roofs. Each house has nine floors and two staircases. On the ground floor a large entrance hall and four residence apartments are situated. There are 6 apartments in each floor 2 to 8. In the top floor, there is the technology-center of the building.

5 Applied Usage and Weather Conditions (Boundary Conditions)

The user profiles of the residents used for the simulation are shown in Figures 4 and 5. The required weather is provided by directorate of weather and climate information, Kazakhstan. As an example, the ground temperature at 1 meter depth is shown in Figure 6 throughout a reference year.

In Table 1, wall construction details of the building as well as heat transfer coefficients are presented. The details of the wall construction are taken from the layout plan of the building. The insulation details of the wall e.g. the wall heat transfer coefficient have been chosen according to the German EnEV standard.

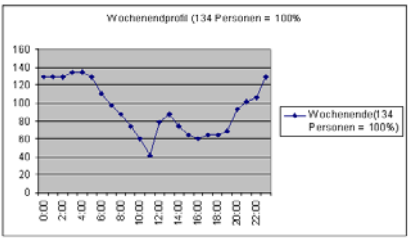

Fig. 4. Weekends profile of the residents

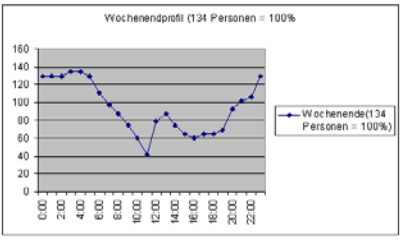

Fig. 5. Weekdays profile of the residents

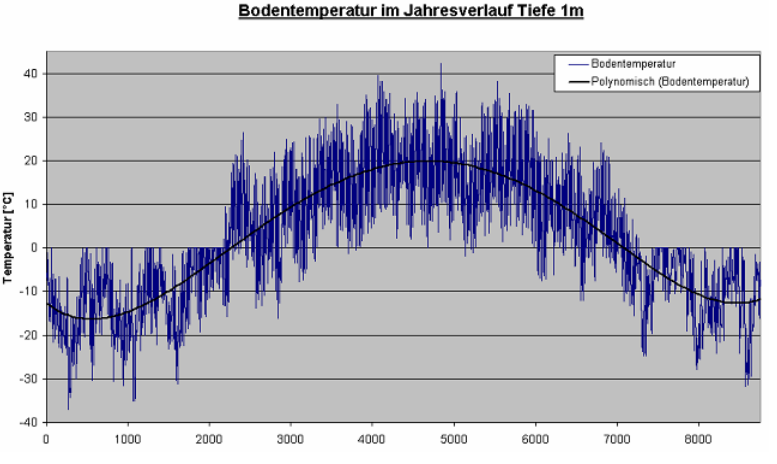

Fig. 6. Yearly changing of the floor temperature (1m deep)

Table 1. Wall construction and heat transfer coefficients (U-values) of the building concerned

2. U-Value - building kazakhstan

Building Part	Floor	Notes	Heat insulation	U-Value	g-Value
				[W/m²K]	
Brick External Wall	EG bis 9. OG	Hollow brick Block 25 cm	WLG 035	0.29	
Concret External Wall	KG bis 9. OG	Precast concret 30 cm	WLG 035	0.29	
Brick Internal Wall	KG bis 9. OG	Hollow brick Block 25 cm	-	1.83	
Concret Internal Wall	KG bis 9. OG	Precast concret 30 cm	-	2.72	
intermediate Floor	KG	Reinforced Concrete 20cm	Foot Fall Sound Insulation	0.74	
Roof	9. OG	Precast concret	WLG 035	0.25	
Window	EG bis 9. OG	-	-	1.70	0.60
External Door	-	-	-	2.40	0.60
Internal Door	-	-		2.50	
Boundary Conditions					
Area	Basement Ceiling (The Basement Heated with primary Insulation)				
Heat Conduction	Optimized with DIN 4108 Bbl.2				
Building Tightness	Without using Blow Door Test (n = 0.5)				

6 Simulation Results of "One-Zone model"

PREBID has been used to define the characteristics of the building e.g. location, orientation and the appropriate climate data as an input. Only One-Zone model has been used in PREBID. The walls of the zone are defined by selecting the right arrangement of layers of materials. All details of the building layout, e.g. windows, doors, floor, inner and outer walls can be defined through PREBID by following the international standards in its given libraries or by user own definitions. After definition of the zone layout, the heating, cooling, ventilation and gains are further inputs of this defined zone. The simulation is corresponding to DIN 4701 (German standard for calculation of the maximum heat requirement). The result of the simulation in PREBID is the heat requirement for the whole building.

ISSIBAT has been used, after knowing the heat requirement of the whole building to find out the relationship between the building and its environment. In Figure 7, the linkage map of the building simulation is depicted.

The required amount of energy in a building is determined with the help of the energy balance. The annual heating requirement is defined as:

$$\text{Heating requirement} = \text{losses} - \text{gains}$$

$$Q_H = Q_T + Q_V - \eta(Q_S + Q_I)$$

Where,

- Q_H: Yearly-Heating requirement [kWh/a]
- Q_T: Transmission loses [kWh/a]
- Q_V: Ventilation loses [kWh/a]
- Q_S: Solar gain [kWh/a]
- Q_I: Internal gains [kWh/a]
- η: Utilization factor[-]: factor, which reduces the monthly or yearly heat gain (internal and passive-solar) in order to get the usable portion of the heat gains.

Figure 9 shows that TRNSYS simulation results are nearly identified to various German standards.

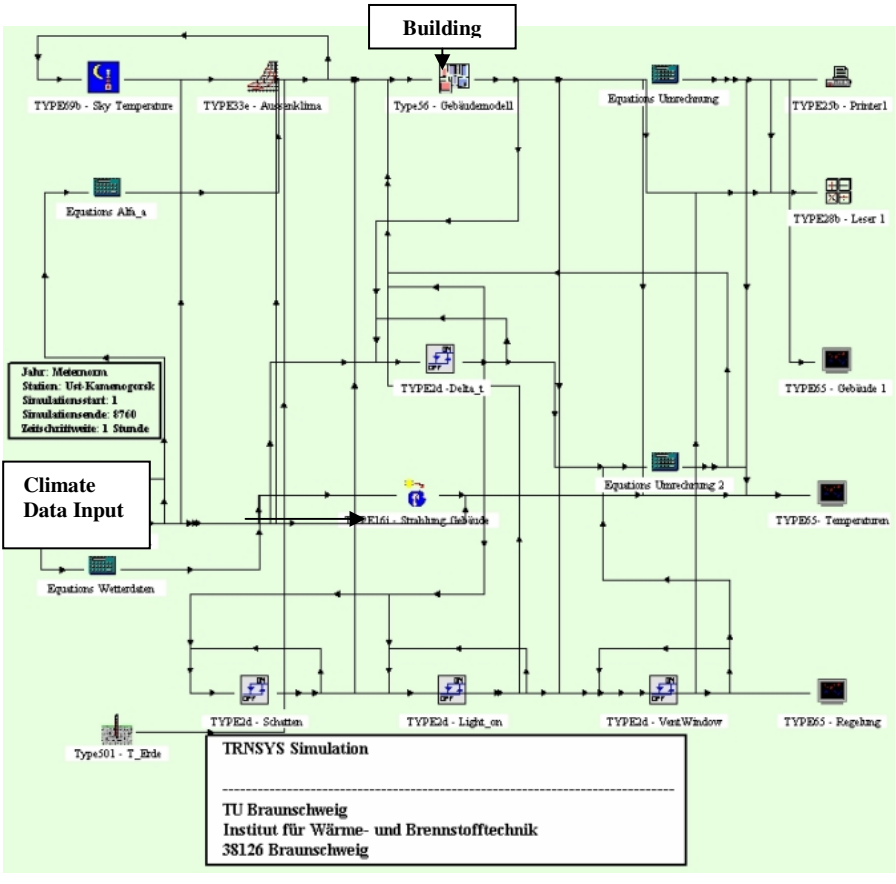

Fig. 7. Linkage map of the building simulation

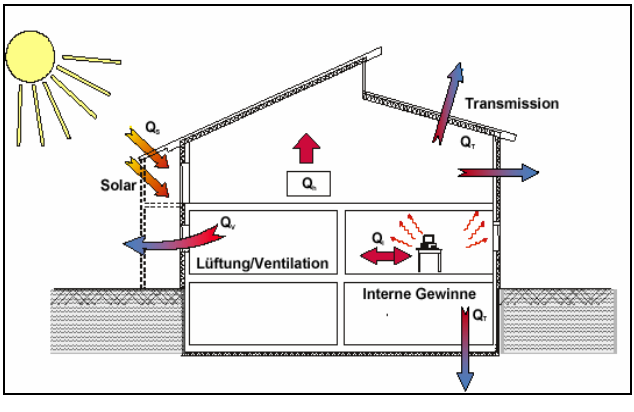

Fig. 8. Heat balance of a building [3]

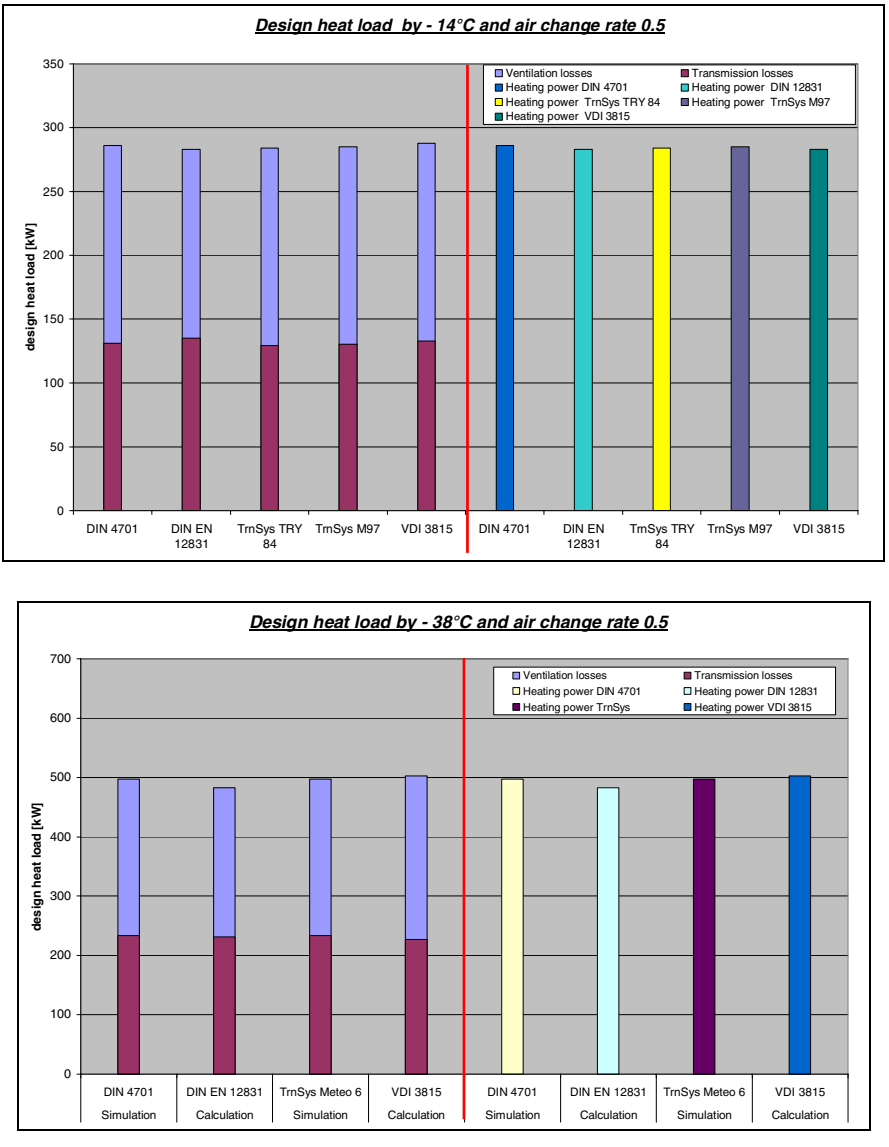

Fig. 9. Identified maximum heat load at -38 ° C

Figure 10 shows the different gains and losses calculated with TRNSYS using weather data from Meteo 6, Meteo 97, TRY 5 and EnEv for Würzburg. The heating demand for the high-rise building with insulation according to German standard EnEV 2007 amounts 365 MWh/a, 468 MWh/a and 533 MWh/a dependant on the used weather data.

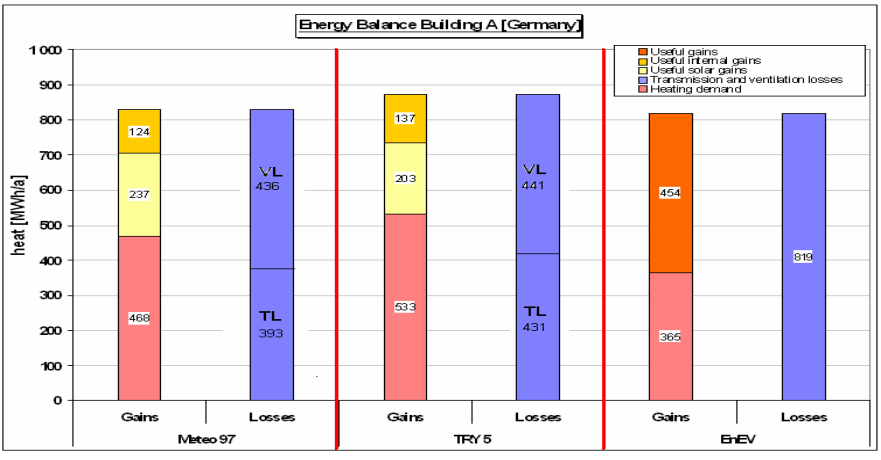

Fig. 10. Energy balance of the building with weather data of Würzburg

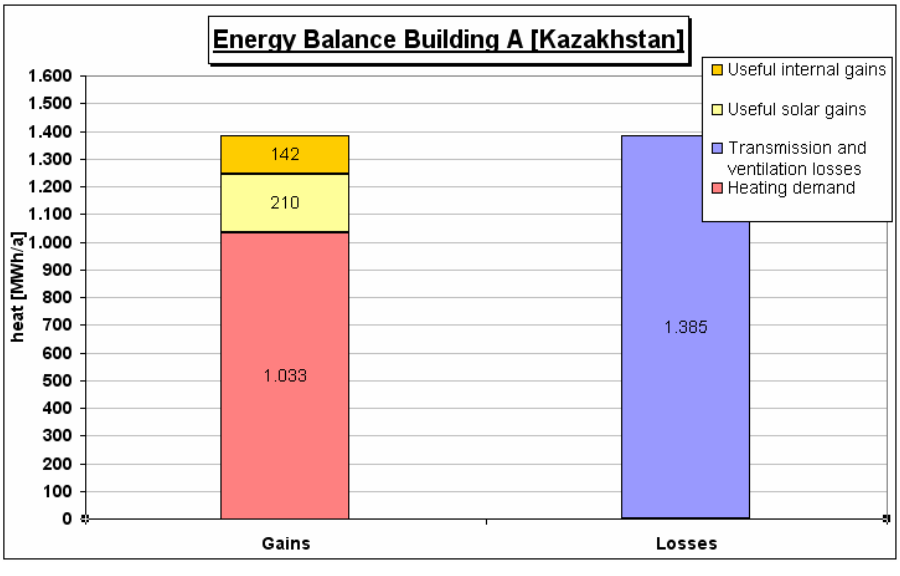

Fig. 11. Energy balance of the building with weather data of Ust- Kamenogorsk, Kazakhstan

Figure 11 shows similar calculations with TRNSYS with weather data of Ust-Kamenogorsk, Kazakhstan. The heat demand of the high-rise building with insulation according to Kazakhstan standards amounts 1033 MWh/a.

A summary of results is presented in the following table 2 where simulation results are compared with energy saving regulation – EnEV.

Table 2. Comparison of the heat consumption

	Simulation TRNSYS	**EnEV**
Concerned living space	8600 m²	8600 m²
Specific heating load [W/m²]	33,4	35…45
Specific heating requirement [kWh/m²a]	52	55…80

7 Future Work – Modeling of Energy System Technology

Since the total heating requirement of the building is now known through simulation, the next important question is to select an appropriate energy supply system. There are many possibilities:

- Decentralized supply by using gas boiler system
- Central supply (local heating supply) by using gas boiler
- Central supply (local heating supply) by using biomass boiler and local heating supply
- Central supply (local heating supply) by using gas boiler and thermal solar energy
- Central supply (local heating supply) by using biomass boiler and thermal solar energy system
- etc.

All these possibilities can be optimized in terms of their costs under local climate conditions and are shown in Figure 12.

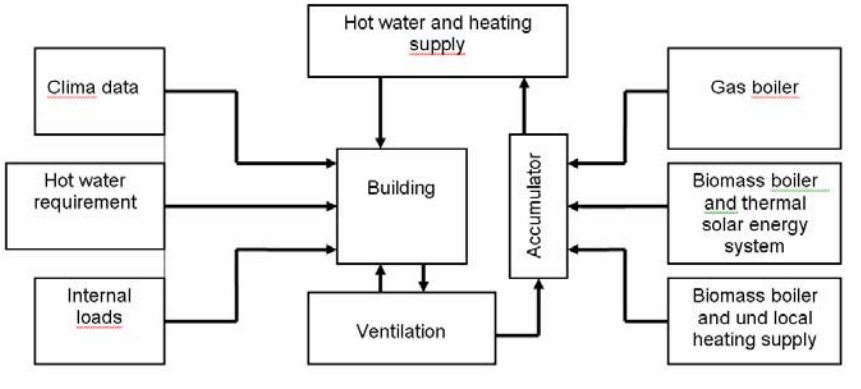

Fig. 12. Energy supply technologies

8 Summary

Within the scope of the work, different variations of the heating supply systems haven been examined for a multi-family building in Kazakhstan. This selected building was simulated using PREBID and IISiBat of TRNSYS. In this model, effect of human presence is also taken into account. The geometry corresponds to a building with heat insulation requirements according to the energy saving regulation valid in Germany. Simulation results are compared with the energy saving regulation – EnEV. The simulation results of the building in Kazakhstan show very high heat requirements because of the weather conditions in Kazakhstan. In the second step, different technology variations for the heating, ventilation and hot-water supply are defined. The objective is the reduction of the primary energy demand and emissions and low operational costs through optimization and by using reasonably competitive renewable energy.

References

1. Zimmermann, M.: Handbuch der passiven Kühlung. Verlag Fraunhofer IRB (2003)
2. Pech, A., Jens, K.: Heizung und Kühlung. Springer, Wien (2005)
3. FISCH, Klimatechnik. Bauphysik Vorlesung (18). Technische Universität Braunschweig (2007)
4. Ihle, C.: Klimatechnik mit Kältetechnik. Verlag Werner. 4. Auflage (2006)
5. Höper, F.: Primärenergetischer Vergleich von Verfahren der solar unterstützen Kühlung zur Gebäudeklimatisierung. Dissertation. Verlag Shaker (1998)
6. Forschungs Verbund Sonnenenergie von Nordrhein-Westfallen, Wärme- und Kälteenergie aus Sonne und Erde. Jahrestagung (2005)
7. Simader, G.R., Rakos, C.: Klimatisierung, Kühlung und Klimaschutz: Technologien, Wirtschaftlichkeit und CO_2-Reduktionspotenziale. Austrian Energy Agency (2005)
8. FISCH, Lüftungsgrundlagen. Bauphysik Vorlesung (11). Technische Universität Braunschweig (2007)
9. http://www.energiepfahl.com
10. Hanschke, T.: Planung, Errichtung und Betrieb von Energiepfahlanlagen. Stuttgarter Geothermietag. H. S. W. Ingenieurbüro für Angewandte und Umweltgeologie Rostock (2008)
11. http://www.asie-centrale.com/kazahkstan
12. Christoffer, J., Deutschländer, T., Webs, M.: Testreferenzjahre von Deutschland für mittlere und extreme Witterungsverhältnisse. Deutscher Wetterdienst (2004)
13. Energieeinsparverordnung und Energieausweise, Rechnerischer Nachweis, Baukonstruktion und Haustechnik für Neubauten und Bauten im Bestand. Verlag Forum (2006)
14. Transsolar Energietechnik GmbH. PREBID. An interface for creating the building description of Type 56 (multi zone building) Version 4.0. Bedienungsanleitung
15. CSTB. IISiBat. The Intelligent Interface for the Simulation of Building. Version 3.0. Bedienungsanleitung

Towards a More Holistic and Complementary Approach to Modelling Energy Consumption in Buildings

Stephen Pullen

School of the Natural and Built Environments, University of South Australia
stephen.pullen@unisa.edu.au

Abstract. The need to reduce energy consumption in buildings is clearly recognised as a necessary contribution to the minimisation of greenhouse gas emissions. To complement the focus on the energy performance of individual buildings, this paper suggests additional approaches which include life cycle energy analysis in combination with urban energy mapping techniques. Commencing with an overview of energy consumption in the built environment, the paper draws attention to other components of urban energy consumption such as the embodied energy of buildings and infrastructure. The different approaches to modifying energy usage are placed in the context of scale in the built environment and complexity of urban energy improvements. Recent attempts to influence energy consumption patterns across this scale are referred to by using the city of Adelaide in South Australia as an example. Some research projects are described which take a range of approaches to modelling energy usage in buildings. These offer potential for analysing changes to overall energy consumption such as the retrofitting of buildings, selection of alternative dwelling forms and the design of urban redevelopments.

1 Introduction

The imperative to moderate energy consumption in buildings is well established in many parts of the world. It is driven by a number of reasons including financial costs, the minimisation of supply dependency and the desire to reduce environmental impact. Buildings which are more energy efficient are being encouraged by minimum performance building regulations and voluntary codes which reward high performers. In addition, technological developments in improved building envelopes, more efficient appliances and novel building services are contributing to this aim. The focus for this effort is on the basic unit of the built environment which is the individual building and this quite justifiably tends to highlight the importance of reducing operational energy consumption in new building designs.

An alternative perspective is to view the urban environment more holistically in tackling the challenge of moderating energy usage. This approach acknowledges new energy efficient buildings but in the context of the substantial existing building stock and urban infrastructure. It has the potential for taking a life cycle approach to energy consumption in the built environment including other energy inputs such as the energy used in construction and materials manufacture as well as operational energy

used in buildings. Furthermore, a more comprehensive analysis provides the possibility of investigating the effects of different residential and non-residential building types, alternative urban configurations and transport infrastructure.

The purpose of this paper is to draw attention to the potential advantages of a more holistic and complementary approach to the analysis of energy consumption in buildings. The first part of the paper considers some of the broader issues of urban energy usage and this is followed by the case study of Adelaide, South Australia which provides an example of specific developments in this field including that of research into modelling.

2 Energy Consumption in Buildings

The benefits of modern urban settlements are self evident in terms of providing housing, employment, education, health services and public transport. However, the construction, operation and maintenance of the buildings and infrastructure require resources, materials and energy (ESCAP, 2007). In particular, the dependence on fossil fuels as the energy source can present a number of disadvantages and the solution to this problem is subject to much research (Droege, 2006).

In developed countries, buildings consume a substantial portion of a nation's energy usage depending on many factors including the structure of the economy and climate. For instance, in a more service oriented economy such as that in the UK, buildings and the activities carried out therein account for approximately 41% of the final national energy consumption (DTI, 2007). These buildings include those in both the domestic sector (households) and the services sector (commercial buildings, public administration, education and health). This compares with approximately one fifth of final national energy consumed in the residential and commercial building sectors in Australia where a significant portion of the economy and energy usage is devoted to primary industries (Ceuvas-Cubria and Riwoe, 2006).

However, regardless of the proportions reported, the statistics relate to the operational energy required for buildings. They are not intended to account for the energy used on construction sites (normally included in the industry sector data), energy used to produce and manufacture building materials and components (also a significant part of the industry sector data) and the energy used to transport building materials (included in the transport sector data). Hence, the energy consumption of buildings has been shown to be even more significant when both the indirect and direct energy usage is considered from the activities of construction, materials production and building operation (Fay et al, 2000; Mithraratne and Vale, 2004). This has implications for the effects of greenhouse gas emissions arising from the full life cycle of buildings in countries where energy generation is dominated by fossil fuel consumption (DECC, 2008).

The life cycle energy analysis approach is useful to ensure that short term energy savings do, in fact, result in reductions in energy usage in the longer term. Consequently, the method has been used for assessing alternative construction materials and components to determine the lower energy options (Treloar, 2000; Treloar et al, 2004; Huberman and Pearlmutter, 2008). The method has also been applied to solar powered water heating services (Crawford and Treloar, 2006) where conventional

appliances were compared with solar alternatives. In New South Wales, Australia, a life cycle energy assessment of 20 schools was carried out to establish environmental performance criteria for the design and construction of future education buildings (Ding, 2007).

Other than operational energy, a significant energy input to the life cycle of buildings is that of the embodied energy of materials and components from which buildings are constructed. This includes both the embodied energy of the materials as used in new buildings (initial) and that of further materials required for refurbishment, renovation and periodic maintenance (recurrent). The life cycle analysis of 20 schools by Ding (2007) indicated that initial and recurrent embodied energy was approximately 38% of the life cycle energy usage (combined embodied and operational). A similar proportion was found by Langston and Langston (2007) in a survey of 30 residential, public, education and medical buildings in Melbourne, Australia. The significance of embodied energy has been recognised in building rating schemes such as BREEAM (UK), LEED (US) and Green Star (Australia) whereby the specification of low embodied materials is rewarded in construction projects by scoring more 'points' (Dickie and Howard, 2000). The quantitative assessment and comparison of operational energy and embodied energy of new buildings is not commonplace. However, this may become more frequent for new 'green' developments as it provides a means of estimating total greenhouse gas emissions and offers a mechanism for attempting to design, construct and operate buildings with a minimal life cycle carbon dioxide output. An example is that of the 'green village' residential development at Lochiel Park in South Australia where biosequestration is being considered to offset life cycle carbon dioxide emissions arising from both operational and embodied energy consumption (Cohen and Oliphant, 2008).

3 Energy Consumption in the Built Environment

The modification of existing buildings and urban form offers great potential for reducing energy consumption and other environmental impacts. A report by the Royal Institution of Chartered Surveyors (McAllister and Sweett, 2007) commented on opportunities and progress by the construction and property industry in the UK in reducing the environmental impact of the existing building stock as follows:

> Typically, these opportunities have been missed and previous efforts to improve environmental performance have primarily targeted new buildings. Existing building stock represents 98-99% of buildings in the UK at any time. New buildings add between 1% and 1.5% to building stock each year. Improving the sustainability performance of existing stock is a key opportunity that should be pursued. (McAllister and Sweett, 2007).

Such opportunities could arise from the construction of new compact and mixed use developments, the densification of older suburbs or the retrofitting of existing buildings. A more holistic approach to the analysis of development offers the potential for exploiting past embodied energy expenditure to lower overall life cycle consumption in the future. There are strong arguments in favour of substantially changing urban form in order to reduce energy consumption as this can include savings in transport and embodied energy as well as moderating the operational energy of buildings. The argument for more dense urban design with less resources is well known and there

has been commentary on possible correlations between building density and materials/energy consumption (Roberts, 2007; Salat, 2007). This also extends to engineering infrastructure since more compact forms of urban development bring about efficiencies in the provision of services (Schiller, 2007). The complexities of designing urban areas within cities to minimise energy consumption have been discussed by Steemers (2003) who showed that the arguments for and against densification were finely balanced when all energy inputs were considered.

There have been a number of examples of the modelling of energy consumption in the built environment to gain a better appreciation of the effects of different building types and alternative urban configurations on energy demand and greenhouse gas emissions including that by Yamaguchi et al (2007) based on Osaka city, Japan. Other researchers have based their models on spatial software platforms thereby providing maps of urban energy consumption or greenhouse gas emissions such as Jones et al (2001) in Cardiff, Wales; Gupta (2005) in Oxford, England and Tornberg & Thuvander (2005) in Goteborg, Sweden. These provide a convenient method of depicting operational energy consumption (or the associated emissions) using geographical information systems.

The combination of life cycle energy analysis and the spatial depiction of energy consumption (and associated emissions) offer the potential for a more comprehensive means of analysing energy consumption in the built environment. It can include the energy required for the provision and operation of urban infrastructure such as water supply and disposal, sewage systems, roads, railways and other transport systems as well as buildings. In addition, the consideration of the existing built form in terms of embodied energy of materials opens up the possibility of including re-used and recycled materials in the energy analysis. This is shown conceptually in Figure 1 which indicates improvements in urban energy usage commencing with new energy efficient buildings through to the retrofitting of existing buildings and finally to increasingly challenging developments which involve the re-use and reconfiguration of the existing built form. There is also an urban design and planning dimension to this as greater integration is required as the scale of development increases.

This implies greater complexity in construction from greenfield development to the exploitation of materials, buildings and infrastructure currently existing on brownfield sites. To achieve the optimum energy outcomes, there needs to be a broadening of the development agenda to embrace a more holistic framework and this requires the analysis of the long term dynamics of building and infrastructure stocks (Kohler, 2007).

The arguments for broadening the agenda for energy modelling in the built environment reflect the more general debate about taking a bottom-up or top-down approach to energy analysis and greenhouse gas emissions. In a review of energy modelling in the context of climate change, Grubb et al (2006) described the separate development of top-down and bottom-up models in the 1980s and 1990s. Since that time, there have been many examples of models combining the two approaches including using bottom-up information in top-down models (Koopmans and te Velde, 2001; McFarland et al, 2004) and coupled bottom-up/top down models (Drouet et al, 2005). The coupled or hybrid approaches can provide a macro perspective in combination with technology sensitive changes occurring at the smaller scale.

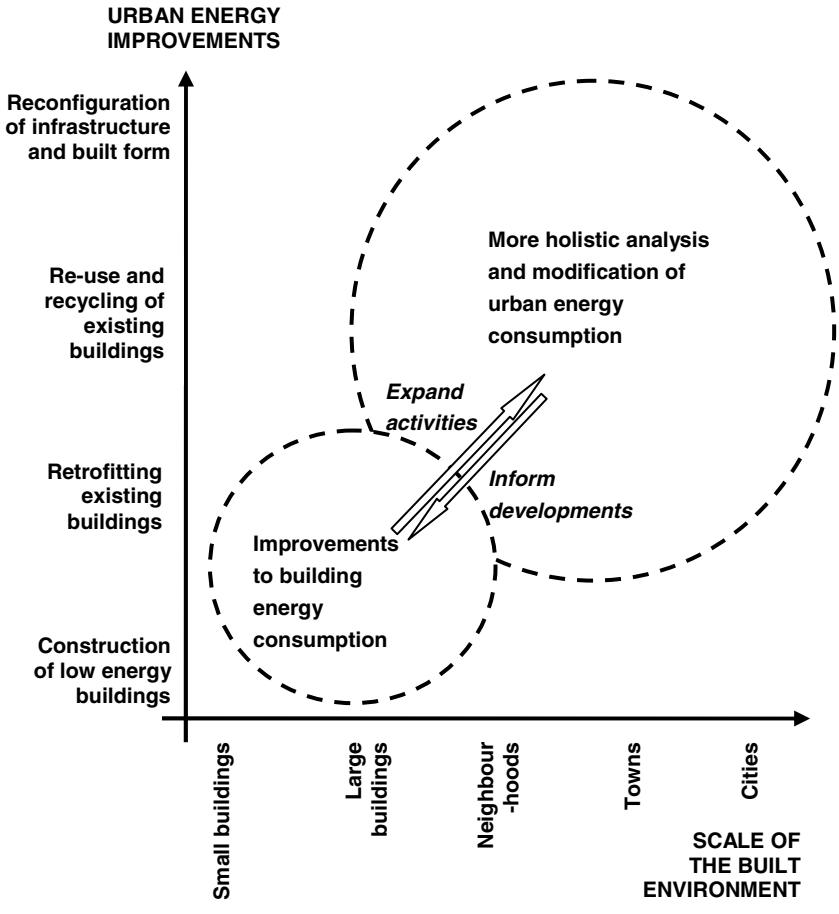

Fig. 1. Relationship between urban energy improvements and built environment scale

The principle of using an integrated approach can also be adopted for energy analysis and energy efficiency improvements in buildings, and a range of initiatives is required across the scale of the built environment. Such initiatives are occurring in many locations and the following section on developments in South Australia provides an example of this.

4 Adelaide, South Australia as an Example – Background

Many nations, states and provinces around the world have now instigated measures aimed at mitigating the effects greenhouse gas emissions and these include the moderation of energy usage in the built environment. This section uses South Australia as an example of such initiatives and describes some of the rapid changes that have

occurred relating to energy consumption and greenhouse gas emissions in the context of climate change. This forms the backdrop for the discussion of some recent research into the more holistic analysis of urban energy consumption.

South Australia is a large state covering nearly 1 million square kilometres but with a small population of around 1.6 million people of which approximately 70% reside in Adelaide which is the state's capital city. Greenhouse gas emissions are estimated to be at about 20 tonnes of carbon dioxide equivalent per person which is 30% lower than the national average but about four times the world average (SA Govt, 2007). In order to contribute to the global effort to moderate greenhouse gas emissions from the consumption of fossil fuels, the South Australian Government passed the Climate Change and Greenhouse Emissions Reduction Act in 2007 making it the first state in Australia to legislate targets for this purpose. The Act details a series of strategies to address climate change and was developed through consultation with over 600 people from industry, the community, academia, local councils and government. It builds upon elements of the state's Strategic Plan which commits to the Kyoto target aiming to reduce emissions by 60% (to 40% of 1990 levels) by 2050 and sets a target of 20% for renewable electrical energy by 2014. The Act describes six sectors in the economy including the Buildings and Transport/Planning sectors with government initiatives spanning the range from innovative building technologies to larger scale urban planning strategies.

With respect to building technologies, the Residential Energy Efficiency Scheme (REES) has been introduced to encourage energy providers to offer householders incentives to adopt energy saving measures such as insulation, draught proofing, retiring second fridges and installation of more efficient lighting and appliances. Furthermore, from the middle of 2008, it was mandated that replacement water heaters installed in most existing homes in South Australia should be low emission types such as high efficiency gas, solar or electric heat pump. In addition, households with solar photovoltaic panels will be rewarded for putting power back into the electricity grid by means of the Electricity Feed-in Scheme which will pay a premium guaranteed tariff of over double the normal price.

A quite separate scheme supported by the Commonwealth Government has selected Adelaide as one of seven regions in Australia for the Solar Cities program which is aimed to change the way individuals, communities, businesses and governments use energy. Focusing on the city centre and northern suburbs, it will trial the latest solar photovoltaic systems, provide innovative financial packages to local residents to make household photovoltaic installations more affordable and supply 'smart meters' so that residents can take advantage of cost and energy saving benefits of new electricity tariffs.

On the scale of larger facilities, new South Australian government buildings have to be constructed to achieve a minimum 5 star rating and the government's building stock must reduce energy consumption by 25% by 2014. The importance of existing commercial buildings has also been recognised in the challenge to moderate energy consumption and these will be targeted in the Building Tune Ups-2012 Project which aims to improve the performance of office accommodation in the Adelaide central business district and reduce greenhouse gas emissions by approximately 70,000 tonnes a year. This follows a Stage 1 trial in which ten central business district buildings owned by both government and the private sector were selected for benchmarking and

improvement in energy and water consumption. New suburban initiatives include a 'green village' at Lochiel Park which has been designed to achieve a 74% reduction in operational greenhouse gas emissions for housing when compared to the average Adelaide home and is likely to become Australia's first proven carbon neutral housing development utilising carbon offsets from trees and plants.

On the broader urban scale, renewable energy sources offer the potential for significant reductions in greenhouse gas emissions. Presently, South Australia generates over half of Australia's wind power (Rann, 2008) and approximately 45% of the country's solar power with a state population which is just 8% of the nation's total. With regard to land use planning, stated priorities for the future recognise the influence that the built form and infrastructure can have on urban energy consumption. The aim is for more compact neighbourhoods with co-location of complementary industries and expansion of services at the local level. The concept of transit oriented developments (TODs) which encourage denser mixed-use buildings in urban centres connected by efficient public transport is seen as a priority for urban redevelopment in the longer term for achieving a more sustainable city. Travel behaviour is a target for change so as to discourage high emission forms of transport and encourage low emission technologies. This will include bicycling programs, public transport service upgrades and urban corridor initiatives. Hence, the example of South Australia demonstrates the scale of measures that can be adopted to modify energy consumption in the built environment ranging from new technologies in particular types of buildings to larger scale urban redevelopments.

5 Research on Energy Consumption Modelling in the Built Environment in South Australia

Research is being carried out in Adelaide, South Australia which provides a more holistic approach to modelling energy consumption. This section describes some of this work and shows that the research spans the scale from individual buildings to urban areas.

To determine the renewable energy potential of installing solar hot water devices and solar photovoltaic panels on the roofs of buildings, Kellett and Hamilton (2008) undertook an analysis of the local government council of Playford which is 346 sq km in area to the north of Adelaide city centre. By using geographical information systems (GIS) techniques, they selected a sample of houses which were used to identify north facing roofs (for maximum solar collection in the southern hemisphere) which amounted to a total area of 1.27 sq km and represented 9.1 PJ of available solar resource. The installation of a solar hot water device and a $8m^2$ (1000W) solar photovoltaic panel on each dwelling would provide approximately 50% of the baseline electricity demand for residential property. Furthermore, it was feasible with larger panels to achieve an output of 1.47 PJ which is similar to the current baseline demand.

Other research has aimed to take a life cycle approach to energy modelling. It was considered that a method to comprehensively model energy consumption in the built environment would have significant advantages for monitoring progress towards a lower emissions future as it may provide alternative options for achieving the same goal. Such a method would need to be able to combine the different urban energy

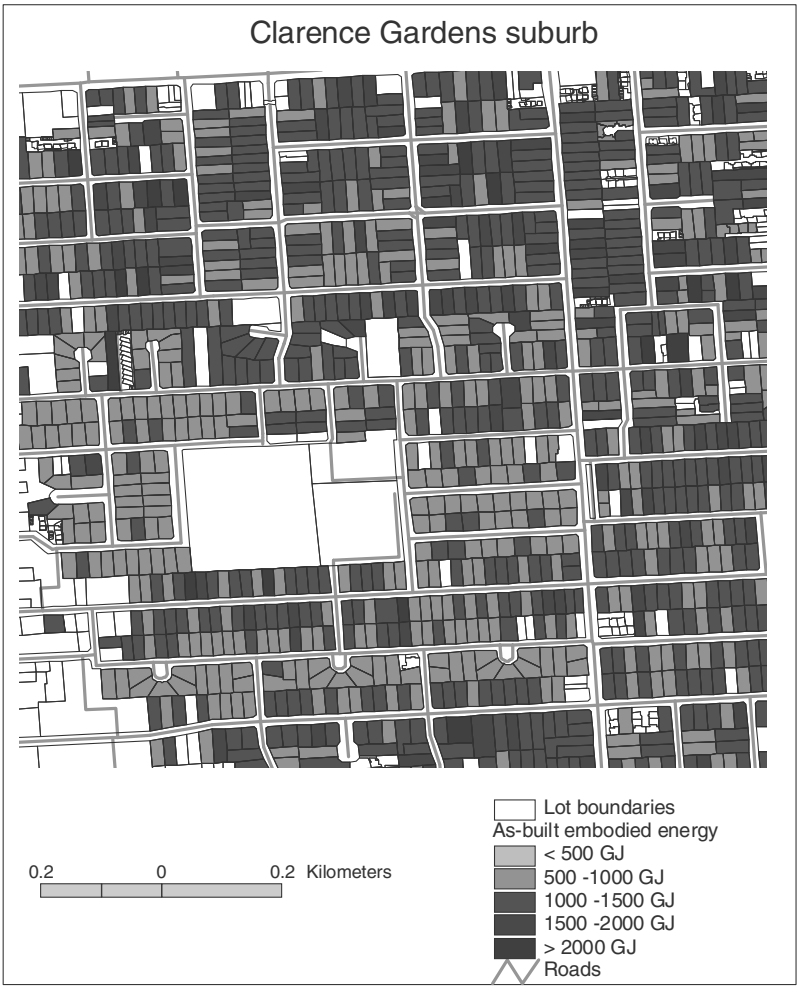

Fig. 2. Embodied energy of single storey detached houses in the Clarence Gardens suburb

inputs consisting of the embodied energy of buildings and infrastructure, operational energy and transport energy. Assuming all of the data could be collected, its depiction could be accommodated using a spatial dimension as provided by GIS software. This would allow for the addition of the various energy inputs by superimposition over the embodied energy usage. The following provides a brief description of a model which spatially represents the embodied energy of residential urban areas in Adelaide, South Australia. A more detailed account of its development including the modelling methodology and sources of data is given elsewhere (Pullen, 2007). Validation of the model has been undertaken by assessing the potential for error in the databases used and will vary depending on the energy system boundary selected.

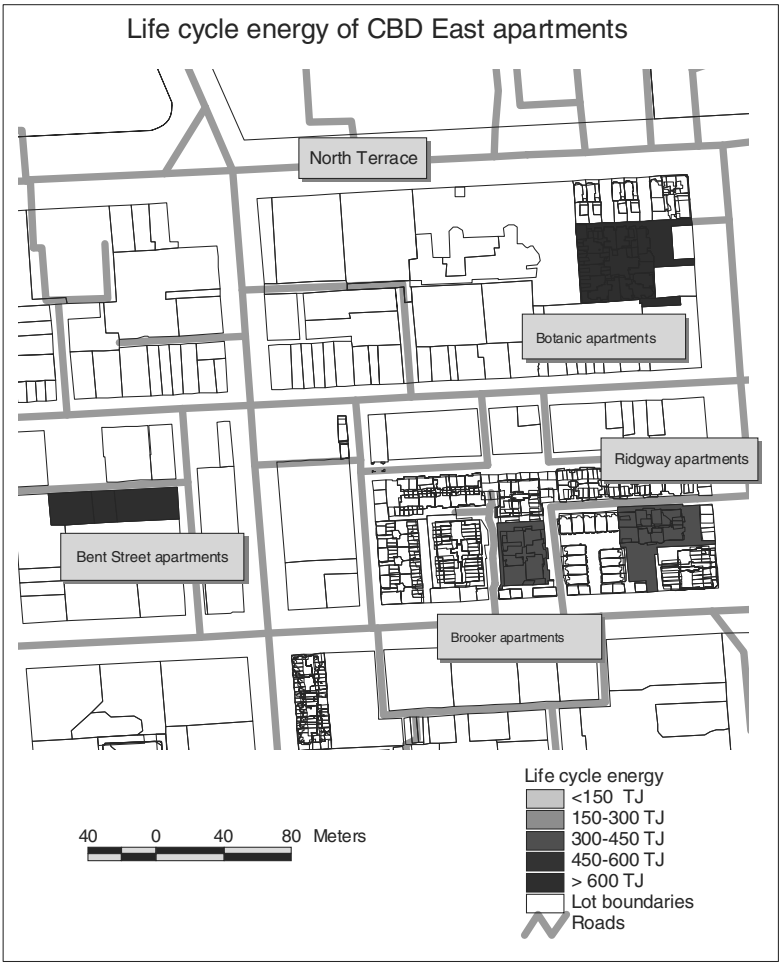

Fig. 3. Life cycle energy of apartment buildings to the east of Adelaide CBD

The model for spatially representing the embodied energy consumption of residential areas has three components which are property register data, embodied energy theory and geographical information systems (GIS) software. The property register provides data about buildings including age, floor area, number of storeys and some basic information on building materials. This information can be used to compile a materials inventory for each building which forms the basis for estimating embodied energy using embodied energy coefficients calculated for individual building materials and components. Each property record requires interrogation using a computer algorithm to extract the necessary information which provides the data files for use with ArcView GIS software. The results for the inner Adelaide suburb of Clarence Gardens are shown in Figure 2 indicating the range of embodied energy consumption for single storey houses in units of GJ. Unshaded plots indicate other types of land use

such as recreational areas or non-residential buildings which have not yet been evaluated for embodied energy mapping. Depending on the availability of property register data, the method used to derive the model can be applied to other urban locations.

Although the embodied energy at the time of construction is shown i.e. as-built embodied energy, it is feasible to depict recurrent embodied energy based on the age of the buildings. In addition, the embodied energy of urban infrastructure such as roads, water supply and disposal systems and sewage pipes associated with each dwelling can be added. For some types of analysis, it may be preferable to spatially depict the greenhouse gas emissions associated with the embodied energy consumption and the model allows for this. If data on operational energy is available for individual buildings, this can be aggregated with the embodied energy data to indicate life cycle energy consumption.

It is envisaged that this type of modelling will be used in the investigation of urban densification and redevelopment to estimate future energy outcomes when all energy inputs are considered. Although higher densities for dwellings in cities are seen as more energy and resource efficient, the findings of some recent research in Adelaide indicate that this relationship may not be entirely clear (Perkins et al, 2007). In this study, the energy consumption and greenhouse gas emissions of households in 41 high density city centre apartments (in the east of the Central Business District) were compared with those from 48 medium density inner suburban households (at Norwood) and 164 low density outer suburban households (at Seaford).

The energy inputs considered for the buildings were the operational energy and embodied energy of dwellings thereby taking a life cycle approach to building energy consumption. Figure 3 depicts the life cycle energy consumption for the four city centre apartment buildings considered. Despite the detailed nature of the South Australian property register, information on multi-storey residential and non-residential properties is limited and it is not possible to interrogate the property register in the same manner as for houses. Hence, the embodied energy of the apartment buildings was derived from first principles. Inventories of the building materials were derived from surveys and inspection of construction drawings and appropriate embodied energy coefficients were used to estimate the as-built embodied energy for each building which was then entered into the GIS data files for depiction as a map. Factors were applied to allow for recurrent embodied energy used in periodic maintenance activities. The annual operational energy for the 2006 period was acquired by means of a questionnaire completed by the sample of apartment households (Perkins et al, 2007).

To form a more comprehensive analysis, transport operational and embodied energy expended by the households were also evaluated. For comparison purposes, annual energy inputs were aggregated and for this reason the embodied energy data for buildings was annualised according to estimates for the expected life of the apartments and houses. The results of the analysis showed that the total emissions *per household* were highest for the outer suburban location as these were strongly influenced by the transport emissions resulting from greater commuting distances. However, when calculated on a *per capita* basis, the households of certain apartment buildings had the highest emissions reflecting the lower number of occupants per apartments and moderately higher embodied energy in high rise buildings. These results indicate that dwelling form and occupancy of inner city developments may be

important in ensuring lower energy outcomes and greater consideration should be given to investigating alternative design configurations.

A more holistic approach to modelling energy consumption has also been proposed for the redevelopment of the regional centre of Noarlunga which is 30km to the south of the Adelaide CBD (Ness et al, 2008). This centre is projected to grow significantly in the future but this needs to occur in a more environmentally sustainable manner using less resources and energy and producing fewer emissions and waste. Currently, the location is characterised by low density development including a shopping centre, education and medical facilities, large car parks and an under utilised railway connection. Urban consolidation is seen as a probable solution by integrating public transport with higher density development. The comparison of alternative redevelopment proposals using analytical techniques such as the model described above, provides a means of indicating the lower overall energy options. These are likely to exploit the use of existing materials, built form and infrastructure with corresponding savings in embodied energy compared with other options based predominantly on demolition and all new facilities. This provides an example of research which is aimed at the larger urban scale of neighbourhoods and regional centres.

6 Conclusions

It is recognised that changes to patterns of energy consumption in the built environment are necessary for various reasons, not least of which is to minimise greenhouse gas emissions arising from the use of fossil fuels. Improvements to the energy efficiency of buildings provide an obvious means by which this can be achieved and this includes better building envelope performance as well as alternative services based on renewable energy sources. Although improved building designs can contribute to this effort, the modification of the existing built form and infrastructure offers considerable scope for further changes. In other words, reducing energy consumption in the built environment requires strategies across the range of urban scale.

The use of models which incorporate life cycle energy analysis and provide a spatial dimension to energy consumption offers a further method for evaluating new building projects. They have the potential for the comparison of inner and outer city developments and different forms of dwellings, for the assessment of energy required for refurbishment and maintenance, and for the modification of the existing building stock to determine lower energy options. This type of modelling and measurement of energy usage, which takes into account other inputs besides operational energy can provide a means for selecting more sustainable options in the redevelopment of existing urban areas. This provides a more holistic approach to the understanding of energy consumption and is a useful complement to other methods for analysing energy usage at the various scales of the urban environment.

Acknowledgments. The contribution of colleagues from the School of the Natural and Built Environments at the University of South Australia to research summarised in the papers by Perkins et al (2007 and Ness et al (2008) and referred to in this paper is gratefully acknowledged.

References

Ceuvas-Cubria, C., Riwoe, D.: Australian Energy. National and State Projections to 2029-30. Australian Bureau of Agricultural and Resource Economics (ABARE) Research Report 06.26, Canberra (December 2006) ISBN 1 920925 81 3

Cohen, L., Oliphant, M.: Lochiel Park and CO_2 Report for Land Management Corporation. South Australian Government by the Australian Carbon Biosequestration Inititiative Ltd. (January 2008)

Crawford, R., Treloar, G.: Life-cycle energy analysis of domestic hot water systems in Melbourne, Australia. In: Proceedings of 40th Annual Conference of the Architectural Science Association, Adelaide (November 2006)

Dickie, I., Howard, N.: Assessing environmental impacts of construction - Industry consensus. BREEAM and UK Ecopoints BRE Press (2000)

Ding, G.: Life Cycle Energy Assessment of Australian Schools. Building Research & Information 35(5), 487–500 (2007)

Droege, P.: Renewable City - a comprehensive guide to an urban revolution. John Wiley and Sons, Chichester (2006)

Droet, L., Haurie, A., Labriet, M., Thalmann, P., Vilee, M., Viguier, L.: A Coupled Bottom-Up/Top-Down Model for GHG Abatement Scenarios in the Swiss Housing Sector. In: Loulou, R., Waaub, J., Zaccour, G. (eds.) Energy and Environment, ch. 2, pp. 27–59. Springer, US (2005)

DTI. Meeting the Energy Challenge: a White Paper on Energy. Department of Trade and Industry. CM7124. HM Government. UK Energy Sector Indicators 2007 supplement (2007), http://www.berr.gov.uk/files/file39511.pdf (accessed January 2, 2009)

DECC. UK Energy Sector Indicators 2008 Background Indicators Fossil fuel dependency in OECD countries and Russia. Chart E5.5 p41. Department of Energy and Climate Change. HM Government (2008), http://www.berr.gov.uk/files/file48502.pdf (accessed January 2, 2009)

ESCAP. Green Growth at a Glance: The Way Forward for Asia and the Pacific. Economic and Social Commission for Asia and the Pacific (ESCAP). United Nations (2007)

Fay, R., Treloar, G., Iyer-Raniga, U.: Life-Cycle Energy Analysis of Buildings: a Case Study. Building Research & Information 28(1), 31–41 (2000)

Grubb, M., Carraro, C., Schellnhuber, J.: Technological Change for Atmospheric Stabilization: Inotroductory Overview to the Innovation Modeling Comparison Project. The Energy Journal. Endogenous Technological Change and Atmpsopheric Stabilisation Special Issue 27, 1–16 (2006)

Gupta, R.: Investigating the potential for local carbon emission reductions: Developing a GIS-based Domestic Energy, Carbon counting and Reduction Model (DECoRuM). In: Proceedings of the 2005 Solar World Congress, Orlando, Florida, USA, August 6-12 (2005)

Huberman, N., Pearlmutter, D.: A Life=Cycle Energy Analysis of Building Materials in the Negev. Desert Energy and Buildings 40(5), 837–848 (2008)

Jones, P., Lannon, S., Williams, J.: Modelling Building Energy Use at Urban Scale. In: Proceedings of the 7th International Building Performance Simulation Association (IPSA), Rio de Janeiro, Brazil (August 2001)

Kellett, J., Hamilton, C.: Low Carbon Futures: Renewable Energy Potential in Playford. In: Proceedings of the Australian Institute of Building Surveyors (AIBS) South Australian Conference - Climate Change: Engaging the Elements, Barossa Valley, South Australia, pp. 1–20 (2008)

Kohler, N.: Long-term Management of Building Stocks. Building Research & Information 35(4), 351–362 (2007)

Koopmans, C., te Velde, D.: Bridging the Energy Efficiency Gap: Using Bottom-Up Information in a Top-Down Energy Demand Model. Energy Economics 23, 57–75 (2001)

Langston, Y., Langston, C.: Building Energy and Cost Performance: and Analysis of Thirty Melbourne Case Studies. The Australasian Journal of Construction Economics and Building 7(1), 1–18 (2007)

Mithraratne, N., Vale, B.: Life Cycle Analysis Model for New Zealand Houses. Building and Environment 39, 483–492 (2004)

McAllister, I., Sweett, C.: Transforming Existing Buildings: the Green Challenge Final Report. Royal Institution of Chartered Surveyors, RICS (March 2007)

McFarland, J., Reilly, J., Herzog, H.: Representing Energy Technologies in Top-Down Economic Models Using Bottom-Up Information. Energy Economics 26, 685–707 (2004)

Ness, D., Kellett, J., Wilson, L., Pullen, S., Karuppamman, S., Sivam, A., Tisato, P., Davidson, K.: Integrated Sustainable Assessment of Urban Development and Infrastructure: Complementarities and Contradictions. In: Proceedings of Sustainable Building Conference SB 2008, Melbourne, Australia (September 2008)

Perkins, A., Hamnett, S., Pullen, S., Zito, R., Trebilcock, D.: Transport, housing and urban form: the life cycle transport and housing impact of city centre apartments compared with suburban dwellings. In: Proceedings of the State of Australian Cities Conference, Adelaide (November 2007)

Pullen, S.: A Tool for Depicting the Embodied Energy of the Adelaide Urban Environment. In: Proceedings of 2007 Australian Institute of Building Surveyors International Transitions Conference, Adelaide, pp. 224–242 (March 2007), http://www.aibs.com.au/aibs_docs/conferences/Session_T2A_Pullen.pdf

Rann, M.: Action Now for the Future Latest News. Government of South Australia (November 2, 2008), http://www.ministers.sa.gov.au/news.php?id=3881 (accessed January 6, 2009)

Roberts, B.: Changes in Urban Density: Its Implications on the Sustainable Development of Australian Cities. In: Proceedings of the State of Australian Cities Conference, Adelaide (November 2007)

SA Govt. Tackling Climate Change. South Australia's Greenhouse Strategy 2007-2020. Office of the Premier. Government of South Australia (2007)

Salat, S.: Energy and ecology efficiency of urban morphologies: a comparative analysis of Asian, American and European Cities. In: Proceedings of SB 2007HK, Sustainable Building Conference, Hong Kong, December 4-5 (2007)

Schiller, G.: Urban infrastructure: challenges for resource efficiency in the building stock. Building Research & Information 35(4), 399–411 (2007)

Steemers, K.: Energy and the city: density, buildings and transport. Energy and Buildings 35, 3–14 (2003)

Tornberg, J., Thuvander, L.: A GIS Model for the Building Stock of Goteborg. In: Proceedings of the 25th Annual ESRI User Conference, San Diego, California (2005) http://gis.esri.com/library/userconf/proc05/index.html (accessed January 5, 2009)

Treloar, G.: Streamlined Life Cycle Assessment of Domestic Structural Wall Members. Journal of Construction Research 1, 69–76 (2000)

Treloar, G., Love, P., Crawford, R.: Hybrid Life-Cycle Inventory for Road Construction and Use. Journal of Construction Engineering and Management 130(1), 43–49 (2004)

Yamaguchi, Y., Shimoda, Y., Mizuno, M.: Proposal of a Modelling Approach Considering Urban Form for Evaluation of City Level Energy Management. Energy and Buildings 39, 580–592 (2007)

Energy Consumption in the Greek Hotel Sector: The Influence of Various Factors on Hotels' Carbon Footprints under the Implementation of the EU and Greek Legislative Framework

Maleviti Eva*, Mulugetta Yacob, and Wehrmeyer Walter

Centre for Environmental Strategy,
University of Surrey, GU2 7XH Guildford, UK
Tel.: +44-1483-689074
e.maleviti@surrey.ac.uk

Abstract. This paper is part of a wider work programme that is looking at the reduction of energy consumption and Greenhouse Gas emissions in the Greek Hotel sector. The Greek Government has recently set specific plans to reduce energy consumption in buildings against a backdrop of the European Union's policies aimed at ensuring its members to meet the Kyoto targets. This study will present the results of energy audits which are carried out on a sample of Greek Hotels focusing on their environmental and energy performance. This research will analyze the environmental effect of the hotel sector in Greece, exploring the successful adoption of Energy Policies and Measures set by Greece and EU, for energy conservation measures in key waste energy areas in buildings. This analysis will constitute an important guide to a forthcoming detailed research on modeling and optimizing energy performance of hotels in different areas in Greece.

Keywords: Greek Hotel sector, Energy policies, Energy Consumption, Energy Performance, Energy Auditing.

1 General Overview

1.1 Introduction

Sustainability of tourism is the focus of this research and in specific, the Greek Hotels. In particular, this research will analyze the energy performance and consumption in Greek Hotels and it will explore possibilities in reduction of energy consumption and environmental effects. This analysis provides insights on improving energy performance in Greek Hotels contributing to an efficient hotel industry, which is also very significant for the country's economy. Energy auditing, in different cases/hotels around Greece, is used in this project in order to collect the appropriate data. The analysis of preliminary data will display the current trend in energy consumption in

* Corresponding author.

Greek Hotels. In order to collect the appropriate data, energy audits has been accomplished in selected cases, and the preliminary data of 4 cases are analyzed in this paper. The fact that Greek Hotels have high energy consumption and they are responsible for the 10% of the total electricity consumed in the country. Therefore, it make sense to tackle with this issue and to find possible ways in reducing Greek Hotels' energy consumption, and provide possible solutions to operate in a more sustainable way.

1.2 Main Objective and Aims of the Research

The main objective of the research is to explore the contribution of the Hotel Sector to a Sustainable Tourism Sector and to the overall country's direction towards a low carbon future.

The first aim of the research is the evaluation of the existing legislative framework on energy measures in buildings and hotels, and the achievement of the suggested targets. The second aim is to measure and evaluate the energy consumption in Greek hotels and identify their most energy consuming parts. The third aim is to identify options for reduction of energy consumption in Greek Hotels and improve their energy performance, using renewable energy technologies and energy efficiency measures. The fourth aim of the research is to explore the influence of different parameters in Hotels' energy performance in long-term. These parameters are the tourism growth rate in the country, the changes of occupancy rates in Greek Hotels, the geographical location of Hotels' and their type of tourism.

2 Methods and Data Analysis

2.1 Research Methodology

The following analysis demonstrates the current trend in energy consumption based on the data collected from the 4 Hotels, without any policy interventions. This analysis represents the Business as Usual Scenario. Energy audits in each hotel and interviews with hotel managers and engineers were made, in order to collect data for this research. The following graphs exhibit future projections on the electricity consumption of the 4 hotels and the CO2 emissions from it. The projections are based on the variability of occupancy rates according to estimates of annual tourism growth in Greek hotels under the World Travel and Tourism Council and World Tourism Organization, and three assumptions are used. The first assumption is based on the estimated modest increase of tourism growth by 2.5% by 2016 in Greek Hotels according to the World Travel and Tourism Council. The second is based again in the World Travel and Tourism Council (2006) and the World Tourism Organization (2005) with an increase of 4.3%, a more unreserved assumption. The third is the actual increase of occupancy ratio during the years 2000-2006, 3.5%. Additionally, since these 4 cases are from different areas around Greece, the type of tourism differs; it is analyzed how this affects the electricity consumption in each case.

2.2 Data Analysis

The data analysis demonstrates the current trend in electricity consumption in the selected case studies. This analysis represents the baseline scenario, without policy interventions, giving approximations and estimates on energy consumption in these 4 case studies. It is interesting to mention that this is an exploratory analysis and demonstrates the electricity consumption in four different cases, which represent a real sample of the Greek Hotels. As indicated in the following table, the 4 cases have different technical characteristics which play a significant role in their energy consumption.

Table 1. Technical Characteristic

	Hotel A	Hotel B	Hotel C	Hotel D
Year of Construction	1980	1900(2003)	1975	1982
Category	5*****	5*****LUX	5*****	3***
Number of Rooms	182	321	255	60
No of Floors	9	8(+2basements)	3	4
Area/floor (m2)	900	2400	2997	450
Total Area (m2)	12000	22776	30239	6700

These characteristics shape the energy consumption and the energy sources consumed in each hotel. The energy sources used in the four hotels are mainly electricity, natural gas to provide hot water and heating, and Hotel C and D use oil for heating. The research demonstrated that Hotels A and C have the same services offered, but different occupancy per year and different total floor area. However, it is examined that they have the same scale of electricity consumption. Then again, Hotel C indicates major differences in electricity consumed in the kitchen and in the laundrette. This is due to the difference in occupancy during summer and winter. On the other hand, Hotel B offers a spa where an important amount of electricity is consumed. In addition, in Hotel B there is a high number of electrical equipment which have higher power capacity comparing to the equipments in the in the other 3 cases. Hotel D has higher electricity consumption in a summer day than in a winter day, without having significant difference in the amount of electricity consumption. This is because it is a small hotel comparing to the other three and in order to cover its customers' needs in a winter day, the amount of electricity consumed is still high.

The main difference in electricity consumption in each hotel appears in the electricity consumption in rooms. This is because the hotels have different occupancy ratio during their annual operation. Hotel A has an average occupancy ratio 70% throughout the year. On the other side, Hotel B has 82% occupancy during summer, 49% during the winter and 75-77% in the spring and autumn. Hotel C shows a 70% during the summer, 31-36% in the winter and autumn and 54% in the spring. Hotel D has an average occupancy ratio in summer around 80%, in autumn 50% and in winter and in spring 30 and 40% respectively. The following graph shows the differences in electricity consumption. The daily use is measured around 8 hours in summer and in winter.

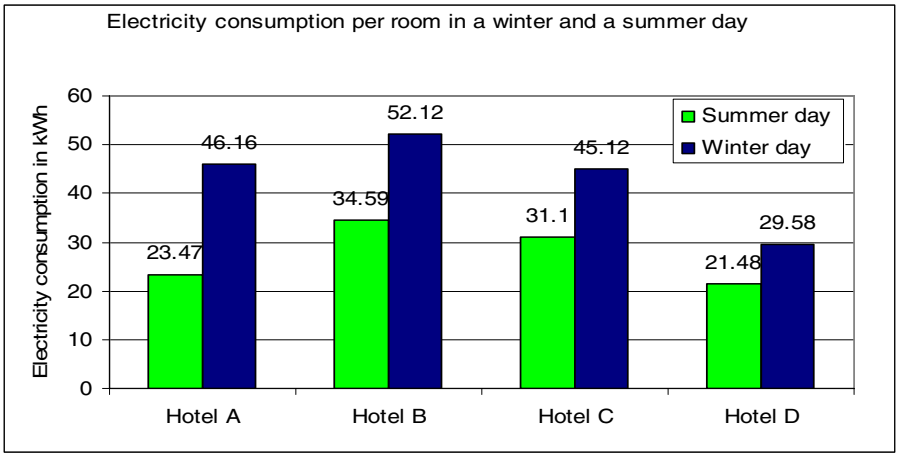

Fig. 1. Electricity Consumption per room in a winter and a summer day

The higher power capacity of the equipment is used to provide heating in the room, justifying the higher consumption of electricity during the same time of operation. For Hotel B, again the large difference in electricity consumption is due to the power capacity of air-conditions and the difference on the daily use in summer and winter. At this point it should be stated that the significant difference in occupancy rates during summer and winter-49% and 82% respectively- affects notably the energy consumption in rooms in total. For Hotel C it can be observed that there is the smallest difference in electricity consumption between a summer and a winter day. During the winter, rooms are heated from the building's central heating, with a maximum 4 hour daily use of air-conditions. For Hotel D, it was observed that the services which are offered to the customers are the basic without luxurious services. In the rooms there are not many equipments include, apart from the television and a small refrigerator. During summer there is a central A/C unit, therefore the electricity consumption is quite low comparing to the use of one A/C unit per room.

Again, the different types of operations, the daily use of rooms' equipment and the type of the equipment used in each hotel explain the differences. As it will be explained below, the occupancy rates influence significantly the electricity consumption and consequently the CO_2 emissions. The following graphs show how electricity consumption in the 4 cases is affected by the increase of tourism growth and thus the increase of occupancy.

The bottom part of the graph represents the trend of electricity consumption for Hotel D. Its mean occupancy ratio in a summer day is 80%. There is no significant change in electricity consumption since under thee assumption and changes in occupancy rates, the hotel will be full after year 2009. Therefore, all rooms are occupied and the electricity consumption in rooms remains stable, since there will not be further increase. This is why the graph in this case is an almost straight line for the three assumptions of increase of the occupancy ratio. The second from the bottom graph represents Hotel A. For this case, the annual growth of occupancy-with 70% of occupancy on a summer day- signifies lower growth rate of electricity consumption

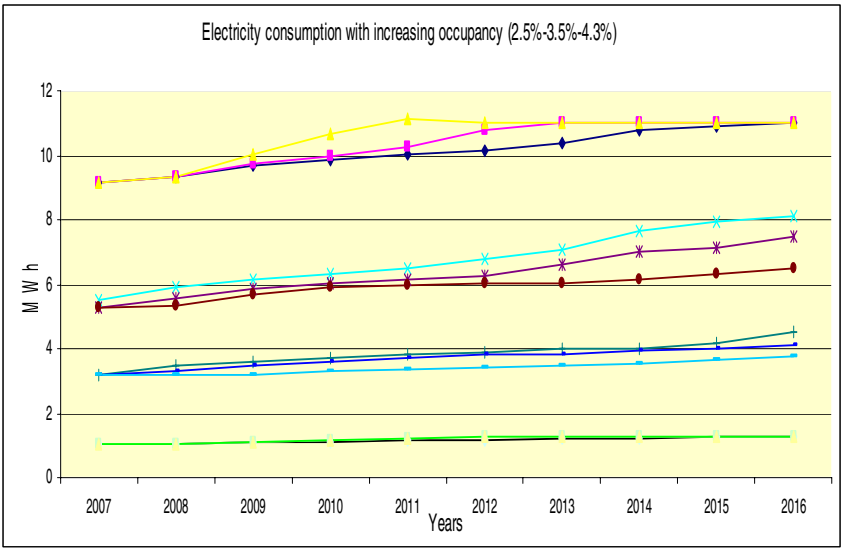

Fig. 2. Electricity consumption with increasing occupancy (2.5%-3.5%-4.3%) (Hotels A-B-C-D)

throughout a ten years period comparing, to a hotel with less annual occupancy. This appears because it is harder for more rooms to be occupied since the hotel has already reached the 70% of its occupied rooms. The third part of this graph represents the electricity consumption in Hotel C and it shows that the increase of the occupancy rate will affect more the increase of electricity consumption. The graph demonstrates that the electricity consumption in Hotel A will not show a high increase of electricity consumption comparing to Hotel C which has less occupancy rate during the same period of the year. Hotel B has very small increase of occupancy rate, having all the rooms occupied at the year 2016. This case justifies as well the link between occupancy ratio and electricity consumption. It shows that during the 10 year period, when the hotel has hypothetically, all the rooms occupied, the electricity consumption remains stable. Therefore, from the above graph could be stated that the growth of occupancy ratio affects the electricity consumption of a hotel when it has smaller number of occupied rooms on an annual basis.

3 Results

3.1 Observations

The main observation of the above analysis is that the occupancy ratio influences electricity consumption of a hotel when fewer rooms are occupied. In making better sense, it is useful to separate total electricity consumption into electricity consumption that does not change significantly with occupancy rate and into electricity consumption that changes significantly with occupancy rates. In specific, electricity consumption in rooms, or electricity consumption from A/C is influenced by the occupancy

ratio. On the other hand, electricity consumption from open space heating, the use of electrical equipment and facilities in the kitchen will remain approximately the same, since there are specific hours of operation. In addition, the electricity consumption for lighting in the reception area and outside of the building is also not influenced by the occupancy ratios.

The following function explains in a more detailed way, why occupancy ratio influences the electricity consumption more, when smaller number rooms are occupied.

TE =FE +VE* X*(total number of rooms). Where **TE** = the total electricity consumption in the hotel, **FE** = the fixed electricity consumption, where it represents the electricity consumption in the areas which are not influenced by the number of occupied rooms (i.e. kitchen, laundry facilities, lighting in reception areas, restaurants, bars, etc.). Therefore, this term will be largely independent from the occupied rooms.

VE= Variable electricity consumption, which largely depends on the occupied rooms.

X= Occupancy factor (a number from 0 to 1).

Modifying this function the total electricity consumption per room will be:

TE/rooms= FE/rooms + VE*X/rooms (eq. 1).

This function shows that the term FE/rooms remains largely stable in any number of occupied rooms. Therefore, the total energy consumption/room will be influenced by the changes of the last term VE*X.

Differentiating eq.1, it would be:

∂ (TE/rooms) = ∂ (FE/rooms) + ∂ (VE*X/rooms), where a significant increase of the last term will strongly influence the term ∂ (TE/rooms), justifying the findings from the data analysis.

Further than that, an important factor which influences the electricity consumption and consequently, influences the total energy consumption in a hotel, is the type of equipment used. Hotel C has obsolete equipment comparing to Hotels A and B, which is an important element for increased CO2 emissions in a 10-year period. Hotel D has the lowest electricity consumption and fewer services offered. In addition, the fact that the buildings are constructed in the last 20-30 years and around 100 for Hotel B indicates the importance of energy efficiency measures to be taken.

4 Conclusions

To conclude, Greek Hotel Sector is a very important element to the country's economy, but with significant environmental effects. Energy audits in 4 Hotels from different areas in Greece, demonstrated their physical and technical characteristics and their trends in energy consumption. Additionally, the influence of changes in occupancy ratio was taken into consideration, exploring how these are influencing the Hotels' electricity consumption. From the data analysis was observed that the occupancy ratio influences electricity consumption of a hotel when fewer rooms are occupied. Additionally, none of the 4 Hotels uses renewable energy technologies or has taken energy efficiency measures. Furthermore, the influence of obsolete equipment in total electricity consumption in each Hotel plays an important role for the total energy consumption. In future research, more case studies will be added supporting this analysis and to give a clearer picture about energy consumption in Greek Hotels and how changes in this sector could lead to a Sustainable Tourism sector for the country.

References

Diakoulaki, D., et al.: A bottom-up decomposition analysis of energy-related CO_2 emissions in Greece. Energy 31(14), 2638–2651 (2006)

European Commission (in cooperation with Eurostat), EU energy and transport in figures, Statistical pocketbook, Luxembourg (2003)

European Commission. Priorities for energy conservation in buildings. 48, European Commission. Ref Type: Report (2006)

IEA, World Energy Outlook, OECD/IEA, Paris (2006b)

Karagiorgas, M., et al.: HOTRES: renewable energies in the hotels. An extensive technical tool for the hotel industry. Renewable and Sustainable Energy Reviews 10(3), 198–224 (2006)

Onut, S., Soner, S.: Energy efficiency assessment for the Antalya Region hotels in Turkey. Energy and Buildings 38(8), 964–971 (2006)

Santamouris, M., et al.: Energy characteristics and savings potential in office buildings. Solar Energy 52(1), 59–66 (1994)

Santamouris, M., et al.: On the impact of urban climate on the energy consumption of buildings. Solar Energy 70(3), 201–216 (2001)

Santamouris, M., et al.: Investigating and analysing the energy and environmental performance of an experimental green roof system installed in a nursery school building in Athens, Greece. Energy 32(9), 1781–1788 (2007)

United Nations Framework Convention on Climate Change, Article I. United Nations Framework Convention on Climate Change (retrieved on 2007-01-15)

World Travel and Tourism Council, Greece: The Impact of Travel and Tourism on Jobs and the Economy (2006)

Investigating the Applicability of Different Thermal Comfort Models in Kuwait Classrooms Operated in Hybrid Air-Conditioning Mode

Khaled E. Al-Rashidi, Dennis L. Loveday, and Nawaf K. Al-Mutawa

[1] Department of Civil and Building Engineering, Loughborough University, UK
K.E.H.Al-Rashidi@lboro.ac.uk, D.L.Loveday@lboro.ac.uk
[2] Department of Mechanical Engineering, Kuwait University, Kuwait
Nawaf@Kuc01.kuniv.edu.ku

Abstract. A field study to investigate the applicability of different thermal comfort indices was conducted in Kuwait classrooms operated in a hybrid air-conditioned mode, to assess thermal conditions during the school day. In Kuwait, the girls' and boys' schools are completely separated at all academic levels thus offering a wide range for investigating differences in thermal comfort sensations between both genders. A modified questionnaire was used to collect responses from lower age groups of pupils while thermal comfort variables were measured at the same time. However, this paper reports on findings for pupils in the age range 11-17 years. Data analyzed suggested that the different thermal comfort indices (PMV, ePMV, PMV_{10} and adaptive model and various comfort equations) under-predicted the students' actual thermal comfort sensation on the warm side of neutral and over-predicted thermal sensation on the cool side of neutral on the ASHRAE comfort scale for both genders. Higher neutral temperatures were also predicted than those resulting from the students' actual mean vote (AMV). A difference in neutral temperature was found between both genders.

Keywords: children, classrooms, Kuwait, thermal comfort.

1 Introduction

1.1 Study Background

Kuwait is a hot and dry country where during summer the temperature can reach 48°C (July and August) in the afternoon and sometimes can exceed 55°C. Furthermore, Kuwait has a desert climate which is characterized by the high percentage of sunshine, wide diurnal temperature extremes and little rainfall with an average summer relative humidity of about 18%, MD (2004). Therefore, most buildings extensively use air-conditioning systems during summer while in winter the weather is cold and dry and in this period the air conditioning systems are not used.

At the beginning of the 1990's, school buildings in Kuwait were extensively constructed or renovated. Air-conditioning systems were installed in those buildings to provide comfortable thermal conditions. The control of those systems is not under the direct control of the students, and this may have a negative effect on comfort sensation in the classroom.

The question of thermal conditions in classrooms has to be seriously considered because children are still physically developing. For example, poor thermal conditions

could affect the children's health and may indirectly affect their learning and performance – this may have detrimental consequences for their and society's future.

In Kuwait, the girls' schools are separate from the boys' schools at all academic levels, which are structured as follows: elementary level which consists of five classroom grades from the 1st class to the 5th class and the students ages are from 6-10 years; intermediate level which consists of 4 classroom grades from the 6th class to the 9th class and the students ages are from 11-14 years; and secondary level which consists of 3 classroom grades from the 10th class to the 12th class and the students ages are from 15-17 years. Students in Kuwait classrooms have a strict code of scholarly clothing which is imposed by the Ministry of Education in Kuwait. The main objectives of the study reported here, and which apply to students between the ages of 11 to 17 years old are:

- To examine the applicability of different thermal comfort indices (PMV, ePMV, PMV_{10} and adaptive model, and various comfort equations) in Kuwait classrooms operated in the hybrid ventilation mode and determine whether one model is more appropriate than the others for thermal comfort prediction in such situations.
- To determine the neutral temperature (t_n) for both student genders during this climatic period in the classrooms.
- To compare findings with similar studies conducted elsewhere and reported in the literature.

Table 1. Thermal comfort research conducted in classrooms in different regions around the world (NV = naturally ventilated; A/C = air-conditioned)

Researcher & published year	Study location	Climatic weather	Study period	Classrooms ventilation Type	Neutral temperature t_n (°C)
Kwok, 1998	Hawaii, USA	tropical	Sept-Oct, 1996 Jan., 1997	NV & A/C	26.8 in NV 27.4 in A/C
Xavier and Lamberts, 2000	Florianopolis –Santa Brazil	tropical	April-Dec., 1997	NV	23.1
Cheong et al., 2003	Singapore	tropical	12th Oct., 1999	A/C	25.8
Wong and Khoo, 2003	Singapore	tropical	21st and 24th August, 2001	NV	28.8
Sh.Ahmad and Ibrahim, 2003	Shah Alam, Malaysia	tropical	16th and 17th January, 2002	FV & A/C	27.6 in NV 26.5 in A/C
Kwok and Chungyoon, 2003	Tokyo, Japan	Sub-tropical	Sept., 2000	NV & A/C	27.5 in NV 23.1 in A/C
Hwang et al., 2006	Center and south Taiwan	Sub-tropical		NV&A/C	26.3

1.2 Field Studies on Thermal Comfort in Classrooms

Many field studies and experiments have been conducted in different regions of the world to investigate and understand the effects of the thermal comfort variables on students occupying classrooms in different building types. A summary description of these studies and the corresponding neural temperature of subjects found in these studies are shown in Table 1.

From the literature review it is clear that in all previous studies that investigated the thermal comfort conditions in classrooms, the work was conducted in subtropical or tropical environments, whilst few, if any, studies have been carried out in classrooms located in hot dry climatic environments like that of Kuwait. The thermal sensations of female and male students were combined in most of the previous studies, whereas the separation of the genders into separate classrooms that is the practice in Kuwait necessitates the investigation of the thermal sensations of each gender separately. This, in turn, can uncover gender effects related to classroom thermal sensation.

2 Methodology

2.1 Timing and Structure of Study

The field study was conducted over the period, 13th - 22nd November, 2005 in Kuwait classrooms. This period in Kuwait is the end of the hot season and the beginning of the cold season. The weather in this period is considered as thermally fluctuating and some of the classrooms are still using air-conditioning systems. In these classrooms the operation of the air-conditioning systems is considered to be in the 'hybrid mode' where the air-conditioning systems are turned on and off during different parts of the day. Kuwait students have limited and restricted scholar clothing codes in summer and winter seasons.

From the beginning of November to the end of March every year, the students wear the winter school dress code and these are different for girls and boys. For girls in the intermediate and secondary levels, there are two winter school dress codes, the first dress code consists of the hejab (hair cover), shirt, long dress and sweater, while the second dress code consists of shirt, short dress and sweater. The boys' winter school dress code is the same for all academic levels and consists of shirt, trousers, thermal underwear and sweater. This study has been conducted in the following school rooms: 4 intermediate boys' classrooms; 3 secondary boys' classrooms; 4 intermediate girls' classrooms and 3 secondary girls' classrooms.

2.2 Objective Measurements

In this field study, a Bruel & Kjaer indoor climate analyzer type 1213 was used to measure the environmental variables (air temperature, air velocity, relative humidity and the mean radiant temperature). The measuring equipment was placed in five different locations within each classroom at two different heights above the floor (1.1 m and 0.6 m) as recommended by ASHRAE and ISO standards. At each position the equipment was left to run for about 3 minutes before the mean values of the environmental parameters were recorded. The metabolic rate of the students in the seated

position was estimated in accordance with ASHRAE 55 and ISO 7730 standards. The metabolic rate used for this study was estimated to represent the sedentary activity which is equal to 1.2 met.

The average clothing insulation value for the intermediate and secondary girls' winter school dress code is 0.95 clo. The average clothing insulation value for the boy's is equal to 1.17 clo for winter. These values were estimated from the data presented in ASHRAE 55 and ISO 7730 standards.

2.3 Subjective Assessment

A simple thermal comfort sensation questionnaire survey was used in the classrooms to evaluate the students' thermal sensation in the different classroom environments. The questionnaire consisted of 6 basic questions which asked the students about their thermal sensation, comfort level, thermal preferences, acceptability level and their feeling toward two environmental variables (airflow and humidity). Students were asked to answer the thermal sensation questions in accordance to the ASHRAE seven-point continuous scale. The comfort question employed asked the students to state their current comfort level and the possible responses to this question were "comfortable; uncomfortable and very uncomfortable". The third question used was the McIntyre thermal preference scale and asked the students if they wanted to be 'cooler; no change or warmer' at this moment. The thermal acceptability was the fourth question and the students were asked to answer the acceptability question as 'acceptable or unacceptable'. Questions about two environmental variables, air movement and humidity, were asked of the student. The possible answers to these questions were 'breezy; just right or still' and 'dry; just right or humid' for air movement and humidity, respectively.

A sample of 336 student subjects, 169 girls and 167 boys, in 14 classrooms in intermediate and secondary academic levels were surveyed to assess their thermal comfort conditions in this period. The total subjects' votes is equal to 336 votes. The questionnaire survey was administered simultaneously with the physical measurements in each classroom. The questionnaire was handed to the students 30 minutes after they had entered the classroom to ensure that the students' metabolic rate has settled and reached the recommended sedentary metabolic rate (1.2 met) and that thermal equilibrium (steady state) was approaching.

3 Results and Discussion

3.1 Analysis of Votes on ASHRAE Scale

The classroom thermal conditions during the hybrid air-conditioned mode for both genders and the occupants' votes on thermal perception are shown in Table 2 and in Fig. 1. From Fig. 1, the percentage of votes around the three central points of the ASHRAE scale (-1 'slightly cool', 0 'neutral' and +1 'slightly warm') is 65.1% for girls with average classrooms temperatures of 23.31^{o}C, and 64.1% for boys with average classrooms temperatures of 22.27^{o}C.

Table 2. Classrooms thermal conditions and students' actual mean votes

Class grade	No. of Students	Age	School Dress Code	t_o (°C)	V_a m/s	RH (%)	mean comfort Votes	(1,0,+1) Votes (%)	Votes distribution according to ASHRAE scale						
									-3	-2	-1	0	+1	+2	+3
Girls	32	11	winter	24.09	0.22	33.6	1.31	53.1	0	0	2	9	6	7	8
Girls	27	12	winter	24.42	0.08	35.6	1.15	44.4	0	2	2	3	7	9	4
Girls	25	13	winter	24.34	0.09	30.6	1.56	68.0	0	0	0	1	16	1	7
Girls	26	14	winter	24.07	0.38	41.8	1.19	84.6	0	0	0	1	21	2	2
Girls	20	15	winter	20.54	0.09	60.8	-1.15	60.0	6	2	4	5	3	0	0
Girls	23	16	winter	24.21	0.08	63.8	1.17	65.2	0	0	0	6	9	6	2
Girls	16	17	winter	21.52	0.10	63.2	0.31	93.8	0	0	1	9	5	1	0
Boys	28	11	winter	24.91	0.04	48.0	1.43	35.7	0	1	1	3	6	14	3
Boys	32	12	winter	22.85	0.07	35.6	0.56	59.4	0	4	5	3	11	7	2
Boys	23	13	winter	21.22	0.07	35.6	-0.13	100	0	0	9	8	6	0	0
Boys	25	14	winter	23.16	0.16	52.6	1.28	36.0	0	1	2	3	4	13	2
Boys	21	15	winter	21.09	0.11	51.0	-0.24	81.0	0	2	9	4	4	2	0
Boys	21	16	winter	20.98	0.07	43.8	0.05	95.2	0	1	2	13	5	0	0
Boys	17	17	winter	21.71	0.11	53.2	0.71	52.9	0	1	3	4	2	6	1
All Girls classrooms	169	11-17	winter	23.31	0.15	47.1	0.79	65.1	6	4	9	34	67	26	23
All Boys classrooms	167	11-17	winter	22.27	0.09	45.7	0.52	64.1	0	10	31	38	38	42	8

Where, to, classroom operative temperature °C; ¼ classroom airflow speed m/s; RH, classroom relative humidity %; (-1,0 and +1) votes, votes around the three central points of ASHRAE scale (slightly cool; neutral and slightly warm) %.

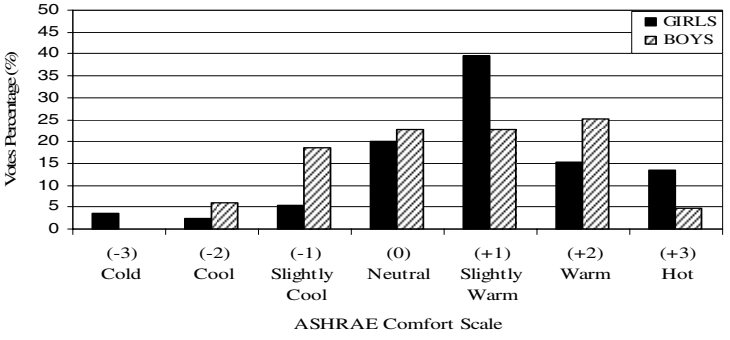

Fig. 1. The total percentage of the girls' and boys' votes along the ASHRAE comfort scale

3.2 Applicability of the Different Thermal Comfort indices in Kuwait Classrooms

A new extended PMV model was proposed by Fanger and Toftum (2002) to give better prediction of the actual thermal sensation of occupants in non-air conditioned buildings in warm climate. This new model takes into account psychological adaption effects and a reduction in metabolic rate. In this model, the authors suggested that the occupants of the non-air-conditioned buildings have a lower expectation toward their thermal environment than those in air-conditioned buildings. An expectancy factor *e* was proposed as a multiplication factor to the PMV model to improve its prediction. Table 3 shows the ranges of the expectation factor proposed by Fanger and Toftum (2002). From this table it is clear that the suitable range for '*e*' in Kuwait classrooms should be 0.9-1.0.

A further approach was taken by the authors of this study which involved reducing the estimated sedentary metabolic rate used in the PMV model (which was originally based on adults) by 10% in order to fit the children's metabolic rate. This modification was based on Havenith (2007) findings. The modified model is called PMV_{10}. The regression lines for the students' actual mean vote (AMV), PMV, the extension to PMV (ePMV) and the PMV with 10% reduction in metabolic rate (PMV_{10}) are shown in Fig. 2 and Fig. 3 for both genders.

Table 3. Ranges of expectancy factor for non air-conditioned buildings in warm climate

Expectation level	Building Classification	Expectancy ranges, *e*
High	Non air-conditioned building located in regions where air-conditioned building are common, warm periods occurring briefly during the summer.	0.9-1.0
Moderate	Non air-conditioned buildings located in regions with some air-conditioned building, warm summer seasons.	0.7-0.9
Low	Non air-conditioned buildings located in regions with few air-conditioned buildings, warm weather during all seasons	0.5-0.7

From these figures it is clear that the PMV and ePMV are identical and under predicted the students' AMV for the warm side of neutral and over-predicted AMV for the cold side of neutral. The PMV_{10} moves parallel to PMV and ePMV with a shift equal to the reduction in the metabolic rate and also under-predicted the students' AMV on the warm side of neutral and over-predicted AMV on the cool side of neutral. The prediction differences between the PMV, ePMV models and the AMV at the neutral situation for both genders is equal to +0.1 units, where the prediction differences between the PMV_{10} model and the AMV at the neutral situation for both genders is equal to -0.2 units.

3.3 Predicting the Neutral Temperature

The values of the AMV and the predicted PMV, ePMV and PMV_{10} for each gender were plotted and regressed against the operative temperature inside the classrooms as shown in Fig.4 and Fig. 5. From these figures it is clear that the predicted neutral temperature by the different prediction models is lower (under-predicted) than that based on prediction by the occupants' actual mean votes on the warm side of neutral and higher (over-predicted) on the cool side of neutral on the ASHRAE scale.

The neutral temperatures that result from the different thermal comfort indices and the recommended neutral temperature in Kuwait using the adaptive model and various equations are tabulated in Table 4.

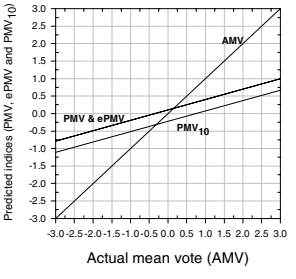

Fig. 2. The regression lines for the girls' actual mean vote (AMV) and the predicted indices (PMV, Epmv, PMV_{10} and PMV_{10})

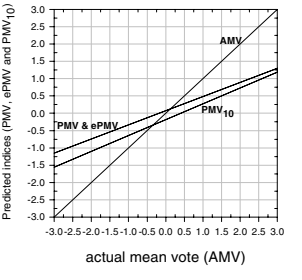

Fig. 3. The regression lines for the boys' actual mean vote (AMV) and the predicted indices (PMV, ePMV and PMV_{10})

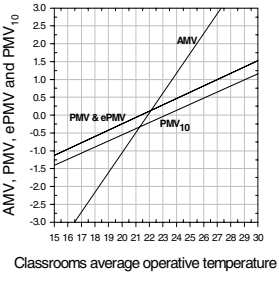

Fig. 4. The regressed neutral temperature (t_n of the girls' AMV and the different predicted indices (PMV, ePMV and PMV_{10})

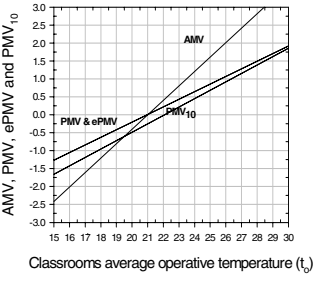

Fig. 5. The regressed neutral temperature (t_n of the boys' AMV and the different predicted indices (PMV, ePMV and PMV_{10})

Table 4. Predicted and recommended neutral temperature using various thermal comfort indices and equations

	AMV	PMV	ePMV	PMV_{10}	De Dear & Brager, 2002	Humphreys, 1978	Auliciems, 1981
					NV	NV	All
Equation					17.8+ $0.31T_{a\ out}$	11.9+ $0.543T_m$	17.6+ $0.31T_m$
Girls	22.0	21.5	21.5	23.3	24.3	22.8	23.8
Boys	21.0	21.0	21.0	22.1	23.4	22.8	23.8
All (ave)	21.5	21.3	21.3	22.7	23.9	22.8	23.8

From Table 4, it is clear that there is a difference of 1°C in the neutral temperature between the girls and boys according to their votes. This finding is in agreement with the findings of Hwang et al. (2006). This difference may be related to the higher clothing insulation values worn by boys compared with the girls. By combining the girls' and boys' votes, the average neutral temperature of both genders is equal to 21.5°C and this value is the same as the average neutral temperature predicted by the PMV and ePMV models.

Reduction of the metabolic rate in this study predicted a 1.3°C higher neutral temperature than that from the normal PMV and the ePMV. All other indices and equations under-predict the neutral temperature for girls and boys. The adaptive approach (De Dear and Brager, 2002) gives a higher neutral temperature than that obtained from the AMVs of the subjects (by 2.4°C). This may be related to the domination of the A/C periods (A/C turn on) during the period of this study. This might suggest that the classroom environment during this hybrid mode can still be considered as an A/C mode, whereas the adaptive approach is more applicable to the naturally ventilated environments.

At first sight, this might suggest that the PMV and ePMV models are the more appropriate thermal comfort indices to predict the thermal comfort sensations of the children in Kuwait classroom during this period. However, this might be related to the fact that the classroom could be considered as more that of an air-conditioned environment instead of being a naturally-ventilated one. Finally, the neutral temperature found in this study during this period is lower than that found in previous studies conducted in classrooms in tropical and sub-tropical climates.

4 Conclusions

- All the thermal comfort indices investigated in this study under-predicted the children's actual thermal sensation on the warm side of neutral on the ASHRAE scale and over-predicted actual thermal sensation on the cool side of neutral on the ASHRAE scale.
- The PMV and ePMV indices give similar results in the Kuwait classroom environment where the expectation level of the occupants is high.

- The hybrid air-conditioned mode could be considered as more that of an air-conditioned mode instead of being a naturally-ventilated mode, where the PMV and ePMV indices are more appropriate to predict the children thermal sensations in Kuwait classrooms in this period than other thermal comfort indices.
- The neutral temperatures of the girls and boys are 22°C and 21°C, respectively, with the difference of 1°C considered to be the result of the difference in clothing ensemble insulation between male and female pupils.
- The average neutral temperature (21.5°C) for both female and male pupils during this period is lower than that found in previous studies conducted in classrooms in subtropical or tropical environments. This may be related to the higher insulation values of the school dress codes as worn by the students in Kuwait classrooms during this period than those worn in the studies in the other countries reported, in addition to the differences in climates.

Acknowledgments. The authors would like to record their gratitude to Loughborough University, UK; Kuwait University, and the Ministry of Education in the State of Kuwait, including their staff and students, for their cooperation during this study.

References

Auliciems, A.: Towards a psycho-physiological model of thermal comfort perception. International Journal of Biometeorology 25, 109–122 (1981)

Cheong, K.W.D., Djunaedy, E., Chua, Y.L., Tham, K.W., Sekhar, S.C., Wong, N.H., Ullah, M.B.: Thermal comfort study of an air-conditioned lecture theatre in the tropics. Building and Environment 38, 63–73 (2003)

De Dear, R.J., Brager, G.S.: Thermal comfort in naturally ventilated buildings: revisions to ASHRAE Standard 55. Energy and Buildings 34(6), 549–561 (2002)

Fanger, P.O., Toftum, J.: Extension of the PMV model to non-air-conditioned buildings in warm climates. Energy and Buildings 34(6), 533–536 (2002)

Havenith, G.: Metabolic rate and clothing insulation data of children and adolescents during various school activities. Ergonomics 50(10), 1689–1701 (2007)

Humphreys, M.A.: Outdoor temperature and comfort indoors. Building Research and Practice 6(2), 92–105 (1978)

Hwang, R., Lin, T., Kuo, N.: Field experiments on thermal comfort in campus classrooms in Taiwan. Energy and Buildings 38, 53–62 (2006)

Kwok, A.G.: Thermal comfort in tropical classrooms. ASHRAE Technical Data Bulletin 14(1), 85–101 (1998)

Kwok, A.G., Chun, C.: Thermal comfort in Japanses schools. Solar Energy 74, 245–252 (2003)

MD: The metrological department annual report, meteorological department, directorate of civil aviation, Kuwait (2004)

Sh.Ahmad, S., Ibrahim, N.: A study on thermal comfort in classrooms in Malaysia. In: PLEA 2003-The 20th Conference on Passive and Low Energy Architecture, Santiago- CHILE, 9-12 November 2003, paper code Ma01, pp. 1–6 (2003)

Wong, N.H., Khoo, S.S.: Thermal comfort in classrooms in the tropics. Energy and Buildings 35, 337–351 (2003)

Xavier, A.A.D., Lamberts, R.: Indices of thermal comfort developed from field survey in Brazil. ASHRAE Transactions 106(1), 45–58 (2000)

Water and Energy Efficient Showers

David Phipps, Rafid Alkhaddar, Roger Morgan, Robert McClelland, and Robert Doherty

Liverpool John Moores University, and Richard Critchley, United Utilities Ltd.

Abstract. The performance of showers was studied in a laboratory, in the homes of volunteers and with focus groups, with a view to identifying key factors which would encourage the reduction of both water and energy consumption. Focus groups defined their principal requirement for a "good shower experience" to be adequate water flow to enjoy the experience of showering (enough volume at the right temperature in order to keep warm and to wash satisfactorily). Laboratory work investigated pressure:flow-rate correlation, spray pattern, temperature and "skin pressure". The pressure:flow-rate relationship followed a simple square-root relationship for most showerheads. Suggestions are made for the use of a Head Factor in design. Showers in homes were modified by temporary insertion of flow restrictors or by replacing conventional shower heads with aerating heads. Flow restrictors proved to be generally unacceptable, while aerating heads were popular. The study has shown a financial payback within a few months for a mixer or pumped shower operating at over 8 l/min by installing a water saving showerhead.

1 Introduction

The Water Research Centre (WRc 2005) estimate that 8% of household water consumption is used for showering. The Market Transformation Programme (MTP 2007a) have estimated that if current trends continue the quantity of water used in showers in the UK will rise from about 650 Ml/d in 2000 to over 1200 Ml/d by 2020. As a result the use of water for showering is likely to become a major component of domestic water consumption, potentially rising to over 15% of total household water consumption by 2020. Any strategy for encouraging water efficiency in homes should therefore include actions for showers as a priority.

2 Focus Group Study

A series of three focus group workshops were held in late 2005 with 30 shower users (10 per seminar), drawn from the Merseyside area of United Utilities' supply area. The groups were questioned surrounding two broad themes: perceptions of the shower experience and attitudes to water efficiency and energy use. The group profiles represented:-

- Mix of gender (13 male, 17 female)
- Householders responsible for paying the water charge

- Mix of 12 metered and 18 unmetered water customers
- A range of adult age groups
- A range of lifestyle types (based on "Values and Lifestyles" groups)

3 Results of Focus Group Studies

The key themes identified were verified by triangulation with at least three supporting separate evidence strands for each theme.

- The focus groups confirmed the key importance of good flow-rate and temperature control. It is perceived as important to have enough water running over the body in order to keep warm in the shower.
- There is a growing trend toward daily or twice daily showering because of the ease of taking a shower.
- Adequate water flow and pressure are perceived as important factors in obtaining comfort, and some find more comfort by having a bath than by taking a shower.
- It was observed that higher pressure is required when taking a cold shower – a cold (or warm) shower is more acceptable if it feels forceful.
- There was often confusion about what is meant by a "power shower". This may be due to shower promotion literature often describing products as "power showers" even if they do not use a pump.

These results are in agreement with a focus group study carried out by the Market Transformation programme (MTP 2007c) with three separate groups of 10 people, increasing the confidence which can be placed in the outcomes of focus groups.

4 Laboratory Testing

An experimental shower was set up that represents as far as possible the standard plumbing practices in the UK. Tests were carried out on over 20 showerheads or flow restrictors in order to compare their physical performance characteristics over a range of pressure/flow conditions.

The key physical characteristics that were evaluated are:-

- Flow-rate
- Spray pattern (or spray distribution)
- Water temperature gradient
- Skin pressure (or velocity of spray)

These have been identified by MTP (2007d) as being key performance measures of shower comfort.

The system was equipped to continuously monitor and record the following key parameters

- Flow-rate (Q) of the cold water feed and the combined water at the showerhead.
- Temperature (T) of the cold water feed, hot water feed and the combined water at the showerhead.

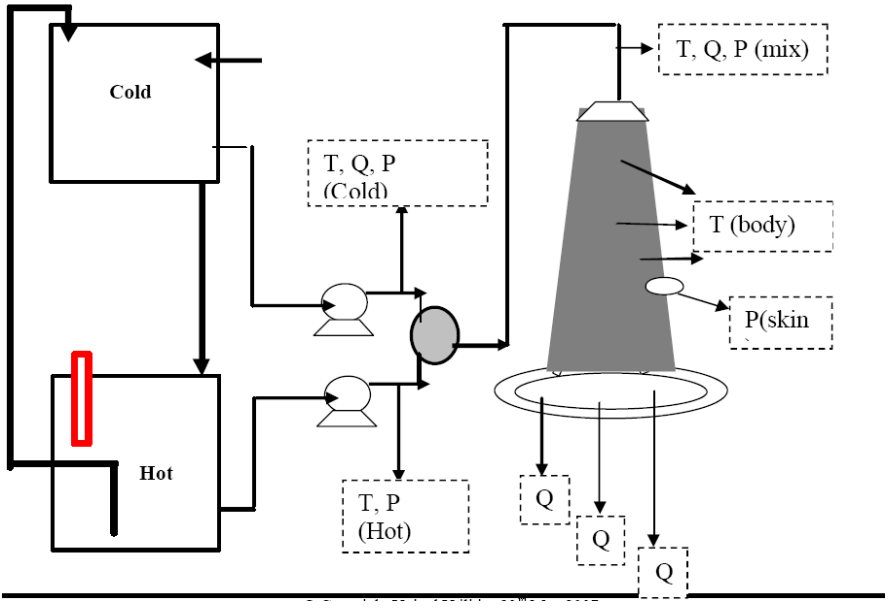

Fig. 1. Schematic view of laboratory trial system

- Vertical temperature profile (T body) in the shower cubicle
- Spray pattern/distribution by measuring the flow entering each segment of a concentric collector. It was measured at high level in accordance with British Standard BS 6340 Part 4, and at the shower base.
- Pressure (P) of the cold water feed, hot water feed and the combined water at the showerhead.
- "Skin pressure" (P_{skin}) to assess the forcefulness of the feel of the water spray on the body.

5 Results from Laboratory Tests

The majority of the showerheads tested obeyed a simple pressure-flow relationship with flow being proportional to the square root of the internal pressure at the showerhead.

$Q = k.P_{int}^{0.5}$, where Q = flow, P_{int} = internal gauge pressure in the showerhead and k is a form of discharge coefficient.

This is in accordance with the theory for turbulent flow through a constriction. The value of the constant k will depend on the nature of the constriction (and also on the units chosen for Q and P).

Pressure-flow- curves were derived for over 20 showerheads and regulators /restrictors. A sample is presented in Figure 2.

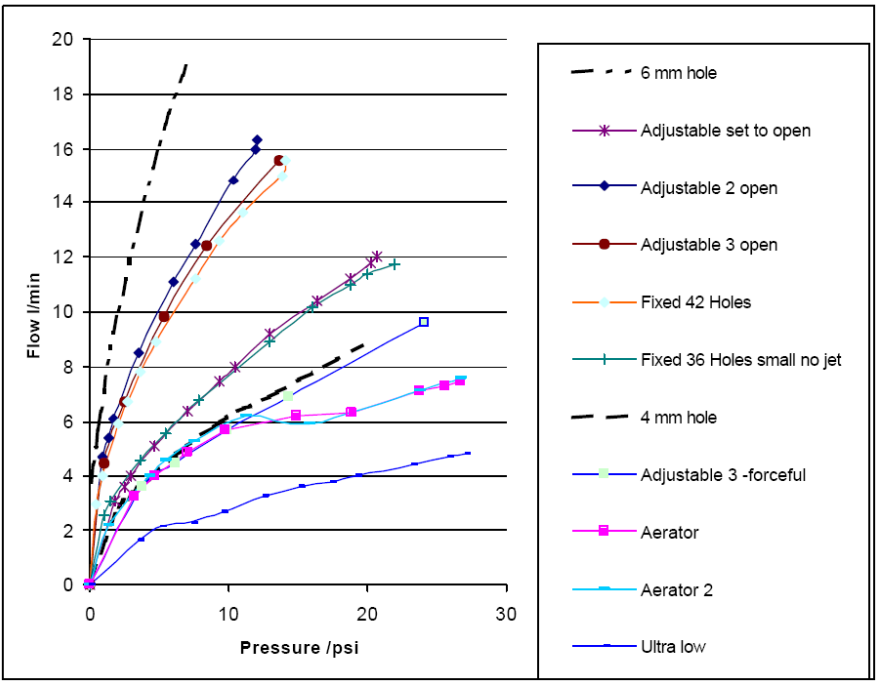

Fig. 2. Pressure-flow relationships. In some cases very high flow rates (over 12 l/min) were achieved at moderate or high pressures, whereas aerated showerheads and low flow showerheads maintained flows below 8 l/min even at the highest pressures.

6 Comparing Flow Rate with Showerhead Characteristics

It would be useful to be able to predict the flow behaviour of the showerhead from appearance or simple measurement. Therefore the performance of the showerheads was first compared to flow through a simple circular orifice in order to see if showerheads could be classified by their equivalent diameter D_e (where D_e is the diameter of a single circular orifice at the pipe outlet which gives the same pressure-flow characteristic as the showerhead itself). Despite the difference between a simple single orifice and the multiple small holes in a typical showerhead it proved possible to establish this relationship. The flow-pressure characteristics of an open orifice of 4mm or 6mm diameter are shown in Figure 3. Unsurprisingly, k and D_e were related, and over the range used showed a simple correlation

$$k = C_1.D_e - C_2$$

where C_1 and C_2 are constants whose value depends on the choice of units.

The form of equation shows that flow effectively ceases at small values of D_e. The coefficient k (and hence D_e) varied widely both between different showerheads and within a single showerhead where it was designed for use with multiple flow regimes. Interestingly, D_e was found to vary between 20 and 80% of the open hole diameter of

the feed pipe, implying that these would produce very different flow characteristics. It is suggested that k could be useful parameter in evaluating comparative flow performance of different showerheads.

7 Spray Pattern

The spray pattern (radial distribution) of different showerheads and the same showerhead operating under different conditions was examined. Widely varying spray distributions were measured either between the same head on different settings (where available) or between heads. Figure 3 shows the behaviour of a typical adjustable showerhead. In this case the pattern of spray distribution was relatively unaffected by the change in flow-rate, but changed with setting as designed. Note that the forceful effect was achieved by directing the spray into a narrow central pattern.

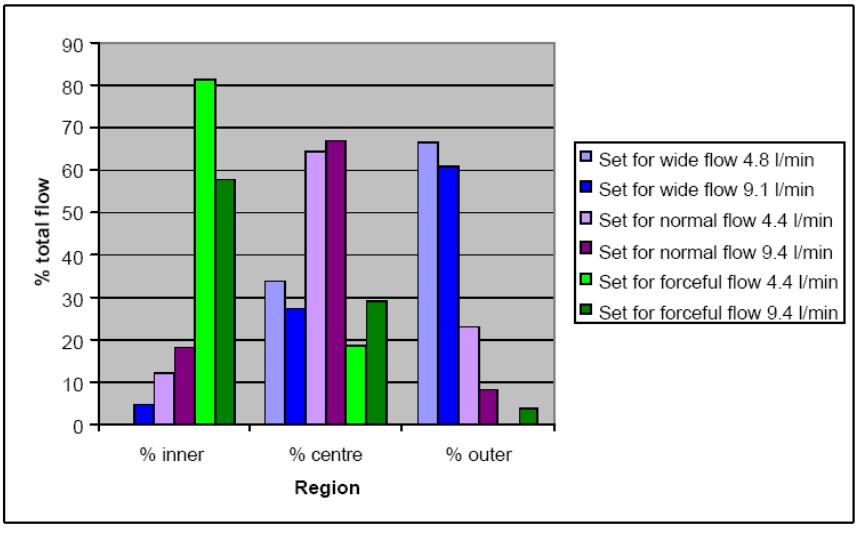

Fig. 3. The effect of flow-rate change in an adjustable shower head

Showerheads varied considerably in their ability to maintain a spray pattern over a range of flows. With some designs, flow distribution changes more significantly with changing flow-rate. Low flow is substantially more centrally directed which might serve to give the impression of a higher flow-rate than is actually occurring. However, overall wetting of the body might be affected which would modify the "shower experience".

8 The Effect of Flow Restriction

The incorporation of a flow restrictor produced effects predictable by the pressure-flow relationship. The form of the empirical pressure-flow relationship was unchanged and

the flow was reduced in proportion to the pressure loss caused by the restrictor. Since the flow characteristic is a function of pressure inside the showerhead itself, any device which is placed before it will simply reduce the pressure and hence the flow. This effect is no different to reducing the flow by turning down the tap on the mixer.

It is important here to differentiate between a simple restrictor that is effectively an orifice plate, and the more sophisticated flow-regulators which have internal restriction which is changes its effectiveness with applied pressure. In effect these latter devices provide a low restriction up to a preset value then rapidly increase thereafter giving a cut-off effect.

The effect on spray distribution will normally be that expected from a reduction in flow, as determined from previous experiments. The difficulty is that different showers heads respond quite differently.

9 Temperature Profile

It is generally agreed that temperature of the water is a major factor in defining shower experience. A modern shower with a well-designed thermostatic mixer is capable of giving very effective temperature stabilisation. However, once the water leaves the showerhead, significant heat losses can occur in a complex process in which droplet size, temperature difference between surrounding air and the water droplet, relative humidity and other variables have a significant role.

The vertical temperature profile of the falling spray in an empty shower cubicle under constant external conditions was examined (Figure 4) and found to differ between shower heads. There was no discernible difference in general between aerated showerheads and conventional showerheads. In general, larger temperature

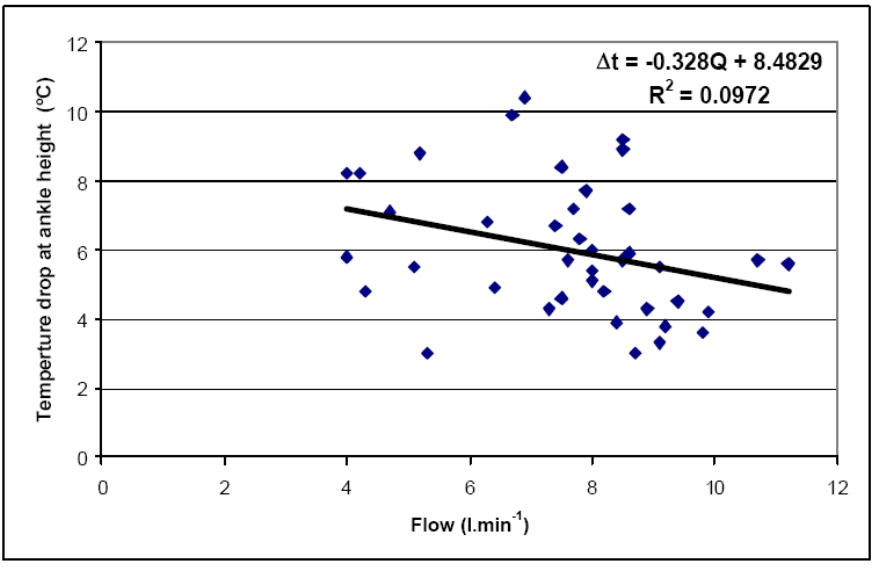

Fig. 4. Vertical temperature drop for different shower heads

drops were found at lower flow-rates. Although the correlation was only weak, it has implications for shower comfort if the flow-rate is deliberately restricted.

10 "Skin Pressure"

One of the factors affecting the shower experience is the sensation caused by the water hitting the skin. This sensation is complex and is affected by flow-rate, droplet

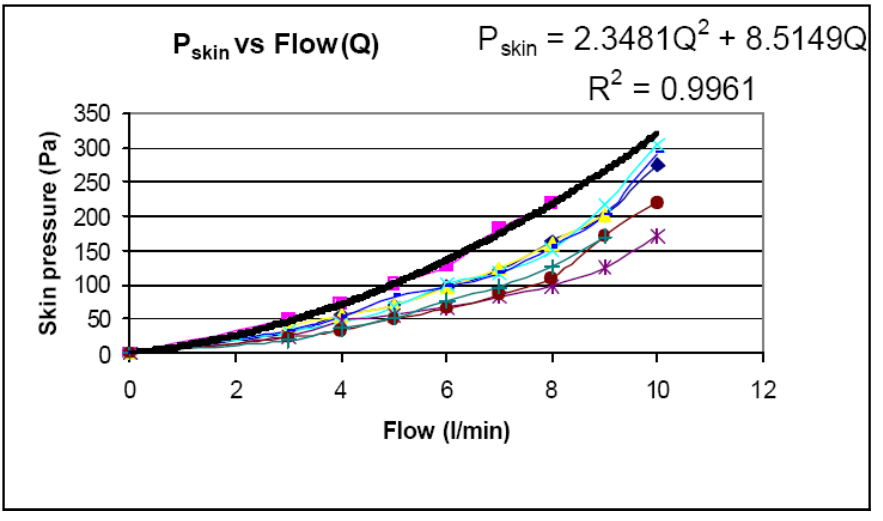

Fig. 5. Skin pressure as a function of flow

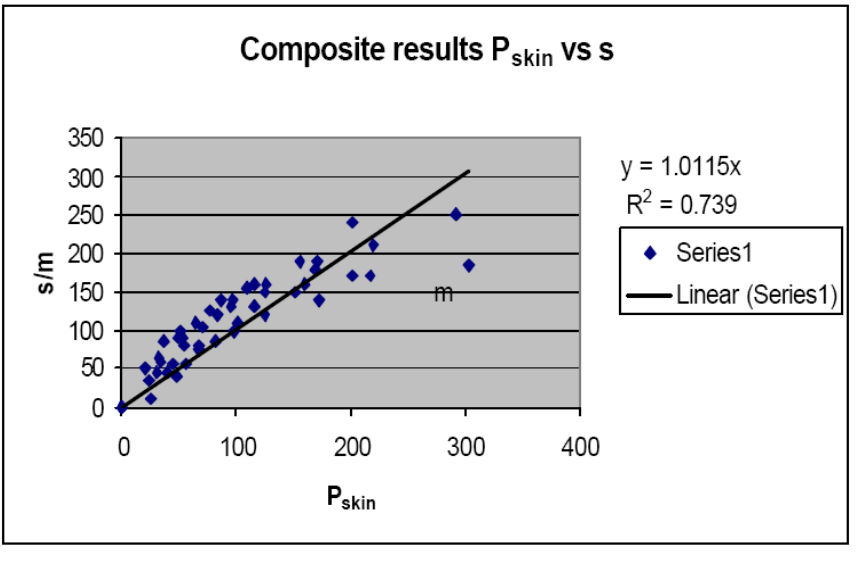

Fig. 6. Skin pressure is related to horizontal projection distance

size and temperature amongst other variables. Showers are often described in terms such as drenching, forceful, gentle, sparkling etc as manufactures promote particular characteristics. Clearly, it would be helpful if a direct measure of skin pressure could be made. In these experiments attempts were made to measure skin pressure using a membrane-sensing element coupled to very sensitive electronic manometer.

The data (figure 5) shows that as expected the skin pressure increases in a non-linear fashion with flow-rate. However, as the perceived effect of impact is not easy to determine the exact meaning of this for shower experience still remains to be resolved.

Although these experiments were successful, in general they are not practicable outside of a specially equipped laboratory. Consequently, a number of methods for indirect measurement were considered. A useful relationship (figure 6) was determined between P_{skin} and s (the horizontal distance of droplets leaving the shower).

11 Head Factor (*Hf*)

The dimensionless ratio P_{skin} / P_{supply} is independent of flow for a given showerhead, but varies widely between different showerheads. This parameter ($P_{skin} / P_{supply} = Hf$) which can be termed the 'head factor' could be of great significance in showerhead design.

Given the difficulty of relating qualitative outcomes such as "shower experience" to any experimentally determined variable it might a useful experiment to try to relate *Hf* to some measure of user satisfaction. If this could be established then the head factor might be a useful design tool.

12 Summary of Laboratory Results

Overall, it is concluded that a reduction of flow would change spray pattern, vertical temperature profile and skin pressure, but the changes in the first two would be different for each type of head. Therefore any process of water-saving which relies solely on flow reduction might change the shower experience in such a way as to render it unacceptable to the user. Consequently, water saving might be better achieved if reduced flow was achieved by adopting a suitable showerhead design, rather than by a simple restriction.

13 Home-Based Evaluations

A home-based evaluation programme was undertaken in order to investigate the extent to which customers are willing to accept a shower water saving device fitted to a mixer or pumped shower.

Water saving devices were tested in 18 homes - flow restrictors were fitted in 9 homes and aerated showerheads were fitted in 9 homes. The trial was designed to allow each household sufficient time (two weeks) to become used to the new system and thus give a more balanced response to the change.

Volunteers were recruited to participate in the project from employees at the university and at one water company office. They were informed that a modification would be made to their shower and that they could choose at the end of 2 weeks whether or not to keep the modification – they were not informed at that stage that the modification would involve water saving. In order to attract volunteers a reward of shopping vouchers to the value of £25 was offered for each home that was used for the tests.

The testing was completed for 18 households. Another 15 homes who were originally contacted were not used because either the shower was unsuitable (10 cases), or there were difficulties in contacting the customer (3 cases) or the customer withdrew during the testing (2 cases). The most common reason for a shower being unsuitable was that the flow-rate was too low, and the impact of the water saving device would be excessive.

Before testing, the 18 volunteer households were asked to complete a satisfaction rating for their shower (see below). At start of the test, the plumber visited each household to measure flow-rate and spray distribution of the shower at the user's preferred settings. He then fitted a water saving device – either a flow restrictor or an aerated showerhead. The households were then given a 2 week period in which to become accustomed to the water saving device. They were then asked to maintain a diary record for up to 2 weeks of each person's use of the shower, recording when the shower was taken, why a shower was taken, and its duration (they were given a digital timer). Two weeks later the plumber revisited the household to measure flow-rate and spray distribution of the shower, with the water saving device fitted, at the user's preferred settings. He asked the customer to complete a new satisfaction rating for the shower with the water saving device. He then either left or removed the water saving device as desired by the customer.

For each of the questions below, please tick the answer that mostly closely describes your satisfaction or experience with your shower.					
How satisfied are you with the overall ease of use and performance of your shower?	Very dissatisfied	Dissatisfied	Satisfied	Very satisfied	Fully satisfied
How easy is it to use your shower?	Very difficult	Difficult	Satisfactory	Good	Excellent
How easy is it to get in and out of your shower?	Very difficult	Difficult	Satisfactory	Good	Excellent
How well does the water flow cover your body?	Very poor	Poor	Satisfactory	Good	Excellent
How satisfied are you with the water flow to wash your hair effectively?	Very poor	Poor	Satisfactory	Good	Excellent
How does the water feel on your skin?	Too gentle or Very forceful		Gentle or Slightly forceful		Just right
How easy is it to get the water temperature right?	Very difficult	Difficult	Satisfactory	Good	Excellent
How satisfactory is the temperature throughout the shower enclosure?	Very cold in parts	Cool in parts	Satisfactory	Good	Excellent throughout

House reference	Shower type	Flow-rate before (l/min)	Flow-rate after (l/min)	Flow-rate reduction (l/min)	Flow-rate reduction (%)	Satisfaction score before	Satisfaction score after	Change in satisfaction score
RESTRICTOR WATER SAVING DEVICE KEPT AFTER TEST								
2	Mixer	12.4	6.6	5.6	45	25	17	-8
4	Pumped	11.0	7.8	3.2	29	30	28	-2
9 (m)	Pumped	18.4	6.0	12.4	67	36	31	-5
RESTRICTOR WATER SAVING DEVICE REMOVED AFTER TEST								
3 (m)	Pumped	11.0	7.8	3.2	29	36	30	-6
10	Mixer	9.4	7.2	2.2	23	28	17	-11
12 (m)	Pumped	12.4	9.8	2.6	21	27	22	-5
13	Mixer	7.8	6.4	1.4	18	27	25	-2
16	Mixer	12.8	7.1	5.7	45	36	17	-19
18	Mixer	12.1	7.4	4.7	39	?	?	?
SHOWERHEAD WATER SAVING DEVICE KEPT AFTER TEST								
1	Mixer	7.8	7.6	0.2	3	30	32	+2
6 (m)	Mixer	11.2	7.2	4.0	36	28	34	+6
7	Pumped	12.8	7.0	5.8	45	31	34	+3
8	Mixer	12.8	7.0	5.8	45	23	33	+10
11 (m)	Mixer	11.6	7.2	4.4	38	?	31	?
14	Mixer	8.1	7.4	0.7	9	27	35	+8
15	Pumped	12.0	8.4	3.6	30	33	32	-1
17	Mixer	8.4	7.2	1.2	14	32	31	-1
SHOWERHEAD WATER SAVING DEVICE REMOVED AFTER TEST								
5 (m)	Mixer	23.6	10.9	12.7	54	23	23	0

Water saving device	Houses choosing to KEEP device fitted	Houses choosing to have device REMOVED
	Number of houses	Number of houses
Restrictor	3	6
Aerated showerhead	8	1
All houses	11	7
	Average flow reduction (l/min)	Average flow reduction (l/min)
Restrictor	3.2	3.3
Aerated showerhead	3.2	12.7*
	Average flow reduction (%)	Average flow reduction (%)
Restrictor	47	29
Aerated showerhead	28	54*
	Average change in satisfaction score (range)	Average change in satisfaction score (range)
Restrictor	-5 (-2 to –8)	-9 (-2 to –19)
Aerated showerhead	+4 (-1 to +10)	0

14 Results of Home-Based Evaluations

The key findings from the home-based evaluations are:-

- The two sets of test households were broadly comparable with average flows of 12 l/min before any modification.
- The reduction for the two sets of households were also very similar (showers 12.0 →7.8 l/min and regulator 12.0 →7.4 l/min).
- Consequently initial flows or flow changes are not the principal determining cause of retention or removal.
- Flow restrictors were effective in reducing flow, but in most cases (6 out of 9) were not acceptable to customers and were asked to be removed.
- Aerated showerheads were effective in reducing flow, and in nearly all cases (8 out of 9) were requested to be kept.
- There is a statistically significant (at the 95% level) association between mode of water saving and the choice to retain. The presence of a water meter or not did not seem to affect the decision whether to retain a water saving device.
- There was no statistically significant difference observed in the flow-rate reduction between fitting of restrictor or showerhead.
- Satisfaction scores were lower in every case after fitting a flow restrictor, whereas satisfaction scores increased or were unchanged in nearly all cases after fitting the water saving showerhead.
- Changes in satisfaction score and the decision to keep or remove the water saving device do not seem to be linked to the reduction in water flow.
- There is a willingness by some customers to accept a water saving device even if it impairs the shower satisfaction.
- There was no marked change in the distribution of water flow by fitting of a flow restrictor or water saving showerhead.

15 Water and Energy Use

Over many years the use of a shower has been promoted as being more water efficient than having a bath. The data from this study and elsewhere indicates that often more water or energy is used by people who wash by shower than by a bath.

The home-based trials demonstrated that replacement of an existing showerhead with of an aerated showerhead saves an average of 28% of the water and energy use, assuming there is no change in the frequency and duration of showering. A customer with a mixer shower could typically expect to save £45 to £69 per year (assuming 5.8 to 9 minute average shower duration) or £103 per year in the case of a pumped shower. The payback period for a customer that purchases and installs an aerated showerhead would therefore usually be 1 to 3 months.

The energy use in homes to heat (and pump) water for personal washing is about 70 times that used by a water company to supply the water and dispose of the wastewater (MTP 2007b). The “carbon footprint” associated with total water use in the home also far exceeds that expended by the water company. Therefore actions to reduce water use, and the associated energy consumption, by showers do not only reduce water abstraction from the environment but also, very importantly, will have a significant effect on the energy and carbon consumption in the home.

Acknowledgements

This work was funded by United Utilities plc under their Social Responsibility Programme.

References

Market Transformation Programme, UK water consumption of showers (2007a)
Market Transformation Programme (in preparation). Energy consumption for household water consumption (2007b)
Market Transformation Programme, Consumer views about showers (2007c)
Market Transformation Programme, Showers water efficiency performance tests (2007d)
Note: all MTP reports,
http://www.mtprog.com/cms/library-programme-reports/
Water Research Centre, Increasing the value of domestic water use data for demand management, WRc Report P6805 (2005)

Research of Solar-Kang Heating Systems Design for Rural House in Cold Areas of China

Chunyan Zhou [1,2] and Hong Jin[*]

[1] School of Architecture, Harbin Institute of Technology, Harbin 150001, China
zhouchunyan1976@yahoo.cn
[2] School of Architecture and Programming, Jilin Institute of Architecture and Civil Engineering, Changchun 130021, China

Abstract. According to doing research on the rural houses in cold areas, this thesis mainly discusses a set of solar-hot-air heating system------Solar-Kang. In the local rural areas, one storey, rectangular and sloping roof are the most important characteristics in shape, and "Kang" is one of the main heating equipment. This heating system combines the characteristics of local houses and peasant's living habits, using slope roof as its heat collection devices, changing the traditional "Kang" into heat storage pond, and utilizing solar energy and cooking heat as heat source. Therefore, the poor indoor thermal environment in traditional rural houses can be improved, and it can reach the purposes of saving energy, ecology, comfort, and environmental protection.

1 Introduction

With the worse condition of energy and environment, solar heating technology has gradually begun to be used in the rural areas, especially in the cold areas where need to consume a large amount of energy for heating in winter. Under current investigation, we are able to see vast majority of solar heating technology is passive. This kind of technology has many merits----- easy operation, less cost, facilitate management, and it can improve indoor thermal comfort in winter to a certain extent. But under the influence of outside climate factors, its efficiency of heat gathering is lower and unstable. Therefore it is the trend for the rural houses to set up the active solar heating system through combining the characteristics of local house and appropriately increasing some active type equipments.

In the chill region of China, solar energy resources are very abundant. According to the Chinese national standard, the annual total solar radiation of the region is classified as level Ⅲ in China. The year-round sunshine duration is about 2200 to 3000 hours long, and the annual total solar radiation per square meter is about 5016 to 5852 *MJ*, which is equivalent to the quantity of heat generated by burning 170 to 200 *kg* of standard coal.

In the local rural areas, the vast majority of rural houses are single-storey detached house. Due to scattering, there are not unified pipe network in house, and both heating and water supplying are self-sufficient.

[*] Corresponding author.

Fig. 1. The traditional Kang in the rural house of China

"Kang" is the one of main living components in the local rural houses. In the first place, it is not only used as sleep furniture, but it is also the most important indoor heating equipment, which is commonly arranged in the bedroom. The hole of Kang connects the cooking stove, so that the Kang can be heated by remaining thermal of cooking, which is used for indoor heating. Much agricultural garbage could be used as fuel, such as straw, crop stalks, and so on. These fuels are adequate and cheap. Secondly, it is the center of activities of daily living. Northern peasants are used to sleeping, dining and doing housework on the Kang, for the surface temperature of the Kang is quite high which is between 33~45℃. While the outdoor temperature is under -30℃ and most space in the house is in quite low temperature which changes with the outdoor temperature rapidly through monitoring. Therefore, the "Kang" is very important in rural houses, and it is good not only for living comfort in winter, but also energy efficiency.

According to peasants' different living habits, "Kang" has many forms, as shown in Fig. 1: a North Kang or South Kang, the ground-Kang, etc. By comparing those different forms of Kang from the level of thermal comfort, energy saving and efficiency of using spaces, the ground-Kang is considered as the best form. Therefore combining the traditional ground-Kang with solar heating technology, it does not only meet the peasants' living habits, but also save the space and cost for the use of solar technology.

2 Systems Design

2.1 Medium Choice

In the active solar heating system, it is usually divided into three types according to different medium in the solar collecting devices: the solar water-collecting and water-heating system; the solar water-collecting and air-heating system; the solar air-collecting and air-heating system etc. Comparing with these heating systems, each of them has its own merit and shortcoming. For the chill region, air system has an advantage over water system.

The reasons are as follows:

- The outdoor temperature of chill region in winter is much lower, which means the freezing phenomenon occurs easily to the water-collecting system.
- The water medium easily makes the equipments decay, thus high quality anticorrosive and hermetic equipments are needed, which increase the cost. Meanwhile, equipment for air heating system is much simpler and cheaper.
- Besides bringing indoor hot air and maintaining comfortable living environment, air-heating system can conveniently control the humidity and ventilation.
- The requirement to the temperature of the medium for air-heating system is not high, 30~50℃ air can make the system run.

Thus, it is recommended taking the solar air collecting and heating system for rural houses in cold areas.

2.2 Solar Collecting Device Design

Through the on-the-spot investigation of the local rural houses, we discovered that the most local houses are slope roof. There will be triangular space in the roof, which is used to ventilating and removing moisture for the house. Accordingly we can make the south of roof into passive solar collecting device for solar heating system. As shown in Fig. 2, we can change the partly materials of the southern roof into glass. Under the sunshine, the greenhouse effect is produced. Then the heated air in the roof is sent to heat storage pond through supply air tube. This solar collecting device is widely used in Northern Europe of higher latitude areas, and also gains an effective result.

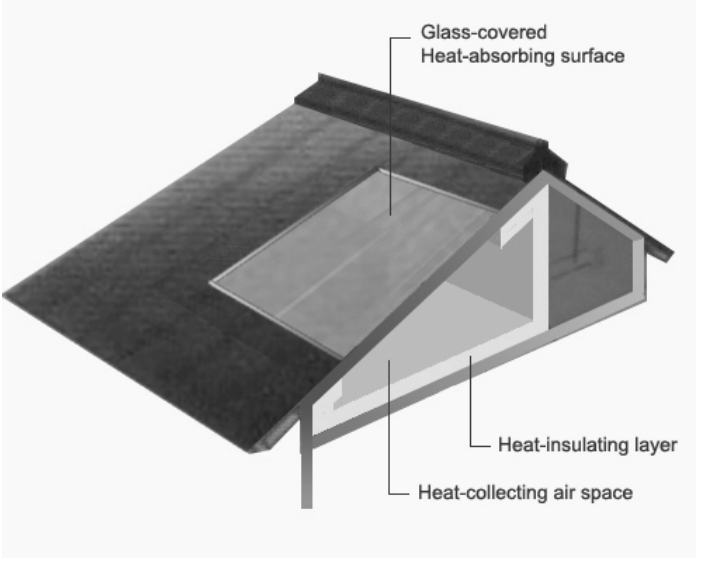

Fig. 2. Solar collecting space

In order to collect the air with high temperature, the solar collecting device must be solar-collecting efficiency. It is recommended adopting these measures:

- Choose special glass material, which has the higher efficiency in solar collecting.
- Make the surface of solar collector vertical with sunlight as far as possible, which can receive the most radiation from sun. So the sloping angle of roof must depend on the solar altitude of needed seasons. On the basis of experience, the best degree of sloping angle is "φ+15°" （"φ"is the local geography latitude）, so the 60°is suitable degree for the sloping angle of roof in the chill region.

On the other hand, good heat insulation for the solar collecting space is needed:

- Choose three-layer glaze.
- Set a zone from north space by using insulation board, it does not only cut down heating space but also reduce heat loss.
- Thick heat-insulating layer should be set on the roof and ceiling.

In addition, the glass for solar collecting should be strong enough to prevent damages from rain, snow and hailstone.

2.3 Heat Storage Pond Design

"Kang" is the most important heating equipment in the local rural houses. Cooking relies on its heating, so it needs connect with the stove directly. For this reason, bedrooms and kitchens are usually adjacent in the layout of house.

The traditional heating time is usually based on the meal time, belonging to the type of intermittent heating. In winter, the peasants generally do the cooking three times a day only, so there are three main heating times. This type of heating needs a longer interval, going through warming-up, constant temperature and cooling, which lead to greater temperature fluctuation and larger energy consumption. A study says: Energy consumed for warm-up period normally is 1.5 times that of temperature constancy period, and indoor temperature is not high. In order to maintain indoor temperature, it is necessary to make a good reservoir heat pond that can store up the thermal which is heated every time.

This principle is the same with the solar heating which is limited by time when receiving. In order to get constant thermal, a good reservoir heat pond is absolutely necessary. When air is adopted as the heating medium, solid material is needed to store heat. Nowadays one of the most popular solid materials is gravel. Because it has the higher ratio of the heat transmission with the air, at the same time it has the lower ratio between them, those are beneficial for heat storage. But compare with the water, the specific heat of gravel is one fourth of water; its density is as two and a half time as water. So on the condition of the same volume, the capacity of heat collection of gravel is as much as a bit more than three-fifth of water. Therefore it needs larger volume gravel when heat capacity is the same.

Combining the traditional heating device of the rural house, Kang space is used as the reservoir heat pond, which can not only avoid the extra occupation of the building space, but can also make use of the surplus heat after cooking.

Although the gravel has stronger heat storage capacity**,** it is necessary to possess a certain volume to achieve the requirements of heat storage, according to the formula:

$$V = \frac{Q}{\rho c \Delta t}$$

Where V ——the volume of the thermal storage material, m^3;

Q ——heat dissipating capacity at night, kJ;

ρ ——The density of materials, kg/m^3;

c ——specific heat capacity, $kJ/(kg \cdot ℃)$;

Δt ——temperature shift, $℃$.

As a rule, heating load of typical rural house is 54.72*kWh* in the whole day in the Northeast. The heat dissipating capacity of "Kang" is relatively less at night, occupying 1 / 3 of heating load. There are two Kangs in a house, so the heating load of each Kang is 9.12*kWh*, which is 32832 *kJ*. If the temperature shift is 5 ℃, the volume of gravel needed about 3 m^3. If the area of the ground Kang is 3*m* × 4.5*m*, the thickness of gravel needs about 200 *mm.*

The specific method of combination is following. Firstly, divide the body of Kang into two layers. The upper layer is solar energy heat storage pond. In order to keep the temperature of the air stable, this layer will be filled with gravels. In addition, the diameter of the gravels also has a very big influence on the heat transmission and circulation. If the diameter is small, the areas of heat transmission are large and the gradient of temperature is small, which is beneficial for heat transmission. But if the diameter is excessively small, the air resistance of the circulation will be strong, what is disadvantageous. So"1 to 1.5 *cm*" is better choice for the diameter of the gravels, at the same time the size of the gravels should be the same as far as possible.

The lower layer of Kang is the smoke tube. It is used to exhaust the smoke that is produced during cooking. The smoke tube is divided into two parts and they are arranged side in side. One is with larger area, used in winter. As shown in Fig. 3, the heat-insulated layer is under the smoke tube, which can decrease the losing of heat. The other one is with smaller area, used in summer when the heat supply is needless. The heat insulated layer is between the storage heat pond and the smoke tube, which is to avoid the heat, producing during cooking, going into indoor, which may cause the excessively high temperature. The material, which separates the two layers, should have both good capacity of heat transmission or heat insulation and certain capacity of sustaining weight. The surface of the Kang will not be taken any measures. It can radiate heat spontaneously. There will be an exhaust air vent under the window of the outer wall, which can form a warm screen for resisting the coldness. At the same time, the air vent should be higher than the ground in case some foreign matters would block it.

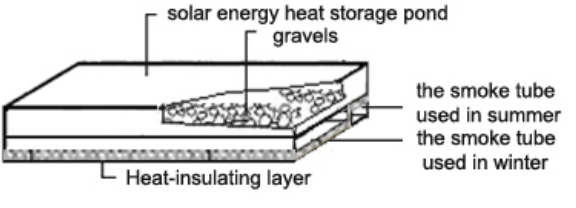

Fig. 3. Heat storage space

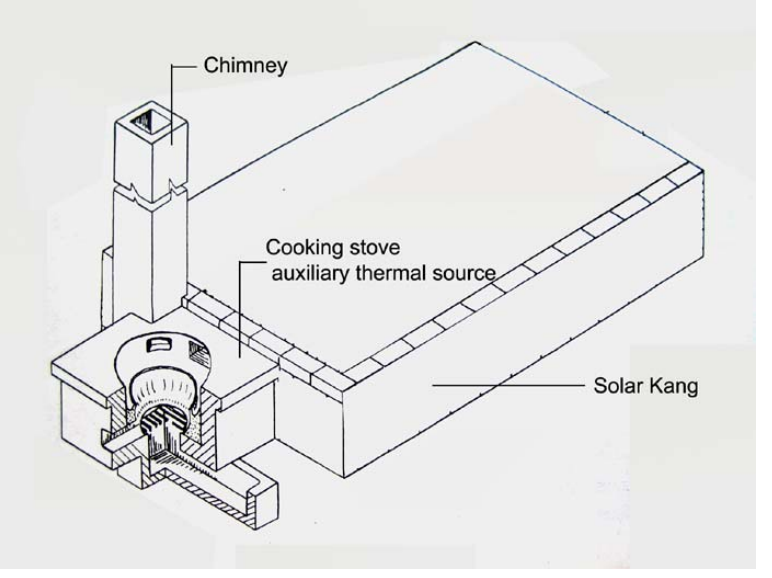

Fig. 4. Auxiliary thermal source

2.4 Auxiliary Thermal Source

In the solar heating system, auxiliary thermal source is a very important component in addition to the solar collector and heat storage devices because when solar radiation is received, it is limited not only by the time, but restricted by the weather. If it is cloudy and the solar radiation is not enough, the remaining heat of cooking could be used to heat up the air of the heat storage pond. If not cook, the furnace should be used to heat up the air that comes from the eaves before it is sent into the heat storage pond.

2.5 Heat-Recycling Devices

One of the main reasons for the loss of heat is the exchange between the outdoor air and the indoor air. So there should be a mechanical air exhaust device with the function of heat recovery. The device can recover the quantity of heat from hot and wet air that is produced during the cooking. On one side, it can exhaust the wet air and decrease the relative humidity; on the other side, during the time when the hot air is exhausted, it can heat the air goes in and reduce the temperature of the air which is exhausted out to the outdoors.

3 Systems Running

3.1 Running Procedure of Heating-Season System

As illustrating in figure 5, fresh air comes into the heat collection device through the eaves firstly, and then goes to the heat storage pond through the tube and stove after it

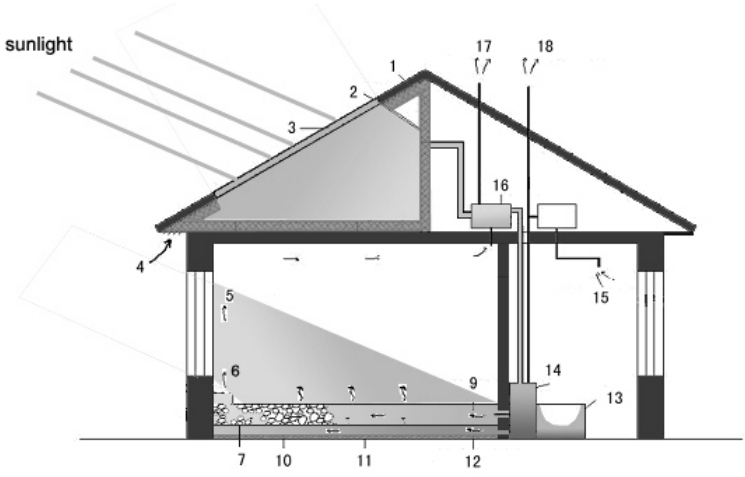

1. Adiabatic and shading board; 2. Closed damper; 3. Heat-gathering glass; 4. Fresh air comes into the heat collection device through the eaves; 5. Hot air screen; 6. Exit for hot air; 7. Gravel storage heat; 8. Thermolysis; 9. Heat from heat-collection device; 10. Flue 11. Heat-insulated layer of flue; 12. Remaining heat of cooking; 13. Cooking stove; 14. Furnace; 15. Smoke and humidity of cooking; 16. Heat-recycling devices; 17. Dirty air; 18. Exit of burning production;

Fig. 5. Running procedure of heating-season system

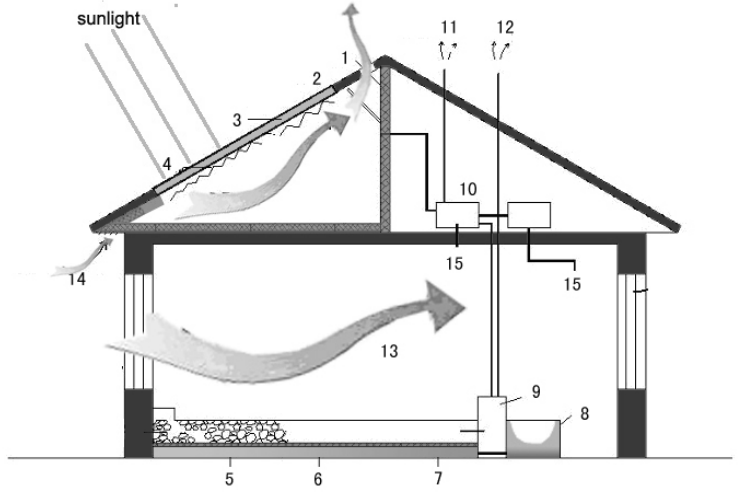

1. Adiabatic and shading board; 2. Opened damper; 3. Heat-gathering glass; 4. Automatic sunshade device; 5. Flue; 6. Heat-insulated layer of flue; 7. Remaining heat of cooking; 8. Cooking stove; 9.furnace; 10. Heat-recycling devices; 11. Dirty air; 12. Exit of burning production; 13. Draught; 14. Fresh air comes into the heat collection device through the eaves; 15. Exit of dirty air

Fig. 6. Running procedure of non-heating-season system

is heated. Then the heat will give off through conduction, convection and radiant. It can heat the room effectively. If the temperature of air that comes from the eaves is too low, the furnace should be used to heat up it before it is sent into the heat storage pond. At last, the dirty air in bedroom and kitchen can be sent outside by aeration system that possesses heat recovery device. The heat recovery pipe inside the system is border on the air-entering pipe. It can heat up the fresh air so that reduce the loss of the heat.

3.2 Running Procedure of Non-heating-Season System

As illustrating in figure 6, damper is set on the top of the heat collection device, and intake is set near the ridge of roof that could be closed in winter and opened in summer in order to make convection. The damper could adopt "memorial metal". When the heat runs over the fixed temperature, the metal will extend and the light damper will be opened. Meanwhile, the inside of the solar-gathering glass should adopt the automatic sunshade device in order to avoid greenhouse effect. In addition, windows should be opened on the inside wall in order to let the air go though.

4 Conclusions

For rural houses in chill region, heating energy in winter is the main part of energy consumption. Previous heating system wasted energy and polluted environment, influenced the peasants' living condition and quality. If combines clean solar energy technology and traditional heating technology, makes full use of the space of roof and Kang, it dose not only reserve peasants' traditional lifestyle, but also save the energy in maximum. Take a point of view on cost, it is much cheaper than those sets of active solar energy heating system, and more suitable for local technology and economy condition in rural areas.

Acknowledgments. This work was supported by the Ministry of Construction of China for the "11th Five-year Plan State science and technology support projects (Serial Number: 2006BAJ04B05-4)".

References

[1] Yunjun, L., et al.: The solar energy utilization technology. China Building Industry Press (2005)
[2] Hong, J., Lingling, Z.: Development and lasting of energy efficient performance in traditional rural house in northern region. New Architecture (2), 17–19 (2002)
[3] Ye, L., Ju-xiang, L., Xin-dong translate, W.: SNGLO, NORTON. The Influence of the solar collector long-term performance caused by habitation mode under northern Europe climate. Foreign Architecture and Country Construction (1), 35–42 (1997)
[4] Yuan-zhe, L.: Passive solar houses thermal design book. Qinghua University Press, China (1993)
[5] Yamad, M.: The thermal insulation for building. Guiqin Jing translate. China Building Industry Press (1987) (Japan)

[6] Feng, J., Jing, W., Xu, Z.: Solar-Kang Heating system for cold areas. Information of China Construction (12), 46 (2005)
[7] Green Architecture Research Center of Xi'an University of Architecture & Technology Green Architecture. China Planning Press (1999)

Research on Energy-Efficient Exterior Walls of Rural Housing in Northern China

Hong Jin and Hua Zhao

School of Architecture, Harbin Institute of Technology, Harbin 150001, China
jinhong_777@yahoo.com.cn

Abstract. The exterior wall of northern rural house in China takes up over 40% of the total thermal dissipation of the house. Inner surface of the exterior walls often freeze seriously with dew and frost. The paper brings forward the optimum fabric of exterior wall and the principle of choosing green insulation material through analyzing the condition of climate, construction and economic of northern rural area in China in order to solve these disadvantage. Therefore, the high quality green rural housing can be built, so that advancing sustainable development of rural housing construction in chill region of China.

Keywords: exterior wall, optimal structure, green building material, sustainable development, rural housing construction in northern China.

1 Introduction

The winter in China's northern regions is extremely cold and long, while the summer is cool and short. Most rural houses here are single-storey detached house with 100 square meters. The exterior wall areas per rural house are larger than that of the residential building in cities. Calculation shows that exterior wall takes up one quarter of the total thermal dissipation in the residential building, while the percent will reach to 40% in rural house.

Nowadays, most exterior walls of rural houses are still made of brick with 490mm thick in northern China. The exterior wall has poor performance in thermal insulation and energy conservation for Heat Transfer Coefficient of the wall is high (1.28 W/m^2•K). Inner surface temperature of exterior wall is usually below zero degree in winter, which leads to dew and frost heavily, shown as Fig. 1. Therefore, it is important to research optimal thermal insulation exterior wall which suits for the condition of rural areas in northern China.

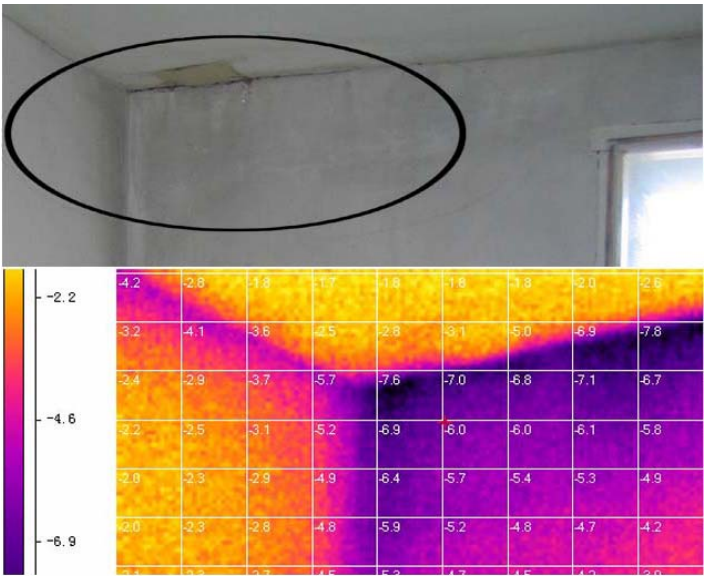

Fig. 1. The status and temperature distribution of interior surface of the exterior walls of traditional rural house in winter in Northern China

2 Optimize the Fabric of Exterior Wall

2.1 Enough Strength and Stability

Most rural houses in northern China are built with brick by local peasants who are skilled in building these houses. The brick wall has been proved to be in a good performance of supporting structure, dampproof, and fireproof through using for several hundreds of years. Therefore, it is suggested to keep on using brick as wall structure, and the thickness drops to 240mm from original 490mm on condition that meet supporting requirement, at the same time, the insulation material can be appended in the spare space.

2.2 Good Thermal Capability

After investigation, we found that causes of dewing on inner surface of exterior wall are as follows: (1) The heat resistance of the exterior wall is insufficient. (2) Heat source in rural houses is heated Kang [1], which cannot provide enough heat for the room by simply relying on the surplus heat of cooking three times a day. The indoor temperature is quite low at night, in the morning, as the hot air comes from kitchen to the cold wall, dew drops start to appear on the surfaces of walls. The heat that walls obtain by exchanges with the indoor air isn't enough to raise the temperature of inner surface of the walls above dew-point temperature while the heat storage coefficient of the material inside the structure of the wall is high.

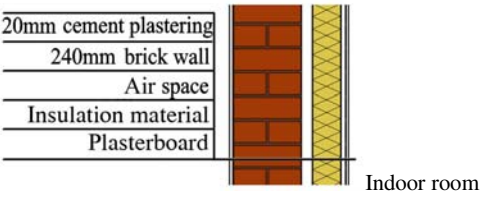

Fig. 2. The fabric of insulation compound wall

Improving the thermal performance of exterior wall, the first of all is to reduce heat transfer coefficient of exterior wall so as to enhance its insulation capability. It is suggested to add insulation materials to the brick walls to form compound walls, shown as Fig. 2. The thickness of insulation layer is based on the local climate and it is suggested to adopt economical thermal resistance to calculate the thickness of insulation materials [2], then be adjusted by the goal of saving 50% energy compared to the local traditional rural house, aiming to reach the goal of cost efficient and energy saving. Second is to decide the position of insulation material. Calculation shows that it is better to lessen attenuation multiple of inner material of exterior wall [3], furthermore, the physical character of the first internal skin of the structure play the most important role, i.e. the less thermal capacity is the inner material of exterior wall, the less energy is needed to raise the temperature of inner surface of exterior wall. This needs that walls are sensitive to fluctuate of indoor temperature. So a new type of wall should be designed not only with enough heat resistance but also with low heat storage capacity. It means that the inner surface temperature of the wall needs to rise beyond dew point as soon as possible after burning the oven, which is good for removing dew and keeping the structure dry.

Compared with the other kinds of walls, inner insulation compound wall will lead to poor indoor thermal stability, for its capability of heat storage is weak. However, rural housing owns heated Kang that made of concrete or bricks, which have large capability of thermal storage. That can maintain the indoor thermal stability. Hence, inner insulation compound wall is suitable to the rural house.

2.3 Good Enduring Performance

In order to enhance the integrate performance of waterproof and fireproof, at same time, advance the durability and applicability of the walls, it is suggested add 120mm brick inside the exterior walls as protection layer, shows as Fig. 3.

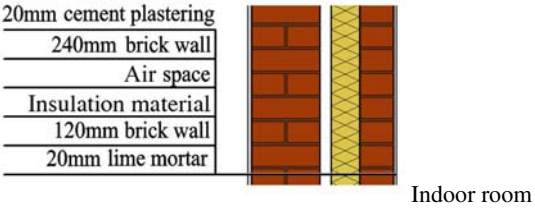

Fig. 3. The fabric of insulation wall with brick protection

3 Choose Suitable Insulation Materials

The best thermal insulation materials should be harmless, renewable, recyclable and degradable during their whole life-cycle. When choosing the thermal insulation materials, it should base on the local condition and follow the principle of "high performance, low cost, simply structured and plentiful", and at same time, another factor should be carefully considered which is called "cost of unit thermal resistance". It represents the relationship between the thermal performance of material and its cost.

Table 1. The analysis on the performance and price of the insulation material

Insulation materials		Prices(yuan/m^3)	Cost of unit thermal resistance Yuan/[m^2•(m^2•K/W)]
Straw panel		71.4	4.284
Straw panel (making by peasants)		42.8	2.568
Styrofoam (10kg/m^3)		210	8.82
Styrofoam with steel net	80mm	80	65
	100mm	100	65

Fig. 4. The straw compound wall under construction

By far, the most widely used insulation materials in the cold rural areas of China are Styrofoam plates, expanded perlite and the wastes of crops (such as the straw, husks and stalks, etc). The performance and price of them can be seen from Table 1, and it shows that the straw panel has the lowest cost. Meanwhile it is plentiful, renewable with low energy cost during the processing and transporting periods.

Recently, several model rural houses with straw wall have been built in cold rural areas in China (Fig. 4), which prove to be in good performance. Obviously, the straw panel will be a perfect thermal insulation material if it is disposed appropriately. Therefore, in the rural areas with plenty of straws, the renewable straw panel is a good choice.

4 Problems and Solutions

4.1 Elimination of Moisture

During the heating season, the water vapor will transfer from inside to outside, for the indoor partial pressure of water vapor is much higher than the outside one, Vapor will get dewed inside the wall during its transfer outwards from indoor room, and a condensational level will happen between these two materials if water vapor resistance of outside material is higher than inside material of the wall. Once condensation happens, the damp insulation materials may decrease their ability of thermal insulation. And for the straw panels, the moisture will not only weaken thermal performance of it, but turn it putrid.

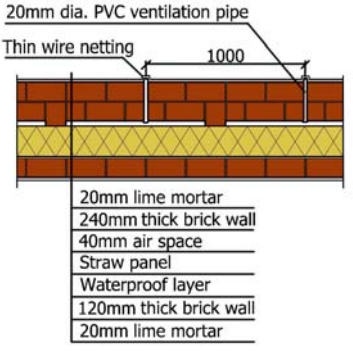

Fig. 5. Detail drawing of wall ventilation

So it is very essential to solve the problem of being moist for the wall. In view of this, it is recommended to place waterproof layer inside the insulation, and at same time, take ventilation measures for the wall. One of the appropriate measures is to add air gap between the brick and insulation material, and 20 mm diameter holes spread apart 1000mm vertically and horizontally, which covered with mosquito wiring at outlet (Fig. 5). Meanwhile, the lime mortar is adopted to finish surface of the wall in order to help with the evaporation of the moisture.

4.2 Disposal of Thermal Bridge

If the wall builds as Fig. 3, the thermal bridge happens in the connecting structure between wall and window, walls and roof, walls and floor. So it is necessary to enhance thermal insulation capability in these areas.

(1) It is recommended to cut off window lintel with insulation materials without decreasing the strength of the structure. And in order to keep the integrity of the structure, reinforcement steels are usually used to connect two lintels, shown as Fig. 6.

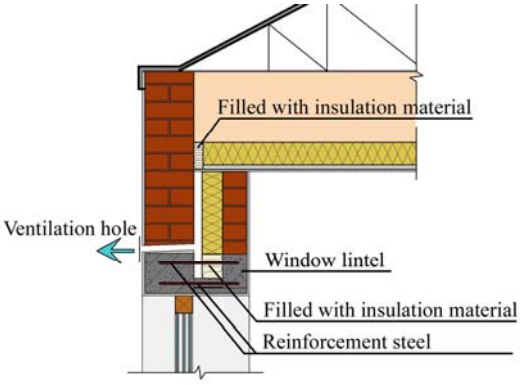

Fig. 6. The connection fabric between exterior wall and roof

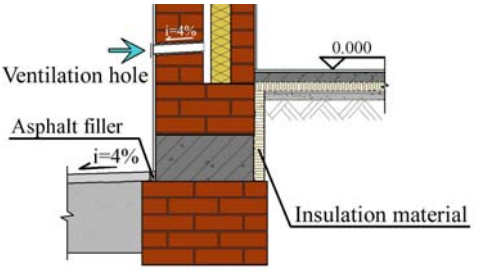

Fig. 7. The connection fabric between exterior wall and floor

(2) Insulation materials should be used to cut off the thermal bridge between the walls and floor, walls and roof to keep thermal insulation property of the envelope, shown as Fig. 6 and Fig. 7.

4.3 Stability and Integrity of Structure

The stability and integrity of insulation compound walls are weak than brick wall. In order to enhance the stability of the compound walls, it is necessary to strengthen the connection between different materials. Steel wall tie should be used to connect the structure of different materials to increase the stability, shown as Fig. 8.

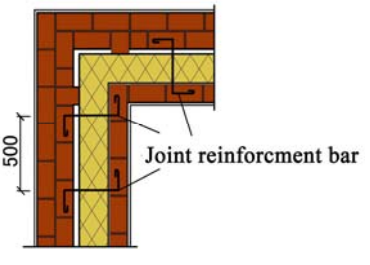

Fig. 8. Connecting structure of the wall

5 Conclusion

A model rural house according to above researches was built in Lindian county, Heilongjiang province. The results showed that the house with inner insulation com-

pound exterior wall had a good thermal performance, which made the house reduce energy consumption to 51.73% compared with the local traditional houses. Also, it solves the thermal disadvantages of traditional rural house such as dewing or frosting on the wall, creates a comfortable indoor environment and provides a good aesthetic appearance. At the same time, as straw penal is produced from crop wastes, it will not only reduce the transportation and energy cost, air pollutions and CO_2 emission, but also help with the sustainable development of rural housing and the environment in the cold region of China.

Acknowledgments. Project is supported by "National Key Project of Scientific and Technical Supporting Programs Funded by Ministry of Science & Technology of China (2006BAJ04B05-4)".

References

[1] Zhang, Y.: Jilin traditional house. Chinese Building Publishing House (1983)
[2] Hua, Z., Hong, J.: Economical Analyse of the compound envelop and materials in the heating buildings. Harbin Architecture University Journal 34(2), 83–85 (2001)
[3] Hong, J., et al.: Analyse the declination of building envelops in the villages of northern part in China. Harbin Architecture University Journal 33(4), 74–79 (2000)
[4] Rule of PRC, Thermal design code for civil building, China (1993)
[5] Rule of PRC, Energy conservation design standard for new heating residential buildings, JGJ26-95, China (1995)
[6] Rule of Heilongjiang, Design standard for energy efficiency of residential buildings in Heilongjiang Province (2008)

Family Thermal Performance Analysis Based on Household Metering

Hua Zhao and Hongxiang Shu

School of Municipal and Environmental Engineering, Harbin Institute of Technology, Harbin, China
zhaohua_hit@sina.com

Abstract. In this paper, we establish the mathematical models of the family thermal performance based on household metering and analyze the regularity of the family thermal performance on the basis of regression analysis. The models reveal the influencing factors of the heating system and individual regulation law of the indoor temperature based on household metering.

Keywords: Household-based heat metering, Regression analysis, Family thermal performance.

1 Introduction

Users regulated indoor temperature at different time of the day is called family thermal performance based on household metering. The regulation law of the indoor temperature of each family is different according to family members' living habits, economic condition and person comfort. The individual regulation will make heating system become a dynamic system, and the traditional operating regulation format is no longer fit. The individual regulation and the analysis of influencing factor of heat user will be the basis for the research of heating system based on household metering. Single room temperature regulation is affected by many factors, which has a certain regularity and randomness.

2 Multiple Regression Analysis

In this paper, regression analysis is used to be analysis method in the study of temperature regulation and functional relation between indoor temperature and other variables. Regression analysis is excellent statistical methods for studying the relationship between the variables. By analyzing a large number of sample data, the mathematical relationship between the variables is determined, and at the same time its credibility is checked by all kinds of statistics, then the significant variables which can influenced a certain specific variable are distinguished from the irrelevant ones. Users regulate the indoor temperature uncertainly, so the indoor temperature may be varied at different times in a day. In order to obtain the universal law, we use the multiple linear regression to establish the mathematical models of the family thermal

performance. In this paper, the data adapted in the process of analyzing are from the survey of the family heating in Harbin in the Master Degree thesis of HIT, "The Users Thermal Performance Based on Household Metering and the Research of System Operation and Regulation".

The regression analysis which is according to many independent variables' optimal combination to establish the regression equation in order to predict dependent variables is called the multiple regression analysis. Generally speaking the relationship between variables can be classified into two kinds: one kind is so called functional relationship in which the relationship among each variable is completely determined. Calculus is the very study of this kind of relationship. The other kind as the former which is also a certain relationship, but the relationship among each variable is incompletely certain. A powerful tool to cope with the relationship during these incompletely certain variables is the regression analysis. When the value of the independent variable is certain, the value of the dependent variable is uncertain, but there is a certain relationship in which uncertain among variables is called correlativity. Controlled variables can freely take given value in certain range. Uncontrolled variables are random, and possess certain probability distribution. The analysis among variable can be called regression analysis when variables are the controlled variables.. It includes linear regression, curve estimation, non-linear regression, logistic regression, and so on. Regression analysis of independent variable more than one is called the multiple regression analysis. The mathematical model of multiple regression analysis is:

$$y = \beta_0 + \beta_1 x_1 + \beta_2 x_2 + \cdots + \beta_p x_p + \varepsilon \tag{1}$$

Formula (1) is p variable linear regression model which includes p explanatory variables. The change of explanatory variable y consists of two parts: One part which caused by the change of p explanatory variables x is linear change that is: $y=\beta_0+\beta_1 x_1+\beta_2 x_2+\ldots\ldots+\beta_P x_P$; Another part which caused by other random factor isε. $\beta_0,\beta_1,\beta_2,\beta_P$ are all unknown parameters which respectively known as regression constant and partial regression coefficient of the model. $\varepsilon$is called accidental error the expectations of which is 0 and the variance is a specific value as the formula (2) requires:

$$\begin{cases} E(\varepsilon) = 0 \\ \mathrm{var}(\varepsilon) = \sigma^2 \end{cases} \tag{2}$$

Regression equation can not be immediately used for the analysis and forecast of actual problems after the establishment by sampled data, as usually needing to carry out various statistical test includes test of goodness of fit and significance test of regression equation, significance test of regression coefficients, residual analysis and so on.

3 Mathematical Models of Family Thermal Performance

In order to study the family thermal performance, multiple regression is adopted to establish mathematical models. Dependent variable is presumed to the linear function of

a number of variables. For example, if there are three variables, theoretical models can be expressed as follows:

$$T = \beta_0 + \beta_1 x_1 + \beta_2 x_2 + \beta_3 x_3 + \varepsilon \tag{3}$$

In Equation, β_0, β_1, β_2, β_3 are predicted regression coefficient; x_1, x_2, $x_3$are independent variable which assumed to influence the dependent variable q; ε is random errors.

Through finding every minimum value of square error between the observed value of dependent variable and the value predicted by regression equation, coefficientβ_j can be determined. In order to access to effective results by ordinary least square method, five basic assumptions of regression model are as follows:

Average is zero: For all the i, Sum(ε_i) or the error of expected value is zero, therefore error of expected value will change around zero at random and then it cancel each other out In a sense.

General changes: For all the i, $Var(\varepsilon_i) = \varphi_2$, error is prescribed constant which unrelated to the value of the dependent variable.

Independence: For all the $i \neq j$, ε_i andε_j are all normal.

Independence x_j: No relationship among independent variables.

Normal: The distribution of the dependent variable is similar to normal.

Two additional conditions are:

(1) Any of the independent variables is not the multi-combination (linear) of other ones;
(2) The known number need to be greater than the undetermined coefficient. When the regression model meet these five basic assumptions, the regression coefficient β, which is unbiased minimum, is determined by least square in the unbiased manner which is considered as the best linear unbiased estimates. If the basic assumptions are not met, the accuracy of least square will weaken.

The analysis of data in the preliminary process of which the samples with data unmatched (such as the one only with the option of indoor temperature without the law of life) and the data error (such as the situation that the temperature at bedtime is lower than temperature of duty) caused possibly by some real problems are rejected and, is based on the large amounts of survey data. In addition, in the study of data, some samples (for example, Users choose the indoor temperature regulation, but the settings of indoor temperature have not changed) which may affect the results of analysis are also deleted, which caused by the discrepancy when residents fill out their income. Due to the precondition that the linear relationship exist between variables, which do not meet the analysis, only one that has linear relationship is retained, the others are deleted.

Users regulated indoor temperature according to their own needs in the system based on household metering, so the indoor temperature $T_{in}=T(\tau,\varphi)$, whereτstands for time, τ=1:00-24:00 and $\varphi$is the factor affected the choice of users at room temperature. In the study of family thermal performance, a day will be divided into 24 sessions, and mathematical model of indoor temperature regulation each time will be

established to study the change rule of indoor temperature, then the daily models of the family thermal performance under normal circumstances will be obtained. The detailed steps of analysis are as follows:

(1) Do the correlation analysis in various time slots and find out the main factors influence the characteristic of heating usage of each session.
(2) Adopt the method of backward screening for the main factors and then remove some of the factors to obtain the main factors of indoor temperature regulation of each session.

Do the regression analysis through the main factors of indoor temperature regulation of each session and the indoor temperature of this session.

According to the above analysis of the data, mathematical models of the characteristic of family thermal performance based on household metering per session per day will be obtained and the results show as formula (4) where $y_1, y_2, \ldots\ldots y_{24}$ stand for the settings of room temperature each time, x_1, building area; x_2, member of the household; x_3, life time; x_4, regulation or not; x_5, Influence of hot price; x_6, age; x_7, educational level; x_8, users' income.

$$Y = AX + B \tag{4}$$

Where $Y=[y_1\ y_2\ \ldots\ldots y_{24}]^T$, $X=[x_1\ x_2\ \ldots\ldots x_{24}]$; A, B are coefficient of matrix; From the above models of the characteristic of thermal performance in different time slots, the influencing factors of the family thermal performance are approximately the same under the same state of life, or some differences exist. It shows that users' regulation which has the certain regularity and randomness is determined by many factors.

$$A = \begin{bmatrix}
0.014 & -0.565 & 0.035 & 0 & 0 & 0 & 0 & 0 \\
0.014 & -0.578 & 0.035 & 0 & 0 & 0 & 0 & 0 \\
0.014 & -0.578 & 0.035 & 0 & 0 & 0 & 0 & 0 \\
0.014 & -0.578 & 0.035 & 0 & 0 & 0 & 0 & 0 \\
0.014 & -0.609 & 0.035 & 0 & 0 & 0 & 0 & 0 \\
0.012 & -0.47 & 0.032 & 0 & 0 & 0 & 0 & 0 \\
0.014 & -0.793 & 0.038 & 0 & 0 & 0 & 0 & 0 \\
0.02 & -4.049 & 0.05 & -2.187 & -1.608 & 0 & 0 & 0 \\
0.026 & -4.77 & 0.094 & -2.618 & -1.81 & 0 & 0 & 0 \\
0.027 & -4.888 & 0.084 & -2.666 & -1.76 & 0 & 0 & 0 \\
0.028 & -4.664 & 0.094 & -2.536 & -1.705 & 0 & 0 & 0 \\
0.021 & -3.343 & 0.057 & -1.674 & 0 & 0 & 0 & 0 \\
0.021 & -3.285 & 0.06 & -1.676 & 0 & 0 & 0 & 0 \\
0.022 & -3.792 & 0.055 & -2.018 & 0 & 0 & 0 & 0 \\
0.027 & -4.759 & 0.094 & -2.633 & -1.692 & 0 & 0 & 0 \\
0.027 & -4.759 & 0.094 & -2.633 & -1.692 & 0 & 0 & 0 \\
0.026 & -4.718 & 0.096 & -2.51 & -2.149 & 0 & 0 & 0 \\
0.01 & -0.609 & 0.051 & 0 & 0 & -0.287 & 0.91 & 0 \\
0.013 & -0.622 & 0.045 & 0 & 0 & -0.291 & 0.902 & 0 \\
0 & 0 & 0 & 0 & 0 & 0 & 5.513 & 0 \\
0.012 & -0.541 & 0.047 & 0 & 0 & -0.311 & 1.022 & 0 \\
0.014 & -0.512 & 0.042 & 0 & 0 & 0 & 1.106 & 0 \\
0 & -2.012 & 0 & 0 & 0 & 0 & 0 & 0.002 \\
0.014 & -0.629 & 0.038 & 0 & 0 & 0 & 0.909 & 0
\end{bmatrix}$$

$$B = \begin{bmatrix}
18.398 \\
18.407 \\
18.407 \\
18.407 \\
18.528 \\
18.9 \\
18.89 \\
23.317 \\
22.744 \\
23.11 \\
22.447 \\
20.65 \\
20.508 \\
21.018 \\
22.545 \\
22.545 \\
22.886 \\
18.944 \\
19.053 \\
17.266 \\
18.834 \\
17.791 \\
17.857 \\
17.903
\end{bmatrix}$$

4 Result Analysis

According to the above mathematical models of the characteristic, we choose different building area, different incomes, different family composition, different education level and the heating price as the different impacting factors. Analyzing the data from the investigation, we get the conclusion that the larger the building area, the higher the mean indoor temperature. And the same with incomes and education level. We also

Table 1. Evaluate law of data input

Influence fator	Description	reference
age	According different range :1, 2, 3	Different age
Family member	Have the elderly or young :1, No: 2	Different condition
Heating style	Radiator:1, floor radiation : 2, others: 3	Different style
Education level	Junior and below: 0.25, senior: 0.5, bachelor: 0.75, master and above: 1	Different level
Know the heating price or not	Unknown: 0, know but wrong answered: 0.5, know and answered correctly: 1	Different level
Regulate or not	cannot: 0, maybe: 0.5, can: 1	Different level
incomes	take the median income range to input	Different level
Influnce from the heating price	no: 0, a little: 0.25, more: 0.75, much more: 1	Different level

Table 2. Investigation data in electron table

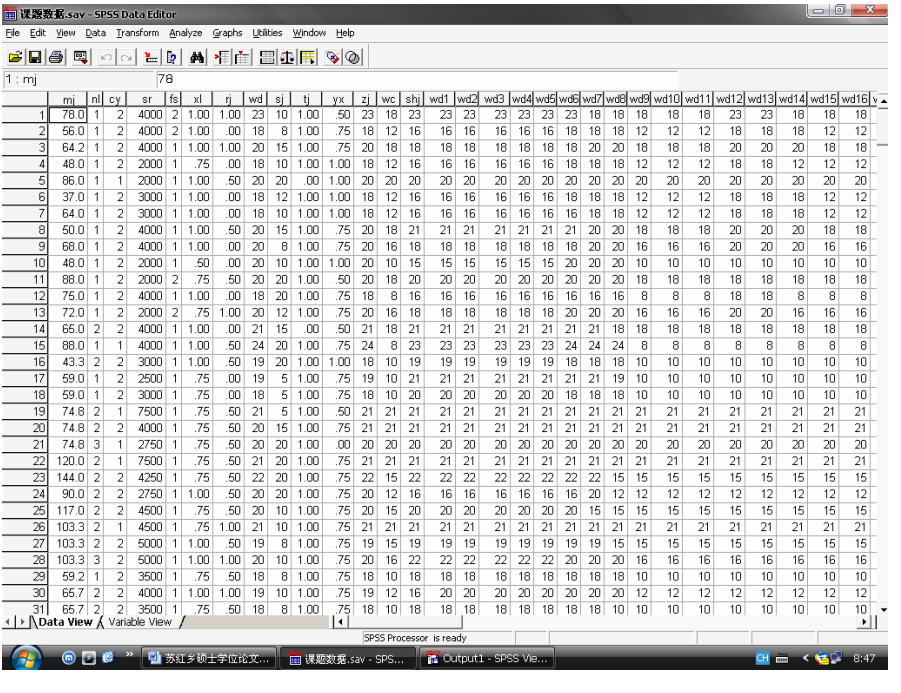

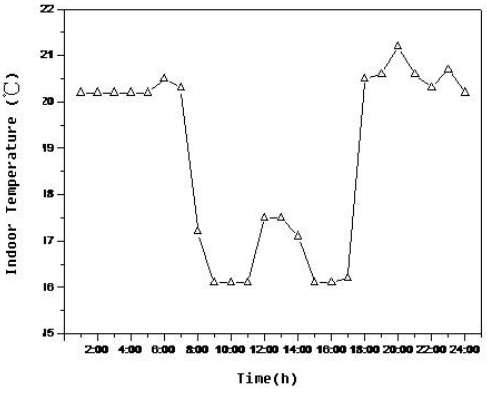

Fig. 1. The regulating characteristic curve of heating usage in family

find that the desire of family indoor temperature including children and elders is higher than that of common family and the mean date. Meanwhlie 70% users agreed that the influence exits on heating price. Deal with the data of the investigation, change them to be the signals and input them to the computer, then we got the table 2.

According to the above mathematical models of the characteristic, the regression, and fitting data of investigation the general model of family thermal performance can be obtained, the regulating characteristic curve of family thermal performance shows in Figure 1. From the curve, the characteristic of family thermal performance based on household metering is as follows:

Users regulated the indoor temperature with obvious stages, so the users should have a regular regulation change mainly according to laws of user's daily life;
Users' regulation of indoor temperature has two obvious process of temperature drop (Around 8:00 am, 13:00 pm) and temperature rise (11:00 am, 17:00 pm), mainly due to the difference of users' commuting time and life situation at this point in time.

From the curve, when the users have a rest or sleeping at home, the regulation of indoor temperature changes little, which shows that users at home regulate the indoor temperature with little probability and indoor temperature is basically stable.

The expected room temperature is higher than its value in the standard, which shows that the setting of indoor temperature should be improved in the heating based on household metering to leave a certain space for the users' regulation.

5 Conclusions

In this paper, according to the analysis of the influencing factors of family thermal performance, we establish the mathematical models of family thermal performance in the condition of users' daily life by using Regression Analysis. From the models, we can see that there are some regularity and randomness in the characteristic of the heating usage in family. The establishment of models will help us understand the

influencing factors of users' thermal performance based on household metering more clearly, and study the regulation law of users heating based on household metering more intuitively, inquire residents' consumption pattern and level of heating based on household metering in northern china more roundly, analyze how the energy consumption of building heating changes on the present basis as well as its change range. All of these will provide basic data and foundation for the government department to formulate the policy and the schedule plan of charge based on thermal measurement.

Acknowledgments

Thanks for the grant by "Key Technology of Energy Efficiency in Heating System" (issue number: 2006BAJ01A04), which is the fourth subtopic of the Science and Technology projects of the "11th Five-Year" plan of the nation".

References

1. Jianying, Y., Xuhong, H.: Statistic and Analysis for Data and Application of SPSS. People's Post Press (2003)
2. Xue, w.: Statistic Analysis and Application for SPSS. Electronics Industry Press (2005)

The Investigation and Analysis of Indoor Temperature Desire of Building Users in Harbin

Hua Zhao and Hongxiang Shu

School of Municipal and Environmental Engineering, Harbin Institute of Technology, Harbin, China
zhaohua_hit@sina.com

Abstract. The desire of building indoor temperature is the basis of heating supply. This paper made research on the desire of indoor temperature in Harbin, and analyzed the influencing factors of the heating desire. In this research, we get the answer from questionnaires on building users, which contains, such as the area of the house, the family in the house, the age of the family, the income of the family, their job, their life, the choice of the indoor temperature and the price of the heating and so on. There are about 14 main questions and 20 subsidiary questions. We can get a law after analyzing the questionnaire, the users' desire of the indoor temperature in the Household Metering System is different from traditional charging by area. The will of the regulating of the users is related to the income of the family, the members of the family, the age of the families, the education that the families income, the area of the building, the price of the heat and their life styles. Generally speaking, the users think the scale of the most comfortable indoor temperature is 18~20℃, mostly prefer 20~22℃. The scale of the living house temperature, the temperature at work and sleeping temperature are respectively 19~22℃, 13.5~17.5℃ and 19~21℃.

Keywords: Household metering, heating, Energy conservation, Indoor temperature.

1 Introduction

With the development of the building energy conservation in china, it is necessary to develop new heating metering system, in which the desire of the indoor temperature and the regulation method is influenced by many factors, and is different from the traditional system. The research on the desire of the users based on household metering will provide important data for the design of the system, the decision of the heating price and some other research.

2 Family Thermal Performance in Harbin

This paper aimed to know influencing factors of user desired indoor temperature, and our group got the useful material by a investigation on users. We take two methods of typical check and spot check, and require the users to answer the questionnaires and

returned immediately. In this way, we can communicate with the users face to face, and know more new problems and try to save them, so the problem from the research could be reasonable. During communicating with the clients, we get more about what they concerned and what the heating metering needs. It is good for the following research on the regulation of users heating requirement. Before the design of the questionnaires, we have referred to papers about others' research in the world, and we can get some popular questions of the influence factors from the users. Every question appears relatively, in this way, the users want to finish our problems, so the investigated time was cut down and the work efficiency will be enhanced.

After the design of the questionnaires and the discussion of all the teacher and students, print a small number of questionnaires and hand them out to some users, from the returned questionnaire, we can find the some disadvantages, then we modified the questionnaires after analyzing the questionnaire from the first handing out and return, finally, we fixed on the format and the content, which contains 14 main questions and 20 subsidiary questions. In order to get the useful points, we have taken many surveying methods in these questionnaires, the popular surveying methods contain willing-research, biding and comparing.

The questions contain many things, such as the square of the house, the family in the house, the age of the family, the income of the family, the choice of the indoor temperature and the price of the heating and so on. The members of the questionnaire handed out 400 papers to the dweller in Harbin, and 380 papers returned during Nov. 2006 and Mar. 2007. In this research we usually get into the users' house to communicate with them, and by the talk face to face, we get a lot of messages which we can get from the questionnaires. In the aspect of area choosing, we consider that in terms of the economy, the development, the surrounding, and the users. In terms of the desire of the research, we considered of building as our main objects, including the living building in colleges, the living building of workers of companies and common merchandise-building. The objects of the research contain many kinds of people, the age from 18 to 70; different education level from blank to postgraduate; the job such as research worker, workers out of job, students and businessman; the building styles modern-building and low building; the style of heating, radiator heating and radiant heating. Besides indoor temperature research, we have also taken social research, and we hand out the questionnaires to the people outside, and they can answer the questions immediately and return the papers back. In this way, we can have a communication with the people face to face, we can get some problems in practice.

This research is mainly on the regulation of the family thermal performance and the influencing factors, which included the heating terminal mode, the income of the family, the living habits, psychological factors of the users and so on.

3 Result Analysis

Analyzed the dates from the investigation, and deleted the swatch which is not suitable (such as just choose the indoor temperature and no life style) and some mistakes caused by problems in practice (such as the sleeping temperature is under the temperature on service). Otherwise, we find that some swatch may influence the analysis results, mainly because the incomes answered by the users are not true. So some swatch was deleted, too. After first processing to the dates, we can get such conclusions.

After implementing household metering, the users can regulate the indoor temperature according to their desire. In the research, we found that the users have three states: free at home, asleep and working. By analyzing the dates from the questionnaires, we can get the desire of indoor temperature in the three states, just as following table.

Table 1. Mean indoor temperature

The style of temperature	Swatch number	Min (℃)	Max (℃)	Mean (℃)	Standard difference
At home	367	18	24	20.70	1.528
Working	367	5	24	15.29	4.446
Sleeping	367	15	24	20.19	1.749
Comfortable	367	18	26	20.72	1.525

From the Table 1, we know that the desire of the indoor temperature based on heating metering: free at home is 20.7℃, working is 15.29℃, sleeping is 20.19℃, and 20.72℃ is the most comfortable. The desire of the indoor temperature is different in different state based on heating metering. The desire of the indoor temperature in the state of free at home and sleeping is higher then present design criterion, which caused some users' indoor temperature lowed because of hydraulic disorder, so the desire of the indoor temperature is high then needs; With the living level improving, indoor temperature raise, too. The desire of the indoor temperature in the state of working is 2.71℃ lower than criteria, and the difference is small, firstly, in order to avoid the indoor temperature fluctuate too much, the users will need higher indoor temperature, secondly, the main reason is that many users cannot make sure whether the heating metering system can make the indoor temperature satisfied their desire, so they don't want to low their indoor temperature.

The influence of the building area to the indoor temperature: the mean indoor temperature in different state and different building area can be found from Table 2, we can get that there are some relations between the building area and the willing mean indoor temperature, generally speaking, the larger the building area, the higher the mean indoor temperature.

The influence of the incomes: from data analysis in Table 3, we can get that the regulation of indoor temperature was affected by incomes, generally speaking, the

Table 2. The mean indoor temperature in different building area

The building area (m^2)	Percent in total (%)	At home (℃)	Working (℃)	Sleeping (℃)	Comfortable (℃)
Mean number	100	20.7	15.29	20.19	20.72
<60	18.0	19.62	12.68	19.00	19.71
60~90	41.7	20.3	14.35	19.71	20.3
90～120	24.8	21.4	17.24	21.00	21.4
Above 120	15.5	21.89	17.72	21.60	21.96

Table 3. The indoor temperature of different incomes

Incomes (Yuan)	Percent in total (%)	At home (℃)	Working (℃)	Sleeping (℃)	Comfortable (℃)
Mean	100	20.7	15.29	20.19	20.72
<1000	1.4	19.60	15.40	19.40	19.60
1000~2500	32.7	20.08	13.54	19.38	20.08
250～3500	36.2	20.69	15.40	20.23	20.68
350～5000	22.9	21.44	16.99	21.07	21.39
Above 5000	6.8	21.84	17.40	21.12	21.72

Table 4. The indoor temperature of different family

The member of the family	Percent in total (%)	At home (℃)	Working (℃)	Sleeping (℃)	Comfortable (℃)
Mean	100	20.70	15.29	20.19	20.72
Elder and children	30	21.40	17.91	20.97	21.42
No elder and children	70	20.40	14.17	19.86	20.43

more the incomes is, the higher the mean indoor temperature is. We cannot find good orderliness from Table 3, because that there is no economic relations between the way of heating charge and users, so the relation between the incomes and the desire of indoor temperature is not evident. therefore, the incomes is a main factor that influence the indoor temperature in different time and the regulating of the users.

The influence of the family members to indoor temperature: in the process of designing the questionnaires, we have considered the influence of the family members to indoor temperature, we divided the family structure into two kinds, the result of the analysis of the date was written in Table 4, we can find that the desire of family indoor temperature including children and elders is higher than that of common family and the mean date, specially the temperature at working. So we can have a conclusion that heating was influenced much by the members of the family.

The influence of the education level to the desire of indoor temperature: in order to know the influence factors of the education level to the desire of indoor temperature, the users were asked to answer their education level before their answering the questionnaires. And take the answerers education level as the family's, which was divided into four kinds, which can be found in Table 5. The results tell us that the higher the education level of the family is, the higher the indoor temperature they need. The desire when free at home and sleeping is higher, but it is lower when they are working outside. All of that mean that the education level has some influence to the habits of the heating and life style. The higher the education level is, the higher the comfortable desire need.

Table 5. Indoor temperature of different education level

Education level	Percent in total (%)	At home (℃)	Working (℃)	Sleeping (℃)	Comfortable (℃)
Mean	100	20.7	15.29	20.19	20.72
Postgraduate	19.4	20.79	14.82	20.23	20.86
Undergraduate/junior college	49.0	20.99	15.94	20.57	21.02
Senior high school Technical secondary school	28.3	20.12	14.16	19.47	20.10
Grade school	3.3	20.92	18.08	20.67	20.83

Table 6. The influence of the heating price to the indoor temperature

The level of the influence	Percent in total (%)	At home (℃)	Working (℃)	Sleeping (℃)	Comfortable (℃)
Mean	100	20.7	15.29	20.19	20.72
Large influence	28.9	20.32	14.58	19.66	20.35
Influence	41.1	20.48	14.65	20.03	20.47
A little	21.3	21.53	17.15	21.10	21.58
Non	8.7	20.97	16.13	20.53	21.09

The influence of the heating price to regulating of indoor temperature: in order to study the influence of the heating price to regulating of indoor temperature, in the questionnaires this question was included, the result of the data analysis was written in Table 6. The data means that 70% users agreed that the influence exits or the influence is large. If the heating price is higher, the indoor temperature will lower than the mean one especial when at work, so the heating price can be seen as the lever of economics. We can regulate the indoor temperature through the heating price. From the table we can know that the comfort of human is not only influenced by the feeling and other subjected factors, but also by some objected factors, such as the heating price and the economic level.

Besides, the regulation of indoor temperature was influenced by other factors, such as the life style of the families, the consciousness of energy saving and the heating ways of the family.

The consciousness of energy saving: in order to achieve energy saving in the building, we must call for the consciousness of energy saving in users. In heating metering system, users can regulate their indoor temperature to satisfy themselves comfortable, turn down the indoor temperature when nobody at home, and the basic indoor temperature can be kept by the heat store of the building, meanwhile, start the temperature control valve when the temperature is too high rather than opening the window. From the data of the questionnaires, about 94% of the users agree with regulating of indoor temperature if it is able to do that. But most of the users' reason to regulate the indoor temperature is that the temperature is far from the expect one in today's design and running of the heating system. The desire of indoor temperature of the users, including the one agreeing with the temperature regulating and the one disagreeing, is written in Table 7.

Table 7. Indoor temperature of the users say yes or no to the regulation of indoor temperature

Regulating or not	Percent in total (%)	At home (℃)	Working (℃)	Sleeping (℃)	Comfortable (℃)
Mean	100	20.7	15.29	20.19	20.72
No	5.7	21.14	19.48	20.76	21.19
Yes	94.3	20.68	15.04	20.16	20.70

From the Table 7, we can get that the desire of the indoor temperature is lower for the users say yes than the one say no, especially in the time of working, the difference is 4.4℃, so we can see that it is obvious to save energy with indoor temperature regulating. In practice, the users don't want to turn down the indoor temperature because they are worried about the long time of warm up for the building, and some users are not used to regulating. From the table 3, many users choose the same temperature asleep when the one free at home, the main reason is that they don't want to regulate the temperature control valve. From this research we can also know that the motivation to regulate the indoor temperature is not all just aiming to save energy, and the level of the indoor temperature exits difference in practice. From another data we can know that 43.1% of the users don't know the heat price at all, 19.6% say know but the answer is wrong, only 37.3% can give us a right answer. Then we can know that the users don't care for the heating price, this may be caused by the heating system, the heating price has no relation to the users' benefit directly, then the consciousness of energy saving was decreased, for users in Harbin, the energy saving is not so popular as the data from the questionnaires, so the potential of energy saving in activity of clients themselves is larger.

4 Household Metering Technical Problems

From the research we find that in order to make users save energy in household metering system, we should solve following problems:

(1) Regulation and control should be simple and convenient. In the research, users doubt for the regulating equipment of indoor temperature (temperature control valve), the metering and control of indoor temperature will influence directly users say yes or no to the regulator of indoor temperature. In heating designs, double-rise and panel heating were used together in buildings, which can finish simple household control, but the setting and regulating of indoor temperature is difficult.

(2) For the problem of heating price. Reasonable heating price can motivate the activities to save energy, turn down the indoor temperature when people are out of the building and keep the indoor temperature by the heat accumulation of the building. Meanwhile the regulating of the indoor temperature will drive the building-energy saving and decrease the energy building used. The existing charging model, charging by areas and under the planned economy system, has not connected the heating with the user's benefit, heat has not been seen as goods. After the household metering, the existing single model of charging for heat should be changed, and we should search for a reasonable heating price and a charge model, for example, allow the difference of the heating price for different users and divide the buildings into different use. Such as the

building on service (living building, office building, teach building) and commercial building (super market, hotel, building for finance and telecom), industrial building and so on, we should make the heating price and constitute correlative policy, charge in terms of the heating quality. To the energy status in china, we should limit the maximum heat use in the basis of satisfying all the users' heating desire, which means that we should make the maximum limit for each kind of building, perfect correlative metering system, evaluating system and rewards and punishment bad system, we should give some punishment to the users whose heating load is higher than the limit, and the one who used least should get some rewards. The consciousness of heating users is improved by the method of law and economy.

(3) For the regulation and control of heating system based on household metering, users' regulation in household metering system will bring variable hydraulic characteristic of the heating network, and how to make sure the heat source and network to adapt to the change and the desire of the users. Generally speaking, the regulation of the indoor temperature contains three steps: turn up the temperature (warm-up), keep the temperature, turn down the temperature. Whether the users can get enough heat in the step one and decrease the warm-up time will influence the activity of the users to regulate the indoor temperature and the fluctuation of the indoor temperature. How to satisfy the users' desire according to the additional heat supply capacity and the combination of different heating system is important.

(4) Rational metering method and evaluating system is need. Impartial and rational heat metering model will influence the users' benefits directly, we should know how to make sure the users pay the heat in terms of the heat use.

5 Conclusions

This paper study the influencing factors of indoor temperature desire from traditional heating system to household metering system by analyzing the questionnaires and the data from the research of the indoor temperature desire in Harbin. The regulation of indoor temperature may be influenced by many factors, the building area, incomes of the family, the members of the family, the heat price, the life style and so on. The relation between the factors and users' desire need a further research.

Acknowledgments

Thanks for the grant by "Key Technology of Energy Efficiency in Heating System" (issue number: 2006BAJ01A04), which is the fourth subtopic of the Science and Technology projects of the "11th Five-Year" plan of the nation".

References

1. Hongkang, F.: The sample survey. Higher Education Press, China (2002)
2. Xiaoping, C.: Common mathematics method of economic forecast. Transaction of Nantong Institute of Technology, China 15(3), 49–52 (1999)

3. Qiuhua, Z., Shuxin, H.: The new problems caused by heat-metering. Chinese housing facilities (12), 44–46 (2004)
4. Feng, W.: The research about the heating load and the disciplinarian of the change of indoor temperature in Household Metering system. MA Dissertation of Taiyuan Polytechnic University, China (2003)

Simulated Performance of Earthtube for Cooling of Office Buildings in the Southeast of UK

Abdullahi Ahmed, Kenneth IP, Andrew Miller, and Kassim Gidado

School of Environment and Technology, University of Brighton, Cockcroft Building, Lewes Road, Brighton, BN2 4GJ, UK
aa1@bton.ac.uk, k.ip@bton.ac.uk, a.miller@bton.ac.uk, k.i.gidado@bton.ac.uk

Abstract. Using the ground-air heat exchanger to reduce the temperature fluctuations of the outdoor air supply to a building is a potential sustainable low carbon emissions building design option where suitable site conditions exist. Although the basic concept of this technology is simple and some thermal models already exist, there is no integrated design tool or published data that can be used directly to predict their dynamic thermal performance. This research reviewed the current state of the art on the thermal models of earthtubes and thermal performance prediction tools. Available soil temperature profiles and earthtube thermal models were evaluated, selected and adopted in component based dynamic thermal simulation software Transient System Simulation Environment (TRNSYS). A system network representing the configuration of a proposed system can be establish which enables parametric and system study of the dynamic thermal behaviour. This computer simulation tool was applied to study the application of earthtube to maintain the summer thermal comfort of an office located at the southeast of UK. The results showed an optimized system configuration with the appropriate pipe diameter, pipe length and airflow rates are necessary to maintain the comfort conditions in the summer.

Keywords: ground-air heat exchanger, low energy cooling, thermal simulation, TRNSYS, low carbon technology, thermal comfort.

1 Introduction

Ground-Air Heat Exchanger (GAHX) is a cooling/heating system that consists of a network of pipes buried below the ground surface, through which ventilation outdoor air supply is passed through before entering the building or the air-handling unit. The concept of using GAHX is well established dating back to Persian and Greek architecture (Argirou 1996). Recent applications of the system however involve the use of fans to drive air through the pipes. Difference in temperature between the pipe wall and the air drives the pre-cooling/pre-heating of the ventilation air. The heat transfer between air and pipe surface is dependent on a number of factors including: ground temperature profile; ambient air temperature; pipe materials and the pipe dimensions; air flow velocity; soil property and pipe buried depth (Pfafferott 2007). As the behaviour of GAHX is affected by the physical, geological and climatic conditions, its dynamic thermal performance is therefore not universal and needs to be studied within these

context (Piechowski 1999). This paper reports on the research development of an integrated computer simulation tool that is capable of studying the thermal performance of GAHX and their impact to the energy use of building and the indoor thermal comfort. The tool was developed within the framework of the TRYSYS software, which already provided some of the basic building thermal analysis components. A critical review was performed to evaluate and select thermal model for the earth tube and ground temperature profile. Components of these were subsequently established. The potential impact of GAHX to the energy use of a building is demonstrated by means of a low-rise office building located in the Southeast of England.

2 Thermal Simulation

A component based building thermal simulation software Transient Systems Simulation Environment (TRNSYS) has been adopted for the thermal analysis in this study. TRNSYS is well-established software that already possesses a number of generic components which can be adapted to create a system simulation, some of the components include: ground-air heat exchanger, soil temperature generator, external climatic, ventilation system and an office (TRNSYS 2005). The thermal model representing the actual system is established by linking the components to form a logical network on the computer screen. System boundary, simulation parameters as well as output options are defined using facilities provided by TRNSYS. TRNSYS requires special training to gain knowledge of its operation, a Windows based user interface has therefore been developed to simplify the input-output procedure and to allow easy change of parameters for repeated analyses. This interface will be useful to users that are not competent in thermal modelling and use of TRNSYS.

3 Simulation Components

The characteristics and the properties of the components used in the simulation are described in the following sections.

3.1 Soil Temperature Generator

In order to study the behaviour of earth-air heat exchangers there is a need to have a clear understanding of how the soil temperature changes with depth and time over the year. Subsurface soil temperature in the UK is lower than ambient air temperature in summer and higher than ambient air temperature in winter. Figure 1 shows the annual profile of soil temperature for seven counties of South East England for the depth of 1m below the surface. Soil temperature within the region varies by about 1 K and 2K in winter and summer respectively, which smaller than the UK wide variations.

Thermal analysis of EAHX requires soil temperature as an input to the simulation. Because of the lack of soil temperature for most locations or depths below 1m, soil temperature predicting models are used to calculate soil temperature using readily available climatic parameters. Empirical correlations have been developed over the years for predicting soil temperature at various depths by Lab (1989). Labs (1989) developed a mathematical model based on the one-dimensional heat transfer in

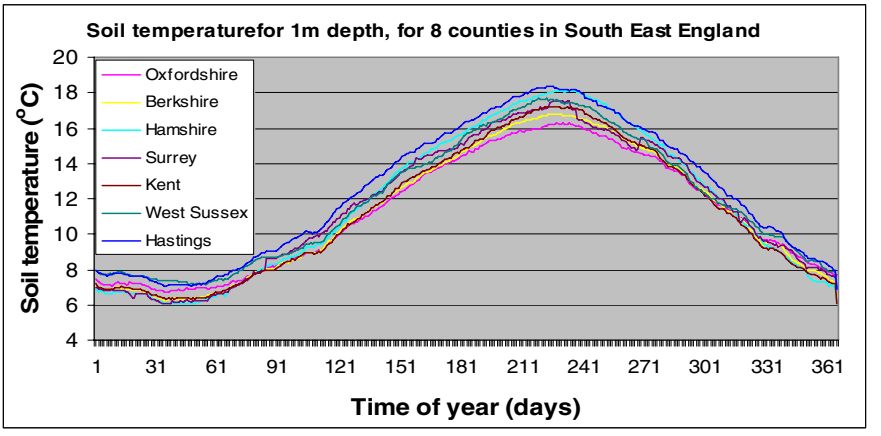

Fig. 1. Annual soil temperature profile for South East, UK

semi-infinite solids shown in Equation 1, which is based on the sinusoidal variation of soil surface temperature over the year. This mathematical model is used for calculating soil temperature for any depth and time of year, using information on ground physical and thermal properties and ground surface temperature, as inputs to the model. Equation 1 calculates soil temperature using available meteorological and soil parameters, and is useful in areas with limited or no soil temperature records. The mathematical model has been validated using soil temperature records of a location in South East United Kingdom and found to be accurate to about 1 K (Ahmed et al 2007).

$$T_{z,t} = T_m - A_s \times \exp\left[-z\left(\frac{\pi}{8760\alpha}\right)^{1/2}\right] Cos\left\{\frac{2\pi}{8760}\left[t - t_0 - \frac{z}{2}\left(\frac{8760}{\pi\alpha}\right)^{1/2}\right]\right\}$$

Equation 1. Soil temperature prediction equation

Where:

T_{zt} Soil temperature at time t and depth z (ºC).
A_s Annual amplitude of ground surface temperature (ºC).
α Thermal diffusivity of soils (m^2/hr).
z Depth below ground surface (m).
t Time elapsed from the beginning of the year (hours).
t_o Hour of the year with minimum soil surface temperature (hours).
T_m Mean annual soil surface temperature.
π 3.1416.

The variation of soil surface temperature at different times of the year is what determines the subsurface soil temperature. This parameter is not measured by most weather stations in the UK. Long term monthly average soil surface temperature from NASA Surface Meteorology and Solar Energy database (NASA 2006) has been collected and used to generate hourly soil surface temperature with TRNSYS Weather

Generator (TYPE 54). The data generated has been used to provide the hourly soil surface temperature at different times of the year.

3.2 Ground-Air Heat Exchanger

Thermal modelling of earth-air heat exchanger has been established by researchers using both analytical and numerical heat transfer analysis. Tzaferis et al. (1992) compared a range of thermal models with short term experimental data and finds significant level of agreement, even though length of the experimental data is not long enough for the thermal storage capacity to be a major influence on the experimental results. Some of these models have limitations such as, the type of configurations that can be modelled, detail of the heat transfer analysis (1, 2, 3 three dimensional approximations) and number and complexity of input and output parameters. The thermal simulation in this research is based on the numerical three dimensional thermal model developed by Holmuller (2001) selected after an in-depth review of existing models. The model is based Finite Difference method of heat transfer analysis in soil and takes account of both sensible and latent heat transfer between pipe surface and air. The model also allows for the dimensioning of multiple configurations of EAHX and non-homogenous soil condition. The disadvantage of the model is the need for a complex set of input parameters in the form of a simulation file that is called by the TRNSYS simulation after each simulation runs. The parameter files consist of thermal properties of soil, pipe, air and the description of the soil and pipe node location and sizes. A pre-processor for the generation of the parameter definition file has been developed as a C++ executable which will significantly reduce the time required for generating the parameter definition file. Thermal simulation has been run for a range

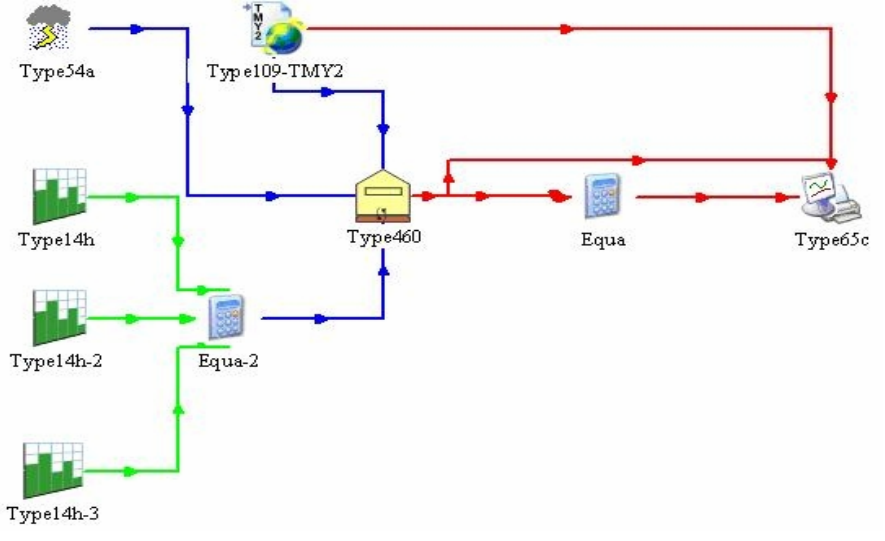

Fig. 2. TRNSYS Earth-air heat exchanger simulation

of earthtube dimensions and air velocity. The Earth-air heat exchanger outlet temperature has been presented as a frequency distribution of the occurrence of outlet air at certain temperature, this provides a measure of comparing outlet air temperature based on the percentage of outlet air temperature that exceed certain temperature during the simulation period in a particular location. Secondly the outlet air temperature profile for different dimensions of earth-air heat exchanger for different locations have been plotted and compared with inlet air temperature. Figure 2 show the TRNSYS simulation project that has been used as the basis for the development of TRNSED Earthtube simulation tool.

Figure 3 shows the frequency distribution of outlet air temperature from 20cm diameter earth-air heat exchanger buried at 2m depth with air velocity of 1 and 3 m/s. With small pipe diameter it is clear from the figure that at low air velocity of 1 m/s 100 % of outlet air of 30-80m EAHX is below 19ºC and for 90% of the time the outlet air temperature was below 17ºC for all lengths. The variation in outlet air temperature reveals that for small diameter pipes the benefit if increase in length does not appear to have any significant thermal benefit on the reduction of outlet air temperature. The total variation of maximum outlet air temperature for 30 to 80m pipes are found to be less that 2.5 K. This variation further reduces between to 1K for the 40-80m length and 0.5 for 50-80m. Figure 3 also shows the annual outlet air temperature for different lengths of earthtubes, which shows that the thermal performance of the system improves with increase in length.

3.3 Office

TRNSYS visual building interface (TRNBLD) allows for the development of a building description file which contains detailed information on the building geometry,

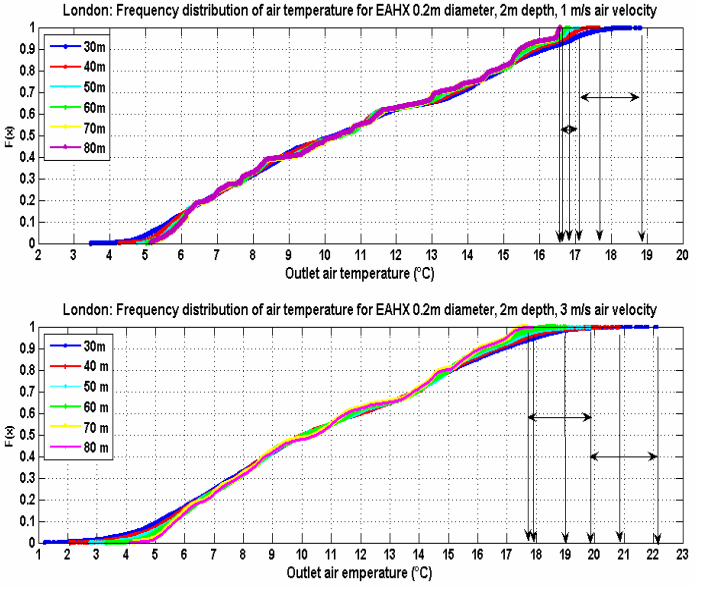

Fig. 3. London: Frequency distribution of Outlet air temperature, 30-80m length

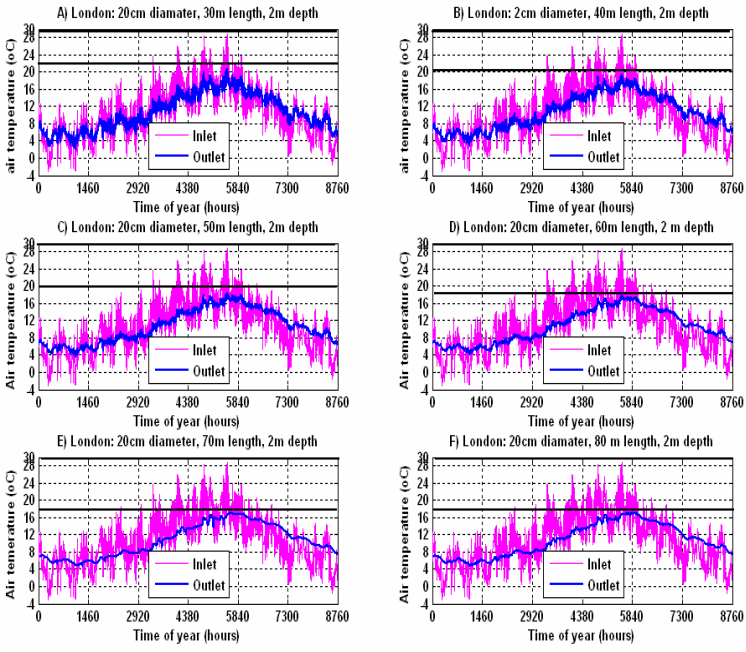

Fig. 4. Air temperature for London; EAHX 30m to 80m long, 2 m/s air velocity

materials, internal loads and connection to other components such as the weather data generators. TRNBLD also allows for the creation of multi-zone buildings, each building zone is a non-geometrical balance models with one air node per zone, which represents the thermal capacity of zone air. Office building of dimensions (20m X 10m X 3m) has been developed and integrated with EAHX simulation, to establish the impact of EAHX on the indoor environment in summer. The TRNSYS building interface (TRNBLD) has been used to develop a building model of the description in Table 1. Values of internal gain recommended by (CIBSE 2006) for office building has been used to describe building internal gains. Climate data for London South East England has been generated and used as input to the simulation using TRNSYS Weather generator (TYPE109). The building ventilation air is supplied through different configuration of EAHX.

3.4 Climate Conditions

The thermal evaluation of Earthtube and building requires input of hourly climate data, ambient air temperature, relative humidity, solar radiation and soil surface temperature. Climate data for this study has been generated using TMY2 files generated using Meteonorm programme and the TRNSYS weather ready (Type109), which generates climate data at any interval using long term monthly average values of any location around the world. Average climate data for London South East England have been used to generate hourly climate data required for earthtube and building simulation.

Table 1. Building description

Parameter	**Values**
Total floor area	200 m^2
Room volume	600 m^3
External wall surface area	180 m^2
Window area: (% of wall area)	
South	40%
North	40%
East	25%
West	25%
Floor area allowance per person	10 m^2 (20 people)
Minimum suggested air supply	8 ($l.s^{-1}.person^{-1}$)

4 Results and Discussions

Because earth-air heat exchanger changes the condition of ambient air to provide ventilation air supply at lower temperature and higher relative humidity to the air handling unit or directly to the building. This study determines the potential of earth-air heat exchanger for improving indoor thermal conditions. In order to achieve this building simulation has been carried out using the integrated Earthtube and building model to simulate a mechanical ventilation system consisting of all air system. The first case utilise ambient air condition as the ventilation air supply using 4 and 5 air changes per hour (ACH). The second case outlet air from 0.3m diameter, 60m long Earthtube as ventilation air supply. Both cases utilized mechanical ventilation system, by using fan to drive air movement through building air handling unit. Figures 5 and 6 shows the building indoor condition for ambient air and earthtube ventilation strategies, which indicates that Earthtube provides significant improvement in building thermal comfort condition throughout the year. The indoor temperature exceeds 30ºC

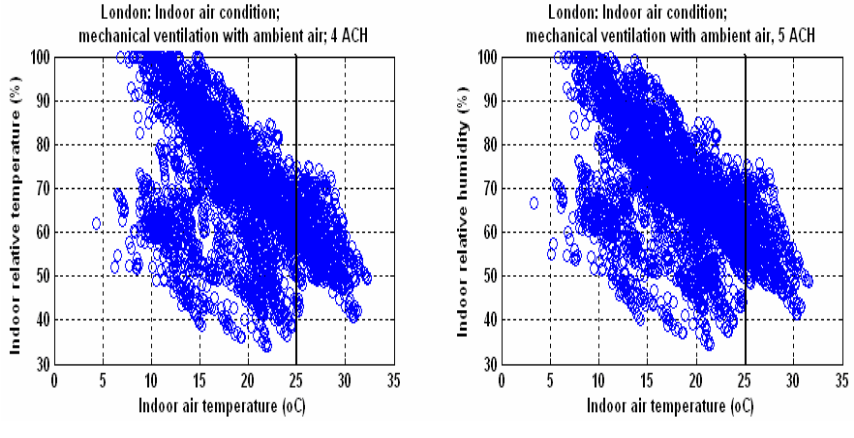

Fig. 5. Indoor air condition for ventilation with ambient air

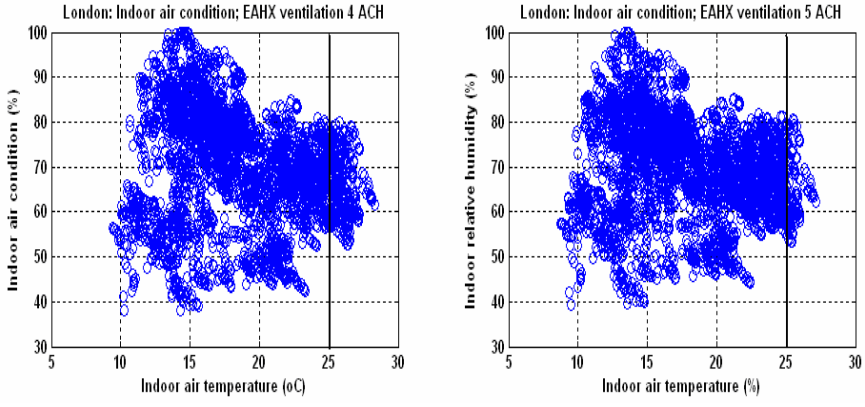

Fig. 6. Indoor air temperature; EAHX ventilation 0.3m diameter, 60m length

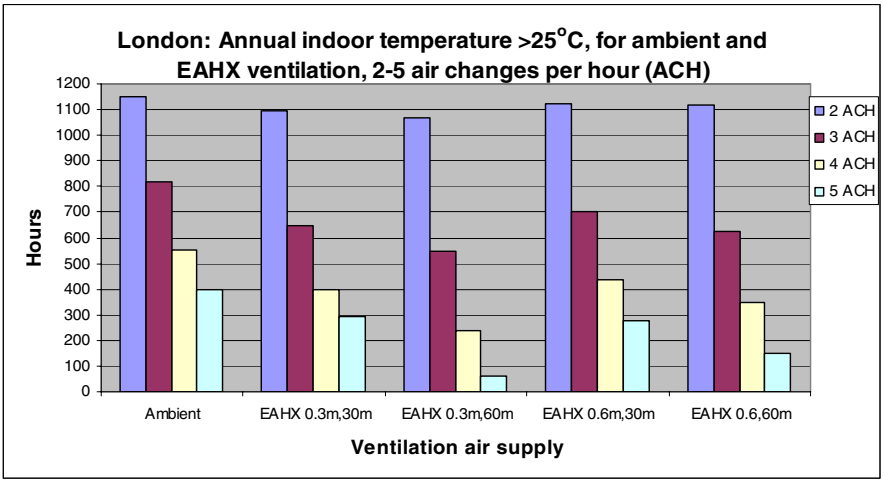

Fig. 7. Indoor temperature exceeding 25ºC, EAHX and ambient air ventilation

with 4-5 air changes per hour for ventilation with ambient air. The indoor conditions remained below 28ºC for 4-5 air changes per hour for similar ventilation with earthtube ventilation.

Figure 7 shows the number of hours exceeding 25ºC set point temperatures for ventilation with ambient air and different configuration of earthtubes. The results reveal that for all ventilation air changes, ventilation with ambient air has the highest number of hours exceeding the set point temperature. While number of hours for ambient air ventilation ranges between 1150 to 400 hours for 2 to 5 air changes, the number of hours for ventilation with 30cm diameter, 60m long EAHX is about 1050 to 60 hours for 2 to 5 air changes ventilation rate. These results show that in South East England, small diameter pipes provide the best option for reducing indoor temperature with at least a ventilation rate of about 5 air changes per hour.

5 Conclusions and Future Work

This research investigates the potential of ground-air heat exchanger under the climate of the Southeast of UK. It has identified and demonstrated the impact of the key parameters on the thermal behaviour of the earth tube system. Soil temperature profile and thermal models for predicting the outlet air conditions of the earth-air heat exchanger have been determined and applied in the thermal simulation software TRNSYS. Simulation of the sensible energy gains for various configurations of the GAHX system and the cooling demand of an office building showed significant benefits in improving indoor thermal conditions and reduction of cooling load if air-conditioning is used. The on-going research will study the performance of the system in other locations around the UK and assess the cooling capacities of various system configurations and boundary conditions.

References

Ahmed, A., Miller, A., Ip, K.: The potential of earth-air heat exchangers for low-energy cooling of buildings. In: Wittkopt, S.K., Kiang, T.B. (eds.) Passive and Low Energy Architecture. National University Singapore, Singapore (2007)

Argiriou, A.: Ground Cooling. In: Santamouris, M., Asimakopolous, D. (eds.) Passive Cooling of Buildings. James and James Ltd., Huddersfield (1996)

CIBSE: CIBSE Guide A: Environmental design, Norwich, Page Bros. (2006)

Hollmuller, P., Lachal, B.: Cooling and preheating with buried pipe systems: monitoring, simulation and economic aspects. Energy and Buildings 33, 509 (2001)

Kumar, R., Ramesh, S., Kaushik, S.C.: Performance evaluation and energy conservation potential of earth-air-tunnel system coupled with non-air-conditioned building. Building and Environment 38, 807 (2003)

Labs, K.: Earth Coupling. In: Cook, J. (ed.) Passive Cooling. MIT Press, Cambridge (1989)

NASA, NASA Surface Meteorology and Solar Energy, NASA (2006)

Pfafferott, J., Walker-Hertkorn, S., Sanner, B.: Ground cooling: Recent progress. In: Santamouris, M. (ed.) Advances in passive cooling, London, Earthscan (2007)

Piechowski, M.: Heat and Mass Transfer Model of a Ground Heat Exchanger: Theoretical Development. International Journal of Energy Research 23, 571–588 (1999)

TRNSYS16.0, A Transient System Simulation Programme. 16.0 ed. Madison, WI. University of Wisconsin (2005)

Tzaferis, A., et al.: Analysis of the accuracy and sensitivity of eight models predict the performance of earth-air heat exchangers. Energy and Buildings 18(1), 35 (1992)

Study on a Novel Hybrid Desiccant Dehumidification and Air Conditioning System

K. Sumathy[1], Li Yong[2], Y.J. Dai[2], and R.Z. Wang[2]

[1] Department of Mechanical Engineering, North Dakota State University, Fargo, ND, USA
[2] Institute of Refrigeration and Cryogenics, Shanghai Jiao Tong University, Shanghai, 200030, P.R. China

Abstract. This paper proposes a novel hybrid desiccant dehumidification and air conditioning system. The aim is to achieve a higher energy efficiency to reduce the use of electricity by utilizing the desiccant dehumidification system to remove latent load, while the vapor-compression and IEC system meeting the sensible heat load. Experimental set-up has been built by combining the rotary desiccant wheel, heat exchangers with compressive cooling system. Tests are carried out at typical operative ranges for air conditioning applications, more specially for high humid regions in southeast China. Two desiccants namely LiCl and composite desiccant are used in the experiments. Results are reported both in terms of COP based on primary energy usage and electrical energy usage. Significant reduction in humidity ratio has been obtained through respective subsystem and thereby effecting a higher COP based on primary energy usage. The composite desiccant can achieve a COP close to that of LiCl while assuring a stable performance. It is found that the hybrid system can achieve a higher energy performance in hot humid regions.

1 Introduction

Buildings comsume more than 30 percent of all energy and 60 percent of electricity in China. HVAC system uses more than 70 percent of these energy in the buildings. Hence, it is important to enhance the energy efficiency of air conditioning system to reduce the energy used in buildings. The idea of hybrid cooling system is to combine two or more cooling systems, to improve the overall system performance and make good use of low grade energy source. The hybrid system, which is the subject of present work, combines a vapor-compression air conditioning system with a desiccant dehumidification system and indirect evaporative cooling (IEC) system. In present hybrid desiccant cooling system, the desiccant dehumidification system is intended to remove latent load, while the vapor-compression and IEC system will meet the sensible heat load. Hence, it is proposed as an alternative to existing conventional vapor compression systems, which could result in a considerable reduction in electircal energy consumption as well as lowering the energy costs.

Several researchers have worked on different hybrid systems [1-3]. The performance of a first generation prototype desiccant integrated hybrid system was investigated through establishing a numerical model of the system by Worek and Moon [4]. Their system utilized waste heat rejected from a vapor compression cycle,

to directly activate a solid desiccant dehumidification cycle. Results showed that at the same level of dehumidification, 60% performance improvement over vapour compression system was obtained at Air-conditioning & Refrigeration Instiute (ARI) design conditions. The performance of hybrid system decreased as the outdoor humidity ratio was increased. Nevertheless, over the range investigated, the performance improvement varied from 44 to 74%. More rencently, Dhar and Singh [5] analyzed the performance of four hybrid cycles for a typical hot-dry and hot-humid weather, based on the analogy method of Maclaine-Cross and Banks [3]. Effect of room sensible heat factor, ventilation mixing ratio, and regeneration temperature were analyzed. Results show that solid desiccant-based hybrid air-conditioning systems can give substantial energy savings, compared to the conventional vapour compression refrigeration based air-conditioning systems.

Though some useful results have been achieved, it can be observed that most previous works were based on theoretical analysis, and experimental research is scarce. Also, most of the working conditions studied in previous work are under mild ARI condition, which is very much different from the prevailing weather conditions in southeast China.

The objective of present work is to stduy the performance of such hybrid system working under hot-humid conditions and check the potential of electrical energy saving when desiccant based air conditioning system is employed as a part of the hybrid system. Hence, in the present work, an experimental hybrid desiccant cooling set-up had been built, and experiments were carried out for a typical hot-humid conditions, reflecting the actual weather in southeast China. The system performance has been evaluated based on two different criteria: (i) COP based on primary energy usuage and (ii) COP based on the electrical energy input. Performance of the system under typical design conditions (regeneration temperature and process air flow rate) was first measured and analyzed. The ability of such system to work under part load has also been investigated.

2 System Description

Figure 1 shows the schematic diagram of the hybrid air-conditioning system operating on an open cycle during ventilation mode. It comprises of three main subsystems: 1) a honeycomb rotary dehumidifier; 2) a cross-flow IEC unit; and 3) a conventional vapor compression air-conditioning unit.

Unlike the conventional desiccant systems, the present hybrid system would have three air streams: (i) process air being delivered to conditioned space; (ii) regeneration air being used to regenerate the desiccant material; and (iii) the ambient air is used to pre-cool the process air exiting from the dehumidifier.

On the process side, initially, moist air gets dehumidified as it flows through the desiccant wheel (state 2); i.e., when the rotating wheel is exposed to regeneration air flow, adsorbed moisture is released from the wheel. Due to the effect of adsorption heat and heat transfer from the regeneration stream via the rotating desiccant wheel, temperature of the dehumidified process air at the outlet of the desiccant wheel (state 2) is significantly higher than at the inlet (state 1). The desiccant wheel is driven by a constant speed motor through a gear. The wheel consists of Lithium Chloride (LiCl)

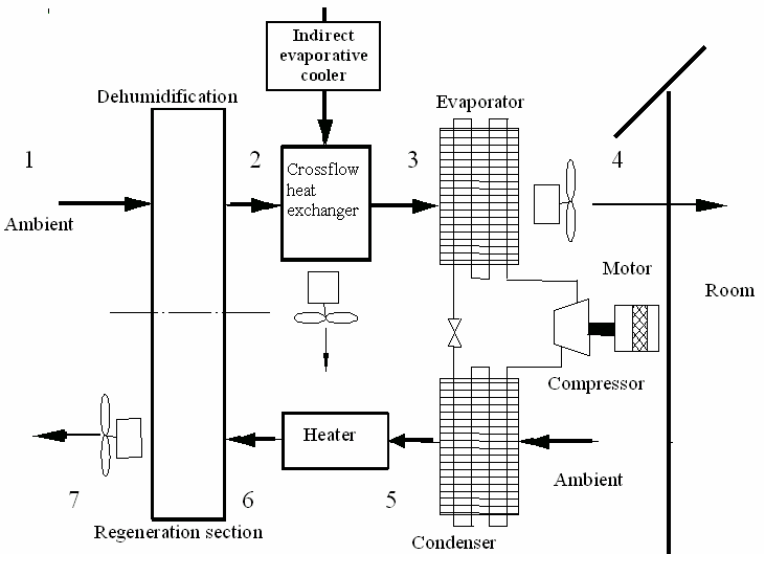

Fig. 1. Schematic of the hybrid system

coated honeycomb air passageways along the length and is equipped with Teflon coated rubber seals to minimize intermixing of the two streams. Once the hot process air leaves the dehumidifier, it is cooled by an indirect evaporative exchanger to state 3 and is further cooled with a conventional vapor compression cooler to attain the required comfort condition (state 4).

On the regeneration side, ambient air initially flows through the condenser of the conventional vapor compression system to recover heat, and gets further heated by an electrical heater to a specific temperature (state 6) in order to regenerate the desiccant.

The flow rate of each air stream is controlled with a damper. Flow areas for the process and regeneration air streams is set to be at a ratio of 3: 1. The process air is heated with an adjustable 8 kW heater and humidified with an adjustable 3 kW humidifier to meet the desired temperature and humidity ratio conditions. Similarly, the regeneration air temperature is controlled with an adjustable 9 kW electrical heater.

The third air stream drawn from the ambient is forced through a falling film evaporative cooler by a fan in order to achieve a lower temperature, and is then allowed to pass through a cross-flow heat exchanger, to pre-cool the process air from the desiccant wheel.

Two desiccant materials are used in the hybrid system. They are LiCl and compound desiccant developed in our lab [6]. The diameter of the desiccant wheel is 320 mm and the length is 200 mm. The rotational speed of the wheel is kept constant at 7 r/h. The temperature and relative humidity is measured by a TNT-N263A high accuracy and multi functioned Digital Thermo/ Hygrometer with an accuracy of ± 0.5 ºC and ± 2% RH. The air flow rate is measured using a Alnor Electronic Balometer system along with a APM 150 meter which could measure airflow rate within an accuracy of ± 12 m^3/h. Galvanometer and a voltmeter are used to measure the power consumed by fans and vapor compression air conditioner unit with an accuracy of 3 V and ± 0.01 A. The various operative conditions are listed in Table 1.

Table 1. Operating conditions of the system

Parameter	Value
Volumetric process air flow rate	400 ~1000 m^3/h
Volumetric regeneration air flow rate	300 m^3/h
Volumetric pre-cooling air flow rate	800 m^3/h
Regeneration air temperature	60 ~120 °C
Ambient air temperature	30 ~38 °C
Ambient air humidity ratio	13 ~22 g/kg dry

Table 2. ASHRAE *Standard* 55 on Thermal Environmental Conditions for a specified temperature range

Temperature (°C)	RH (%)	w (g/kg dry air)
23	76	13.4
24	69.6	13
25	63	12.6
26	57.9	12.2

Once temperature and humidity of the system attains steady state conditions, various measurements are made. It takes about thirty minutes for the system to attain steady state. Flow rate and pressure drop measurements have been repeated two times to ensure consistency. The present hybrid system is mainly considered for ventilation applications, and hence, different weather conditions in hot humid region were tested. It should be mentioned here that, it is impossible to achieve a constant output of process air at state 4 (ideal condition) for the given experimental set-up. Therefore, the comfort zones listed in Table 2, as specified by the ASHRAE *Standard* 55 on Thermal Environmental Conditions for Human Occupancy [7], are identified as the upper limit of the designed output conditions.

3 Performance Analysis

The objective of developing this hybrid system is to use the low-grade heat such as waste heat or solar thermal energy and reduce the consumption of electrical energy. Hence, the coefficient of performance based on electrical energy input (utilized vapor compression air conditioner and fans) is defined to evaluate the energy efficiency of this system:

$$COP_e = \frac{Q_c}{E} \tag{1}$$

In the above equation, Q_c is the cooling capacity and is defined as:

$$Q_c = \dot{m}_{pa} (h_4 - h_1) \tag{2}$$

'*E*' represents the electrical power used to drive the hybrid system. Fans are employed to force circulate the regeneration air as well as process air streams and also for the

indirect evaporative cooling unit. In our experimental study, it is found that this portion of energy is very significant and can not be neglected. Hence, E is calculated including the electrical power for driving the fans:

$$E = E_{com} + E_{fan1} + E_{fan2} + E_{fan3} \tag{3}$$

In this experiment, the power of process air fan E_{fan1} is 0.5 kW. The power of precooling air fan E_{fan2} and regeneration air fan E_{fan3} are the same in the range of 0.15 kW. This hybrid system is driven both by thermal energy as well as electrical energy. To evaluate the performance of this system based on different energy input, the electrical and thermal energy must be expressed on a common basis. The sum of the fossil fuel equivalent of the electrical energy use and corresponding equivalent of the thermal energy input is referred to as the primary energy use, which is defined as [8,9]:

$$Q_p = \frac{Q_{th}}{\eta_{th}} + \frac{E}{\eta_e} \tag{4}$$

$$Q_{th} = \dot{m}_{pr} (h_6 - h_5) \tag{5}$$

In this study, η_{th} and η_e were taken to be 1.0 and 0.3, respectively [10]. Q_{th} represents the heat utilized for regeneration process. It should be pointed out that, even though the regeneration air stream is heated by an electrical heater, for practical applications, low grade thermal energy such as solar energy or waste heat can be used. Hence, in the present analysis, the portion of energy used to regenerate the desiccant is classfied as "thermal energy". A detailed error analysis indicated an overall accuracy within ± 13.5% for COP_p and ± 11.7% for COP_e.

4 Results and Discussion

Table 3 lists the measured dry- and wet-bulb temperatures and calculated properties for the process air during a typical operation. It can be found that the humidity ratio of process air is reduced to the required inlet value after the steam flows through the desiccant wheel. Furthermore, the temperature of process air is lowered to nearly its original inlet value at state 3 (Fig. 1) due to the cooling effect of Indirect Evaporative Cooling (IEC). The enthalpy reduction ratio between the desiccant subsystem (state1~3) to the compressive subsystem (state 3~4) is 1.5. This demonstrates that the latent heat can effectively be removed by the desiccant rotary wheel, and the sensible heat can be released using a heat exchanger along with the conventional vapor compression unit.

Table 4 illustrates the energy performances of hybrid system using two different desiccant wheels under typical ambient and working condition (m_{pa} = 750 m^3/h, T_{rga} = 100 °C, m_{rga} = 300 m^3/h, T_{amb}= 30°C, w_{amb} = 19 g/kg dry air), the COP_p turns out to be 0.49 and 0.47 for LiCl and compound desiccant respectively. Hence, COP_p of the present hybrid system is higher compared to the previous simple desiccant cooling system (COP_p = 0.45) [8]. This may be due to high efficiency of the two subsystems such as the desiccant subsystem and the IEC unit.

Table 3. The typical measured and calculated state properties of the system shown in Fig. 1

Desiccant : LiCl, m_{pa} = 750 m^3/h T_{rga} = 100 °C m_{rga} = 300 m^3/h

State	T (°C)	RH (%)	w (g /kg dry air)	h (kJ/kg dry air)
1	30	70.5	19	78.5
2	52	14	11.7	83
3	32	40	11.8	62.6
4	21	76	11.9	51.1
5	45	36.9	19	93
6	100	2.5	19	150
7	51	20	38	148

Table 4. Energy performances of hybrid system using two different desiccant wheels

m_{pa} = 750 m^3/h T_{rga} = 100 °C m_{rga} = 300 m^3/h

Desiccant	COP_p	COP_e
LiCl	0.49	3
Composite	0.47	2.6

For the given system, the COP_e turns out to be 3 which is lower than reported (COP_e ~ 5) in the literature[8]. This is because: (i) in their work, the electricity energy utilized by fans was neglected. However, in the present study, it is found that this portion of energy significantly accounts to more than 30% of total electricity consumed by the system; (ii) the actual COP of the conventional vapor compression unit in present study is lower than their assumed COP.

Besides the investigation of the system under typical working conditions, (m_{pa} = 750 m^3/h, T_{rga}= 30°C) the effects of flow rate of process air (m_{pa}) and regeneration temperature (T_{rga}) on the system performance were also studied. Figure 2 shows the variation in system performance with the process air flow rate for a given T_{rga} and m_{rga}. It is seen that the COP_p increases significantly when the flow rate is lower than 900 m^3/h. This is due to the fact that: (i) for low values of m_{pa}, moisture removal increases significantly with m_{pa} without any addition in regeneration energy. (ii) In the present system, the flow rate is varied by adjusting the outlet opening of the damper. Hence, for low values of m_{pa}, electrical energy input to the fans and vapor compression AC marginally reduces compared to its nominal value (in 750 m^3/h). Therefore, the total energy input remains almost unchanged and the increase in system performance is dictated only by the cooling power. However, it should be noted that, when the flow rate is further increased beyond 900 m^3/h, there exists no appreciable increase in COP_p, because the increase in rate of moisture removal as well as sensible cooling effect is not pronounced.

The effects of regeneration temperature (T_{rga}) on the COP_p are illustrated in Fig. 3. An interesting trend is observed in COP_p for desiccant LiCl. That is, with an increase in T_{rg}, COP_p increases, reaching a maximum value of 0.5; but with a further increase in T_{rg} beyond 100 °C, COP_p reduces, gradually. This can be

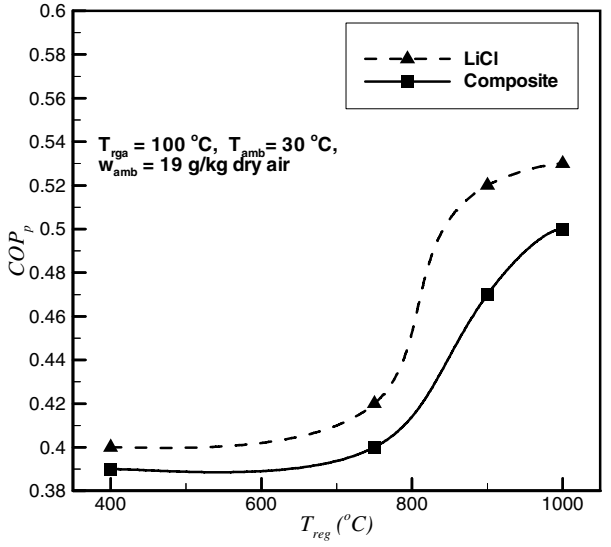

Fig. 2. Effect of process air flow rate on the hybrid system's performance

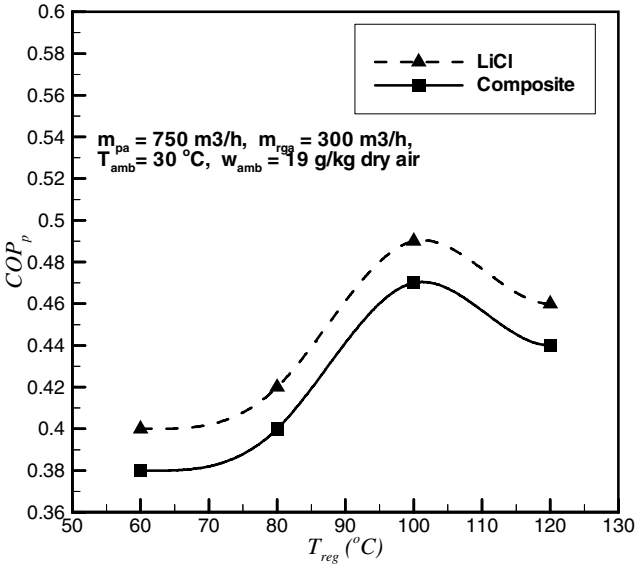

Fig. 3. Regeneration temperature vs. system performance

attributed to the fact that when T_{rg} is low, dehumidification ability of the desiccant wheel increases with regeneration temperature, in turn effecting to an increase in system performance. However, with an increase in regeneration temperature (T_{rg} > 100 °C), sensible heat transferred to the process air stream becomes much higher,

resulting in a higher outlet temperature of the process air; this in turn has to be cooled by the heat exchanger along with the conventional AC unit, which affects the COP_p.

A similar trend can be found for COP_p of composite desiccant developed in our lab. However, the reduction in COP_p value obtained by the composite desiccant is not significant (less than 5%). Considering the fact of stability and no crystallization process happening when used at high water concentrations, the composite desiccant wheel can be a promising component used for hybrid system.

5 Conclusion

A hybrid desiccant dehumidification and air conditioning system is built and tested to study performance and its feasibility in hot-humid regions. It is found that, the latent heat can be released by desiccant wheel, while the sensible heat could effectively be removed by indirect evaporative cooling unit and conventional air conditioner. The system could attain a maximum performance of 0.5 and 3 measured on the basis of primary energy input and electrical energy input, respectively. Results have shown that, the flow rate of process air as well as regeneration temperature have greater influence on the system performance and when regeneration temperature is beyond 100 ºC, the performance declines. The composite desiccant which is more stable than LiCl can be used in hybrid system with a marginal reduction in energy efficiency.

Nomenclature

COP_p	coefficient of performance based on primary energy use
COP_e	coefficient of performance based on electrical energy input (vapor compression air conditioner & fans)
E	electrical power (W)
h	enthalpy of moist air (J/kg dry air)
m	volume flow rate of air (m^3/h)
p	pressure (Pa)
Q	heat energy (J)
RH	relative humidity
T	temperature (ºC)
w	humidity ratio (g water/kg dry air)

Greek letters

η_e	conversion efficiency of electricity from fuel at the point of generation to electricity at the point of use, assumed to be 0.29.
η_{th}	conversion efficiency from fuel to thermal energy, assumed to be unity.

Subscripts

c	cooling capacity
e	electrical energy
ia	indirect evaporative heat exchanger secondary air stream
o	ambient air

p	primary resource energy
pa	process air stream
rga	regeneration air stream
th	thermal energy

References

[1] Burns, P.R., Mitchell, J.W., Beckman, W.A.: Hybrid desiccant cooling systems in super market applications. ASHRAE Trans. 91, Part-1B, 457–468 (1985)
[2] Sheridan, J.C., Mitchell, J.W.: Hybrid solar desiccant cooling system. Solar Energy 34(2), 187–193 (1985)
[3] Maclaine-Cross, I.L., Banks, P.J.: Coupled heat and mass transfer in regenerators predictions using an analogy with heat transfer. Int. J. of Heat and Mass Transfer 15, 1225–1241 (1972)
[4] Worek, W.M., Moon, C.J.: Desiccant integrated hybrid vapour compression cooling — performance sensitivity to outdoor conditions. Heat Recovery Systems and CHP 8(6), 489–501 (1988)
[5] Dhar, P.L., Singh, S.K.: Studies on solid desiccant based hybrid air-conditioning systems. Applied Thermal Engineering 21, 119–134 (2001)
[6] Dai, Y.J., Jia, C.X., Wang, R.Z., Wu, J.Y.: Use of compund desiccant to develop high performance desiccant cooling system. International Journal of Refrigeration 30, 345–353 (2007)
[7] ASHRAE, ASHRAE Handbook of Fundamentals, American Society of Heating, Refrigerating and Air Conditioning Engineers, Atlanta (1997)
[8] Jurinak, J.J., Mitchell, J.W., Beckman, W.A.: Open cycle desiccant air conditioning as an alternative to vapor compression cooling in residential applications. Journal of Solar Energy Engineering 106(3), 252–260 (1984)
[9] Dai, Y.J., Wang, R.Z., Zhang, H.F., Yu, J.D.: Use of liquid desiccant cooling to improve the performance of vapor compression air conditioning. Applied Thermal Engineering 21(12), 1185–1202 (2001)

Author Index